Journal of Diabetes Research

Animal Models of Diabetes and Its Associated Complications

Guest Editors: Md. Shahidul Islam, Daisuke Koya, and Bernard Portha

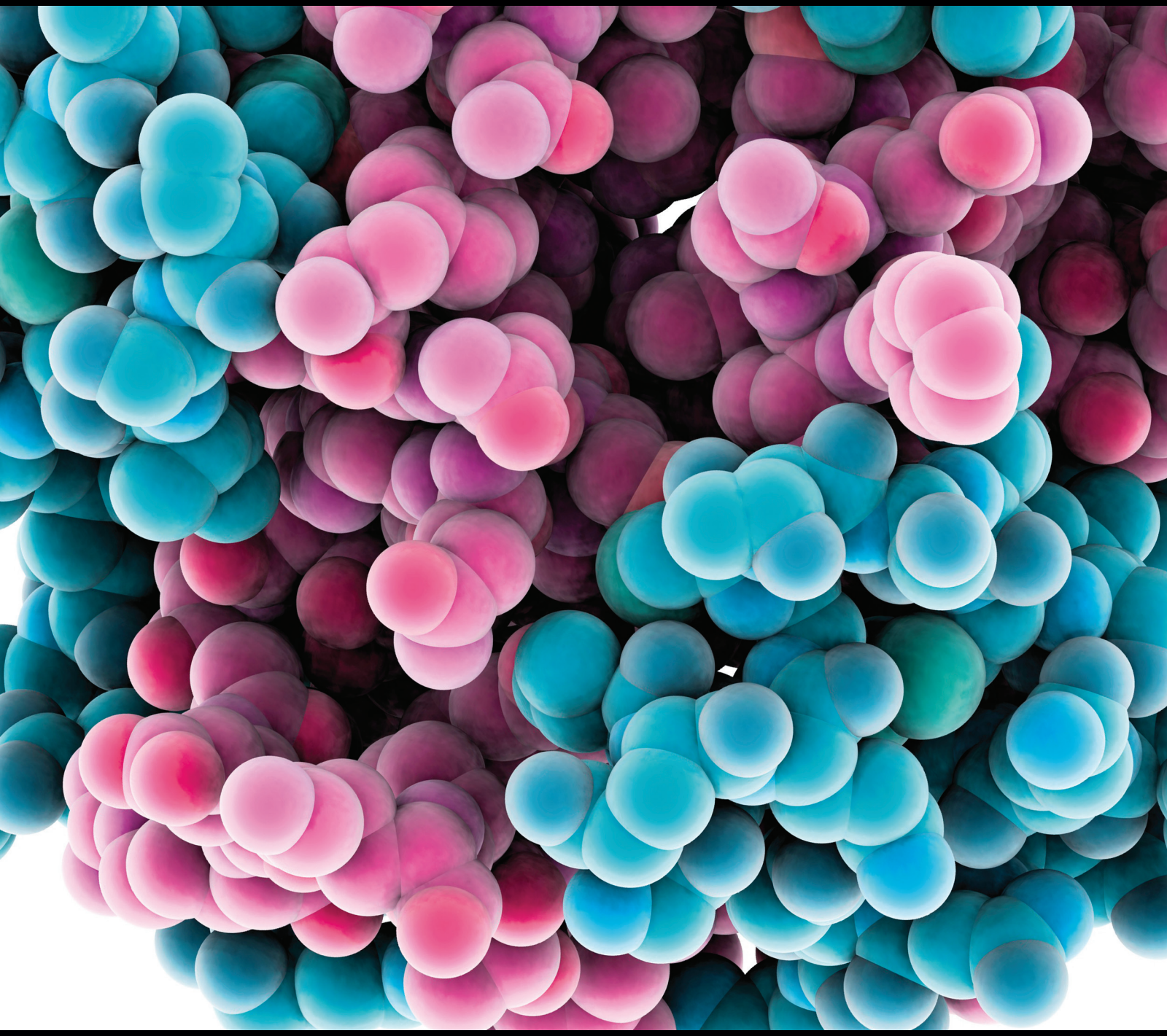

Animal Models of Diabetes and Its Associated Complications

Journal of Diabetes Research

Animal Models of Diabetes and Its Associated Complications

Guest Editors: Md. Shahidul Islam, Daisuke Koya, and Bernard Portha

Editorial Board

Contents

Hindawi Publishing Corporation
Journal of Diabetes Research
Volume 2013, Article ID 593204, 1 page
http://dx.doi.org/10.1155/2013/593204

Editorial

Animal Models of Diabetes and Its Associated Complications

Md. Shahidul Islam,[1] Daisuke Koya,[2] and Bernard Portha[3]

[1] *Department of Biochemistry, School of Life Sciences, University of KwaZulu-Natal (Westville Campus), Durban 4000, South Africa*
[2] *Department of Diabetology & Endocrinology, Kanazawa Medical University, Kahoku-gun, Ishikawa 920-0293, Japan*
[3] *Laboratory of Biology and Pathology of the Endocrine Pancreas, University of Paris-Diderot and CNRS, 75013 Paris, France*

Correspondence should be addressed to Md. Shahidul Islam; islamd@ukzn.ac.za

Received 18 September 2013; Accepted 18 September 2013

Diabetes is a major threat to global public health. According to the latest data from the International Diabetes Federation (IDF), at least 366 million people are living with diabetes and this number is projected to be 552 million by 2030. At least 50% of people with diabetes suffer from one or two major diabetic complications such as diabetic cardiomyopathy, nephropathy, neuropathy, retinopathy, and diabetic foot diseases. Development of an authentic model of each type of diabetes and their associated complications, which exactly mimic the human pathogenesis, is very crucial not only for a better understanding of the core causes of the diseases but also for the development and routine pharmacological screening of novel anti-diabetic drugs. A number of genetic and nongenetic animal models of the different types of diabetes and their associated complications have been developed in last three decades but none of them are without limitations.

This special issue of the Journal of Diabetes Research has been designed to publish original and review articles with novel approaches of the development of animal model of diabetes and its associated complications. Almost all areas of the animal models of diabetes and its associated complications have been covered by this issue. Among the reviews: the animal models of diabetic retinopathy by A. K. W. Lai and A. Lo, animal models of diabetic neuropathy by M. S. Islam, murine models of diabetic neuropathy by L. L. Kong et al., methods and models for metabolic assessment by G. Pacini et al., and porcine models of accelerated coronary atherosclerosis by D. Hamamdzic et al. contributed significantly by summarizing the advantages, disadvantages, and suitability of animal models developed to study the above-mentioned diabetic complications. Many other original papers such as role of adrenomedulin in the renal NADPH oxidase and (pro)renin in diabetic mice by M. Hayashi et al., development of glomerulopathy in the KK.Cg-Ay/J mouse with the pathology of diabetic nephropathy by P. Stephen et al., and the role of ERK/MAPK and TGF-beta/Smad signaling pathways in the kidney fibrosis of diabetic mice by X. Cheng et al. contributed novel information in the pathogenesis of diabetic nephropathy, a major and common complications of diabetes mellitus. Finally, an exceptional paper has been contributed by E. Hillhouse et al. on the effect of nearby construction on the progress to overt autoimmune diabetes in NOD mice. As a whole, papers from almost every aspects of the animals models of diabetes and its associated complications have been published in this special issue so it can be a special interest of diabetes researchers particularly those who are working in the different areas of diabetic complications.

Md. Shahidul Islam
Daisuke Koya
Bernard Portha

Hindawi Publishing Corporation
Journal of Diabetes Research
Volume 2013, Article ID 106594, 29 pages
http://dx.doi.org/10.1155/2013/106594

Review Article

Animal Models of Diabetic Retinopathy: Summary and Comparison

Angela Ka Wai Lai[1] and Amy C. Y. Lo[1,2]

[1] *Department of Ophthalmology, Li Ka Shing Faculty of Medicine, The University of Hong Kong, Hong Kong*
[2] *Research Center of Heart, Brain, Hormone and Healthy Aging, Li Ka Shing Faculty of Medicine, The University of Hong Kong, Hong Kong*

Correspondence should be addressed to Amy C. Y. Lo; amylo@hkucc.hku.hk

Received 10 January 2013; Revised 2 September 2013; Accepted 2 September 2013

Academic Editor: Bernard Portha

Diabetic retinopathy (DR) is a microvascular complication associated with chronic exposure to hyperglycemia and is a major cause of blindness worldwide. Although clinical assessment and retinal autopsy of diabetic patients provide information on the features and progression of DR, its underlying pathophysiological mechanism cannot be deduced. In order to have a better understanding of the development of DR at the molecular and cellular levels, a variety of animal models have been developed. They include pharmacological induction of hyperglycemia and spontaneous diabetic rodents as well as models of angiogenesis without diabetes (to compensate for the absence of proliferative DR symptoms). In this review, we summarize the existing protocols to induce diabetes using STZ. We also describe and compare the pathological presentations, in both morphological and functional aspects, of the currently available DR animal models. The advantages and disadvantages of using different animals, ranging from zebrafish, rodents to other higher-order mammals, are also discussed. Until now, there is no single model that displays all the clinical features of DR as seen in human. Yet, with the understanding of the pathological findings in these animal models, researchers can select the most suitable models for mechanistic studies or drug screening.

1. Introduction

Diabetic retinopathy (DR) is a one of the most common microvascular complications of diabetes. In 2012, there are more than 371 million people suffering from diabetes, and it is being projected that the number of diabetic patients will reach 550 million in 2030 (http://www.eatlas.idf.org/; assessed 29-Nov-2012). Diabetes can be generally divided into two types: type 1 (insulin dependent) and type 2 (insulin independent), although patients of both types will have hyperglycemia. A study reported that about one-third of the diabetic patients have signs of DR and about one-tenth of them even have vision-threatening retinopathy [1]. Nearly 60% and 35% of DR patients progress to proliferative DR and severe vision loss in 10 years, respectively [2].

Clinically, DR can be classified into nonproliferative (NPDR) and proliferative (PDR) [3]. NPDR can be further graded into mild, moderate, and severe and is characterized by the presence of microaneurysms, hemorrhages, hard exudates (liquid deposits), cotton wool spots, intraretinal microvascular abnormalities, venous beading, and loop formation. NPDR may develop into PDR, where hallmarks of neovascularization of the retina and vitreous hemorrhage are found. Vision loss can be resulted from retinal detachment if patients are left untreated. Moreover, maculopathy, including macular edema and ischemia, can occur at any stage of DR; it accounts for the majority of the blindness due to DR. In fact, the growing number of diabetic patients and a longer life span in the aging population imply an increase in patients suffering from DR, which not only affects the quality of life of the individuals and their families but also increases the medical and economical burden to the society. As a consequence, effective therapy is urgently needed.

In order to develop effective drugs, detailed understanding of the pathophysiological progression of DR is required. Over half a century ago, histological studies have been

performed in postmortem retinas of diabetic patients. In retinal vessels and capillaries, selective endothelial and mural cells loss, presence of mural cell ghosts, endothelial clusters, acellularity, and microaneurysms were found to be increased in diabetic patients [4, 5]. Basement membrane thickening, presence of hemorrhage in the inner nuclear layer (INL), and outer plexiform layer (OPL) as well as eosinophilic exudates in the OPL were also reported [5].

Nowadays, immunological studies evidenced an increased glial fibrillary acidic protein (GFAP) expression in the Müller cell processes throughout the inner and outer diabetic retina, suggesting that these cells were hypertrophied [6]. There was also increased apoptosis in diabetic retina [7]. Abu El-Asrar et al. [8] further showed that proapoptotic molecules were expressed in ganglion cells, together with the activation of glial cells, which expressed several antiapoptotic molecules. Elevated vascular endothelial growth factor (VEGF) immunoreactivity was found in retinal blood vessels in diabetic humans with preproliferative or no retinopathy, further consolidated the role of VEGF in angiogenesis and vascular permeability [9]. Alternation in other factors, including somatostatin [10], cortistatin [11], αA and αB-crystallins, advanced glycation end products (AGEs), and receptor for AGE (RAGE) [12] as well as apolipoprotein A1 (ApoA1) [13], were also observed in the postmortem tissues. Somatostatin and cortistatin, which are neuropeptides with a very similar structure, were both downregulated in diabetic retinas, and their expression levels are inversely correlated with glial activation and apoptosis. On the other hand, upregulations of αA-, αB-crystallin, AGE, RAGE, and ApoA1 in the diabetic retinal tissue were reported. These morphological studies provide a better picture, yet without the mechanistic pathway, of the pathogenesis of DR at a cellular level. Moreover, advanced technologies further allow us to study the mRNA or protein expressions of various chemokines [14–17], cytokines [15–18], inflammatory markers [16, 19, 20], angiogenic factors [16, 17, 19–21], and other factors [19, 22, 23] in aqueous humor, serum, or urine from diabetic patients, thereby predicting the pathological pathways of DR. With the aid of the sophisticated computerized equipments and technologies, clinicians would even be able to monitor or predict the progression structural lesion [24–29] as well as functional defects [30, 31] in live patients with DR.

Although a lot of important information or clues on the development of DR can be obtained from human studies, the mechanisms of DR development still cannot be elucidated. Emergence of animal models, therefore, not only enables us to have a more comprehensive understanding of the etiology of DR at a molecular level in a controlled manner, but also fulfills the need for drug screening tools. With these models, we may even be able to discover the early markers for DR in the body fluids from diabetic patients. This not only allows a faster and more convenient screening but also serves as an alarm for diabetic patients before the presence of cellular or functional lesion. Until now, many studies on the pathogenesis of DR have been carried out in animal models. A cascade of events, including oxidative stress, inflammation, protein kinase C (PKC) activation, accumulation of AGE and sorbitol, and upregulation of rennin-angiotensin system (RAS) and VEGF, contribute to retinal vascular endothelial dysfunction as a result of hyperglycemia [3]. Based on the mechanistic studies, drugs targeting different molecules in the cascade are being developed. In order to evaluate the effect of the drug properly, reliable and appropriate animal models are required. Throughout the years, many animal models of DR have been developed; however, none of them can mimic the entire pathophysiological progression as observed in human. While most animal models only show the early symptoms of DR, some show the late stage proliferative angiogenesis. Researchers have to select an appropriate model or models which can compensate each other in order to address their research questions. In this review, we focus on the animal models of DR that researchers have used, briefly describe how the models were generated, highlight the morphological and functional changes in the retina, and finally discuss the strengths and weaknesses of each model.

2. Animal Models

2.1. Mouse Models of DR. In general, mice have been routinely used in many *in vivo* studies since they are small in size and therefore easy to handle and inexpensive to house. They also have relatively short life span that allows a shorter experimental turnover time. Indeed, mechanistic studies of DR have been carried out extensively in mice as these models share similar symptoms of early DR as in human. More importantly, the availability of a collection of transgenic and knockout mice allows researchers to study the role of particular genes, which may even be cell type specific, in the development and pathophysiological progression of DR. There are three main types of mouse models to study DR; the first two involve mice with hyperglycemia development either via pharmacological induction or inbreeding of mice with endogenous mutation while the third type focuses on pathological angiogenesis found in transgenic animals or induced by experimental procedures, in mice without diabetes.

2.1.1. Pharmacologically Induced Mouse Models of DR. Type 1 diabetes can be induced in mice by injection of chemicals, including streptozotocin (STZ) and alloxan, both of which are toxic to and therefore destroy the β-cells in the pancreatic islets. Hyperglycemia can also be induced in mice by feeding with galactose.

STZ-induced mice have been routinely used as a DR model in a lot of mechanistic studies and therapeutic drug testing for a long period of time owing to the abundant reports on the phenotypes. Depending on the injection dosage, the onset of diabetes can be achieved within a few days after injection in the wild-type animals, making it a popular diabetic model. Nevertheless, there are many variations in the injection protocol in terms of dosage, route of injection, and with or without insulin compensation that are usually based on the practice in individual laboratories; nonetheless, all mice end up with hyperglycemia in 1 to 4 weeks after STZ injection. For an easy reference, a summary of DR studies

using STZ-induced mice in the past five years is presented in Table 1. This table aims to provide the researchers with a general idea of the appropriate dosage or injection method in mice of different age and/or with genetic background. Amongst these methods, intraperitoneal injection of single high-dose injection of 150 mg/kg and multiple low doses of 50 mg/kg for 5 consecutive days to C57Bl/6 mice without insulin compensation are the standard protocols recommended by the Animal Models of Diabetic Complications Consortium (http://www.diacomp.org/; accessed on 9-Dec-2012). In the STZ-induced diabetic mice, transient astrocyte activation [32] as well as increased astrocyte number [33] was observed at 4 to 5 weeks of hyperglycemia. GFAP upregulation in glial cells and reactive gliosis were also evidenced at the same time [33]. Retinal ganglion cells (RGCs) are reduced starting from 6 weeks [34, 35] while thinning of INL and ONL were observed at 10 weeks of hyperglycemia [35]. Apoptosis of RGCs and vascular cells can be identified at 6 weeks [35] and 6 months [32] of hyperglycemia, respectively. Yet, some studies showed that there is no significant in ganglion cell death even after a long time, up to 9 to 10 months of hyperglycemia [36–39]. Increased leukocyte number [40], together with leukostasis [38], was reported at 8 weeks of hyperglycemia. For vascular pathogenesis, upregulation of vascular permeability was being observed as early as 8 days of hyperglycemia [41], resulting in vessel leakage at 2 months [42]. After 17 weeks of hyperglycemia, thickening of capillary basal lamina [43] and neovascularization [44] were reported. Acellular capillaries and pericyte ghosts were found in retina in mice after 6 to 9 [32, 37] months of hyperglycemia. Decreased retinal arteriolar and venular RBC velocities, retinal arteriolar and venular blood flow rates, and arterial velocity were observed in mice after 4 weeks of hyperglycemia [45–47]. Although decreased arteriolar and venular diameters were also reported in mice after 4 weeks of hyperglycemia [48], it is controversial in other studies. Functional defects were described in some electroretinography (ERG) studies including decreased OP3 and ΣOPs, prolonged implicit time of OP2-3 at 4 weeks of hyperglycemia [49, 50]; decreased a-waves and b-waves at 6 months of hyperglycemia [37]; and decreased pattern ERG amplitude at 7 weeks of hyperglycemia [51]. The variations in the above observations may be due to difference in mouse strains [52], STZ dosage, or observation time points. Moreover, individual animals may be resistant to STZ and fail in hyperglycemia induction; therefore, it is essential for the experimenters to confirm the blood glucose level of the animals and exclude those without hyperglycemia development.

On the other hand, alloxan is less commonly used in mice, which may be due to the absence of the inducible cellular and vascular lesions associated with hyperglycemia. Morphologically, the dendrites of microglial cells were found to be shortened without any ganglion cell apoptosis after 3 months of hyperglycemia [128]. At the same time, vessel diffusion and density of the retinal capillary network remained unchanged [128]. Functional abnormalities, however, were being reported in ERG, in which b-wave amplitude [129, 130] and b/a wave amplitude ratio [128] were found to be decreased at 3 weeks and 3 months of hyperglycemia, respectively. Nevertheless, cellular and vascular lesions are possibly detectable after a longer period of hyperglycemia as suggested by the presence of functional defects in this model.

Feeding with galactose is another method to induce hyperglycemia. Here, the blood aldohexose concentration is elevated in the animal without affecting other metabolic abnormalities, such as alterations in concentrations of insulin, glucose, fatty acids, and amino acids. This allows the researchers to study the consequential retinal complications solely due to the elevation of hexose concentration. Galactose-fed mice have a longer life span than other diabetic models; therefore, an extended monitoring period of up to 26 months can be allowed [131–133]. Endothelial cell loss and increased acellular capillaries were observed starting from 15 months of hyperglycemia. For a further 6 months of hyperglycemia, other morphological lesions including the presence of pericyte ghosts, saccular microaneurysms as well as basement membrane thickening of retinal capillaries were also evidenced [131–133]. Amongst the mouse models currently available, the animals in this model have the least mortality at around 2 years old of age, which allows a longer period of hyperglycemia, and therefore phenotypes associated with increment of hexose concentration can be targeted. Researchers should be aware that it takes a relatively longer period of time to develop retinopathy in these mice, which in turn leads to a higher cost.

2.1.2. Diabetic Mouse Models Carrying Endogenous Mutation. Apart from injection or intake of chemicals, spontaneous hyperglycemia can be found in mice carrying endogenous mutation. By inbreeding the mutated mice with the wild-type animals, researchers can further expand the colonies and use them as mouse models for diabetes studies. Although breeding is a time-consuming process, further manipulations, such as injections and feeding with specialized chow, are avoided. Retinopathies in terms of morphological and functional lesions have been observed in a few type 1 and type 2 diabetic models, including $Ins2^{Akita}$, nonobese diabetic (NOD), db/db, and KKA^{y} mice. In these animals, onset of hyperglycemia takes place spontaneously as a result of the presence of the transgene or mutation; a relatively consistent phenotype as well as a higher success rate in induction of hyperglycemia can be obtained.

The $Ins2^{Akita}$ mice represent one of the spontaneous type 1 diabetic models. These mice carry a point mutation in the insulin2 gene, which causes a conformational change in the protein that accumulates in the pancreatic β-cells, and ultimately leads to cell death. Retinopathy in heterozygous $Ins2^{Akita}$ mice is well characterized in a few studies. Cellular lesions, such as reactive microglia, are evidenced as early as 8 weeks of diabetes [134]. By 12 weeks of onset of hyperglycemia, immunological studies showed abnormal swelling in somas, axons, and dendrites of RGCs, and the number of these cells was reduced in the peripheral region; while more dendritic terminals, increased total dendrite length, and greater dendritic density were observed in the ON-type RGCs [135]. It has been reported that the number of RGCs was significantly reduced in the peripheral regions after 22

weeks of hyperglycemia [135]; yet, another study showed that there was no ganglion cell death in these mice even up to 10 months of hyperglycemia [39]. Morphological change in astrocytes was also observed where they had short projections and became in less contact with the vessels [134]. Moreover, the IPL and INL became thinner, which may be due to the decrease of the cholinergic and dopaminergic amacrine cells as evidenced in retina after 6 months of hyperglycemia [136]. Vascular lesions such as increased of leukocyte number are already found in mice upon 8 weeks of hyperglycemia and retinal vascular permeability was increased in 12 weeks of hyperglycemia. The presence of acellular capillaries [134] and neovascularization [137] were described after 8 to 9 months of hyperglycemia. Abnormal vascular functions were also reported in a study which showed that the arteriolar and venular RBC velocity, shear rate, and retinal blood flow rate were significantly decreased in the diabetic animals with 26 weeks of hyperglycemia [138]. A decrease of a- and b-wave amplitudes in the ERG after 8 month indicates functional problem associated with the cellular defects or degeneration [137]. Although the diabetic animals have an average life span of 305 days, they provide a stable induction of hyperglycemia while projecting the early and some of the late DR symptoms in human. Thus, this model could be very useful in drug screening, and it has received more attention in the field of DR.

The NOD mice are another model of type 1 diabetes, in which pancreatic β-cells were destroyed via an autoimmune process by the $CD4^+$ and $CD8^+$ cells. The onset of hyperglycemia in these animals is 12 weeks of age, and the frequency of having hyperglycemia at the age of 30 weeks old is about 80% in female and less than 20% in male [139]. Owing to the low induction rate and inconsistency in the male mice, female NOD mice were commonly used. Using transmission electron microscopy, ultrastructural changes including apoptosis of pericytes, endothelial cells, and RGCs, perivascular edema, and retinal capillary basement membrane thickening were reported as early as 4 weeks of hyperglycemia, and these retinopathogeneses became more obvious after 12 weeks of hyperglycemia [140]. At about 4 months of hyperglycemia, vascular abnormalities were described in the NOD mice. Vasoconstriction or degeneration was observed in some of the major vessels, together with the presence of poorly defined microvessels and disordered focal proliferation of the new vessels [141]. The presence of these vascular pathologies and the etiology of the development of type 1 diabetes in the NOD mice are relatively similar to those of human, making this model unique. However, there is a big variation in the time of onset of diabetes; frequent and regular monitoring of the blood glucose levels is therefore required. More importantly, since female animals were used in these studies, estrogen, which plays a role in regulation of metabolism [142], may have a protective function in DR. This further complicates the mechanistic studies or contributes unknown effects in drug screening, thereby affecting the accuracy.

The db/db mice spontaneously develop type 2 diabetes owing to the deficiency in the leptin receptor. Hyperglycemia and obesity were observed in the homozygous mice at 4 to 8 weeks old [143]. Reduction of RGC number and thickness of the central total retina, INL, and photoreceptor layers were identified in the histological sections of mice after 6 weeks of hyperglycemia [144]. After 18 weeks [145] and 13 months of onset of hyperglycemia [146], pericyte loss and glial reactivation were reported, respectively. Vascular lesions including capillary basement membrane thickening [147], the presence of acellular capillaries [145], increased vessel density in the INL, and vessel leakage [146] were observed in the diabetic retina. Compared with other mouse models, the reported glial reactivation and vessel leakage occurred relatively late in db/db mice, which could be explained by a relative late time point chosen in a long-term study [146]. The use of db/db mice to study DR is not very popular, potentially due to a low birth rate resulting from the unsatisfactory mating performance in the male homozygotes and failure to reproduce in the female homozygotes (http://jaxmice.jax.org/; accessed on 15-Dec-2012).

KKA^y mouse is a combined model made by the introduction of the yellow obese gene, A^y, into the KK mouse, in which moderate diabetic traits are thought to be inherited by polygenes. These mice spontaneously develop diabetic characteristics, such as hyperglycemia, hyperinsulinemia, and obesity, at around 6 to 8 weeks of age, but revert to normal at the age of 40 weeks [148]. Of the limited DR studies using this mouse model, increased apoptosis of the retinal neuronal cells was found in the RGC layer and the INL in mice after 4 weeks and 3 months of hyperglycemia, respectively. Capillary basement membrane thickening was also observed in ultrastructural study [149]. Owing to the limited retinopathologic findings and the uncertain etiology of this model, this model is not popularly used in DR studies.

2.1.3. Mouse Models of Proliferative Retinopathy. In order to compensate for the lack of proliferative pathogenesis in the retinal vasculature in most of the above diabetic mouse models, researchers developed a number of nondiabetic models, which allow them to specifically target neovascularization in the ocular region. When using these models, however, researchers should be aware of the fact that the etiology of the progression of vascular abnormalities is different owing to the absence of classical systemic characteristics as seen in diabetes. Proliferative retinopathy can be achieved mainly from two approaches: the first one is via introduction of ischemia to the eyes, such as oxygen-induced retinopathy (OIR) and retinal occlusion [150]; the second one is by direct injection or genetically induction of the angiogenic factor, VEGF, into the ocular region.

OIR originally is an animal model of retinopathy of prematurity in newborns. Owing to the presence of neovascularization, this model is also adapted for studying the angiogenesis as seen in proliferative DR [150]. In brief, postnatal day 7 (P7) neonatal mice were put into a 75% oxygen chamber for five days and then returned to room air [151, 152]. Vessel loss in the central area of retina, which is associated with hypoxic challenged, is observed immediately at this time. Neovascularization extending from the inner retina into the vitreous begins at two days after the return to room air, peaks on P17 [152], and is gradually regressed

and spontaneously resolved by P25 [151]. A comprehensive study was carried out in this model, in which mice at P18 were analyzed [153]. Morphologically, more gliotic Müller cells and reactivated microglia can be observed. The total retinal thickness was reduced in the midperipheral region, while the IPL and the outer segment length were reduced in the central and midperipheral regions. The number of vessels was also reduced in the IPL in the central region; and in the deep plexus in the central and midperipheral regions. Aberrant intravitreal neovascularization was observed across all eccentricities. Retinal function was examined by ERG, in which reductions in the amplitudes of a-wave, b-wave, OP3, and OP4, and delayed b-wave implicit time were revealed. Mouse OIR model showed a number of vascular, neuronal, and glial changes in the retina; however, the spontaneous regression of the neovascularization within a week confines its application in therapeutic drug research.

Since DR can also be considered as an ischemic disorder in the retina, retinal occlusion models, such as unilateral ligation of pterygopalatine artery (PPA) and external carotid artery (ECA) [154], branch retinal vein occlusion [155], and elevating the intraocular pressure (IOP) [156], were also applied in studies of vasculature abnormalities. In these occlusion models, increased apoptotic cells, reduced thickness of retinal cell layers, reduced a-wave, b-wave, and OPs amplitudes of the ERG were evidenced. Nevertheless, the acute induction of ischemia, particularly those followed by reperfusion, to the retinal tissue makes these models less appropriate for studying DR, in which chronic ischemia is persistently involved.

Kimba (trVEGF029) is a transgenic mouse model of neovascularization, as a result of transient overexpression of human $VEGF_{165}$ in the rhodopsin-expressing cells with which it peaks at P10 to P15 and declines at P20. Characterization studies have been carried out as early as at P7 [157]. At that time, reduced thickness of the RGC layer, INL, outer nuclear layer (ONL), and the total retinal layer was observed. By P28, such reduction was found in IPL, the outer segment, and the total retinal layer. Microaneurysms, intraretinal microvascular abnormalities, and capillary dropout were evident by P28 [157]. Vascular leakage was also observed at P28 [157], but it ceased at 9 weeks of age potentially due to the absence of over-expression of VEGF [158]. Increased adhered leukocytes were found in veins and capillaries, together with increased acellular capillaries by 6 weeks of age. Topological and fractal analysis of retinal vasculature showed that vessel-covered area, vessel length, and crossing points in the 9-week-old Kimba mice were reduced. Vessel tortuosity and pericyte loss were also evident at this time point [158]. Varied degrees of the pathogenesis were being reported, which were separated into two groups based on the assessment of fundus fluorescein angiography. The phenotypic observations of the relatively severe group were presented in this review. Since this transgenic mouse is not commercially available, it is not a popular model in DR.

In order to generate an ideal mouse model to study DR, a new mouse model of DR was created by crossing the Kimba mice with the $Ins2^{Akita}$ mice, named Akimba [159]. These mice inherit the key systemic diabetic phenotypes from their parental strains, making it a unique model. At 8 weeks of age, optical coherence tomography (OCT) showed uneven thickness in the retina. Retinal edema and reduced photoreceptor layer thickness, together with retinal detachment, were observed. RGCs number and neural retinal thickness were reduced by 24 weeks of age. Abnormal microvasculature, including microaneurysms, capillary dropout, hemorrhage, neovascularization, venous loops, vessel tortuosity, vessel beading, vascular dilatation, and vascular leakage, were also evident in mice of 8 weeks old, although the leakage stopped by 20 weeks of age. The Akimba mouse model displays a number of vascular changes; however, more complete mechanistic studies are essential before its utilization in therapeutic drug studies.

A summary of the earliest reported morphological and functional lesions in different mouse models of DR is shown in Table 2.

2.2. Rat Models of DR. Although rats have a slightly bigger size than mice, they are still easy to handle with a low cost of maintenance, making them to be another popular animal frequently used in *in vivo* studies. The use of rats in DR study is particularly common owing to a relatively larger tissue size, with which functional assessment and morphological and molecular analyses can be done. Similar to DR studies in mice, three types of rat models were used; these include pharmacological induction of hyperglycemia, spontaneous diabetic rats, and models of angiogenesis without diabetes. A summary of the morphological and functional lesions in different rat models of DR is shown in Table 3.

2.2.1. Pharmacologically Induced Rat Models of DR. Similar to mice, hyperglycemia can be induced in rats by injection of STZ or alloxan or by ingestion of galactose.

Compared to mice, rats are more susceptible to the toxicity of STZ; therefore, usually a much lower dosage of STZ is used. In order to minimize the mortality, insulin complementation may also be administered. Table 1 summarized most of the induction method of STZ in the past 3 years and served as a reference for the researchers to select the most appropriate dosage, injection paradigm, and rats with different genetic background for their studies. Amongst the methods, a single dose of 60–65 mg/kg of weight is the most popular one. Variation of the retinal lesions was reported, which can be explained by the genetic background. Indeed, a comparative study showed a strain difference in the rate of developing early DR symptoms in rats upon STZ challenge [120]. After 8 months of hyperglycemia, Lewis rats displayed accelerated degeneration of retinal capillaries and RGC loss, whereas Wistar rats only showed the capillary degeneration and Sprague-Dawley (SD) rats showed no morphological defects to a significant level. Increased apoptotic cells were detected throughout the retina as soon as 2 weeks after hyperglycemia [136]. After 1 month of hyperglycemia, the number of astrocytes in the peripheral region was reduced; however, the number of Müller cells and microglial cells is increased [160, 161] with the accompany of microglial hypertrophy

Table 1: Existing methods for induction of diabetes in rodents using STZ.

	Compensation of insulin	Dosage	Animal strain, age or weight	Onset of hyperglycemia
Mouse				
Single dose	No	150 mg/kg, i.p.	C57Bl/6, 8–10 wk old	6 wk* [53]
	No	150–180 mg/kg, i.p.	C57Bl/6, 10–12 wk old	2 wk [54]
	No	180 mg/kg, i.p.	C57Bl/6, 10 wk old	1 day [41, 55]
	No	200 mg/kg, i.p.	C57Bl/6J, 10 wk old [56]; F1 hybrid (BALBc/129Sv × C57Bl/6J), 16 wk old [43]	3 days [56]
	Yes	180 mg/kg, i.p.	C57Bl/6, 9–12 wk old	1 wk [45, 48, 57, 58]
	Yes	200 mg/kg, i.p.	C57Bl/6, 12 wk old	1 wk [47]
Multiple dose	No	40 mg/kg, i.p., for 5 consecutive days	C57Bl/6, 10 wk old	1 wk [59]
	No	45 mg/kg, i.p., for 5 consecutive days	C57Bl/6, 7-8 wk old	3 days [60]
	No	50 mg/kg, i.p., for 5 consecutive days	C57Bl/6J, 4-5 wk old [61]; C57Bl/6J, 8-9 wk old [46, 62]; C57Bl/6 [63]	1 wk [46]
	No	55 mg/kg, i.p., for 5 consecutive days	C57Bl/6, 8–10 wk old [42, 64–66]	1 wk [42, 64, 66]; 2 wk [65]
	No	60 mg/kg, i.p., for 3 consecutive days	C57Bl/6, 5–8 wk old [34, 49, 50]	1 wk [34, 49, 50]
	No	60 mg/kg, i.p., for 5 consecutive days	C57Bl/6, 6 wk old [40]; C57Bl/6J, 22 g [44]; C57Bl/6, 22 wk old [67]	1 wk [40, 44]; 2 wk [67]
	No	75 mg/kg, i.p., for 3 consecutive days	C57Bl/6, 3–5 months old	5 wk* [68]
	No	80 mg/kg, i.p., for 3 consecutive days	C57Bl/6, 6–8 wk	1 wk [69]
	No	80 mg/kg, i.p., for 5 consecutive days	F1 hybrid mice (FVB/N × C57Bl/6J), 10 wk old	1 wk [33]
	No	100 mg/kg, i.p., for 2 consecutive days	C57Bl/6J, 6–8 wk old	1 wk [70]
	Yes	50 mg/kg, i.p., for 3 alternate days	C57Bl/6, 23–36 g	4 wk* [71]
	Yes	50 mg/kg, i.p., for 5 consecutive days	C57Bl/6 [72]	Did not mentioned
	Yes	60 mg/kg, i.p., for 5 consecutive days	C57Bl/6 [73]; C57Bl/6J [38]	1-2 wk [38, 73]
Rat				
Single dose	No	30 mg/kg, i.v.	Wistar rats, 6 wk old	3 wks [74]
	No	45 mg/kg, i.p.	Sprague-Dawley (SD) rats, 200–250 g [75, 76]; Wistar rats, 220–250 g [77]	1 day [77]; 3 days [76]; 1 wk [75]
	No	45 mg/kg, i.v.	Wistar rats, 130–150 g	1 day [78]
	No	50 mg/kg, i.p.	Brown Norway (BN) rats, 8 wk old	2 days [79]
	No	55 mg/kg, i.p.	Wistar rats, 8–12 wk old [80, 81]	3 days [80, 81]

Table 1: Continued.

Compensation of insulin	Dosage	Animal strain, age or weight	Onset of hyperglycemia
No	60 mg/kg	Lewis rats [82]	Did not mentioned
No	60 mg/kg, i.p.	BN rats, 200–250 g [83]; SD rats, 6–8 wk old [84–91]; SD rats, 230–350 g [92, 93]; SD rats [94]; Wistar rats, 140–200 g [95–97]; Wistar rats, 200–300 g [98–100]; Long-Evens (LE) rats, 250–300 g [101]	1 day [83, 89]; 2 days [86–88, 91, 100]; 3 days [84, 85, 92, 93, 97, 98] 1 wk [90, 96]
No	65 mg/kg, i.p.	SD rats, 150–200 g [102–106]; SD rats, 240–275 g [107, 108]; Wistar rats, 8-9 wk old [109–111]	1 day [106]; 2 days [107, 109–111]; 3 days [102, 103]; 1 wk [104, 105]
No	65 mg/kg, i.v.	BN rats, 150–200 g [112]; LE rats, 150–200 g [112]; Wistar rats, 160–170 g [113, 114]	3 days [112]; 2 wk* [113, 114]
No	70 mg/kg, i.p.	SD rats, 8 wk old	12 wk* [115]
No	75 mg/kg, i.p.	LE rats, 200–250 g	2 days [116]
No	80 mg/kg, i.p.	LE rats, 6–8 wk old	1 wk [69]
Yes	45 mg/kg, i.v.	Wistar rats, 12 wk old	3 days [117]
Yes	50 mg/kg, i.p.	SD rats, 6 wk old	2 wk [118]
Yes	55 mg/kg, i.p.	SD rats, 200 g	2-3 days [119]
Yes	55 mg/kg	Lewis rats, 200 g [120, 121]; SD rats, 200 g [120]; Wistar rats, 200 g [120]	2 wk* [120, 121]
Yes	60 mg/kg, i.p.	Wistar rats, 129–170 g [58] Wistar rats, 240–280 g** [122]	1 day [122]; 1 wk [58]
Yes	65 mg/kg, i.p.	SD rats, 260 g	4 wk* [123]
Yes	65 mg/kg, i.v.	SD rats, 200 g	4 wk* [124]
Yes	70 mg/kg, i.p.	LE rats, 8 wk old	3 days [125, 126]
Yes**	80 mg/kg, i.p.	SD rats, 200 g	1 wk [127]

*Indicates the earliest time point being mentioned by the authors.
**Comparison between the insulin-treated versus untreated animals.

[160]. The density of astrocyte was further reduced in the central region, together with the reduction of astrocyte processes in the peripheral region after 6 weeks of hyperglycemia [118]. Decreased total retinal thickness [163], as well as decreased number of cells in the RGC layer [160], the ONL [163], and the INL [160] was also reported. Regarding the vascular changes, blood-retinal-barrier (BRB) breakdown was evident at 2 weeks of hyperglycemia [161, 163]. Increased adherent leukocytes [164] and arterial or venous capillaries basement membrane thickening [165] were observed at 8 weeks and 12 months after hyperglycemia, respectively. Retinal function was affected from 2 weeks after the onset of hyperglycemia as reflected by the ERG. Reduced b-wave [166], OPs [167], and a-wave [166] amplitudes were progressively found at 2 weeks, 8 weeks, and 10 weeks of hyperglycemia. At around the same time, the a-wave implicit time and OPs were delayed [168]. Morphological and functional studies suggested that STZ-induced diabetic rats only showed early DR symptoms, which is comparable to those in STZ-induced mice.

The use of alloxan in DR studies is not very common nowadays, and the existing morphological studies were mainly focused on the vascular lesions. Neovascularization was already observed from 2 months of induction of hyperglycemia starting from the midperiphery region and progressing to the whole retina after 9 months of hyperglycemia [170]. Extravascular macrophage accumulation and capillary endothelial cells swelling were also identified after 2 months and 5 months of hyperglycemia, respectively [170]. By 8 months, increased cell death in the retinal microvasculature was evident [171]. Acellular capillaries, basement membrane

Table 2: Comparison of the morphological and functional lesions in mouse models of DR.

Animal model	Type of diabetes	Onset of hyperglycemia	Temporal morphological lesions in retina upon development of hyperglycemia		Temporal functional lesions in retina upon development of hyperglycemia (ERG, SLO, fMRI)
			Cellular	Vascular	
STZ injection	Type 1	Within 1 wk of injection	4 wk: astrocyte activation [32] 5 wk: (i) Increased astrocyte number [33] (ii) Reactive gliosis [33] 6 wk: apoptosis of RGCs [35] 6–14 wk: reduced RGCs [34, 35]* 10 wk: reduced thickness of INL and ONL [35] 6–9 mth: pericytes loss [32, 37]	8 days: upregulation of vascular permeability [41] 4 wk: (i) Decreased retinal arteriolar and venular RBC velocity [45, 46] (ii) Decreased retinal arteriolar and venular blood flow rate [45, 46] (iii) Decreased arterial velocity [47] (iv) Decreased arteriolar and venular diameters [48] 8 wk: (i) Vessel leakage [42] (ii) Increased leukocyte number [40] (iii) Leukostasis [38] 17 wk: (i) Capillary basal laminar thickening [43] (ii) Neovascularization [44] 6 mth: apoptosis of vascular cells [32] 6–9 mth: acellular capillaries [32, 37]	4 wk: (i) Decreased OP3 and ΣOPs in ERG [49, 50] (ii) Prolonged implicit time of OP2-3 in ERG [50] 7 wk: decreased pattern of ERG amplitude [51] 6 mth: decreased a-wave and b-wave amplitudes [37]
Alloxan injection	Type 1	Within 4 days of injection	3 mth: shortening of dendrites of microglial cells [128]		3 wk: decreased b-wave in ERG [129, 130] 3 mth: (i) Decreased b/a wave amplitude ratio in ERG [128] (ii) Delayed OPs in ERG [128]
Galactose-fed	—	—	16–22 mth: decreased endothelial cell [132, 133] 20–26 mth: pericyte loss [131, 133]	15–21 mth: acellular capillaries [131–133] 21 mth: saccular microaneurysms [131] 21-22 mth: capillary basal laminar thickening [131, 132]	
$Ins2^{Akita}$	Type 1	4 wk of age	8 wk: reactivated microglia [134] 12 wk: (i) Increased apoptosis [136] (ii) Reduced RGCs in the peripheral retina [135] (iii) Changes in dendrite of ON-type RGCs [135] (iv) Abnormal swelling on somas, axons, and dendrites in RGCs [135] 22 wk: (i) Change in astrocyte morphology and less contact with the vessels [134] (ii) Reduced thickness of IPL and INL [134] (iii) Reduced RGCs [134]* 6 mth: decreased cholinergic and dopaminergic amacrine cells [136]	8 wk: increased leukocyte number [134] 12 wk: increased retinal vascular permeability [134] 26 wk: decreased arteriolar and venular RBC velocity, shear rate, and flow rate [138] 31–36 wk: increased acellular capillaries [134] 8 mth: (i) Retinal neovascularization [137] (ii) Formation of new capillary beds [137] (iii) Formation of new blood vessels in OPL [137]	8 mth: decreased a-wave and b-wave amplitudes in ERG [137]

Table 2: Continued.

Animal model	Type of diabetes	Onset of hyperglycemia	Temporal morphological lesions in retina upon development of hyperglycemia		Temporal functional lesions in retina upon development of hyperglycemia (ERG, SLO, fMRI)
			Cellular	Vascular	
NOD	Type 1	12–30 wk of age	4 wk: apoptosis of pericytes, endothelial cells, and RGCs [140]	4 wk: (i) Capillary basement membrane thickening [140] (ii) Perivascular edema [140] 4 mth: (i) Vasoconstriction or degeneration in some of the major vessels [141] (ii) Poorly defined microvessels [141] (iii) Disordered focal proliferation of new vessels [141]	
db/db	Type 2	8 wks of age	6 wk: (i) Reduced RGC number [144] (ii) Reduced thickness of the central total retina, INL, and photoreceptor layers [144] 18 wk: pericyte loss [145] 13 mth: glial reactivation [146]	14 wk: basement membrane thickening [147] 26 wk: acellular capillaries [145] 13 mth: (i) Vessel leakage [146] (ii) Increased vessel density in the INL [146]	
KKA^{y}	Type 2	6–8 wk of age	4 wk: increased neuroretinal apoptotic cells in RGC layer [149] 3 mth: increased neuroretinal apoptotic cells in the INL [149]	3 mth: basement membrane thickening [149]	
OIR	—	—	P18: (i) Reduced thickness of total retinal [153] (ii) Reduced thickness of IPL [153] (iii) Absence of the deep plexus [153] (iv) Reduced outer segment length [153] (v) Microglial reactivation [153] (vi) Increased gliotic Müller cells and microglia [153]	P18: (i) Aberrant intravitreal neovascularization across all eccentricities [153] (ii) Reduced vessels in the deep plexus [153] (iii) Reduced vessels in the inner retinal plexus [153]	P18: (i) Reduced a-wave and b-wave amplitudes in ERG [153] (ii) Delayed b-wave implicit time in ERG [153] (iii) Reduced OP3 and OP4 in ERG [153]
Kimba	—	—	9 wk of age: pericyte loss [158]	P28 of age: (i) Microaneurysms [157] (ii) Vascular leakage [157], but stops at 9 wk of age [158] (iii) Capillary blockage, dropout, and hemorrhage [157] 6 wk of age: (i) Leukostasis in veins and capillaries [158] (ii) Acellular capillaries [158] 9 wk of age: (i) Reduced vessel covered area [158] (ii) Reduced vessel length [158] (iii) Reduced crossing points [158] (iv) Vessel tortuosity [158]	
Akimba	Type 1	4 wk of age	8 wk of age: (i) Uneven thickness in the retina in OCT [159] (ii) Reduced photoreceptor layer thickness [159] (iii) Retinal edema [159] (iv) Retinal detachment [159] 24 wk of age: reduced RGCs number and neural retinal thickness [159]	8 wk of age: (i) Capillary dropout [159] (ii) Microaneurysm [159] (iii) Hemorrhage [159] (iv) Vascular leakage, stops by 20 wk of age [159] (v) Vascular dilatation [159] (vi) Venous loops [159] (vii) Vessel tortuosity [159] (viii) Vessel beading [159] (ix) Neovascularization [159]	

*Some studies reported absence of reduction of RGCs [36–39].
The observations reported at a particular time point, which was chosen by the authors, may not totally reflect the sequential processes.

Table 3: Comparison of the cellular and functional lesions in rat models of DR.

Animal model	Type of diabetes	Onset of hyperglycemia	Temporal morphological lesions in retina upon development of hyperglycemia		Temporal functional lesions in retina upon development of hyperglycemia (ERG, SLO, fMRI)
			Cellular	Vascular	
STZ injection	Type 1	Within 1 wk of injection	2 wk: increased apoptotic cells [136] 1 mth: (i) Microglial cells hypertrophy [160] (ii) Increased Müller cells and microglia cell number [160, 161] (iii) Reduced astrocyte number [161] (iv) Apoptosis of a few photoreceptor cells [162] 6 wk: (i) Reduced astrocyte number [118] (ii) Reduced astrocyte processes [118] (iii) Reduced NeuN-positive ganglion cells in GCL [160] (iv) Reduced cells in the ONL [163] (v) Reduced total retinal thickness [163] 4 mth: reduced NeuN-positive neurons in INL [160]	2 wk: BRB breakdown [161, 163] 8 wk: increased adherent leukocytes [164] 12 mth: arterial or venous capillaries basement membrane thickening [165]	2 wk: reduced b-wave amplitudes in ERG [166] 4 wk: decreased positive scotopic threshold response in ERG [167] 8 wk: decreased OPs in ERG [167] 10 wk: reduced a-wave amplitudes in ERG [166] 11 wk: (i) Reduced a-wave implicit time in ERG [168] (ii) Delayed OPs in ERG [168]
Alloxan injection	Type 1	Within 1 wk of injection	12 mth: pericyte loss [169]	2 mth: (i) Neovascularization limited to the midperipheryregion [170] (ii) Extravascular accumulation of monocytes and granulocytes [170] 5 mth: (i) Neovascularization in the midperipheryregion and the center [170] (ii) Capillary endothelial cells swelling [170] 8 mth: retinal microvascular cell death [171] 9 mth: neovascularization in all regions [170] 12 mth: (i) Acellular capillaries [169] (ii) Basement membrane thickening [169]	
Galactose-fed	—	—	12 mth: pericyte loss [169] 28 mth: (i) Gliosis [172] (ii) Disruption of retinal layers [172]	6 mth: retinal microvascular cell death [171] 12 mth: (i) Acellular capillaries [169] (ii) Basement membrane thickening [169] 28 mth: (i) Capillary dilation [172] (ii) Microaneurysm formation in the IPL and the INL [172]	
BB	Type 1	3-4 mth of age	4 mth: absence of infolding or derangement of the basal plasmalemma of the RPE [173] 8 mth: (i) Reduced pericyte number [174] (ii) Reduced pericyte to endothelial cell ratio [174]	2 mth: capillary dilation [175] 4 mth: basement membrane thickening [175] 8 mth: microinfarctions with areas of nonperfusion [175]	

Table 3: Continued.

Animal model	Type of diabetes	Onset of hyperglycemia	Temporal morphological lesions in retina upon development of hyperglycemia		Temporal functional lesions in retina upon development of hyperglycemia (ERG, SLO, fMRI)
			Cellular	Vascular	
WBN/Kob	Type 2	9–12 mth of age	5 mth of age (prediabetic): reduced thickness of outer segments and ONL [176] 2 mth: (i) Reduced thickness of total retinal layer, OPL [176] (ii) Visual cells disappeared [176]	1 mth: capillaries clustered into small tortuous knots [177] 5 mth: capillary basement membrane thickening [176] 6 mth: (i) Increased capillary loop [177] (ii) Reduced number of capillary [177] 12 mth: (i) Increased fibrovascular element proliferation in the vitreous [178] (ii) Increased intraretinal neovascularization [178] (iii) Increased hyalinization of intraretinal vessels [178]	
ZDF	Type 2	6-7 wk of age	6 mth: (i) Increased apoptotic pericytes [179] (ii) Increased pericyte ghosts [179]	5 mth: (i) Capillary basement membrane thickening [180, 181] (ii) Increased capillary cell nuclear density [180, 181] 6 mth: (i) Increased apoptotic endothelial cells [179] (ii) Acellular capillaries [179]	
OLETF	Type 2	5 mth of age	9 mth: (i) Damaged endothelial cells [182] (ii) Reduced ratio of pericyte area to the total capillary cross-sectional area [183] 14 mth: (i) Decreased thickness of INL [182] (ii) Decreased thickness of photoreceptor layer [182] (iii) RPE decreased in height [182] (iv) Basal infoldings were poorly developed [182]	6 wk: leukostasis [184] 9 mth: (i) Capillary basement membrane thickening [182, 183] (ii) Caliber irregularity [183, 185] (iii) Narrowing of arteries [185] 9–12 mth: (i) Tortuosity [182, 183, 185] (ii) Microaneurysms [182, 183, 185] (iii) Loop formation in capillary [182, 183, 185]	
GK	Type 2, nonobese	4–6 wk of age	7 mth: increased endothelial/pericyte ratio [186]	1 mth: (i) Reduced retinal segmental blood flows [186] (ii) Increased retinal mean circulation time [186] 3 mth: increased BRB permeability [187]	
SDT	Type 2, nonobese	5 mth of age	20 wk: increased apoptotic cells in the GCL and the INL [188] 48 wk: distortion of retina and protruded optic disc [189] 50 wk: tractional retinal detachment with fibrous proliferation [190] 15 mth: (i) Proliferative retinopathy without vascular nonperfusion (53% of rats) [191] (ii) Traction retinal folds [191]	24 wk: leukostasis [192] 48 wk: leakage of fluorescein around the optic disc [189]	4 wk: delayed peak latency of the ΣOPs in ERG [189] 24 wk: (i) Reduced a-wave, b-wave, and OPs amplitudes in ERG [193] (ii) Prolonged implicit times in a-wave, b-wave, and OPs in ERG [193]
OIR	—	—	P18: (i) Reduced thickness in INL, IPL, and total retinal layer [194] (ii) Müller cell gliosis in peripheral region [194] (iii) Reduced astrocyte number [195] (iv) Impaired pericyte endothelial interactions [195] (v) Disorganized and thinning of the outer segment [196]	P18: (i) Intravitreal neovascularization [195] (ii) Underdevelopment of the outer vascular plexus [195] (iii) Increased tortuosity in arterioles [197]	P16: reduced a-wave and b-wave amplitudes in ERG [197]

The observations reported at a particular time point, which was chosen by the authors, may not totally reflect the sequential processes.

thickening, and pericyte loss were also reported upon 12 months of hyperglycemia [169]. Nevertheless, appearance of the lesions varied between studies; it would be due to the different time points selected by the authors or different dosage of alloxan being injected. Reported lesions with the "earliest onset" were listed in this review.

Similar to mice, DR can be studied in rats fed with galactose, with the equivalent advantage of longer life span [172, 198]. Studies showed increased retinal microvascular cell death in 6 months after hyperglycemia [171]. Other vascular lesions, such as acellular capillaries and basement membrane thickening as well as pericyte loss, were observed after 12 months of feeding with galactose [169]. A long-term study demonstrated cellular lesions, including gliosis and disruption of retinal layers, together with vascular abnormalities, capillary dilation and microaneurysm formation in the inner plexiform layer (IPL) and the INL, in rats fed with galactose for 28 months [172]. Owing to the differences in galactose concentration and time points selected by various studies, the "earliest onsets" of the lesions were listed in this review.

2.2.2. Diabetic Rat Models Carrying Endogenous Mutation. A number of rats with spontaneous onset of diabetes have been identified. These include type 1 diabetic model: biobreeding (BB) as well as type 2 diabetic model: Wistar Bonn/Kobori (WBN/Kob) rats, Zucker diabetic fatty (ZDF) rats, Otsuka Long-Evans Tokushima fatty (OLETF) rats, nonobese Goto-Kakizaki (GK) rats, and nonobese spontaneously diabetic Torii (SDT) rats.

Like NOD mice, the BB rats spontaneously develop polygenic autoimmune type 1 diabetes, in which the pancreatic β-cells were selective destroyed [175, 199]. After 4 months of hyperglycemia, absence of infolding and derangement of the basal plasma lemma of the RPE were also observed [173]. The number of pericyte and the pericyte to endothelial cell ratio were reduced [174, 175] after 8 months of hyperglycemia. Lesions associated with the retinal microvasculature, including capillary dilation and basement membrane thickening, were found from 2 months and 4 months of hyperglycemia, respectively [175]. Microinfarctions with areas of nonperfusion were evident whereas no neovascularization was detected up to 11 months [175]. Several inbred and outbred lines, such as BB/Wor, BB/E, and BB/Ph, have been produced and named based on the origin of the breeding colony. Since genetic variations and potential differential phenotypes are introduced, researchers should select the appropriate stain carefully.

The WBN/Kob rats are a type 2 diabetes model owing to endo-exocrine pancreatic insufficiency, and only male offspring develop diabetic symptoms [200]. Retinal degeneration was already observed before the animal becomes hyperglycemic at around 9 to 12 months of age. Thickness of outer segments and ONL was reduced in WBN/Kob rats at 5 months of age whereas high blood glucose was evident in these rats at 10 months old [176]. About 2 months after becoming hyperglycemic, these rats also showed reduction in the visual cells, the OPL, and the total retinal layer [176]. Vascular lesions were also identified, and capillaries clustered into small tortuous knots after about 1 month of hyperglycemia [177]. After 5 to 6 months of diabetes, capillary basement membrane thickening [176], increased capillary loop, and reduced number of capillary [177] were also observed. After a prolonged hyperglycemia of 12 months, some rats showed increased proliferation of fibrovascular element in the vitreous, intraretinal neovascularization, and hyalinization of intraretinal vessels [178]. WBN/Kob rats, which display the symptoms of the progressive DR, may serve as a model for testing therapeutic drug targeting angiogenesis. However, the early onset of neuronal degeneration (before hyperglycemia commencement) suggests that the etiology of retinal degeneration may not be the same as that in human; therefore, further studies need to be carried out before this can be used as a model for DR.

The ZDF rats are also a genetic model of type 2 diabetes. They carry an inherited obesity gene mutation, which results in impairment of glucose tolerance and insulin resistance (http://www.criver.com/SiteCollectionDocuments/ZDF.pdf; accessed on 19-Nov-2012). Excessive body weight gain was observed in male ZDF rats in the first 6 months of life, but the weight decrease to a level similar to the lean controls afterwards [201]. Hyperglycemia starts at 6 to 7 weeks of age and maintains high throughout their life [180]. Retinopathological studies in these rats mainly focused on the vasculature. Thickening of the capillary basement membrane and increased capillary cell nuclear density were reported in rats after 5 months of hyperglycemia [180, 181]. Apoptosis of endothelial cells and pericytes was higher in these rats compared to the lean controls, together with an increased number of acellular capillaries and pericyte ghosts upon 6 months of diabetes [179]. Retinal functional analysis and long-term morphological studies of the retinal neuronal and glial cells of these rats remain to be elucidated.

Another type 2 diabetic rat model is OLETF rats; they significantly gained more weight from 1 to 6 months of age, but they lost weight from 9 to 10 months of age. Elevated blood glucose was observed from 5 months of age and it maintained high [182, 183]. After about 6 months of hyperglycemia, despite no significant difference in the number of acellular capillaries and pericyte ghosts [202], OLETF rats with 9 months of hyperglycemia showed reduced ratio of pericyte area to the total capillary cross-sectional area [183] and damaged endothelial cells [182]. By 14 months of hyperglycemia, the INL and the photoreceptor layer became thinner, accompanied with shortening of the RPE height and poorly developed basal infoldings [182]. Relatively early microvessel-related symptoms were reported in these rats, in which leukocyte entrapment was evident in rats after 6 weeks of hyperglycemia [184]. Other abnormalities, including thickening of capillary basement membrane, tortuosity, microaneurysms, loop formation in capillary, caliber irregularity and narrowing of arteries, were also described in rats after 9 to 12 months of diabetes [182, 183, 185]. No hemorrhages, emboli, and exudates were found in these rats up to 14 months of diabetes [182]. Moreover, ERG revealed that OLETF rats fed with sucrose for 8 weeks had a prolonged peak latency of $\sum$ OPs [203]. The absence of acellular capillaries as well as the

late onset of diabetes and the related symptoms diminished the popularity of using this model to study DR.

The GK rat is a spontaneous model of non-insulin-dependent diabetes without obesity. These rats are originated from normal Wistar rats and they were selected via repeated inbreeding exercise using glucose intolerance as a selection index [186, 204]. Rats at 4–6 weeks of age develop hyperglycemia [186, 187]; they also showed reduction of retinal segmental blood flows and prolonged retinal mean circulation time after 1 month of hyperglycemia [186]. Increased BRB permeability [187] and endothelial/pericyte ratio [186] were also evident in 3 months and 7 months after the onset of hyperglycemia. No significant differences were observed in the retinal arterial and venous diameters [186]. Owing to the limited publications on the retinopathology in the GK rats, further characterizations on the non-vascular-related lesions need to be performed.

The SDT rat, which is a substrain of the SD rat, is another model of nonobese type 2 diabetes. Glucose intolerance and impaired insulin secretion were demonstrated in the male SDT rats at 14 weeks, followed by hyperglycemia and glucosuria at 5 months of age. These rats showed a sexual differentiation in the development of diabetes that the cumulative incident is about 100% in males at 40 weeks of age and only about 33% in females up to 65 weeks of age [190, 205]. Retinal dysfunction was observed after 4 weeks of hyperglycemia, as evident by delayed peak latency of the $\sum$OPs [189]. The amplitudes of a-wave, b-wave, and $\sum$OPs were significantly reduced with prolonged implicit times at 24 weeks of hyperglycemia [193]. At the same time, leukostasis [192] and the number of apoptotic cells in the GCL and the INL [188] were increased in the retinas of SDT rats. Vascular lesions, such as acellular capillaries and pericyte loss, have been described by Kakehashi et al. [206]. Advanced lesions, including leakage of fluorescein around the optic disc as well as distortion of retina and protruded optic disc, were also observed after 48 weeks of hyperglycemia [189]. More importantly, a few studies showed that proliferative DR can be detected in some of the aged SDT rats, which have been exposed to hyperglycemia for more than 48 weeks [190, 191, 205, 206]. The reported symptoms include retinal hemorrhages, tortuous vessels, capillary nonperfusion, neovascularization, and tractional retinal detachment with fibrous proliferation. Amongst the diabetic rat models mentioned in this review, the SDT rat is the only one that shows severe ocular complications similar to those seen in human. Although some common phenotypes in human DR, such as microaneurysms and development of avascular area, are rare in this model, this is a unique model to study proliferative DR [205, 207].

2.2.3. Rat Models for Angiogenesis Study. Similar to the mouse models for studying angiogenesis, OIR and occlusion models were also applicable to rats. Owing to the relevance of ischemic-induced neovascularization, we will focus on the OIR in this section.

The basic principle of OIR in rats is very similar to that in mice, which involves the induction of neurovascularization in nondiabetic animals. Different from the "standard" protocol of OIR in mice, several paradigms with varied oxygen concentrations and duration of the exposure period have been applied in rats. In brief, the newborn pups are exposed in alternative hyperoxia-hypoxia cycles for 11 to 14 days and then returned to room air [194, 195, 208–210]. Peripheral astrocyte degeneration was observed soon after the rats were exposed to room air [195]. At P18, the number of astrocyte was reduced almost throughout the whole retina [195] with prominent Müller cell reactivity in the regions that are devoid of intraretinal blood vessels [194]. Reduction of thickness in the INL, the IPL, and the total retinal layers was evident [194]; the outer segment layer also became thinner and disorganized [196]. While the number of pericytes was comparable to the room air control, the pericyte-endothelial interactions were impaired [195]. Intravitreal neovascularization, incomplete development of the outer vascular plexus and extension of the abnormal endothelial "tufts" toward the vitreous were observed in the OIR rats [195]. Functional lesions were also studied using ERG, in which the a- and b-wave amplitudes were reduced [197]. This model is useful in therapeutic drug screening or in the study of the mechanisms in angiogenesis, yet special equipments are required. Moreover, strain-dependent difference in the degree of retinal vascularization and abnormalities in vascular morphology have been reported [208]. The albino SD, the pigmented Dark Agouti, and Hooded Wister rats were more prone to the hyperoxia-hypoxia challenge, and they showed severe vascular attenuation following the oxygen exposure as well as severe vascular pathologies when compared to other strains.

In summary, rodents are very popular models to study the pathogenesis and examine the efficiency of therapeutic drugs of DR in laboratories. They have the advantage of being small in size which allows easier handling; however, this also makes *in vivo* examinations, such as fundus photography, fundus fluorescein angiography, and optical coherence tomography, difficult. Despite the lack of proliferative DR symptoms as described in most of the models mentioned above, researchers also focus on other animals in order to obtain the most representative model of DR, which ideally displays the comparable DR symptoms as seen in human patients. Higher mammals not only can serve as a platform for easier examinations but also allow easier treatment particularly those involving sophisticated surgical procedures. In these animals, sampling of body fluid, for example, vitreous and blood, can also be performed routinely.

2.3. Rabbit Models of DR. Similar approaches have been applied to rabbits to induce DR; these include pharmacologically induced and dietary-induced diabetic models as well as VEGF-induced angiogenesis in the retina without affecting the blood glucose level.

2.3.1. Pharmacologically Induced Rabbit Models of DR. Hyperglycemia can be induced in rabbit by STZ, although this method is not very frequently used. A study showed that intravenous injection of STZ (100 mg/kg) in rabbits can elevate their blood glucose level [211]. Fundus examination was done after 19 weeks of hyperglycemia and all eyes showed

certain degree of retinopathy, of which 50% showed proliferant retinopathy; 40% showed serious vasculopathy with serious retinal and preretinal hemorrhages, vascular lesions, hemovitreous and venous thrombosis; and the remaining 10% showed moderate vasculopathy with hard or soft exudates and widespread hemorrhages. Variation in the extent of the retinopathogenesis limits the use of this model.

2.3.2. Diet-Induced Rabbit Models of DR. Early DR can be found in rabbit models of diet-induced impaired glucose tolerance plus hyperlipidaemia [212]. Rabbits were fed with standard chow with 10% lard, 40% sucrose, and 0.1–0.5% cholesterol for a period of 24 weeks. The blood glucose level slightly elevated in the animals after feeding with 12 weeks of the special diet, and they became hyperglycemic by the end of the study period. Histological findings suggested that increased microaneurysms and hyperfluorescent dots were already present before the rabbit becomes hyperglycemic, while those pathological symptoms further progressed with prolonged feeding. Although this model mimics the natural development of type 2 diabetes in human, the drawback is the slow progression of DR symptoms.

2.3.3. Rabbit Models for Angiogenesis Study. In brief, a polymeric pellet containing human recombinant VEGF was implanted into the vitreous cavity of the rabbit [213]. After 7 days of implementation, increased dilation and tortuosity of retinal vessels were observed. During 14 to 21 days after implementation, fluorescein angiography further showed profuse leakage of dye, together with the presence of numerous small tortuous blood vessels, suggesting induction of neovascularization. However, such vascular changes stopped afterwards and neovascularization almost totally regressed after 35 days of implementation. The authors suggested that the regression of vessels may be due to depletion of the VEGF, implying that choosing the experimental endpoint is crucial when screening therapeutic agents in this model. Therefore, another group generated a similar model, in which human recombinant basic fibroblast growth factor (bFGF) was also incorporated into the polymeric pellet besides the human recombinant VEGF [214]. In this model, similar retinopathologies were observed but they only required approximately half of the time to develop when compared with the VEGF-induced model previously described. In addition, hemorrhage from the new vessels and even total traction retinal detachment were also observed. Moreover, differential retinal angiogenic response to VEGF/bFGF was reported in different rabbit strains, where Dutch belt rabbits are more susceptible than the NZW/Black satin cross rabbit [215].

It is evident that vascular retinopathy could be observed in the rabbit models mentioned above; however, researchers should be aware of the fact that retinal vasculature in the rabbit differs from those in other species. In rabbit, the optic artery branches into major blood vessels in a bidirectional horizontal manner; they further arborized into capillaries, forming a ring-like network. Moreover, the visual streak of rabbit is located below this region; functional defects may not be able to be detected if the lesion site is in the medullary ray where the blood vessels are. As compared with other animals, such vascular system is only present in a small area of the retina in rabbit; therefore, the global deleterious contributions by the vessels may be underestimated. On the other hand, if researchers aim to study the vessel-to-cell interaction at a molecular level, this model provides an alternative choice with an additional advantage of a bigger eyeball size than rodents. Therefore, more precise and delicate experiments can be performed, but the problem of limited housing space needs to be attended to.

2.4. Cat Model of DR. The majority of the DR studies in cats are induced by pancreatectomy with or without alloxan injection. The animal will become hyperglycemic 1 to 2 weeks after the surgery [216–218]. Capillary basement membrane thickening was first described from 3 months of pancreatectomy, where no change was observed in the number of endothelial cells and pericytes as well as the contacts between endothelial cells and pericytes up to 10 months [218]. A case report showed that microaneurysm was first observed in one eye in a diabetic cat after 5 years of pancreatectomy; and by 6.5 years, both eyes showed microaneurysms and small intraretinal hemorrhages in the area centralis [216]. Region of capillary nonperfusion and intraretinal microvascular abnormalities (IRMA) were also evident from 7.5 years. At 8.5 years, presence of small foci of neovascularization was suggested. Cotton-wool spots, venous beading, extensive preretinal neovascularization, or microvascular changes were not found in the peripheral retina. On the other hand, another study showed that only one out of two experimental diabetic cats showed microaneurysms, but not hemorrhages or area of nonperfusion, after 7 years of pancreatectomy, while the other diabetic cat did not show any microaneurysm or hemorrhage in the retina [217]. Cats only showed mild cataracts upon diabetes, thereby allowing visualization of the fundus angiography and ERG. However, the studies of DR in cat are very limited and the described phenotypes are less consistent. A long follow-up period for the development of retinal pathology and lack of reagents in molecular studies may be the drawbacks for using this animal model.

2.5. Dog Model of DR. Attempts of using dogs for studying DR have also been made, in which most of them are about inducible hyperglycemia either by injection of STZ or alloxan or feeding the animals with galactose. It has been suggested that galactose-fed dog is the animal model that shares the retinal lesions morphologically and clinically as those developed in human diabetic patients [219].

2.5.1. Pharmacologically Induced Dog Models of DR. Induction of diabetes in dogs by intravenous injection of STZ and alloxan resulted in basement membrane thickening in 3 years of injection, and it was recognized in some vessels from the first year [220]. Loss of pericytes and smooth muscle cells was observed in the retinal arterioles from 4 years of postinjection; no microaneurysm was noted towards the end of this 5-year study. Moreover, a comparative study showed

that increased microaneurysms, acellular capillaries, pericyte ghosts, endothelial cells to pericytes ratio, and basement membrane thickening were evident in the dogs after 5 years of galactosemia than those of alloxan-induced diabetes [221].

In the galactose-induced DR model, experimental dogs were continuously fed with normal diet supplemented with 30% galactose. Cellular lesions such as presence of pericyte ghosts and uneven distribution of endothelial cells were observed in retina of dogs after feeding with galactose for 19 and 24 months, respectively, followed by the formation of microaneurysms [222, 223]. Dot and blot hemorrhages were found from 33 months, which became more confluent, progressing to the preretinal and intravitreal regions after 66 months of feeding [222]. Nonperfusion was evident in dogs from 37 months of feeding [223, 224], and the area was broadened with time [222]. After 36-month feeding of galactose, acellular capillaries and endothelial cells to pericytes ratio were increased [225]. Other vascular lesions, such as abnormalities in intraretinal microvessels, occlusion of arterioles, presence of large arteriovenous shunts, and node formation on arterial and arteriolar walls, were also reported after feeding for about 5 years. At about the same time, presence of soft exudates and gliosis in the nerve fiber layer was reported [222]. Further advanced retinopathy of neovascularization was described in dogs being galactose fed for 68 to 84 months [222, 224]. It has been suggested that the onset of DR symptoms is age dependent in galactose-fed dogs; younger animals develop DR symptoms earlier than the older ones [225]. This may explain the variation of the onsets of the lesions mentioned above.

The biggest advantage of using dogs as a model is that they develop similar retinal morphological lesions as compared with human. Routine *in vivo* vasculature assessments, however, were impeded owing to the spontaneous diabetic cataract, particularly in the galactose-fed model; additional lensectomy is necessary [219, 223, 224]. Moreover, high maintenance cost, long-term follow-up period, and lack of molecular reagents, such as antibodies, make this model less commonly used for studying DR.

2.6. Swine Model of DR. Pig eye has become a useful tool in eye research because of its close similarities in the size as well as the basic retinal structure and vasculature to the human eye [226]. A number of models have been generated in order to study the retinopathy in swine upon diabetes, which include alloxan- and STZ-induced type 1 diabetic models. There is also a recently developed model of proliferative vitreoretinopathy that involved surgical procedures and intravitreal injection of retinal pigment epithelial (RPE) cells.

2.6.1. Pharmacologically Induced Swine Models of DR. There are only limited reports on the retinal morphology of the chemically induced diabetic pigs. Instead, researchers make use of the large amount of specific retinal cells and vitreous available in the pig eyes for *in vitro* experiments [227, 228]. Nevertheless, reactivation of Müller cells was evident from the increased GFAP immunoreactivity from the ONL extending to the outer limiting membrane [227] in 2 to 3 months after onset of alloxan-induced diabetes. At around 4 months of hyperglycemia, pericyte degeneration in parallel to reduced the total number of BRB capillaries and capillary collapse were also observed [229]. Retinal vascular lesions, such as basement membrane thickening [230, 231] and rarefaction [231], were reported in pigs after 18 weeks of STZ-induced diabetes. Development of hyperglycemic cataract was also reported in this animal after 32 weeks of hyperglycemia that constrain the visualization of the vasculatures, such as fundus angiography [231].

2.6.2. Swine Model for Angiogenesis Study. Recently, a new swine model of proliferative vitreoretinopathy has been described [232]. In brief, vitreal and retinal detachments were initially induced by vitrectomy and injection of subretinal fluid, respectively, prior to injection of cultured RPE cells into the vitreous cavity. Formation of contractile membranes on the inner retinal surface as well as localized tractional retinal detachments was evident and maintained after 14 days of induction while the retina reattached in the control animals at 3 days after the surgery. Further characterization of this model needs to be carried out before its use in therapeutic drug screening.

Although pig is a valuable model for disease study in human, high maintenance cost, requirement of special housing facilities, and lack of biochemical reagents make this model less commonly being used.

2.7. Monkey Model of DR. Monkey, a nonhuman primate, is considered to be a potential model in eye research owing to its structural similarity to human and, in particular, the presence of macula. The studies of DR in monkey can be divided into 3 groups: type 1 diabetic model, type 2 diabetic model, and model of VEGF-induced neovascularization.

2.7.1. Type 1 Diabetic Monkey Models. In an attempt to produce DR in monkeys, monkeys with type 1 diabetes that developed spontaneously as well as that resulted from total pancreatectomy or STZ injection were being used [233]. Unexpectedly, 37 out of 39 of these monkeys did not show any significant DR within 5 years of hyperglycemia. Animals with hyperglycemia of 6 to 15 years only showed mild disruption of the blood-retinal barrier. On the other hand, spontaneous or pharmacological induction of hypertension in the hyperglycemic monkeys, either by STZ injection or with spontaneous diabetes, resulted in ischemic retinopathies, such as cotton-wool spots which were found in the peripapillary region, microaneurysms, capillary dropout, capillary dilatation, focal intraretinal capillary leakage spots, arteriolar and venular occlusions, and atrophic macula, between 6 and 15 years of diabetes. The authors suggested that the fluctuating blood glucose levels and systemic blood pressure, but not hyperglycemic alone, play a role in the pathogenesis of DR.

2.7.2. Type 2 Diabetic Monkey Models. DR studies have also been carried out in monkeys that spontaneously develop type 2 diabetes. While moderate retinal lesions can be identified in a case of monkey with 3 years of diabetic history, no

detectable retinopathy was reported in a monkey with 15 years of diabetes [234]. The presence of these lesions was variable in individual animals, making it hard to deduce the precise onset of symptoms based on the diabetic duration. Among those showing retinopathies, cotton-wool spots, intraretinal hemorrhages, and nonperfused areas were the early observations. Progressive lesions, such as growing nonperfused area, which are associated with the formation small IRMAs and microaneurysms, as well as macular edema were also evident. Similar observations were also reported in another case study in which the subject is a monkey with at least 5 years of diabetes [235]. The authors have mentioned other histological abnormalities, including reduction of the thickness of the ONL and the inner and outer segments of the photoreceptor layers. Functional lesions were suggested by a loss in the amplitudes in the multifocal ERG, and they were virtually correlated to the nonperfused areas. Progressive reduction of amplitudes and delayed a-waves were also observed in the dark-adapted Ganzfeld ERG, suggesting a loss of function in the both inner and outer retina and reduced sensitivity in the photoreceptors, respectively. Moreover, it is reported that the occurrence of retinopathy is correlated with hypertension [234], which is coincidently similar to the descriptions in the type 1 diabetic monkey model.

2.7.3. Monkey Models for Angiogenesis Study. VEGF-induced proliferative retinopathy has also been carried out in nonhuman primates [213]. In brief, a pellet containing human recombinant VEGF was implanted into the vitreous cavity of the animal. At 2 weeks after the implementation, severe BRB breakdown was noted. Retinal vascular dilation and tortuosity were further observed in 3 weeks. The abnormalities peaked at 3 weeks and regressed afterwards. Neovascularization was not detected in this model.

There are many limitations in using monkeys in DR studies. Apart from the variations in the onset of morphological abnormalities and the absence of advanced retinopathies, low birth rate, high cost, long duration of study, and the heightened ethical concern make this model unfeasible for the purpose of drug screening.

2.8. Zebrafish Model of DR. Despite the enormous ethical concern in the laboratory use of the mammals mentioned above, in particular the primates, the recent emergence of zebrafish can resolve this complication. Zebrafish is extensively used in the study of visual development and impairments owing to its similarity to those seen in human [236]. The distinctive pattern of the mammalian retinal cell layers, ranging from ganglion cell layer to retinal pigment epithelium, is observed in zebrafish [236]. The retinal vasculature is rather complex in adult zebrafish [237]. Blood supply to the retina is supported by the optic artery, which branches into four to nine major blood vessels. These vessels further arborize into smaller vessels towards the peripheral of the retina where anastomosis between the neighboring capillaries is present. This radial vascular network covers the entirely inner surface retina with direct contact with the GCL. Oxygen-deprived blood is collected in the circumferential vein surrounding the retina where the cilliary marginal zone is. DR can be studied in zebrafish via direct elevation of glucose in the surrounding as well as angiogenesis without the involvement of glucose.

2.8.1. Glucose-Induced Diabetic Model of DR. In brief, zebrafish was exposed to freshwater with alternation between 2% and 0% glucose in every 24 hours for 30 days [238]. Hyperglycemia can be achieved in the animal in 1 day of immersion in the 2% glucose freshwater and maintained for at least 30 days with repeated hyperglycemic spikes every time after the removal from the glucose-freshwater. After 28 days of persistent hyperglycemia, the thickness of the IPL was significantly decreased, and yet no other abnormality has been observed [238]. The mechanism of glucose uptake in zebrafish is regulated by osmoregulation, in which influx of water, together with glucose, goes into their body as a result of high internal salt concentration. It has been reported that teleosts also have endocrine islet tissue containing hormone-producing cells which converge in the fish body, and the secretory teleost insulin is functional and is homologous to the human insulin [239]. This further validates the potential use of glucose-induced diabetic zebrafish in studying the retinopathy. Yet, morphological studies associated with the retinal vessels remained to be performed.

2.8.2. Zebrafish Models for Angiogenesis Study. Two models to study angiogenesis in zebrafish are described below, namely, environmentally and transgenic-induced models.

Retinal neovascularization can be achieved by keeping the zebrafish in hypoxic aquaria where the air saturation is gradually reduced to 10% (820 bbp) over a course of 48 to 72 hours and maintained for 12 days [240, 241]. In these studies, *fli*-EGFP-Tg zebrafish, which is a transgenic line that overexpresses EGFP in the vascular endothelium, was used for easy visualizing and imaging of the blood vessels. After 12 days of hypoxic challenge, neovascularization was observed in the retina evident by increased number of branch points, sprouts, and vascular area as well as reduced intercapillary distance [240]. This model can be useful for studying the development of angiogenesis or possibly for screening antiangiogenic pharmacological agents.

Retinal angiogenesis can also be induced in zebrafish via transgenic approach. Zebrafish carrying $vhl^{-/-}$ mutation displays an upregulation of hypoxia-inducible factor, which in turns triggers VEGF production and expression of the VEGF receptors [242]. By 5.75 days after fertilization (dpf), increased hyaloids and choroidal vascular networks were observed, followed by vascular leakage at 7.25 dpf. Excessive blood vessels were evident in the IPL, together with severe macular edema and retinal detachment at 7.5 dpf. However, this model is not commercially available, which limits its use in the field even though severe neovascularization and proliferative retinopathy are observed.

Zebrafish is very small in size; therefore, its maintenance is simple, convenient, and inexpensive. They have a short life span and a large breeding size, which in turn allow a shorter experimental turnover time. Moreover, a number

Table 4: Comparison of the morphological and functional lesions in models of DR other than rodents.

Animal model	Type of diabetes	Onset of hyperglycemia	Temporal morphological lesions in retina upon development of hyperglycemia		Temporal functional lesions in retina upon development of hyperglycemia (ERG, SLO, fMRI)
			Cellular	Vascular	
Rabbit					
STZ injection	Type 1	Did not mentioned	19 wk: (i) Moderate vasculopathy with hard or soft exudates, widespread hemorrhages in 10% of eyes [211] (ii) Serious vasculopathy with serious retinal and preretinal hemorrhages, vascular lesions, hemovitreous, and venous thrombosis in 40% of eyes [211] (iii) Proliferant retinopathy in 50% of eyes [211]		
Diet-induced	Type 2	Between 12 and 24 wk of diet		12 wk of special diet: (i) Increased microaneurysms [212] (ii) Presence of hyperfluorescent dots consistent with microaneurysms [212]	
VEGF implant	—	—		7 days after implementation: increased dilation and tortuosity of retinal vessels [213] 14 days after implementation: (i) Presence of numerous small tortuous blood vessels [213] (ii) Leakage of blood vessels [213] 21 days after implementation: neovascularization [213]	
Cat					
Pancreatectomy	Type 1	1-2 wk after surgery		3–10 mth: basement membrane thickening [218] 5 yr: microaneurysms [216] 6.5 yr: small intraretinal hemorrhages [216] 7.5 yr: (i) Presence of area of capillary nonperfusion [216] (ii) IRMA [216] 8.5 yr: small foci of neovascularization [216]	

Table 4: Continued.

Animal model	Type of diabetes	Onset of hyperglycemia	Temporal morphological lesions in retina upon development of hyperglycemia		Temporal functional lesions in retina upon development of hyperglycemia (ERG, SLO, fMRI)
			Cellular	Vascular	
Dogs					
Galactose-fed	—	—	19 mth of feeding: pericyte loss [222] 24 mth of feeding: uneven distribution of endothelial cells [222] 60 mth of feeding: (i) Soft exudates [222] (ii) Gliosis in the nerve fiber layer [222]	27-28 mth of feeding: microaneurysm formation [222, 223] 33 mth of feeding: (i) Dot and blot hemorrhages [222] (ii) Degenerated microaneurysms and varicose enlargements [222] 36 mth of feeding: (i) Confluent hemorrhages [222] (ii) Increased acellular capillaries [225] (iii) Increased endothelial cells to pericytes ratio [225] 37–46 mth of feeding: nonperfusion [223, 224] 56 mth of feeding: (i) Preretinal hemorrhage [222] (ii) Broad areas of nonperfusion [222] (iii) IRMA [222] 60 mth of feeding: (i) Occluded arterioles [222] (ii) Large arteriovenous shunts [222] (iii) Node formation on arterial and arteriolar walls [222] 66 mth of feeding: (i) Intravitreal hemorrhage [222] (ii) Partial posterior vitreous detachment [222] 68 mth of feeding: neovascularization [224] 84 mth of feeding: intravitreal retinal-vascular growth [222]	
STZ/alloxan injection			4 yr: (i) Pericytes loss [220] (ii) Loss of smooth muscle cells [220]	3 yr: basement membrane thickening [220]	
Pigs					
Alloxan injection	Type 1	15 days	90 days: Müller cells reactivation [227] 20 wk: pericyte loss [229]	20 wk: (i) Reduced total number of BRB capillaries [229] (ii) Capillary collapse [229]	
STZ injection	Type 1	1 wk		18 wk: (i) Basement membrane thickening [230, 231] (ii) Rarefaction [231]	
Surgery + RPE injection	—	—	14 days: (i) Formation of contractile membranes on the inner retinal surface [232] (ii) Localized traction retinal detachments [232]		

Table 4: Continued.

Animal model	Type of diabetes	Onset of hyperglycemia	Temporal morphological lesions in retina upon development of hyperglycemia		Temporal functional lesions in retina upon development of hyperglycemia (ERG, SLO, fMRI)
			Cellular	Vascular	
Monkey					
Spontaneous, STZ-induced, or pancreatectomy	Type 1	—	6–15 yr: atrophic macula [233]	6–15 yr: (i) Cotton-wool spots in the peripapillary region [233] (ii) Microaneurysms [233] (iii) Capillary dropout [233] (iv) Capillary dilatation [233] (v) Focal intraretinal capillary leakage spots [233] (vi) Arteriolar and venular occlusions [233]	
Spontaneous obese	Type 2	—	3–8 yr: (i) Macular edema [234] (ii) Reduction thickness of ONL [235] (iii) Reduction thickness of inner and outer segments of the photoreceptor layers [235]	3–8 yr: (i) Cotton-wool spots [234] (ii) Intraretinal hemorrhages [234] (iii) Nonperfused areas [234] (iv) Small IRMAs [234] (v) Microaneurysms [234]	5 yr: (i) Amplitude loss in multifocal ERG [235] (ii) Reduced amplitudes in ERG [235] (iii) Delayed a-waves in ERG [235]
VEGF implant	—	—		2 wk after implementation: severe BRB breakdown [213] 3 wk after implementation: retinal vascular dilation and tortuosity [213]	
Zebrafish					
Glucose-induced	Type 1	1 day	28 d: decreased IPL thickness [238]		
Hypoxia-induced	—	—		12 days: (i) Increased branch points [240] (ii) Increased number of sprouts [240] (iii) Reduced intercapillary distance [240] (iv) Increased vascular area [240]	
Vhl$^{-/-}$	—	—		5.75 dpf: increased hyaloid and choroidal vascular networks [242] 7.25 dpf: vascular leakage [242] 7.5 dpf: (i) Presence of blood vessels in the IPL [242] (ii) Severe macular edema [242] (iii) Retinal detachment [242]	

The observations reported at a particular time point, which was chosen by the authors, may not totally reflect the sequential processes.

Table 5: Comparison of the strengths and weaknesses of different animal models of DR.

Animal	Strength	Weakness
Mouse	(i) Cellular lesions are extensively studied (ii) Availablility of many transgenic models, which allows the study of the role of particular genes in the development and pathophysiological progression of DR (iii) Duration of developing early DR symptoms is short (i.e., within weeks to months) (iv) Small in size, easy to handle and house (v) A wide range of molecular reagents are available	(i) Only early DR lesions were observed (ii) PDR does not spontaneously occur and it can only be induced with the aid of models of angiogenesis (e.g., OIR, occlusion, and VEGF-induced models)
Rat	(i) Cellular lesions are extensively studied (ii) Duration of developing early DR symptoms is short (i.e., within weeks to months) (iii) Small to medium in size, relatively easy to handle and house (iv) A wide range of molecular reagents are available	(i) Only early DR lesions were observed, except in SDT rats (ii) PDR will not spontaneously occur and it can only be induced with the aid of models of angiogenesis (e.g., OIR, I/R models)
Higher-order mammals including rabbit, cat, dog, pig, and nonhuman primates	(i) Relatively similar to the pathophysiology of DR in human (ii) Larger tissues which allow easier *in vivo* examinations (iii) Routine sampling of body fluids is allowed	(i) Longer life span, require longer period of time to develop DR (ii) Large in size, difficult to handle and house (iii) Lack of reagents for molecular studies (iv) Heightened ethical concern
Zebrafish	(i) Genes of interest can be easily targeted induced, deleted, or overexpressed (ii) Maintenance is simple, convenient, and inexpensive (iii) Short life span and large breeding size, which allow shorter experimental turnover time (iv) Minimal ethical concern	(i) Thickness of retinal layers and retinal vasculature is different (ii) Retina is anatomically less similar to human (iii) Skillful technique is required due to small size of tissue (iv) Lack of reagents for molecular studies (v) Not being widely used

of studies showed that genes of interest can be specifically induced, deleted, or overexpressed in zebrafish, allowing mechanistic studies of diseases [243]. As a consequence, researchers have developed certain zebrafish models in order to study DR, including glucose-induced diabetic model and models specifically of angiogenesis. However, the retinal cells layers differ in thickness and thereby the number of cells, the findings may under- or overestimate the contribution of a specific cell type in regard to the pathogenesis of DR. In terms of the vasculature in zebrafish, the growth of the tertiary plexus of blood vessels in the INL is absent and the venous system is different from those in human. Therefore, researchers should be aware that using zebrafish may lead to potential discrepancy in cellular and vascular aspects and may not truly reflect the pathological development of DR in patients. Moreover, owing to the limited supply of tissue from a single animal, skillful techniques and a large quantity of eyeballs are required in dissection and for molecular analysis.

A summary of the temporal morphological and functional lesions of the animal models, other than rodents, described above is shown in Table 4. Table 5 displays general comparisons of the use of different animals in studying DR.

3. Conclusions

Animal models are very important in understanding the pathogenesis of diseases in human, defining novel therapeutic targets as well as screening of novel therapeutic drugs. In this review, a number of animal models of DR have been described and compared, ranging from different species to different induction methods of diabetes or angiogenesis, together with their corresponding temporal morphological and functional lesions. Up to date, there is no single model which can mimic the development of DR as in human, that is, from the very early cellular and vascular abnormalities to the proliferative stage, and subsequently retinal detachment, as a result of prolonged hyperglycemia. Rodents have been extensively used in DR studies owing to their small size and the ability to develop retinopathies within a relatively short period of time. The availability of a collection of transgenic mice further aids in elucidating the role of target molecules in DR. Since the STZ-induced diabetic rodents are the most frequently used models in studying the associated retinopathy, we have summarized the administration dosage and paradigm published in the recent years as a reference to other researchers. Nevertheless, a majority of the diabetic rodent models only demonstrated the early symptoms of DR, which restricts their applications in mechanistic studies and drugs screening targeting the early progression of DR. Some higher-order animals showed relatively advanced retinopathies, such as neovascularization, upon induction of diabetes, yet they still cannot imitate the later stage of DR as seen in human. Moreover, high maintenance cost, long duration of study, and lack of molecular reagents, such as antibodies, as well as ethical concern further limit their use in studies. Zebrafish is another model that emerged recently in studies of DR; however, further characterization needs to be done. The presence of neovascularization is controversial in some animal models; such variation may come from animals of different strain and age, individual variation, and/or even the detection methods. Therefore, we suggested that researchers should have a bigger sample size, use at least two detection methods, such as fluorescence angiography, immunohistochemical staining of blood vessel marker on retinal flat mounts or cross-sections in combination with molecular analysis, in order to have a more convincing claim. Furthermore, overexposure of the fluorescence staining and "cleanness" of the section, particularly in the flat mounts, are other issues that researchers should be aware of. Although neovascularization can be observed in animals overexpressing VEGF, either via transgenic approach or direct introduction, the development of neovascularization is not caused by prolonged hyperglycemia. Therefore, using these models in studies of the etiology of the disease or the development of preretinal neovascularization should be avoided. Another approach for induction of neovascularization is by hypoxic challenge in rodents; however, regression was reported within a few days, which may limit the duration of the drug treatment versus the formation of new vessels. As outlined in this review, individual model of DR has different strengths and weaknesses; careful consideration should be made in choosing appropriate models to address the research questions.

References

[1] J. B. Saaddine, A. A. Honeycutt, K. M. V. Narayan, X. Zhang, R. Klein, and J. P. Boyle, "Projection of diabetic retinopathy and other major eye diseases among people with diabetes mellitus: United States, 2005–2050," *Archives of Ophthalmology*, vol. 126, no. 12, pp. 1740–1747, 2008.

[2] T. Y. Wong, M. Mwamburi, R. Klein et al., "Rates of progression in diabetic retinopathy during different time periods: a systematic review and meta-analysis," *Diabetes Care*, vol. 32, no. 12, pp. 2307–2313, 2009.

[3] N. Cheung, P. Mitchell, and T. Y. Wong, "Diabetic retinopathy," *The Lancet*, vol. 376, no. 9735, pp. 124–136, 2010.

[4] R. Levene, G. Horton, and R. Gorn, "Flat-mount studies of human retinal vessels," *American Journal of Ophthalmology*, vol. 61, no. 2, pp. 283–289, 1966.

[5] M. Yanoff, "Ocular pathology of diabetes mellitus," *American Journal of Ophthalmology*, vol. 67, no. 1, pp. 21–38, 1969.

[6] M. Mizutani, C. Gerhardinger, and M. Lorenzi, "Muller cell changes in human diabetic retinopathy," *Diabetes*, vol. 47, no. 3, pp. 445–449, 1998.

[7] A. J. Barber, E. Lieth, S. A. Khin, D. A. Antonetti, A. G. Buchanan, and T. W. Gardner, "Neural apoptosis in the retina during experimental and human diabetes: early onset and effect of insulin," *Journal of Clinical Investigation*, vol. 102, no. 4, pp. 783–791, 1998.

[8] A. M. Abu El-Asrar, L. Dralands, L. Missotten, I. A. Al-Jadaan, and K. Geboes, "Expression of apoptosis markers in the retinas of human subjects with diabetes," *Investigative Ophthalmology & Visual Science*, vol. 45, no. 8, pp. 2760–2766, 2004.

[9] G. A. Lutty, D. S. McLeod, C. Merges, A. Diggs, and J. Plouét, "Localization of vascular endothelial growth factor in human retina and choroid," *Archives of Ophthalmology*, vol. 114, no. 8, pp. 971–977, 1996.

[10] E. Carrasco, C. Hernández, A. Miralles, P. Huguet, J. Farrés, and R. Simó, "Lower somatostatin expression is an early event in diabetic retinopathy and is associated with retinal neurodegeneration," *Diabetes Care*, vol. 30, no. 11, pp. 2902–2908, 2007.

[11] E. Carrasco, C. Hernández, I. de Torres, J. Farrés, and R. Simó, "Lowered cortistatin expression is an early event in the human diabetic retina and is associated with apoptosis and glial activation," *Molecular Vision*, vol. 14, pp. 1496–1502, 2008.

[12] S. Kase, S. Ishida, and N. A. Rao, "Increased expression of áA-crystallin in human diabetic eye," *International Journal of Molecular Medicine*, vol. 28, no. 4, pp. 505–511, 2011.

[13] R. Simo, M. García-Ramírez, M. Higuera, and C. Hernández, "Apolipoprotein A1 is overexpressed in the retina of diabetic patients," *American Journal of Ophthalmology*, vol. 147, no. 2, pp. 319–325, 2009.

[14] A. M. Abu El-Asrar, S. Struyf, D. Kangave, K. Geboes, and J. van Damme, "Chemokines in proliferative diabetic retinopathy and proliferative vitreoretinopathy," *European Cytokine Network*, vol. 17, no. 3, pp. 155–165, 2006.

[15] C. M. Cheung, M. Vania, M. Ang, S. P. Chee, and J. Li, "Comparison of aqueous humor cytokine and chemokine levels in diabetic patients with and without retinopathy," *Molecular Vision*, vol. 18, pp. 830–837, 2012.

[16] Y. Suzuki, M. Nakazawa, K. Suzuki, H. Yamazaki, and Y. Miyagawa, "Expression profiles of cytokines and chemokines in vitreous fluid in diabetic retinopathy and central retinal vein occlusion," *Japanese Journal of Ophthalmology*, vol. 55, no. 3, pp. 256–263, 2011.

[17] Y. Wakabayashi, Y. Usui, Y. Okunuki et al., "Correlation of vascular endothelial growth factor with chemokines in the vitreous in diabetic retinopathy," *Retina*, vol. 30, no. 2, pp. 339–344, 2010.

[18] S. Doganay, C. Evereklioglu, H. Er et al., "Comparison of serum NO, TNF-α, IL-1β, sIL-2R, IL-6 and IL-8 levels with grades of retinopathy in patients with diabetes mellitus," *Eye*, vol. 16, no. 2, pp. 163–170, 2002.

[19] M. L. Schwartzman, P. Iserovich, K. Gotlinger et al., "Profile of lipid and protein autacoids in diabetic vitreous correlates with the progression of diabetic retinopathy," *Diabetes*, vol. 59, no. 7, pp. 1780–1788, 2010.

[20] I. K. Oh, S. W. Kim, J. Oh, T. S. Lee, and K. Huh, "Inflammatory and angiogenic factors in the aqueous humor and the relationship to diabetic retinopathy," *Current Eye Research*, vol. 35, no. 12, pp. 1116–1127, 2010.

[21] L. P. Aiello, R. L. Avery, P. G. Arrigg et al., "Vascular endothelial growth factor in ocular fluid of patients with diabetic retinopathy and other retinal disorders," *New England Journal of Medicine*, vol. 331, no. 22, pp. 1480–1487, 1994.

[22] M. Beránek, P. Kolar, S. Tschoplova, K. Kankova, and A. Vasku, "Genetic variations and plasma levels of gelatinase A (matrix metalloproteinase-2) and gelatinase B (matrix metalloproteinase-9) in proliferative diabetic retinopathy," *Molecular Vision*, vol. 14, pp. 1114–1121, 2008.

[23] M. Myśliwiec, K. Zorena, A. Balcerska, J. Myśliwska, P. Lipowski, and K. Raczyńska, "The activity of N-acetyl-beta-d-glucosaminidase and tumor necrosis factor-alpha at early stage of diabetic retinopathy development in type 1 diabetes mellitus children," *Clinical Biochemistry*, vol. 39, no. 8, pp. 851–856, 2006.

[24] P. S. Silva, J. D. Cavallerano, J. K. Sun, J. Noble, L. M. Aiello, and L. P. Aiello, "Nonmydriatic ultrawide field retinal imaging compared with dilated standard 7-field 35-mm photography and retinal specialist examination for evaluation of diabetic retinopathy," *American Journal of Ophthalmology*, vol. 154, no. 3, pp. 549–559, 2012.

[25] J. Tam, K. P. Dhamdhere, P. Tiruveedhula et al., "Subclinical capillary changes in non-proliferative diabetic retinopathy," *Optometry & Vision Science*, vol. 89, no. 5, pp. E692–E703, 2012.

[26] H. Wang, J. Chhablani, W. R. Freeman et al., "Characterization of diabetic microaneurysms by simultaneous fluorescein angiography and spectral-domain optical coherence tomography," *American Journal of Ophthalmology*, vol. 153, no. 5, pp. 861–867, 2012.

[27] J. Ding, M. K. Ikram, C. Y. Cheung, and T. Y. Wong, "Retinal vascular calibre as a predictor of incidence and progression of diabetic retinopathy," *Clinical and Experimental Optometry*, vol. 95, no. 3, pp. 290–296, 2012.

[28] S. H. Byeon, Y. K. Chu, Y. T. Hong, M. Kim, H. M. Kang, and O. W. Kwon, "New insights into the pathoanatomy of diabetic macular edema: angiographic patterns and optical coherence tomography," *Retina*, vol. 32, no. 6, pp. 1087–1099, 2012.

[29] R. Bernardes, P. Serranho, and C. Lobo, "Digital ocular fundus imaging: a review," *Ophthalmologica*, vol. 226, no. 4, pp. 161–181, 2011.

[30] M. A. Bearse Jr., A. J. Adams, Y. Han et al., "A multifocal electroretinogram model predicting the development of diabetic retinopathy," *Progress in Retinal and Eye Research*, vol. 25, no. 5, pp. 425–448, 2006.

[31] J. Kizawa, S. Machida, T. Kobayashi, Y. Gotoh, and D. Kurosaka, "Changes of oscillatory potentials and photopic negative response in patients with early diabetic retinopathy," *Japanese Journal of Ophthalmology*, vol. 50, no. 4, pp. 367–373, 2006.

[32] R. A. Feit-Leichman, R. Kinouchi, M. Takeda et al., "Vascular damage in a mouse model of diabetic retinopathy: relation to neuronal and glial changes," *Investigative Ophthalmology & Visual Science*, vol. 46, no. 11, pp. 4281–4287, 2005.

[33] S. Kumar and L. Zhuo, "Longitudinal in vivo imaging of retinal gliosis in a diabetic mouse model," *Experimental Eye Research*, vol. 91, no. 4, pp. 530–536, 2010.

[34] Y. Yang, D. Mao, X. Chen et al., "Decrease in retinal neuronal cells in streptozotocin-induced diabetic mice," *Molecular Vision*, vol. 18, pp. 1411–1420, 2012.

[35] P. M. Martin, P. Roon, T. K. van Ells, V. Ganapathy, and S. B. Smith, "Death of retinal neurons in streptozotocin-induced diabetic mice," *Investigative Ophthalmology & Visual Science*, vol. 45, no. 9, pp. 3330–3336, 2004.

[36] R. A. Gubitosi-Klug, R. Talahalli, Y. Du, J. L. Nadler, and T. S. Kern, "5-Lipoxygenase, but not 12/15-lipoxygenase, contributes to degeneration of retinal capillaries in a mouse model of diabetic retinopathy," *Diabetes*, vol. 57, no. 5, pp. 1387–1393, 2008.

[37] L. Zheng, Y. Du, C. Miller et al., "Critical role of inducible nitric oxide synthase in degeneration of retinal capillaries in mice with streptozotocin-induced diabetes," *Diabetologia*, vol. 50, no. 9, pp. 1987–1996, 2007.

[38] G. Li, J. Tang, Y. Du, C. A. Lee, and T. S. Kern, "Beneficial effects of a novel RAGE inhibitor on early diabetic retinopathy and tactile allodynia," *Molecular Vision*, vol. 17, pp. 3156–3165, 2011.

[39] S. J. Howell, M. N. Mekhail, R. Azem, N. L. Ward, and T. S. Kern, "Degeneration of retinal ganglion cells in diabetic dogs and mice: relationship to glycemic control and retinal capillary degeneration," *Molecular Vision*, vol. 19, pp. 1413–1421, 2013.

[40] S. Kubota, Y. Ozawa, T. Kurihara et al., "Roles of AMP-activated protein kinase in diabetes-induced retinal inflammation," *Investigative Ophthalmology & Visual Science*, vol. 52, no. 12, pp. 9142–9148, 2011.

[41] J. H. Kim, J. H. Kim, Y. S. Yu, C. S. Cho, and K. W. Kim, "Blockade of angiotensin II attenuates VEGF-mediated blood-retinal barrier breakdown in diabetic retinopathy," *Journal of Cerebral Blood Flow and Metabolism*, vol. 29, no. 3, pp. 621–628, 2009.

[42] Y. H. Kim, Y. S. Kim, G. S. Roh, W. S. Choi, and G. J. Cho, "Resveratrol blocks diabetes-induced early vascular lesions and vascular endothelial growth factor induction in mouse retinas," *Acta Ophthalmologica*, vol. 90, no. 1, pp. e31–e37, 2012.

[43] E. J. Kuiper, R. van Zijderveld, P. Roestenberg et al., "Connective tissue growth factor is necessary for retinal capillary basal lamina thickening in diabetic mice," *Journal of Histochemistry and Cytochemistry*, vol. 56, no. 8, pp. 785–792, 2008.

[44] L. Su, J. Ji, J. Bian, Y. Fu, Y. Ge, and Z. Yuan, "Tacrolimus (FK506) prevents early retinal neovascularization in streptozotocin-induced diabetic mice," *International Immunopharmacology*, vol. 14, no. 4, pp. 606–612, 2012.

[45] Z. Wang, A. S. Yadav, W. Leskova, and N. R. Harris, "Attenuation of streptozotocin-induced microvascular changes in the mouse retina with the endothelin receptor A antagonist atrasentan," *Experimental Eye Research*, vol. 91, no. 5, pp. 670–675, 2010.

[46] Z. Wang, A. S. Yadav, W. Leskova, and N. R. Harris, "Inhibition of 20-HETE attenuates diabetes-induced decreases in retinal hemodynamics," *Experimental Eye Research*, vol. 93, no. 1, pp. 108–113, 2011.

[47] W. S. Wright and N. R. Harris, "Ozagrel attenuates early streptozotocin-induced constriction of arterioles in the mouse retina," *Experimental Eye Research*, vol. 86, no. 3, pp. 528–536, 2008.

[48] W. S. Wright, J. E. Messina, and N. R. Harris, "Attenuation of diabetes-induced retinal vasoconstriction by a thromboxane receptor antagonist," *Experimental Eye Research*, vol. 88, no. 1, pp. 106–112, 2009.

[49] M. Sasaki, Y. Ozawa, T. Kurihara et al., "Neurodegenerative influence of oxidative stress in the retina of a murine model of diabetes," *Diabetologia*, vol. 53, no. 5, pp. 971–979, 2010.

[50] T. Kurihara, Y. Ozawa, N. Nagai et al., "Angiotensin II type 1 receptor signaling contributes to synaptophysin degradation and neuronal dysfunction in the diabetic retina," *Diabetes*, vol. 57, no. 8, pp. 2191–2198, 2008.

[51] S. S. Zhu, Y. Ren, M. Zhang et al., "WldS protects against peripheral neuropathy and retinopathy in an experimental model of diabetes in mice," *Diabetologia*, vol. 54, no. 9, pp. 2440–2450, 2011.

[52] A. A. Rossini, M. C. Appel, R. M. Williams, and A. A. Like, "Genetic influence of the streptozotocin-induced insulitis and hyperglycemia," *Diabetes*, vol. 26, no. 10, pp. 916–920, 1977.

[53] X. Qin, Z. Zhang, H. Xu, and Y. Wu, "Notch signaling protects retina from nuclear factor-κB- and poly-ADP-ribose-polymerase-mediated apoptosis under high-glucose stimulation," *Acta Biochimica et Biophysica Sinica*, vol. 43, no. 9, pp. 703–711, 2011.

[54] A. M. Serra, J. Waddell, A. Manivannan, H. Xu, M. Cotter, and J. V. Forrester, "CD11b+ bone marrow-derived monocytes are the major leukocyte subset responsible for retinal capillary leukostasis in experimental diabetes in mouse and express high levels of CCR5 in the circulation," *American Journal of Pathology*, vol. 181, no. 2, pp. 719–727, 2012.

[55] J. H. Kim, J. H. Kim, Y. S. Yu, B. H. Min, and K. W. Kim, "Protective effect of clusterin on blood-retinal barrier breakdown in diabetic retinopathy," *Investigative Ophthalmology & Visual Science*, vol. 51, no. 3, pp. 1659–1665, 2010.

[56] S. Kumar and L. Zhuo, "Quantitative analysis of pupillary light reflex by real-time autofluorescent imaging in a diabetic mouse model," *Experimental Eye Research*, vol. 92, no. 3, pp. 164–172, 2011.

[57] A. S. Yadav and N. R. Harris, "Effect of tempol on diabetes-induced decreases in retinal blood flow in the mouse," *Current Eye Research*, vol. 36, no. 5, pp. 456–461, 2011.

[58] W. S. Wright, R. M. McElhatten, J. E. Messina, and N. R. Harris, "Hypoxia and the expression of HIF-1α and HIF-2α in the retina of streptozotocin-injected mice and rats," *Experimental Eye Research*, vol. 90, no. 3, pp. 405–412, 2010.

[59] A. Y. Shanab, T. Nakazawa, M. Ryu et al., "Metabolic stress response implicated in diabetic retinopathy: the role of calpain, and the therapeutic impact of calpain inhibitor," *Neurobiology of Disease*, vol. 48, no. 3, pp. 556–567, 2012.

[60] B. B. Gao, J. A. Phipps, D. Bursell, A. C. Clermont, and E. P. Feener, "Angiotensin AT1 receptor antagonism ameliorates murine retinal proteome changes induced by diabetes," *Journal of Proteome Research*, vol. 8, no. 12, pp. 5541–5549, 2009.

[61] W. M. Freeman, G. V. Bixler, R. M. Brucklacher et al., "Transcriptomic comparison of the retina in two mouse models of diabetes," *Journal of Ocular Biology, Diseases, and Informatics*, vol. 2, no. 4, pp. 202–213, 2009.

[62] Y. Zhong, J. Li, Y. Chen, J. J. Wang, R. Ratan, and S. X. Zhang, "Activation of endoplasmic reticulum stress by hyperglycemia is essential for Müller cell-derived inflammatory cytokine production in diabetes," *Diabetes*, vol. 61, no. 2, pp. 492–504, 2012.

[63] M. K. Losiewicz and P. E. Fort, "Diabetes impairs the neuroprotective properties of retinal alpha-crystallins," *Investigative Ophthalmology & Visual Science*, vol. 52, no. 9, pp. 5034–5042, 2011.

[64] Y. H. Kim, S. Y. Park, J. Park et al., "Reduction of experimental diabetic vascular leakage and pericyte apoptosis in mice by delivery of alphaA-crystallin with a recombinant adenovirus," *Diabetologia*, vol. 55, no. 10, pp. 2835–2844, 2012.

[65] S. Pinach, D. Burt, E. Berrone et al., "Retinal heat shock protein 25 in early experimental diabetes," *Acta Diabetologica*, 2011.

[66] C. Tikellis, K. Bialkowski, J. Pete et al., "ACE2 deficiency modifies renoprotection afforded by ACE inhibition in experimental diabetes," *Diabetes*, vol. 57, no. 4, pp. 1018–1025, 2008.

[67] C. Gustavsson, C. D. Agardh, A. V. Zetterqvist, J. Nilsson, E. Agardh, and M. F. Gomez, "Vascular cellular adhesion molecule-1 (VCAM-1) expression in mice retinal vessels is affected by both hyperglycemia and hyperlipidemia," *PLoS ONE*, vol. 5, no. 9, Article ID e12699, 2010.

[68] T. J. Giove, M. M. Deshpande, C. S. Gagen, and W. D. Eldred, "Increased neuronal nitric oxide synthase activity in retinal neurons in early diabetic retinopathy," *Molecular Vision*, vol. 15, pp. 2249–2258, 2009.

[69] S. Satofuka, A. Ichihara, N. Nagai et al., "(Pro)renin receptor-mediated signal transduction and tissue renin-angiotensin system contribute to diabetes-induced retinal inflammation," *Diabetes*, vol. 58, no. 7, pp. 1625–1633, 2009.

[70] Q. Li, A. Verma, P. Y. Han et al., "Diabetic eNOS-knockout mice develop accelerated retinopathy," *Investigative Ophthalmology & Visual Science*, vol. 51, no. 10, pp. 5240–5246, 2010.

[71] S. Sen, S. Chen, Y. Wu, B. Feng, E. K. Lui, and S. Chakrabarti, "Preventive effects of North American ginseng (Panax quinquefolius) on diabetic retinopathy and cardiomyopathy," *Phytotherapy Research*, vol. 27, no. 2, pp. 290–298, 2013.

[72] M. W. Bobbie, S. Roy, K. Trudeau, S. J. Munger, A. M. Simon, and S. Roy, "Reduced connexin 43 expression and its effect on the development of vascular lesions in retinas of diabetic mice," *Investigative Ophthalmology & Visual Science*, vol. 51, no. 7, pp. 3758–3763, 2010.

[73] R. P. Kandpal, H. K. Rajasimha, M. J. Brooks et al., "Transcriptome analysis using next generation sequencing reveals molecular signatures of diabetic retinopathy and efficacy of candidate drugs," *Molecular Vision*, vol. 18, pp. 1123–1146, 2012.

[74] Q. Wang, S. Gorbey, F. Pfister et al., "Long-term treatment with suberythropoietic epo is vaso- and neuroprotective in experimental diabetic retinopathy," *Cellular Physiology and Biochemistry*, vol. 27, no. 6, pp. 769–782, 2011.

[75] D. Luo, Y. Fan, and X. Xu, "The effects of aminoguanidine on retinopathy in STZ-induced diabetic rats," *Bioorganic & Medicinal Chemistry Letters*, vol. 22, no. 13, pp. 4386–4390, 2012.

[76] L. N. Hao, Y. Q. Zhang, Y. H. Shen et al., "Effect of puerarin on retinal pigment epithelial cells apoptosis induced partly by peroxynitrite via Fas/FasL pathway," *International Journal of Ophthalmology*, vol. 3, no. 4, pp. 283–287, 2010.

[77] S. K. Gupta, B. Kumar, T. C. Nag et al., "Curcumin prevents experimental diabetic retinopathy in rats through its hypoglycemic, antioxidant, and anti-inflammatory mechanisms," *Journal of Ocular Pharmacology and Therapeutics*, vol. 27, no. 2, pp. 123–130, 2011.

[78] V. A. O. Silva, A. Polesskaya, T. A. Sousa et al., "Expression and cellular localization of microRNA-29b and RAX, an activator of the RNA-dependent protein kinase (PKR), in the retina of streptozotocin-induced diabetic rats," *Molecular Vision*, vol. 17, pp. 2228–2240, 2011.

[79] B. Zhang, K. K. Zhou, and J. X. Ma, "Inhibition of connective tissue growth factor overexpression in diabetic retinopathy by SERPINA3K via blocking the WNT/β-catenin pathway," *Diabetes*, vol. 59, no. 7, pp. 1809–1816, 2010.

[80] O. Catanzaro, E. Labal, A. Andornino, J. A. Capponi, I. Di Martino, and P. Sirois, "Blockade of early and late retinal biochemical alterations associated with diabetes development by the selective bradykinin B1 receptor antagonist R-954," *Peptides*, vol. 34, no. 2, pp. 349–352, 2012.

[81] A. S. Yar, S. Menevse, I. Dogan et al., "Investigation of ocular neovascularization-related genes and oxidative stress in diabetic rat eye tissues after resveratrol treatment," *Journal of Medicinal Food*, vol. 15, no. 4, pp. 391–398, 2012.

[82] Y. Jiang, R. J. Walker, T. S. Kern, and J. J. Steinle, "Application of isoproterenol inhibits diabetic-like changes in the rat retina," *Experimental Eye Research*, vol. 91, no. 2, pp. 171–179, 2010.

[83] A. Thakur, R. I. Scheinman, V. R. Rao, and U. B. Kompella, "Pazopanib, a multitargeted tyrosine kinase inhibitor, reduces diabetic retinal vascular leukostasis and leakage," *Microvascular Research*, vol. 82, no. 3, pp. 346–350, 2011.

[84] Q. Chu, J. Zhang, Y. Wu et al., "Differential gene expression pattern of diabetic rat retinas after intravitreal injection of erythropoietin," *Clinical and Experimental Ophthalmology*, vol. 39, no. 2, pp. 142–151, 2011.

[85] P. Li, X. Xu, Z. Zheng, B. Zhu, Y. Shi, and K. Liu, "Protective effects of rosiglitazone on retinal neuronal damage in diabetic rats," *Current Eye Research*, vol. 36, no. 7, pp. 673–679, 2011.

[86] S. G. Lee, J. L. Kim, H. K. Lee et al., "Simvastatin suppresses expression of angiogenic factors in the retinas of rats with streptozotocin-induced diabetes," *Graefe's Archive for Clinical and Experimental Ophthalmology*, vol. 249, no. 3, pp. 389–397, 2011.

[87] S. G. Lee, C. G. Lee, I. H. Yun, D. Y. Hur, J. W. Yang, and H. W. Kim, "Effect of lipoic acid on expression of angiogenic factors in diabetic rat retina," *Clinical and Experimental Ophthalmology*, vol. 40, no. 1, pp. e47–e57, 2012.

[88] B. Cui, J. H. Sun, F. F. Xiang, L. Liu, and W. J. Li, "Aquaporin 4 knockdown exacerbates streptozotocin-induced diabetic retinopathy through aggravating inflammatory response," *Experimental Eye Research*, vol. 98, no. 1, pp. 37–43, 2012.

[89] L. Xu, Y. M. Liu, Z. J. Yao et al., "Generation of trans-arachidonic acid under nitrative stress is associated with upregulation of thromponsdin-1 in diabetic rats," *Chinese Medical Journal*, vol. 124, no. 12, pp. 1885–1889, 2011.

[90] J. Y. Wang, Q. Lu, Y. Tao, Y. R. Jiang, and J. B. Jonas, "Intraocular expression of thymosin β4 in proliferative diabetic retinopathy," *Acta Ophthalmologica*, vol. 89, no. 5, pp. e396–e403, 2011.

[91] P. Ma, Y. Luo, X. Zhu, T. Li, J. Hu, and S. Tang, "Retinal heparanase expression in streptozotocin-induced diabetic rats," *Canadian Journal of Ophthalmology*, vol. 45, no. 1, pp. 46–51, 2010.

[92] X. Ye, G. Xu, Q. Chang et al., "ERK1/2 signaling pathways involved in VEGF release in diabetic rat retina," *Investigative Ophthalmology & Visual Science*, vol. 51, no. 10, pp. 5226–5233, 2010.

[93] Y. Zhu, X. L. Zhang, B. F. Zhu, and Y. N. Ding, "Effect of antioxidant N-acetylcysteine on diabetic retinopathy and expression of VEGF and ICAM-1 from retinal blood vessels of diabetic rats," *Molecular Biology Reports*, vol. 39, no. 4, pp. 3727–3735, 2012.

[94] A. S. Ibrahim, A. B. El-Remessy, S. Matragoon et al., "Retinal microglial activation and inflammation induced by amadori-glycated albumin in a rat model of diabetes," *Diabetes*, vol. 60, no. 4, pp. 1122–1133, 2011.

[95] W. S. Wright, R. M. McElhatten, and N. R. Harris, "Increase in retinal hypoxia-inducible factor-2α, but not hypoxia, early in the progression of diabetes in the rat," *Experimental Eye Research*, vol. 93, no. 4, pp. 437–441, 2011.

[96] Z. Yang, K. Li, X. Yan, F. Dong, and C. Zhao, "Amelioration of diabetic retinopathy by engrafted human adipose-derived mesenchymal stem cells in streptozotocin diabetic rats," *Graefe's Archive for Clinical and Experimental Ophthalmology*, vol. 248, no. 10, pp. 1415–1422, 2010.

[97] H. Yang, Y. Huang, X. Chen et al., "The role of CTGF in the diabetic rat retina and its relationship with VEGF and TGF-β2, elucidated by treatment with CTGFsiRNA," *Acta Ophthalmologica*, vol. 88, no. 6, pp. 652–659, 2010.

[98] H. Xin, F. Zhou, T. Liu et al., "Icariin ameliorates streptozotocin-induced diabetic retinopathy in vitro and in vivo," *International Journal of Molecular Sciences*, vol. 13, no. 1, pp. 866–878, 2012.

[99] E. Arnold, J. C. Rivera, S. Thebault et al., "High levels of serum prolactin protect against diabetic retinopathy by increasing ocular vasoinhibins," *Diabetes*, vol. 59, no. 12, pp. 3192–3197, 2010.

[100] M. Ramírez, Z. Wu, B. Moreno-Carranza et al., "Vasoinhibin gene transfer by adenoassociated virus type 2 protects against VEGF- and diabetes-induced retinal vasopermeability," *Investigative Ophthalmology & Visual Science*, vol. 52, no. 12, pp. 8944–8950, 2011.

[101] I. Semkova, M. Huemmeke, M. S. Ho et al., "Retinal localization of the glutamate receptor GluR2 and GluR2-regulating proteins in diabetic rats," *Experimental Eye Research*, vol. 90, no. 2, pp. 244–253, 2010.

[102] S. Yan, C. Zheng, Z. Q. Chen et al., "Expression of endoplasmic reticulum stress-related factors in the retinas of diabetic rats," *Experimental Diabetes Research*, vol. 2012, Article ID 743780, 11 pages, 2012.

[103] H. Yang, R. Liu, Z. Cui et al., "Functional characterization of 58-kilodalton inhibitor of protein kinase in protecting against diabetic retinopathy via the endoplasmic reticulum stress pathway," *Molecular Vision*, vol. 17, pp. 78–84, 2011.

[104] C. M. McVicar, R. Hamilton, L. M. Colhoun et al., "Intervention with an erythropoietin-derived peptide protects against neuroglial and vascular degeneration during diabetic retinopathy," *Diabetes*, vol. 60, no. 11, pp. 2995–3005, 2011.

[105] T. E. Fox, M. M. Young, M. M. Pedersen, X. Han, T. W. Gardner, and M. Kester, "Diabetes diminishes phosphatidic acid in the retina: a putative mediator for reduced mTOR signaling and increased neuronal cell death," *Investigative Ophthalmology & Visual Science*, vol. 53, no. 11, pp. 7257–7267, 2012.

[106] X. Xiao, J. Cai, J. Xu et al., "Protective effects of hydrogen saline on diabetic retinopathy in a streptozotocin-induced diabetic rat model," *Journal of Ocular Pharmacology and Therapeutics*, vol. 28, no. 1, pp. 76–82, 2012.

[107] X. Zhang, M. Chen, and M. C. Gillies, "Two isoforms of Flk-1 transcripts in early diabetic rat retinas," *Current Eye Research*, vol. 37, no. 1, pp. 73–79, 2012.

[108] T. S. Devi, I. Lee, M. Hüttemann, A. Kumar, K. D. Nantwi, and L. P. Singh, "TXNIP links innate host defense mechanisms to oxidative stress and inflammation in retinal muller glia under chronic hyperglycemia: implications for diabetic retinopathy," *Experimental Diabetes Research*, vol. 2012, Article ID 438238, 19 pages, 2012.

[109] A. F. Castilho, J. T. Liberal, F. I. Baptista, J. M. Gaspar, A. L. Carvalho, and A. F. Ambrósio, "Elevated glucose concentration changes the content and cellular localization of AMPA receptors in the retina but not in the hippocampus," *Neuroscience*, vol. 219, pp. 23–32, 2012.

[110] A. R. Santiago, M. J. Garrido, A. J. Cristóvão, J. M. N. Duarte, R. A. Carvalho, and A. F. Ambrósio, "Evaluation of the impact of diabetes on retinal metabolites by NMR spectroscopy," *Current Eye Research*, vol. 35, no. 11, pp. 992–1001, 2010.

[111] E. C. Leal, J. Martins, P. Voabil et al., "Calcium dobesilate inhibits the alterations in tight junction proteins and leukocyte adhesion to retinal endothelial cells induced by diabetes," *Diabetes*, vol. 59, no. 10, pp. 2637–2645, 2010.

[112] J. Kusari, S. X. Zhou, E. Padillo, K. G. Clarke, and D. W. Gil, "Inhibition of vitreoretinal VEGF elevation and blood-retinal barrier breakdown in streptozotocin-induced diabetic rats by brimonidine," *Investigative Ophthalmology & Visual Science*, vol. 51, no. 2, pp. 1044–1051, 2010.

[113] A. Mori, T. Miwa, K. Sakamoto, T. Nakahara, and K. Ishii, "Pharmacological evidence for the presence of functional β3-adrenoceptors in rat retinal blood vessels," *Naunyn-Schmiedeberg's Archives of Pharmacology*, vol. 382, no. 2, pp. 119–126, 2010.

[114] A. Mori, S. Suzuki, K. Sakamoto, T. Nakahara, and K. Ishii, "Vasodilation of retinal arterioles induced by activation of BKCa channels is attenuated in diabetic rats," *European Journal of Pharmacology*, vol. 669, no. 1–3, pp. 94–99, 2011.

[115] H. Jiang, J. Fang, B. Wu et al., "Overexpression of serine racemase in retina and overproduction of D-serine in eyes of streptozotocin-induced diabetic retinopathy," *Journal of Neuroinflammation*, vol. 8, article 119, 2011.

[116] T. Hattori, A. Matsubara, K. Taniguchi, and Y. Ogura, "Aldose reductase inhibitor fidarestat attenuates leukocyte-endothelial interactions in experimental diabetic rat retina in vivo," *Current Eye Research*, vol. 35, no. 2, pp. 146–154, 2010.

[117] J. Ma, T. Zhu, X. Tang, P. Ye, and Z. Zhang, "Effect of an intravitreal injection of bevacizumab on the expression of VEGF and CD34 in the retina of diabetic rats," *Clinical and Experimental Ophthalmology*, vol. 38, no. 9, pp. 875–884, 2010.

[118] A. Ly, P. Yee, K. A. Vessey, J. A. Phipps, A. I. Jobling, and E. L. Fletcher, "Early inner retinal astrocyte dysfunction during diabetes and development of hypoxia, retinal stress, and neuronal functional loss," *Investigative Ophthalmology & Visual Science*, vol. 52, no. 13, pp. 9316–9326, 2011.

[119] A. Chronopoulos, A. Tang, E. Beglova, P. C. Trackman, and S. Roy, "High glucose increases lysyl oxidase expression and activity in retinal endothelial cells: mechanism for compromised extracellular matrix barrier function," *Diabetes*, vol. 59, no. 12, pp. 3159–3166, 2010.

[120] T. S. Kern, C. M. Miller, J. Tang, Y. Du, S. L. Ball, and L. Berti-Matera, "Comparison of three strains of diabetic rats with respect to the rate at which retinopathy and tactile allodynia develop," *Molecular Vision*, vol. 16, pp. 1629–1639, 2010.

[121] Y. Du, J. Tang, G. Li et al., "Effects of p38 MAPK inhibition on early stages of diabetic retinopathy and sensory nerve function," *Investigative Ophthalmology & Visual Science*, vol. 51, no. 4, pp. 2158–2164, 2010.

[122] D. do Carmo Buonfiglio, R. A. Peliciari-Garcia, F. G. do Amaral et al., "Early-stage retinal melatonin synthesis impairment in streptozotocin-induced diabetic wistar rats," *Investigative Ophthalmology & Visual Science*, vol. 52, no. 10, pp. 7416–7422, 2011.

[123] M. Opreanu, M. Tikhonenko, S. Bozack et al., "The unconventional role of acid sphingomyelinase in regulation of retinal microangiopathy in diabetic human and animal models," *Diabetes*, vol. 60, no. 9, pp. 2370–2378, 2011.

[124] C. Wang, B. George, S. Chen, B. Feng, X. Li, and S. Chakrabarti, "Genotoxic stress and activation of novel DNA repair enzymes in human endothelial cells and in the retinas and kidneys of streptozotocin diabetic rats," *Diabetes/Metabolism Research and Reviews*, vol. 28, no. 4, pp. 329–337, 2012.

[125] A. Mishra and E. A. Newman, "Inhibition of inducible nitric oxide synthase reverses the loss of functional hyperemia in diabetic retinopathy," *Glia*, vol. 58, no. 16, pp. 1996–2004, 2010.

[126] A. Mishra and E. A. Newman, "Aminoguanidine reverses the loss of functional hyperemia in a rat model of diabetic retinopathy," *Front Neuroenergetics*, vol. 3, article 10, 2011.

[127] J. L. Winkler, M. H. Kedees, Y. Guz, and G. Teitelman, "Inhibition of connective tissue growth factor by small interfering ribonucleic acid prevents increase in extracellular matrix molecules in a rodent model of diabetic retinopathy," *Molecular Vision*, vol. 18, pp. 874–886, 2012.

[128] D. Gaucher, J. A. Chiappore, M. Pâques et al., "Microglial changes occur without neural cell death in diabetic retinopathy," *Vision Research*, vol. 47, no. 5, pp. 612–623, 2007.

[129] S. Johnsen-Soriano, M. Garcia-Pous, E. Arnal et al., "Early lipoic acid intake protects retina of diabetic mice," *Free Radical Research*, vol. 42, no. 7, pp. 613–617, 2008.

[130] M. Miranda, M. Muriach, I. Almansa et al., "CR-6 protects glutathione peroxidase activity in experimental diabetes," *Free Radical Biology and Medicine*, vol. 43, no. 11, pp. 1494–1498, 2007.

[131] T. S. Kern and R. L. Engerman, "A mouse model of diabetic retinopathy," *Archives of Ophthalmology*, vol. 114, no. 8, pp. 986–990, 1996.

[132] A. M. Joussen, V. Poulaki, M. L. Le et al., "A central role for inflammation in the pathogenesis of diabetic retinopathy," *FASEB Journal*, vol. 18, no. 12, pp. 1450–1452, 2004.

[133] A. M. Joussen, S. Doehmen, M. L. Le et al., "TNF-α mediated apoptosis plays an important role in the development of early diabetic retinopathy and long-term histopathological alterations," *Molecular Vision*, vol. 15, pp. 1418–1428, 2009.

[134] A. J. Barber, D. A. Antonetti, T. S. Kern et al., "The Ins2Akita mouse as a model of early retinal complications in diabetes," *Investigative Ophthalmology & Visual Science*, vol. 46, no. 6, pp. 2210–2218, 2005.

[135] M. J. Gastinger, A. R. Kunselman, E. E. Conboy, S. K. Bronson, and A. J. Barber, "Dendrite remodeling and other abnormalities in the retinal ganglion cells of Ins2Akita diabetic mice," *Investigative Ophthalmology & Visual Science*, vol. 49, no. 6, pp. 2635–2642, 2008.

[136] M. J. Gastinger, R. S. J. Singh, and A. J. Barber, "Loss of cholinergic and dopaminergic amacrine cells in streptozotocin-diabetic rat and Ins2Akita-diabetic mouse retinas," *Investigative Ophthalmology & Visual Science*, vol. 47, no. 7, pp. 3143–3150, 2006.

[137] Z. Han, J. Guo, S. M. Conley, and M. I. Naash, "Retinal angiogenesis in the Ins2Akita mouse model of diabetic retinopathy," *Investigative Ophthalmology & Visual Science*, vol. 54, no. 1, pp. 574–584, 2013.

[138] W. S. Wright, A. Singh Yadav, R. M. McElhatten, and N. R. Harris, "Retinal blood flow abnormalities following six months of hyperglycemia in the Ins2(Akita) mouse," *Experimental Eye Research*, vol. 98, no. 1, pp. 9–15, 2012.

[139] S. Makino, K. Kunimoto, and Y. Muraoka, "Breeding of a non-obese, diabetic strain of mice," *Experimental Animals*, vol. 29, no. 1, pp. 1–13, 1980.

[140] C. R. Li and S. G. Sun, "VEGF expression and cell apoptosis in NOD mouse retina," *International Journal of Ophthalmology*, vol. 3, no. 3, pp. 224–227, 2010.

[141] S. G. Shaw, J. P. Boden, E. Biecker, J. Reichen, and B. Rothen, "Endothelin antagonism prevents diabetic retinopathy in NOD mice: a potential role of the angiogenic factor adrenomedullin," *Experimental Biology and Medicine*, vol. 231, no. 6, pp. 1101–1105, 2006.

[142] M. H. Faulds, C. Zhao, K. Dahlman-Wright, and J. Å. Gustafsson, "The diversity of sex steroid action: regulation of metabolism by estrogen signaling," *Journal of Endocrinology*, vol. 212, no. 1, pp. 3–12, 2012.

[143] K. P. Hummel, M. M. Dickie, and D. L. Coleman, "Diabetes, a new mutation in the mouse," *Science*, vol. 153, no. 3740, pp. 1127–1128, 1966.

[144] L. Tang, Y. Zhang, Y. Jiang et al., "Dietary wolfberry ameliorates retinal structure abnormalities in db/db mice at the early stage of diabetes," *Experimental Biology and Medicine*, vol. 236, no. 9, pp. 1051–1063, 2011.

[145] E. Midena, T. Segato, S. Radin et al., "Studies on the retina of the diabetic db/db mouse. I. Endothelial cell-pericyte ratio," *Ophthalmic Research*, vol. 21, no. 2, pp. 106–111, 1989.

[146] A. K. H. Cheung, M. K. L. Fung, A. C. Y. Lo et al., "Aldose reductase deficiency prevents diabetes-induced blood-retinal barrier breakdown, apoptosis, and glial reactivation in the retina of db/db mice," *Diabetes*, vol. 54, no. 11, pp. 3119–3125, 2005.

[147] R. S. Clements Jr., W. G. Robison Jr., and M. P. Cohen, "Anti-glycated albumin therapy ameliorates early retinal microvascular pathology in db/db mice," *Journal of Diabetes and Its Complications*, vol. 12, no. 1, pp. 28–33, 1998.

[148] S. Taketomi, "Chapter 16: KK and KKAy mice: models of type 2 diabetes with obesity," in *Animal Models of Diabetes : Frontiers in Research*, CRC Press, Boca Raton, Fla, USA, 2nd edition, 2007.

[149] X. Ning, Q. Baoyu, L. Yuzhen, S. Shuli, E. Reed, and Q. Q. Li, "Neuro-optic cell apoptosis and microangiopathy in KKAY mouse retina," *International Journal of Molecular Medicine*, vol. 13, no. 1, pp. 87–92, 2004.

[150] H. E. Grossniklaus, S. J. Kang, and L. Berglin, "Animal models of choroidal and retinal neovascularization," *Progress in Retinal and Eye Research*, vol. 29, no. 6, pp. 500–519, 2010.

[151] L. E. H. Smith, E. Wesolowski, A. McLellan et al., "Oxygen-induced retinopathy in the mouse," *Investigative Ophthalmology & Visual Science*, vol. 35, no. 1, pp. 101–111, 1994.

[152] Z. J. Fu, S. Y. Li, N. Kociok, D. Wong, S. K. Chung, and A. C. Lo, "Aldose reductase deficiency reduced vascular changes in neonatal mouse retina in oxygen-induced retinopathy," *Investigative Ophthalmology & Visual Science*, vol. 53, no. 9, pp. 5698–5712, 2012.

[153] K. A. Vessey, J. L. Wilkinson-Berka, and E. L. Fletcher, "Characterization of retinal function and glial cell response in a mouse model of oxygen-induced retinopathy," *Journal of Comparative Neurology*, vol. 519, no. 3, pp. 506–527, 2011.

[154] H. Ogishima, S. Nakamura, T. Nakanishi et al., "Ligation of the pterygopalatine and external carotid arteries induces ischemic damage in the murine retina," *Investigative Ophthalmology & Visual Science*, vol. 52, no. 13, pp. 9710–9720, 2011.

[155] H. Zhang, K. H. Sonoda, H. Qiao, T. Oshima, T. Hisatomi, and T. Ishibashi, "Development of a new mouse model of branch retinal vein occlusion and retinal neovascularization," *Japanese Journal of Ophthalmology*, vol. 51, no. 4, pp. 251–257, 2007.

[156] Y. Inokuchi, M. Shimazawa, Y. Nakajima et al., "A Na+/Ca2+ exchanger isoform, NCX1, is involved in retinal cell death after N-methyl-D-aspartate injection and ischemia-reperfusion," *Journal of Neuroscience Research*, vol. 87, no. 4, pp. 906–917, 2009.

[157] P. E. van Eeden, L. B. G. Tee, S. Lukehurst et al., "Early vascular and neuronal changes in a VEGF transgenic mouse model of retinal neovascularization," *Investigative Ophthalmology & Visual Science*, vol. 47, no. 10, pp. 4638–4645, 2006.

[158] W. Y. Shen, C. M. Lai, C. E. Graham et al., "Long-term global retinal microvascular changes in a transgenic vascular endothelial growth factor mouse model," *Diabetologia*, vol. 49, no. 7, pp. 1690–1701, 2006.

[159] E. P. Rakoczy, I. S. Ali Rahman, N. Binz et al., "Characterization of a mouse model of hyperglycemia and retinal neovascularization," *American Journal of Pathology*, vol. 177, no. 5, pp. 2659–2670, 2010.

[160] X. X. Zeng, Y. K. Ng, and E. A. Ling, "Neuronal and microglial response in the retina of streptozotocin-induced diabetic rats," *Visual Neuroscience*, vol. 17, no. 3, pp. 463–471, 2000.

[161] E. Rungger-Brändle, A. A. Dosso, and P. M. Leuenberger, "Glial reactivity, an early feature of diabetic retinopathy," *Investigative*

Ophthalmology & Visual Science, vol. 41, no. 7, pp. 1971–1980, 2000.

[162] S. H. Park, J. W. Park, S. J. Park et al., "Apoptotic death of photoreceptors in the streptozotocin-induced diabetic rat retina," *Diabetologia*, vol. 46, no. 9, pp. 1260–1268, 2003.

[163] J. Zhang, Y. Wu, Y. Jin et al., "Intravitreal injection of erythropoietin protects both retinal vascular and neuronal cells in early diabetes," *Investigative Ophthalmology & Visual Science*, vol. 49, no. 2, pp. 732–742, 2008.

[164] A. Jariyapongskul, T. Rungjaroen, N. Kasetsuwan, S. Patumraj, J. Seki, and H. Niimi, "Long-term effects of oral vitamin C supplementation on the endothelial dysfunction in the iris microvessels of diabetic rats," *Microvascular Research*, vol. 74, no. 1, pp. 32–38, 2007.

[165] H. R. Anderson, A. W. Stitt, T. A. Gardiner, and D. B. Archer, "Diabetic retinopathy: morphometric analysis of basement membrane thickening of capillaries in different retinal layers within arterial and venous environments," *British Journal of Ophthalmology*, vol. 79, no. 12, pp. 1120–1123, 1995.

[166] Q. Li, E. Zemel, B. Miller, and I. Perlman, "Early retinal damage in experimental diabetes: electroretinographical and morphological observations," *Experimental Eye Research*, vol. 74, no. 5, pp. 615–625, 2002.

[167] K. Kohzaki, A. J. Vingrys, and B. V. Bui, "Early inner retinal dysfunction in streptozotocin-induced diabetic rats," *Investigative Ophthalmology & Visual Science*, vol. 49, no. 8, pp. 3595–3604, 2008.

[168] H. A. Hancock and T. W. Kraft, "Oscillatory potential analysis and ERGs of normal and diabetic rats," *Investigative Ophthalmology & Visual Science*, vol. 45, no. 3, pp. 1002–1008, 2004.

[169] R. A. Kowluru, J. Tang, and T. S. Kern, "Abnormalities of retinal metabolism in diabetes and experimental galactosemia. VII: effect of long-term administration of antioxidants on the development of retinopathy," *Diabetes*, vol. 50, no. 8, pp. 1938–1942, 2001.

[170] S. Schroder, W. Palinski, and G. W. Schmid-Schonbein, "Activated monocytes and granulocytes, capillary nonperfusion, and neovascularization in diabetic retinopathy," *American Journal of Pathology*, vol. 139, no. 1, pp. 81–100, 1991.

[171] T. S. Kern, J. Tang, M. Mizutani et al., "Response of capillary cell death to aminoguanidine predicts the development of retinopathy: comparison of diabetes and galactosemia," *Investigative Ophthalmology & Visual Science*, vol. 41, no. 12, pp. 3972–3978, 2000.

[172] W. G. Robison Jr., T. N. Tillis, N. Laver, and J. H. Kinoshita, "Diabetes-related histopathologies of the rat retina prevented with an aldose reductase inhibitor," *Experimental Eye Research*, vol. 50, no. 4, pp. 355–366, 1990.

[173] N. P. Blair, M. O. M. Tso, and J. T. Dodge, "Pathologic studies on the blood-retinal barrier in the spontaneously diabetic BB rat," *Investigative Ophthalmology & Visual Science*, vol. 25, no. 3, pp. 302–311, 1984.

[174] A. A. F. Sima, R. Garcia Salinas, and P. K. Basu, "The BB Wistar rat: an experimental model for the study of diabetic retinopathy," *Metabolism*, vol. 32, no. 7, supplement 1, pp. 136–140, 1983.

[175] A. A. F. Sima, S. Chakrabarti, R. Garcia-Salinas, and P. K. Basu, "The BB rat; an authentic model of human diabetic retinopathy," *Current Eye Research*, vol. 4, no. 10, pp. 1087–1092, 1985.

[176] N. Miyamura and T. Amemiya, "Lens and retinal changes in the WBN/Kob rat (spontaneously diabetic strain). Electron-microscopic study," *Ophthalmic Research*, vol. 30, no. 4, pp. 221–232, 1998.

[177] I. A. Bhutto, N. Miyamura, and T. Amemiya, "Vascular architecture of degenerated retina in WBN/Kob rats: corrosion cast and electron microscopic study," *Ophthalmic Research*, vol. 31, no. 5, pp. 367–377, 1999.

[178] N. Tsuji, T. Matsuura, K. Ozaki, T. Sano, and I. Narama, "Diabetic retinopathy and choroidal angiopathy in diabetic rats (WBN/Kob)," *Experimental Animals*, vol. 58, no. 5, pp. 481–487, 2009.

[179] Y. Behl, P. Krothapalli, T. Desta, A. DiPiazza, S. Roy, and D. T. Graves, "Diabetes-enhanced tumor necrosis factor-α production promotes apoptosis and the loss of retinal microvascular cells in type 1 and type 2 models of diabetic retinopathy," *American Journal of Pathology*, vol. 172, no. 5, pp. 1411–1418, 2008.

[180] R. P. Danis and Y. Yang, "Microvascular retinopathy in the Zucker diabetic fatty rat," *Investigative Ophthalmology & Visual Science*, vol. 34, no. 7, pp. 2367–2371, 1993.

[181] Y. S. Yang, R. P. Danis, R. G. Peterson, P. L. Dolan, and Y. Q. Wu, "Acarbose partially inhibits microvascular retinopathy in the Zucker Diabetic Fatty rat (ZDF/Gmi(TM)-fa)," *Journal of Ocular Pharmacology and Therapeutics*, vol. 16, no. 5, pp. 471–479, 2000.

[182] Z. Y. Lu, I. A. Bhutto, and T. Amemiya, "Retinal changes in Otsuka long-evans Tokushima Fatty rats (spontaneously diabetic rat)—possibility of a new experimental model for diabetic retinopathy," *Japanese Journal of Ophthalmology*, vol. 47, no. 1, pp. 28–35, 2003.

[183] N. Miyamura, I. A. Bhutto, and T. Amemiya, "Retinal capillary changes in Otsuka Long-Evans Tokushima fatty rats (spontaneously diabetic strain). Electron-microscopic study," *Ophthalmic Research*, vol. 31, no. 5, pp. 358–366, 1999.

[184] K. Miyamoto, N. Hiroshiba, A. Tsujikawa, and Y. Ogura, "In vivo demonstration of increased leukocyte entrapment in retinal microcirculation of diabetic rats," *Investigative Ophthalmology & Visual Science*, vol. 39, no. 11, pp. 2190–2194, 1998.

[185] I. A. Bhutto, Z. Y. Lu, Y. Takami, and T. Amemiya, "Retinal and choroidal vasculature in rats with spontaneous diabetes type 2 treated with the angiotensin-converting enzyme inhibitor cilazapril: corrosion cast and electron-microscopic study," *Ophthalmic Research*, vol. 34, no. 4, pp. 220–231, 2002.

[186] K. Miyamoto, Y. Ogura, H. Nishiwaki et al., "Evaluation of retinal microcirculatory alterations in the goto-Kakizaki rat: a spontaneous model of non-insulin-dependent diabetes," *Investigative Ophthalmology & Visual Science*, vol. 37, no. 5, pp. 898–905, 1996.

[187] A. Carmo, J. G. Cunha-Vaz, A. P. Carvalho, and M. C. Lopes, "Nitric oxide synthase activity in retinas from non-insulin-dependent diabetic Goto-Kakizaki rats: correlation with blood-retinal barrier permeability," *Nitric Oxide*, vol. 4, no. 6, pp. 590–596, 2000.

[188] M. Fukuda, Y. Nakanishi, M. Fuse et al., "Altered expression of aquaporins 1 and 4 coincides with neurodegenerative events in retinas of spontaneously diabetic Torii rats," *Experimental Eye Research*, vol. 90, no. 1, pp. 17–25, 2010.

[189] T. Sasase, H. Morinaga, T. Abe et al., "Protein kinase c beta inhibitor prevents diabetic peripheral neuropathy, but not histopathological abnormalities of retina in spontaneously

diabetic torii rat," *Diabetes, Obesity and Metabolism*, vol. 11, no. 11, pp. 1084–1087, 2009.

[190] M. Shinohara, T. Masuyama, T. Shoda et al., "A new spontaneously diabetic non-obese torii rat strain with severe ocular complications," *Experimental Diabesity Research*, vol. 1, no. 2, pp. 89–100, 2000.

[191] H. Yamada, E. Yamada, A. Higuchi, and M. Matsumura, "Retinal neovascularisation without ischaemia in the spontaneously diabetic Torii rat," *Diabetologia*, vol. 48, no. 8, pp. 1663–1668, 2005.

[192] M. Matsuoka, N. Ogata, K. Minamino, and M. Matsumura, "Leukostatis and pigment epithelium-derived factor in rat models of diabetic retinopathy," *Molecular Vision*, vol. 13, pp. 1058–1065, 2007.

[193] T. Okuno, H. Oku, T. Sugiyama, and T. Ikeda, "Electroretinographic study of spontaneously diabetic Torii rats," *Documenta Ophthalmologica*, vol. 117, no. 3, pp. 191–196, 2008.

[194] L. E. Downie, M. J. Pianta, A. J. Vingrys, J. L. Wilkinson-Berka, and E. L. Fletcher, "Neuronal and glial cell changes are determined by retinal vascularization in retinopathy of prematurity," *Journal of Comparative Neurology*, vol. 504, no. 4, pp. 404–417, 2007.

[195] L. E. Downie, M. J. Pianta, A. J. Vingrys, J. L. Wilkinson-Berka, and E. L. Fletcher, "AT1 receptor inhibition prevents astrocyte degeneration and restores vascular growth in oxygen-induced retinopathy," *Glia*, vol. 56, no. 10, pp. 1076–1090, 2008.

[196] A. B. Fulton, X. Reynaud, R. M. Hansen, C. A. Lemere, C. Parker, and T. P. Williams, "Rod photoreceptors in infant rats with a history of oxygen exposure," *Investigative Ophthalmology & Visual Science*, vol. 40, no. 1, pp. 168–174, 1999.

[197] K. Liu, J. D. Akula, C. Falk, R. M. Hansen, and A. B. Fulton, "The retinal vasculature and function of the neural retina in a rat model of retinopathy of prematurity," *Investigative Ophthalmology & Visual Science*, vol. 47, no. 6, pp. 2639–2647, 2006.

[198] T. S. Kern and R. L. Engerman, "Galactose-induced retinal microangiopathy in rats," *Investigative Ophthalmology & Visual Science*, vol. 36, no. 2, pp. 490–496, 1995.

[199] R. H. Wallis, K. Wang, L. Marandi et al., "Type 1 diabetes in the BB rat: a polygenic disease," *Diabetes*, vol. 58, no. 4, pp. 1007–1017, 2009.

[200] Y. Mori, J. Yokoyama, M. Nishimura, H. Oka, S. Mochio, and Y. Ikeda, "Development of diabetic complications in a new diabetic strain of rat (WBN/Kob)," *Pancreas*, vol. 7, no. 5, pp. 569–577, 1992.

[201] R. E. Schmidt, D. A. Dorsey, L. N. Beaudet, and R. G. Peterson, "Analysis of the Zucker Diabetic Fatty (ZDF) type 2 diabetic rat model suggests a neurotrophic role for insulin/IGF-I in diabetic autonomic neuropathy," *American Journal of Pathology*, vol. 163, no. 1, pp. 21–28, 2003.

[202] T. Matsuura, S. Yamagishi, Y. Kodama, R. Shibata, S. Ueda, and I. Narama, "Otsuka Long-Evans Tokushima Fatty (OLETF) rat is not a suitable animal model for the study of angiopathic diabetic retinopathy," *International Journal of Tissue Reactions*, vol. 27, no. 2, pp. 59–62, 2005.

[203] N. Hotta, J. Nakamura, F. Sakakibara et al., "Electroretinogram in sucrose-fed diabetic rats treated with an aldose reductase inhibitor or an anticoagulant," *American Journal of Physiology—Endocrinology and Metabolism*, vol. 273, no. 5, part 1, pp. E965–E971, 1997.

[204] C. G. Ostenson, "Chapter 5: the Goto-Kakizaki rat," in *Animal Models of Diabetes : Frontiers in Research*, CRC Press, Boca Raton, Fla, USA, 2nd edition, 2007.

[205] M. Shinohara, T. Masuyama, and A. Kakehashi, "Chapter 14: the spontaneously diabetic torii (SDT) rat with retinopathy lesions resembling those of humans," in *Animal Models of Diabetes : Frontiers in Research*, CRC Press, Boca Raton, Fla, USA, 2nd edition, 2007.

[206] A. Kakehashi, Y. Saito, K. Mori et al., "Characteristics of diabetic retinopathy in SDT rats," *Diabetes/Metabolism Research and Reviews*, vol. 22, no. 6, pp. 455–461, 2006.

[207] T. Sasase, "Pathophysiological characteristics of diabetic ocular complications in spontaneously diabetic torii rat," *Journal of Ophthalmology*, vol. 2010, Article ID 615641, 7 pages, 2010.

[208] P. van Wijngaarden, D. J. Coster, H. M. Brereton, I. L. Gibbins, and K. A. Williams, "Strain-dependent differences in oxygen-induced retinopathy in the inbred rat," *Investigative Ophthalmology & Visual Science*, vol. 46, no. 4, pp. 1445–1452, 2005.

[209] J. S. Penn, B. L. Tolman, and M. M. Henry, "Oxygen-induced retinopathy in the rat: relationship of retinal nonperfusion to subsequent neovascularization," *Investigative Ophthalmology & Visual Science*, vol. 35, no. 9, pp. 3429–3435, 1994.

[210] J. S. Penn, M. M. Henry, and B. L. Tolman, "Exposure to alternating hypoxia and hyperoxia causes severe proliferative retinopathy in the newborn rat," *Pediatric Research*, vol. 36, no. 6, pp. 724–731, 1994.

[211] F. Drago, C. La Manna, I. Emmi, and A. Marino, "Effects of sulfinpyrazone on retinae damage induced by experimental diabetes mellitus in rabbits," *Pharmacological Research*, vol. 38, no. 2, pp. 97–100, 1998.

[212] T. Helfenstein, F. A. Fonseca, S. S. Ihara et al., "Impaired glucose tolerance plus hyperlipidaemia induced by diet promotes retina microaneurysms in New Zealand rabbits," *International Journal of Experimental Pathology*, vol. 92, no. 1, pp. 40–49, 2011.

[213] H. Ozaki, H. Hayashi, S. A. Vinores, Y. Moromizato, P. A. Campochiaro, and K. Oshima, "Intravitreal sustained release of VEGF causes retinal neovascularization in rabbits and breakdown of the blood-retinal barrier in rabbits and primates," *Experimental Eye Research*, vol. 64, no. 4, pp. 505–517, 1997.

[214] C. G. Wong, K. A. Rich, L. H. L. Liaw, H. T. Hsu, and M. W. Berns, "Intravitreal VEGF and bFGF produce florid retinal neovascularization and hemorrhage in the rabbit," *Current Eye Research*, vol. 22, no. 2, pp. 140–147, 2001.

[215] M. H. Erb, C. E. Sioulis, B. D. Kuppermann, K. Osann, and C. G. Wong, "Differential retinal angiogenic response to sustained intravitreal release of VEGF and bFGF in different pigmented rabbit breeds," *Current Eye Research*, vol. 24, no. 4, pp. 245–252, 2002.

[216] D. L. Hatchell, C. A. Toth, C. A. Barden, and P. Saloupis, "Diabetic retinopathy in a cat," *Experimental Eye Research*, vol. 60, no. 5, pp. 591–593, 1995.

[217] R. A. Linsenmeier, R. D. Braun, M. A. McRipley et al., "Retinal hypoxia in long-term diabetic cats," *Investigative Ophthalmology & Visual Science*, vol. 39, no. 9, pp. 1647–1657, 1998.

[218] S. Z. Mansour, "Reduction of basement membrane thickening in diabetic cat retina by sulindac," *Investigative Ophthalmology & Visual Science*, vol. 31, no. 3, pp. 457–463, 1990.

[219] P. F. Kador, K. Blessing, J. Randazzo, J. Makita, and M. Wyman, "Evaluation of the vascular targeting agent combretastatin A-4 prodrug on retinal neovascularization in the galactose-fed dog," *Journal of Ocular Pharmacology and Therapeutics*, vol. 23, no. 2, pp. 132–142, 2007.

[220] T. A. Gardiner, A. W. Stitt, H. R. Anderson, and D. B. Archer, "Selective loss of vascular smooth muscle cells in the retinal microcirculation of diabetic dogs," *British Journal of Ophthalmology*, vol. 78, no. 1, pp. 54–60, 1994.

[221] T. S. Kern and R. L. Engerman, "Capillary lesions develop in retina rather than cerebral cortex in diabetes and experimental galactosemia," *Archives of Ophthalmology*, vol. 114, no. 3, pp. 306–310, 1996.

[222] P. F. Kador, Y. Takahashi, M. Wyman, and F. Ferris III, "Diabeteslike proliferative retinal changes in galactose-fed dogs," *Archives of Ophthalmology*, vol. 113, no. 3, pp. 352–354, 1995.

[223] T. Kobayashi, E. Kubo, Y. Takahashi, T. Kasahara, H. Yonezawa, and Y. Akagi, "Retinal vessel changes in galactose-fed dogs," *Archives of Ophthalmology*, vol. 116, no. 6, pp. 785–789, 1998.

[224] M. Cusick, E. Y. Chew, F. Ferris III, T. A. Cox, C. C. Chan, and P. F. Kador, "Effects of aldose reductase inhibitors and galactose withdrawal on fluorescein angiographic lesions in galactose-fed dogs," *Archives of Ophthalmology*, vol. 121, no. 12, pp. 1745–1751, 2003.

[225] P. F. Kador, Y. Takahashi, Y. Akagi, K. Blessing, J. Randazzo, and M. Wyman, "Age-dependent retinal capillary pericyte degeneration in galactose-fed dogs," *Journal of Ocular Pharmacology and Therapeutics*, vol. 23, no. 1, pp. 63–69, 2007.

[226] I. Sanchez, R. Martin, F. Ussa, and I. Fernandez-Bueno, "The parameters of the porcine eyeball," *Graefe's Archive for Clinical and Experimental Ophthalmology*, vol. 249, no. 4, pp. 475–482, 2011.

[227] J. L. King, J. O. Mason 3rd., S. C. Cartner, and C. Guidry, "The influence of alloxan-induced diabetes on Müller cell contraction-promoting activities in vitreous," *Investigative Ophthalmology & Visual Science*, vol. 52, no. 10, pp. 7485–7491, 2011.

[228] J. L. King and C. Guidry, "Vitreous IGFBP-3 effects on Müller cell proliferation and tractional force generation," *Investigative Ophthalmology & Visual Science*, vol. 53, no. 1, pp. 93–99, 2012.

[229] Y. Yang, M. R. Hayden, S. Sowers, S. V. Bagree, and J. R. Sowers, "Retinal redox stress and remodeling in cardiometabolic syndrome and diabetes," *Oxidative Medicine and Cellular Longevity*, vol. 3, no. 6, pp. 392–403, 2010.

[230] D. P. Hainsworth, M. L. Katz, D. A. Sanders, D. N. Sanders, E. J. Wright, and M. Sturek, "Retinal capillary basement membrane thickening in a porcine model of diabetes mellitus," *Comparative Medicine*, vol. 52, no. 6, pp. 523–529, 2002.

[231] S. E. Lee, W. Ma, E. M. Rattigan et al., "Ultrastructural features of retinal capillary basement membrane thickening in diabetic swine," *Ultrastructural Pathology*, vol. 34, no. 1, pp. 35–41, 2010.

[232] K. Umazume, Y. Barak, K. McDonald, L. Liu, H. J. Kaplan, and S. Tamiya, "Proliferative vitreoretinopathy in the Swine-a new model," *Investigative Ophthalmology & Visual Science*, vol. 53, no. 8, pp. 4910–4916, 2012.

[233] M. O. M. Tso, A. Kurosawa, E. Benhamou et al., "Microangiopathic retinopathy in experimental diabetic monkeys," *Transactions of the American Ophthalmological Society*, vol. 86, pp. 389–421, 1988.

[234] S. Y. Kim, M. A. Johnson, D. S. McLeod et al., "Retinopathy in monkeys with spontaneous type 2 diabetes," *Investigative Ophthalmology & Visual Science*, vol. 45, no. 12, pp. 4543–4553, 2004.

[235] M. A. Johnson, G. A. Lutty, D. S. McLeod et al., "Ocular structure and function in an aged monkey with spontaneous diabetes mellitus," *Experimental Eye Research*, vol. 80, no. 1, pp. 37–42, 2005.

[236] P. Goldsmith and W. A. Harris, "The zebrafish as a tool for understanding the biology of visual disorders," *Seminars in Cell and Developmental Biology*, vol. 14, no. 1, pp. 11–18, 2003.

[237] Y. Alvarez, M. L. Cederlund, D. C. Cottell et al., "Genetic determinants of hyaloid and retinal vasculature in zebrafish," *BMC Developmental Biology*, vol. 7, article 114, 2007.

[238] M. Gleeson, V. Connaughton, and L. S. Arneson, "Induction of hyperglycaemia in zebrafish (Danio rerio) leads to morphological changes in the retina," *Acta Diabetologica*, vol. 44, no. 3, pp. 157–163, 2007.

[239] T. W. Moon, "Glucose intolerance in teleost fish: fact or fiction?" *Comparative Biochemistry and Physiology*, vol. 129, no. 2-3, pp. 243–249, 2001.

[240] R. Cao, L. D. E. Jensen, I. Söll, G. Hauptmann, and Y. Cao, "Hypoxia-induced retinal angiogenesis in zebrafish as a model to study retinopathy," *PLoS ONE*, vol. 3, no. 7, Article ID e2748, 2008.

[241] Z. Cao, L. D. Jensen, P. Rouhi et al., "Hypoxia-induced retinopathy model in adult zebrafish," *Nature Protocols*, vol. 5, no. 12, pp. 1903–1910, 2010.

[242] E. van Rooijen, E. E. Voest, I. Logister et al., "Von Hippel-Lindau tumor suppressor mutants faithfully model pathological hypoxia-driven angiogenesis and vascular retinopathies in zebrafish," *Disease Models and Mechanisms*, vol. 3, no. 5-6, pp. 343–353, 2010.

[243] R. F. Collery, M. L. Cederlund, V. A. Smyth, and B. N. Kennedy, "Applying transgenic zebrafish technology to study the retina," *Advances in Experimental Medicine and Biology*, vol. 572, pp. 201–207, 2006.

Hindawi Publishing Corporation
Journal of Diabetes Research
Volume 2013, Article ID 254529, 8 pages
http://dx.doi.org/10.1155/2013/254529

Research Article

Outcome of Acute Renal Injury in Diabetic Mice with Experimental Endotoxemia: Role of Hypoxia-Inducible Factor-1α

A. Ortega,[1] A. Fernández,[1] M. I. Arenas,[1] P. López-Luna,[2] C. Muñóz-Moreno,[2] I. Arribas,[3] N. Olea,[2] L. García-Bermejo,[4] J. Lucio-Cazana,[2] and R. J. Bosch[1,2]

[1] *Laboratory of Renal Physiology and Experimental Nephrology, Department of Biological Systems/Physiology Unit, University of Alcalá, Alcalá de Henares, Madrid, Spain*
[2] *Department of Biological Systems/Physiology Unit, University of Alcalá, Alcalá de Henares, Madrid, Spain*
[3] *Department of Clinical Chemistry University Hospital "Príncipe de Asturias", University of Alcalá, Alcalá de Henares, Spain*
[4] *Cell Response to Ischemia Laboratory, Department of Systems Disorders and Cancer, Instituto Ramón y Cajal de Investigación Sanitaria, Madrid, Spain*

Correspondence should be addressed to R. J. Bosch; ricardoj.bosch@uah.es

Received 15 January 2013; Accepted 5 July 2013

Academic Editor: Shahidul Islam

The role of diabetic nephropathy in the outcome of acute renal injury (AKI) is not well defined. Herein we evaluate the outcome of lipopolysaccharide- (LPS-) induced AKI in streptozotocin-induced diabetes, as well as the potential role of Hypoxia Inducible Factor (HIF-1α) in this condition. Although 6 h after LPS injection all mice developed a decrease in renal function, proteinuric diabetic mice showed a better recovery of this parameter throughout the study (72 h). Both HIF-1α and vascular endothelium growth factor (VEGF) were found to be upregulated in diabetic mice. After LPS injection, all animals showed an upregulation of these factors, although it was higher in the diabetic group. Glycated albumin (GA) was found to upregulate HIF-1α in HK-2 cells, which resulted in increased production of VEGF. Interestingly, LPS cooperated with GA to induce HIF-1α upregulation. In conclusion, diabetic mice display a better recovery of AKI after experimental endotoxemia. Moreover, these animals showed an increased expression of both HIF-1α and VEGF that was reproduced by incubating renal cells with GA. Since VEGF is considered a survival factor for tubular cells, our findings suggest that diabetes displays HIF-1α upregulation that might function as a "precondition state" offering protection from endotoxic AKI.

1. Introduction

The role of diabetes in the outcome of acute renal injury (AKI) is not well understood and may depend upon the cause of the injury as well as on the stage of diabetic renal involvement. Among the various causes of AKI, endotoxemia, a major component of sepsis, remains an elusive and challenging condition which is still lacking treatment. Although it is known that rodents with experimental diabetes are protected from certain nephrotoxic agents [1–3], diabetes has been recognized as an independent risk factor for the development of AKI in a variety of clinical settings, including sepsis [4–8].

Hypoxia-inducible factor (HIF-1α) allows the adaptive response to hypoxia by stimulating the expression of target genes such as erythropoietin, enzymes involved in glucose metabolism, and the vascular endothelial growth factor A (VEGF-A) [9]. The later has been recognized as a survival factor for proximal tubular cells [10].

HIF-1α is a heterodimer transcription factor consisting of a constitutively expressed β subunit and two α subunits, HIF-1α or HIF-2α. In normoxia, HIF-1α is continuously synthesized but rapidly ubiquitinated and subsequently degraded by the cellular proteasome [11]. Under hypoxia, the HIF-1α ubiquitination is suppressed. HIF-1α protein is thereby stabilized, it translocates to the nucleus, and together with the β subunit and transcriptional coactivators, it binds to hypoxia-responsive elements (HRE) in target genes [12, 13]. Besides hypoxia, several physiological regulators such as

growth factors, hormones, stress factors, and inflammatory mediators, increase HIF-1α expression in normoxia [14]. Moreover, HIF-1α is also induced upon diabetic condition with a potential role in wound healing [15]. Activation of HIF-1α by cobalt chloride has therapeutic benefit in several kidney disease models including ischemia reperfusion, cisplatin nephropathy, remnant kidney, progressive anti-Thy1 nephritis, and diabetic nephropathy, reviewed by Nangaku et al. [16]. Less is known about the potential role of HIF-1α in AKI due to endotoxemia. Moreover, most of the available data are based upon experimental models of early diabetic stage, which might not recapitulate a long-term disease such as diabetic nephropathy, a condition characterized by an increase in urinary albumin excretion (UAE) [17]. There is also tubular injury, which is due to several factors, particularly high glucose levels, albuminuria, and the presence of advanced glycation end-product (AGE-) modified proteins [17, 18].

The aim of the present study was to evaluate the outcome of AKI in animals with experimental diabetes after the development of an increase in the UAE. Moreover, we also investigate the potential role of HIF-1α in this outcome.

2. Material and Methods

In all of the experiments, adult CD-1 mice (4–8 months old, n = 10–15 per group, total 104) were used. The experimental procedures were previously approved by the Committee for Animal Ethics of Alcalá University, in accordance with the Spanish and European Guidelines. AKI was induced by intraperitoneal injection of lipopolysaccharide (LPS) (10 mg/Kg) (from *E. Coli*, Sigma) in mice at different periods (6–72 h). In some animals, diabetes was induced by three consecutive daily intraperitoneal injections of streptozotocin (STZ) (Sigma, St. Louis, MO, USA), 65 mg/kg body weight in citrate buffer, pH 4.5 (vehicle) 6 weeks before LPS injury. This is a previously reported model of early diabetic nephropathy characterized by increased UAE during the first month of diabetes [19]. After the last STZ injection, induction of diabetes was confirmed by measurement of blood glucose levels. Animals with blood glucose >300 mg/dL were included in the study.

Animals were individually housed in metabolic cages with free access to food and tap water, and 24-hour urine was collected for protein measurement. Blood was taken by cardiac puncture under ether anaesthesia, and plasma glucose was determined [19]. Urinary albumin excretion (UAE), endogenous creatinine clearance (CCr), urinary volume (UV), and fractional excretion of sodium (NaFE) ($Na_u \times Cr_s$)]/[$Na_s \times Cr_u$] × 100) were analyzed. One kidney of each animal was removed, weighed, frozen in liquid nitrogen, and stored at −80°C for subsequent total protein and RNA extraction. The remaining kidney was fixed in 10% (v/v) formaldehyde in PBS, embedded in paraffin, and sectioned at 5 μm for morphological and immunohistochemistry studies.

2.1. Renal Expression and Immunolocalization of HIF-1α and VEGF-A. Western blotting in tissue was performed as previously described [20]. Briefly, a small piece of kidney was lysed in RIPA buffer and centrifuged for preclearance, and total protein was loaded into 8% acrylamide SDS gels and transferred to PVDF membrane. The membrane was incubated with anti-mouse anti-HIF-1α (R&D Systems, Inc, MN, USA), 1/500 and appropriate HRP-conjugated secondary antibody.

Sections were deparaffinised, rehydrated, and placed in 10 mM sodium citrate buffer, pH 6.0, and heated in a pressure cooker for 2 min. The sections were allowed to cool for 20 min. After rinsing with distilled water, the sections were washed twice in TBS buffer, pH 7.6, for 5 min. The endogenous peroxidase activity was inhibited by incubation with 3% H_2O_2 for 20 min. Sections were washed with H_2O and TBS and incubated with 3% normal donkey serum plus 0.05% Triton X-100 in TBS, pH 7.6, at room temperature for 45 min, to prevent nonspecific binding of the first antibody. Afterwards, the sections were incubated overnight at 4°C, with the following rabbit polyclonal antibodies: HIF-1α (Abcam, Cambridge, UK) diluted 1 : 300 and VEGF-A (Santa Cruz Biotechnology, Lamecula, CA, USA) diluted 1 : 500 in the blocking solution diluted 1 : 9. Then, the sections were washed in TBS, and detection was made by the conventional labelled-streptavidin-biotin method (LSAB-kit, Dako). The peroxidase activity was detected using the DAB kit (Master Diagnostica, Granada, Spain). Tissue sections were counterstained with hematoxylin, dehydrated, cleared in xylene, and mounted in Entellan (Merck, Darmstadt, Germany). Two independent observers in a blinded manner scored both HIF-1α and VEGF-A renal staining as negative, mild, moderate, and intense. The final score was the mean of the two evaluations.

2.2. Cell Culture. Human kidney HK-2 cells were purchased from American Type Culture Collection (Rockville, MD, USA). YC-1 was purchased from Sigma Chemical Co. (St. Louis, MO, USA), monoclonal HIF-1α (1 : 1000) (Transduction Laboratories, BD Biosciences, Palo Alto, CA, USA); polyclonal β-actin (1 : 10000) was obtained from Sigma. Cells were maintained in DMEM supplemented with 10% foetal bovine serum (FBS), 1% penicillin/streptomycin/amphotericin B (Invitrogen, Carlsbad, CA, USA) and 1% Insulin-Transferrin-Selenium (Sigma, St. Louis, MO, USA). Cells were routinely cultured in 95% air, 5% CO_2 (normoxic conditions) at 37°C. In all experiments, cells were plated at 70–90% confluence, and when completely attached, they were treated with LPS in serum complete media. When necessary, cells were also treated with AGE, albumin, or YC-1 under the conditions specified in the legends to figures.

2.3. Single-Step Real-Time Quantitative RT-PCR. Total cell RNA from HK-2 cells was isolated with TriReagent (Sigma, St. Louis, MO, USA), and real-time quantitative RT-PCR analysis was performed in 2 ng samples using SYBR Green PCR master mix (Applied Biosystems), in one-step RT-PCR protocol as previously described [20]. Primer sequences for genes were as follows (sequences 5′-3′): VEGF165 sense: GACAAGAAAATCCCTGTGGGCAAC, antisense: GCGAGTCTGTGTTTTTGC; β-actin sense: AGAAGGATTCCTATGTGGGCG and antisense: CATGTC CCAGTTGGTGAC.

2.4. Protein Isolation and Western Blotting. HK-2 cells were incubated with albumin or AGE (100 μg/mL each) or in combination with LPS (1 μg/mL) for different periods. Cells were washed twice with ice-cold PBS, then harvested, scraped into ice-cold PBS, and then pelleted by centrifugation at 500 ×g for 5 min at 4°C. In order to obtain cell lysates, the cells were kept on ice for 30 min in a solution containing 50 mM Tris-HCl (pH 7.5), 150 mM NaCl, 1% Triton X-100, 0.5% sodium deoxycholate, and protease inhibitors. Thereafter, the cells were pelleted by centrifugation at 4000 ×g for 5 min at 4°C. Proteins from cell lysates were denatured by heating. Then, they were resolved by 10% SDS-PAGE and blotted on a nitrocellulose membrane (BioTrace/NT) overnight in 50 mM Tris-HCl, 380 mM glycin, 0.1% SDS, and 20% methanol. Mouse anti-HIF-1α (1 : 1000) antibody (BD Biosciences, CA, USA) was added followed by incubation overnight at 4°C. After treatment for 1 h at room temperature with the corresponding secondary antiserum (1 : 4000), the signals were detected with enhanced chemiluminescence reagent (GE Healthcare-Life Science, NJ, USA) using β-actin antibody (Calbiochem-Merk Bioscience, USA) as loading control.

For HIF-1α inhibition, we used HIF-1α siRNA sc-44225 (Santa Cruz Biotechnologies, CA, USA) for HIF-1α containing 3 sequences against 3 different HIF-1α exons and scramble siRNA AM4637 (Ambion) as a control as previously described [16]. HK-2 cells at 70% of confluence were transfected with 100 nM HIF-1α siRNA or 100 nM scramble siRNA. According to the manufacturer's protocol, we used Lipofectamine 2000 to get the transfection. HIF-1α interference was evaluated by qRT-PCR for HIF-1α mRNA.

2.5. Statistical Analysis. Results are expressed as mean ± SEM throughout the text. Animal data was analyzed by either the Kruskal-Wallis test or Mann-Whitney test, when appropriate. Unless otherwise specified, in vitro experiments were repeated at least three times, and the statistical analysis was performed by the Bonferroni test. In all cases, a $P < 0.05$ was considered statistically significant.

3. Results

3.1. Characterization of LPS-Induced AKI in Diabetic Mice Model. As shown in Figure 1, diabetic animals after 6 weeks of STZ display a significant increase in the UAE throughout the study. Both groups of animals also showed a significant increase of this parameter at 18–24 h after LPS injection. Although six hour after LPS, diabetic and nondiabetic mice developed a similar degree of decrease of renal function, only diabetic animals showed a recovery of this parameter at 24 h to a level not significantly different from those of the control animals (Figure 2). On the contrary, nondiabetic mice did not show a complete recovery of the renal function throughout the period of the study (72 h) (Figure 2). As expected, these changes were associated with an increased Urine Volume (UV) in diabetic mice, and a decrease in the UV in nondiabetic mice (Figure 3). Moreover, while diabetic mice did not show any significant changes in the NaFE throughout the study, nondiabetic mice displayed a significant decrease in this parameter (Figure 4). This maintained renal sodium reabsorption capacity observed in the diabetic mice is in accordance with a functional or mild form of AKI [21].

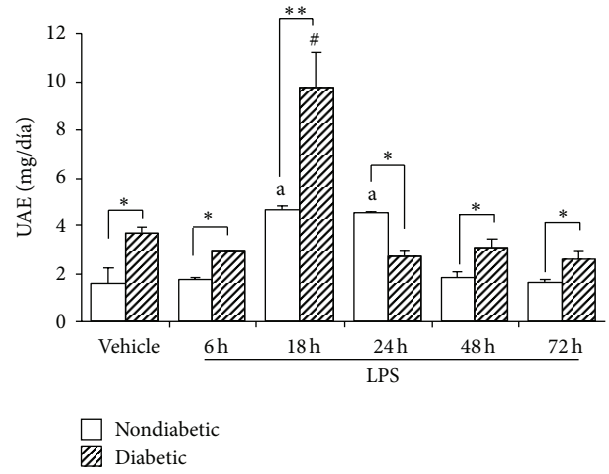

Figure 1: Urinary Albumin Excretion (UAE) in diabetic and nondiabetic LPS-injected mice. Values are mean ± SEM. $^{*}P < 0.05$ versus control value, $^{**}P < 0.01$ versus control value, $^{\#}P < 0.01$ versus diabetic, and a $P < 0.01$ versus nondiabetic.

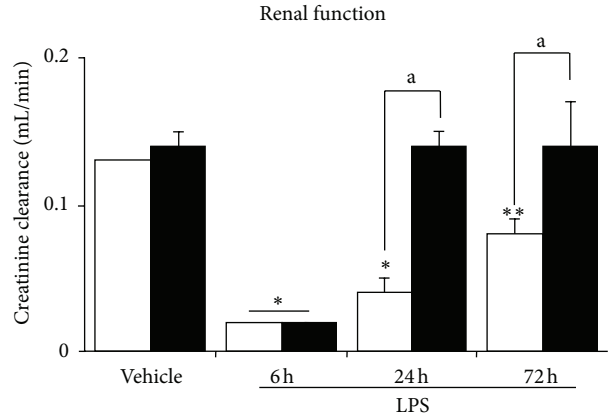

Figure 2: Renal function (endogenous creatinine clearance (CCr) in diabetic (black bars) and nondiabetic (open bars) LPS-injected mice. Values are mean ± SEM. $^{*}P < 0.05$ versus control value, $^{**}P < 0.01$ versus control value, and a $P < 0.01$ versus nondiabetic.

3.2. Renal Expression and Immunolocalization of HIF-1α and VEGF-A. Western-blotting analysis revels that LPS increased the expression of HIF-1α in both groups of animals, albeit it was even higher in the diabetic group (Figure 5(a)). Interestingly, the condition of diabetes itself was able to induce a significant upregulation of this protein.

In the kidney of control animals, an intense immunoexpression to HIF-1α was observed in the cytoplasm and several nuclei of the proximal convoluted tubules, and a weak signal was observed in the nuclei of distal tubules (Figure 5(b), I). By contrast, 5 weeks after diabetes induction, the mouse kidney displayed a higher number of positive tubuloepithelial nuclei, showing an increase in the cytoplasm immunoreactivity (Figure 5(b), II).

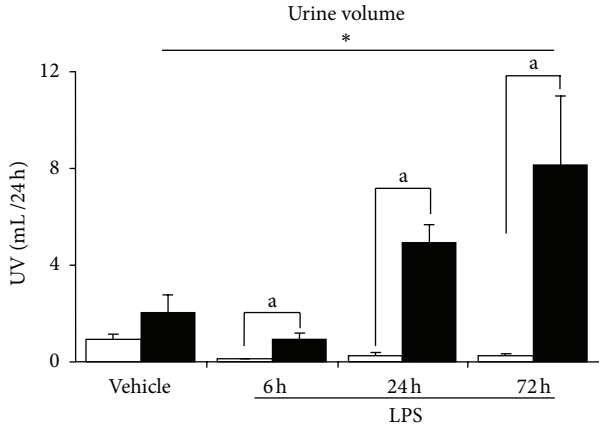

Figure 3: Urinary volume in diabetic (black bars) and nondiabetic (open bars) LPS-injected mice. Values are mean ± SEM. $^{*}P < 0.05$ versus control value and a $P < 0.01$ versus nondiabetic.

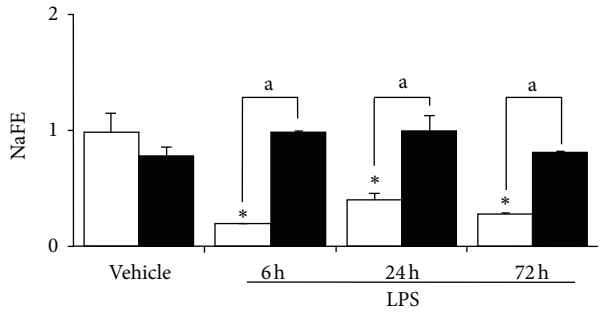

Figure 4: Fractional excretion of sodium (NaFE) in diabetic (black bars) and nondiabetic (open bars) LPS-injected mice. Values are mean ± SEM. $^{*}P < 0.05$ versus control value and a $P < 0.01$ versus nondiabetic.

In LPS-treated mice, both the nucleus and cytoplasm of renal tubules showed a strong immunoexpression to HIF-1α antibody (Figure 5(b), III) and this labelling was even greater in diabetic LPS-treated mice (Figure 5(b), IV).

To analyze if the observed HIF-1α upregulation was transcriptionally active in vivo, we analyzed the expression of the HIF-1α target gene VEGF-A, by immunostaining in mice kidneys. We first observed that while control mice did not show VEGF-A staining, diabetic mice display some degree of expression of this protein. Although all LPS-treated mice display a significant increase in the expression of VEGF-A in comparison with their respective controls, diabetic LPS-treated mice showed the highest immunolabeling (Figure 6).

3.3. Glycated Albumin Synergizes with LPS to Upregulate HIF-1α in HK-2 Renal Cells. We then performed an in vitro approach in order to get inside into the cellular mechanism responsible for the observed upregulation of both HIF-1α and VEGF-A in the kidney of diabetic mice. It has been previously described that AGE increases VEGF expression in retinal epithelial cells through activation of HIF-1α [22]. AGE is the major form of circulating glycated proteins in vivo, and its levels are increased in diabetes [23, 24]. Furthermore, AGE elicits pathobiological effects in cultured renal cells that are identical to those of high glucose ambient [23]. Therefore, in order to assess the effect of the diabetic milieu on the expression of HIF-1α in proximal tubular cells, HK-2 cells were incubated with 100 μg/mL AGE or albumin for up to 6 h. In these conditions, HIF-1α was upregulated in a time-dependent manner in AGE-treated cells, but not in cells treated with albumin, and its expression reached its maximum after 4 h incubation (Figure 7(a)).

We then assessed whether LPS affects AGE-induced HIF-1α upregulation, since a hypothetical synergy for HIF-1α expression in the proximal tubule could contribute to better recovery of renal function in diabetic mice after experimental endotoxemia. HK-2 cells were preincubated with either 100 μg/mL AGE or 100 μg/mL albumin for 1 h and then with 1 μg/mL LPS for 5 h. Expression of HIF-1α was increased to a similar degree by AGE and LPS, but it was dramatically enhanced in cells which were incubated with both agents (Figure 7(b)). These results suggest that AGE and LPS increased HIF-1α expression in the proximal tubules, in a synergistic manner.

3.4. Glycated Albumin-Induced HIF-1α Promotes the Upregulation of the Renoprotective VEGF-A in HK-2 Renal Cells. To demonstrate that AGE-induced HIF-1α was transcriptionally active, we determined by Q-RT-PCR the mRNA levels of VEGF-A in HK-2 cells treated with either 100 μg/mL GA or 100 μg/mL albumin for 5 h. VEGF mRNA expression (Figure 8) was substantially increased by AGE but not by albumin. In order to establish the dependency on HIF-1α of AGE-induced increase in VEGF-A mRNA expression, cells were preincubated with HIF-1α inhibitor YC-1 or transfected with specific HIF-1α siRNA. Both treatments abolished AGE-induced increase in VEGF-A mRNA expression (Figure 8), which confirmed that the AGE effect on VEGF-A expression is dependent on HIF-1α.

4. Discussion

Although it is known that rodents with experimental diabetes are protected from certain nephrotoxic agents [1–3], most of the available data are based upon experimental models of an early diabetic stage, condition characterized by the presence of renal cell proliferation, and thus renal cells are not quiescent as occurred in adult subjects [25, 26]. Thus, as reported by Zhang et al. [25], an inherently proproliferative state of the diabetic kidney may explain the observed lower expansion of renal injury on the one hand and recovery due to higher proliferative response after injury on the other. The same also accounts for HIF-1α where available data is limited to an early diabetic stage. Thus, herein we studied the role of HIF-1α in the outcome of AKI in diabetic animals after the development of proteinuria.

AKI is a syndrome defined by an abrupt change in the renal function and/or urine output which could range from overt tubular necrosis to mild perturbations in renal function without significant pathologic changes (prerenal azotemia) [18]. In our study, we observed that diabetic mice, besides an increase in the UAE, display better recovery of renal

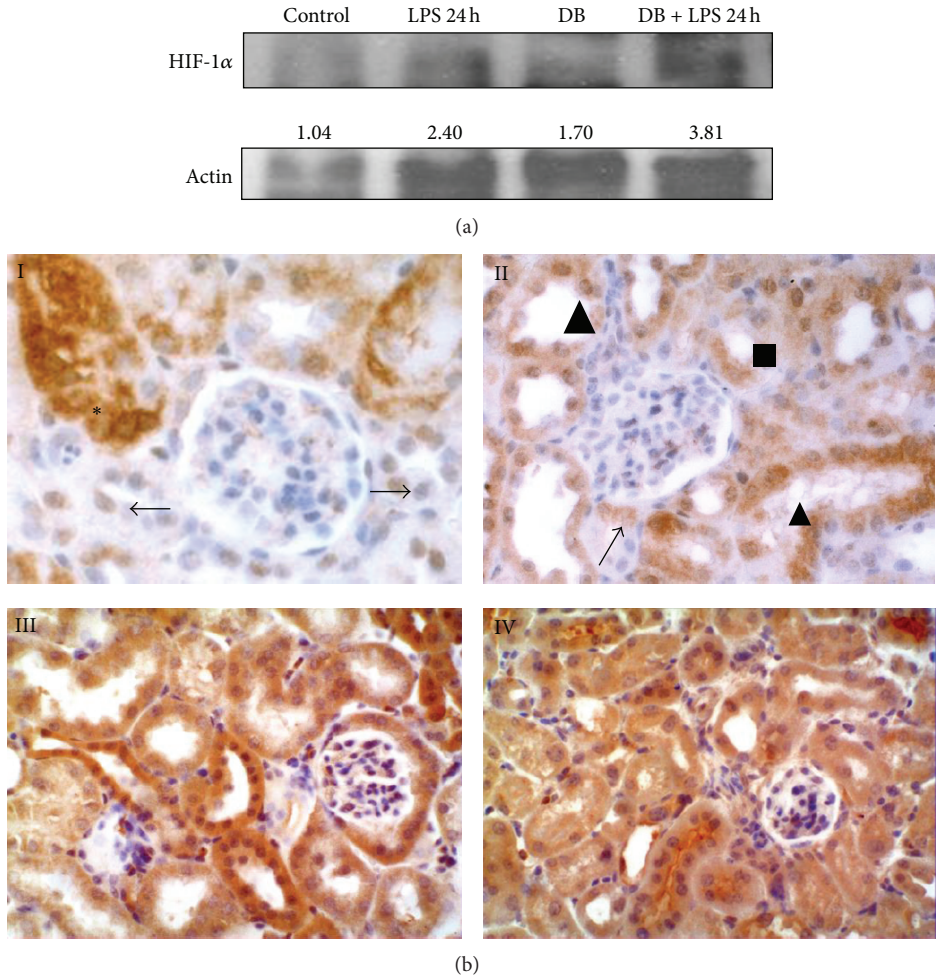

Figure 5: (a) Western-blotting analysis of HIF-1α in renal tissue. Quantification of HIF-1 α signal normalized by β-actin signal is also shown. (b) HIF-1α immunohistochemistry. I: control kidney. An intense immunoexpression of HIF-1α was detected in the cytoplasm of proximal convoluted tubules (∗), and in the nuclei of distal tubules, the labelling was weaker (→). II: diabetic mice. Proximal tubules showed positive reaction to HIF-1α in the cytoplasm (■). Both nucleus and cytoplasm of distal convoluted tubules cells (▲) presented a positive reaction to HIF-1α. The arrow points to the urinary pole with moderate reaction to this antibody. III: LPS-treated mice. Both convoluted tubules showed a strong immunolabelling to HIF-1α. IV: diabetic LPS-treated mice. The highest reaction to HIF-1α was encountered in the kidney of diabetic mice treated with endotoxin. Magnification: I and II: ×600; III and IV: ×300.

function after experimental endotoxemia. The maintained renal sodium reabsorption capacity observed in the diabetic mice is in accordance with a functional or mild form of AKI [21]. Furthermore, no alterations of the renal structure in any of the animal groups studied were found.

This is interesting due to the fact that proteinuria is a well-known factor involved in the progression of renal damage by mechanisms which include alterations in tubuloepithelial cell growth, apoptosis, gene transcription, and inflammatory cytokine production [27]. Furthermore, multiple clinical trials have indicated that antiproteinuric strategies are, in general, renoprotective [27]. Herein we demonstrate that in the diabetic kidney, endotoxemia could trigger the upregulation of HIF1-1α even in the proteinuric stage of the disease.

It is known that renal proximal tubular epithelial cells are targets for LPS during sepsis and renal infections. Septic AKI is characterized by a paucity of tubular cell death despite often severe impairment of global function. Accumulating data suggest that the renal tubules are also heavily involved in the pathogenesis of diabetic nephropathy [16]. In diabetes, tubular injury in the kidney is due to several factors, particularly high glucose levels, albuminuria, and the presence of advanced glycation end-product modified proteins. We show here that either LPS or AGE increases the expression of HIF-1α in HK-2 cells to a similar extent, and that exposure of AGE-treated cells to LPS results in overexpression of HIF-1α. Interestingly, renal expression of HIF-1α was also increased in several areas, including proximal tubules, in both diabetic and LPS-treated mice, and maximal renal HIF-1α upregulation was found in diabetic mice treated with LPS.

Accumulating evidence indicates that there is a fine line between the potential benefit and harmful side effects of HIF-1α activation. For instance, among the noxious effects of HIF-1α, which is related to our experimental setting, it is worth

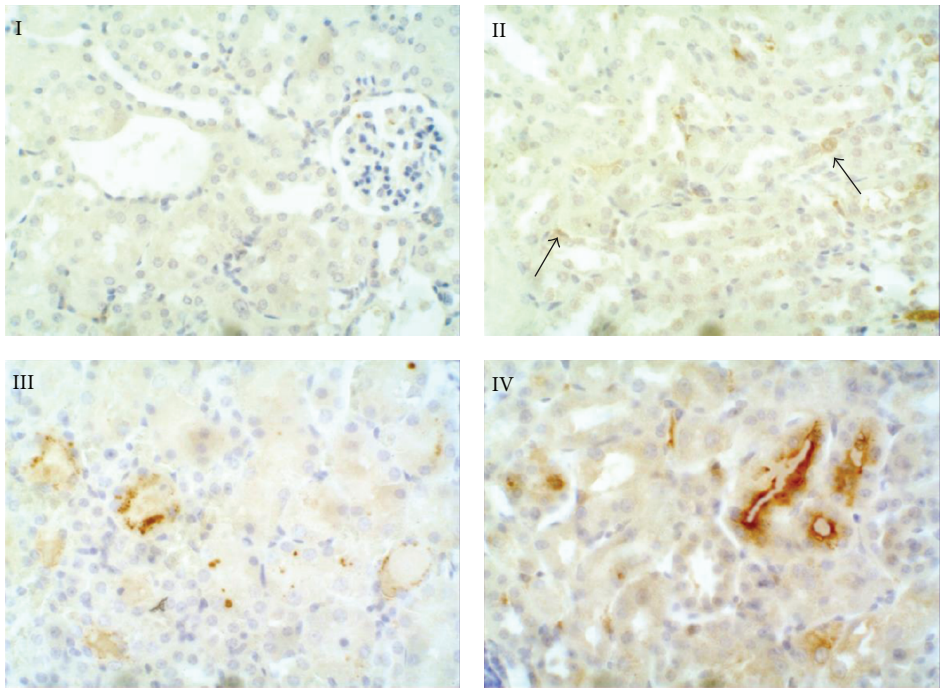

Figure 6: VEGF-A immunohistochemistry. I: control kidney. VEGF-A was not detected in the kidney of control mice. II: diabetic mice. Some of proximal tubules cells showed positive reaction to VEGF-A in the cytoplasm (right arrow). Endothelial cells were also immunostained (left arrow). III: LPS-treated mice. In some cells of convoluted tubules, VEGF-A was located in the cytoplasm with a granular pattern; in the other tubules, VEGF-A antibody showed a diffuse labelling. IV: diabetic LPS-treated mice. The highest reaction to VEGF-A was encountered in the kidney of diabetic mice treated with endotoxin. Magnification ×300.

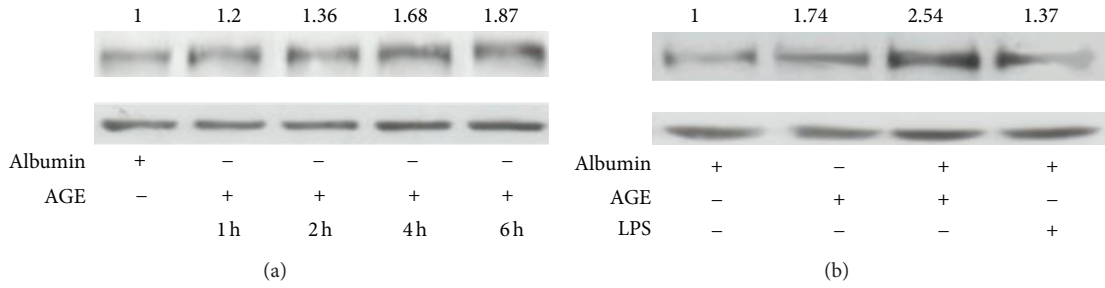

Figure 7: AGE and LPS induce HIF-1α upregulation and cooperate to over-increase HIF-1α expression. (a) AGE induces HIF-1α upregulation. (b) LPS induces HIF-1α upregulation and synergizes with AGE to over-increase HIF-1α expression. Equal protein loading was confirmed by probing with an anti-β-actin antibody. Normalized density ratio of HIF-1α over β-actin is indicated for each band.

mentioning that hypoxia-dependent increased tubular activity of HIF-1α has been proposed as a contributing factor in the development of tubulointerstitial fibrosis in diabetes mellitus [16]. In addition, HIF-1α has been shown to play an essential role in the development of LPS-induced sepsis in mice, so that targeted deletion of HIF-1α has a protective effect [28]. On the other hand, HIF-1α inducer cobalt chloride improves disease manifestations in a variety of kidney disease models including diabetic nephropathy and hypoxic preconditioning ameliorates LPS-induced renal dysfunction [29]. Moreover, it has been recently published that HIF-1α promotes renal ischemic injury regeneration [30]. According to the latter observation, it is tempting to speculate that the increased renal expression of HIF-1α in diabetic mice, particularly in the proximal tubules, might contribute to better recovery of renal function after experimental endotoxemia.

Regarding potential mechanisms triggered by HIF-1α for contributing to renal recovery in our model, it is conceivable that VEGF induction as HIF-1α target gene might be mediating. VEGF has been described as a survival factor for proximal tubule cells [23] and critical for maintenance of renal vasculature during kidney damage including AKI [31]. Our present data indicating that VEGF is induced in LPS-treated diabetic mice further support this notion.

In conclusion, we have found that mice with diabetic nephropathy display better recovery of renal function after experimental endotoxemia than their control littermates. This finding was associated with an increased expression of

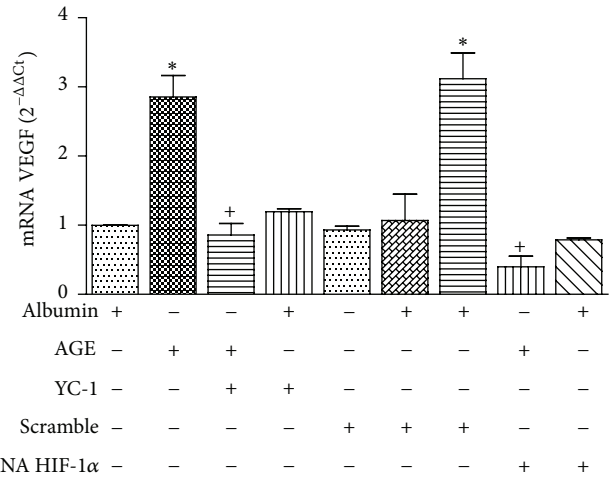

Figure 8: AGE increases VEGF mRNA expression in a HIF-1α-dependent manner. Cells were preincubated with HIF-1α inhibitor YC-1 or transfected with HIF-1α siRNA or control siRNA (scramble) as indicated in Section 2. Then they were incubated with albumin or AGE, and VEGF mRNA expression was quantified by Q-RT-PCR. Bars are the mean ± SD of 3 different experiments. $^{*}P < 0.01$ versus albumin; $^{+}P < 0.01$ versus AGE.

both HIF-1α and VEGF-A in the tubule epithelium of the diabetic mice. Furthermore, in these cells, AGE was found to be capable of upregulating HIF-1α as well as VEGF-A, a survival factor for these cells. Our findings suggest that even in the presence of an increased UAE, the diabetic condition may display upregulation of HIF-1α that might function as a "precondition state" capable of protecting from renal damage such as endotoxic AKI.

Conflict of Interests

The authors declared that they have no conflict of interests.

Acknowledgments

N. Olea is recipient of a Research Contract from Comunidad Autónoma de Madrid, Programa de Actividades I+D en Biociencias 2010 (S2010/BMD-2378). A. Fernández is the recipient of a postdoctoral fellowship from the Junta de Comunidades de Castilla-La Mancha. This work was supported in part by Grants from Ministerio de Ciencia e Innovación (SAF2009-12009-C02-01), SAF2011-26838, Junta de Comunidades de Castilla-La Mancha (POII10-0034-0322), Instituto Salud Carlos III (PI12/02825), FIS PS 09/02183, and the Eugenio Rodríguez Pascual Foundation.

References

[1] W. C. Elliott, D. C. Houghton, and D. N. Gilbert, "Experimental gentamicin nephrotoxicity: effect of streptozotocin-induced diabetes," *Journal of Pharmacology and Experimental Therapeutics*, vol. 233, no. 1, pp. 264–270, 1985.

[2] K. Hamilton, E. J. Eaton, H. O. Garland, and S. Old, "Effect of experimental diabetes mellitus on gentamicin-induced acute renal functional changes in the anaesthetized rat," *Clinical and Experimental Pharmacology and Physiology*, vol. 25, no. 3-4, pp. 231–235, 1998.

[3] A. V. Dnyanmote, S. P. Sawant, E. A. Lock, J. R. Latendresse, A. A. Warbritton, and H. M. Mehendale, "Diabetic mice are protected from normally lethal nephrotoxicity of S-1,2-dichlorovinyl-L-cysteine (DCVC): role of nephrogenic tissue repair," *Toxicology and Applied Pharmacology*, vol. 211, no. 2, pp. 133–147, 2006.

[4] M. R. Rudnick, S. Goldfarb, L. Wexler et al., "Nephrotoxicity of ionic and nonionic contrast media in 1196 patients: a randomized trial," *Kidney International*, vol. 47, no. 1, pp. 254–261, 1995.

[5] P. A. McCullough, R. Wolyn, L. L. Rocher, R. N. Levin, and W. W. O'Neill, "Acute renal failure after coronary intervention: incidence, risk factors, and relationship to mortality," *American Journal of Medicine*, vol. 103, no. 5, pp. 368–375, 1997.

[6] C. V. Thakar, S. Arrigain, S. Worley, J.-P. Yared, and E. P. Paganini, "A clinical score to predict acute renal failure after cardiac surgery," *Journal of the American Society of Nephrology*, vol. 16, no. 1, pp. 162–168, 2005.

[7] M. H. Rosner and M. D. Okusa, "Acute kidney injury associated with cardiac surgery," *Clinical Journal of the American Society of Nephrology*, vol. 1, no. 1, pp. 19–32, 2006.

[8] M. D. Griffin, E. J. Bergstralh, and T. S. Larson, "Renal papillary necrosis a sixteen-year clinical experience," *Journal of the American Society of Nephrology*, vol. 6, no. 2, pp. 248–256, 1995.

[9] G. L. Semenza, "Signal transduction to hypoxia-inducible factor 1," *Biochemical Pharmacology*, vol. 64, no. 5-6, pp. 993–998, 2002.

[10] J. Kanellis, S. Fraser, M. Katerelos, and D. A. Power, "Vascular endothelial growth factor is a survival factor for renal tubular epithelial cells," *American Journal of Physiology*, vol. 278, no. 6, pp. F905–F915, 2000.

[11] P. Jaakkola, D. R. Mole, Y.-M. Tian et al., "Targeting of HIF-α to the von Hippel-Lindau ubiquitylation complex by O_2-regulated prolyl hydroxylation," *Science*, vol. 292, no. 5516, pp. 468–472, 2001.

[12] M. Ivan, K. Kondo, H. Yang et al., "HIFα targeted for VHL-mediated destruction by proline hydroxylation: implications for O_2 sensing," *Science*, vol. 292, no. 5516, pp. 464–468, 2001.

[13] S. Kaluz, M. Kaluzová, and E. J. Stanbridge, "Regulation of gene expression by hypoxia: integration of the HIF-transduced hypoxic signal at the hypoxia-responsive element," *Clinica Chimica Acta*, vol. 395, no. 1-2, pp. 6–13, 2008.

[14] J. Zhou and B. Brune, "Cytokines and hormones in the regulation of hypoxia inducible factor-1alpha (HIF-1alpha)," *Cardiovascular & Hematological Agents in Medicinal Chemistry*, vol. 4, no. 3, pp. 189–197, 2006.

[15] I. R. Botusan, V. G. Sunkari, O. Savu et al., "Stabilization of HIF-1α is critical to improve wound healing in diabetic mice," *Proceedings of the National Academy of Sciences of the United States of America*, vol. 105, no. 49, pp. 19426–19431, 2008.

[16] M. Nangaku, R. Inagi, T. Miyata, and T. Fujita, "Hypoxia and hypoxia-inducible factor in renal disease," *Nephron*, vol. 110, no. 1, article e1, 2008.

[17] C. C. Tisher and T. H. Hostetter, "Diabetic nephropathy," in *Renal Pathology*, C. C. Tisher and B. M. Brenner, Eds., vol. 2, JB Lippincott, Philadelphia, Pa, USA, 1994.

[18] C. E. Guthrow, M. A. Morris, and J. F. Day, "Enhanced nonenzymatic glucosylation of human serum albumin in diabetes

mellitus," *Proceedings of the National Academy of Sciences of the United States of America*, vol. 76, no. 9, pp. 4258–4261, 1979.

[19] A. Izquierdo, P. López-Luna, A. Ortega et al., "The parathyroid hormone-related protein system and diabetic nephropathy outcome in streptozotocin-induced diabetes," *Kidney International*, vol. 69, no. 12, pp. 2171–2178, 2006.

[20] A. B. Fernandez-Martinez, M. I. Jimenez, I. S. Hernandez et al., "Mutual regulation of hypoxic and retinoic acid related signalling in tubular proximal cells," *International Journal of Biochemistry & Cell Biology*, vol. 43, no. 8, pp. 1198–1207, 2011.

[21] A. A. Sharfuddin and B. A. Molitoris, "Pathophysiology of ischemic acute kidney injury," *Nature Reviews Nephrology*, vol. 7, no. 4, pp. 189–200, 2011.

[22] C. Treins, S. Giorgetti-Peraldi, J. Murdaca, and E. Van Obberghen, "Regulation of vascular endothelial growth factor expression by advanced glycation end products," *Journal of Biological Chemistry*, vol. 276, no. 47, pp. 43836–43841, 2001.

[23] C. E. Guthrow, M. A. Morris, and J. F. Day, "Enhanced nonenzymatic glucosylation of human serum albumin in diabetes mellitus," *Proceedings of the National Academy of Sciences of the United States of America*, vol. 76, no. 9, pp. 4258–4261, 1979.

[24] M. P. Cohen and F. N. Ziyadeh, "Role of Amadori-modified nonenzymatically glycated serum proteins in the pathogenesis of diabetic nephropathy," *Journal of the American Society of Nephrology*, vol. 7, no. 2, pp. 183–190, 1996.

[25] Y. Zhang, Y. Shi, Y. Liu et al., "Growth pattern switch of renal cells and expression of cell cycle related proteins at the early stage of diabetic nephropathy," *Biochemical and Biophysical Research Communications*, vol. 363, no. 1, pp. 159–164, 2007.

[26] S. V. Griffin and S. J. Shankland, "Renal hyperplasia and hypertrophy: role of cell cylce regulatory proteins," in *The Kidney Physiology and Pathophysiology*, R. J. Alpern and S. C. Hebert, Eds., chapter 27, pp. 723–742, New York, NY, USA, 2008.

[27] R. J. Baines and N. J. Brunskill, "Tubular toxicity of proteinuria," *Nature Reviews Nephrology*, vol. 7, no. 3, pp. 177–180, 2011.

[28] M. Thiel, C. C. Caldwell, S. Kreth et al., "Targeted deletion of HIF-1α gene in T cells prevents their inhibition in hypoxic inflamed tissues and improves septic mice survival," *PLoS ONE*, vol. 2, no. 9, article e853, 2007.

[29] S. Ohtomo, M. Nangaku, Y. Izuhara, S. Takizawa, C. V. Y. D. Strihou, and T. Miyata, "Cobalt ameliorates renal injury in an obese, hypertensive type 2 diabetes rat model," *Nephrology Dialysis Transplantation*, vol. 23, no. 4, pp. 1166–1172, 2008.

[30] E. Conde, L. Alegre, I. Blanco-Sánchez et al., "Hypoxia inducible factor 1-alpha (hif-1 alpha) is induced during reperfusion after renal ischemia and is critical for proximal tubule cell survival," *PLoS ONE*, vol. 7, no. 3, Article ID e33258, 2012.

[31] E. C. Leonard, J. L. Friedrich, and D. P. Basile, "VEGF-121 preserves renal microvessel structure and ameliorates secondary renal disease following acute kidney injury," *American Journal of Physiology*, vol. 295, no. 6, pp. F1648–F1657, 2008.

Hindawi Publishing Corporation
Journal of Diabetes Research
Volume 2013, Article ID 162846, 6 pages
http://dx.doi.org/10.1155/2013/162846

Review Article

Novel Role of Parathyroid Hormone-Related Protein in the Pathophysiology of the Diabetic Kidney: Evidence from Experimental and Human Diabetic Nephropathy

Montserrat Romero,[1] Arantxa Ortega,[1] Nuria Olea,[1] María Isabel Arenas,[2] Adriana Izquierdo,[1] Jordi Bover,[3] Pedro Esbrit,[4] and Ricardo J. Bosch[1,2]

[1] *Laboratory of Renal Physiology and Experimental Nephrology, Department of Biological Systems/Physiology Unit, University of Alcalá, Alcalá de Henares, Madrid, Spain*
[2] *Department of Biomedicine and Biotechnology/Cell Biology Unit, University of Alcalá, Alcalá de Henares, Madrid, Spain*
[3] *Nephrology Department, Fundació Puigvert, Barcelona, Spain*
[4] *Bone and Mineral Metabolism Laboratory, Instituto de Investigación Sanitaria-Fundación Jiménez Díaz, Madrid, Spain*

Correspondence should be addressed to Ricardo J. Bosch; ricardoj.bosch@uah.es

Received 17 December 2012; Accepted 4 July 2013

Academic Editor: Bernard Portha

Parathyroid hormone-related protein (PTHrP) and its receptor type 1 (PTH1R) are extensively expressed in the kidney, where they are able to modulate renal function. Renal PTHrP is known to be overexpressed in acute renal injury. Recently, we hypothesized that PTHrP involvement in the mechanisms of renal injury might not be limited to conditions with predominant damage of the renal tubulointerstitium and might be extended to glomerular diseases, such as diabetic nephropathy (DN). In experimental DN, the overexpression of both PTHrP and the PTH1R contributes to the development of renal hypertrophy as well as proteinuria. More recent data have shown, for the first time, that PTHrP is upregulated in the kidney from patients with DN. Collectively, animal and human studies have shown that PTHrP acts as an important mediator of diabetic renal cell hypertrophy by a mechanism which involves the modulation of cell cycle regulatory proteins and TGF-β1. Furthermore, angiotensin II (Ang II), a critical factor in the progression of renal injury, appears to be responsible for PTHrP upregulation in these conditions. These findings provide novel insights into the well-known protective effects of Ang II antagonists in renal diseases, paving the way for new therapeutic approaches.

1. Diabetic Nephropathy (DN)

End-stage renal failure due to diabetes mellitus, especially type 2 diabetes, has been recently described as a medical catastrophe of worldwide dimensions [1]. Diabetic nephropathy (DN) is characterized by the development of proteinuria and subsequent glomerulosclerosis, conditions which are always preceded by renal cell hypertrophy [2]. Although the diabetic kidney is extremely variable, from near normal size to even small fibrotic kidney, renal enlargement due to cellular hypertrophy and hyperplasia is an early feature of the disease both in human and in experimental animal models, especially in the absence of insulin treatment. Hypertrophy of tubuloepithelial as well as glomerular cells, including both visceral epithelial (podocytes) and mesangial cells, is an early hallmark of diabetes renal involvement [3–5]. Over time, glomerular cell hypertrophy might become a maladaptive response leading to glomerulosclerosis.

Although the mechanisms by which high glucose (HG) leads to renal cell hypertrophy are still not completely understood, they appear to involve cell entry into the cell cycle—associated with cyclin D_1 kinase activation early in G_1—and subsequent arrest at the G_1/S interphase, implicating inhibition or insufficient activation of cyclin E kinase, to permit progression into S phase, and therefore, arrest of cell cycle progression followed by an increase in cell protein synthesis [6].

Recent studies have shown that HG-induced hypertrophy involves an early activation of the renin angiotensin system,

followed by an induction of TGF-β_1, which in turn activates a cell cycle regulatory protein, the cyclin dependent kinase inhibitor (CDKI) $p27^{Kip1}$ [7–9]. The interaction of $p27^{Kip1}$ with the cyclin E kinase has been implicated in the inhibition of this late complex and thus the G_1 progression [10].

2. The Renal PTH/PTHrP System

In the adult kidney, both parathyroid hormone- (PTH-) related protein (PTHrP) and the PTH1 receptor (PTH1R) are abundant throughout the renal parenchyma, including the intrarenal vasculature [11–13]. In the kidney, PTHrP appears to modulate renal plasma flow and glomerular filtration rate and induces proliferative effects on both glomerular mesangial and tubuloepithelial cells [11–17]. Renal PTHrP is overexpressed in several experimental nephropathies, including acute renal injury, obstructive nephropathy, and a rat model of tubulointerstitial scarring after protein overload, associated with the development of proteinuria [12, 18]. The recent development of a transgenic mouse model characterized by PTHrP overexpression in the renal proximal tubule made it possible to explore the functional consequences of chronic PTHrP overexpression in experimental models of renal damage (reviewed in [19]). This novel approach has provided valuable data which have helped to disclose the true roles of PTHrP in the damaged kidney. The following paragraphs describe the latest results in experimental as well as in human DN.

3. PTHrP in Experimental DN

Recently, we hypothesized that PTHrP involvement in the mechanisms of renal injury might not be limited to conditions with predominant damage of the renal tubulointerstitium and might be extended to glomerular diseases, such as DN. Using an experimental model of DN induced by streptozotocin (STZ) [20], we studied the possible changes in the PTHrP/PTH1R system associated with the outcome of this nephropathy, characterized by an initial phase of renal hypertrophy at both tubular and glomerular levels, followed by an increase in urinary albumin excretion (UAE) (proteinuria) [21, 22]. DN was induced in Swiss-CD1 (CD1) mice as well as in PTHrP-overexpressing mice. In the diabetic CD-1 mice, a significant increase in the expression of both PTHrP and PTH1R was observed, at both glomerular and tubular levels, associated with the development of an increase in the UAE [20]. On the other hand, diabetic PTHrP-overexpressing mice, in comparison to their control littermates, have increased renal hypertrophy, a significantly higher UAE, and lower total plasma protein levels. A significant association among the renal expression of PTHrP, PTH1R, and UAE was found to occur in the diabetic mice. Furthermore, there was a 6-fold increase in the risk of developing proteinuria in those mice with the higher PTHrP and PTH1R levels, according to the logistic regression analysis [20]. It is interesting to mention that albeit the STZ model has limitations for assessing long-term histomorphological changes in the diabetic kidney [21], the aforementioned findings might have pathophysiological implications since the amount of proteinuria is a reliable predictor of diabetic nephropathy [22]. Thus, these studies indicate that the renal PTHrP/PTH1R system is upregulated in STZ-induced diabetic mice, where it appears to be involved in renal hypertrophy and adversely affects the outcome of DN.

More recently, the putative role of PTHrP in the hypertrophy of the diabetic kidney was explored. In this way Romero et al. observed that PTHrP plays a key role in the mechanisms of HG-induced podocyte hypertrophy. It is worth mentioning that podocytes are thought to be terminally differentiated cell and hence not able to regenerate *in vivo*. In these studies, HG-induced podocyte hypertrophy was inhibited by the presence of a specific PTHrP neutralizing antibody. Interestingly, in this condition HG also failed to upregulate the expression of the hypertrophy factor TGF-β_1 [23].

Although PTHrP does not seem to affect podocyte apoptosis, it was shown to be able to modulate the expression of several positive as well as negative cell cycle regulatory proteins. In this way, while PTHrP (1–36) was shown to stimulate cyclin D_1, thus promoting podocytes to enter into G_1, it also downregulates cyclin E, hence blocking the cell cycle later in G_1. Moreover, PTHrP is able to upregulate the negative cell cycle regulatory protein $p27^{Kip1}$ which plays a key role in diabetic cell hypertrophy by preventing activation of cyclin E activity and arresting the cell cycle later in G_1 [4, 23]. Interestingly, Romero et al. [23] found that the pharmacological blockade of the PTH1R inhibited the $p27^{Kip1}$ upregulation induced by both HG and AngII. Taken together, these data suggest that PTHrP might mediate the hypertrophic signaling acting in an autocrine/intracrine fashion through the PTH1R receptor.

To discern the mechanism involved in the stimulation of $p27^{Kip1}$ induced by both PTHrP and TGF-β_1, Romero et al. [23] performed two experimental approaches. First, they found that using a PTHrP siRNA inhibited the ability of HG and AngII to stimulate the upregulation of $p27^{Kip1}$, albeit it could not prevent the TGF-β_1 upregulation of this protein. Secondly, on TGF-β_1 siRNA transfected podocytes, PTHrP (1–36) failed to induce both $p27^{Kip1}$ overexpression and hypertrophy, thus suggesting that TGF-β_1 mediates both $p27^{Kip1}$ upregulation and the hypertrophy response induced by PTHrP on HG conditions.

Interestingly, Romero et al. [23] observed that the glomerular expression of both TGF-β_1 and $p27^{Kip1}$ are constitutively upregulated in PTHrP-overexpressing mice, albeit the latter was not accompanied by renal hypertrophy [24]. This result seems plausible since the hypertrophic mechanism requires the entry into the cell cycle and subsequent arrest at the G_1/S interphase. Several studies have demonstrated that in glomerular mesangial cells grown in HG ambient, initially, self-limited proliferation occurs due to generation of HG-induced growth factors, followed by cell cycle arrest in the G_1 due to the expression of factors that block the checkpoint G_1-S interphase and undergo cellular hypertrophy [4, 25–27]. Of considerable interest is the fact that previous studies on PTHrP-overexpressing mice have revealed the constitutive upregulation of various proinflammatory mediators [28], including the vascular endothelial growth factor-1 [29]

without evidence of kidney damage in the absence of a renal insult. In any case, these data strongly suggest that PTHrP might participate in the upregulation of glomerular TGF-β_1 and $p27^{Kip1}$. Collectively, these results indicate that the renal PTHrP/PTH1R system is upregulated in streptozotocin-induced diabetes in mice and appears to be involved with renal hypertrophy and adversely affects the outcome of DN.

4. PTHrP in Human DN

In order to extend our studies into human DN, we developed two experimental approaches (30). We first assessed whether PTHrP might be upregulated in the kidney from patients with DN. And secondly, we analyzed the potential role of PTHrP in the mechanisms of HG-induced hypertrophy in another glomerular cell line known to be affected in this condition, such as human mesangial cells (HMC).

By using immunohistochemistry in kidney sections from patients with clinical and histopathological diagnosis of DN, we observed an intense PTHrP upregulation in both glomerular and tubuloepithelial cells, including a remarkable nuclear immunolocalization in the latter cells. Interestingly, the kidneys of these patients displayed a similar pattern of PTHrP immunolocalization to that previously observed in a diabetic mouse model [23]. Although the human diabetic kidney is extremely variable in size, renal enlargement due to hypertrophy and hyperplasia is an early feature of the disease as measured by several imaging techniques [1, 30]. Due to the fact that kidney size measurement is not regularly assessed in the clinical setting, this parameter was not available in the studied human cohort. However, the fact that all of these patients presented a pattern of PTHrP staining similar to that observed in the mouse model referred to previously, together with present *in vitro* data in HMC, strongly suggests that PTHrP may be an important factor in the pathophysiology of glomerular mesangial cell hypertrophy in diabetic patients (Figure 1).

In vitro studies have established that prolonged exposure of human as well as rodent MC to HG in the absence of exogenous growth factors triggers hypertrophy after a brief self-limited mitogenic effect [31]. We and other investigators previously reported that the N-terminal fragment of PTHrP is mitogenic for these cells [13, 16]. Our data herein show that HG-induced HMC hypertrophy was associated with a progressive increase in PTHrP protein expression between 24 and 72 h. Moreover, exogenous PTHrP (1–36) displays an early (24 h) proliferative effect followed by a hypertrophy response at 72 h. Thus, PTHrP seems to recapitulate the proliferative as well as the hypertrophy response induced by HG on cultured HMC (30).

In order to study the mechanism whereby PTHrP (1–36) was able to switch its initial mitogenic stimulus into hypertrophy, we assessed the expression of several cell cycle regulatory proteins known to modulate this cellular effect. Both HG and PTHrP (1–36) were initially (24 h) shown to trigger HMC to enter the cell cycle, associated with an increase of both cyclins D1 and E and cdk2 activity. Later, at 72 h, only cyclin D1 remained increased, together with cyclin E/cdk2 inactivation. In this sense, it is well accepted that while cyclin D governs the physical growth of the cell, cyclin E determines whether the growth pattern of renal cells will be one of hyperplasia (cyclin E upregulation) or hypertrophy (cyclin E downregulation) [32]. The cdk inhibitor $p27^{Kip1}$ is also known to play a key role in the mechanisms of HG-induced MC hypertrophy by regulating (inhibiting) the activity of the cyclin E/cdk2 complex [33, 34]. Interestingly, we also show that PTHrP (1–36) was able to upregulate $p27^{Kip1}$ in a similar fashion and time frame as HG medium. Collectively, our findings indicate that the observed decrease in cyclin E/cdk2 complex kinase activity elicited by either HG or PTHrP (1–36) related to HMC hypertrophy is likely a consequence of both cyclin E downregulation and $p27^{Kip1}$ upregulation. In addition, these data strongly suggest that HG and PTHrP (1–36) interact with a common cellular pathway leading to hypertrophy in HMC (30).

The potential role of PTHrP on the mechanisms of HG-induced HMC hypertrophy was further assessed by observing that antagonizing the PTHrP system abolished the latter, together with reversal of the hypertrophy-related changes in the cell cycle (30). As we previously observed in a mouse podocyte cell line, we find that PTHrP is also able to stimulate the protein expression of TGF-β_1 and its type II receptor in HMC, and a neutralizing TGF-β_1 antibody abrogated HMC hypertrophy induced by PTHrP (1–36). Moreover, blockade of the PTHrP system abolished TGF-β_1 upregulation but not that of its type II receptor by HG in these cells. In this regard, upregulation of the latter receptor has been shown to be associated with increased TGF-β-mediated growth inhibition [35], whereas its reduced expression contributes to the loss of sensitivity to TGF-β and the increased proliferation of some cancer cells [36, 37]. Therefore, it is likely that the TGF-β system might also be activated, contributing to HMC hypertrophy by a PTHrP-independent mechanism. In any event, these findings indicate that TGF-β1 is a downstream mediator of PTHrP (1–36) to induce hypertrophy in HMCs, as previously discussed in mouse podocytes [23].

5. Interaction between PTHrP and Angiotensin II in the Damaged Kidney

The renin-angiotensin system is well known for playing an important pathogenic role in the mechanisms of renal injury [38, 39]. Local activation of components of this system, including Ang II, in the kidney has shown to occur early in various experimental models of ARF, for example, folic acid-induced nephrotoxicity and ischemia/reperfusion [11, 39, 40]. Moreover, Ang II antagonists exert beneficial effects on renal function in these models [39, 41, 42].

Recent data strongly suggest that PTHrP might be involved in the mechanisms related to Ang II-induced renal injury. Exogenously administered Ang II, via its type 1 (AT1) receptor, increases PTHrP expression in glomerular and tubular cells as well as in vascular smooth muscle cells both *in vivo* and *in vitro* [43, 44]. Interestingly, a significant correlation between PTHrP overexpression and tubular damage and fibrosis was observed in the rat kidney after systemic Ang II infusion [43]. Furthermore, in nephrotoxic ARF, the improvement of renal function by Ang II antagonists

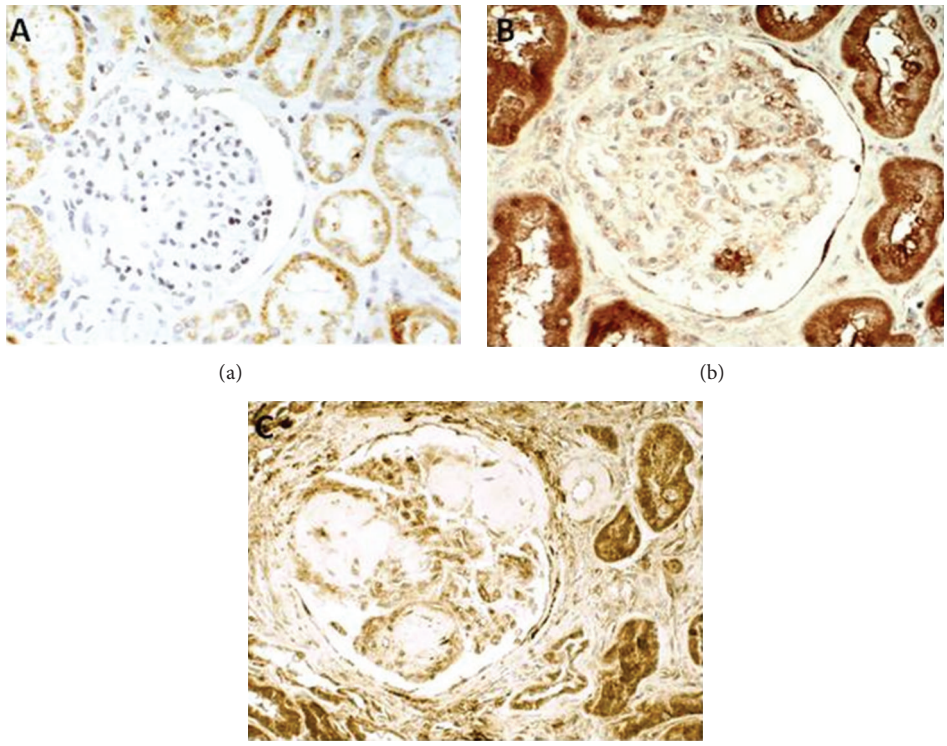

(a) (b)

(c)

Figure 1: Immunostaining for PTHrP in the kidney of patients with diabetic nephropathy. PTHrP was detected by using a goat α-PTHrP antibody (Santa Cruz Biotechnology) in kidney tissue sections from patients with clinical and histological diagnosis of DN. (a) Section from normal kidney showing PTHrP immunostaining restricted to the epithelial cells cytoplasm of convoluted renal tubules. (b, c) Kidney samples from two diabetic patients with different degree of DN: one patient with moderate (b) or more severe (c) diabetic glomerulosclerosis. PTHrP labelling was present in both the glomeruli and the tubuloepithelial cells. Original magnifications ×300.

was associated with inhibition of PTHrP overexpression [38]. These aggregated data suggest that Ang II is a likely candidate responsible for PTHrP overexpression, and this might contribute to the deleterious effects of Ang II in the damaged kidney. These findings could provide novel insights into the well-known protective effects of Ang II antagonists in renal diseases, possibly leading the way to new therapeutic approaches.

6. Conclusion

Collectively, these results indicate that the renal PTHrP/PTH1R system is upregulated in experimental as well human diabetes, appears to be involved with renal hypertrophy, and adversely affects the outcome of DN. PTHrP also participates in the hypertrophic signalling triggered by HG on glomerular cells. In this condition, AngII induces the upregulation of PTHrP, which might induce the expression of TGF-β_1 and $p27^{Kip1}$. These findings provide new insights into the protective effects of AngII antagonists in DN, paving the way for new forms of intervention.

Acknowledgments

N. Olea is the recipient of a Research Contract from the Comunidad Autónoma de Madrid (S-BIO-2083-2006) and the University of Alcalá. A. Izquierdo is currently Assistant Professor at the Rey Juan Carlos University, Alcorcón, Madrid. This work was supported in part by Grants from Ministerio de Educación y Cultura of Spain (SAF2002-04356-C03-01, -02, and -03) Ministerio de Ciencia e Innovación (SAF2009-12009-C02-01), Instituto de Salud Carlos III (RETICEF RD06/0013/1002 and RD12/0043/0008 and PI12/02825), the Spanish Society of Nephrology, and the Eugenio Rodríguez Pascual Foundation.

References

[1] E. Ritz, I. Rychlik, F. Locatelli, and S. Halimi, "End-stage renal failure in type 2 diabetes: a medical catastrophe of worldwide dimensions," *American Journal of Kidney Diseases*, vol. 34, no. 5, pp. 795–808, 1999.

[2] G. Wolf and F. N. Ziyadeh, "Molecular mechanisms of diabetic renal hypertrophy," *Kidney International*, vol. 56, no. 2, pp. 393–405, 1999.

[3] A. C. Powers, "Diabetes Mellitus," in *Harrison's principles of Internal Medicine*, D. L. Kasper, E. Braunwald, A. S. Fauci, S. L. Hauser, D. L. Longo, and J. L. Jamerson, Eds., pp. 2152–2180, McGRaw-Hill, New York, NY, USA, 16th edition, 2005.

[4] C. C. Tisher and T. H. Hostetter, "Diabetic nephropathy," in *Renal Pathology*, C. C. Tisher and B. M. Brenner, Eds., vol. 2, p. 1387, JB Lippincott, Philadelphia, Pa, USA, 1994.

[5] G. Wolf, "New insights into the pathophysiology of diabetic nephrophathy: from haemodynamics to molecular pathology," *European Journal of Clinical Investigation*, vol. 34, no. 12, pp. 785–796, 2004.

[6] H. C. Huang and P. A. Preisig, "G1 kinases and transforming growth factor-β signaling are associated with a growth pattern switch in diabetes-induced renal growth," *Kidney International*, vol. 58, no. 1, pp. 162–172, 2000.

[7] Z. Xu, T. Yoo, D. Ryu et al., "Angiotensin II receptor blocker inhibits p27Kip1 expression in glucose-stimulated podocytes and in diabetic glomeruli," *Kidney International*, vol. 67, no. 3, pp. 944–952, 2005.

[8] T. Pantsulaia, "Role of TGF-beta in pathogenesis of diabetic nephropathy," *Georgian medical news.*, no. 131, pp. 13–18, 2006.

[9] G. Wolf, R. Schroeder, F. Thaiss, F. N. Ziyadeh, U. Helmchen, and R. A. K. Stahl, "Glomerular expression of p27(Kip1) in diabetic db/db mouse: role of hyperglycemia," *Kidney International*, vol. 53, no. 4, pp. 869–879, 1998.

[10] S. V. Ekholm and S. I. Reed, "Regulation of G1 cyclin-dependent kinases in the mammalian cell cycle," *Current Opinion in Cell Biology*, vol. 12, no. 6, pp. 676–684, 2000.

[11] S. Santos, R. J. Bosch, A. Ortega et al., "Up-regulation of parathyroid hormone-related protein in folic acid-induced acute renal failure," *Kidney International*, vol. 60, no. 3, pp. 982–995, 2001.

[12] P. Esbrit, S. Santos, A. Ortega et al., "Parathyroid hormone-related protein as a renal regulating factor: from vessels to glomeruli and tubular epithelium," *American Journal of Nephrology*, vol. 21, no. 3, pp. 179–184, 2001.

[13] R. J. Bosch, P. Rojo-Linares, G. Torrecillas-Casamayor, M. C. Iglesias-Cruz, D. Rodríguez-Puyol, and M. Rodríguez-Puyol, "Effects of parathyroid hormone-related protein on human mesangial cells in culture," *American Journal of Physiology*, vol. 277, no. 6, pp. E990–E995, 1999.

[14] T. Massfelder, N. Parekh, K. Endlich, C. Saussine, M. Steinhausen, and J. Helwig, "Effect of intrarenally infused parathyroid hormone-related protein on renal blood flow and glomerular filtration rate in the anaesthetized rat," *British Journal of Pharmacology*, vol. 118, no. 8, pp. 1995–2000, 1996.

[15] N. Endlich, R. Nobiling, W. Kriz, and K. Endlich, "Expression and signaling of parathyroid hormone-related protein in cultured podocytes," *Experimental Nephrology*, vol. 9, no. 6, pp. 436–443, 2001.

[16] N. E. Soifer, S. K. Van Why, M. B. Ganz, M. Kashgarian, N. J. Siegel, and A. F. Stewart, "Expression of parathyroid hormone-related protein in the rat glomerulus and tubule during recovery from renal ischemia," *Journal of Clinical Investigation*, vol. 92, no. 6, pp. 2850–2857, 1993.

[17] A. Garcia-Ocana, F. De Miguel, C. Penaranda, J. P. Albar, J. L. Sarasa, and P. Esbrit, "Parathyroid hormone-related protein is an autocrine modulator of rabbit proximal tubule cell growth," *Journal of Bone and Mineral Research*, vol. 10, no. 12, pp. 1875–1884, 1995.

[18] R. Largo, D. Gómez-Garre, S. Santos et al., "Renal expression of parathyroid hormone-related protein (PTHrP) and PTH/PTHrP receptor in a rat model of tubulointerstitial damage," *Kidney International*, vol. 55, no. 1, pp. 82–90, 1999.

[19] R. J. Bosch, A. Ortega, A. Izquierdo, I. Arribas, J. Bover, and P. Esbrit, "A transgenic mouse model for studying the role of the parathyroid hormone-related protein system in renal injury," *Journal of Biomedicine and Biotechnology*, vol. 2011, Article ID 290874, 7 pages, 2011.

[20] A. Izquierdo, P. López-Luna, A. Ortega et al., "The parathyroid hormone-related protein system and diabetic nephropathy outcome in streptozotocin-induced diabetes," *Kidney International*, vol. 69, no. 12, pp. 2171–2178, 2006.

[21] M. L. Gross, E. Ritz, A. Schoof et al., "Comparison of renal morphology in the Streptozotocin and the SHR/N-cp models of diabetes," *Laboratory Investigation*, vol. 84, no. 4, pp. 452–464, 2004.

[22] M. P. O'Donnell, C. C. Chao, G. Gekker, K. S. Modi, B. L. Kasiske, and W. F. Keane, "Renal cell cytokine production stimulates HIV-1 expression in chronically HIV-1-infected monocytes," *Kidney International*, vol. 53, no. 3, pp. 593–597, 1998.

[23] M. Romero, A. Ortega, A. Izquierdo, P. López-Luna, and R. J. Bosch, "Parathyroid hormone-related protein induces hypertrophy in podocytes via TGF-β1 and p27Kip1: Implications for diabetic nephropathy," *Nephrology Dialysis Transplantation*, vol. 25, no. 8, pp. 2447–2457, 2010.

[24] N. M. Fiaschi-Taesch, S. Santos, V. Reddy et al., "Prevention of acute ischemic renal failure by targeted delivery of growth factors to the proximal tubule in transgenic mice: the efficacy of parathyroid hormone-related protein and hepatocyte growth factor," *Journal of the American Society of Nephrology*, vol. 15, no. 1, pp. 112–125, 2004.

[25] G. Wolf, K. Sharma, Y. Chen, M. Ericksen, and F. N. Ziyadeh, "High glucose-induced proliferation in mesangial cells is reversed by autocrine TGF-β," *Kidney International*, vol. 42, no. 3, pp. 647–656, 1992.

[26] F. G. Cosio, "Effects of high glucose concentrations on human mesangial cell proliferation," *Journal of the American Society of Nephrology*, vol. 5, no. 8, pp. 1600–1609, 1995.

[27] M. Isono, A. Mogyorósi, D. C. Han, B. B. Hoffman, and F. N. Ziyadeh, "Stimulation of TGF-β type II receptor by high glucose in mouse mesangial cells and in diabetic kidney," *American Journal of Physiology*, vol. 278, no. 5, pp. F830–F838, 2000.

[28] D. Rámila, J. A. Ardura, V. Esteban et al., "Parathyroid hormone-related protein promotes inflammation in the kidney with an obstructed ureter," *Kidney International*, vol. 73, no. 7, pp. 835–847, 2008.

[29] J. A. Ardura, R. Berruguete, D. Rámila, M. V. Alvarez-Arroyo, and P. Esbrit, "Parathyroid hormone-related protein interacts with vascular endothelial growth factor to promote fibrogenesis in the obstructed mouse kidney," *American Journal of Physiology*, vol. 295, no. 2, pp. F415–F425, 2008.

[30] G. Wolf and F. N. Ziyadeh, "Molecular mechanisms of diabetic renal hypertrophy," *Kidney International*, vol. 56, no. 2, pp. 393–405, 1999.

[31] J. Sun, Y. Xu, H. Deng, S. Sun, Z. Dai, and Y. Sun, "Involvement of osteopontin upregulation on mesangial cells growth and collagen synthesis induced by intermittent high glucose," *Journal of Cellular Biochemistry*, vol. 109, no. 6, pp. 1210–1221, 2010.

[32] G. Wolf, "Cell cycle regulation in diabetic nephropathy," *Kidney Internationa*, vol. 58, no. 77, pp. S59–S66, 2000.

[33] L. Hengst and S. I. Reed, "Inhibitors of the Cip/Kip family," *Current Topics in Microbiology and Immunology*, vol. 227, pp. 25–41, 1997.

[34] G. Wolf, R. Schroeder, F. N. Ziyadeh, F. Thaiss, G. Zahner, and R. A. K. Stahl, "High glucose stimulates expression of p27(Kip1) in cultured mouse mesangial cells: relationship to hypertrophy," *American Journal of Physiology*, vol. 273, no. 3, pp. F348–F356, 1997.

[35] Y. Nishikawa, M. Wang, and B. I. Carr, "Changes in TGF-beta receptors of rat hepatocytes during primary culture and

liver regeneration: increased expression of TGF-beta receptors associated with increased sensitivity to TGF-beta-mediated growth inhibition," *Journal of Cellular Physiology*, vol. 176, pp. 612–623, 1998.

[36] M. E. Kadin, M. W. Cavaille-Coll, R. Gertz, J. Massagué, S. Cheifetz, and D. George, "Loss of receptors for transforming growth factor β in human T-cell malignancies," *Proceedings of the National Academy of Sciences of the United States of America*, vol. 91, no. 13, pp. 6002–6006, 1994.

[37] J. Wang, W. Han, E. Zborowska et al., "Reduced expression of transforming growth factor β type I receptor contributes to the malignancy of human colon carcinoma cells," *The Journal of Biological Chemistry*, vol. 271, no. 29, pp. 17366–17371, 1996.

[38] R. C. Harris and M. Martinez-Maldonado, "Angiotensin II-mediated renal injury," *Mineral and Electrolyte Metabolism*, vol. 21, no. 4-5, pp. 328–335, 1995.

[39] A. Ortega, D. Rámila, A. Izquierdo et al., "Role of the renin-angiotensin system on the parathyroid hormone-related protein overexpression induced by nephrotoxic acute renal failure in the rat," *Journal of the American Society of Nephrology*, vol. 16, no. 4, pp. 939–949, 2005.

[40] J. Kontogiannis and K. D. Burns, "Role of AT1 angiotensin II receptors in renal ischemic injury," *American Journal of Physiology*, vol. 274, no. 1, pp. F79–F90, 1998.

[41] G. W. Long, D. C. Misra, R. Juleff, G. Blossom, P. F. Czako, and J. L. Glover, "Protective effects of enalaprilat against postischemic renal failure," *Journal of Surgical Research*, vol. 54, no. 3, pp. 254–257, 1993.

[42] R. C. Abdulkader, M. M. Yuki, A. C. M. Paiva, and M. Marcondes, "Prolonged inhibition of angiotensin II attenuates glycerol-induced acute renal failure," *Brazilian Journal of Medical and Biological Research*, vol. 21, no. 2, pp. 233–239, 1988.

[43] O. Lorenzo, M. Ruiz-Ortega, P. Esbrit et al., "Angiotensin II increases parathyroid hormone-related protein (PTHrP) and the type 1 PTH/PTHrP receptor in the kidney," *Journal of the American Society of Nephrology*, vol. 13, no. 6, pp. 1595–1607, 2002.

[44] M. Nodat, T. Katoh, N. Takuwa, M. Kumada, K. Kurokawa, and Y. Takuwa, "Synergistic stimulation of parathyroid hormone-related peptide gene expression by mechanical stretch and angiotensin II in rat aortic smooth muscle cells," *The Journal of Biological Chemistry*, vol. 269, no. 27, pp. 17911–17917, 1994.

Hindawi Publishing Corporation
Journal of Diabetes Research
Volume 2013, Article ID 149452, 9 pages
http://dx.doi.org/10.1155/2013/149452

Review Article

Animal Models of Diabetic Neuropathy: Progress Since 1960s

Md. Shahidul Islam

Department of Biochemistry, School of Life Sciences, University of KwaZulu-Natal (Westville Campus), Durban 4000, South Africa

Correspondence should be addressed to Md. Shahidul Islam; islamd@ukzn.ac.za

Received 30 May 2013; Accepted 9 July 2013

Academic Editor: Daisuke Koya

Diabetic or peripheral diabetic neuropathy (PDN) is one of the major complications among some other diabetic complications such as diabetic nephropathy, diabetic retinopathy, and diabetic cardiomyopathy. The use of animal models in the research of diabetes and diabetic complications is very common when rats and mice are most commonly used for many reasons. A numbers of animal models of diabetic and PDN have been developed in the last several decades such as streptozotocin-induced diabetic rat models, conventional or genetically modified or high-fat diet-fed C57BL/Ks (db/db) mice models, streptozotocin-induced C57BL6/J and ddY mice models, Chinese hamster neuropathic model, rhesus monkey PDN model, spontaneously diabetic WBN/Kob rat model, L-fucose-induced neropathic rat model, partial sciatic nerve ligated rat model, nonobese diabetic (NOD) mice model, spontaneously induced Ins2 Akita mice model, leptin-deficient (ob/ob) mice model, Otsuka Long-Evans Tokushima Fatty (OLETF) rat model, surgically-induced neuropathic model, and genetically modified Spontaneously Diabetic Torii (SDT) rat model, none of which are without limitations. An animal model of diabetic or PDN should mimic the all major pathogeneses of human diabetic neuropathy. Hence, this review comparatively evaluates the animal models of diabetic and PDN which are developed since 1960s with their advantages and disadvantages to help diabetic research groups in order to more accurately choose an appropriate model to meet their specific research objectives.

1. Introduction

The term "diabetes" was first coined by Araetus of Cappodocia (81-133AD). Later, the word "mellitus" (honey sweet) was added by Thomas Willis (Britain) in 1675 after rediscovering the sweetness of urine and blood of patients (first noticed by the ancient Indians) [1]. In 1776, Dobson (Britain) for the first time confirmed the presence of excess sugar in urine and blood as a cause of their sweetness. Depending on the pathogenesis, diabetes is classified as type 1 and type 2. The first widely accepted classification of diabetes mellitus was published by World Health Organization (WHO) in 1980 [2] and, in modified form, in 1985 [3]. In 1980, the WHO Expert Committee proposed two major classes of diabetes mellitus, namely: Insulin Dependent Diabetes Mellitus (IDDM) or Type 1 and Noninsulin Dependent Diabetes Mellitus (NIDDM) or Type 2 diabetes (T2D). In 1985, the WHO expert committee omitted the terms Type 1 and Type 2, but the terms IDDM and NIDDM were retained, and a class of Malnutrition-Related Diabetes Mellitus (MRDM) was introduced [3]. In both reports (1980 and 1985), other classes of diabetes were also included, for example, Impaired Glucose Tolerance (IGT) and Gestational Diabetes Mellitus (GDM) [2, 3]. These were reflected in the subsequent International Nomenclature of Disease (IND) in 1991 and in the tenth revision of the International Classification of Diseases (ICD-10) in 1992. The 1985 classification was widely accepted and used internationally even today.

Since last few decades, diagnosis of diabetes is not only limited in blood and urine sugar levels but also in many other parameters and factors such as serum insulin levels, blood glycated haemoglobin and proteins, glucose tolerance ability, insulin sensitivity or insulin resistance, pancreatic beta-cell function, and so forth. Apart from above-mentioned parameters related abnormalities, diabetes patients are often suffered from other diabetes related complications such as—diabetic neuropathy, diabetic cardiomyopathy, diabetic nephropathy (DN), and diabetic retinopathy. These are usually caused by the poor glycemic control or improper management of diabetes mellitus. About 50% of people with diabetes are affected with one or more of the above complications. Amongst others, diabetic neuropathy is one the leading and painful

complications usually suffered by many diabetic patients; however, the pathogenesis of this complication is still not fully understood due to the absence of an authentic animal model which fully mimics the complications of human diabetic neuropathy.

Animal models in diabetes research are very common when most of the existing models are developed as a conventional model either for Type 1 or for T2D. But very often a conventional model of diabetes cannot demonstrate the specific pathogenesis of diabetes related complications. Therefore, the necessity of the individual and specific model for diabetic complications has been raised in the recent years to achieve the authentic outcomes of specific research aims. A number of animal models of diabetic neuropathy have been developed in last few decades approaching from diverse point of views. However, most of them did not receive much popularity because of their considerable number of limitations and disadvantages. In a comprehensive review, Harati [4] reported that the major handicap in studying diabetic neuropathies is the lack of a suitable animal model that addresses acute and chronic events leading to diabetic neuropathy. Hence, in this review, the pathogenesis, advantages, disadvantages, and limitations of several genetic and nongenetic animal models of diabetic neuropathy have been discussed to substantiate their efficacy for human study and in order to guide diabetes research groups to more accurately select the most appropriate models to address their specific research questions.

2. Animal Models in Diabetic Neuropathy

Peripheral diabetic neuropathy (PDN) is a shattering complication of diabetes and leading cause of foot exclusion [5]. Clinical indications of PDN include increased vibration and thermal perception thresholds that progress to sensory loss, occurring in conjunction with degeneration of all fiber types in the peripheral nerve [6]. A proportion of patients with PDN also describe abnormal sensations such as paresthesia, allodynia, hyperalgesia, and spontaneous pain that sometimes coexist with loss of normal sensory function [7]. According to a recent review, a number of studies have investigated and described DN in mice, but it is difficult to compare these studies with each other or with human DN due to experimental differences including the animal strain, type of diabetes, method of induction, duration of diabetes, animal age, and gender [8]. Although two review articles [9, 10] on animal models of diabetic and some other neuropathies are published recently, none of them suggested the most suitable model in order to study the further pathogenesis of diabetic neuropathy and also for the pharmacological screening and development of antidiabetic or anti-neuropathic drug in their reviews. Shaikh and Somani [9] simply reviewed the behavioral, structural, functional, and molecular markers of Type 1 and Type 2 diabetic neurophaty while Höke [10] briefly reviewed the physiological changes in diabetic and some other peripheral neuropathies such as chemotherapy-induced peripheral neuropathy and human-immunodeficiency virus-associated sensory neuropathies. This review precisely discussed the progress with the animal models of diabetic neuropathy which have been developed in last few decades since early 1960s with their advantages, disadvantages, and limitations in order to assist scientists to more appropriately choose a model based on their specific research aims. Additionally, the characterization of neuropathy or advantages and limitations or disadvantages of most of the models are summarized in Table 1.

2.1. Models Developed during 1960s and 1970s. The nerve conduction and regenerative changes in experimental diabetes were first noticed by Eliasson during 1964-1965 [11, 12]; however, the first peripheral neuropathy in alloxan-diabetic rats was reported by Preston in 1967 [13] then Lovelace in 1968 [14]. After that a number of scientists reported diabetic neurophaty mostly in alloxan-induced diabetic models. A complete animal (rat) model of diabetic neuropathy (DN) was first reported by Jakobsen and Lundbeck in 1976 [15] with reduced sizes of nerve fiber, axon, and myelin sheath, which contribute in impaired motor function in streptozotocin (STZ)-induced diabetic rats. After a couple of years, during 1978–1980, animal model of PDN was first reported as well as evaluated by Sima and Robertson in several studies conducted in streptozotocin-induced diabetic rats and mutant diabetic [C57BL/Ks (db/db)] mice [16–18]. The PDN was initially characterized by severely decreased motor nerve conduction velocity (MNCV), absence of large myelinated fibers, and axonal atrophy in this mouse model. In the further evaluation studies, axonal changes as well as axonal dystrophy were observed in the myelinated and unmyelinated fibers followed by loss, shrinkage, and breakdown of myelin sheath in the later stage. However, the major limitation is that none of these models have been evaluated by using anti-diabetic or antineuropathic drugs.

2.2. Models Developed during 1980s. In early 1980s, PDN was assessed in diabetic Chinese hamster by Kennedy and colleagues [19]. Conduction velocities in both motor and sensory components of the hind lamb nerves were reduced 16–22% in diabetic compared to control animals. However, there was no reduction in nerve fiber diameters or other signs of abnormal morphology that could be correlated with these physiological effects. However, PDN in diabetic hamster is less severe than human DN in its clinical stage. Hence, further study is warranted to use this animal as a model for human PDN. Cornblath et al. [20] tried to develop a primate model of PDN in rhesus monkey. They found significantly reduced motor nerve conduction velocities and prolonged F-wave latencies in diabetic animals compared to nondiabetic control animals, while motor-evoked amplitudes did not differ. Additionally, nerve conduction times were increased in motor fibers of diabetic animals two years after the onset of diabetic hyperglycemia. Although these abnormalities are similar to those seen in humans, further study is needed to establish this primate model for human PDN since these models have not been evaluated by any antineuropathic drugs. Additionally, after comparing with diabetic and hypoglycaemic neuropathy, Sima et al. [21] reported that diabetic neuropathy is not associated with nerve cell loss but showed marked axonal

Table 1: Characterization criteria (advantages) and limitations (disadvantages) of some selective animal models of diabetic neuropathy developed since 1960s.

Animals models	References	Characterization of diabetic neuropathy/advantages	Limitations/disadvantages
Streptozotocin-induced rat model (classic)	Jakobsen and Lundbeck [15].	(i) Reduced sizes of nerve fiber, axon, and myelin sheath. (ii) Impaired motor function.	Not validated by antineuropathic drug.
Streptozotocin-induced rat model (recent)	Filho and Fazan [22].	(i) Significantly reduced right and left fascicular areas and myelination of phrenic nerves. (ii) Validated by insulin (s.c.).	(i) Some major pathogenesis of diabetic neuropathy has not been characterized. (ii) Although validated by insulin (s.c.), no antineuropathic drug has been used.
C57BL/Ks (db/db) mice model (classic)	Sima and Robertson [16, 17]; Robertson and Sima [18].	(i) Severely decreased motor nerve conduction velocity (MNCV). (ii) Absence of large myelinated fibers. (iii) Axonal atrophy. (iv) Axonal dystrophy in myelinated and unmyelinated fibers. (v) Loss, shrinkage, and breakdown of myeline sheath.	Not evaluated by any anti-diabetic or antineuropathic drug.
Genetically modified C57BL/Ks (db/db) mice model (recent)	Hinder et al. [23].	(i) Increased body weight, hyperglycemia, and hyperlipidemia. (ii) Lower tail flick response to heat stimulus, sciatic motor nerve conduction velocity, and intraepididymal nerve fiber velocity.	(i) Mismatched results were observed for body weight, blood glucose, plasma lipids, and blood glycated hemoglobin. (ii) Not validated by anti-diabetic or antineuropathic drugs.
Streptozotocin-induced C57BL6/J mice model	Vareniuk et al. [24].	(i) Peroxynitrite injury in peripheral nerve and dorsal root ganglion neurons. (ii) Motor and sensory nerve conduction velocity deficits, thermal and mechanical hyperplasia, tactile allodynia, and loss of intraepidermal nerve fibers.	Not validated by using antineuropathic drug.
Streptozotocin-induced diabetic sensory neuropathic ddY mice model	Murakami et al. [25].	(i) Significantly lower sensory nerve conduction velocity, higher nociceptive threshold, hypoalgesia, and unmyelinated fiber atrophy. (ii) Successfully evaluated by insulin treatment. (iii) Can be a better model to study the human sensory polyneuropathy.	No significant change was found in the myelinated nerve fiber areas.
Chinese hamster neuropathic model	Kennedy et al. [19].	Reduced conduction velocity of both motor and sensory components of hind lamb nerves (16–22%).	(i) Peripheral diabetic neuropathy (PDN) was less severe than human diabetic neuropathy. (ii) Further study needed for proper validation.
Rhesus monkey model of PDN	Cornblath et al. [20].	(i) Significantly reduced motor conduction velocity. (ii) Prolonged F-wave latencies. (iii) Pathogeneses' resembles to humans.	(i) No difference in motor-evoked amplitudes. (ii) Prolonged nerve conduction induction time (2 years). (iii) Not validated by antineuropathic drug.

Table 1: Continued.

Animals models	References	Characterization of diabetic neuropathy/advantages	Limitations/disadvantages
Spontaneously diabetic WBN/Kob rat model	Yagihashi et al. [26].	(i) Slower motor nerve conduction and temporal dispersion of compound muscle action potential. (ii) Structural de- and remyelination in the sciatic and tibial nerves at 12 month. (iii) Axonal degeneration, dystrophy, and reduced myelinated fiber at 20 month. (iv) Resembles human pathogenesis of PDN.	Not validated by antineuropathic drug.
L-fucose induced neuropathic rat model	Sima et al. [27].	(i) Reduced Na^+-K^+-ATPase activity. (ii) Reduced nerve conduction velocity. (iii) Axonal dystrophy. (iv) Paranodal swelling and demyelination without increasing Walleran degeneration of nerve fiber loss.	Not validated by antineuropathic drug.
Partial sciatic nerve ligated rat model	Fox et al. [28].	(i) Produced long-lasting mechanical, but thermal hyperalgesia. (ii) Evaluated by ant-diabetic neuropathic drugs.	Major pathogenesis was not characterized.
Nonobese diabetic (NOD) mice model	Schmidt et al. [29]; Homs et al. [30].	(i) Short induction period. (ii) Markedly swollen axons and dendrites (neurotic dystrophy). (iii) Consistent with the pathogenesis of other rodent models of PDN and human PDN. (iv) Suggested as a better model than ICR mice particularly in terms of nerve regeneration.	Not validated by antineuropathic drug.
Spontaneously induced Ins2 Akita mouse model	Choeiri et al. [31]; Schmidt et al. [32].	(i) Spontaneously induced diabetic model. (ii) Progressive and sustained chronic hyperglycemia. (iii) Reduced sensory nerve conduction velocity. (iv) Markedly swollen axons and dendrites (neurotic dystrophy). (v) Consistent with the pathogenesis of other rodent models of PDN and human PDN.	Not validated by anti-diabetic or antineuropathic drug.
Leptin-deficient (ob/ob) mice model	Drel et al. [6].	(i) Clearly manifested thermal hypoalgesia. (ii) Relatively higher nonfasting blood glucose level (20 mmol/L). (iii) Slow motor and sensory nerve conduction. (iv) Significant reduction of intraepidermal nerve fiber. (v) Validated by antiperipheral diabetic neuropathic drug.	May not be widely available for routine pharmacological screening of anti-diabetic or anti-neuropathic drugs.
Otsuka Long-Evans Tokushima Fatty (OLETF) rats model	Kamenov et al. [33].	(i) Significantly higher blood glucose and HbA1c levels. (ii) Reduced motor nerve conduction velocity and thermal nociception.	(i) Some major pathogenesis of PDN has not been characterized. (ii) Not validated by anti-diabetic neuropathic drugs.
Rat insulin I promoter/human interferon-beta (RIP/IFNβ) transgenic ICR mice model	Serafín et al. [34].	(i) Significantly hyperglycemia, slower tibial sensory nerve conduction velocity. (ii) Reduced nerve fiber density and increased motor latencies.	(i) A sophisticated surgical approach has been used to develop the model. (ii) Not validated by anti-diabetic or antineuropathic drugs.

Table 1: Continued.

Animals models	References	Characterization of diabetic neuropathy/advantages	Limitations/disadvantages
High-fat diet-fed female C57BL6/J mice model	Obrosova et al. [35].	(i) Deficit of motor and sensory nerve conductions, tactile allodynia, and thermal hypoalgesia. (ii) Can be used as model for prediabetic or obesity related neuropathy.	(i) Intradermal nerve fiber loss, and axonal atrophy was absent. (ii) Cannot be used for chronic diabetic neuropathy. (iii) Not validated by antineuropathic drugs.
Surgically-induced neuropathic model	Muthuraman et al. [36].	(i) Thermal and mechanical hyperalgesia in paw and tail. (ii) Reduced nerve fiber density and nerve conduction velocity. (iii) Very short induction period.	(i) Not validated by using antineuropathic drug. (ii) Not suitable to study the human diabetic neuropathy.
Genetically modified SDT fatty rat model	Yamaguchi et al. [37].	(i) Sustained hyperglycemia and dyslipidemia with delayed and reduced motor nerve conduction velocity. (ii) Lower number of sural nerve fibers and thickened epinural arterioles. (iii) Successfully validated by anti-diabetic drug such as pioglitazone.	Some pathogenesis was induced only after a long period of time such as 40 weeks.

atrophy involving predominantly sensory fibers. So this particular factor needs to be considered before choosing any animal model for a diabetic neuropathic study.

2.3. Models Developed during 1990s

2.3.1. Spontaneously Diabetic WBN/Kob Rat Model. In early 1990s, the model of PDN further developed in a spontaneously diabetic WBN/Kob rats via examining electrophysiologic, biochemical, and structural changes of peripheral nerves at 12 and 20 months of ages [26]. This model was characterized by slower motor nerve conduction and temporal dispersion of compound muscle action potential. Structural de- and remyelinations were observed in the sciatic and tibial nerves in 12-month-old rats, while 20-month-old rats additionally showed axonal degeneration and dystrophy, reduced myelinated fiber occupancy, and decreased mean myelinated fiber size. Additionally, these neuropathic manifestations are unique as compared with those found in other spontaneously diabetic animal models. This model of WBN/Kob rats is further supported by Ozaki et al. [38], because this model of PDN develops primary segmental demyelination and secondary axonal degeneration, which are similar to those in human patients with diabetes mellitus and unlike those in rodents with streptozotocin-induced diabetes [38]. Hence, spontaneously diabetic WBN/Kob rats can be a better model to study the human PDN.

2.3.2. L-Fucose-Induced Rat Model. In late 1990s, it has been reported that L-fucose, a competitive inhibitor of sodium-dependent myoinositol transport, has been shown effective to induce diabetic neuropathy in normal rats mediated by Na^+-K^+-ATPase activity and conduction of nerve velocity [27]. To further validate, long-term feeding of L-fucose has been studied in this model and evaluated by nerve Na^+-K^+-ATPase activity, conduction velocity, and myelinated nerve fiber pathology. After 24-week supplementation of L-fucose enriched (10 or 20%) diets, Na^+-K^+-ATPase activity was significantly decreased, associated with a 25–30% reduction in nerve conduction velocity. Twenty percent L-fucose diet resulted in significant axonal atrophy, paranodal swelling, and paranodal demyelination without increasing Walleran degeneration or nerve fiber loss. After this study, it has been recommended that this L-fucose model can serve as an experimental tool to study the diabetic neuropathy.

2.3.3. Partial Sciatic-Nerve Ligated Rat Model. In another study, partial ligation of sciatic nerve method has been used to induce PDN and compared with a usual STZ-induced rat model of PDN [28]. STZ-induced diabetic animals were chronically ill, with reduced growth rate, polyuria, diarrhoea, and enlarged and distended bladders when these symptoms were not found in sciatic nerve ligated model. This sciatic nerve ligated model has also been evaluated with antineuropathic drugs (Morphine and L-Baclofen), which produce greater reversal of mechanical hyperalgesia following partial nerve ligation. They also added that STZ-induced diabetes in rats produces long-lasting mechanical but not thermal hyperalgesia. Although evaluated by antineuropathic drugs, further study is needed to understand the induction of the major pathogenesis of PDN.

2.4. Models Developed during 2000s

2.4.1. Nonobese Diabetic (NOD) Mice Models. Diabetic autonomic neuropathy has been examined in the nonobese diabetic (NOD), and streptozotocin (STZ)-induced diabetic mice, two models of Type 1 diabetes, and the db/db mouse,

a model of Type 2 diabetes [29]. It was found that after only 3–5 weeks of diabetes, NOD mice developed markedly swollen axons and dendrites (neurotic dystrophy) in the prevertebral superior mesenteric and celiac ganglia (SMG-CG), similar to the pathology described in diabetic STZ- and BBW-rat and human. STZ-induced diabetic mice develop identical changes, although at a much slower pace and to a lesser degree than NOD mice. Chronically diabetic Type 2 db/db mice fail to develop neurotic dystrophy, suggesting that hyperglycaemia alone may not be the crucial and sufficient element. Therefore, NOD mouse appears to be a valuable model of diabetic sympathetic autonomic neuropathy which is consistent with the pathogenesis of other rodent models and human. It has been further supported by a very recently published comparative study on peripheral neuropathy between NOD and ICR diabetic mice [30] where NOD mice have been suggested as a better model than ICR mice particularly in terms of nerve regeneration.

2.4.2. Genetic Rodent Models. The development of peripheral diabetic neuropathy has been assessed by longitudinal memory performance in spontaneously induced Type 1 diabetic Ins2C96Y Akita mice by Choeiri et al. [31]. This model was characterized by reduced number of beta cells with hypoinsulinemia, progressive hyperglycemia, and reduced sensory nerve conduction velocity; however no significant deficit has been detected as Morris water maze trial compared to the control group, and many other diabetic neuropathy-related major parameters have not been measured. Later, after measuring a number of diabetic neuropathy related parameters, Schmidt et al. [32] reported that Ins2 Akita mouse is a robust model of diabetic sympathetic autonomic neuropathy which closely corresponds to the characteristics pathology of other rodent models and humans. This model has been evaluated by progressively developed markedly swollen axons and dendrites which are the common signs of neurotic dystrophy. According to the above-mentioned studies, although Ins2 Akita mice can be a proper genetic model of diabetic neuropathy, this model needs to be evaluated by antidiabetic and antineuropathic drugs.

Drel et al. [6] reported that leptin-deficient (ob/ob) mice clearly manifest thermal hypoalgesia, the condition observed in human subjects, which is a transient phenomenon in PDN in humans [39] and, non-fasting blood glucose was not more than 20 mmol/L which was found very higher, ~30 mmol/L, in Zucker Diabetic Fatty (ZDF) rats [39]. The ob/ob mice developed a clearly manifested slow motor and sensory nerve conduction and accumulation of peripheral nerve sorbitol pathway intermediate when fed a regular mouse diet to maintain moderated hyperglycaemia [6]. Usually subject with Type 1 or Type 2 diabetes display epidermal nerve fiber loss, and it was found that 11-week-old ob/ob mice developed a dramatic reduction (78%) in intraepidermal nerve fiber compared with age-matched nondiabetic controls [6]. This animal model was also successfully evaluated by a potent inhibitor of PDN such as aldose reductase inhibitor which normalized motor and sensory nerve conduction velocity. The results of this study suggest that leptin-deficient ob/ob mice can be better for PDN.

On the other hand, Kamenov et al. [33] compared the complications of diabetic neuropathy between Otsuka Long-Evans Tokushima Fatty (OLETF) rats and Long-Evans Tokushima Otsuka (LETO) rats, where OLETF is a spontaneous animal model of T2D. In this regard, each type of animal has been divided into 2 subgroups and fed with or without sucrose-containing diets for 2 months and found that the blood glucose and HbA1c levels were significantly higher in OLETF rats, when compared with those in control LETO rats. Motor nerve conduction velocity and thermal nociception were significantly decreased in OLETF rats in their 10 months of age, while the values of the tail pressure test did not differ compared with those from LETO rats. It was concluded that signs of diabetic neuropathy appear in LETO rats after a longer period of time compared to OLETF rats. Therefore OLETF rat can be a better animal model for Type 2 diabetic neuropathy than the LETO rats.

Recently, Serafín et al. [34] developed a model of diabetic neuropathy in 6-week-old rat insulin I promoter/human interferon-beta (RIP/IFNβ) transgenic ICR mice with a low dose of STZ injection (30 mg/kg BW) for 5 consecutive days. Additionally, in order to induce nerve damage, after 4 weeks of sustained hyperglycemia, the left sciatic nerve was exposed by blunt dissection and crushed at the femur major trochanter level for three times in succession for 30 seconds in anaesthetized animals when intact contralateral nerve was used as a control. This transgenic model was evaluated by significant hyperglycemia, slower tibial sensory nerve conduction velocity (SNCV) and increased motor latencies and duration of compound muscle potential, reduced nerve fiber density, and so on. The slower recovery of nerve conduction velocities were observed in the diabetic transgenic mice group compared to the control. Although this model has been displayed most of the major pathogenesis of peripheral diabetic neuropathy, a sophisticated surgical approach has been used with multiple STZ injections to develop this model, and it has not been evaluated by any antidiabetic or antineuropathic drugs.

2.4.3. Experimentally-Induced Models. Filho and Fazan [22] developed a streptozotocin (STZ)-induced model of phrenic nerve neuropathy in rats. Diabetes was induced by a single injection of streptozotocin to penile vein, and higher blood glucose level confirmed the diabetic state. Left and right fascicular areas and diameter of the phrenic nerves were significantly decreased in the proximal segments and right segments, respectively. The phrenic nerves of diabetic rats showed smaller myelinated axon diameters compared to controls. The g ratio for diabetic rats was significantly lower than the controls when these changes have been restored by the daily injection (s.c.) of insulin (9 U/kg body weight). Although this model has been evaluated by insulin, no antineuropathic drug has been used for the evaluation of this model.

After a year, Obrosova and colleagues [35] tried to develop a neuropathy model in female C57BL6/J mice by feeding high-fat diet for a 16-week period. This model was characterized by the deficit of motor and sensory nerve conductions, tactile allodynia, and thermal hypoalgesia; however intradermal nerve fiber loss or axonal atrophy was absent in

this model. Although plasma FFA and insulin concentrations were increased and glucose tolerance was impaired, the frank hyperglycemia was absent in this model. According to the data, although this model can be used for prediabetes and obesity related neuropathy, it cannot be used for chronic diabetic neuropathy. This model has also not been evaluated by any antineuropathic drug, and the duration of model development time is one of the major concerns.

In 2008, Hong and Kang [40] published a very special finding on auditory neuropathy in streptozotocin-induced diabetic ICR mice in order to understand the possible auditory damage. The diabetes was induced by the different dosages of STZ (50, 100, and 150 mg/kg BW) dissolved in citrate buffer (pH 4.5) in 7-week-old male animals. The auditory diabetic neuropathy in this particular model has been evaluated by significantly increased absolute latencies of IV, and the interpeak latencies of I–III and I–IV of auditory brainstem response (ABR), and dose dependent induction of Pa latency of auditory middle latency response (AMLR) in STZ treated mice compared to control mice. In terms of ABR, best results were observed for the dose of 100 mg/kg BW of STZ compared to other two STZ dosages. From the data of this study, authors suggested that the STZ-induced mouse can be used for the evaluation of auditory pathway impairment via ABR and AMLR tests, however this model has not been evaluated by any antidiabetic or antineuropathic drugs.

At the same year, Vareniuk et al. [24] compared the pathogenesis of peripheral diabetic neuropathy in STZ-induced wild-type and inducible nitric oxide synthase (iNOS) gene deficient mice with C57BL6/J background. The model was developed by injecting single doses (100 mg/kg BW) of STZ injection (i.p.) to nonfasted wild-type and iNOS (also known as Nos2) deficient (iNos (−/−)) mice and maintained for a 6-week experimental period. Although STZ-injected wild-type mice displayed peroxynitrite injury in peripheral nerve and dorsal root ganglion neurons and developed motor and sensory nerve conduction velocity deficits, thermal and mechanical hypoalgesia, tactile allodynia, and approximately 36% loss of intraepidermal nerve fibers, the STZ-injected iNOS (−/−) mice did not display most of the above-mentioned pathogenesis except nitrosative stress in dorsal root ganglia with normal nerve conduction velocities and less severe small fiber sensory neuropathy. Although the STZ injected model was not evaluated by any antidiabetic or antineuropathic drugs, but from this study it is clear that iNOS gene plays a major role in the induction or peripheral diabetic neuropathy which can be future research and drug development target.

Recently, Muthuraman and colleagues [36] developed a rat model of vasculatic neuropathy by ischemic perfusion in the rat femoral artery. This model was validated after 2, 4, and 6 h of ischemia followed by prolonged reperfusion. The model has been characterized by thermal and mechanical hyperalgesia in paw and tail which are associated with peripheral and central neuropathic pain, respectively. The serum IL-10, nerve fiber density, and nerve conduction velocity were lower, and serum nitrate, malondialdehyde (MDA) and TNF-alpha levels were higher in this model. Although neuropathy induction period of this model is very short and has similar pathogenesis with human diabetic neuropathy, the pathogenesis of neuropathy have not been developed here via hyperglycaemia, what is usually happened in diabetic neuropathy, but via ischemic perfusion in the animal femoral artery. Hence, this model cannot be a better model to study human peripheral diabetic neuropathy. Additionally, this model has not been evaluated by using any antineuropathic drugs.

2.5. Models Developed during 2010s

2.5.1. Genetically Modified SDT Rat Model. Recently, Yamaguchi et al. [37] developed diabetic peripheral neuropathy in Spontaneously Diabetic Torii (SDT) fatty rats by introducing *fa* allele of Zucker Diabetic Fatty (ZDF) rats since SDT rats develop delayed hyperglycemia compared to diabetic complications. Apart from common diabetic abnormalities such as sustained hyperglycemia and dyslipidemia, this diabetic peripheral neuropathic model was further characterized by significantly delayed and lower motor nerve conduction velocity from 24 weeks and significantly lower number of sural nerve fibers at the end of the 40-week experimental period. Additionally, thickened epineurial arterioles were frequently found in this model. This model was further evaluated by an antidiabetic drug such as pioglitazone which could significantly improve the motor nerve conduction velocity and blood HbA1c level when fed food admixture at a dose of 10 mg/kg/day for a 6-week period. So this model can be a better diabetic peripheral neuropathic model not only to understand the pathogenesis of diabetic peripheral neuropathy but also to screen and develop antidiabetic peripheral neuropathic drug, particularly for Type 2 diabetes.

2.5.2. Genetically Modified C57BLKS Mice Model. Very recently, Hinder et al. [23] developed a dyslipidemia-induced mouse model of diabetic neuropathy by some genetic manipulation. This model was developed by knockout of ApoE and ApoB48 genes in db/db or ob/ob mice C57BLKS background which mimicked the neuropathic plasma lipid profile in diabetic humans. It was also characterized by increased body weight, hyperlipidemia, hyperglycemia, and the evidence of neuropathy; however this model was not delivered by lipid profile usually seen in translational diabetic neuropathy. Although this model has been characterized by significantly lower tail flick response to heat stimulus, sciatic motor nerve conduction velocity, and intraepididymal nerve fiber velocity, mismatched results were observed for the body weight, blood glucose, plasma lipids, and total blood glycated haemoglobin. From the results of this study, authors suggested that the overall effects of ApoE knockout, either directly upon nerve structure and function or indirectly on lipid metabolism, are insufficient to significantly alter the course of translational diabetic neuropathy research, and further therapeutic intervention is necessary in this regard. Apart from the above limitations, this model was also not evaluated by any antidiabetic or antineuropathic drug.

2.5.3. Streptozotocin-Induced Diabetic Sensory Neuropathy Mice Model. Most recently, Murakami et al. [25] developed

a sensory neuropathy model in STZ-induced 8-week-old ddY mice. Diabetes was developed by a single injection (i.p.) of STZ and confirmed by blood glucose level >16.7 mmol/L one week after the STZ injection. This model has been evaluated by significantly lower sensory nerve conduction velocity (SNCV), higher nociceptive threshold, hypoalgesia, and reduced axon area of unmyelinated nerve fibers or unmyelinated fiber atrophy. Although no difference was found for the myelinated nerve fiber areas between the diabetic and healthy mice, this model has been successfully evaluated by insulin treatment. Since the unmyelinated nerve fibers were more affected than myelinated nerve fibers and it has been successfully evaluated with insulin treatment, so it can be a better model to study the human sensory polyneuropathy.

3. Conclusion

As per this review, although a number of approaches have been used to develop the diabetic neuropathic models in different strains of animals in last five decades, none of them are without limitations. Several models such as conventional and genetically modified C57BL/Ks (db/db) mice, streptozotocin-induced C57BL6/J and ddY mice, spontaneously diabetic WBN/Kob rats, L-fucose induced neuropathic rats, nonobese diabetic (NOD) rats, spontaneously induced InS2 Akita mice, leptin-deficient (ob/ob) mice, high-fat diet-fed female C57BL6/J mice, and genetically modified SDT fatty rats have been shown to develop major pathogenesis of diabetic neuropathy or peripheral diabetic neuropathy; however most of them were not validated either by antidiabetic or antineuropathic drugs. Some models such as streptozotocin-induced rats, Chinese hamster, rhesus monkey, partial sciatic nerve ligated rats, and Otsuka Long-Evans Tokushima Fatty (OLETF) rats developed very few major or some minor pathogenesis of diabetic neuropathy and peripheral diabetic neuropathy and the model development time for some of these models were very long. The best model of diabetic neuropathy or peripheral diabetic neuropathy should have some major criteria such as: (1) the model should have all major pathogenesis of diabetic neuropathy or PDN with other minor pathogenesis which is normally found in human diabetic neuropathic patients, (2) the model should be sensitive to antidiabetic or anti-neuropathic drugs, and (3) the model needs to be suitable to study the pathogenesis of disease as well as for routine pharmacological screening of antidiabetic anti-neuropathic drugs. Although most of the genetic or genetically modified models of diabetic neuropathy or PDN discussed in this review are suitable for studying the pathogenesis of the diseases, the C57BL/Ks (db/db) mice, streptozotocin-induced C57BL6/J and ddY mice, spontaneously diabetic WBN/Kob rats, nonobese diabetic mice, spontaneously induced Ins2 Akita mice, and leptin-deficient (ob/ob) mice have been found as better models for human diabetic neuropathy when high-fat diet-fed female C57BL6/J mice have been suggested to use for prediabetic or obesity related diabetic neuropathy. Although L-fucose induced neuropathic rats, OLETF rats, and genetically modified SDT rats have shown some promising pathogenesis of diabetic and PDN, further studies are needed to understand the suitability and usefulness of these models for diabetic or peripheral diabetic neuropathic researches.

List of Abbreviations (in Alphabetical Order)

DN: Diabetic neuropathy
GDM: Gestational diabetes mellitus
ICD: International classification of diseases
IDDM: Insulin dependent diabetes mellitus
IFN: Interferon
IGT: Impaired glucose tolerance
IND: International nomenclature of diseases
iNOS: Inducible nitric oxide synthase
LETO: Long Evans Tokushima obese
MNCV: Motor nerve conduction velocity
MRDM: Malnutrition related diabetes mellitus
NIDDM: Noninsulin dependent diabetes mellitus
NOD: Nonobese diabetic
OLETF: Otsuka long Evans Tokushima fatty
PDN: Peripheral diabetic neuropathy
SDT: Spontaneously diabetic torii
SNCV: Sensory nerve conduction velocity
STZ: Streptozotocin
T2D: Type 2 diabetes
WHO: World health organization
ZDF: Zucker diabetic fatty.

Acknowledgments

This work was supported by a Competitive Research Grant from Research Office of the University of KwaZulu-Natal, Durban and an Incentive Grant for Rated Researchers and a Grant Support for Women and Young researchers from the National Research Foundation (NRF), Pretoria, South Africa.

References

[1] A. M. Ahmed, "History of diabetes mellitus," *Saudi Medical Journal*, vol. 23, no. 4, pp. 373–378, 2002.

[2] *WHO Expert Committee on Diabetes Mellitus. Second Report*, vol. 646 of *WHO Technical Report Series*, Geneva, Switzerland, 1980.

[3] World Health Organization (WHO), *DiAbetes Mellitus: Report of a WHO Study Group*, vol. 727 of *WHO Technical Report Series*, Geneva, Switzerland, 1985.

[4] Y. Harati, "Diabetic neuropathies: unanswered questions," *Neurologic Clinics*, vol. 25, no. 1, pp. 303–317, 2007.

[5] A. J. M. Boulton, "The diabetic foot: from art to science. The 18th Camillo Golgi lecture," *Diabetologia*, vol. 47, no. 8, pp. 1343–1353, 2004.

[6] V. R. Drel, N. Mashtalir, O. Ilnytska et al., "The leptin-deficient (ob/ob) mouse: a new animal model of peripheral neuropathy of type 2 diabetes and obesity," *Diabetes*, vol. 55, no. 12, pp. 3335–3343, 2006.

[7] N. A. Calcutt, "Potential mechanisms of neuropathic pain in diabetes," *International Review of Neurobiology*, vol. 50, pp. 205–228, 2002.

[8] K. A. Sullivan, S. I. Lentz, J. L. Roberts Jr., and E. L. Feldman, "Criteria for creating and assessing mouse models of diabetic neuropathy," *Current Drug Targets*, vol. 9, no. 1, pp. 3–13, 2008.

[9] A. S. Shaikh and R. S. Somani, "Animal models and biomarkers of neuropathy in diabetic rodents," *Indian Journal of Pharmacology*, vol. 42, no. 3, pp. 129–134, 2010.

[10] A. Höke, "Animal models of peripheral neuropathies," *Neurotherapeutics*, vol. 9, no. 2, pp. 262–269, 2012.

[11] S. G. Eliasson, "Nerve conduction changes in experimental diabetes," *The Journal of Clinical Investigation*, vol. 43, pp. 2353–2358, 1964.

[12] S. G. Eliasson, "Regenerative processes in experimental diabetic neuropathy," *Transactions of the American Neurological Association*, vol. 90, pp. 35–37, 1965.

[13] G. M. Preston, "Peripheral neuropathy in the alloxan-diabetic rat," *Journal of Physiology*, vol. 189, no. 2, 1967.

[14] R. E. Lovelace, "Experimental neuropathy in rats made diabetic with alloxan," *Electroencephalography and Clinical Neurophysiology*, vol. 25, no. 4, p. 399, 1968.

[15] J. Jakobsen and K. Lundbeck, "Neuropathy in experimental diabetes: an animal model," *British Medical Journal*, vol. 2, no. 6030, pp. 278–279, 1976.

[16] A. A. F. Sima and D. M. Robertson, "Peripheral neuropathy in mutant diabetic mouse [C57BL/Ks(db/db)]," *Acta Neuropathologica*, vol. 41, no. 2, pp. 85–89, 1978.

[17] A. A. F. Sima and D. M. Robertson, "Peripheral neuropathy in the diabetic mutant mouse. An ultrastructural study," *Laboratory Investigation*, vol. 40, no. 6, pp. 627–632, 1979.

[18] D. M. Robertson and A. A. F. Sima, "Diabetic neuropathy in the mutant mouse [C57BL/ks(db/db)]. A morphometric study," *Diabetes*, vol. 29, no. 1, pp. 60–67, 1980.

[19] W. R. Kennedy, D. C. Quick, T. Miyoshi, and G. C. Gerritsen, "Peripheral neurology of the diabetic Chinese hamster," *Diabetologia*, vol. 23, no. 5, pp. 445–451, 1982.

[20] D. R. Cornblath, M. A. Hillman, J. S. Striffler, C. N. Herman, and B. C. Hansen, "Peripheral neuropathy in diabetic monkeys," *Diabetes*, vol. 38, no. 11, pp. 1365–1370, 1989.

[21] A. A. F. Sima, W.-X. Zhang, and D. A. Greene, "Diabetic and hypoglycemic neuropathy—a comparison in the BB rat," *Diabetes Research and Clinical Practice*, vol. 6, no. 4, pp. 279–296, 1989.

[22] O. A. R. Filho and V. P. S. Fazan, "Streptozotocin induced diabetes as a model of phrenic nerve neuropathy in rats," *Journal of Neuroscience Methods*, vol. 151, no. 2, pp. 131–138, 2006.

[23] L. M. Hinder, A. M. Vincent, J. M. Hayes, L. L. McLean, and E. L. Feldman, "Apolipoprotein E knockout as the basis of mouse models of dyslipidemia-induced neuropathy," *Experimental Neurology*, vol. 293, pp. 102–110, 2013.

[24] I. Vareniuk, I. A. Pavlov, and I. G. Obrosova, "Inducible nitric oxide synthase gene deficiency counteracts multiple manifestations of peripheral neuropathy in a streptozotocin-induced mouse model of diabetes," *Diabetologia*, vol. 51, no. 11, pp. 2126–2133, 2008.

[25] T. Murakami, T. Iwanaga, Y. Ogawa et al., "Development of sensory neuropathy in streptozotocin-induced diabetic mice," *Brain and Behavior*, vol. 3, no. 1, pp. 35–41, 2013.

[26] S. Yagihashi, R.-I. Wada, M. Kamijo, and K. Nagai, "Peripheral neuropathy in the WBN/Kob rat with chronic pancreatitis and spontaneous diabetes," *Laboratory Investigation*, vol. 68, no. 3, pp. 296–307, 1993.

[27] A. A. F. Sima, J. A. Dunlap, E. P. Davidson et al., "Supplemental myo-inositol prevents L-fucose-induced diabetic neuropathy," *Diabetes*, vol. 46, no. 2, pp. 301–306, 1997.

[28] A. Fox, C. Eastwood, C. Gentry, D. Manning, and L. Urban, "Critical evaluation of the streptozotocin model of painful diabetic neuropathy in the rat," *Pain*, vol. 81, no. 3, pp. 307–316, 1999.

[29] R. E. Schmidt, D. A. Dorsey, L. N. Beaudet et al., "Non-obese diabetic mice rapidly develop dramatic sympathetic neuritic dystrophy: a new experimental model of diabetic autonomic neuropathy," *American Journal of Pathology*, vol. 163, no. 5, pp. 2077–2091, 2003.

[30] J. Homs, L. Ariza, G. Pagès et al., "Comparative study of peripheral neuropathy and nerve regeneration in NOD and ICR diabetic mice," *Journal of the Peripheral Nervous System*, vol. 16, no. 3, pp. 213–227, 2011.

[31] C. Choeiri, K. Hewitt, J. Durkin, C. J. Simard, J.-M. Renaud, and C. Messier, "Longitudinal evaluation of memory performance and peripheral neuropathy in the Ins2C96Y Akita mice," *Behavioural Brain Research*, vol. 157, no. 1, pp. 31–38, 2005.

[32] R. E. Schmidt, K. G. Green, L. L. Snipes, and D. Feng, "Neuritic dystrophy and neuronopathy in Akita (Ins2Akita) diabetic mouse sympathetic ganglia," *Experimental Neurology*, vol. 216, no. 1, pp. 207–218, 2009.

[33] Z. Kamenov, H. Higashino, M. Todorova, N. Kajimoto, and A. Suzuki, "Physiological characteristics of diabetic neuropathy in sucrose-fed Otsuka Long-Evans Tokushima fatty rats," *Methods and Findings in Experimental and Clinical Pharmacology*, vol. 28, no. 1, pp. 13–18, 2006.

[34] A. Serafín, J. Molín, M. Márquez et al., "Diabetic neuropathy: electrophysiologicaland morphological study of peripheral nerve degenerationand regeneration in transgenic mice that express IFNβ in β cells," *Muscle and Nerve*, vol. 41, no. 5, pp. 630–641, 2010.

[35] I. G. Obrosova, O. Ilnytska, V. V. Lyzogubov et al., "High-fat diet-induced neuropathy of pre-diabetes and obesity: effects of "healthy" diet and aldose reductase inhibition," *Diabetes*, vol. 56, no. 10, pp. 2598–2608, 2007.

[36] A. Muthuraman, M. Ramesh, and S. Sood, "Development of animal model for vasculatic neuropathy: induction by ischemic-reperfusion in the rat femoral artery," *Journal of Neuroscience Methods*, vol. 186, no. 2, pp. 215–221, 2010.

[37] T. Yamaguchi, T. Sasase, Y. Mera et al., "Diabetic peripheral neuropathy in spontaneously diabetic tori-Lepr (fa) (SDT Faty) rats," *Journal of Veterinary Medical Science*, vol. 74, no. 12, pp. 1669–1673, 2012.

[38] K. Ozaki, K. Miura, M. Tsuchitani, and I. Narama, "Peripheral neuropathy in the spontaneously diabetic WBN/Kob rat," *Acta Neuropathologica*, vol. 92, no. 6, pp. 603–607, 1996.

[39] P. J. Dyck, P. J. B. Dyck, J. A. Velosa, T. S. Larson, and P. C. O'Brien, "Patterns of quantitative sensation testing of hypoesthesia and hyperalgesia are predictive of diabetic polyneuropathy: a study of three cohorts," *Diabetes Care*, vol. 23, no. 4, pp. 510–517, 2000.

[40] B. N. Hong and T. H. Kang, "Auditory neuropathy in streptozotocin-induced diabetic mouse," *Neuroscience Letters*, vol. 431, no. 3, pp. 268–272, 2008.

Hindawi Publishing Corporation
Journal of Diabetes Research
Volume 2013, Article ID 342479, 9 pages
http://dx.doi.org/10.1155/2013/342479

Research Article

IL-10 Induction from Implants Delivering Pancreatic Islets and Hyaluronan

Paul L. Bollyky,[1] Robert B. Vernon,[2] Ben A. Falk,[1] Anton Preisinger,[2] Michel D. Gooden,[2] Gerald T. Nepom,[2] and John A. Gebe[2]

[1] *Division of Infectious Diseases and Geographic Medicine, Department of Medicine, Stanford University School of Medicine, Grant Building, 300 Pasteur Drive, Stanford, CA 94305-5107, USA*
[2] *Benaroya Research Institute, 1201 Ninth Avenue, Seattle, WA 98101-2795, USA*

Correspondence should be addressed to John A. Gebe; jgebe@benaroyaresearch.org

Received 5 February 2013; Revised 8 June 2013; Accepted 13 June 2013

Academic Editor: Shahidul Islam

Local induction of pro-tolerogenic cytokines, such as IL-10, is an appealing strategy to help facilitate transplantation of islets and other tissues. Here, we describe a pair of implantable devices that capitalize on our recent finding that hyaluronan (HA) promotes IL-10 production by activated T cells. The first device is an injectable hydrogel made of crosslinked HA and heparan sulfate loaded with anti-CD3/anti-CD28 antibodies and IL-2. T cells embedded within this hydrogel prior to polymerization go on to produce IL-10 *in vivo*. The second device is a bioengineered implant consisting of a polyvinyl alcohol sponge scaffold, supportive collagen hydrogel, and alginate spheres mediating sustained release of HA in fluid form. Pancreatic islets that expressed ovalbumin (OVA) antigen were implanted within this device for 14 days into immunodeficient mice that received OVA-specific DO.11.10 T cells and a subsequent immunization with OVA peptide. Splenocytes harvested from these mice produced IL-10 upon re-challenge with OVA or anti-CD3 antibodies. Both of these devices represent model systems that will be used, in future studies, to further evaluate IL-10 induction by HA, with the objective of improving the survival and function of transplanted islets in the setting of autoimmune (type 1) diabetes.

1. Introduction

Interleukin 10 (IL-10) is a potent immunosuppressive cytokine made by regulatory T cells (Tregs) and other cell types [1–3]. IL-10 inhibits antigen-specific immune responses in part *via* suppression of activated macrophage and monocyte functions, which include cytokine synthesis and expression of class II MHC and costimulatory molecules such as IL-12 and CD80/CD86 [4].

IL-10 has important roles in transplant biology. Endogenous IL-10 production is correlated with transplant acceptance in multiple animal models and human tissues [5–8]. IL-10 has been evaluated as a treatment to improve the survival of engrafted islets, which has been accomplished by transfer of IL-10-producing Tregs [6], gene therapy [9, 10] or direct administration of IL-10 alone, or in conjunction with immunomodulatory drugs [11–13]. It is noteworthy that systemic IL-10 treatment has failed to support islet engraftment in mice in the setting of established autoimmunity [14] and may induce immune suppression. These results suggest that an alternative approach that provides a sustained, local presence of IL-10 at the graft site might be more effective at preventing islet rejection.

We recently reported a role for the extracellular matrix (ECM) macromolecule *hyaluronan* (HA) in regulating IL-10 production by T cells. HA is a simple, long-chain glycosaminoglycan polymer made up of repeating disaccharides of N-acetyl glucosamine and glucuronic acid. HA is an important structural component of many tissues, but also has important roles in inflammation and tissue repair [15–18]. Short HA oligomers (<30 kDa) generated through tissue catabolism are typically proinflammatory [16–18]. Conversely, plate-bound HA or chemically crosslinked HA is anti-inflammatory and promotes IL-10 production by FoxP3(+)

natural Tregs (nTregs) [19] and conventional T cells *in vitro* [20]. Induction of IL-10 in these systems was mediated by crosslinking of CD44, the primary receptor for HA [20]. We have proposed that plate-bound HA and HA hydrogels may function as biomimetics of HA-containing tissue matrices. However, the minimum size for HA-mediated CD44 crosslinking and IL-10 production by T cells is unknown. Additional support for a role for HA in IL-10 production is provided by observations of HA-induced upregulation of IL-10 by cultured synoviocytes [21] and elevated IL-10 levels in intestinal biopsies of mice given oral HA [22]. However, HA alone does not appear to promote IL-10 induction by T cells *in vitro*. Indeed, our data suggest that concomitant antigenic stimulation through the T cell receptor (TCR) complex is required for efficient IL-10 induction in the presence of HA.

HA preparations are currently used as treatments for arthritis [23], atopic dermatitis [24], prevention of abdominal adhesions [25, 26] and are under evaluation as an experimental treatment for burns and wounds [27, 28]. In most of these preparations, HA is crosslinked to promote its stability and efficacy [29]. Crosslinking (as well as plate-binding or sustained release from alginate) may also limit the generation of pro-inflammatory HA fragments. Building upon these findings, we have evaluated whether HA has utility in promoting IL-10 production *in vivo*.

Here, we describe and evaluate a pair of technologies that both provide antigenic stimulation in the context of HA. First, we have asked whether cells implanted within a crosslinked HA hydrogel that incorporates a supplemental complex to induce polyclonal TCR stimulation could enhance production of IL-10 *in vivo*. Second, we have developed a bioengineered implant capable of delivering an antigenic signal along with sustained release of HA in fluid form. These technologies represent parallel strategies for delivering HA as a medium to promote IL-10 production *in vivo*, with the ultimate objective of inducing durable immune tolerance to transplanted islets in individuals with autoimmune diabetes.

2. Materials and Methods

2.1. Transgenic Mice. C57BL/6 green fluorescent protein (GFP)-FoxP3 knock-in and RIPmOVA/Rag2$^{-/-}$ mice were the kind gifts of Dr. A. Rudensky (Memorial Sloan-Kettering Cancer Center, New York, NY, USA) and Dr. Steve Ziegler (Benaroya Research Institute—BRI), respectively. DO11.10 mice were purchased from Taconic Farms. All mice were maintained in a specific pathogen-free, AAALAC-accredited facility at BRI, and all experiments were approved by the BRI Institutional Animal Care and Use Committee (IACUC), protocol approval number 10116.

2.2. Isolation of Leukocyte Populations. Mouse lymphocyte populations were prepared as previously described [19]. In brief, for the *in vitro* experiments, CD4(+) cells were isolated using MACS kits (Miltenyi, Inc.), and the GFP-FoxP3(−) fraction was isolated from the CD4(+) population using a FACS Vantage cell-sorter (BD Biosciences). CD4(+)/GFP-FoxP3(−) T cells were used to ensure that any IL-10 production we measured would be from conventional T cells, rather than from activated GFP-FoxP3(+) nTregs. Cells were cultured in Opti-MEM (Invitrogen) serum-free media supplemented with 100 μg/mL penicillin and 100 U/mL streptomycin (P/S). Where specifically noted, cells were cultured in complete media consisting of Dulbecco's Modified Eagle's Medium (DMEM)-10 (Invitrogen) supplemented with 10% fetal bovine serum (FBS) (Hyclone), P/S, 50 μM β-mercaptoethanol, 2 mM glutamine, and 1 mM Na pyruvate (Invitrogen).

2.3. In Vitro T Cell Activation Using Plate-Bound Antibodies and HA. Cell culture plates (96-well) were coated with 0.5 μg/mL of anti-CD3 antibody (145-2C11, BD Biosciences), washed, and then subsequently coated with either 0.2 mg/mL bovine serum albumin (BSA)- conjugated HA (1.5×10^6 Da) HA (Genzyme) or 10% BSA. CD4(+)/GFP-FoxP3(−) T cells (2×10^5 per well) were cultured for 96 hours on these plates, followed by collection of the culture supernatants for analysis. Measurement of cytokines in the cell culture supernatants was performed using enzyme-linked immunosorbent assays (ELISAs) or cytometric bead assays (BD Biosciences).

2.4. In Vitro T Cell Activation Using HA Hydrogels. Hydrogels were made from thiolated constituents (HA, heparin sulfate [HS], and collagen) crosslinked with polyethylene glycol S-S diacrylate (PEGSSDA). These reagents are available as a kit (Extracel-HP, Glycosan/Biotime) and were used per the manufacturer's instructions. Of note, our understanding from communications with the manufacturer is that HA of $> 1 \times 10^6$ Da is used in the kits. Prior to addition of the crosslinker, the mixture was supplemented with 10 μg/mL of streptavidin (Sigma Aldrich), 10 μg/mL each of biotinylated anti-CD3 and anti-CD28 antibodies (145-2C11, 37.51, BD Biosciences), and 20 IU/mL of IL-2. Hydrogels of this formulation are referred to here as *"supplemented HA hydrogels."* For *in vitro* cell culture experiments, 2×10^5 CD4(+)/GFP-FoxP3(−) T cells were layered on top of 25 μL volumes of the hydrogel. After 96 hours of culture, cells and culture supernates were collected for analysis. To control the collagen constituent of the HA hydrogels, a set of hydrogels lacking HA/HS was made by replacing the thiolated HA/HS with an equivalent volume of thiolated collagen. These controls are referred to as *"supplemented collagen hydrogels."*

2.5. Implantation of T Cells and HA. 3×10^6 CD4(+)/GFP-FoxP3(−) T cells were dispersed in supplemented HA hydrogels of 300 μL volume prior to crosslinking with PEGSSDA, which was initiated 30 min prior to intraperitoneal injection into mice. For these studies *in vivo*, the supplemented HA hydrogels incorporated 360 IU/mL of IL-2. Four days after injection of the supplemented HA hydrogels, the mice were sacrificed and lymphoid tissues were harvested. Residual hydrogel material in the peritoneal cavity was also removed and dissolved by mild reduction of the PEGSSDA (per the manufacturer's instructions) in order to retrieve cells for analysis. Intracellular staining of these cells for IL-10 and subsequent flow cytometry assays utilized antibodies and equipment as previously described [19].

2.6. Isolation of Islets. Islets were isolated as described previously [30]. Briefly, C57Bl/6 mice of 12–24 weeks age were anesthetized with 2,2,2-tribromoethanol in phosphate-buffered saline (PBS). The descending aorta of each anesthetized mouse was transected, the bile duct clamped at its distal (intestinal) end, and a 30-gauge needle was used to inflate each pancreas through the common bile duct with 4 mL of 4°C *Islet Medium* comprised of RPMI 1640 containing 1.0 g $NaHCO_3$, 10% FBS (Atlanta Biologicals, cat. number S12450H), 1 mM Na-pyruvate, and P/S. The Islet Medium was supplemented with 0.8 mg/mL of collagenase P (Roche, cat. number 11-249-002-001) and filtered at 0.22 μm prior to injection. Subsequently, 2-3 excised pancreata were placed in separate 50 mL conical centrifuge tubes and incubated in 5 mL of Islet Medium for 13 min at 37°C. The medium was then decanted, fresh 4°C Islet Medium was added, and the tubes were shaken vigorously to disrupt the pancreata. The tissue suspensions were filtered through a 30-mesh metal screen to remove large debris, the filtrates were pelleted by centrifugation, and the pellets resuspended in 4°C Islet Medium. The resuspended material was centrifuged through Histopaque 1077 to isolate the islets, which were washed, resuspended in Islet Medium, and placed in a tissue culture (TC) incubator. After all pancreata were processed, the isolated islets were hand picked, cultured overnight, and picked again the next day before being placed in bioengineered implants. Average yields were 100–150 islets per mouse.

2.7. Fabrication of Bioengineered Implants (BIs)

2.7.1. Polyvinyl Alcohol (PVA) Scaffolds. Biopsy punches (Sklar Instruments) were used to cut 10 mm diameter disks from 2 mm thick sheets of PVA sponge (Type CF90, 500 μm average pore size with no surfactant treatment—a generous gift from Merocel/Medtronic, Inc.). Subsequently, each disk was through-punched with a single central hole of 2 mm diameter and six peripheral holes of 1.5 mm diameter, using correspondingly sized biopsy punches (Acuderm, Inc.). The punched disks were washed 5 × 10 min on a rocker in 50 mL centrifuge tubes filled with 40 mL of sterile distilled water, then air-dried on Whatman filter paper, transferred to 60 mm dishes, sterilized by gamma irradiation, and stored until needed for BI assembly.

2.7.2. Type I Collagen Solution. One volume of a stock solution of rat tail native type I collagen in dilute (0.02 N) acetic acid (BD Biosciences) was combined with 1/9 volume of 10-strength $NaHCO_3$-saturated Medium 199 (Invitrogen) and sufficient DMEM and normal mouse serum (NMS) to yield a working solution containing 2.5 mg/mL collagen and 10% NMS [30]. The working solution was prepared just prior to assembly of the BIs and kept on ice until needed.

2.7.3. Alginate Spheres. An aqueous stock solution of 4% alginate (Sigma-Aldrich, cat. number A0682), filtered at 0.45 μm, was used for preparation of spheres for sustained release of vascular endothelial growth factor (VEGF) and HA. Spheres incorporating human recombinant $VEGF_{165}$ (Peprotech, cat. number 100-20) were prepared as described previously [30]. Briefly, a mixture of 2% alginate and 5 ng/μL VEGF was formed into 10 μL (2.2 mm diameter) spheres using a gravity-drop method, crosslinked into a hydrogel for 15 min in 0.1 M $CaCl_2$, washed 2 × 2 min in 0.15 M NaCl/25 mM HEPES/2 mM $CaCl_2$, pH 7.2 (saline/HEPES/Ca), transferred to serum-free DMEM/P/S, and kept in a tissue culture incubator until needed for BI assembly.

Fabrication of HA spheres was similar to that of the VEGF constructs, with replacement of the VEGF with 50 μg of 120 kDa HA (Genzyme). HA of this size (approximately 317 disaccharide units) was chosen to facilitate a complete delivery of HA from the spheres within a 2 week experimental time period.

2.7.4. Assembly of BIs. Dry PVA sponge scaffolds were allowed to swell for 5 min in sterile DMEM/P/S. Subsequently, a single, freshly prepared alginate sphere containing VEGF and five spheres containing HA were gently pressed into the 6 peripheral holes of each expanded scaffold. The scaffolds were then blotted on sterile Whatman filter paper, transferred to 60 mm plastic cell culture dishes lined with UV-sterilized Parafilm M, and flooded with 60 μL of type I collagen working solution containing suspended islets. The PVA sponges absorbed the collagen solution, with the majority of the islets entering the 2 mm diameter central hole of the scaffold. Subsequently, the dishes were covered with dish tops (lined with moist filter paper) and placed in a tissue culture incubator for 30 min to polymerize the collagen into a hydrogel. The completed BIs were placed in DMEM/10% NMS/P/S in 24-well cell culture plates and kept in a tissue culture incubator prior to implantation in mice.

2.7.5. Measurement of Release of HA from Alginate Spheres In Vitro. To measure the kinetics of release of HA from alginate hydrogels *in vitro*, spheres containing 2% alginate and 2.5 μg of fluorescein isothiocyanate (FITC)-conjugated 120 kDa HA or 1.5×10^6 Da HA were prepared as described previously. The spheres were placed in 96-well cell culture plates (one sphere per well) that had each of the wells filled with 200 μL of Dulbecco's Ca/Mg PBS (DPBS Ca/Mg, Invitrogen). The plates were placed in a tissue culture incubator, and 100 μL volumes of the media were removed from each well at specific time points (up to 14 days) and analyzed by fluorescence spectrophotometry to quantify released FITC-HA, using a standard curve of fluorescence *versus* known concentration of FITC-HA. Following removal of the medium at each time point, the residual medium in each well was discarded, and each well was refilled with 200 μL of fresh medium.

To determine the percentage of HA retained in alginate spheres during their fabrication, freshly prepared spheres containing 2.5 μg of FITC-HA were dissolved in PBS/100 mM ethylenediaminetetraacetic acid (EDTA), and the resultant solution was analyzed by fluorescence spectrophotometry to quantify total FITC-HA per sphere.

2.7.6. Implantation of BIs In Vivo. BIs were implanted into mesenteric pockets of RIPmOVA/$Rag2^{-/-}$ mice (one BI per

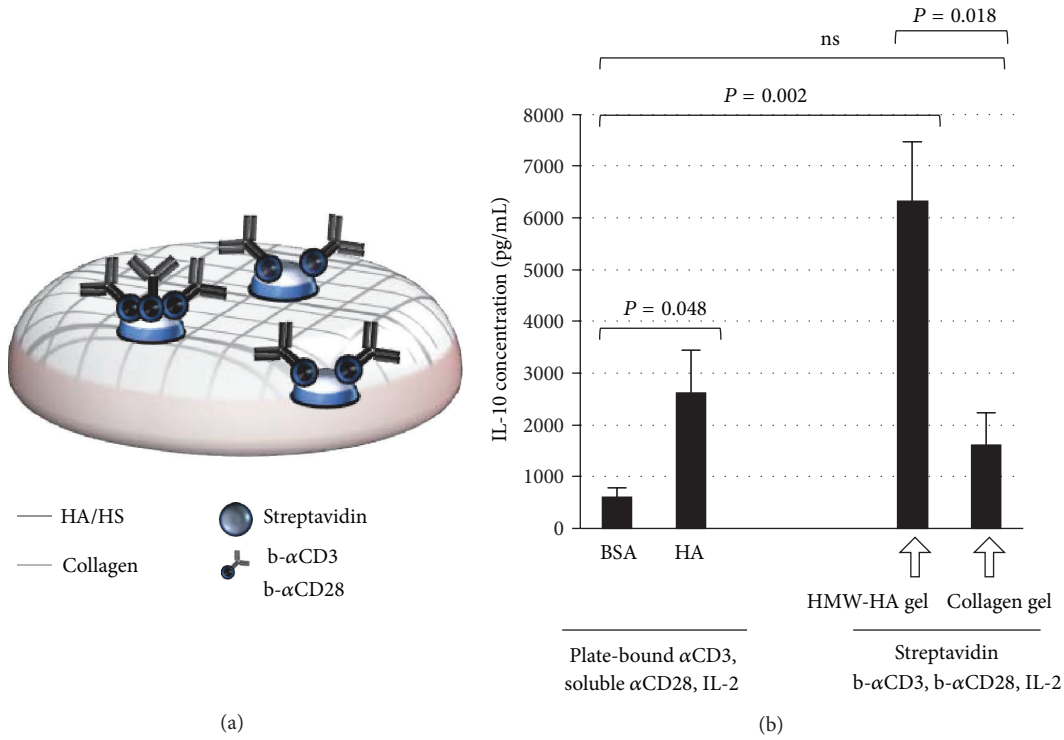

Figure 1: Induction of IL-10 by supplemented HA hydrogels *in vitro*. (a) Schematic for the design of a hydrogel capable of delivering a TCR stimulus in association with an HA signal. The "supplemented HA hydrogel" incorporates a crosslinked matrix of thiolated high molecular weight (HMW)-HA, HS, and collagen to which we have added streptavidin and biotinylated anti-CD3 and anti-CD28 antibodies (b-αCD3, b-αCD28) to deliver an activating signal through the TCR. (b) Concentration of IL-10 in supernates taken from T cell cultures 96 hours after either plate-based (left side of graph) or hydrogel-based (right side of graph) activation (cells were cultured on top of the hydrogels for the latter experiments). Supplemented collagen hydrogels that lacked HA were used as a negative control. $n = 5$ independent experiments.

mouse) using previously described protocols [30], followed by injection of the mice 24 hours later with 1×10^5 purified OVA-specific CD4(+) DO11.10 T cells.

2.8. Statistical Analyses. Statistical comparison of samples was made using Student's *t*-test.

3. Results

3.1. Supplemented HA Hydrogels Promote IL-10 Production In Vitro. We previously demonstrated that plate-bound HA together with an antigenic signal promotes IL-10 production by CD4(+)/GFP-FoxP3(−) T cells. This led us to ask whether we could develop this finding into a tool for use in promoting IL-10 production *in vivo*.

To this end, we modified a HA-based hydrogel to deliver a polyclonal antigenic stimulus through addition of streptavidin, biotinylated anti-CD3/CD28 antibodies, and IL-2. A schematic of this hydrogel design is shown in Figure 1(a). We have previously shown that a similar form of supplemented HA hydrogel is an efficient way to elicit IL-10 production from T cells *in vitro* [20].

We found that CD4(+)/GFP-FoxP3(−) T cells exposed to the supplemented HA hydrogels produced IL-10 at significantly higher levels than did corresponding T cells activated with anti-CD3/CD28 antibodies and IL-2 on cell culture plates (Figure 1(b)). This was the case whether the cells were cultured on top of the gels (as shown) or embedded within the gels (data not shown). Omission of either streptavidin or anti-CD3 antibody from the gel mixture likewise abrogated IL-10 production (data not shown), indicating that CD3 was required for the stimulus and suggesting that streptavidin was necessary to retain CD3 in the hydrogel lattice. Streptavidin, biotinylated anti-CD3/CD28 antibodies, and IL-2 incorporated into a hydrogel lacking HA (supplemented collagen hydrogel) did not significantly increase IL-10 production over plate-bound activation by these agents (Figure 1(b)), which demonstrated the potentiating influence of HA on IL-10 production. The unique capability of HA to stimulate IL-10 production by T cells is underscored by the observation that hydrogels made from other types of ECM, including basement membrane components (Matrigel) and fibrin, are not stimulatory *in vitro* [20].

3.2. Supplemented HA Hydrogels Promote IL-10 Production In Vivo. To evaluate whether supplemented HA hydrogels could be used to induce IL-10 production *in vivo*, the gels were populated with 3×10^6 CD4(+)/GFP-FoxP3(−) T cells from CD45.2 mice and injected into the peritoneal cavities of CD45.1 mice. By use of the CD45.1 and CD45.2 allelic

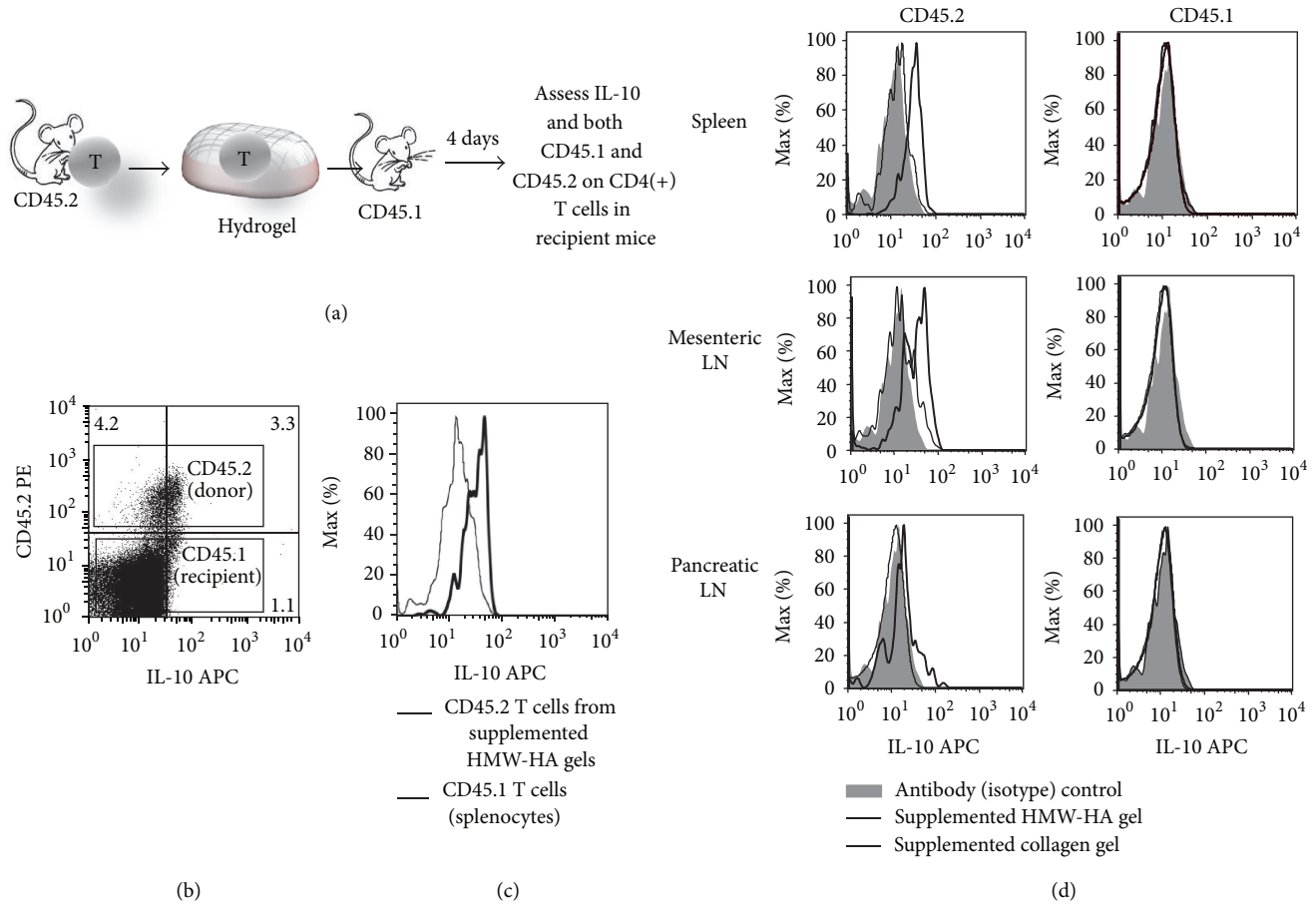

Figure 2: Supplemented HA hydrogels induce IL-10 *in vivo*. (a) Diagram of the experiment. Supplemented HA hydrogels, or control collagen hydrogels lacking HA, were populated with 3×10^6 CD4(+)/GFP-FoxP3(−)/CD45.2 donor cells and injected into the peritoneal cavities of CD45.1 recipient mice. Four days after implantation, lymphoid tissues were harvested, processed, and stained for intracellular IL-10 and CD markers. (b) Gating indicates relative IL-10 expression by CD45.2 donor and CD45.1 host T cells. (c) IL-10 expression by CD45.2 donor T cells harvested from HA hydrogel residue removed from the peritoneal cavity is substantially greater than that of CD45.1 host T cells from the spleen. (d) IL-10 staining of CD3(+)/CD4(+) T cells harvested from the spleen and mesenteric/pancreatic lymph nodes (LN). The donor T cells from mice that received the supplemented HA hydrogels expressed higher levels of IL-10 than corresponding donor T cells from mice that received the control supplemented collagen hydrogels. Host T cells from these two groups of mice did not express IL-10 above levels of the nonspecific antibody (isotype) controls. In (c), and (d), data are representative of three experiments each.

markers, the donor and recipient cell populations could be distinguished. A schematic of this transfer protocol is shown in Figure 2(a). Four days after implantation, spleens and lymph nodes were harvested, processed, the released cells stained for intracellular IL-10 and CD markers, and gating performed to distinguish donor T cells from host T cells (Figure 2(b)). As controls, analogous supplemented collagen hydrogels lacking HA were populated with cells and injected into a designated set of mice.

After 4 days, a substantial volume of residual HA hydrogel was found within the peritoneal cavities of the treated mice; however, the control collagen hydrogels had dissolved. In separate experiments, we found that after 7 days no implanted HA hydrogels were identifiable, indicating that extensive catabolism of the hydrogels takes place *in vivo*.

The cells within the HA hydrogel residue 4 days after implantation were primarily CD45.2(+) and expressed IL-10 at a high level relative to host T cells from the spleen (Figure 2(c)). These cells remained FoxP3(−) (data not shown), consistent with our previous report that HA does not induce FoxP3 expression [19]. Cell isolates from the spleens and lymph nodes of the transplanted mice contained CD45.2(+) donor T cells (Figure 2(d)), which indicated that the T cells embedded in the hydrogels had migrated into lymphoid tissues. Donor T cells that migrated from the supplemented HA hydrogels expressed higher levels of IL-10 than the corresponding donor T cells that migrated from the control collagen hydrogels. Host T cells from these two groups of mice did not express IL-10 above levels of the nonspecific antibody controls (Figure 2(d)). These data indicate that HA hydrogels providing endogenous TCR stimuli can be used as platforms to induce IL-10 production *in vivo*.

While supplemented HA hydrogels are a novel system for inducing implantable T cell populations that produce IL-10, we sought to devise an implantable platform that would elicit IL-10 production from endogenous T cells in

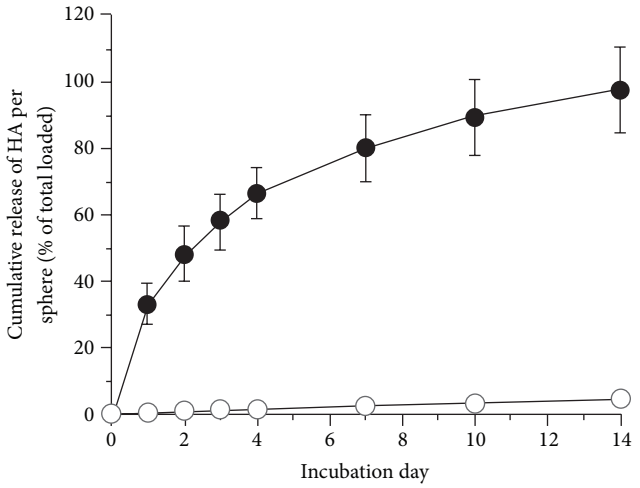

Figure 3: Kinetics of release of HA from alginate *in vitro*. Alginate spheres (2% alginate/10 μL volume/2.2 mm diameter) incorporating 2.5 μg of FITC-labeled 120 kDa HA (closed circles) or FITC-labeled 1.5×10^6 Da HA (open circles) were cultured at 37°C in DPBS Ca/Mg, and the media collected at specific time points for measurement of released HA. Essentially all (98%) of the 120 kDa HA was released over 14 days, whereas less than 5% of the 1.5×10^6 Da HA was released during this time period. Error bars = standard deviations (error bars for the 1.5×10^6 Da group are within the diameter of the open circles). n = 10 spheres for each group.

an antigen-specific manner. To this end, we adapted a novel *bioengineered implant (BI)* we had developed from an earlier study to combine the antigenic stimulus with sustained release of HA within the same construct.

3.3. Sustained Release of HA from BIs Induces IL-10 Production In Vivo. We recently reported on the development of the BI as a model system to explore improved approaches for islet transplantation [30]. The BI, sized for mesenteric or subcutaneous implantation in mice, consists of a disk-shaped PVA sponge infused with a type I collagen hydrogel that contains dispersed donor islets. To promote islet vascularization, the BI incorporates a spherical alginate construct for delivery of VEGF. Previously, we used syngeneic mice to demonstrate that BIs containing 450–500 islets and 20 ng of VEGF could reverse streptozotocin (STZ)-induced diabetes in 100% of recipients [30]. Notably, none of these mice required exogenous insulin therapy once the BIs began to fully regulate levels of blood glucose. Moreover, the transplanted mice responded to glucose challenge in a near-normal manner.

Induction of pro-tolerogenic cytokines, such as IL-10, is an appealing strategy to help facilitate transplantation of islets. Here, we have adapted our BI device to evaluate the capacity of HA in fluid form (i.e., HA not crosslinked to form a hydrogel) to elicit IL-10 production in an autoimmune setting. To test this model, we loaded the BI with islets expressing the OVA antigen, transferred in OVA-specific T cells, immunized the recipient mice with OVA, and asked whether these cells expressed IL-10 in an OVA or TCR-specific manner.

We first evaluated the kinetics of release of HA from 2 mm diameter, 2% alginate spheres under physiological conditions *in vitro* (Figure 3). We found that release of 1.5×10^6 Da HA was linear, but relatively slow—less than 5% was released after 14 days. In contrast, the release of 120 kDa HA was much more rapid—essentially 100% was released within 14 days, which was a useful time frame in which to analyze post-transplantation immune responses. We found that over 60% (63.7% ± 6.1%) of the 120 kDa HA loaded into each sphere was retained by the alginate after crosslinking with calcium. The BIs we designed for our experiments *in vivo* (Figure 4) incorporated a single alginate sphere containing 20 ng of VEGF and 5 spheres that contained a total of 160 μg of 120 kDa HA (the total is derived from a value of 32 μg of HA per sphere, based on 64% retention of the 50 μg of HA present in each sphere prior to calcium crosslinking). A set of control BIs incorporated one VEGF sphere and 5 spheres loaded with saline in place of the HA. The central hole of the BI was infused with a type I collagen hydrogel containing islets from RIPmOVA mice, which express chicken ovalbumin driven by the rat insulin promoter (RIP). BIs of this design were implanted into mesenteric pockets of RIPmOVA/Rag2$^{-/-}$ mice (one BI per mouse), followed by injection of the mice 24 hours later with 1×10^5 purified OVA-specific CD4(+) DO11.10 T cells. Forty-eight hours after implantation, each mouse was immunized with 100 μg of OVA peptide (aa 323–339). On day 14 after implantation, splenocytes were isolated from the mice and assayed for IL-10 production *in vitro* after 96 hours of stimulation with either anti-CD3/anti-CD28 antibodies or antigen-specific OVA peptide (Figure 5(a)). In this assay, the splenocytes from the mice treated with HA produced more IL-10 than the splenocytes from the control mice that were not exposed to HA. This differential response was observed when the splenocytes were given either a nonspecific stimulus with CD3/CD28 (Figure 5(b)) or a specific stimulus with OVA peptide (Figure 5(c)). Unfortunately, these data do not allow us to discern which cells are the source of IL-10 in this assay and specifically whether the cells in question are FoxP3(+) Tregs or FoxP3(−) conventional T cells.

4. Discussion

We demonstrate, using two separate model systems, that delivery of HA together with antigenic signals promotes the production of IL-10 *in vivo*. Our data suggest a potential clinical application for HA-mediated induction of IL-10-producing T cells using injectable hydrogels. HA hydrogel platforms are in development for a variety of applications, including drug delivery and wound dressings, and are noted for their biocompatibility [31, 32]. In the present study, we have shown that augmentation of HA hydrogels with a complex of biomolecules that provide TCR stimulation in addition to the HA signal can deliver the requisite cues for IL-10 induction, both *in vitro* and *in vivo*.

In treatments of diabetic patients that involve transplantation of islets, controlling rejection is typically accomplished by systemic immunosuppressive compounds. Dosing

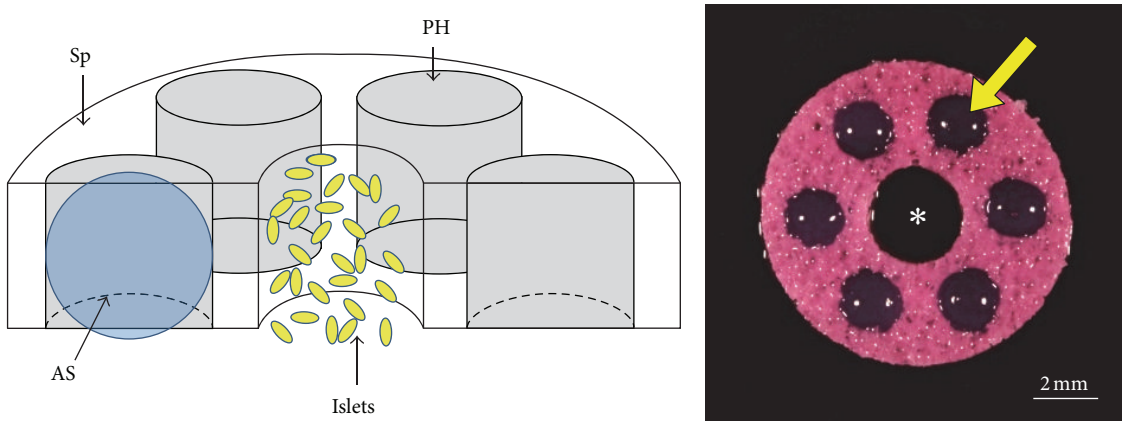

Figure 4: BI designed for evaluation of immune modulation by HA *in vivo*. (a) Cut-away diagram of the BI. A disk-shaped PVA sponge (Sp) scaffold provides mechanical support. Alginate spheres (AS-blue) occupy the six peripheral holes (PH) of the sponge. A central hole in the sponge contains islets (yellow) suspended in a type 1 collagen hydrogel (not shown). The collagen hydrogel also infuses the sponge. For clarity, the pores of the sponge are not depicted. (b) A PVA sponge scaffold (stained pink from culture medium) is oriented to show the empty central hole (asterisk) and the six peripheral holes, which each contain an alginate sphere (e.g., arrow). The scaffold is 10 mm in diameter × 2 mm thick.

of these compounds is a difficult balance—levels must be low enough to permit a reasonable degree of protective immunity against pathogenic organisms, but high enough to effectively suppress allo- and autoimmune activity. In the case of simultaneous pancreas-kidney (SPK) transplants, some current immunosuppression regimens are inadequate to control autoimmunity [33, 34]. Moreover, no matter what the dose, systemic immunosuppression can be accompanied by a variety of undesirable side-effects on tissue and organ systems that are not directly associated with the transplant. In light of the problems associated with systemic treatments, an alternative approach would be to confine the delivery of immunotherapy to the implant itself. In this way, immunomodulatory compounds could be delivered at relatively high concentrations, but within the limited volume of the implant, thereby minimizing side-effects on tissues and organs outside the zone of delivery. To this end, the BI described here includes a mechanically-supportive scaffold and ECM hydrogel that concentrates the islets in a small volume, and a sustained-release component for local delivery of immunomodulatory compounds.

In the present study, we have adapted our BI to release HA in fluid form. Rather than using HA of 1–1.5 × 10^6 Da that is typically incorporated into HA hydrogels, we used HA with a 10-fold lower MW (120 kDa) to provide release kinetics that were optimal for the 14-day duration of our experiments *in vivo*. Of note, we observed that this shorter HA could induce an IL-10 response from host mice. To our knowledge, this observation is the first demonstration of IL-10 production by HA of this weight class. It is possible that the 120 kDa HA is crosslinked into higher MW forms after its release into tissue from alginate, which could be accomplished by HA-binding molecules such as inter-alpha-trypsin inhibitor (IαI) and/or tumor necrosis factor-stimulated gene-6 protein (TSG-6) which are present at sites of inflammation and which are known to crosslink HA into macromolecular assemblies [35–37]. Such crosslinking could result not only in a functional increase in the MW of HA, but also promote the retention of HA in the fibrovascular tissue that invades the BI [30] and in the tissues immediately surrounding the implant. Our future studies will continue to use BIs as platforms to evaluate the effectiveness of HA and other specific ECM and cytokine environments on islet survival and reversal of diabetes in the setting of autoimmunity.

Abbreviations

HA: hyaluronan;
BRI: Benaroya Research Institute;
BI: bioengineered implant;
GFP: green fluorescent protein;
IL-2, IL-10: interleukin-2, -10;
HS: heparan sulfate;
NMS: normal mouse serum;
TCR: T cell receptor complex;
Tregs: regulatory T cells;
VEGF: vascular endothelial growth factor.

Conflicts of Interest

The authors acknowledge no competing financial interests. Specifically, the authors have no conflict of interest with any trademark mentioned in this manuscript.

Acknowledgments

The authors wish to thank Drs. Susan Potter-Perigo and Thomas N. Wight for providing the FITC-HA used in our studies. This work was supported in part by National Institutes of Health grants R01 DK096087, R01 HL113294, and

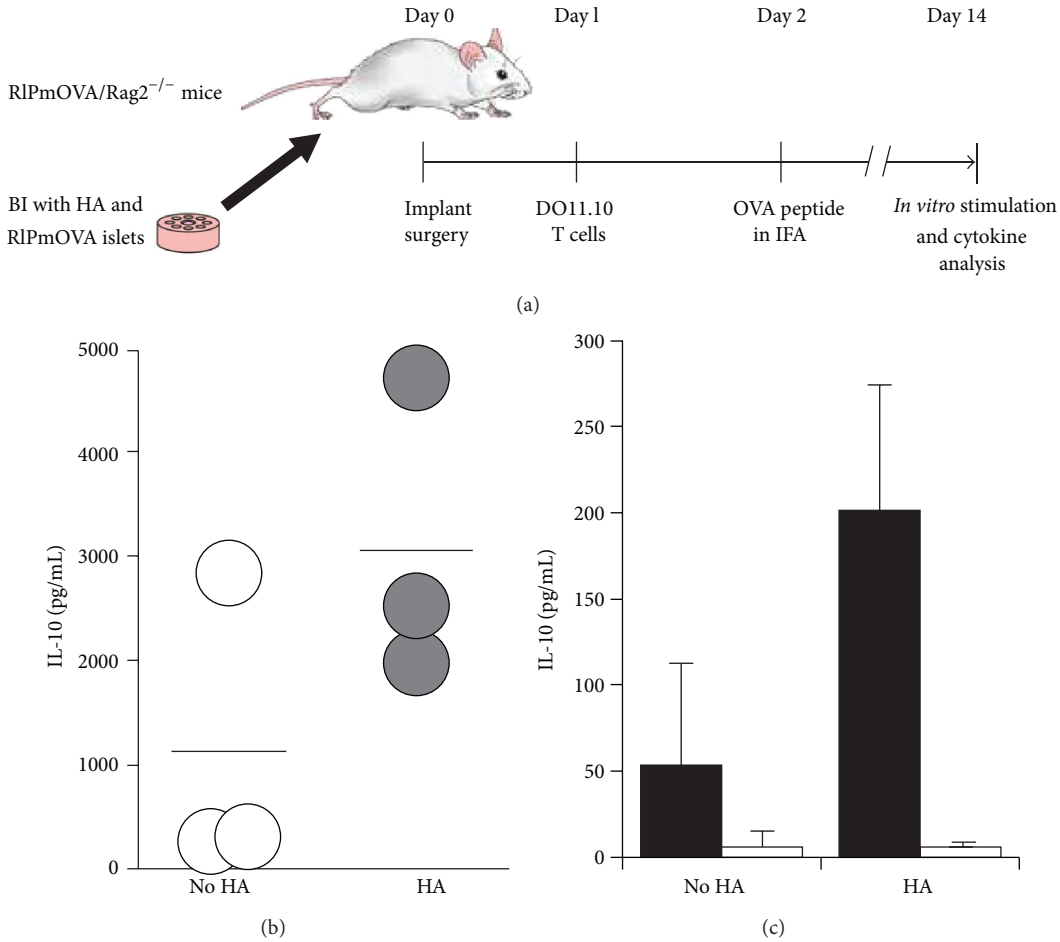

Figure 5: Local release of fluid HA from BIs generates IL-10 producing T cells *in vivo*. (a) Diagram of the experiment. BIs incorporating RIPmOVA islets and alginate spheres loaded with HA or saline (controls) were implanted in RIPmOVA /Rag2$^{-/-}$ mice, followed by injection of OVA-specific DO11.10 T cells on day 1 and 100 μg of OVA peptide in incomplete Freund's adjuvant (IFA) on day 2. On day 14, splenocytes were harvested and assayed for IL-10 production in response to antigenic stimulation *in vitro*. (b) IL-10 production by splenocytes from recipient animals in response to stimulation with anti-CD3/CD28 antibodies. (c) IL-10 production in response to OVA peptide (black bars) or no peptide (white bars). In (b) and (c), cells were stimulated for 96 hours, and culture supernates in contact with the stimulated cells for 72 hours were assayed by ELISA. Data are representative of 2 experiments totaling 5 mice in each group.

U01 AI101984 to Paul L. Bollyky; the Klorfine Foundation and Gilbertson Foundation (to Robert B. Vernon); and USAMRAA/DOD W81XWH-10-1-0149 and Washington State Life Sciences Discovery Fund Grant no. 4553677 to Gerald T. Nepom.

References

[1] C. Asseman, S. Mauze, M. W. Leach, R. L. Coffman, and F. Powrie, "An essential role for interleukin 10 in the function of regulatory T cells that inhibit intestinal inflammation," *Journal of Experimental Medicine*, vol. 190, no. 7, pp. 995–1004, 1999.

[2] E.-O. Glocker, D. Kotlarz, K. Boztug et al., "Inflammatory bowel disease and mutations affecting the interleukin-10 receptor," *The New England Journal of Medicine*, vol. 361, no. 21, pp. 2033–2045, 2009.

[3] M. G. Roncarolo, S. Gregori, M. Battaglia, R. Bacchetta, K. Fleischhauer, and M. K. Levings, "Interleukin-10-secreting type 1 regulatory T cells in rodents and humans," *Immunological Reviews*, vol. 212, pp. 28–50, 2006.

[4] K. W. Moore, M. R. de Waal, R. L. Coffman, and A. O'Garra, "Interleukin-10 and the interleukin-10 receptor," *Annual Review of Immunology*, vol. 19, pp. 683–765, 2001.

[5] A. M. VanBuskirk, W. J. Burlingham, E. Jankowska-Gan et al., "Human allograft acceptance is associated with immune regulation," *Journal of Clinical Investigation*, vol. 106, no. 1, pp. 145–155, 2000.

[6] S. Yi, M. Ji, J. Wu et al., "Adoptive transfer with in vitro expanded human regulatory T cells protects against porcine islet xenograft rejection via interleukin-10 in humanized mice," *Diabetes*, vol. 61, no. 5, pp. 1180–1191, 2012.

[7] K. S. Baker, M.-G. Roncarolo, C. Peters, M. Bigler, T. DeFor, and B. R. Blazar, "High spontaneous IL-10 production in unrelated bone marrow transplant recipients is associated with fewer transplant-related complications and early deaths," *Bone Marrow Transplantation*, vol. 23, no. 11, pp. 1123–1129, 1999.

[8] V. Daniel, C. Naujokat, M. Sadeghi, M. Wiesel, O. Hergesell, and G. Opelz, "Association of circulating interleukin (IL)-12- and IL-10-producing dendritic cells with time posttransplant, dose of

immunosuppression, and plasma cytokines in renal-transplant recipients," *Transplantation*, vol. 79, no. 11, pp. 1498–1506, 2005.

[9] Y. C. Zhang, A. Pileggi, A. Agarwal et al., "Adeno-associated virus-mediated IL-10 gene therapy inhibits diabetes recurrence in syngeneic islet cell transplantation of NOD mice," *Diabetes*, vol. 52, no. 3, pp. 708–716, 2003.

[10] Y.-H. Kim, D.-G. Lim, Y.-M. Wee et al., "Viral IL-10 gene transfer prolongs rat islet allograft survival," *Cell Transplantation*, vol. 17, no. 6, pp. 609–618, 2008.

[11] A. Rabinovitch, W. L. Suarez-Pinzon, O. Sorensen, R. V. Rajotte, and R. F. Power, "Combination therapy with cyclosporine and interleukin-4 or interleukin- 10 prolongs survival of syngeneic pancreatic islet grafts in nonobese diabetic mice: islet graft survival does not correlate with mRNA levels of type 1 or type 2 cytokines, or transforming growth factor-β in the islet grafts," *Transplantation*, vol. 64, no. 11, pp. 1525–1531, 1997.

[12] M. Battaglia, A. Stabilini, E. Draghici et al., "Rapamycin and interleukin-10 treatment induces T regulatory type 1 cells that mediate antigen-specific transplantation tolerance," *Diabetes*, vol. 55, no. 1, pp. 40–49, 2006.

[13] N. Gagliani, S. Gregori, T. Jofra et al., "Rapamycin combined with anti-CD45RB mAB and IL-10 or with G-CSF induces tolerance in a stringent mouse model of islet transplantation," *PloS One*, vol. 6, no. 12, article e28434, 2011.

[14] Y. C. Zhang, A. Pileggi, R. D. Molano et al., "Systemic overexpression of interleukin-10 fails to protect allogeneic islet transplants in nonobese diabetic mice," *Transplantation*, vol. 80, no. 4, pp. 530–533, 2005.

[15] T. C. Laurent and J. R. E. Fraser, "Hyaluronan," *The FASEB Journal*, vol. 6, no. 7, pp. 2397–2404, 1992.

[16] D. Jiang, J. Liang, J. Fan et al., "Regulation of lung injury and repair by Toll-like receptors and hyaluronan," *Nature Medicine*, vol. 11, no. 11, pp. 1173–1179, 2005.

[17] C. Termeer, F. Benedix, J. Sleeman et al., "Oligosaccharides of hyaluronan activate dendritic cells via Toll-like receptor 4," *Journal of Experimental Medicine*, vol. 195, no. 1, pp. 99–111, 2002.

[18] J. D. Powell and M. R. Horton, "Threat matrix: low-molecular-weight hyaluronan (HA) as a danger signal," *Immunologic Research*, vol. 31, no. 3, pp. 207–218, 2005.

[19] P. L. Bollyky, B. A. Falk, S. A. Long et al., "CD44 costimulation promotes FoxP3+ regulatory T cell persistence and function via production of IL-2, IL-10, and TGF-β," *Journal of Immunology*, vol. 183, no. 4, pp. 2232–2241, 2009.

[20] P. L. Bollyky, R. P. Wu, B. A. Falk et al., "ECM components guide IL-10 producing regulatory T-cell (TR1) induction from effector memory T-cell precursors," *Proceedings of the National Academy of Sciences of the United States of America*, vol. 108, no. 19, pp. 7938–7943, 2011.

[21] T.-L. Huang, H.-C. Hsu, K.-C. Yang, and F.-H. Lin, "Hyaluronan up-regulates IL-10 expression in fibroblast-like synoviocytes from patients with tibia plateau fracture," *Journal of Orthopaedic Research*, vol. 29, no. 4, pp. 495–500, 2011.

[22] A. Asari, T. Kanemitsu, and H. Kurihara, "Oral administration of high molecular weight hyaluronan (900 kDa) controls immune system via toll-like receptor 4 in the intestinal epithelium," *Journal of Biological Chemistry*, vol. 285, no. 32, pp. 24751–24758, 2010.

[23] A. Gigante and L. Callegari, "The role of intra-articular hyaluronan (Sinovial) in the treatment of osteoarthritis," *Rheumatology International*, vol. 31, no. 4, pp. 427–444, 2011.

[24] Y. Kim, Y.-S. Lee, J.-H. Hahn et al., "Hyaluronic acid targets CD44 and inhibits FcεRI signaling involving PKCδ, Rac1, ROS, and MAPK to exert anti-allergic effect," *Molecular Immunology*, vol. 45, no. 9, pp. 2537–2547, 2008.

[25] Q. Zeng, Z. Yu, J. You, and Q. Zhang, "Efficacy and safety of seprafilm for preventing postoperative abdominal adhesion: systematic review and meta-analysis," *World Journal of Surgery*, vol. 31, no. 11, pp. 2125–2131, 2007.

[26] G. Kogan, L. Šoltés, R. Stern, and P. Gemeiner, "Hyaluronic acid: a natural biopolymer with a broad range of biomedical and industrial applications," *Biotechnology Letters*, vol. 29, no. 1, pp. 17–25, 2007.

[27] R. D. Price, V. Das-Gupta, I. M. Leigh, and H. A. Navsaria, "A comparison of tissue-engineered hyaluronic acid dermal matrices in a human wound model," *Tissue Engineering*, vol. 12, no. 10, pp. 2985–2995, 2006.

[28] G. Gravante, R. Sorge, A. Merone et al., "Hyalomatrix PA in burn care practice: results from a national retrospective survey, 2005 to 2006," *Annals of Plastic Surgery*, vol. 64, no. 1, pp. 69–79, 2010.

[29] G. D. Prestwich, X. Z. Shu, Y. Liu et al., "Injectable synthetic extracellular matrices for tissue engineering and repair," *Advances in Experimental Medicine and Biology*, vol. 585, pp. 125–133, 2006.

[30] R. B. Vernon, A. Preisinger, M. D. Gooden et al., "Reversal of diabetes in mice with a bioengineered islet implant incorporating a type I collagen hydrogel and sustained release of vascular endothelial growth factor," *Cell Transplantation*, vol. 21, no. 10, pp. 2099–2110, 2012.

[31] M. A. Serban, A. Scott, and G. D. Prestwich, "Use of hyaluronan-derived hydrogels for three-dimensional cell culture and tumor xenografts," *Current Protocols in Cell Biology*, chapter 10, unit 10.14, 2008.

[32] K. R. Kirker, Y. Luo, J. H. Nielson, J. Shelby, and G. D. Prestwich, "Glycosaminoglycan hydrogel films as bio-interactive dressings for wound healing," *Biomaterials*, vol. 23, no. 17, pp. 3661–3671, 2002.

[33] E. Laughlin, G. Burke, A. Pugliese, B. Falk, and G. Nepom, "Recurrence of autoreactive antigen-specific CD4+ T cells in autoimmune diabetes after pancreas transplantation," *Clinical Immunology*, vol. 128, pp. 23–30, 2008.

[34] F. Vendrame, A. Pileggi, E. Laughlin et al., "Recurrence of type 1 diabetes after simultaneous pancreas-kidney transplantation, despite immunosuppression, is associated with autoantibodies and pathogenic autoreactive CD4 T-cells," *Diabetes*, vol. 59, pp. 947–957, 2010.

[35] M. S. Rugg, A. C. Willis, D. Mukhopadhyay et al., "Characterization of complexes formed between TSG-6 and inter-α-inhibitor that act as intermediates in the covalent transfer of heavy chains onto hyaluronan," *Journal of Biological Chemistry*, vol. 280, no. 27, pp. 25674–25686, 2005.

[36] L. Zhuo and K. Kimata, "Structure and function of inter-α-trypsin inhibitor heavy chains," *Connective Tissue Research*, vol. 49, no. 5, pp. 311–320, 2008.

[37] D. Mukhopadhyay, A. Asari, M. S. Rugg, A. J. Day, and C. Fülöp, "Specificity of the tumor necrosis factor-induced protein 6-mediated heavy chain transfer from inter-α-trypsin inhibitor to hyaluronan: implications for the assembly of the cumulus extracellular matrix," *Journal of Biological Chemistry*, vol. 279, no. 12, pp. 11119–11128, 2004.

Hindawi Publishing Corporation
Journal of Diabetes Research
Volume 2013, Article ID 134395, 8 pages
http://dx.doi.org/10.1155/2013/134395

Research Article

The Role of Adrenomedullin in the Renal NADPH Oxidase and (Pro)renin in Diabetic Mice

Michio Hayashi,[1] Akihiro Tojo,[2] Tatsuo Shimosawa,[1] and Toshiro Fujita[1]

[1] *Department of Internal Medicine, University of Tokyo, 7-3-1 Hongo, Bunkyo-ku, Tokyo 113-8655, Japan*
[2] *Division of Nephrology and Endocrinology, Department of Internal Medicine, University of Tokyo, 7-3-1 Hongo, Bunkyo-ku, Tokyo 113-8655, Japan*

Correspondence should be addressed to Akihiro Tojo; akitojo-tky@umin.ac.jp

Received 4 February 2013; Accepted 25 June 2013

Academic Editor: Bernard Portha

Adrenomedullin has an antioxidative action and protects organs in various diseases. To clarify the role of adrenomedullin in diabetic nephropathy, we investigated the NADPH oxidase expression, renin-secreting granular cell (GC) hyperplasia, and glomerular matrix expansion in the streptozotocin (STZ)-induced diabetic adrenomedullin gene knockout (AMKO) mice compared with the STZ-diabetic wild mice at 10 weeks. The NADPH oxidase p47phox expression and lipid peroxidation products were enhanced in the glomeruli of the diabetic mice compared with that observed in the controls in both wild and AMKO mice. These changes were more obvious in the AMKO mice than in the wild mice. Glomerular mesangial matrix expansion was more severe in the diabetic AMKO mice than in the diabetic wild mice and exhibited a positive correlation with the degree of lipid peroxidation products in the glomeruli. Proteinuria was significantly higher in the diabetic AMKO mice than in the diabetic wild mice. The GC hyperplasia score and the renal prorenin expression were significantly increased in the diabetic AMKO mice than in the diabetic wild mice, and a positive correlation was observed with the NADPH oxidase expression in the macula densa. The endogenous adrenomedullin gene exhibits an antioxidant action via the inhibition of NADPH oxidase probably by suppressing the local renin-angiotensin system.

1. Introduction

Adrenomedullin is a potent vasodilating peptide that is upregulated in cardiovascular diseases to counteract the disease process with its diverse physiological actions including antioxidative stress actions [1–6]. The plasma concentration of adrenomedullin also increased in the diabetic patients, and hyperglycemia increases the production of adrenomedullin in the vasculature [7, 8]. The receptors for adrenomedullin are expressed in the kidneys, especially in the glomerulus and distal nephron, and the local action of adrenomedullin is increased in diabetic rats [9], thus suggesting that adrenomedullin may contribute to the dilatation of the glomerular capillary in the early phase of diabetic nephropathy. Although the organoprotective effects of adrenomedullin have been demonstrated in various cardiovascular diseases, the mechanisms underlying its renoprotection in diabetic nephropathy are still unclear.

Hyperglycemia accelerates the formation of advanced glycation end products (AGE), while also upregulating the protein kinase C (PKC) activity, accelerating the polyol pathway, and promoting sorbitol deposition [10]. These pathways are related to the increased oxidative stress, which plays a significant pathogenetic role in diabetic complications. In the kidneys of diabetic animals, the expression of NADPH oxidase and its oxidative products is observed to increase, and the suppression of NADPH oxidase ameliorates renal damage and endothelial dysfunction in diabetics [11–16]. Adrenomedullin has been demonstrated to possess an antioxidant action; however, the relationship between NADPH oxidase and adrenomedullin in the kidneys of diabetic nephropathy remains to be elucidated.

In this study, we applied the streptozotocin (STZ)-induced diabetic adrenomedullin gene knockout (AMKO) mice to clarify the role of adrenomedullin in the NADPH

oxidase expression and its oxidative products in diabetic nephropathy, and we also investigated the relationship between adrenomedullin and the renin-angiotensin system that stimulates NADPH oxidase and oxidative stress.

2. Materials and Methods

2.1. Animals. The AMKO mice were generated in our laboratory as previously described [4]. The homoknockout of the adrenomedullin gene is embryonically lethal; therefore, we used the adrenomedullin gene heteroknockout mice in the experiments. The genotyping was performed with polymerase chain reaction (PCR) using the tail genomic DNA as a template and the +/+ littermates as wild controls. All mice were kept in a 12-hour light/12-hour dark room and fed mice pellets and tap water *ad libitum*. STZ at a dose of 50 mg/kg BW in citrate buffer (pH 4.5) was injected intraperitoneally at six weeks ($n = 4$ in each group) after 18 hours of fasting for five consecutive days. Four weeks after the last STZ injection, 24-hour urine samples were collected, and the mice were anesthetized with pentobarbital (5 mg/mouse). After abdominal incisions were created, blood samples were collected from the inferior vena cava, and the mice were then perfused with phosphate buffered saline (PBS) to wash out the blood, followed by 4% paraformaldehyde. The kidneys were excised and subjected to a histological examination. All procedures were performed in accordance with our university guidelines for animal handling.

2.2. Immunohistochemistry and Morphometry. The procedure for immunohistochemistry has been described previously [13, 17, 18]. Briefly, 2-μm sections of kidney blocks were incubated with 3% H_2O_2 and blocking serum. The sections were incubated with a monoclonal antibody for NADPH oxidase component p47phox (Transduction Laboratories, Lexington, KY, USA) and a rabbit polyclonal antibody for malondialdehyde (MDA, Alpha Diagnostic International, San Antonio, TX, USA) at 1 : 100 dilution overnight. Sections were incubated with a biotinylated secondary antibody against mouse immunoglobulin for NADPH oxidase p47phox or with a biotinylated secondary antibody against rabbit immunoglobulin for MDA (Dako, Glostrup, Denmark) for two hours, followed by incubation with a horseradish peroxidase (HRP)-conjugated streptavidin solution. HRP labeling was detected using incubation with peroxidase substrate solution and diaminobenzidine (DAB, 0.8 mM, Dojindo Laboratories, Kumamoto, Japan). The sections were counterstained with hematoxylin. For a negative control, sections were processed in the same way without the primary antibody. Immunoreactivity for p47phox in the macula densa and for MDA in the glomerular mesangial area was scored as 0 for no staining, 1 for mild staining, 2 for moderate staining, and 3 for strong staining [18]. The scores from four animals were pooled in each group. The juxtaglomerular apparatus (JGA) was observed using periodic acid methenamine silver (PAM) staining. The presence of renin-secreting granular cells (GC) around the afferent arteriole was scored as 0 for no renin granules, 1 for few segmental cells containing renin granules in the JGA, 2 for all cells containing renin granules around the afferent arteriole, and 3 for renin-containing cells extended to the proximal portion of the afferent arteriole. The GC scores of four mice were pooled in each group. The correlation between the GC score in the JGA and the NADPH oxides expression score in the macula densa was calculated using a linear regression analysis. The degree of glomerular matrix expansion was scored in each glomerulus as previously described [19], and the correlation with the glomerular MDA immunostaining score was calculated using a linear regression analysis.

2.3. Western Blot for Prorenin. As described previously [13], the kidneys were homogenized, and samples containing 50 mg of protein were separated using SDS-polyacrylamide gel electrophoresis on a 4/20% gel and electroblotted on a nitrocellulose membrane. Western blotting was performed with rabbit anti-prorenin antibodies (Yanaihara Institute Inc., Shizuoka, Japan, 1 : 250 dilution) as the primary antibody and HRP-conjugated swine anti-rabbit immunoglobulin (Dako, Glostrup, Denmark) as the secondary antibody at 1 : 1,000 dilution. Next, the membrane was incubated with 0.8 mmol/L of diaminobenzidine (DAB; Dojindo Laboratories, Kumamoto, Japan) with 0.01% H_2O_2 and 3 mmol/L of $NiCl_2$ to detect blots. The area and density of the bands of each stained protein were measured using the NIH image software package.

2.4. Measurements for Blood Glucose, Urinary Protein, and Plasma and Renal Angiotensin II. Blood glucose was measured by Glutest E II (Kyoto Dai-iti Kagaku, Kyoto, Japan), and urinary protein was measured by the Bradford method and corrected by urinary creatinine measured by Jaffe method using spectrophotometer [15]. Plasma and renal angiotensin II concentration was assessed by the radioimmunoassay method and corrected by the kidney weight [20].

2.5. Statistics. The values were expressed as the mean ± standard error. An analysis of variance was used for statistical comparisons among the four groups followed by a Bonferroni post hoc analysis. P values of less than 0.05 were considered to be statistically significant.

3. Results

3.1. Diabetes in AMKO Mice. Four weeks after STZ injection, the blood glucose levels significantly increased in both the wild DM mice and the AMKO-DM mice compared with those observed in the control wild and AMKO mice, and there were no differences in the blood glucose levels between the wild DM mice and the AMKO-DM mice (Table 1). The urinary protein excretion corrected for the level of urinary creatinine was significantly higher in the AMKO DM mice than in the wild DM mice (Table 1). It was impossible to measure the urinary protein levels of wild and AMKO control mice due to their extremely low urinary volume.

Table 1: Physiological data.

	Wild-control	Wild-DM	AMKO-control	AMKO-DM
Body weight (g)	22.0 ± 0.4	16.9 ± 1.1^{**++}	24.5 ± 0.6	18.9 ± 0.9^{*++}
Blood glucose (mg/dL)	109 ± 3	361 ± 45^{**++}	161 ± 16	410 ± 27^{**++}
Urinary protein (mg/mg Cr)	ND	29 ± 3	ND	44 ± 4$^{\#}$
Plasma angiotensin II (pg/mL)	33.3 ± 11.0	19.0 ± 3.9	34.5 ± 1.5	59.3 ± 19.0$^{\#}$
Renal angiotensin II (pg/g kidney)	615 ± 102	685 ± 71^{++}	269 ± 32*	458 ± 81$^{\#}$

$^{*}P < 0.05$, $^{**}P < 0.001$ versus Wild control, $^{+}P < 0.05$, $^{++}P < 0.001$ versus AMKO control, $^{\#}P < 0.05$ versus Wild-DM. $N = 4$ in each group.

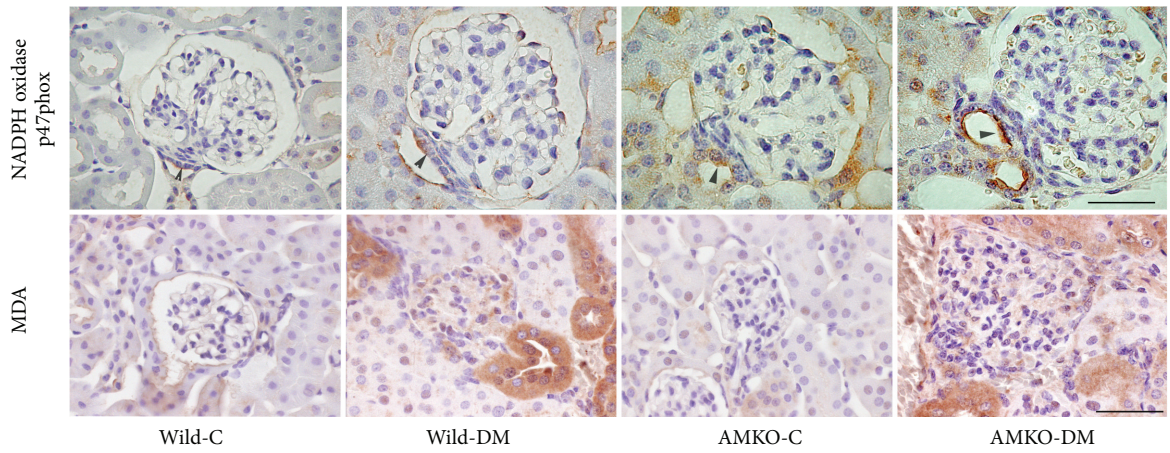

Figure 1: Immunohistochemistry of NADPH oxidase p47phox and malondialdehyde (MDA) in the kidneys of the control (C) and streptozotocin-induced diabetic (DM) in wild and adrenomedullin gene knockout (AMKO) mice. Immunoreactivity for p47phox and its product MDA was stronger in the glomeruli and distal tubules, including the macula densa (arrowhead), in the DM mice compared with that observed in the controls in both wild and AMKO mice, and was stronger in the AMKO-DM mice than in the wild-DM. The bar indicates 50 μm.

3.2. The NADPH Oxidase Expression and Lipid Peroxidation Products in the Kidneys. Immunoreactivity for the NADPH oxidase p47phox in the glomerulus and distal tubules, including the macula densa, was increased in the wild-DM mice compared with that observed in the wild-control mice, and while the AMKO-DM mice exhibited further increases in NADPH oxidase p47phox compared with the AMKO-control mice (Figure 1). Associated with the changes in the NADPH oxidase expression, the lipid peroxidation products evaluated with MDA were increased in the glomeruli and distal tubules in both the wild-DM and AMKO-DM mice compared with that observed in each control, and the immunoreactivity for MDA was stronger in the AMKO-DM mice than in the wild-DM mice (Figure 1).

3.3. Glomerular Matrix Expansion Was Correlated with Lipid Peroxidation Products in Glomeruli. PAS staining demonstrated glomerular mesangial matrix expansion in the diabetic mice compared with that observed in the control wild and control AMKO mice (Figure 2(a)). The glomerular mesangial expansion scores were significantly higher in the diabetic mice than in the controls in both wild mice (0.83 ± 0.05 versus 0.40 ± 0.07, $P < 0.005$) and AMKO mice (1.20 ± 0.12, versus 0.46 ± 0.07, $P < 0.0001$), and the AMKO-DM mice exhibited further increases in mesangial matrix expansion than the wild-DM mice ($P < 0.01$, Figure 2(b)). There was a significant positive correlation between the glomerular MDA staining scores and the mesangial matrix expansion scores (Figure 2(c)).

3.4. Renin-Secreting Granular Cells and the NADPH Oxidase Expression. PAM staining identified the renin-secreting granular cells (GC) around the distal portion of the afferent arteriole in the juxtaglomerular apparatus with small granules (Figure 3(a)). The diabetic mice displayed GC hyperplasia compared with that observed in the controls in both wild (1.16 ± 0.12 versus 0.68 ± 0.14, $P < 0.005$) and AMKO mice (1.66 ± 0.12 versus 0.96 ± 0.11, $P < 0.001$), and the GC hyperplasia scores were significantly higher in the AMKO-DM mice than in the wild-DM mice ($P < 0.01$, Figure 3(b)). Western blotting of renal prorenin confirmed the increased renal prorenin production in AMKO-DM mice compared with that observed in the wild-DM mice (Figure 4). Plasma angiotensin II was significantly increased in AMKO-DM mice compared with that in wild-DM mice, and renal angiotensin II was significantly increased in AMKO-DM mice compared with that in AMKO-C mice. There was a significant positive correlation between the GC hyperplasia

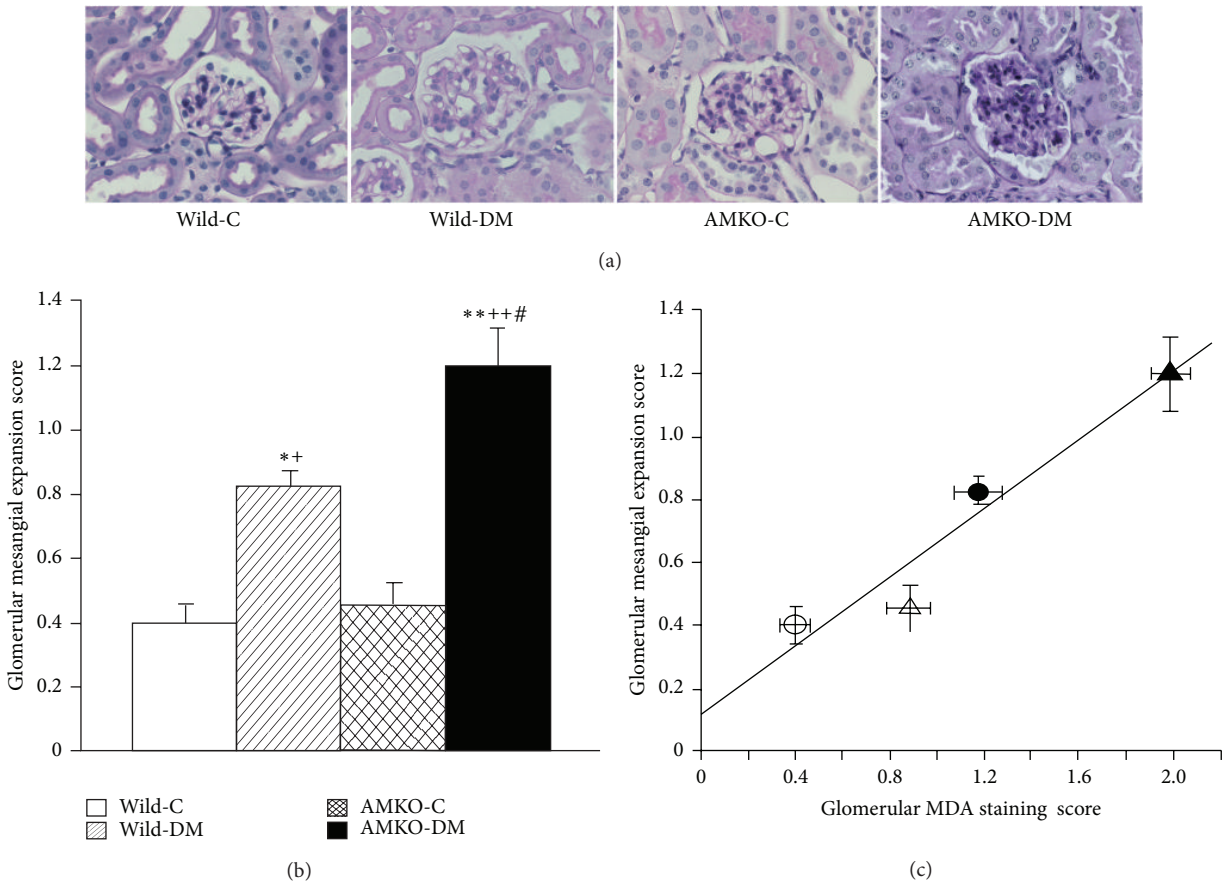

Figure 2: PAS staining of the glomerulus (a). The glomerular matrix expansion score (b) and its correlation with the glomerular malondialdehyde (MDA) staining score (c). The mesangial matrix was segmentally increased in both the STZ-induced diabetic wild mice (Wild-DM) and the diabetic adrenomedullin gene knockout (AMKO) mice (AMKO-DM) compared with that observed in the control mice (Wild-C and AMKO-C). (a) The bar indicates 50 μm. (b) The AMKO-DM mice exhibited a significant increase in the mesangial matrix expansion score compared with the wild-DM mice. Four mice in each group. $^{*}P < 0.005$, $^{**}P < 0.0001$ versus Wild-C, $^{+}P < 0.01$, $^{++}P < 0.0001$ versus AMKO-C, and $^{\#}P < 0.01$ versus Wild-DM. (c) The white circles indicate wild-control mice, the black circles, diabetic wild mice, the white triangles indicate adrenomedullin gene knockout (AMKO)-control mice, and the black triangles indicate diabetic AMKO mice. $R = 0.96$, $P < 0.05$.

scores and the NADPH oxidase p47phox expression scores in the macula densa (Figure 3(c)).

4. Discussion

In the present study, we revealed that diabetic AMKO mice exhibit significant increases in the NADPH oxidase expression and lipid peroxidation product formation in the kidneys compared with diabetic wild mice. The presence of increased lipid peroxidation products in the glomeruli exhibited a positive correlation with the presence of mesangial matrix expansion. This indicates that endogenous adrenomedullin plays an important role in protecting against oxidative stress in the kidneys via the suppression of NADPH oxidase and can prevent glomerulosclerosis. This is consistent with our previous observation that the antioxidative stress action of adrenomedullin plays an important role in organ protection in cardiovascular disease [4, 6].

It has been shown that the production of adrenomedullin is increased in the vasculature in patients with diabetes [7, 8] and that the local action of adrenomedullin in the kidneys is upregulated in the early phase of diabetic nephropathy [9]. However, the role of adrenomedullin in diabetic nephropathy has not been clearly elucidated. To clarify the role of adrenomedullin in diabetic nephropathy, we induced diabetes using STZ in AMKO mice. We demonstrated that proteinuria and glomerular matrix expansion are more severe in the diabetic AMKO mice than in the diabetic wild mice. Therefore, we hypothesize that endogenous adrenomedullin in diabetes may act to protect against the development of diabetic nephropathy. This is supported by evidence showing that the genetic predisposition to develop diabetic nephropathy is associated with the microsatellite DNA polymorphism of the adrenomedullin gene [21].

Endogenous adrenomedullin plays a role in renoprotection by suppressing oxidative stress in the diabetic condition

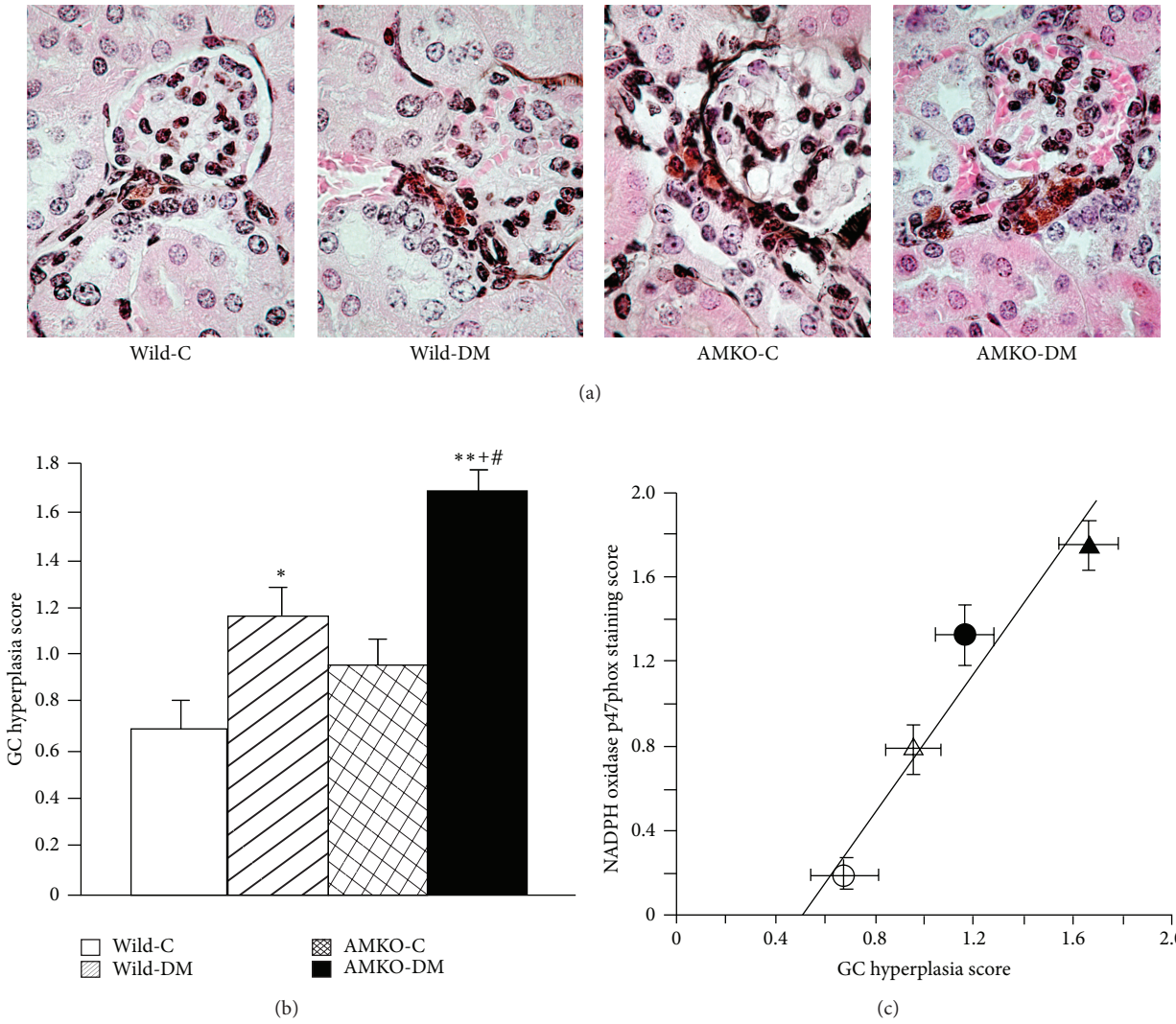

FIGURE 3: Renin-secreting granular cells in the juxtaglomerular apparatus and their correlation with the NADPH oxidase expression in the macula densa. (a) PAM staining illustrating granular cells in the juxtaglomerular apparatus with silver stained renin granules and reddish cytoplasm. The bar indicates 50 μm. (b) The granular cell (GC) hyperplasia scores were increased in the STZ-induced diabetic wild mice (Wild-DM) and the adrenomedullin gene knockout (AMKO) mice (AMKO-DM) compared with those observed in the control mice (Wild-C and AMKO-C). The AMKO-DM mice exhibited further increases in granular cells compared with the Wild-DM mice. Four mice in each group. $^{*}P < 0.005$, $^{**}P < 0.0001$ versus Wild-C, $^{+}P < 0.001$ versus AMKO-C, and $^{\#}P < 0.01$ versus Wild-DM. (c) The correlation between the renin-secreting granular cells (GC) hyperplasia score in the juxtaglomerular apparatus and the NADPH oxidase p47phox immunoreactivity score in the macula densa. The white circles indicate wild-control mice, the black circles indicate diabetic wild mice, the white triangles indicate adrenomedullin gene knockout (AMKO)-control mice, and the black triangles indicate diabetic AMKO mice. $R = 0.96$, $P < 0.03$.

because we showed that oxidative stress production via NADPH oxidase is increased in diabetic adrenomedullin gene-deficient mice compared to that observed in diabetic wild type mice and that renal MDA production has a positive correlation with glomerular mesangial matrix expansion. Among several pathogenetic mechanisms of diabetic nephropathy including advanced glycated end-product formation, an enhanced PKC pathway, the polyol pathway, the hexosamine pathway, and the renin-angiotensin (RA) system [10], oxidative stress plays an important role in the development of diabetic nephropathy, while the suppression of oxidative stress ameliorates renal damage [12–15]. In this study, the NADPH oxidase expression in the glomeruli and distal tubules, including the macula densa, was increased in diabetic wild mice compared to that observed in control wild mice, confirming the findings of our previous study showing that the expression of p47phox, the regulatory component of NADPH oxidase, is increased in the kidneys of diabetic rats [13, 15]. The diabetic AMKO mice demonstrated further increases in the NADPH oxidase in glomeruli and distal

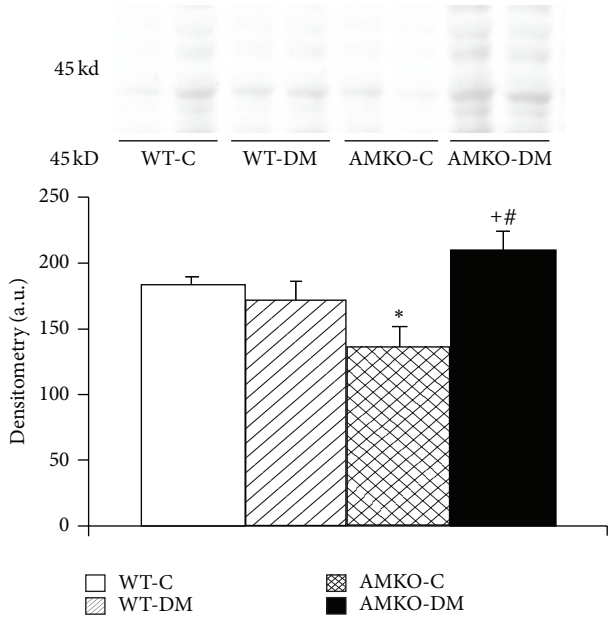

Figure 4: Western blotting of prorenin in the kidneys. The bands for prorenin are demonstrated at the molecular weight of 45 kD, and the densitometry of the bands is shown below ($n = 4$). Wild-C: wild-control mice, Wild-DM: wild mice with streptozotocin-induced diabetes, AMKO-C: adrenomedullin gene knockout (AMKO) mice without treatment (control), and AMKO-DM: AMKO mice with streptozotocin-induced diabetes. $^{*}P < 0.05$ versus Wild-C, $^{+}P < 0.01$ versus AMKO-C, and $^{\#}P < 0.05$ versus Wild-DM.

tubules, indicating that endogenous adrenomedullin may suppress the NADPH oxidase expression and its oxidative products in the diabetic kidneys.

In contrast, oxidative stress can induce adrenomedullin production [1, 22, 23], and it is possible that adrenomedullin increases in patients with diabetes to counterbalance increased oxidative stress. Indeed, increased oxidative stress is associated with elevated plasma levels of adrenomedullin in hypertensive diabetic patients [24]. The induction of adrenomedullin by high levels of glucose is dependent on PKC activation [8], while PKC also activates NADPH oxidase via translocation of p47phox and p67phox to the membrane components and produces oxidative stress [25] that further increases adrenomedullin production. Moreover, the NADPH oxidase expression and renal MDA production did not show significant differences between the AMKO mice and the wild type mice in the control condition in the present study, suggesting that the role of endogenous adrenomedullin is not obvious in the control condition without stimuli to enhance oxidative stress. Based on our results, it is possible to assume that endogenous adrenomedullin exerts a negative feedback action on oxidative stress via the suppression of NADPH oxidase.

Hyperplasia of renin-secreting granular cells in the JGA indicates the activation of the renin-angiotensin system in the kidneys. Enhanced production of renal angiotensin II increases the mesangial matrix via TGF-β and is also well known to stimulate NADPH oxidase activity and radical production [26, 27]. In the present study, we showed that the scores of granular cell hyperplasia were higher in the diabetic animals compared with those observed in the controls in both wild and AMKO mice. This finding is consistent with those of previous reports showing that the JGA is enlarged in the early stage of type 1 diabetes [28, 29]. It has been reported that the level of local angiotensin II is increased in the kidneys of diabetes, although the circulating levels of renin are normal or even low in diabetic patients [30–33]. Interestingly, in this study, the diabetic AMKO mice exhibited an exaggerated enlargement of renin-secreting granular cells and renal prorenin compared with the diabetic wild mice. This suggests an interaction between adrenomedullin and the renin-angiotensin system. Some reports have demonstrated that adrenomedullin increases the plasma renin concentration [34] and also increases the release of renin from isolated perfused kidneys as well as from primary cultured granular cells [35]. On the other hand, chronic adrenomedullin administration in Dahl salt-sensitive rats inhibits increases in the plasma renin concentration, the aldosterone level, and the renal tissue angiotensin II levels [2]. Although renal angiotensin II level was suppressed in the AMKO-mice in the normal condition, our histological findings of increased granular cell hyperplasia and renal prorenin in AMKO-DM mice compared with those of Wild-DM mice and the findings of renal angiotensin II suppression in the chronic adrenomedullin-infused-Dahl salt sensitive rats raise the hypothesis that adrenomedullin counteracts the pathological activation of JGA and the renal renin-angiotensin system in diabetes and hypertension. In this study, there was a positive correlation between the granular cell hyperplasia score and the NADPH oxidase expression in the macula densa, indicating that increases in the renal renin-angiotensin system stimulate the NADPH oxidase expression in the kidneys of diabetic AMKO mice.

In conclusion, adrenomedullin gene knockout exaggerates diabetic mesangial matrix expansion and the NADPH oxidase expression and is associated with increased renin-secreting granular cell hyperplasia and renal prorenin. Therefore, we believe that endogenous adrenomedullin counteracts the pathogenesis of diabetic nephropathy possibly through an antioxidative stress action via the suppression of NADPH oxidase and the renin-angiotensin system. The activation of an endogenous adrenomedullin may therefore be a novel therapeutic approach for effective treating of diabetic nephropathy.

Acknowledgment

This work was partly supported by Grants-in-Aid for scientific research from the Japan Society for the Promotion of Science to AT (C2-16590780, C-23591214).

References

[1] T. Saito, H. Itoh, T.-H. Chun et al., "Coordinate regulation of endothelin and adrenomedullin secretion by oxidative stress in endothelial cells," *American Journal of Physiology*, vol. 281, no. 3, pp. H1364–H1371, 2001.

[2] T. Nishikimi, Y. Mori, N. Kobayashi et al., "Renoprotective effect of chronic adrenomedullin infusion in Dahl salt-sensitive rats," *Hypertension*, vol. 39, no. 6, pp. 1077–1082, 2002.

[3] H. Nishimatsu, Y. Hirata, T. Shindo et al., "Role of endogenous adrenomedullin in the regulation of vascular tone and ischemic renal injury: studies on transgenic/knockout mice of adrenomedullin gene," *Circulation Research*, vol. 90, no. 6, pp. 657–663, 2002.

[4] T. Shimosawa, Y. Shibagaki, K. Ishibashi et al., "Ad-ren-om-ed-ull-in, an endogenous peptide, counteracts cardiovascular damage," *Circulation*, vol. 105, no. 1, pp. 106–111, 2002.

[5] T. Tsuruda and J. C. Burnett Jr., "Adrenomedullin: an autocrine/paracrine factor for cardiorenal protection," *Circulation Research*, vol. 90, no. 6, pp. 625–627, 2002.

[6] J. Kawai, K. Ando, A. Tojo et al., "Endogenous adrenomedullin protects against vascular response to injury in mice," *Circulation*, vol. 109, no. 9, pp. 1147–1153, 2004.

[7] M. Hayashi, T. Shimosawa, M.-A. Isaka, S. Yamada, R. Fujita, and T. Fujita, "Plasma adrenomedullin in diabetes," *The Lancet*, vol. 350, no. 9089, pp. 1449–1450, 1997.

[8] M. Hayashi, T. Shimosawa, and T. Fujita, "Hyperglycemia increases vascular adrenomedullin expression," *Biochemical and Biophysical Research Communications*, vol. 258, no. 2, pp. 453–456, 1999.

[9] K. Hiragushi, J. Wada, J. Eguchi et al., "The role of adrenomedullin and receptors in glomerular hyperfiltration in streptozotocin-induced diabetic rats," *Kidney International*, vol. 65, no. 2, pp. 540–550, 2004.

[10] M. Brownlee, "Biochemistry and molecular cell biology of diabetic complications," *Nature*, vol. 414, no. 6865, pp. 813–820, 2001.

[11] C. G. Schnackenberg and C. S. Wilcox, "The SOD mimetic tempol restores vasodilation in afferent arterioles of experimental diabetes," *Kidney International*, vol. 59, no. 5, pp. 1859–1864, 2001.

[12] T. Nassar, B. Kadery, C. Lotan, N. Da'as, Y. Kleinman, and A. Haj-Yehia, "Effects of the superoxide dismutase-mimetic compound tempol on endothelial dysfunction in streptozotocin-induced diabetic rats," *European Journal of Pharmacology*, vol. 436, no. 1-2, pp. 111–118, 2002.

[13] M. L. Onozato, A. Tojo, A. Goto, T. Fujita, and C. S. Wilcox, "Oxidative stress and nitric oxide synthase in rat diabetic nephropathy: effects of ACEI and ARB," *Kidney International*, vol. 61, no. 1, pp. 186–194, 2002.

[14] M. W. Brands, T. D. Bell, and B. Gibson, "Nitric oxide may prevent hypertension early in diabetes by counteracting renal actions of superoxide," *Hypertension*, vol. 43, no. 1, pp. 57–63, 2004.

[15] M. L. Onozato, A. Tojo, A. Goto, and T. Fujita, "Radical scavenging effect of gliclazide in diabetic rats fed with a high cholesterol diet," *Kidney International*, vol. 65, no. 3, pp. 951–960, 2004.

[16] K. Asaba, A. Tojo, M. L. Onozato et al., "Effects of NADPH oxidase inhibitor in diabetic nephropathy," *Kidney International*, vol. 67, no. 5, pp. 1890–1898, 2005.

[17] A. Tojo, M. L. Onozato, N. Kobayashi, A. Goto, H. Matsuoka, and T. Fujita, "Angiotensin II and oxidative stress in Dahl salt-sensitive rat with heart failure," *Hypertension*, vol. 40, no. 6, pp. 834–839, 2002.

[18] A. Tojo, M. L. Onozato, S. Fukuda, K. Asaba, K. Kimura, and T. Fujita, "Nitric oxide generated by nNOS in the macula densa regulates the afferent arteriolar diameter in rat kidney," *Medical Electron Microscopy*, vol. 37, no. 4, pp. 236–241, 2004.

[19] A. Tojo, K. Kimura, S. Nanba, H. Matsuoka, and T. Sugimoto, "Variations in renal arteriolar diameter in deoxycorticosterone acetate-salt hypertensive rats. A microvascular cast study," *Virchows Archiv A*, vol. 417, no. 5, pp. 389–393, 1990.

[20] M. L. Onozato, A. Tojo, J. Leiper, T. Fujita, F. Palm, and C. S. Wilcox, "Expression of NG,NG-dimethylarginine dimethylaminohydrolase and protein arginine N-methyltransferase isoforms in diabetic rat kidney effects of angiotensin II receptor blockers," *Diabetes*, vol. 57, no. 1, pp. 172–180, 2008.

[21] T. Ishimitsu, K. Tsukada, J. Minami et al., "Microsatellite DNA polymorphism of human adrenomedullin gene in type 2 diabetic patients with renal failure," *Kidney International*, vol. 63, no. 6, pp. 2230–2235, 2003.

[22] T.-H. Chun, H. Itoh, T. Saito et al., "Oxidative stress augments secretion of endothelium-derived relaxing peptides, C-type natriuretic peptide and adrenomedullin," *Journal of Hypertension*, vol. 18, no. 5, pp. 575–580, 2000.

[23] F. Yoshihara, T. Horio, T. Nishikimi, H. Matsuo, and K. Kangawa, "Possible involvement of oxidative stress in hypoxia-induced adrenomedullin secretion in cultured rat cardiomyocytes," *European Journal of Pharmacology*, vol. 436, no. 1-2, pp. 1–6, 2002.

[24] A. Katsuki, Y. Sumida, H. Urakawa et al., "Increased oxidative stress is associated with elevated plasma levels of adrenomedullin in hypertensive patients with type 2 diabetes," *Diabetes Care*, vol. 26, no. 5, pp. 1642–1643, 2003.

[25] M. Kitada, D. Koya, T. Sugimoto et al., "Translocation of glomerular p47phox and p67phox by protein kinase C-β activation is required for oxidative stress in diabetic nephropathy," *Diabetes*, vol. 52, no. 10, pp. 2603–2614, 2003.

[26] K. K. Griendling, C. A. Minieri, J. D. Ollerenshaw, and R. W. Alexander, "Angiotensin II stimulates NADH and NADPH oxidase activity in cultured vascular smooth muscle cells," *Circulation Research*, vol. 74, no. 6, pp. 1141–1148, 1994.

[27] P. N. Seshiah, D. S. Weber, P. Rocic, L. Valppu, Y. Taniyama, and K. K. Griendling, "Angiotensin II stimulation of NAD(P)H oxidase activity: upstream mediators," *Circulation Research*, vol. 91, no. 5, pp. 406–413, 2002.

[28] C. Gulmann, S. Rudberg, G. Nyberg, and R. Østerby, "Enlargement of the juxtaglomerular apparatus in insulin-dependent diabetes mellitus patients with microalbuminuria," *Virchows Archiv*, vol. 433, no. 1, pp. 63–67, 1998.

[29] C. Gulmann, R. Østerby, H.-J. Bangstad, and S. Rudberg, "The juxtaglomerular apparatus in young type-1 diabetic patients with microalbuminuria: effect of antihypertensive treatment," *Virchows Archiv*, vol. 438, no. 6, pp. 618–623, 2001.

[30] E. Ritz and R. Dikow, "Angiontensin receptor antagonists in patients with nephropathy due to type 2 diabetes," *Annals of Medicine*, vol. 34, no. 7-8, pp. 507–513, 2002.

[31] R. E. Gilbert, H. Krum, J. Wilkinson-Berka, and D. J. Kelly, "The renin-angiotensin system and the long-term complications of diabetes: pathophysiological and therapeutic considerations," *Diabetic Medicine*, vol. 20, no. 8, pp. 607–621, 2003.

[32] S. Mezzano, A. Droguett, M. E. Burgos et al., "Renin-angiotensin system activation and interstitial inflammation in human diabetic nephropathy," *Kidney International, Supplement*, vol. 64, no. 86, pp. S64–S70, 2003.

[33] R. Moriya, J. C. Manivel, and M. Mauer, "Juxtaglomerular apparatus T-cell infiltration affects glomerular structure in type 1 diabetic patients," *Diabetologia*, vol. 47, no. 1, pp. 82–88, 2004.

[34] C. J. Charles, J. G. Lainchbury, M. G. Nicholls, M. T. Rademaker, A. M. Richards, and R. W. Troughton, "Adrenomedullin and the renin-angiotensin-aldosterone system," *Regulatory Peptides*, vol. 112, no. 1–3, pp. 41–49, 2003.

[35] B. L. Jensen, B. K. Krämer, and A. Kurtz, "Adrenomedullin stimulates renin release and renin mRNA in mouse juxtaglomerular granular cells," *Hypertension*, vol. 29, no. 5, pp. 1148–1155, 1997.

Hindawi Publishing Corporation
Journal of Diabetes Research
Volume 2013, Article ID 463740, 8 pages
http://dx.doi.org/10.1155/2013/463740

Research Article

Both ERK/MAPK and TGF-Beta/Smad Signaling Pathways Play a Role in the Kidney Fibrosis of Diabetic Mice Accelerated by Blood Glucose Fluctuation

Xiaoyun Cheng,[1] Wenke Gao,[2] Yongyan Dang,[2] Xia Liu,[2] Yujuan Li,[2] Xu Peng,[2] and Xiyun Ye[2]

[1] *Department of Endocrinology, Shanghai Tenth People's Hospital, Tongji University School of Medicine, Shanghai 200072, China*
[2] *Shanghai Key Laboratory of Regulatory Biology, Institute of Biomedical Sciences and School of Life Sciences, East China Normal University, 500 Dongchuan Road, Shanghai 200241, China*

Correspondence should be addressed to Xiyun Ye; xyye@bio.ecnu.edu.cn

Received 9 October 2012; Revised 18 April 2013; Accepted 15 May 2013

Academic Editor: Shahidul Islam

Background. The notion that diabetic nephropathy is the leading cause of renal fibrosis prompted us to investigate the effects of blood glucose fluctuation (BGF) under high glucose condition on kidney in the mice. *Methods*. The diabetic and BGF animal models were established in this study. Immunohistochemistry, Western blot, and RT-PCR analysis were applied to detect the expression of type I collagen, matrix metalloproteinase-1 (MMP1), metalloproteinase inhibitor 1 (TIMP1), transforming growth factor beta 1 (TGF-β1), phosphorylated-ERK, p38, smad2/3, and Akt. *Results*. BGF treatment increased type I collagen synthesis by two times compared with the control. The expression of MMP1 was reduced markedly while TIMP1 synthesis was enhanced after BGF treatment. ERK phosphorylation exhibits a significant increase in the mice treated with BGF. Furthermore, BGF can markedly upregulate TGF-β1 expression. The p-smad2 showed 2-fold increases compared with the only diabetic mice. However, p-AKT levels were unchanged after BGF treatment. *Conclusions*. These data demonstrate that BGF can accelerate the trend of kidney fibrosis in diabetic mice by increasing collagen production and inhibiting collagen degradation. Both ERK/MAPK and TGF-β/smad signaling pathways seem to play a role in the development of kidney fibrosis accelerated by blood glucose fluctuation.

1. Introduction

Diabetes can cause a wide range of health complications such as atherosclerosis, cardiac dysfunction, retinopathy, and nephropathy. Hyperglycemia is a major sign of diabetes mellitus (DM) and the main cause for its various complications. The side effects of hyperglycemia can be categorized into two types, persistent elevation of blood glucose (BG) levels and blood glucose fluctuation (BGF) [1], which are closely correlated with the DM prognosis, pathogenesis, and complications. Larger BGF is associated with a higher incidence of chronic diabetic complications and a poorer prognosis [2]. Clinical studies have shown that the risks associated with long-term BGF were much more detrimental than that of chronic elevation of BG levels [3]. Furthermore, there are some evidences that intermittent fluctuation of high glucose can induce lesions of varying degrees in glomerular mesangial and vascular endothelial cells *in vitro* [4–6]. Thus, the effects of BGF on diabetic complications need to be determined.

Diabetic nephropathy (DN) is the leading cause of renal fibrosis and chronic renal failure [7]. Renal fibrosis was characterized by glomerulosclerosis and tubulointerstitial fibrosis, which would reduce excretory renal function [8]. Although considerable advances have been made to understand that hyperglycemia can promote chronic diabetic nephropathy, there are no published data to describe the effects of BGF under high glucose condition on renal fibrosis.

It is well known that fibroblast proliferation, altered expression and overdeposition of extracellular matrix contribute to progressive diabetic renal fibrosis. Collagen overproduction, as the major contributor of renal fibrosis, is regulated by several fibrogenic factors such as transforming growth factor-beta1 (TGF-β1) and matrix metalloproteinases (MMPs). To study the different effects of hyperglycemia and BGF under hyperglycemia conditions on collagen synthesis and degradation in the kidney of diabetic mice, we establish the diabetic and repetitive BGF animal models, respectively.

The inhibition of p38 mitogen-activated protein kinase has been reported to ameliorate renal fibrosis in obstructive nephropathy [9]. TGF-beta is the primary cytokine driving fibrosis in kidney and other organs susceptible to fibrotic injury such as lung and liver. Members of the TGF-β superfamily transduce intracellular signals by smad proteins. Smad2 and smad3 act in the TGF-β/activin pathway, whereas smad1, smad5, and smad8 are thought to act as bone-morphogenetic-protein- (BMP-) specific smads. Smad2/3 form heteromeric complexes with smad4 and translocate into the nucleus to regulate transcription of target genes. A study demonstrates that TGF-β signals can mediate renal fibrosis through smad2/3 [10]. However, the underlying cellular mechanisms by which BGF leads to matrix accumulation in the renal tissue are less well understood.

Therefore, this study investigates whether blood glucose fluctuation in the diabetic mice could accelerate the development and progression of diabetic renal fibrosis *in vivo*. Moreover, we also examine the underlying mechanisms of BGF-associated renal changes to further study the therapeutic potential of inhibiting BGF in diabetic renal fibrosis.

2. Methods

2.1. Animals. Male Kunming mice (25–28 g) were purchased from Shanghai SLAC Laboratory Animal Co. (Shanghai, China). They were housed in pathogen-free conditions with water and standard mouse chow freely available. Mice were randomly divided into 3 groups (n = 10/group): (i) Controls (C), (ii) Diabetic (D), and (iii) Diabetic with BGF (D + BGF).

2.2. Diabetic Mouse Model. Animals were fasted overnight and then injected i.v. into the tail vein with 50 mg/kg alloxan that was freshly prepared in normal saline and used within 10 min, whereas controls received saline only. Five days later, mice were fasted for 6 h and then peripheral blood was harvested from the tail vein. Blood glucose levels were determined using a glucose kit and only mice with concentrations between 18 to 21 mM were used for the studies.

2.3. BGF Mouse Model. Glucose delivered via i.p. injection was used to establish the BGF model. Diabetic mice were injected i.p. with 2 g/kg of glucose three times a day every 4 h starting at 8 a.m. for 6 weeks. Control and only diabetic mice received saline injections instead of glucose. Blood glucose levels were measured at 7 time points throughout the day for each week to test the regularity of fluctuations as shown in Figure 1. After the animal models were established, ten mice remained in each group for the further experiments.

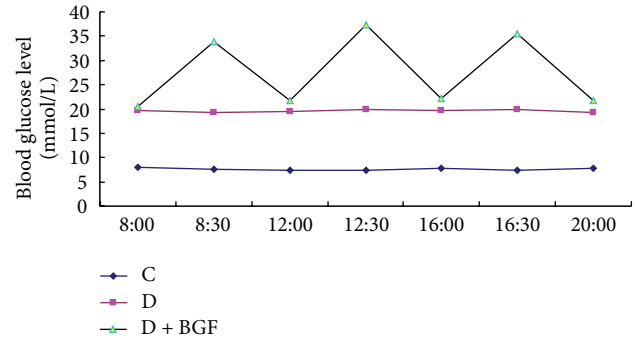

Figure 1: Blood glucose level in the mice at one day after eight-week BGF treatment.

2.4. RT-PCR. After the mice was killed by cervical dislocation, kidney tissue was taken and then weighed for 100 mg. The 100 mg samples were quick-frozen and crushed to powder in a mortar under liquid nitrogen. Total RNA was isolated using Trizol reagent (Invitrogen, USA) according to the instructions of manufacture. RNA samples were quantified by using BioPhotometer (Eppendorf, Germany), and 2 μg total RNA was reverse transcribed into cDNA in 20 μL reaction volume containing 2 μL of random oligonucleotide primer, AMV reverse transcriptase (Invitrogen, USA), and 2 mM dNTP mix. Reverse transcription was performed using a thermal program of 30°C for 10 min, 42°C for 20 min, 99°C for 5 min, and 4°C for 5 min. Then, 1 μL cDNA was used as the templates for PCR amplification in a thermal cycler. The specific primers sequences for human collagen I(α2), MMP1, TIMP1, TGF-β1, and GAPDH were as provided in Table 1. The cycling program used was 95°C for 10 min followed by 35 cycles of 95°C for 30 s, 58°C for 30 s, and 72°C for 45 s. PCR products were electrophoresed at 100 V for 30 min by using a 1% agarose gel, stained with 0.5 μg/mL ethidium bromide, and further visualized by UV illumination (Shanghai, China). The bands were then recorded and analyzed on a digital imaging system (Quantity One software). Levels of gene expression were expressed as the intensity of PCR products normalized that of the GAPDH in the same sample.

2.5. Western Blot. Frozen tissue was crushed in liquid nitrogen, homogenized in 100 μL RIPA lysis buffer (50 mM Tris-Cl, pH 8.0, 150 mM NaCl, 1% (v/v) Nonidet P-40, 0.5% Sodium deoxycholate, 0.1% SDS) on ice for 30 m. Protein was quantified by using the BCA Protein Assay Kit. Samples were run on a 10% denaturing polyacrylamide gel at 80 V, transferred to a nitrocellulose membrane (Millipore) and immunoblotted with anticollagen (Santa Cruz, CA, USA) at 1 : 1000, anti-MMP1 (Santa Cruz, CA, USA) at 1 : 1000, anti-TIMP1 (Santa Cruz, CA, USA) at 1 : 1000, anti-phospho-AKT at 1 : 1000, anti-phospho-ERK (Santa Cruz, CA, USA) at 1 : 1000, and anti-β-actin (Santa Cruz, CA, USA) at 1 : 5000. The fluorescently labeled secondary antibodies (Santa Cruz, CA, USA) were diluted 1 : 5000 into phosphate-buffered

Table 1: Primers for PCR.

Gene	Primer sequence-forward	Primer sequence-reverse
GAPDH	GGAGACAACCTGGTCCTCAG	ACCCAGAAGACTGTGGATGG
Col I(α2)	CTTGTGGCTTCTGACTATCT	AGGAAAATGAGGCTGTTA
MMP1	TTCTGAAACCCTGAGTGC	AAGCCTGGATGCGATTA
TIMP1	AGTGGGGTCTGTGAGGT	CAAAAGAGGGAGTGCTG
TGF-β	CGGTGCTCGCTTTGTA	GCCACTCAGGCGTATC

saline—0.05% Tween (PBST)—1% ovalbumin. Antigen-antibody complexes were visualized with fluorescent labeled secondary antibodies and LI-COR Odyssey Infrared Imaging System.

2.6. Immunohistochemistry. Kidney tissues were fixed in 4% paraformaldehyde at room temperature for 24 h. The samples were then dehydrated with 50%, 70%, 80%, 90%, 95%, and two times of 100% alcohol, cleared with xylene, and embedded in paraffin wax. Also, 5 μm sections were cut in a microtome (Leica, Germany), deparaffinized with xylene, and rehydrated in a series of ethanols. Endogenous peroxidase was blocked by 3% hydrogen peroxide in methanol for 30 m. For epitope retrieval, slides were heated in a microwave oven at 92°C for 20 m in a PBS buffer. They were then incubated overnight at 4°C with the primary antibodies anticollagen I, MMP1 at 1 : 250 (Santa Cruz, CA, USA). Sections were subsequently incubated for 1 h with biotinylated goat anti-rabbit antibody IgG and then for 30 m with Streptavidin-HRP peroxidase (Santa Cruz, CA, USA). Color reaction product was visualized by using diaminobenzidine-(DAB-) H_2O_2 as substrate for peroxidase. All sections were counterstained with hematoxylin, dehydrated, and covered. Incubations with phosphate-buffered saline containing 1% bovine serum albumin were used as negative controls. The positivity of immunoreactivity was evaluated semiquantitatively in a double-blind manner.

2.7. Statistical Analysis. Statistical analyses were performed with SPSS 15.0 software. Differences among different groups were evaluated with the student's t-test, and $P < 0.05$ was considered to be statistically significant.

3. Results

3.1. Blood Glucose Fluctuation Accelerate Type I Collagen Synthesis of Diabetic Mice. To examine whether blood glucose fluctuation could affect the expression of extracellular protein, RT-PCR analysis was performed. The results showed that type I collagen expression in the kidney increased markedly after BGF treatment when compared with the only diabetic mice and controls (Figure 2(a)). The increase rate of type I collagen in the D + BGF group was 2-fold higher than in the D group ($P < 0.05$) (Figure 2(b)).

The expression of type I collagen at the protein level was determined by Western blots. Compared with the D and C groups, BGF treatments induced the maximal increase in the protein level of type I collagen (Figure 2(c)). The results were similar to those obtained by RT-PCR.

To further test the effects of BGF on the kidney of diabetic mice, we performed the immunohistochemical analysis. Collagen expression was positive in 80% of the tissue in the BGF group, 50% of diabetic tissue, and 40% of controls (Figure 2(d)). Therefore, it is obvious that collagen expression was increased significantly in the D + BGF group compared with the D and control groups.

3.2. Blood Glucose Fluctuation Reduce Type I Collagen Degradation of Diabetic Mice. RT-PCR results showed that MMP1 mRNA levels were significantly decreased in the D + BGF group (Figure 3(a)). Although the mRNA level of MMP1 in the D group was also lower than the control, more decrease was observed in the D + BGF group than in only diabetic group ($P < 0.05$) (Figure 3(b)). In contrast, TIMP1 mRNA expression in the D + BGF group was elevated markedly compared with the D and C groups (Figures 3(a) and 3(b)). The proteins of MMP1 and TIMP1 were also evaluated by Western blot analysis. As expected, the protein production of MMP1 in the D + BGF group was markedly inhibited compared with the control and diabetic mice, while the TIMP1 level was higher than the other groups (Figure 3(c)).

A decrease of MMP1 positivity was observed simultaneously in the tissues of the BGF group by immunohistological staining. The MMP1 positive staining presents in 30% of tissue in BGF group, while the control mice showed 80% MMP1 positivity in the kidney (Figure 3(d)). Thus, consistent with the PCR and Western blotting analyses, immunohistological staining supported that collagen synthesis was rather increased while collagen degradation was quite reduced in the D + BGF group.

3.3. ERK Was Activated by Blood Glucose Fluctuation of Diabetic Mice. To determine whether blood glucose fluctuation might increase collagen synthesis in the kidney by activating extracellular signal-regulated kinase/mitogen-activated protein kinase (ERK/MAPK) signaling pathway, the effect of blood glucose fluctuation on the phosphorylation of ERK1/2 was examined. As seen in Figure 4, blood glucose fluctuation markedly induced MAPK/ERK activation. The activation of ERK was increased by twofold when compared with the only D group. Although the diabetes could also elevate the level of phospho-ERK1/2, the increase rate is far less than that of BGF treatment. Western blot analyses showed that the total protein levels of ERK in the BGF group were the same as the D and C groups. However, p38 showed little sensitivity to BGF treatment in the mice. The level of phosphor-p38 was almost unchanged in the control, diabetic, and the BGF mice.

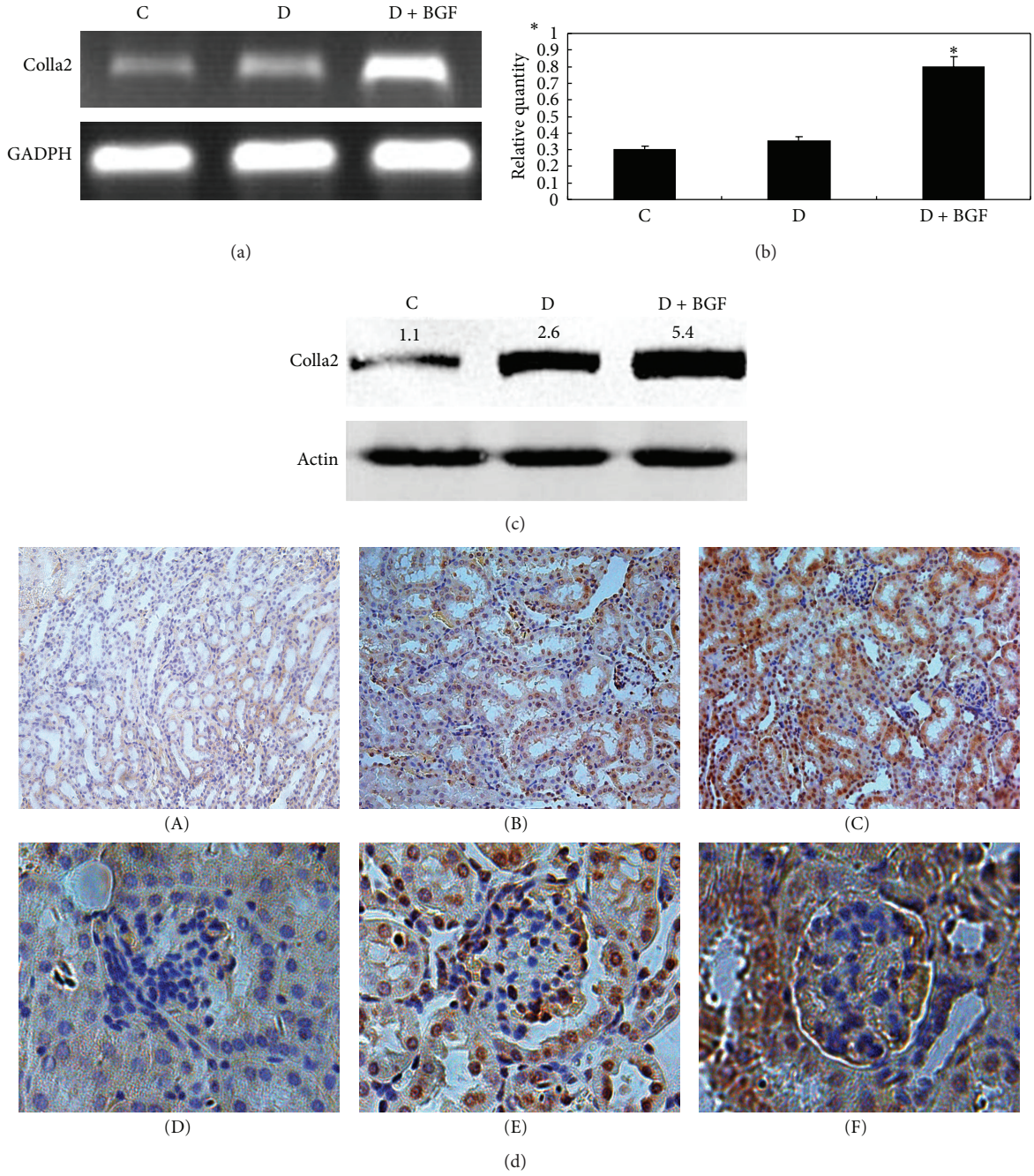

Figure 2: BGF treatment increased the synthesis of type I collagen. (a) Total RNA was extracted and analyzed for the expression of collagen in the kidney by RT-PCR. (b) GAPDH was used as an internal control. PCR products were semiquantified according to the ratio of type I procollagen mRNA to GAPDH mRNA. (b) Data are expressed as the mean ± SEM of three separate experiments. $^{*}P < 0.05$ as compared to the control. (c) Western blot analysis depicted protein level of collagen in the kidney of mice. (d) Immunohistological staining of type I collagen in the kidney tissue of normal ((A), (D)), diabetic ((B), (E)), and BGF-treated ((C), (F)) mice. The rate of collagen positivity in the BGF-treated mice is higher than the other groups. Magnification: 200x.

3.4. Blood Glucose Fluctuation Increased TGF-β and p-Smad2 Expression of Diabetic Mice. Blood fluctuation significantly increased TFG-β1 mRNA expression compared with the untreated mice (Figure 5(a)). The TGF-β1 levels in the kidney treated with BGF for eight weeks were 8 times the control (Figure 5(b)). Compared with the only diabetic mice, the TGF-β1 mRNA expression of D + BGF mice increased twofold ($P < 0.05$). So, blood glucose fluctuation caused more increase of TGF-β level than only diabetes.

To elucidate whether smad activity was increased by the upregulated expression of TGF-β1, the detection of phosphorylation of smad2 and smad3 was carried out. Figure 5(c)

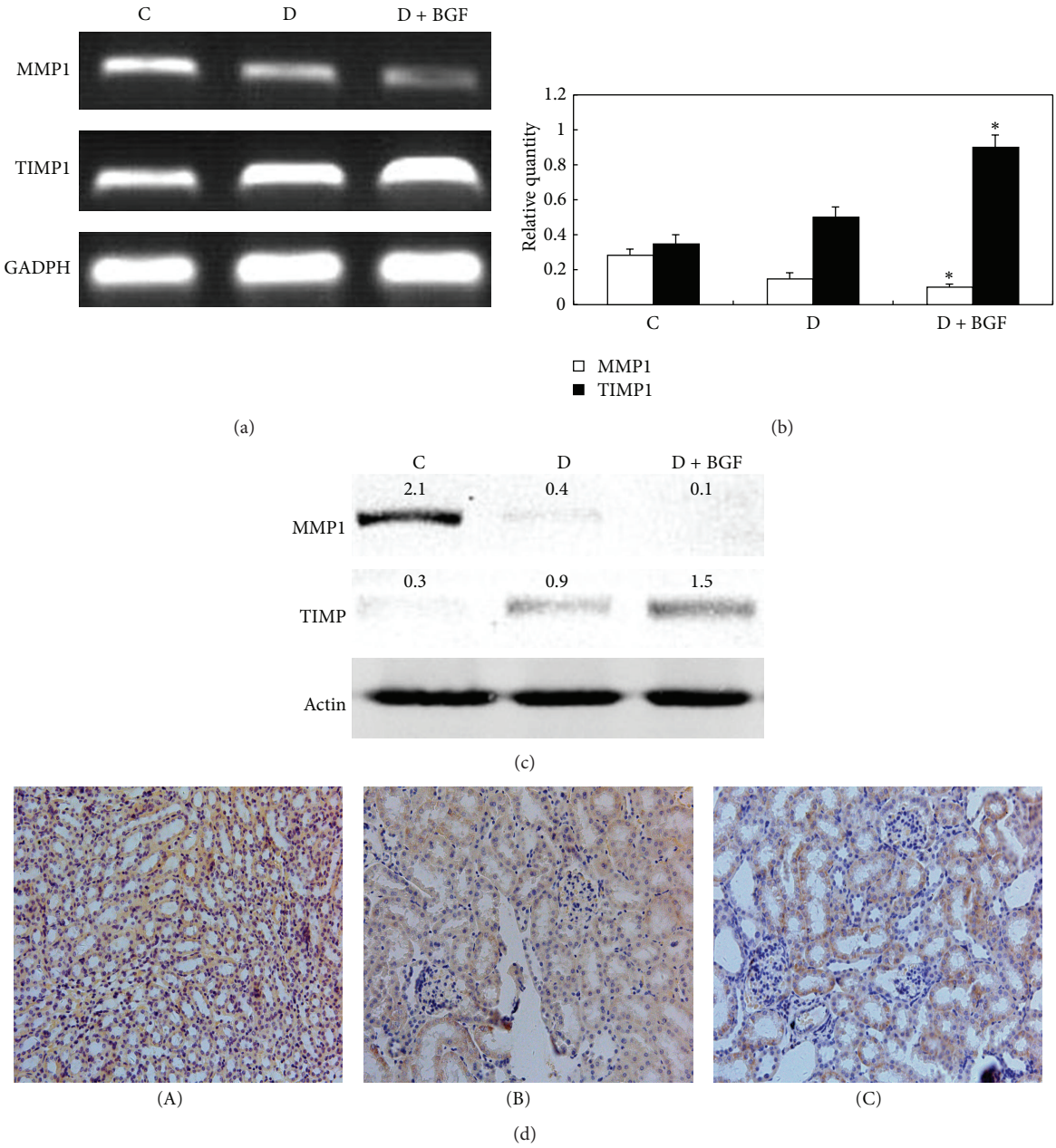

Figure 3: BGF treatment inhibited MMP1 and activated TIMP1. (a) MMP1 and TIMP1 expression in the kidney was evaluated by RT-PCR. (b) GAPDH was used as an internal control. PCR products were semiquantified according to the ratio of type I procollagen mRNA to GAPDH mRNA (b). Data are expressed as the mean ± SEM of three separate experiments. $^{*}P < 0.05$ as compared to the control. (c) Western blot analysis depicted protein levels of MMP1 and TIMP1 in the kidney of mice. (d) Immunohistological staining of MMP1 in the kidney of mice. The rate of MMP1 positivity in the BGF-treated mice (C) was lower than the normal (A) and diabetic (B) mice. Magnification: 200x.

clearly showed that the expression of p-smad2 in the kidney of BGF-treated mice was markedly increased compared with the controls. The elevation of p-smad2 was evident as a 2-fold increase in the kidneys of diabetic mice. The expression of p-smad3 also demonstrated a marked increase compared with controls. However, p-smad3 was similar between the diabetic mice and BGF-treated mice. These results showed that the increase of p-smad2 induced by BGF was more strongly than that of diabetes.

3.5. AKT Was Not Affected by Blood Glucose Fluctuation of Diabetic Mice. PKB/AKT signaling molecules have been reported to be activated by TGF-β1 and play a role in renal fibrosis during diabetic nephropathy. To determine the effects of blood glucose fluctuation on the activation of this signal pathway, phosphospecific antibody to AKT was used in Western blot. As shown in Figure 6, the level of AKT phosphorylation in the kidneys of BGF-treated mice is similar with the control. No differences in AKT

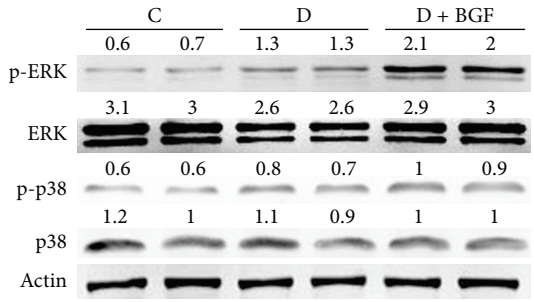

Figure 4: BGF treatment enhanced ERK1/2 phosphorylation in the kidney of mice. The p38 activity was not sensitive to BGF treatment. Whole cell lysates were collected and subjected to Western blot analysis for phosphorylated ERK1/2, p38 and total ERK 1/2, p38.

phosphorylation among the BGF-treated group, consistent hyperglycemia group and controls, were noted.

4. Discussion

Previous study indicates that repetitive postprandial fluctuation in glucose concentration evokes monocyte adhesion to endothelial cells, enhances endothelial cell apoptosis, and accelerates atherosclerosis that was worse than that induced by stable hyperglycemia *in vivo* [11–13]. Glucose fluctuations during postprandial periods also exhibited a more specific triggering effect on oxidative stress than chronic sustained hyperglycemia [14]. Moreover, BGF was demonstrated to damage skin collagen metabolism in mouse skin [15]. In this study, we find that treatments with BGF resulted in increased expression and deposition of type I collagen and decreased collagen degradation when compared to the stable hyperglycemia mice. The overproduction of the interstitial matrix components such as type I and type III collagen and fibronectin is thought to be the most important event in naturally occurring renal fibrosis [8]. Decreased MMPs and increased expression of TIMP1 participate in the excessive collagen deposit during the evolution of experimental interstitial renal fibrosis [16]. Thus, our data indicated that BGF may be related with the development of renal fibrosis in diabetic mice. BGF seems to produce more deleterious effects on accelerating of renal fibrosis of diabetic mice than only consistent hyperglycemia. Therefore, besides the traditional therapeutic methods for DN, more attention should be payed to inhibiting BGF in the diabetes.

Renal fibrosis is characterized by the increased accumulation of extracellular matrix (ECM) within renal tissue. An abnormal matrix deposition may be due to increased synthesis or decreased degradation of ECM. Our present study demonstrated that BGF not only induces the expression of ECM, but also inhibits its degradation by inhibiting matrix metalloproteases (MMPs) and activating the tissue inhibitor of metalloproteinases (TIMPs), which supported the importance of BGF in the progress of renal fibrosis in the diabetes. A previous study demonstrated that short-term peaks in glucose increased the production of collagen type IV, fibronectin, MMP2, MMP9, and TGF-1 in human renal

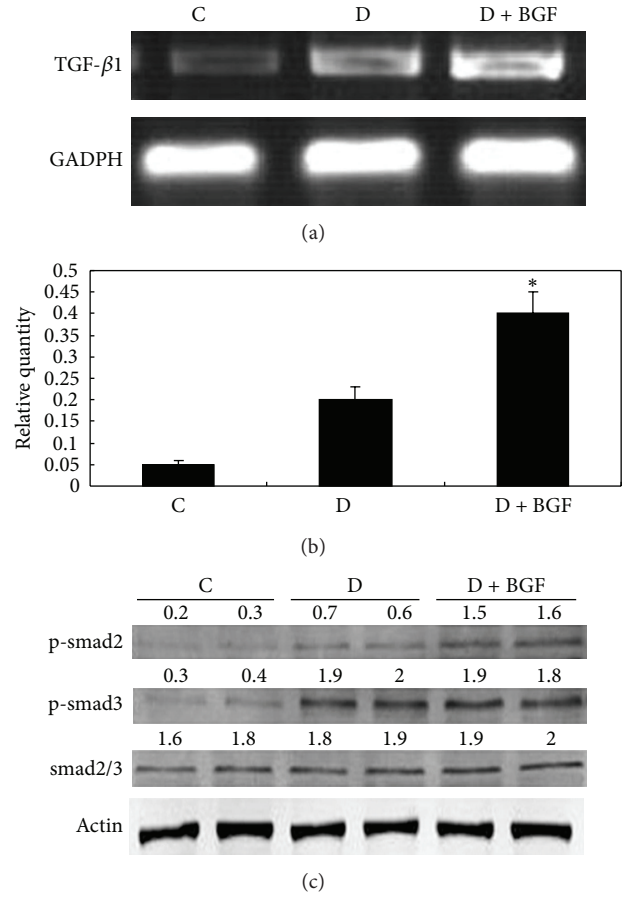

Figure 5: BGF treatment upregulated TGF-β1 expression and activated TGF-β1-induced smad signaling. (a) TGF-β1 expression in the kidney of mice was evaluated by RT-PCR. (b) Data are expressed as the mean ± SEM of three separate experiments. $^{*}P < 0.05$ as compared to the control. (c) The phosphorylated forms of smad2 and smad3 were analyzed by Western blot, using either rabbit anti-p-smad2 or rabbit anti-p-smad3 and total rabbit anti-smad2/3 antibody.

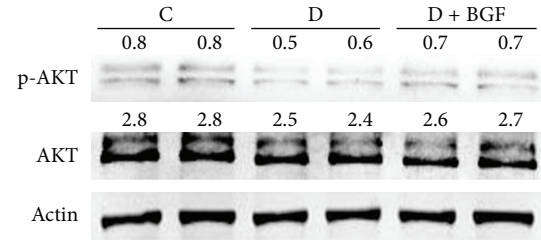

Figure 6: The activity of PIP3/AKT signal pathway was unchanged after BGF treatment. The phosphorylated and total AKT levels were evaluated by Western blot analysis.

cortical fibroblasts [17]. Thus, they concluded that exposure to fluctuating glucose concentrations increases renal interstitial fibrosis *in vitro*, which is consistent with our results *in vivo*.

However, the mechanisms by which BGF affects renal fibrosis remain unclear. The MAPK pathways are well characterized in regulating ECM expression. A previous report

showed that the single blockade of p38 MAPK after the emergence of established fibrosis is effective to reduce subsequent renal fibrosis in the model of unilateral ureteral obstruction [18]. We had some indication, in renal fibrosis, that MAPK pathway may have some roles in promoting BGF-induced abnormal deposition of ECM. Western blot analysis indicated that the level of the phosphorylation of ERK1/2 increased significantly in comparison with the controls and the stable hyperglycemia group. Consistent with the increased collagen synthesis, treatments with only hyperglycemia also cause the activation of ERK pathway compared to controls, but the effect was less than that of BGF treatment. The positive relationship between pERK and collagen overproduction indicated that it is possible that BGF accelerated renal fibrosis by activating the ERK pathway. However, our results showed that the role of p38 in the BGF-induced renal fibrosis can be neglected. It is regrettable that we could not detect the p-JNK expression. We assumed that the role of JNK signaling in the process of BGF-induced renal fibrosis may be minimal.

A previous study has demonstrated that TGF-β was a key mediator of hyperglycemia-induced increase in ECM accumulation [19]. In addition, blocking TGF-β's function has been described to suppress excess ECM accumulation and glomerulosclerosis [20]. Similar with the previous results, we found that hyperglycemia indeed increased the expression of TGF-β1 when compared to the controls. However, the level of TGF-β1 in the D + BGF group was more than that of stable hyperglycemia group, indicating that BGF can accelerate the accumulation of ECM than only diabetes. Several data showed that both smad2 and smad3 mediate the signal transduction from TGF-β1 [21, 22]. Thus, we detected the phosphorylation of smad2 and smad3 by Western blot. We observed BGF markedly increased the levels of p-samd2 when compared the hyperglycemia mice. Our results indicated that BGF-accelerated renal fibrosis also appears to be related with the activation of TGF-β/smad signal pathway. However, p-smad3 showed the similar increases in the BGF-treated and only diabetic mice compared with the controls. Smad7 is an inhibitory smad that functions to block smad2/3 activation by degrading the TβRI and smads [23]. Also, it can inhibit NF-κB-driven inflammatory response by inducing IκBα [24]. Kidney-targeting smad7 gene transfer inhibits renal TGF-β/MAD homologue (smad) and nuclear factor κB (NF-κB) signalling pathways and improves diabetic nephropathy in mice [25]. Thus, expression of smad7 and NF-κB in response to blood glucose fluctuations should be performed in our further experiments. Further studies are also needed to determine the exact relationship between ERK/MAPK and TGF-β/smad signaling in the development and progression of diabetic renal fibrosis.

Another previous study showed that TGF-β-mediated PKB/Akt activation may be important in renal fibrosis during diabetic nephropathy [26]. The activated PI3-K/Akt was found to participate in regulation of HSC migration, proliferation, collagen secretion, and adhesion. However, we could not find any elevation of phosphorylated-AKT in the hyperglycemia mice and BGF-treated mice compared with the controls. Thus, these data showed that Akt may not serve as a mediator of BGF induced renal fibrosis during the pathogenesis of DN.

In summary, we have shown in this present study that BGF could accelerate the progress of renal fibrosis under high glucose conditions by increasing extracellular matrix protein synthesis and inhibiting its degradation. Furthermore, we demonstrate that both ERK/MAPK and TGF-β/smad signaling pathways seem to play a role in the kidney fibrosis of diabetic mice accelerated by blood glucose fluctuation. The data suggest that inhibition of fluctuations in glucose concentrations may be of potential benefit in preventing the renal fibrosis in the diabetic patients. However, diabetic nephropathy as well as interstitial fibrosis is a late occurrence during the development of diabetes. So, it is worthwhile to make a long-term animal model to confirm the results in this study.

Conflict of Interests

The authors declare that they have no conflict of interests.

Acknowledgments

This work was supported by the Grants from the National Basic Research Program of China (2012CB910400), the Grants from National Natural Science Foundation of China (no. 81272226), and the Grants from the Ministry of Science and Technology (2010CB945400).

References

[1] S. del Prato, "In search of normoglycaemia in diabetes: controlling postprandial glucose," *International Journal of Obesity*, vol. 26, no. 3, pp. S9–S17, 2002.

[2] A. Ceriello, "The emerging role of post-prandial hyperglycaemic spikes in the pathogenesis of diabetic complications," *Diabetic Medicine*, vol. 15, pp. 188–193, 1998.

[3] E. Bonora and M. Muggeo, "Postprandial blood glucose as a risk factor for cardiovascular disease in Type II diabetes: the epidemiological evidence," *Diabetologia*, vol. 44, no. 12, pp. 2107–2114, 2001.

[4] L. Piconi, L. Quagliaro, R. da Ros et al., "Intermittent high glucose enhances ICAM-1, VCAM-1, E-selectin and interleukin-6 expression in human umbilical endothelial cells in culture: the role of poly(ADP-ribose) polymerase," *Journal of Thrombosis and Haemostasis*, vol. 2, no. 8, pp. 1453–1459, 2004.

[5] L. Quagliaro, L. Piconi, R. Assaloni, L. Martinelli, E. Motz, and A. Ceriello, "Intermittent high glucose enhances apoptosis related to oxidative stress in human umbilical vein endothelial cells: the role of protein kinase C and NAD(P)H-oxidase activation," *Diabetes*, vol. 52, no. 11, pp. 2795–2804, 2003.

[6] L. Quagliaro, L. Piconi, R. Assaloni et al., "Intermittent high glucose enhances ICAM-1, VCAM-1 and E-selectin expression in human umbilical vein endothelial cells in culture: the distinct role of protein kinase C and mitochondrial superoxide production," *Atherosclerosis*, vol. 183, no. 2, pp. 259–267, 2005.

[7] J. L. Gross, M. J. de Azevedo, S. P. Silveiro, L. H. Canani, M. L. Caramori, and T. Zelmanovitz, "Diabetic nephropathy: diagnosis, prevention, and treatment," *Diabetes Care*, vol. 28, no. 1, pp. 164–176, 2005.

[8] Y. Liu, "Renal fibrosis: new insights into the pathogenesis and therapeutics," *Kidney International*, vol. 69, no. 2, pp. 213–217, 2006.

[9] M. Nishida, Y. Okumura, H. Sato, and K. Hamaoka, "Delayed inhibition of p38 mitogen-activated protein kinase ameliorates renal fibrosis in obstructive nephropathy," *Nephrology Dialysis Transplantation*, vol. 23, no. 8, pp. 2520–2524, 2008.

[10] W. Wang, V. Koka, and H. Y. Lan, "Transforming growth factor-β and Smad signalling in kidney diseases," *Nephrology*, vol. 10, no. 1, pp. 48–56, 2005.

[11] K. Azuma, R. Kawamori, Y. Toyofuku et al., "Repetitive fluctuations in blood glucose enhance monocyte adhesion to the endothelium of rat thoracic aorta," *Arteriosclerosis, Thrombosis, and Vascular Biology*, vol. 26, no. 10, pp. 2275–2280, 2006.

[12] L. Piconi, L. Quagliaro, R. Assaloni et al., "Constant and intermittent high glucose enhances endothelial cell apoptosis through mitochondrial superoxide overproduction," *Diabetes/Metabolism Research and Reviews*, vol. 22, no. 3, pp. 198–203, 2006.

[13] A. Risso, F. Mercuri, L. Quagliaro, G. Damante, and A. Ceriello, "Intermittent high glucose enhances apoptosis in human umbilical vein endothelial cells in culture," *American Journal of Physiology—Endocrinology and Metabolism*, vol. 281, no. 5, pp. E924–E930, 2001.

[14] L. Monnier, E. Mas, C. Ginet et al., "Activation of oxidative stress by acute glucose fluctuations compared with sustained chronic hyperglycemia in patients with type 2 diabetes," *Journal of the American Medical Association*, vol. 295, no. 14, pp. 1681–1687, 2006.

[15] X. Ye, Z. Tong, Y. Dang et al., "Effects of blood glucose fluctuation on skin biophysical properties, structure and antioxidant status in an animal model," *Clinical and Experimental Dermatology*, vol. 35, no. 1, pp. 78–82, 2010.

[16] G. González-Avila, C. Iturria, F. Vadillo-Ortega, C. Ovalle, and M. Montaño, "Changes in matrix metalloproteinases during the evolution of interstitial renal fibrosis in a rat experimental model," *Pathobiology*, vol. 66, no. 5, pp. 196–204, 1998.

[17] T. S. Polhill, S. Saad, P. Poronnik, G. R. Fulcher, and C. A. Pollock, "Short-term peaks in glucose promote renal fibrogenesis independently of total glucose exposure," *American Journal of Physiology—Renal Physiology*, vol. 287, no. 2, pp. F268–F273, 2004.

[18] C. Stambe, R. C. Atkins, G. H. Tesch, T. Masaki, G. F. Schreiner, and D. J. Nikolic-Paterson, "The role of p38α mitogen-activated protein kinase activation in renal fibrosis," *Journal of the American Society of Nephrology*, vol. 15, no. 2, pp. 370–379, 2004.

[19] E. Sugaru, M. Sakai, K. Horigome et al., "SMP-534 inhibits TGF-β-induced ECM production in fibroblast cells and reduces mesangial matrix accumulation in experimental glomerulonephritis," *American Journal of Physiology—Renal Physiology*, vol. 289, no. 5, pp. F998–F1004, 2005.

[20] R. Chen, C. Huang, T. A. Morinelli, M. Trojanowska, and R. V. Paul, "Blockade of the effects of TGF-β1 on mesangial cells by overexpression of Smad7," *Journal of the American Society of Nephrology*, vol. 13, no. 4, pp. 887–893, 2002.

[21] E. Kalo, Y. Buganim, K. E. Shapira et al., "Mutant p53 attenuates the SMAD-dependent transforming growth factor β1 (TGF-β1) signaling pathway by repressing the expression of TGF-β receptor type II," *Molecular and Cellular Biology*, vol. 27, no. 23, pp. 8228–8242, 2007.

[22] C.-H. Heldin, K. Miyazono, and P. Ten Dijke, "TGF-β signalling from cell membrane to nucleus through SMAD proteins," *Nature*, vol. 390, no. 6659, pp. 465–471, 1997.

[23] T. Ebisawa, M. Fukuchi, G. Murakami et al., "Smurf1 interacts with transforming growth factor-β type I receptor through smad7 and induces receptor degradation," *Journal of Biological Chemistry*, vol. 276, no. 16, pp. 12477–12480, 2001.

[24] H. Y. Chen, X. R. Huang, W. Wang et al., "The protective role of Smad7 in diabetic kidney disease: mechanism and therapeutic potential," *Diabetes*, vol. 60, no. 2, pp. 590–601, 2011.

[25] S. M. Ka, Y. C. Yeh, X. R. Huang et al., "Kidney-targeting Smad7 gene transfer inhibits renal TGF-β/MAD homologue (SMAD) and nuclear factor κb (NF-κB) signalling pathways, and improves diabetic nephropathy in mice," *Diabetologia*, vol. 55, no. 2, pp. 509–519, 2012.

[26] J. J. Kattla, R. M. Carew, M. Heljić, C. Godson, and D. P. Brazil, "Protein kinase B/Akt activity is involved in renal TGF-β1-driven epithelial-mesenchymal transition in vitro and in vivo," *American Journal of Physiology—Renal Physiology*, vol. 295, no. 1, pp. F215–F225, 2008.

Hindawi Publishing Corporation
Journal of Diabetes Research
Volume 2013, Article ID 473575, 9 pages
http://dx.doi.org/10.1155/2013/473575

Review Article

Mild Diabetes Models and Their Maternal-Fetal Repercussions

D. C. Damasceno, Y. K. Sinzato, A. Bueno, A. O. Netto, B. Dallaqua, F. Q. Gallego, I. L. Iessi, S. B. Corvino, R. G. Serrano, G. Marini, F. Piculo, I. M. P. Calderon, and M. V. C. Rudge

Laboratory of Experimental Research on Gynecology and Obstetrics, Department of Gynecology and Obstetrics, Botucatu Medical School, Universidade Estadual Paulista (Unesp), 18618-970 Botucatu, SP, Brazil

Correspondence should be addressed to M. V. C. Rudge; marilzarudge@ig.com.br

Received 4 January 2013; Revised 10 June 2013; Accepted 11 June 2013

Academic Editor: Daisuke Koya

The presence of diabetes in pregnancy leads to hormonal and metabolic changes making inappropriate intrauterine environment, favoring the onset of maternal and fetal complications. Human studies that explore mechanisms responsible for changes caused by diabetes are limited not only for ethical reasons but also by the many uncontrollable variables. Thus, there is a need to develop appropriate experimental models. The diabetes induced in laboratory animals can be performed by different methods depending on dose, route of administration, and the strain and age of animal used. Many of these studies are carried out in neonatal period or during pregnancy, but the results presented are controversial. So this paper, addresses the review about the different models of mild diabetes induction using streptozotocin in pregnant rats and their repercussions on the maternal and fetal organisms to propose an adequate model for each approached issue.

1. Introduction

Diabetes mellitus (DM) is considered a chronic disease characterized by hyperglycemia resulting from insulin resistance and/or insulin secondary deficiency caused by failure in beta cells (β) pancreatic [1]. DM1 is an autoimmune disease in which there are deficiency of insulin and loss of control of blood glucose, caused by the destruction of pancreatic β cells mediated by T cells [2]. DM2 is characterized by β-cell dysfunction and decreased insulin action in some tissues [3]. Another classification is the gestational DM, which occurs by glucose intolerance with variable magnitude. It is first diagnosed during pregnancy and may or may not persist after delivery [4].

Human studies that explore mechanisms responsible for changes caused by diabetes are limited not only for ethical reasons but also by the many uncontrollable variables (diet, socioeconomic factors, nutrition, and genetic factors) that can alter the intrauterine environment and increase congenital malformations. So there is a need to develop a suitable experimental model [5]. The use of animal models provides an essential tool for investigating the molecular mechanisms that control cell growth. The maternal-fetal interface is no exception. Although there are some differences in the organization of rodent versus primate maternal-fetal interface, there are many similarities in the functions and in cell lines that compose it. The induction of experimental diabetes by cytotoxic drugs such as beta-streptozotocin (STZ) is well characterized [6]. Depending on the animal strain used, dose, route of drug administration, and the life period in which STZ is administered in rats, different glycemic intensities are achieved: severe diabetes (blood glucose superior to 200/300 mg/dL) [7–13] or mild diabetes (glycemia between 120 and 200/300 mg/dL) [14–18].

An ideal experimental model of gestational diabetes should have normal glycemia levels before gestation but glucose intolerance and impaired insulin secretion and/or function after midpregnancy, which leads to alterations in both glucose and lipid metabolism in the mother and consequently in the fetus [19]. Therefore, mild diabetes is employed in experimental studies to reproduce blood glucose levels as observed in human pregnancy.

This paper addresses a review about the different models of mild diabetes induction in rat pregnancy. This review includes repercussions on the endocrine pancreas, early embryo development, reproductive performance, oxidative stress, structural analysis of the extracellular matrix and urethral striated muscle, and transgenerational effects.

2. Models of Mild Diabetes Induction and Repercussions on the Maternal and Fetal Organisms

2.1. Endocrine Pancreas. Studies about the effects of diabetes in the endocrine pancreas address β-cell regeneration by different mechanisms like neogenesis, proliferation, and transdifferentiation of these cells in animals. Neogenesis consists in generation of new cells from undifferentiated cells. When a differentiated cell undergoes transgression and becomes another type of cell, this is termed transdifferentiation. Proliferation consists in cell replication itself [20, 21].

The regeneration of β cells in STZ-treated pancreata has already been demonstrated in neonatal rats [22]. To evaluate the relationship among the morphology of the pancreatic islets, plasmatic glucose, and insulin, Bonner-Weir et al. [23] intraperitoneally induced diabetes by streptozotocin administration at a dose of 90 mg/kg on day 2 of life in rats. At day 4 of life, the rats presented hyperglycemia and reduced β cells number. At day 10 of life, there were partial recovery of the β cells and normoglycemia. However, after six-weeks, return of hyperglycemia and decreased β-cell volume were observed, therefore, suggesting that these cells are able to partially regenerate.

STZ administration (100 mg/Kg, saphenous vein) on the day of birth of the neonate rats [14, 15] caused high mortality (30 to 50%) [14]. These animals showed decreased pancreatic insulin and hyperglycemia (200–300 mg/dL) [14, 15]. Diabetes presented a quick and spontaneous remission observed by gradual increase of pancreatic insulin of these animals [14], however, during adult life, the animals showed a decrease of insulin secretion [15]. It was concluded that the STZ administered in neonatal life causes regeneration, however, there is a partial loss of β-cell mass and its function. Thus, it suggests that the STZ administered in newborns can not only be used for experimental diabetes but can also be used as a model for studies on neogenesis and/or proliferation of beta cells [14]. Similarly, Movassat et al. [24] intraperitoneally used the same dose of STZ (100 mg/Kg) and observed three days after treatment that the newborn rats exhibited diabetes, decreased body weight, and reduced β cells number. Seven days after administration of STZ, all animals showed increased proliferation of β cells, but the group treated with insulin presented a higher number of cell replication. The insulin-favored regeneration of the β cells reflects both an increased replication from differentiated β cells and an increased neogenesis from precursor/stem cells, with this last pathway being preferentially activated.

Thyssen et al. [25], Nicholson et al. [26], and Liang et al. [27] used 70 mg/kg STZ intraperitoneally on day 4 of postnatal life of rats, and the hyperglycemia (200–300 mg/dL) was verified two days after induction of diabetes. The animals that received the drug presented increased glycemia and partial destruction of β cells [25–27] accompanied by a relative loss of the nucleus islet microvasculature of rats [26]. There was a decrease in pancreatic beta cell mass, but these cells showed rapid regeneration because hyperglycemia was transient. This fact suggests that generation of new islets and restructuring of existing islets may occur [25–27]. Thus, a rapid regeneration that appears to involve the generation of new islets [25], the restructuring of preexisting islets [26], or transdifferentiation of the alpha cell to beta cell was documented [27], but studies indicate that age may limit the mechanism of cell regeneration [25].

Thus, the different studies showed that, regardless of the doses and route of streptozotocin administered in neonatal period, the transient hyperglycemia is resulting from partial regeneration of the beta cell. However, the pathophysiological mechanism involved in this regeneration is unclear.

2.2. Reproductive Performance. The hyperglycemia of gestational diabetes can lead to changes in maternal reproductive performance and embry-ofetal development [28]. Perhaps one of the most devastating diabetes complications is diabetic embryopathy, in which the offspring of a mother with diabetes predating a pregnancy presents congenital malformations. These malformations can affect multiple organ systems, including the brain and spinal cord, the heart and major vessel, kidneys, gut, and skeletal structures [29, 30], and result in pre- or postnatal mortality or disability.

The cellular damage that occurs in differentiated tissues leading to disease may also occur in differentiating embryo tissues but, in addition, malformation may result because signaling caused by excess glucose metabolism interferes with tissue morphogenesis. Because the observations of structures were formed, the factors involved in the malformation appearance cannot be determined. It is important to identify and intermediate in these factors in preimplantation period to prevent fetal malformations.

A unique characteristic of preimplantation development of mammals is that the embryo at this stage is self-regulative; that is, during the first three cleavages, the embryo is highly adaptable and can resist insults with the removal, addition, or rearrangement of its blastomeres [31–33]. Even so, changes that occur in the first stage of embryonic development have an impact on pre-and postimplantation [34]. In addition, initial embryos are able to grow in synthetic culture medium for several days without presenting changes even after being returned to the uterus [35]. Thus, most studies related to diabetes and embryo development use this ability of the embryo as a tool to monitor embryo development in vitro, trying to justify the low implantation rates and the malformation occurrence in diabetic women. As a result, several models are used to explore the pathophysiological mechanisms involved. Although this review has been focused on the models of mild diabetes induction, we studied in vivo model of the mild diabetes, and there are few published articles on the effects/consequences of this type of diabetes at the beginning of embryonic development. Therefore, this section shows an

overview of the studies and in vitro models of diabetes with high glycemic intensity (severe diabetes).

Mihajlik et al. [36] used embryos recovered (day 3) from females mice that received different doses of streptozotocin (130 or 160 mg/kg ip), 14–17 days before mating. These embryos were transferred to the environment in vitro and analyzed after 48 hours of cultivation. The embryos from mice that received STZ 130 mg/kg showed delay in cell proliferation, and those from mice given 160 mg/kg STZ exhibited a high degree of degeneration. However, on day 3 of pregnancy, these animals showed similar blood glucose levels to the control group. After glucose overload, both groups missed reestablishing initial glucose levels, suggesting that changes in maternal insulin levels may affect the embryo in the preimplantation resulting in alteration of cellular distribution during cultivation in vitro and in highest dose of beta-cytotoxic drug, inhibiting the progression of embryonic development after the third cleavage which reinforces the idea that the plasticity of embryonic cells decreases as the embryo develops.

The culture of mouse embryos in serum of women with diabetes [37] results in decreased viability, however, caused no developmental delay. Changes in embryonic growth are found in vitro models as in the study proposed by Wyman et al. [34] that involves embryos exposed to high glucose concentrations in vitro at the fertilization period and, after that, transferred to the uterus of control rats or on the model proposed by Pampfer et al. [38], using uterine cells from diabetic rats as component of the culture medium in which the embryos are developed. Fraser et al. [39] exposed embryos to different glucose concentrations and showed that at high concentrations (15.56 and 25.56 mM glucose) the numbers of blastocysts and cells per blastocyst were reduced at the 5th day of pregnancy; however, the apoptosis rate of these cells was unaltered. In contrast, other investigators describe a relation between decreased cellular number and increased apoptosis in embryos exposed to hyperglycemic environment [40, 41]. Furthermore, increased glucose concentration alters the distribution of embryonic cells causing a decrease in the inner cells mass number while causing an increase in trophoectoderm cells number [39].

These in vitro results could explain the low implantation rate and increased losses and embryonic malformations in pregnancy complicated by diabetes. However, when the zygote is transferred from diabetic uterus to healthy uterus, developmental delay occurs in addition to malformations (neural tube, ribs, and abdominal wall defects), although the exposure time in hyperglycemic environment is short. When the zygote is submitted to high glucose concentrations in vitro for the same period and transferred to the uterus of a female healthy, embryos exhibit reduced capacity for development, demonstrated by an increase in the rate of reabsorption and decreased sites of embryo implantation [34]. While in vitro analysis of embryos allows monitoring normal morphology [42], recent studies indicate that culture of embryos can break embryonic epigenetic control mechanisms leading to altered expression of some genes [43, 44], resulting in embryos that respond differently from those which develop in the in vivo environment.

Furthermore, while high concentrations of glucose are used in vitro studies, many researchers have developed models of diabetes in animals to reproduce DM2 and/or DM gestational to better understand the pathophysiology. A single in vivo study has associated the increased number of morulae and increased number of blastocysts at 5th day of pregnancy at lower doses of streptozotocin to rats with moderate diabetes (glycemia between 120 and 300 mg/dL). Changes in early development in vivo demonstrate that embryos arising from rats with moderate diabetes have developmental delay, similar to embryos from rats with severe diabetes. Moreover, when maternal hyperglycemia increases, the embryos show higher apoptosis rate [45]. Since metabolic insults, such as diabetes, can permanently affect the initial development [34], the use of in vivo models can be a way to clarify the possible mechanisms involved in the increased embryonic loss and malformation in type 2 DM.

Our research group aimed to induce the mild diabetes in laboratory animals. In this regard, female offspring received STZ (100 mg/kg, sc) at first day of life. At adult stage, the Wistar rats presented at term pregnancy increased embryonic losses before and after the implantation process, reduced corpora lutea number and decreased number of live fetuses [46, 47], increased weight and placental index, reduced rates of fetuses with appropriate weights for gestational age, and decreased degree of ossification, showing delay in fetal somatic maturation [46]. Dallaqua et al. [48], using the same model of diabetes induction but with another stain (Sprague Dawley), found a reduction in the number of live fetuses, fetal viability index, and increased number of embryonic deaths. In other study, mild diabetes was induced using STZ (70 mg/kg ip) in female rats on day 5 of postnatal life, and the results showed altered maternal lipid profile, increased oxidative stress, and increased frequency fetal visceral anomalies [49]. The same research group verified similar alteration when STZ was administered at birth (100 mg/kg, sc) and at day 7 of pregnancy (20 mg/kg, ip), confirming that glycemic alterations may impair ovulation and the early stages of embryonic development. Besides, intrauterine growth restriction (IUGR) in the fetuses from these rats was also observed. Regarding the analysis of skeletal fetuses of diabetic rats, the sterna showed abnormal morphology and absent cervical nuclei [50].

Another model using STZ (70 mg/kg, ip) on the 5th day of life in female rats showed a reduction in the number of corpora lutea, lower maternal weight due to higher rates of fetuses with small weight for gestational age, and a lower rate of fetuses large for gestational age [51]. In addition, there was an increase in the number of fetuses with visceral abnormalities (hydronephrosis and hydroureter) [18].

Kervran et al. [52], in order to analyze the development and maturation of β cells in fetuses from mothers with mild diabetes, administered different doses of STZ (from 30 to 50 mg/kg, iv) in adult rats before mating and verified that rats showed an increase in placental weight, but not in fetal weight, even with high levels of plasma insulin. These conflicting results could be explained by the shorter duration of pregnancy of the animals and the existence of a reduced fat mass of fetuses compared to human, which does not allow

the verification of macrosomia in fetuses of rats with mild diabetes.

When STZ (37 mg/kg, ip) was administered at day 5 of pregnancy, it was found that diabetic rats presented reduced insulin levels during the last week of pregnancy. Moreover, most of the fetuses presented macrosomia and high levels of plasma glucose and insulin at first day of life [53].

López-Soldado and Herrera [54] used different doses of streptozotocin (25, 30, and 35 mg/kg, iv), at the onset of pregnancy in rats. It was observed that, on the day of birth, the rat newborns of diabetic dams presented elevated plasma insulin and macrosomia. Caluwaerts et al. [55] also tested different single doses of STZ (30, 35, 40, or 50 mg/kg, ip) on the first day of pregnancy and on two other groups of rats with two lower doses of STZ (one given two days prior to mating and one on the first day of pregnancy: from 30 to 20 or from 30 to 30 mg/kg, ip). There was a reduced maternal weight gain during pregnancy in groups 35 and 50 STZ, and only STZ groups 30/30 and 50 showed fetuses with hyperglycemia on the first day of life. On the first day of birth, fetuses of STZ groups 30/30, 40, and 50 were small and showed larger placentas. Only, STZ groups 30, 30/20, in 35 and there was an increase in plasma insulin.

Some studies cited regarding the induction of diabetes between day 0 and 5 of pregnancy were successful as an ideal model, since the doses and routes of administration resulted similarity in results when compared to gestational diabetes in human, besides the induction period, which is corresponding to the preimplantation, thus avoiding the transfer of β-cytotoxic drug (STZ) from mother to fetus through the placenta and its possible influence on the development of the offspring. The experiments that had failed during the same period can be explained by dose and route of administration. In the first case one should take into consideration that high doses in ways which favor the release of the drug over a prolonged period cause lasting action, and in the second case, the administration of a drug intravenously favors this movement directly into the bloodstream, which leads to faster and more potent compared to other routes of administration.

The literature investigations that employ or have employed different models of induction of mild diabetes (blood glucose between 120 and 300 mg/dL) analyzed maternal and perinatal repercussions by vaginal delivery few days after birth, which contributes to the findings of macrosomia in offspring from diabetic dams, due to their greater adipose tissue during this period [54]. However, because of our research group to assess the diabetes effects in dams and fetus by laparotomy, it was evidenced higher percentage of pups with growth restriction, which does not corroborate with clinical diabetic mothers found.

In general, studies show that the diabetes induction by STZ before and after mating led to an exacerbated hyperglycemia, which features a severe diabetes and not mild diabetes. If we consider that this hyperglycemia in early pregnancy can influence embryonic development, this model should not be used to study maternal reproductive performance. The diabetes induction of STZ at the birth of rats caused glucose intolerance in adulthood and during pregnancy, becoming a model for the study of the effects of mild diabetes in the maternal and embryonic organisms. When the STZ administration was performed on the 5th day of life, our results showed favorable glucose levels for characterization of mild diabetes model. The induction on the 5th day of pregnancy, as established by the research group Merzouk et al. [16], shows excellent results with regard to blood glucose levels and rates of macrosomic newborns. However, these authors did not evaluate the developing embryo, which undertakes the study of reproductive performance.

2.3. Oxidative Stress. Oxidative stress occurs when the production of free radicals is higher than the capacity of the antioxidant defense system. This state is characterized by molecular and structural damage in the cell, such as membranes, DNA, lipid, and protein. Studies have shown that hyperglycemia and pregnancy induce increased production of reactive oxygen [56] and nitrogen species [57]. The first line of defense against oxidative damage is the endogenous enzymatic antioxidants: superoxide dismutase (SOD), catalase, and glutathione system, among them are glutathione reductase (GSH-Rd) and glutathione peroxidase (GSH-Px). There are also nonenzymatic antioxidants that are liposoluble (tocopherols, carotenoids, quinones, and bilirubin) or hydrosoluble (ascorbic acid, uric acid, and proteins bound to metals) [58, 59].

To evaluate the oxidative stress status in mild diabetic models, diabetes was induced by streptozotocin (100 mg/kg sc) in Sprague Dawley rats on the day of birth. At term pregnancy, higher MDA concentration and no change on the SOD and GSH-Px enzymatic activities and concentration of thiol groups was observed, showing an exacerbated oxidative stress [48]. In other study, mild diabetes was induced using STZ (70 mg/kg ip) in female Wistar rats on day 5 of postnatal life. At the end of pregnancy, the mild diabetic rats showed that SOD enzymatic activity was reduced and MDA concentration (lipid peroxidation) was slightly increased, confirming oxidative stress status [18]. Yessoufou et al. [60] showed that the diabetes induced on t day 5 of pregnancy using STZ (40 mg/kg ip) caused mild diabetes on days 12 and 21 of pregnancy, decreased SOD, GSH-Rd, and GSH-Px enzymatic activities, and increased TBARS concentration, showing elevated oxidative stress in diabetic animals.

Although there are different models to induce mild diabetes, an exacerbated oxidative stress status was found in several studies. However, the existing differences are altered/unaltered scavenger activities in these investigations.

2.4. Morphological Analysis of the Extracellular Matrix and Urethral Striated Muscle. Diabetes mellitus during pregnancy is associated with high urinary incontinence levels and pelvic floor muscle dysfunction, but the exact pathophysiology of urinary incontinence (UI) has not been well characterized. UI is known to be multifactorial in origin, including malfunction of the urethral sphincter [61, 62]. The development of animal models is essential for understanding these events and developing preventive interventions [63].

Based on the hypothesis that the muscle and connective tissue integration are intimately related to urinary continence, diabetic animals have great chances to present changes in these tissues. Therefore, a study with mild diabetes model in pregnant rats that received neonatally streptozotocin (100 mg/kg, sc) was conducted. At term pregnancy, the morphological analysis of the extracellular matrix and urethral striated muscle from urethrovaginal tissues showed that the urethral layers were thin, disorganized, and atrophic and there were more fibrosis replacement and collagen fiber deposition associated to muscle atrophy. In addition to structural analyses, one of the most significant findings was the colocalization of fast and slow fibers and a steady decrease in the proportion of fast to slow fibers by immunohistochemical examination in the mild diabetic pregnant rats [64]. Diabetes is related to accumulation of reactive oxygen species, and tissue ischemia which can interactively or independently contribute to the myopathy causes of skeletal muscle dysfunctions [65, 66]. It is well established that the muscle fibers are able of altering their physiological and biochemical properties according to stimulus which they are submitted, reflecting on amount or type of muscle proteins [67]. These changes are often associated with altered glucose metabolism, diabetes and obesity. Skeletal muscle can adapt to functional and metabolic demands by remodeling with fiber type switches to maintain a normal energy balance and utilization of nutrients [68].

Vascular complications are also associated with the progressive severity of diabetes [69] which showed a significant increase in blood vessels in the urethra of mild diabetic pregnant rats. The literature describes the diabetic time-dependent alterations in macrovascular structure and cellular function, suggesting that one of the underlying mechanisms responsible for diabetes-induced vascular disease is uncoupled mitochondria, with increased electron leak and the generation of reactive oxygen species [69].

The mild diabetic pregnant rats also showed an increased interstitial collagen in the ultrastructural analysis. Glycogen granules, lipid droplets, and numerous mitochondria were apparent in the striated muscle cells [64]. Lipid droplets are not membrane bound, and their number and size may vary considerably among different muscle types. They are frequently associated with mitochondria and sometimes completely encircled by them. Experimental enzyme deficiencies in mitochondrial energy metabolism induced the accumulation of giant mitochondria and numerous lipid droplets. This has led to the suggestion that mitochondria may use lipids as a source of energy for muscular contraction. The increased number of lipid droplets in the diabetic pregnant rats indicates that lipids may be an important energy source for striated muscle [70].

These results indicate that mild diabetes in pregnant rats can lead to time-dependent disorder and tissue remodeling in which the urethral striated muscle and extracellular matrix has a fundamental function [64]. Since this is a unique study, there is no description of a best model or comparison with other models in order to reach a conclusion. These findings show that there is a relation between the changes found in the urethra-vagina tissue that would be similar to which occur in the urethra of diabetic women with UI.

2.5. Another Model to Obtain Mild Diabetes. In mammals, the growth and development in fetal intrauterine environment are completely dependent on the nutrients provided by the mother. The maternal requirement of carbohydrates, proteins, and lipids increases considerably during this period [71, 72]. In rats, as in humans, glucose is the main substrate for the development of the fetus, which comes from the maternal circulation. Whereas the insulin is the main growth hormone to the fetus, which is responsible for 50% of fetal weight [73].

An inappropriate maternal-fetal food supply or nutrient flow leads to marked changes in maternal metabolism by modifying isolated fetal nutrition. Thus, further adjustments are needed during development in utero environment [74, 75]. Without these adjustments the postnatal growth is impaired. Health conditions in the course of adulthood result from the combination between genotype and phenotype, which begins in the prenatal period. This effect is known as "fetal origins of adult disease" [29, 30, 76].

The literature studies show transgenerational effects in animal models of hyperglycemia. When female Wistar rats received STZ (30 mg/kg) on the day of mating, it was observed that these rats presented a mean blood glucose 250 mg/dL at the end of pregnancy. The authors found that maternal hyperglycemia impaired glucose metabolism in subsequent generations [77–81]. The first-generation fetuses showed hyperglycemia, and at adulthood (100 days old) these rats showed normal glucose basal levels and endocrine pancreas morphology. However, when glucose load (glucose infusion) was administered, some animals showed glucose intolerance and others presented mild diabetes during pregnancy [82, 83]. The subsequent generation was affected by unfavorable maternal intrauterine environment, and their fetuses showed hyperplasia of pancreatic islets, beta-cell hyperactivity, hyperinsulinemia, and macrosomia [77]. It was verified that the fetal hyperinsulinemia was due to the low levels of amino acids, which can be explained by higher amino acid uptake by placental unit, which can be coresponsible for the decreased insulin response [83]. According to some authors, the transgenerational effect of diabetes crosses through the generations only by the female offspring. However, even if the male present impaired glucose tolerance, there is no transmission to their descendants.

When STZ (40 mg/Kg ip) was administered at day 5 of pregnancy, the animals presented glycemic levels from 100 to 300 mg/dL, confirming mild diabetes. At birth, pups from mild diabetic dams presented higher mean weight compared to control pups, confirming macrosomia. The macrosomic fetus presented higher serum insulin, glucose, and lipid levels and maintained accelerate postnatal growth combined with high adipose tissue weight up to 12 weeks of age without being hyperphagic. This metabolic disturbances varied according to age and sex. At 2 months of age, hepatic and serum triacylglycerol levels were higher in macrosomic females than in controls. By 3 months, macrosomic rats (males and females) had development insulin resistance with

hyperinsulinemia, hyperglycaemia, and higher serum and hepatic lipids [16]. The same research group demonstrated that fetal obesity is associated with alterations in VLDL lipid fatty acid composition and represents an important risk factor for adult obesity and diabetes [84]. Besides these results, it was observed that obese offspring (3 months) presented higher serum lipoprotein concentration, typical of obese and diabetic woman begins [85].

To induce mild diabetes, Sprague Dawley rats received STZ (35 mg/Kg ip) at day 5 of pregnancy. The pups born to the mild diabetic dams had higher birth weight (macrosomia), pancreatic insulin content, plasma insulin, and C-peptide concentrations compared to those pups born to control dams. At 6 weeks of age, an accelerated growth in the female rats was associated with higher fat weight. At adulthood, higher plasma insulin and glycemia in macrosomic rats, only the female macrosomic rats, showed abnormal glucose response due to peripheral insulin resistance. In the male rats, a higher plasma insulin concentration in the macrosomic group was associated with a normal plasma glucose response to oral glucose challenge. This study showed that maternal mild diabetes in rats led to fetal hyperinsulinemia and accelerated fetal growth [86]. To study the cross-generation effect of newborn rats in the mild diabetes model, similar methodology was used. The first generation of rats presented glycemic levels from 100 to 300 mg/dL, confirming mild diabetes. These dams had macrosomic pups presenting hyperinsulinemia and accelerated growth. The second-generation macrosomic males and females and nonmacrosomic males and females were mated to obtain the third generation. It was observed that the pups from macrosomic parents presented higher birth weight and plasma insulin levels. At adulthood, these animals presented an accelerated growth and higher fat tissue weight compared the control pups, showing that an abnormal intrauterine metabolic environment can lead to obesity and glucose intolerance across generations in rats [87].

Another model to induce mild diabetes was employed by our group, who administered STZ (40 mg/Kg iv) in the first generation of adult Wistar rats before the mating period. During pregnancy, these rats presented glycemia higher than 300 mg/dL, characterizing an abnormal intrauterine environment. The offspring from these dams presented glucose intolerance at adulthood, showing impaired repercussions of maternal hyperglycemia [88, 89].

The different models of mild diabetes induction to study the cross-generation effect are important to demonstrate that transgenerational effect from an abnormal intrauterine environment causes metabolic alterations across further generations.

3. Conclusion

Many models mentioned to induce diabetes lead to similar characteristics compared to those resulting from human gestational diabetes. Thus, according to the targeted objectives, each researcher should choose the best model of diabetes induction for the study.

References

[1] American Diabetes Association, "Diagnosis and classification of diabetes mellitus," *Diabetes Care*, vol. 33, supplement 1, pp. S62–S69, 2010.

[2] K. Pechhold, K. Koczwara, X. Zhu et al., "Blood glucose levels regulate pancreatic β-cell proliferation during experimentally-induced and spontaneous autoimmune diabetes in mice," *PLoS ONE*, vol. 4, no. 3, Article ID e4827, 2009.

[3] R. Scharfmann, V. Duvillie, M. Stetsyuk, G. Attali, G. Filhoulaud, and G. Guillemain, "β-cell development: the role of intercellular signals," *Diabetes, Obesity and Metabolism*, vol. 10, no. 4, pp. 195–200, 2008.

[4] Sociedade Brasileira de Diabetes, "Diagnóstico e classificação do diabetes mellitus e tratamento do diabetes mellitus tipo 2," *Consenso Brasileiro Sobre Diabetes*, pp. 1–60, 2011.

[5] I. López-Soldado and E. Herrera, "Different diabetogenic response to moderate doses of streptozotocin in pregnant rats, and its long-term consequences in the offspring," *Experimental Diabesity Research*, vol. 4, no. 2, pp. 107–118, 2003.

[6] D. T. Ward, S. K. Yau, A. P. Mee et al., "Functional, molecular, and biochemical characterization of streptozotocin-induced diabetes," *Journal of the American Society of Nephrology*, vol. 12, no. 4, pp. 779–790, 2001.

[7] U. J. Eriksson, L. A. H. Borg, J. Cederberg et al., "Pathogenesis of diabetes-induced congenital malformations," *Upsala Journal of Medical Sciences*, vol. 105, no. 2, pp. 53–84, 2000.

[8] U. J. Eriksson, J. Cederberg, and P. Wentzel, "Congenital malformations in offspring of diabetic mothers—animal and human studies," *Reviews in Endocrine and Metabolic Disorders*, vol. 4, no. 1, pp. 79–93, 2003.

[9] D. C. Damasceno, G. T. Volpato, I. M. Calderon, R. Aguilar, and M. V. C. Rudge, "Effect of Bauhinia forficata extract in diabetic pregnant rats: maternal repercussions," *Phytomedicine*, vol. 11, no. 2-3, pp. 196–201, 2004.

[10] M. V. C. Rudge, D. C. Damasceno, G. T. Volpato, F. C. G. Almeida, I. M. P. Calderon, and I. P. Lemonica, "Effect of Ginkgo biloba on the reproductive outcome and oxidative stress biomarkers of streptozotocin-induced diabetic rats," *Brazilian Journal of Medical and Biological Research*, vol. 40, no. 8, pp. 1095–1099, 2007.

[11] G. T. Volpato, D. C. Damasceno, M. V. C. Rudge, C. R. Padovani, and I. M. P. Calderon, "Effect of Bauhinia forficata aqueous extract on the maternal-fetal outcome and oxidative stress biomarkers of streptozotocin-induced diabetic rats," *Journal of Ethnopharmacology*, vol. 116, no. 1, pp. 131–137, 2008.

[12] M. da Silva Soares de Souza, P. H. O. Lima, Y. K. Sinzato, M. V. C. Rudge, O. C. M. Pereira, and D. C. Damasceno, "Effects of cigarette smoke exposure on pregnancy outcome and offspring of diabetic rats," *Reproductive BioMedicine Online*, vol. 18, no. 4, pp. 562–567, 2009.

[13] M. D. S. S. de Souza, Y. K. Sinzato, P. H. O. Lima, I. M. P. Calderon, M. V. C. Rudge, and D. C. Damasceno, "Oxidative stress status and lipid profiles of diabetic pregnant rats exposed to cigarette smoke," *Reproductive BioMedicine Online*, vol. 20, no. 4, pp. 547–552, 2010.

[14] B. Portha, C. Levacher, L. Picon, and G. Rosselin, "Diabetogenic effect of streptozotocin in the rat during the perinatal period," *Diabetes*, vol. 23, no. 11, pp. 889–895, 1974.

[15] K. Tsuji, T. Taminato, M. Usami et al., "Characteristic features of insulin secretion in the streptozotocin-induced NIDDM rat model," *Metabolism*, vol. 37, no. 11, pp. 1040–1044, 1988.

[16] H. Merzouk, S. Madani, D. C. Sari, J. Prost, M. Bouchenak, and J. Belleville, "Time course of changes in serum glucose, insulin, lipids and tissue lipase activities in macrosomic offspring of rats with streptozotocin-induced diabetes," *Clinical Science*, vol. 98, no. 1, pp. 21–30, 2000.

[17] Y. K. Sinzato, P. H. O. Lima, K. E. de Campos, A. C. I. Kiss, M. V. C. Rudge, and D. C. Damascene, "Neonatally-induced diabetes: lipid profile outcomes and oxidative stress status in adult rats," *Revista da Associacao Medica Brasileira*, vol. 55, no. 4, pp. 384–388, 2009.

[18] D. C. Damasceno, A. C. I. Kiss, Y. K. Sinzato et al., "Maternal-fetal outcome, lipid profile and oxidative stress of diabetic rats neonatally exposed to streptozotocin," *Experimental and Clinical Endocrinology and Diabetes*, vol. 119, no. 7, pp. 408–413, 2011.

[19] A. Jawerbaum and V. White, "Animal models in diabetes and pregnancy," *Endocrine Reviews*, vol. 31, no. 5, pp. 680–701, 2010.

[20] K. Minami and S. Seino, "Regeneration of the pancreas," *Japanese Journal of Clinical Medicine*, vol. 66, no. 5, pp. 926–931, 2008.

[21] S. Bonner-Weir and G. C. Weir, "New sources of pancreatic β-cells," *Nature Biotechnology*, vol. 23, no. 7, pp. 857–861, 2005.

[22] R. N. Wang, L. Bouwens, and G. Klöppel, "Beta-cell proliferation in normal and streptozotocin-treated newborn rats: site, dynamics and capacity," *Diabetologia*, vol. 37, no. 11, pp. 1088–1096, 1994.

[23] S. Bonner-Weir, D. F. Trent, R. N. Honey, and G. C. Weir, "Responses of neonatal rat islets to streptozotocin. Limited B-cell regeneration and hyperglycemia," *Diabetes*, vol. 30, no. 1, pp. 64–69, 1981.

[24] J. Movassat, C. Saulnier, and B. Portha, "Insulin administration enhances growth of the β-cell mass in streptozotocin-treated newborn rats," *Diabetes*, vol. 46, no. 9, pp. 1445–1452, 1997.

[25] S. Thyssen, E. Arany, and D. J. Hill, "Ontogeny of regeneration of β-cells in the neonatal rat after treatment with streptozotocin," *Endocrinology*, vol. 147, no. 5, pp. 2346–2356, 2006.

[26] J. M. Nicholson, E. J. Arany, and D. J. Hill, "Changes in islet microvasculature following streptozotocin-induced β-cell loss and subsequent replacement in the neonatal rat," *Experimental Biology and Medicine*, vol. 235, no. 2, pp. 189–198, 2010.

[27] X.-D. Liang, Y.-Y. Guo, M. Sun et al., "Streptozotocin-induced expression of Ngn3 and Pax4 in neonatal rat pancreatic α-cells," *World Journal of Gastroenterology*, vol. 17, no. 23, pp. 2812–2820, 2011.

[28] R. J. Jarrett, "Gestational diabetes: a non-entity?" *British Medical Journal*, vol. 306, no. 6869, pp. 37–38, 1993.

[29] D. J. P. Barker, "Maternal nutrition, fetal nutrition, and disease in later life," *Nutrition*, vol. 13, no. 9, pp. 807–813, 1997.

[30] C. Kanaka-Gantenbein, "Fetal origins of adult diabetes," *Annals of the New York Academy of Sciences*, vol. 1205, pp. 99–105, 2010.

[31] B. Hogan and R. Tilly, "In vitro development of inner cell masses isolated immunosurgically from mouse blastocysts. II. Inner cell masses from 3.5- to 4.0-day p.c. blastocysts," *Journal of Embryology and Experimental Morphology*, vol. 45, pp. 107–121, 1978.

[32] N. Hillman, M. I. Sherman, and C. Graham, "The effect of spatial arrangement on cell determination during mouse development," *Journal of Embryology and Experimental Morphology*, vol. 28, no. 2, pp. 263–278, 1972.

[33] A. K. Tarkowski and J. Wróblewska, "Development of blastomeres of mouse eggs isolated at the 4- and 8-cell stage," *Journal of Embryology and Experimental Morphology*, vol. 18, no. 1, pp. 155–180, 1967.

[34] A. Wyman, A. B. Pinto, R. Sheridan, and K. H. Moley, "One-cell zygote transfer from diabetic to nondiabetic mouse results in congenital malformations and growth retardation in offspring," *Endocrinology*, vol. 149, no. 2, pp. 466–469, 2008.

[35] J. M. Goldberg, T. Falcone, and M. Attaran, "In vitro fertilization update," *Cleveland Clinic Journal of Medicine*, vol. 74, pp. 329–338, 2007.

[36] J. Mihajlik, P. Rehák, J. Veselá, Š. Čikoš, V. Baran, and J. Koppel, "Preimplantation embryo development in ICR mice after streptozotocin treatment," *Physiological Research*, vol. 47, no. 1, pp. 67–72, 1998.

[37] A. Ornoy, D. Kimyagarov, P. Yaffee, R. Abir, I. Raz, and R. Kohen, "Role of reactive oxygen species in diabetes-induced embryotoxicity: studies on pre-implantation mouse embryos cultured in serum from diabetic pregnant women," *Israel Journal of Medical Sciences*, vol. 32, no. 11, pp. 1066–1073, 1996.

[38] S. Pampfer, I. Vanderheyden, Y.-D. Wuu, L. Baufays, O. Maillet, and R. De Hertogh, "Possible role for TNF-α in early embryopathy associated with maternal diabetes in the rat," *Diabetes*, vol. 44, no. 5, pp. 531–536, 1995.

[39] R. B. Fraser, S. L. Waite, K. A. Wood, and K. L. Martin, "Impact of hyperglycemia on early embryo development and embryopathy: in vitro experiments using a mouse model," *Human Reproduction*, vol. 22, no. 12, pp. 3059–3068, 2007.

[40] S. Pampfer, I. Vanderheyden, J. E. McCracken, J. Vesela, and R. De Hertogh, "Increased cell death in rat blastocysts exposed to maternal diabetes in utero and to high glucose or tumor necrosis factor-α in vitro," *Development*, vol. 124, no. 23, pp. 4827–4836, 1997.

[41] K. H. Moley, M. M.-Y. Chi, C. M. Knudson, S. J. Korsmeyer, and M. M. Mueckler, "Hyperglycemia induces apoptosis in pre-implantation embryos through cell death effector pathways," *Nature Medicine*, vol. 4, no. 12, pp. 1421–1424, 1998.

[42] D. K. Gardner, M. Lane, J. Stevens, T. Schlenker, and W. B. Schoolcraft, "Blastocyst score affects implantation and pregnancy outcome: towards a single blastocyst transfer," *Fertil Steril*, vol. 73, pp. 1155–1158, 2000.

[43] C. Gicquel, V. Gaston, J. Mandelbaum, J. P. Siffroi, A. Flahault, and Y. Le Bouc, "In vitro fertilization may increase the risk of Beckwith-Wiedemann syndrome related to the abnormal imprinting of the KCN1OT gene," *The American Journal of Human Genetics*, vol. 72, pp. 1338–1341, 2003.

[44] E. R. Maher, L. A. Brueton, S. C. Bowdin et al., "Beckwith-Wiedemann syndrome and assisted reproduction technology (ART)," *Journal of Medical Genetics*, vol. 40, pp. 62–64, 2003.

[45] A. Bueno, Y. K. Sinzato, M. J. Sudano et al., "Diabetic intrauterine environment: relationship betweenmaternal TNF-alpha and rat early embryonic development," Submitted.

[46] I. L. Iessi, A. Bueno, Y. K. Sinzato, K. N. Taylor, M. V. Rudge, and D. C. Damasceno, "Evaluation of neonatally-induced mild diabetes in rats: maternal and fetal repercussions," *Diabetology and Metabolic Syndrome*, vol. 2, no. 1, article 37, 2010.

[47] Y. K. Sinzato, G. T. Volpato, I. L. Iessi et al., "Neonatally induced mild diabetes in rats and its effect on maternal, placental, and fetal parameters," *Experimental Diabetes Research*, vol. 2012, Article ID 108163, 7 pages, 2012.

[48] B. Dallaqua, F. H. Saito, T. Rodrigues et al., "Treatment with Azadirachta indica in diabetic pregnant rats: negative effects on maternal outcome," *J Ethnopharmacol*, vol. 143, no. 3, pp. 805–811, 2012.

[49] D. C. Damasceno, A. C. I. Kiss, Y. K. Sinzato et al., "Maternal-fetal outcome, lipid profile and oxidative stress of diabetic rats neonatally exposed to streptozotocin," *Experimental and Clinical Endocrinology and Diabetes*, vol. 119, no. 7, pp. 408–413, 2011.

[50] F. H. Saito, D. C. Damasceno, W. G. Kempinas et al., "Repercussions of mild diabetes on pregnancy in Wistar rats and on the fetal development," *Diabetology and Metabolic Syndrome*, vol. 2, no. 1, article 26, 2010.

[51] A. C. Kiss, P. H. Lima, Y. K. Sinzato et al., "Animal models for clinical and gestational diabetes: maternal and fetal outcomes," *Diabetol Metab Syndr*, vol. 1, no. 1, article 21, 2009.

[52] A. Kervran, M. Guillaume, and A. Jost, "The endocrine pancreas of the fetus from diabetic pregnant rat," *Diabetologia*, vol. 15, no. 5, pp. 387–393, 1978.

[53] N. L. Gelardi, C.-J. M. Cha, and W. Oh, "Glucose metabolism in adipocytes of obese offspring of mild hyperglycemic rats," *Pediatric Research*, vol. 28, no. 6, pp. 641–645, 1990.

[54] I. López-Soldado and E. Herrera, "Different diabetogenic response to moderate doses of streptozotocin in pregnant rats, and its long-term consequences in the offspring," *Experimental Diabesity Research*, vol. 4, no. 2, pp. 107–118, 2003.

[55] S. Caluwaerts, K. Holemans, R. Van Bree, J. Verhaeghe, and F. A. Van Assche, "Is low-dose streptozotocin in rats an adequate model for gestational diabetes mellitus?" *Journal of the Society for Gynecologic Investigation*, vol. 10, no. 4, pp. 216–221, 2003.

[56] M. Brownlee, "Biochemistry and molecular cell biology of diabetic complications," *Nature*, vol. 414, no. 6865, pp. 813–820, 2001.

[57] Z. Z. Chong, F. Li, and K. Maiese, "Oxidative stress in the brain: novel cellular targets that govern survival during neurodegenerative disease," *Progress in Neurobiology*, vol. 75, no. 3, pp. 207–246, 2005.

[58] D. C. Damasceno, G. T. Volpato, I. D. M. Paranhos Calderon, and M. V. Cunha Rudge, "Oxidative stress and diabetes in pregnant rats," *Animal Reproduction Science*, vol. 72, no. 3-4, pp. 235–244, 2002.

[59] B. Halliwell and J. M. C. Gutteridge, *Free Radicals in Biology and Medicine*, Oxford University Press, Oxford, UK, 3th edition, 1999.

[60] A. Yessoufou, N. Soulaimann, S. A. Merzouk et al., "N-3 fatty acids modulate antioxidant status in diabetic rats and their macrosomic offspring," *International Journal of Obesity*, vol. 30, no. 5, pp. 739–750, 2006.

[61] J. P. F. A. Heesakkers and R. R. R. Gerretsen, "Urinary incontinence: sphincter functioning from a urological perspective," *Digestion*, vol. 69, no. 2, pp. 93–101, 2004.

[62] J.-M. Yang, S.-H. Yang, S.-Y. Yang, E. Yang, W.-C. Huang, and C.-R. Tzeng, "Clinical and pathophysiological correlates of the symptom severity of stress urinary incontinence," *International Urogynecology Journal and Pelvic Floor Dysfunction*, vol. 21, no. 6, pp. 637–643, 2010.

[63] D. M. Morgan, W. Umek, K. Guire, H. K. Morgan, A. Garabrant, and J. O. L. DeLancey, "Urethral sphincter morphology and function with and without stress incontinence," *Journal of Urology*, vol. 182, no. 1, pp. 203–209, 2009.

[64] F. Piculo, G. Marini, A. M. P. Barbosa et al., "Urethral striated muscle and extracellular matrix morphologic characteristics among mild diabetic pregnant rats," submitted to *International Urogynecology Journal*.

[65] R. Mastrocola, P. Reffo, F. Penna et al., "Muscle wasting in diabetic and in tumor-bearing rats: role of oxidative stress," *Free Radical Biology and Medicine*, vol. 44, no. 4, pp. 584–593, 2008.

[66] H. Andersen, "Muscular endurance in long-term IDDM patients," *Diabetes Care*, vol. 21, no. 4, pp. 604–609, 1998.

[67] H. Andersen, P. L. Poulsen, C. E. Mogensen, and J. Jakobsen, "Isokinetic muscle strength in long-term IDDM patients in relation to diabetic complications," *Diabetes*, vol. 45, no. 4, pp. 440–445, 1996.

[68] A. Oberbach, Y. Bossenz, S. Lehmann et al., "Altered fiber distribution and fiber-specific glycolytic and oxidative enzyme activity in skeletal muscle of patients with type 2 diabetes," *Diabetes Care*, vol. 29, no. 4, pp. 895–900, 2006.

[69] B. Chen and J. Yeh, "Alterations in connective tissue metabolism in stress incontinence and prolapse," *Journal of Urology*, vol. 186, no. 5, pp. 1768–1772, 2011.

[70] C. C. G. Chen, A. Hijaz, J. A. Drazba, M. S. Damaser, and F. Daneshgari, "Collagen remodeling and suburethral inflammation might account for preserved anti-incontinence effects of cut polypropylene sling in rat model," *Urology*, vol. 73, no. 2, pp. 415–420, 2009.

[71] L. Aerts and F. A. Van Assche, "Animal evidence for the transgenerational development of diabetes mellitus," *International Journal of Biochemistry and Cell Biology*, vol. 38, no. 5-6, pp. 894–903, 2006.

[72] M. V. C. Rudge, I. D. M. P. Calderon, M. D. Ramos, J. F. Abbade, and L. M. S. S. Rugolo, "Perinatal outcome of pregnancies complicated by diabetes and by maternal daily hyperglycemia not related to diabetes: a retrospective 10-year analysis," *Gynecologic and Obstetric Investigation*, vol. 50, no. 2, pp. 108–112, 2000.

[73] A. L. Fowden, "The role of insulin in fetal growth," *Early Human Development*, vol. 29, no. 1–3, pp. 177–181, 1992.

[74] K. Holemans, L. Aerts, and F. A. Van Assche, "Fetal growth restriction and consequences for the offspring in animal models," *Journal of the Society for Gynecologic Investigation*, vol. 10, no. 7, pp. 392–399, 2003.

[75] S. Caluwaerts, K. Holemans, R. Van Bree, J. Verhaeghe, and F. A. Van Assche, "Aging does not aggravate the pregnancy-induced adaptations in glucose tolerance in rats," *Metabolism*, vol. 55, no. 3, pp. 409–414, 2006.

[76] M. A. Hanson and P. D. Gluckman, "Developmental origins of health and disease: moving from biological concepts to interventions and policy," *International Journal of Gynecology and Obstetrics*, vol. 115, no. 11, pp. 60003–60009, 2011.

[77] L. Aerts and F. A. Van Assche, "Rat foetal endocrine pancreas in experimental diabetes," *Journal of Endocrinology*, vol. 73, no. 2, pp. 339–346, 1977.

[78] L. Aerts and F. A. Van Assche, "Endocrine pancreas in the offspring of rats with experimentally induced diabetes," *Journal of Endocrinology*, vol. 88, no. 1, pp. 81–88, 1981.

[79] L. Aerts and F. A. Van Assche, "Transmission of experimentally induced diabetes in pregnant rats to their offspring in subsequent generations: a morphometric study of maternal and fetal endocrine pancreas at histological and ultrastructural level," in *Lessons From Animal Diabetes*, E. Shalfrir and A. E. Renold, Eds., pp. 705–710, Libbey, London, UK, 1984.

[80] F. A. Van Assche and L. Aerts, "Long term effect of diabetes and pregnancy in the rat: is acquired insulin resistanse responsible?" in *Diabetes*, M. Serrano-Rios and P. J. Lefebvre, Eds., pp. 590–597, Amsterdam, The Netherlands, 1986.

[81] A. O. Martin, J. L. Simpson, C. Ober, and N. Freinkel, "Frequency of diabetes mellitus in mothers of probands with gestational diabetes: possible maternal influence on the predisposition to gestational diabetes," *American Journal of Obstetrics and Gynecology*, vol. 151, no. 4, pp. 471–475, 1985.

[82] L. Aerts and F. A. Van Assche, "Is gestational diabetes an acquired condition?" *Journal of Developmental Physiology*, vol. 1, no. 3, pp. 219–225, 1979.

[83] L. Aerts, R. Van Bree, V. Feytons, W. Rombauts, and F. A. Van Assche, "Plasma amino acids in diabetic pregnant rats and in their fetal and adult offspring," *Biology of the Neonate*, vol. 56, no. 1, pp. 31–39, 1989.

[84] H. Merzouk, S. Madani, A. Hichami, J. Prost, J. Belleville, and N. A. Khan, "Age-related changes in fatty acids in obese offspring of streptozotocin-induced diabetic rats," *Obesity Research*, vol. 10, no. 7, pp. 703–714, 2002.

[85] H. Merzouk, S. Madani, A. Hichami et al., "Impaired lipoprotein metabolism in obese offspring of streptozotocin-induced diabetic rats," *Lipids*, vol. 37, no. 8, pp. 773–781, 2002.

[86] W. Oh, N. L. Gelardi, and C.-J. Cha, "Maternal hyperglycemia in pregnant rats: its effect on growth and carbohydrate metabolism in the offspring," *Metabolism*, vol. 37, no. 12, pp. 1146–1151, 1988.

[87] W. Oh, N. L. Gelardi, and C.-J. M. Cha, "The cross-generation effect of neonatal macrosomia in rat pups of streptozotocin-induced diabetes," *Pediatric Research*, vol. 29, no. 6, pp. 606–610, 1991.

[88] S. B. Corvino, *Exercício físico no diabete transgeracional de ratas: efeito a performance reprodutiva e nos hormônios sexuais [Ph.D. dissertation]*, Faculdade de Medicina de Botucatu, Universidade Estadual Paulista, Botucatu, Brazil, 2012.

[89] A. O. Netto, *Análise de genotoxicidade: otimização de método laboratorial e avaliação em recém-nascidos de mães com restrição de crescimento intrauterino exercitadas durante a prenhez [Ph.D. dissertation]*, Faculdade de Medicina de Botucatu, Universidade Estadual Paulista, Botucatu, Brazil, 2013.

Hindawi Publishing Corporation
Journal of Diabetes Research
Volume 2013, Article ID 716219, 8 pages
http://dx.doi.org/10.1155/2013/716219

Research Article

Antioxidant N-Acetylcysteine Attenuates the Reduction of Brg1 Protein Expression in the Myocardium of Type 1 Diabetic Rats

Jinjin Xu,[1] Shaoqing Lei,[1,2] Yanan Liu,[1] Xia Gao,[1] Michael G. Irwin,[1] Zhong-yuan Xia,[2] Ziqing Hei,[3] Xiaoliang Gan,[3] Tingting Wang,[1,4] and Zhengyuan Xia[1,5]

[1] *Department of Anaesthesiology, The University of Hong Kong, HKSAR, Hong Kong*
[2] *Department of Anaesthesiology, Renmin Hospital of Wuhan University, Wuhan 430060, China*
[3] *Department of Anesthesiology, 3rd Affiliated Hospital of Sun Yat-sen University, Guangzhou 510630, China*
[4] *Department of Anesthesiology and Critical Care, Union Hospital, Tongji Medical College, Huazhong University of Science and Technology, 1277 Jiefang Avenue, Wuhan, China*
[5] *Department of Anesthesiology, Affiliated Hospital of Guangdong Medical College, Zhanjiang 524001, China*

Correspondence should be addressed to Tingting Wang; wangtingting721@yahoo.com and Zhengyuan Xia; zyxia@hku.hk

Received 24 December 2012; Accepted 1 June 2013

Academic Editor: Bernard Portha

Brahma-related gene 1 (Brg1) is a key gene in inducing the expression of important endogenous antioxidant enzymes, including heme oxygenase-1 (HO-1) which is central to cardioprotection, while cardiac HO-1 expression is reduced in diabetes. It is unknown whether or not cardiac Brg1 expression is reduced in diabetes. We hypothesize that cardiac Brg1 expression is reduced in diabetes which can be restored by antioxidant treatment with N-acetylcysteine (NAC). Control (C) and streptozotocin-induced diabetic (D) rats were treated with NAC in drinking water or placebo for 4 weeks. Plasma and cardiac free15-F2t-isoprostane in diabetic rats were increased, accompanied with increased plasma levels of tumor necrosis factor-alpha (TNF-alpha) and interleukin 6 (IL-6), while cardiac Brg1, p-STAT3 and HO-1 protein expression levels were significantly decreased. Left ventricle weight/body weight ratio was higher, while the peak velocities of early (E) and late (A) flow ratio was lower in diabetic than in C rats. NAC normalized tissue and plasma levels of 15-F2t-isoprostane, significantly increased cardiac Brg1, HO-1 and p-STAT3 protein expression levels and reduced TNF-alpha and IL-6, resulting in improved cardiac function. In conclusion, myocardial Brg1 is reduced in diabetes and enhancement of cardiac Brg1 expression may represent a novel mechanism whereby NAC confers cardioprotection.

1. Introduction

Diabetes mellitus-induced cardiovascular complication is a growing life-threatening disease worldwide. Diabetic cardiomyopathy (DCM) is a diabetes-associated ventricular dysfunction, resulted from abnormal ventricular structural alteration that is independent of other etiological factors such as hypertension [1]. Studies have shown that hyperglycemia-induced oxidative stress and the subsequent inflammation play critical roles in the development and progression of diabetic cardiomyopathy [2, 3]. Hyperglycemia-induced oxidative stress mainly results from increased production of reactive oxygen species (ROS) with or without concomitantly damped antioxidant defense system [4, 5]. Our previous study found that the major endogenous antioxidant enzyme superoxide dismutase (SOD), which plays an important role in balancing ROS generation and the overall tissue antioxidant capacity, was increased in both the plasma and heart tissue of rats at a relatively early stage (4 weeks) of diabetes, but tissue and plasma levels of free 15-F_{2t}-isoprostane, a specific marker of lipid peroxidation, were also increased [6]. This indicates that the upregulation of SOD is not sufficient to resist hyperglycemia-induced oxidative stress. Of note, another important enzyme, heme oxygenase-1 (HO-1), a stress-inducible cytoprotective defense enzyme, has been shown to exert cytoprotective effect against oxidative insults [7]. Also, studies showed that enhancing myocardial HO-1 expression could attenuate diabetes-induced cardiac

dysfunction. However, in contrast to the compensatory increase of SOD during early diabetes mellitus, a number of studies showed that myocardial HO-1 expression was significantly decreased in the myocardium of diabetic rats [8, 9]. Thus, unveiling the underlying mechanisms governing the reduction of myocardial HO-1 in diabetes should lead to the development of novel therapies to upregulate HO-1 expression in diabetic heart.

It has been reported that, in response to oxidative stress, Brahma-related gene 1 (Brg1) is necessarily required in Nuclear factor-E2 related factor 2 (Nrf2)/ARE-mediated induction of HO-1 [10]. Brg1 is the core ATPases in the SWI/SNF complex, which plays a central role in the activation and transcription of genes in mammalian cells [11]. The deficiency of Brg1 results in the dissolution of discrete heterochromatin domains, aberrant mitotic progression, and genomic instability, which eventually induces cell death or cell apoptosis [12]. A recent study showed that Brg1 can bind to the promoters of antioxidant defense genes and protect cells from oxidative damage [13], which means that Brg1 can exert antioxidative effect. Furthermore, increasing evidence shows that Brg1 can regulate gene expression during cardiac growth, differentiation, and hypertrophy [14–16]. Brg1 null mice embryos die when cardiomyocytes expansion and maturation begin, while in adult cardiomyocytes, Brg1 is activated by cardiac stresses and assembles a chromatin complex to activate downstream signal transduction, including HO-1 and signal transducer and activator of transcription 3 (STAT3) [10, 16–18], which are protective against ROS-induced cardiomyopathy. Studies by us and others found that myocardial HO-1 expression is reduced in diabetic rats [8, 9] which is accompanied with reduced phosphorylation of STAT3 (p-STAT3, the activated status of STAT3) [19]. We postulated that reductions in myocardial HO-1 and STAT3 in diabetes may be a consequence of reduction in cardiac Brg1 expression subsequent to hyperglycemia-induced oxidative stress.

Accumulated evidence proves that therapies that can reduce oxidative stress are effective to attenuate the development of diabetic cardiomyopathy [20, 21]. Our previous study also found that treatment with the antioxidant N-acetylcysteine (NAC) could attenuate the increase in inflammation factors tumor necrosis factor-alpha (TNF-alpha) and interleukin 6 (IL-6) [6] and ameliorate myocardial dysfunction [2] in diabetic rats. Moderate levels of TNF-alpha or IL-6 have been shown to initiate the activation of STAT3, a key protein in cardioprotective signaling pathway, whose activation is Brg1 dependent [22, 23]. Therefore, the current study was designed to test the hypothesis that myocardial Brg1 is reduced in diabetes and antioxidant NAC may enhance cardiac Brg1 expression and concomitantly increase cardiac STAT3 activation and confer cardioprotection in diabetes.

2. Materials and Methods

2.1. Animals and Introduction of Diabetes. Sprague-Dawley male rats (220 ± 20 g, 8 weeks of age) were obtained from the Laboratory Animal Service Center (University of Hong Kong). All rats were allowed to adapt in their houses and have free access to standard chow and water according to the principles of Animal Care of the University of Hong Kong. The experiment procedures were approved by the Committee on the Use of Live Animals in Teaching and Research (CULATR). Diabetes was induced by a single tail vein injection of streptozotocin (STZ) at the dose of 65 mg/kg body weight (Sigma-Aldrich, St. Louis, MO), freshly dissolved in 0.1 M citrate buffer (PH 4.5) under anesthesia with sodium pentobarbital (65 mg/kg body weight), while control rats were given equal volume of citrate buffer alone. After three days of injection, blood glucose was measured using a Glucose Analyzer (Bayer Healthcare, Bayer AG, Germany), and rats with blood glucose over 16.7 mM were considered diabetic.

2.2. Experimental Protocol. Rats were randomly divided into three groups ($n = 6$ per group): control (C); diabetes (D); diabetes treated with NAC (1.5 g/kg/day) (D + NAC). NAC was administered to the D + NAC group dissolved in drinking water for 4 weeks after induction of diabetes starting one week after the onset of diabetes. Upon completion of treatment, the rats were anticoagulated with heparin (1000 IU/kg) and then anaesthetized with pentobarbital sodium (65 mg/kg body weight). Blood samples were obtained from the inferior vena cava, and plasma was separated and stored at −80°C for further analysis. Rats were sacrificed after completion of echocardiographic assessment of cardiac function, and hearts were harvested and rinsed with ice-cold phosphate buffer saline, dried, and weighted.

2.3. Echocardiography. At the end of 4-week treatment, the rats were examined by echocardiography using a High Resolution Imaging System (Vevo 770, VisualSonics Inc., Canada) equipped with a 17.5-MHz liner array transducer. The following validated parameters were automatically calculated by the ultrasound machine: LV end-diastolic volumes (LVVd), LV end-systolic volume (LVVs), fractional shortening (FS), ejection fraction (EF), and stroke volume (SV). M-mode images were recorded to detect heart rate (HR), LV internal diameter in systole (LVIDs) and diastole (LVIDd), interventricular septal thickness in systole (IVSs) and in diastole (IVSd), and LV posterior wall thickness in systole (LVPWs) and diastole (LVPWd). LV mass was assessed by calculating the formula: LV mass = $1.053\,[(\text{LVIDd} + \text{LVPWd} + \text{IVSd})^3 - \text{LVIDd}^3] \times 0.8$. The peak velocities of early (E) and late (A) flows were obtained from the apical four-chamber view. The E/A ratio and the isovolumetric relaxation time (IVRT) were used as indices of LV diastolic function.

All recordings were performed in rats that underwent inhalation of 3% isopentane in air throughout the whole process, and echocardiography was conducted by investigators who were blinded to the experimental group as we reported [24].

2.4. Measurement of Free 15-F_{2t}-Isoprostane, TNF-Alpha, and IL-6. Free 15-F_{2t}-isoprostane (15-F_{2t}-IsoP), a specific

marker of oxidative stress, was measured by using an enzyme-linked immunoassay kit (Cayman chemical, Ann Arbor, MI) as described [20]. Plasma samples and homogenized heart tissue (in PBS) were purified using Affinity Sorbent and Affinity Column (Cayman chemical, Ann Arbor, MI), then processed for analysis, according to the protocol provided by the manufacturer. The values of plasma or cardiac free 15-F_{2t}-IsoP were expressed as pg/mL in plasma or pg/mg protein in cardiac homogenates, respectively.

Plasma levels of TNF-alpha and IL-6 were determined by using the commercially available rat ELISA kit (Bender Med, Vienna, Austria).

2.5. Western Blot Assay for HO-1, STAT3, and p-STAT3. Frozen heart tissue was homogenized using lysis buffer (20 mmol/L Tris-HCl PH = 7.5, 50 mmol/L 2-mercaptoethanol, 5 mmol/L EGTA, 2 mmol/L EDTA, 1% NP40, 0.1% sodium dodecyl sulfonate (SDS), 0.5% deoxycholic acid, 10 mmol/L NaF, 1 mmol/L PMSF, 25 mg/mL leupeptin, and 2 mg/mL aprotinin) for 30 min and then sonicated and centrifuged at 12000 g for 20 min at 4°C. Protein concentrations were determined using the Bradford assay (Bio-Rad, USA). Samples containing equal amounts were separated on a 10% SDS-polyacrylamide gel, and then proteins were transferred to PVDF membrane overnight at 4°C. Membranes were blocked with 5% nonfat milk in Tris-Buffered Saline (TBS)-Tween for 1 hour and were incubated with anti-Brg1 (Abcam, USA) or anti-STAT3, anti-phospho-STAT3 (T705), anti-HO-1 antibodies (Cell Signaling Technology, Beverly, MA, USA), and GAPDH (Cell Signaling Technology, Beverly, MA, USA) at 1 : 1000 dilution for overnight at 4°C. After washing with phosphate buffered saline-tween (PBST) three times for 30 min, membranes were then incubated with horseradish-peroxidase- (HRP-) conjugated anti-rabbit IgG at 1 : 2000 dilution for 1 hour. Protein bands were developed with enzymatic chemiluminescence, and images were measured by a densitometer with analysis software.

2.6. Statistical Analysis. Data are presented as means ± standard error of the mean (S.E.M.). Data were analysed by the ANOVA within the same group and between groups. Multiple comparisons of group means were analyzed by Tukey's test. The analysis was performed using statistical software package (GraphPad Prism, San Diego, CA, USA). Significant difference was defined as $P \leq 0.05$.

3. Results

3.1. General Characteristics and Effects of NAC Treatment. Administration of STZ resulted in increased plasma glucose and food and fluid intake and reduced body weight gain as compared with age-matched control rats (all $P < 0.05$, Table 1). Treatment with NAC for 4 weeks significantly reduced food consumption and water intake in diabetic rats ($P < 0.05$, D + NAC versus D) but did not have significant effect on glucose levels and body weight gain.

Table 1: General Characteristics of Rats at the End of the Study.

	C	D	D + NAC
Water intake (mL/kg/day)	121.1 ± 8.3	840.3 ± 10.7*	421.1 ± 7.1*
Food intake (g/kg/day)	66.0 ± 1.3	195.1 ± 3.8*	145.5 ± 3.5*
Body weight (g)	486.3 ± 12.7	310.9 ± 17.2*	304.5 ± 12.5*
Plasma glucose (mM)	6.2 ± 0.8	27.7 ± 1.7*	26.1 ± 1.5*

All values are expressed as Mean ± S.E.M. $n = 6$ per group. Control (C) or STZ-induced diabetic rats with untreated (D) or treated with NAC (1.5 g/kg/day) for 4 weeks. $^{*}P < 0.05$ versus C; $^{\#}P < 0.05$ versus D.

Table 2: Effects of NAC treatment on the level of free 15-F_{2t}-isoprostane in plasma and heart tissue.

	C	D	D + NAC
Plasma (pg/mL)	125.1 ± 18.9	245.0 ± 19.1**	150.7 ± 21.4#
Heart tissue (pg/mg protein)	101.3 ± 17.3	208.5 ± 20.6*	167.2 ± 18.5#

All values are expressed as Mean ± S.E.M. $n = 6$ per group. Control (C) or STZ-induced diabetic rats with untreated (D) or treated with NAC (1.5 g/kg/day) for 4 weeks. $^{*}P < 0.05$ versus C; $^{\#}P < 0.05$ versus D.

3.2. Oxidative Stress Marker Free 15-F_{2t}-IsoP Levels. Compared with the control group, the levels of free 15-F_{2t}-IsoP were significantly increased in both the plasma and cardiac tissues of diabetic rats ($P < 0.01$ or $P < 0.05$ versus C, Table 2). NAC treatment reduced plasma and cardiac tissue 15-F_{2t}-IsoP to a level comparable to that in the control ($P < 0.05$ versus D, $P > 0.05$ D + NAC versus C, Table 2).

3.3. Effect of NAC on Left Ventricular Dimension and Function. As shown in Table 3, LVM was much lower in diabetic rats ($P < 0.05$ versus C), despite the fact that there were no significant differences in IVSd, IVSs, LVIDs, LVPWd, and LVPWs between the control and the diabetic rats. However, LVM to body weight ratio, an indicator of myocardial hypertrophy, was remarkably increased in diabetic rats ($P < 0.05$ versus C). NAC reduced LVM to body weight ratio to a level comparable to that in the control ($P < 0.05$, D + NAC versus D; $P > 0.05$ D + NAC versus C, Table 3). The HRs of diabetic rats were significantly decreased as compared to those of the controls ($P < 0.05$ versus C Table 3). NAC had no effect on HR. LVVd and the E/A ratio in diabetic rats were significantly decreased, while IVRT increased (all $P < 0.01$ versus C Table 3). This is indicative of compromised LV relaxation, which may contribute to the significantly reduced SV ($P < 0.05$ D versus C, Table 3). NAC treatment did not have significant effects on LVVd and IVRT nor did it improve SV ($P > 0.05$ D + NAC versus D, Table 3) but remarkably increased E/A ratio which primarily resulted from a reduction in MVA ($P < 0.05$ D + NAC versus D, Table 3). There was no difference in values of FS and EF between the control and diabetic rats.

3.4. Plasma Il-6 and TNF-α. As shown in Figures 1(a) and 1(b), the plasma levels of TNF-α and IL-6 in diabetic rats were significantly increased as compared with the control group

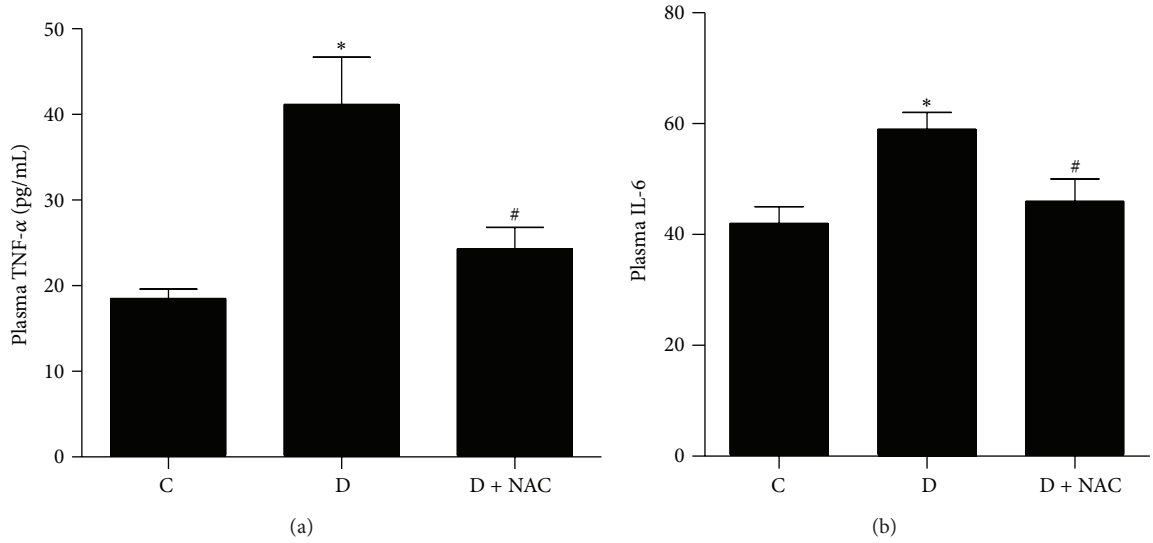

Figure 1: Effects of N-acetylcysteine (NAC) treatment on the level of TNF-alpha (a) and IL-6 (b) in plasma. Control (C) or STZ-induced diabetic rats without treatment (D) or with NAC treatment (1.5 g/kg/day, D + NAC) for 4 weeks. All values are expressed as mean ± S.E.M. $n = 6$ per group. $^{*}P < 0.05$ versus C; $^{\#}P < 0.05$ versus D.

Table 3: M-mode Echocardiographic and transmitral Doppler flow velocity indices of LV dimensions and functions.

	C	D	NAC
LVIDd (mm)	8.30 ± 0.17	7.90 ± 0.15	7.75 ± 0.15*
LVIDs (mm)	4.80 ± 0.14	4.55 ± 0.13	4.65 ± 0.25
IVSs (mm)	2.25 ± 0.11	2.24 ± 0.08	2.08 ± 0.06
IVSd (mm)	1.72 ± 0.06	1.78 ± 0.05	1.60 ± 0.05
LVPWs (mm)	3.06 ± 0.07	2.92 ± 0.05	2.57 ± 0.05*
LVPWd (mm)	1.92 ± 0.04	1.87 ± 0.05	1.62 ± 0.03$^{\#}$
LVM (mg)	964 ± 27.5	812 ± 14.3*	707 ± 18.7*
LVM/body weight (mg/g)	1.90 ± 0.04	2.44 ± 0.07*	2.17 ± 0.04$^{\#}$
HR (bpm)	323 ± 7.8	285 ± 10.8*	286 ± 9.2*
LVVd (μL)	372.7 ± 23.4	318.5 ± 24.2*	319.7 ± 18.4
LVVs (μL)	107.8 ± 10.6	93.7 ± 9.8	101.5 ± 13.2
IVRT (ms)	21.6 ± 1.6	32.5 ± 1.8*	28.5 ± 1.4*
MV *E* (cm/s)	133.2 ± 58.3	1217 ± 30.2	1181.7 ± 62.2
MV *A* (cm/s)	909.5 ± 36.2	1028.9 ± 36.1	838.6 ± 63.8$^{\#}$
E/A	1.49 ± 0.09	1.19 ± 0.03*	1.45 ± 0.07$^{\#}$
SV (μL)	277.8 ± 17.8	226.7 ± 17.4*	218.3 ± 12.2*
FS (%)	42.5 ± 0.9	42.1 ± 0.8	40.7 ± 1.0
EF (%)	71.6 ± 1.7	72.2 ± 1.7	68.8 ± 3.0

All values are expressed as Mean ± S.E.M. $n = 6$ per group. M-mode Echocardiographic and transmitral Doppler flow velocity indices of LV dimensions and functions in Control (C), Diabeties (D), Ruboxistaurin (RBX), N-acetylcysteine (NAC) rats. $^{*}P < 0.05$ or 0.01 versus C; $^{\#}P < 0.05$ or 0.01 versus D. LVIDd: LV internal diastolic diameter; LVIDs: LV internal systolic diameter; IVSs: systolic interventricularseptal thickness; IVSd: diastolic interventricularseptal thickness; LVPWs: LV systolic posterior wall thickness; LVPWd: LV diastolic posterior wall thickness; LVM: LV mass; HR: heart rate; LVVd: LV end-diastolic volume; LVVs: LV end-systolic volume; IVRT: isovolumetric relaxation time; SV: stroke volume; FS: fractional shortening; EF: ejection fraction.

($P < 0.05$). NAC treatment reduced plasma TNF-α and IL-6 to a level comparable to that in the control ($P < 0.05$ versus D; $P > 0.05$ versus C) although they were slightly higher than that in the control rats.

3.5. Effect of NAC on Protein Expression of Brg1. To investigate whether the cardiac protein expression of Brg1 is altered in diabetic rats at an early stage of the disease and whether or not it can be affected by antioxidants, we explored the effects of NAC on cardiac levels of Brg1 in STZ-induced diabetic rats 4 weeks after the establishment of diabetes. As shown in Figure 2(a), the protein expression of Brg1 was significantly decreased in diabetic rats as compared to that of control group ($P < 0.01$). NAC treatment partially but significantly restored the protein expression of Brg1.

3.6. Effect of NAC on Protein Expression of STAT3 and HO-1. Recent study demonstrated that Brg1 is required to establish chromatin accessibility at STAT3 binding targets [18], which is essential to enable these sites to respond to downstream signaling. Therefore, in addition to exploring the changes of myocardial Brg1 protein in diabetes, we also investigated the myocardial protein levels and phosphorylation/activation status of STAT3 in diabetic heart. As shown in Figures 2(c) and 2(d), the protein expression of p-STAT3 (Tyr705 and Ser727) but not total STAT3 was significantly reduced in the myocardium of diabetic rats, accompanied with concomitant reduction of cardiac protein expression of HO-1 (all $P < 0.05$ versus C, Figure 2(b)), an important signaling protein downstream of Brg1. NAC completely restored myocardial p-STAT3 at site Tyr705 and HO-1 protein expression and partially but significantly enhanced p-STAT3 at site Ser-727 in diabetic rats ($P < 0.01$ versus D; $P < 0.05$, $P < 0.01$ versus C).

4. Discussion

Consistent with our previous studies, we have shown in the current study that oxidative stress increased in the early stage (at 4 weeks) rats with STZ-induced type 1 diabetes

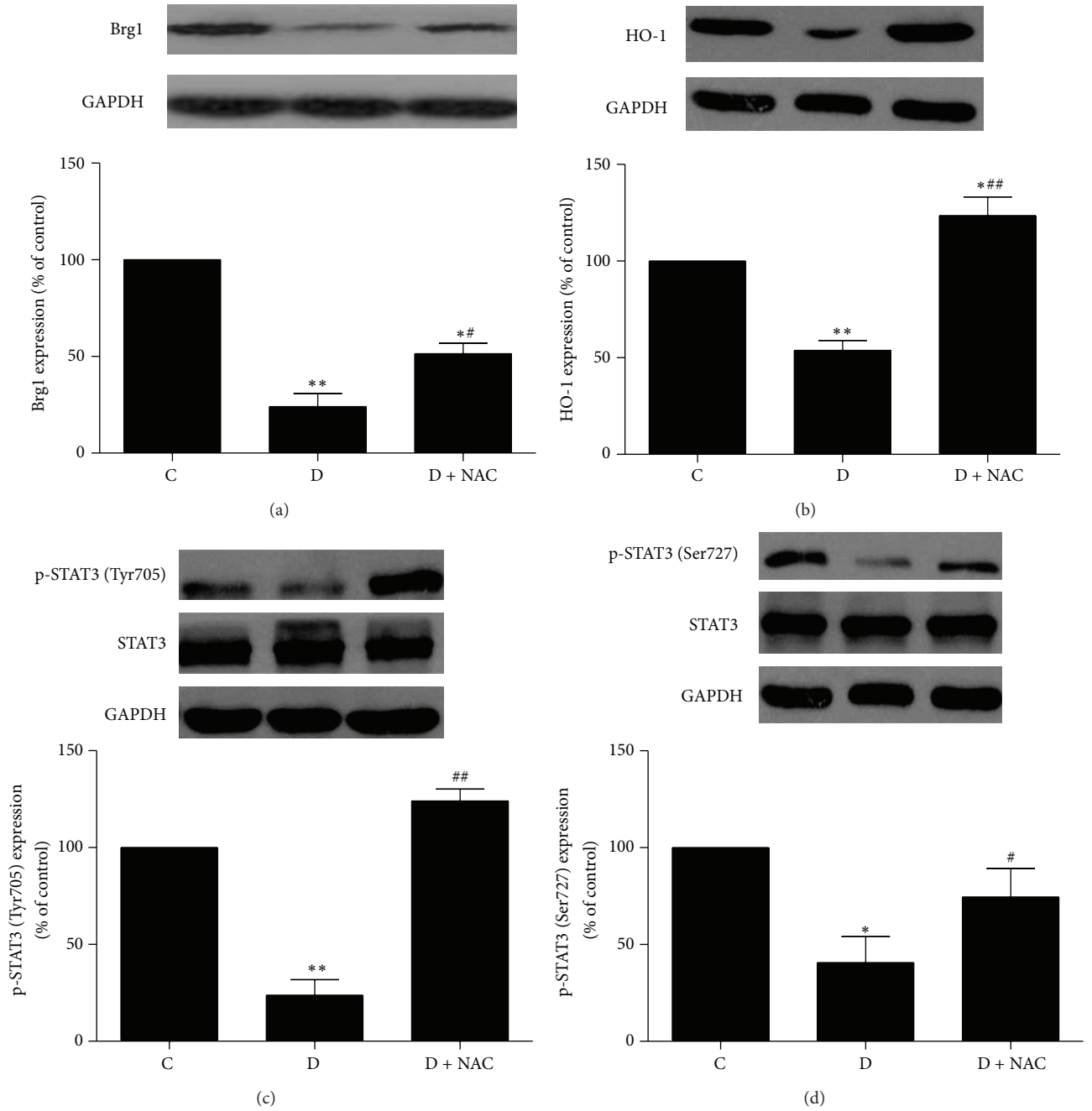

Figure 2: Effects of N-acetylcysteine (NAC) treatment on the protein expression of Brg1 (a), HO-1 (b), and p-STAT3 ((c), (d)) in myocardium. Control (C) or STZ-induced diabetic rats without treatment (D) or with NAC treatment (1.5 g/kg/day, D + NAC) for 4 weeks. All values are expressed as mean ± S.E.M. $n = 6$ per group. $^{*}P < 0.05$, $^{**}P < 0.01$ versus C; $^{\#}P < 0.05$, $^{\#\#}P < 0.01$ versus D.

as indicated by a significant increase in both plasma and heart tissue levels of free 15-F_{2t}-isoprostane, a specific index of oxidative stress [25]. Enhanced levels of oxidative stress were accompanied by increased TNF-alpha and IL-6. In the current study, we further discovered that diabetic rat hearts exhibited decreased expression of Brg1, which was coincident with decreased cardiac expressions of p-STAT3 and HO-1 and compromised cardiac diastolic function as assessed by echocardiography. Effective antioxidant treatment with NAC evidenced as complete prevention of hyperglycemia-induced increases in plasma and heart tissue free 15-F_{2t}-isoprostane significantly attenuated the reduction of myocardial Brg1 protein expression, subsequently significantly enhanced myocardial p-STAT3 and HO-1, and improved cardiac relaxation in diabetic rats. To our knowledge, this is the first study to explore the changes of cardiac Brg1 in diabetic rats and the effectiveness of antioxidant treatment on Brg-1 cardiac expression in diabetes.

Oxidative stress occurs in diabetes as a consequence of hyperglycemia-induced abnormalities, including glucose autooxidation, the formation of advanced glycation end products, and impairment of antioxidant defense system [4]. We previously reported that the heart tissue SOD activity was compensatorily increased, but both the plasma and heart tissue levels of free 15-F_{2t}-isoprostanes were still increased in diabetic rats at the early stage of 4-week diabetes [6], which indicates that, during early stage of diabetes, compensatory increase in myocardial SOD was not sufficient to combat hyperglycemia-induced oxidative stress. While in our current study conducted in the same model of early stage of 4-week diabetes [6], we showed that the protein expression of HO-1, another important antioxidative enzyme, was decreased significantly in the myocardium of diabetic rats, which suggests that a decrease in HO-1 expression may be a major contributor to hyperglycemia-induced oxidative stress in early diabetes. Many studies confirmed that HO-1 plays a central role in cardiovascular protection [26]. It has been shown that, in response to oxidative stress, HO-1 expression can be induced through the Nrf2/ARE signaling pathway, while, effective Nrf2/ARE signaling needs the participation of Brg1 [10]. However, as we showed in the current study, cardiac Brg1 expression in rats at the 4th week after STZ-induced type 1 diabetes was significantly reduced, which might be the major reason why cardiac protein expression of HO-1 was significantly decreased. Antioxidant NAC normalized cardiac free 15-F_{2t}-isoprostanes in diabetic rats and enhanced myocardium Brg1 expression, leading to full restoration of cardiac HO-1 expression. This finding suggests that enhancing Brg1 may represent a novel mechanism whereby NAC confers its antioxidant protection at least in early diabetes.

Consistent with our recent study findings [24], we showed in the current study that ventricular dysfunction occurs during early stage of diabetes manifested as abnormal relaxation function that was coincident with significant reduction in myocardial Brg1 protein expression. This finding is similar in nature to a previous study which showed that mice with cardiac-specific deletion of Brg1 developed impaired cardiac relaxation evidenced as reduction in E/A ratio as determined by ultrasound [15]. The findings by us and others [15] point out the importance of Brg1 in the maintenance of normal cardiac function. In our study, NAC treatment mediated improvement in cardiac diastolic function manifested as significant elevation of E/A ratio in diabetes which may be contributable to enhancement of cardiac Brg1 protein expression.

The risk of progression to heart failure after myocardial ischemia and reperfusion was significantly higher in diabetes compared with nondiabetes [27]. Myocardial STAT3 is an important transcription factor in the SAFE pathway (i.e., JAK2/STAT3 signaling cascade), especially during myocardium ischemia reperfusion injury [28], but cardiac p-STAT3 is reduced in diabetes [19]. Further, STAT3-deficient mice spontaneously develop a form of dilated cardiomyopathy similar to that which occurred in diabetic mice [29], indicating that reduced STAT3 activation may lead to myocardial remodeling. Brg1 is necessarily required to establish chromatin restructure for the activation of STAT3,

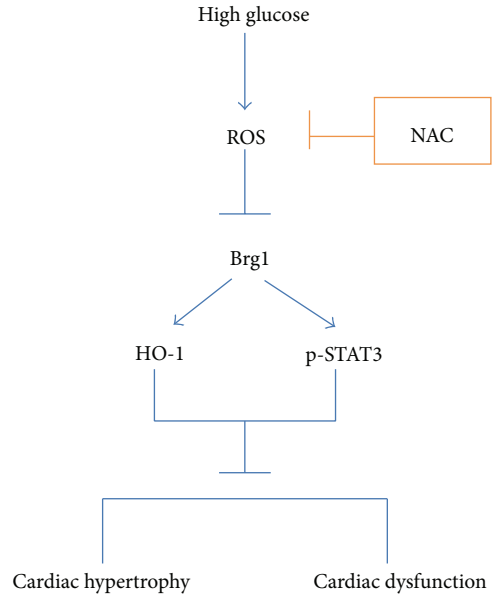

Figure 3: Schematic diagram proposing that Enhancement of cardiac Brg1 expression represents a novel mechanism whereby antioxidant N-acetylcysteine (NAC) enhanced cardiac HO-1 and p-STAT3 expression, and attenuated cardiac diastolic dysfunction in diabetes.

especially STAT3 phosphorylation at site Try705 in various cells such as cancer cell and macrophagocyte [30], and for STAT3 signaling transduction. In the current study, we also found that STAT3 phosphorylation at both Ser727 and Try705 was dramatically reduced in the hearts of diabetic rats, which was concomitant with decreased Brg1 expression. NAC treatment increased the expression of Brg1 and consequently enhanced p-STAT3 at both Try705 and Ser727 in the myocardium of diabetic rats. Based on the fact that Brg1 is a needed component for STAT3 activation [30], our findings suggest that Brg1 may play a key role in the transcriptional induction of cardiac STAT3, especially at Try705 in diabetic rats. NAC may have increased STAT3 phosphorylation in diabetes through enhancing Brg1 expression, although further study is needed to confirm this hypothesis.

Inflammation has been considered as an important process in the progression of diabetes [31, 32]. Elevation of TNF-alpha and IL-6 was detected in diabetes, which was related to the progression of diabetic complications [33]. In the current study, we showed that plasma levels of TNF-alpha and IL-6 were remarkably elevated in diabetic rats at 4 weeks after the establishment of diabetes, and NAC treatment decreased them, indicating that NAC can inhibit the inflammation reaction in diabetes. Studies found that moderate levels of TNF-alpha or IL-6 can increase the phosphorylation of STAT3 at Try705, and this is Brg1 dependent [22, 23]. In our study, we found that the levels of TNF-alpha and IL-6 in NAC-treated diabetic rats were significantly lower than that in the untreated diabetes, but still slightly higher than that in nondiabetic rats. These remaining slight elevations in TNF-alpha and IL-6 after NAC treatment should have contributed to the enhancement of cardiac p-STAT3 as seems

to be in the NAC treated group, which added to the effect of Brg1 in enhancing cardiac Brg1-mediated STAT3 activation as previously mentioned. This explains why NAC treatment did not completely restore cardiac Brg1 protein expression in diabetic rats but completely restored cardiac p-STAT3 at site Try705.

In summary, we first report that the expression of Brg1 was decreased significantly in the myocardium of diabetic rats, which may be responsible at least in part for the reduced expressions of HO-1 and p-STAT3 and impairment of cardiac diastolic function as summarized in the schematic diagram (Figure 3). Enhancement of cardiac Brg1 expression may thus represent a novel mechanism whereby NAC enhanced cardiac HO-1 and p-STAT3 expressions and attenuated cardiac diastolic dysfunction in diabetes.

Conflict of Interests

The authors have no potential conflict of interests to declare.

Acknowledgments

This study was supported by the Hong Kong Research Grant Council (RGC), GRF Grant (782910), and NSFC Grants (81200609, 81270899).

References

[1] I. Falcão-Pires and A. F. Leite-Moreira, "Diabetic cardiomyopathy: understanding the molecular and cellular basis to progress in diagnosis and treatment," *Heart Failure Reviews*, vol. 17, no. 3, pp. 325–344, 2012.

[2] Y. Liu, S. Lei, X. Gao et al., "PKCβ inhibition with ruboxistaurin reduces oxidative stress and attenuates left ventricular hypertrophy and dysfuntion in rats with streptozotocin-induced diabetes," *Clinical Science*, vol. 122, no. 4, pp. 161–173, 2012.

[3] M. Rajesh, P. Mukhopadhyay, S. Btkai et al., "Cannabidiol attenuates cardiac dysfunction, oxidative stress, fibrosis, and inflammatory and cell death signaling pathways in diabetic cardiomyopathy," *Journal of the American College of Cardiology*, vol. 56, no. 25, pp. 2115–2125, 2010.

[4] L. E. Wold, A. F. Ceylan-Isik, and J. Ren, "Oxidative stress and stress signaling: menace of diabetic cardiomyopathy," *Acta Pharmacologica Sinica*, vol. 26, no. 8, pp. 908–917, 2005.

[5] D. Du, Y.-H. Shi, and G.-W. Le, "Oxidative stress induced by high-glucose diet in liver of C57BL/6J mice and its underlying mechanism," *Molecular Biology Reports*, vol. 37, no. 8, pp. 3833–3839, 2010.

[6] S. Lei, Y. Liu, H. Liu, H. Yu, H. Wang, and Z. Xia, "Effects of N-acetylcysteine on nicotinamide dinucleotide phosphate oxidase activation and antioxidant status in heart, lung, liver and kidney in streptozotocin-induced diabetic rats," *Yonsei Medical Journal*, vol. 53, no. 2, pp. 294–303, 2012.

[7] J. A. Araujo, M. Zhang, and F. Yin, "Heme oxygenase-1, oxidation, inflammation, and atherosclerosis," *Frontiers in Pharmacology*, vol. 3, article 119, 2012.

[8] C. Kusmic, A. L'Abbate, G. Sambuceti et al., "Improved myocardial perfusion in chronic diabetic mice by the up-regulation of pLKB1 and AMPK signaling," *Journal of Cellular Biochemistry*, vol. 109, no. 5, pp. 1033–1044, 2010.

[9] V. Selvaraju, M. Joshi, S. Suresh, J. A. Sanchez, N. Maulik, and G. Maulik, "Diabetes, oxidative stress, molecular mechanism, and cardiovascular disease-an overview," *Toxicology Mechanisms and Methods*, vol. 22, pp. 330–335, 2012.

[10] J. Zhang, T. Ohta, A. Maruyama et al., "BRG1 interacts with Nrf2 to selectively mediate HO-1 induction in response to oxidative stress," *Molecular and Cellular Biology*, vol. 26, no. 21, pp. 7942–7952, 2006.

[11] L. Mohrmann and C. P. Verrijzer, "Composition and functional specificity of SWI2/SNF2 class chromatin remodeling complexes," *Biochimica et Biophysica Acta*, vol. 1681, no. 2-3, pp. 59–73, 2005.

[12] R. J. Bourgo, H. Siddiqui, S. Fox et al., "SWI/SNF deficiency results in aberrant chromatin organization, mitotic failure, and diminished proliferative capacity," *Molecular Biology of the Cell*, vol. 20, no. 14, pp. 3192–3199, 2009.

[13] W. Du, R. Rani, J. Sipple et al., "The FA pathway counteracts oxidative stress through selective protection of antioxidant defense gene promoters," *Blood*, vol. 119, no. 18, pp. 4142–4151, 2012.

[14] M. Vallaster, C. D. Vallaster, and S. M. Wu, "Epigenetic mechanisms in cardiac development and disease," *Acta Biochimica et Biophysica Sinica*, vol. 44, no. 1, pp. 92–102, 2012.

[15] J. K. Takeuchi, X. Lou, J. M. Alexander et al., "Chromatin remodelling complex dosage modulates transcription factor function in heart development," *Nature Communications*, vol. 2, article 187, 2011.

[16] C. T. Hang, J. Yang, P. Han et al., "Chromatin regulation by Brg1 underlies heart muscle development and disease," *Nature*, vol. 475, no. 7357, p. 532, 2011.

[17] M. S. Willis, J. W. Homeister, G. B. Rosson et al., "Functional redundancy of SWI/SNF catalytic subunits in maintaining vascular endothelial cells in the adult heart," *Circulation Research*, vol. 111, no. 5, pp. e111–e122, 2012.

[18] L. Ho, E. L. Miller, J. L. Ronan, W. Q. Ho, R. Jothi, and G. R. Crabtree, "EsBAF facilitates pluripotency by conditioning the genome for LIF/STAT3 signalling and by regulating polycomb function," *Nature Cell Biology*, vol. 13, no. 8, pp. 903–913, 2011.

[19] T. Wang, S. Qiao, S. Lei et al., "N-acetylcysteine and allopurinol synergistically enhance cardiac adiponectin content and reduce myocardial reperfusion injury in diabetic rats," *PLoS ONE*, vol. 6, no. 8, Article ID e23967, 2011.

[20] Z. Xia, K.-H. Kuo, P. R. Nagareddy et al., "N-acetylcysteine attenuates PKCβ2 overexpression and myocardial hypertrophy in streptozotocin-induced diabetic rats," *Cardiovascular Research*, vol. 73, no. 4, pp. 770–782, 2007.

[21] V. Ramakrishna and R. Jailkhani, "Oxidative stress in non-insulin-dependent diabetes mellitus (NIDDM) patients," *Acta Diabetologica*, vol. 45, no. 1, pp. 41–46, 2008.

[22] M. N. Ndlovu, C. Van Lint, K. Van Wesemael et al., "Hyperactivated NF-κB and AP-1 transcription factors promote highly accessible chromatin and constitutive transcription across the interleukin-6 gene promoter in metastatic breast cancer cells," *Molecular and Cellular Biology*, vol. 29, no. 20, pp. 5488–5504, 2009.

[23] Z. Ni and R. Bremner, "Brahma-related gene 1-dependent STAT3 recruitment at IL-6-inducible genes," *Journal of Immunology*, vol. 178, no. 1, pp. 345–351, 2007.

[24] X. Gao, Y. Xu, B. Xu et al., "Allopurinol attenuates left ventricular dysfunction in rats with early stages of streptozotocin-induced diabetes," *Diabetes/Metabolism Research and Reviews*, vol. 28, no. 5, pp. 409–417, 2012.

[25] P. Faure, C. Polge, D. Monneret, A. Favier, and S. Halimi, "Plasma 15-F2t isoprostane concentrations are increased during acute fructose loading in type 2 diabetes," *Diabetes and Metabolism*, vol. 34, no. 2, pp. 148–154, 2008.

[26] M.-L. Wu, Y.-C. Ho, and S.-F. Yet, "A central role of heme oxygenase-1 in cardiovascular protection," *Antioxidants and Redox Signaling*, vol. 15, no. 7, pp. 1835–1846, 2011.

[27] M. J. Garcia, P. M. McNamara, T. Gordon, and W. B. Kannell, "Morbidity and mortality in diabetics in the Framingham population. Sixteen year follow up study," *Diabetes*, vol. 23, no. 2, pp. 105–111, 1974.

[28] B. Drenger, I. A. Ostrovsky, M. Barak, Y. Nechemia-Arbely, E. Ziv, and J. H. Axelrod, "Diabetes blockade of sevoflurane postconditioning is not restored by insulin in the rat heart: phosphorylated signal transducer and activator of transcription 3- and phosphatidylinositol 3-kinase-mediated inhibition," *Anesthesiology*, vol. 114, no. 6, pp. 1364–1372, 2011.

[29] D. Hilfiker-Kleiner, A. Hilfiker, M. Fuchs et al., "Signal transducer and activator of transcription 3 is required for myocardial capillary growth, control of interstitial matrix deposition, and heart protection from ischemic injury," *Circulation Research*, vol. 95, no. 2, pp. 187–195, 2004.

[30] S. Giraud, A. Hurlstone, S. Avril, and O. Coqueret, "Implication of BRG1 and cdk9 in the STAT3-mediated activation of the p21waf1 gene," *Oncogene*, vol. 23, no. 44, pp. 7391–7398, 2004.

[31] G. S. Hotamisligil, "Endoplasmic reticulum stress and the inflammatory basis of metabolic disease," *Cell*, vol. 140, no. 6, pp. 900–917, 2010.

[32] P. Casas-Agustench, M. Bulló, and J. Salas-Salvadó, "Nuts, inflammation and insulin resistance," *Asia Pacific Journal of Clinical Nutrition*, vol. 19, no. 1, pp. 124–130, 2010.

[33] J. F. Navarro-González, C. Mora-Fernández, M. Gómez-Chinchón, M. Muros, H. Herrera, and J. Garcia, "Serum and gene expression profile of tumor necrosis factor-α and interleukin-6 in hypertensive diabetic patients: effect of amlodipine administration," *International Journal of Immunopathology and Pharmacology*, vol. 23, no. 1, pp. 51–59, 2010.

Hindawi Publishing Corporation
Journal of Diabetes Research
Volume 2013, Article ID 797548, 10 pages
http://dx.doi.org/10.1155/2013/797548

Review Article

Advances in Murine Models of Diabetic Nephropathy

Li-li Kong, Hao Wu, Wen-peng Cui, Wen-hua Zhou, Ping Luo, Jing Sun, Hang Yuan, and Li-ning Miao

Department of Nephrology, The Second Hospital of Jilin University, Changchun 130041, China

Correspondence should be addressed to Li-ning Miao; miaolining@yahoo.com.cn

Received 2 February 2013; Accepted 21 May 2013

Academic Editor: Shahidul Islam

Diabetic nephropathy (DN) is one of the microvascular complications of both type 1 and type 2 diabetes, which is also associated with a poor life expectancy of diabetic patients. However, the pathogenesis of DN is still unclear. Thus, it is of great use to establish appropriate animal models of DN for doing research on pathogenesis and developing novel therapeutic strategies. Although a large number of murine models of DN including artificially induced, spontaneous, and genetically engineered (knockout and transgenic) animal models have been developed, none of them develops renal changes sufficiently reflecting those seen in humans. Here we review the identified murine models of DN from the aspects of genetic background, type of diabetes, method of induction, gene deficiency, animal age and gender, kidney histopathology, and phenotypic alterations in the hope of enhancing our comprehension of genetic susceptibility and molecular mechanisms responsible for this disease and providing new clues as to how to choose appropriate animal models of DN.

1. Introduction

DN, as one complication of diabetes, is one of the leading causes of end-stage renal disease (ESRD) worldwide. The value of animal models in the study of pathogenesis is beyond doubt. Although great progress has been made in the study of animal models, none of the models can reproduce all the structural and functional changes of human DN. Murine models have substantial advantages over other species in the studies on pathogenesis of DN, including lower cost, murine repositories that bear multiple mutations, plentiful inbred strains, and an available map of murine genomic sequence on the Internet. The Animal Models of Diabetic Complications Consortium (AMDCC) proposes the following three criteria for a desirable murine model of DN: (1) more than 50% decline in glomerular filtration rate (GFR) over the lifetime of the animal; (2) greater than 10-fold increase in albuminuria compared with controls for that strain at the same age and gender; (3) histopathology findings which include mesangial sclerosis (a 50% increase in mesangial volume), any degree of arteriolar hyalinosis, glomerular basement membrane (GBM) thickening (a >25% increase compared with baseline by electron microscopy morphometry), and tubulointerstitial fibrosis. In fact, there are no murine models that meet all of the three criteria. Here we review the identified murine models of DN including artificially induced, spontaneous, and genetically engineered (knockout and transgenic) animal models and compare their advantages and deficiencies. Some of the key issues, such as strain, genetic background, type of diabetes, method of induction, gene deficiency, animal age and gender, kidney histopathology, and phenotypic alterations, are all included in this review. We hope this review could enhance our understanding of genetic susceptibility and molecular mechanisms responsible for DN, as well as provide new clues as to how to choose appropriate animal models of DN.

2. Artificially Induced Murine Models of DN

2.1. Murine Models of DN from Type 1 Diabetes Mellitus (T1DM). Alloxan and streptozotocin (STZ) are widely used for producing artificially induced T1DM which causes kidney damage with similarities to human DN. Both of them are glucose analogues that enter the insulin-producing beta-cells via a glucose transporter. The diabetogenic actions of alloxan and

STZ are mediated by reactive oxygen species (ROS). However, they are generated through different approaches in the case of alloxan and STZ. In the presence of glutathione, alloxan and its reduction product, dialuric acid, generate superoxide radicals in a cyclic redox reaction which undergo dismutation to hydrogen peroxide afterwards. Then Fenton reaction ensues with the formation of highly reactive hydroxyl radicals. After being taken into pancreatic beta-cells, STZ is broken down into its glucose and methylnitrosourea moiety. The latter modifies DNA fragments due to its alkylating properties. DNA damage causes the activation of poly ADP-ribosylation which leads to depletion of cellular NAD^+ and ATP. Enhanced ATP dephosphorylation provides substrate for xanthine oxidase. As a result, superoxide radicals are formed. ROS and a simultaneous cytosolic calcium overload lead to acute necrosis of pancreatic beta-cells [1, 2]. So both of the two diabetogenic agents induce diabetes secondary to the necrosis of pancreatic beta-cells. As time progresses, hyperglycaemia eventually leads to diabetic kidney damage. These STZ-treated models develop a modest degree of proteinuria and serum creatinine increase, as well as minimal mesangial matrix expansion, depending on the genetic background [3, 4]. Animal models of STZ-induced DN are usually performed in mice, Sprague-Dawley and Wistar-Kyoto rats.

2.1.1. Moderate and High-Dose STZ. Given the mouse strains which are resistant to a single dose of STZ (≥200 mg/kg) or a two-dose regimen of STZ (2 × 100–2 × 125 mg/kg), greater cytotoxicity to pancreatic beta-cells and collateral tissue occurs, resulting in a higher incidence and severity of diabetes [4–7]. Because of the severe hyperglycaemia, the diabetic models need to be monitored for blood glucose and administrated insulin. Several months later, a modest degree of proteinuria can be detected. Some investigators optimize the animal models of STZ-induced DN by uninephrectomy in advance which lead to compensatory hypertrophy of the remaining kidney and acceleration of the disease progression. However, owing to the nephrotoxicity of STZ, it is difficult to differentiate between the direct toxic effect of STZ and lesions caused by hyperglycaemia [8, 9]. Some studies on mouse models of DN show that high-dose STZ-treated mice exhibit more albuminuria than those which receive low-dose STZ, despite of similar blood glucose [10]. Besides, evidence for acute kidney injury caused by high-dose STZ in mice and rats has been reported [9, 11]. Although STZ-treated models result in hypoinsulinemia and hyperglycaemia, they do not share autoimmune features like patients with T1DM.

2.1.2. Low-Dose STZ. In order to reduce nonspecific nephrotoxicity of STZ, the regimen of multiple low-dose injections of STZ to induce diabetes has been performed, that is daily intraperitoneally injections of 40–60 mg/kg STZ for five consecutive days [4, 12–14] which usually induces repetitive low-grade beta cell damage accompanied by secondary autoimmune insulitis [15, 16]. It is quite different among inbred strains of mice in susceptibility to both pancreatic beta cell toxicity [17] and the direct nephrotoxicity of low-dose STZ [12]. It is reported by Gurley et al. [18] that there is a hierarchical response of blood glucose level to multiple low doses of STZ (DBA/2 > C57BL/6 > MRL/MP > 129/SvEv > BALB/c). His research results also show that males are more susceptible to diabetes induced by this STZ regimen than females. Generally, given strain-appropriate doses of STZ, mice that receive low-dose STZ develop parallel levels of hyperglycemia to those that receive high-dose STZ [9]; the levels of albuminuria, by contrast, are generally lower as a result of reduced direct nephrotoxicity of STZ [19, 20]. Moreover, evidence for nontoxicity on podocytes has been reported. The US-based AMDCC also recommends a standard low-dose model for STZ-induced diabetic complications which include DN. According to this recommendation, mouse models of DN should be induced by daily intraperitoneally injections of 50 mg/kg STZ for five consecutive days. However, studies show that only 50% of C57BL/6 mice develop overt diabetes through this approach. Therefore, whether it will be adopted by relevant experts is not yet determined.

2.2. Murine Models of DN from Type 2 Diabetes Mellitus (T2DM). The protocol of high-fat diet is widely used to induce insulin resistance and obesity [21–23]. It is also of great use for the research of accelerated atherosclerosis [24–26], although inbred strains of mice exhibit significant differences in response to the effect of high-fat diet. C57BL6 mice respond strongly to high-fat diet; A/J mice, by contrast, are relatively resistant [21]. Sugano et al. [27] have reported a new rat model of DN induced by high-fat diet, multiple low-dose injections of STZ, and uninephrectomy. This model exhibits most features of human DN from T2DM including hyperglycemia, hypoinsulinemia, hyperlipidaemia, hypertension, and microalbuminuria followed by overt albuminuria, mesangial expansion, and terminal glomerular sclerosis.

3. Spontaneous Murine Models of DN

Spontaneous animal models of DN are established by selective breeding from animals which spontaneously develop DN due to genetic abnormality. Renal abnormalities in these models resemble human diseases; therefore, these models provide an experimental platform for studying pathogenesis and genetic susceptibility responsible for DN. Although these models are difficult to feed and breed, not widely available, and with long modeling cycle and higher cost, the application of them is becoming increasingly extensive. Table 1 lists some common murine models of spontaneous DN.

3.1. Murine Models of Spontaneous DN from T1DM

3.1.1. Nonobese Diabetic (NOD) Mouse. The spontaneous murine model of T1DM that has been studied most extensively is the NOD mouse. Due to pathogenic and genetic similarities to the human disease, the model serves as a useful tool to study the etiology, pathology, and progression of disease. NOD mouse was derived from the Jcl: ICR cataract mouse 30 years ago in Japan [28]. These mice develop spontaneous insulitis at the age of 4-5 weeks, and overt

Table 1: Murine models of spontaneous DN.

Models (Ref)	Strains	Defects	Phenotypic alterations	Kidney pathology
NOD mouse [10, 28–32]	Inbred line derived from ICR (outbred line)	Autoimmune insulitis caused by polygenes including specific MHC class II alleles and many non-MHC loci	T1DM, hyperglycemia, albuminuria, autoimmune insulitis, and other autoimmune manifestations	Related reports are few, enlarged glomeruli, and mesangial sclerosis
Insulin-2 Akita mouse [10, 18, 33]	C57BL/6, C3H	Autosomal dominant mutation in the Ins-2 gene causes misfolding of insulin protein	T1DM, hyperglycemia, and modest levels of albuminuria	Increased mesangial matrix, GBM thickening, and no mesangiolysis or widespread marked or nodular mesangial sclerosis
db/db mouse [10, 20, 33–37]	C57BL/6, C57BLKS, DBA, FVB, CBA	G-to-T mutation in the gene coding the leptin receptor (*db/db*)	T2DM, hyperglycemia, obesity,and albuminuria	Glomerular hypertrophy, mesangial matrix expansion, GBM thickening, and no mesangiolysis or nodular mesangial sclerosis
OLETF rat [38–40]	Long-Evans	Poor pancreatic proliferation caused by multiple genes including several QTLs and the gene encoding CCKAR	T2DM, mild obesity, late-onset hyperglycemia, macroalbuminuria, hypertension, and dyslipidemia	Glomerular hypertrophy, GBM thickening, extracellular matrix expansion, nodular lesions, diffuse glomerulosclerosis, and severe tubulointerstitial fibrosis
GK rat [41–45]	Wistar	Pancreatic beta-cell deficit caused by polygenes	T2DM, hypertension, moderate hyperglycemia, albuminuria, nonobesity, nonhyperlipidemia	Glomerular hypertrophy and GBM thickening by 35 weeks; segmental glomerulosclerosis and tubulointerstitial fibrosis at 24 months of age
BTBR *ob/ob* mouse [46–48]	BTBR	*ob/ob* mutation (a recessive mutation in the gene coding leptin) in BTBR strain	T2DM, severe hyperglycemia, pancreatic islet hypertrophy, macroalbuminuria, hypercholesterolemia, elevated triglycerides, obesity, and decreased GFR	Glomerular hypertrophy, mesangial matrix expansion, GBM thickening, loss of podocytes, diffuse mesangial sclerosis (focally approaching nodular glomerulosclerosis), focal mild interstitial fibrosis, focal arteriolar hyalinosis, and mesangiolysis
NZO mouse [10, 49]	NZO	Obesity/diabetes caused by polygenes including QTLs on chromosomes 1, 2, 4, 5, 6, 7, 11, 12, 13, 15, 17, and 18	T2DM, obesity, hyperglycemia, albuminuria, low-titer IgM antibodies to the insulin receptor, and susceptibility to lupus nephritis	Glomerular proliferation, mesangial deposits, mild GBM thickening, glomerulosclerosis, eosinophilic nodules in some glomeruli, occasional hyalinization of the glomerular arterioles, and healing arteriolar inflammation
KK-Ay mouse [10, 50–53]	KK, C57BL, C3H, FVB	Yellow/obese/diabetic phenotype caused by polygenes including dominant mutation in agouti yellow (Ay) gene	T2DM, hyperglycemia, obesity, albuminuria, hypertriglyceridemia, and obstructive uropathy	Glomerular hypertrophy, mild and moderated mesangial matrix expansion, and segmental proliferative glomerular nephritis
ZDF rat [54–62]	Zuker	Missense mutation in the gene coding the leptin receptor (*fa/fa*)	T2DM, hyperglycemia, obesity, hyperlipidemia, hypertension, and macroalbuminuria	mesangial expansion, focal segmental glomerulosclerosis, macrophage infiltration, and interstitial fibrosis

CCKAR: cholecystokinin type A receptor; GFR: glomerular filtration rate; GBM: glomerular basement membrane; MHC: major histocompatibility complex; QTLs: quantitative trait loci.

diabetes emerges at the age of 24–30 weeks when most of pancreatic β-cells are destroyed. Female incidence of diabetes is four times higher than the male in NOD mice [10]. This model exhibits a number of clinical features of human T1DM including hyperglycaemia, glycosuria, polyuria, and polydipsia; however, it is more resistant to ketoacidosis. Without insulin administration, NOD mice usually die of dehydration, rather than ketoacidosis. Like in humans, the major histocompatibility complex (MHC) alleles are closely related to susceptibility to T1DM. Moreover, some MHC alleles must be accompanied by other non-MHC genes for the development of T1DM [29, 30], which is also the same in human disease. Even so, NOD mice are not the perfect animal model for human T1DM. As an inbred strain, they have a fixed genetic risk for T1DM and develop T1DM in a predictable fashion [31], whereas human T1DM develops as a result of deleterious interactions between relevant genes and from external environmental factors.

Despite of the extensive study of the genetic and immunologic pathogenesis of T1DM in NOD mouse, few investigators choose NOD mouse to do research on DN because of the complicated genetics, the late and variable age of onset of T1DM, and the requirement for insulin administration [10]. Even so, one of the few studies shows that the amount of albuminuria in hyperglycemic NOD mice is seven times higher than that in NOD mice before the development of hyperglycemia [32]. The results of renal lesions in acute phase of T1DM in NOD mice show mild changes in glomeruli and structural alteration of the proximal straight tubules. The study also points out that increased neuronal nitric oxide synthase may represent one of the pathogenic factors of DN [70]. Besides, there are also studies using NOD mice demonstrating that transforming growth factor-β (TGF-β) and advanced glycosylation endproducts (AGE) take an important role in mesangial proliferation and sclerosis [71–73], which is also the same in human DN.

3.1.2. Insulin-2 Akita Mouse. Akita mice develop T1DM because of the spontaneous mutation in Ins-2 gene. The mutation leads to the misfolding of insulin protein, which is toxic to pancreatic β-cell. Consequently, the capacity of β-cell to secrete insulin is largely decreased. The Ins-2 Akita mutation which is autosomal dominant was originally found in C57BL/6 mice in Akita, Japan. Mice heterozygous for the mutation develop significant hyperglycemia as a result of severe insulin deficiency at 3 to 4 weeks of age, but homozygotus mice usually die in perinatal period. Males develop substantially worse insulin deficiency than females. Mice with Ins-2 Akita mutation exhibit modest levels of albuminuria and mild-to-moderate glomerular mesangial expansion [18]. Nonetheless, Akita mice have higher levels of hyperglycemia, albuminuria, blood pressure, and more consistent structural changes of kidney compared with STZ-induced DN [18]. Gurley et al. have found that renal phenotype of Akita mice is largely dependent on their genetic background strains [18]. It means that genetic factors might influence susceptibility to DN in Akita mice which is the same in human disease. Thus, mice bearing Ins-2 Akita mutation have significant advantages as a model of T1DM.

3.2. Murine Models of Spontaneous DN from T2DM

3.2.1. Db/db Mouse. The *db/db* mouse which has a G-to-T mutation in the gene coding the leptin receptor develops obesity, insulin resistance, and T2DM spontaneously. The *db/db* mutation which is autosomal recessive was initially recognized from an obese and hyperphagic mouse in the C57BLKS/J strain and was subsequently backcrossed to a pure C57BL/6J background. Mice in the C57BLKS/J stain exhibit hyperinsulinemia at 10 days of age and slight hyperglycemia at 1 month of age. Overt hyperglycemia is noted by 8 weeks of age [20]. Manifestations of DN are albuminuria, glomerular hypertrophy, mesangial matrix expansion, and GBM thickening [20]. Albuminuria can be detected as early as 3 to 4 weeks after the onset of hyperglycemia [3]. The level of albuminuria in the *db/db* male mouse is 68–600 μg/24 h [20, 34–37] which is only 4–21 μg/24 h [34, 37] in the age-matched heterozygous littermate. The *db/db* mice display an increase in glomerular size and mesangial matrix by 5-6 months of age [20]. By 18–20 months, the glomerular and mesangial matrix enlargements become more remarkable, and thickening of the GBM is observed [20]. In general, *db/db* mice do not develop mesangiolysis, nodular mesangial sclerosis, and progressive renal insufficiency [33]. However, they are good models of early changes in human DN. Hyperglycemia, and renal changes of *db/db* mice in C57BLKS/J stain are usually worse than in the C57BL/6 background. Hence, investigations of DN in *db/db* mice are more widely conducted with the C57BLKS/J strain. Nonetheless, *db/db* mice in the C57BL/6 stain which have been intercrossed with gene knockout and transgenic mice [74, 75] provide new strains to identify pathogenesis of DN.

3.2.2. Otsuka Long-Evans Tokushima Fatty (OLETF) Rat. The OLETF rat is an identified murine model of T2DM. The model is characterized by hyperphagia, mild obesity, late-onset hyperglycemia, hypertension, dyslipidemia and advanced DN. Multiple recessive genes are associated with the induction of diabetes, including *odb-1* on X-chromosome of OLETF rats. It is also reported that a major quantitative trait locus colocalizing with cholecystokinin type A receptor gene influences poor pancreatic proliferation in OLETF rats [38]. The progression of T2DM in OLETF rats can be prevented by exercise [76] and calorie-restricted diet [77] as human disease. At 12–20 weeks of age, OLETF rats exhibit mild obesity and hyperinsulinemia [39]. Late-onset hyperglycemia is noted by 18 weeks of age [39]. At 22 weeks of age, the OLETF rats develop overt albuminuria, and at 54 weeks, advanced renal changes such as macroalbuminuria, nodular lesions, diffuse glomerulosclerosis, and tubulointerstitial fibrosis are noted like human DN [40]. Therefore, OLETF rat is considered as one of the best murine models to study DN.

3.2.3. GK Rat. Goto Kakizaki (GK) rat, a spontaneous polygenic model of T2DM, is established by repeated inbreeding of glucose-intolerant Wistar rats over many generations [78]. This model is characterized by moderate hyperglycemia, peripheral insulin resistance, and nonhyperlipidemia, and

nonobese phenotype. It is recognized that T2DM in GK rat is primarily caused by beta-cell deficit. In order to identify the origin of the abnormality, Miralles and Porthe [79] compared the development of the embryo in GK and Wistar rats. They found a decrease in pancreatic cell proliferation from embryonic day 16 to 20 (E16–E20) and a wave of pancreatic cell apoptosis from E16 to E18. By E16, the number of pancreatic beta-cells in the GK rats is half of the Wistar rats, and this difference was sustained until birth. GK rat exhibits morphological changes which can be seen in early stage of human DN such as glomerular hypertrophy and GBM thickening [41]. It does not develop overt proteinuria or progressive nephropathy by 8 months of age [41], even being treated with some initiators to promote renal injury [42, 43]. However, Sato et al. [44] have reported advanced renal changes in GK rats such as segmental glomerulosclerosis and tubulointerstitial fibrosis at 24 months of age. At that time, albuminuria increases notably. Thus, they draw the conclusion that renal changes in GK rats at a late stage were similar to those of progressive human DN. Therefore, GK rat serves a useful tool for studying T2DM and DN.

3.2.4. Ob/ob and BTBR ob/ob Mice. Compared with *db/db* mouse, *ob/ob* mouse develops T2DM caused by the spontaneous recessive mutation in leptin [46], the ligand for the leptin receptor. The *ob/ob* mutation exists in C57BL/6J, DBA2/J, and FVB strains. This model exhibits only mild functional and morphological changes in C57BL/6J strains [80]. Thus, it is not widely used as an animal model of DN.

However, a new mouse model that mimics progressive DN has been developed in BTBR strain with the *ob/ob* mutation [47]. Its characteristics are insulin resistance, hyperinsulinemia, pancreatic islet hypertrophy, severe hyperglycemia, obesity, hypercholesterolemia, and elevated triglycerides. The BTBR *ob/ob* mice are largely resistant to the hypoglycemic effect of insulin administration and rapidly develop pathological changes of both early and advanced human DN [48]. The mice develop progressive proteinuria by 4 weeks of age. Characteristics of early DN such as glomerular hypertrophy, accumulation of mesangial matrix, and loss of podocytes are detectable by 8 weeks of age [48]. Glomerular lesions of progressive, advanced DN are present by 20 weeks. By 22 weeks, morphological characteristics of renal injury has 20% increase in GBM thickness, 50% increase in mesangial matrix, mesangiolysis, diffuse mesangial sclerosis, focal arteriolar hyalinosis, and focal mild interstitial fibrosis [48]. On the one hand, the advantage of BTBR *ob/ob* mice over other animal models is the relatively short period for the development of advanced DN. On the other hand, compared with *db/db* mice (with deficiency of the leptin receptor), BTBR *ob/ob* mice provide a new tool for testing therapeutic effect of leptin administration in DN, whereas the mice have apparent limitations, such as their high cost and infertility [33]. Besides, due to the limited study on BTBR strain, investigators have to pay great attention to the time-consuming backcrossing strategies in order to induce specific genetic mutations into these mice [33]. Nonetheless, BTBR *ob/ob* mouse is fairly valuable for testing therapeutic interventions.

3.2.5. New Zealand Obese (NZO) Mouse. The NZO mouse is established by selective breeding from polygenic mice of obesity and T2DM in New Zealand. It is characterized by obesity, T2DM, and low-titer IgM antibodies to the insulin receptor [49]. The QTLs on chromosomes 1, 2, 4, 5, 6, 7, 11, 12, 13, 15, 17, and 18 [81–83] are responsible for the disease. NZO mice are prone to autoimmune disease and develop circulating antibodies to both native DNA and single-stranded DNA [49]. By 6 months of age, the antibody levels in NZO mice are comparable to those found in the mouse models of systemic lupus erythematosus [49]. NZO mice exhibit morphological features of both diabetic and lupus nephropathies, such as glomerular proliferation, mesangial deposits, mild GBM thickening, glomerulosclerosis, eosinophilic nodules in some glomeruli, occasional hyalinization of the glomerular arterioles, and healing arteriolar inflammation [49]. Thus, given the evidence of immune disorder, NZO mouse offers a unique opportunity to study the relationship among T2DM, autoimmunity, and obesity.

3.2.6. KK-Ay Mouse. KK-Ay mice develop T2DM caused by the dominant mutation in agouti yellow (Ay) gene. The Ay gene is expressed in the hair follicle, where the gene product acts as an antagonist of melanocyte stimulating hormone receptor resulting in the inhibition of melanogenesis and yellow fur [50]. Besides, an agouti-related protein influences weight regulation [51]. It is widely recognized that Ay gene is crucial to the yellow obese phenotype. KK-Ay mice spontaneously exhibit severe, early-onset hyperinsulinemia, hyperglycemia, obesity, hypertriglyceridemia, fatty liver, and albuminuria. KK-Ay mice develop morphological changes of early DN, such as glomerular hypertrophy, mild and moderated mesangial matrix expansion, and segmental proliferative glomerular nephritis [52]. Therefore, KK-Ay mouse might be a useful murine model of the early stage of DN. It is notable, though, that most of male KK-Ay mice die of obstructive uropathy associated with hydronephrosis between 7 and 14 months of age without unknown causes [53]. Partly for this reason, KK-Ay mouse is not widely used as animal model of DN.

3.2.7. Zucker Diabetic Fatty (ZDF) Rat. The ZDF rat which has a missense mutation in the gene coding the leptin receptor (fa/fa) [54] spontaneously develops insulin resistance, T2DM, hyperlipidemia, both moderate hypertension and obesity, and progressive renal injury. Studies of the ZDF rats show that the hyperglycemia is sexually dimorphic. Although female ZDF rats have similar levels of insulin resistance and degrees of obesity to male ZDF rats, they develop hyperglycaemia only when administered with diabetogenic diet [84]. Thus, the ZDF male rats are more widely used as the animal models of T2DM and DN. Histopathologic changes of kidney [55–60] have been described as focal segmental glomerulosclerosis, mild mesangial expansion, macrophage infiltration, and interstitial fibrosis. Hyperglycaemia in ZDF rats is manifested by 12 weeks [61]. These rats develop albuminuria at 14 weeks [62] and focal segmental glomerulosclerosis at 18–20 weeks of age [56, 57]. Macroalbuminuria ultimately leads to chronic renal insufficiency by 22 weeks of age [62]. The

Table 2: Genetically engineered murine models of DN.

Models (Ref)	Strains	Molecular background	Phenotypic alterations	Kidney pathology
OVE26 mice [63–65]	FVB	β-cell-specific damage due to overexpression of calmodulin transgene regulated by the insulin promoter	T1DM, hyperglycemia, hypertension, albuminuria, hypoalbuminemia, and GFR increased first and then decreased	Enlarged glomeruli, enlarging mesangium with diffuse and nodular expansion of mesangial matrix, GBM thickening, diffuse and nodular glomerulosclerosis, nodules similar to typical K-W nodules, expansion of the tubules, atrophy of tubular cells, interstitial infiltration of mononuclear cells, tubulointerstitial fibrosis
eNOS$^{-/-}$/*db/db* mice [66–68]	C57/B6 × C57BLKS/J (BKS)	BKS-*db/db* mice cross with eNOS$^{-/-}$ mice	T2DM, obesity, hyperglycemia, hypertension, albuminuria, and decreased GFR	Mesangial expansion, GBM thickening, arteriolar hyalinosis, mesangiolysis, microaneurysms, focal segmental and nodular glomerulosclerosis, nodules that resemble K-W nodules, striking fibronectin accumulation in glomeruli, minimal tubulointerstitial fibrosis
RAGE/iNOS mice [45]	CD-1	Transgenic mice that overexpress human RAGE in vascular cells crossbreed with another transgenic line carrying human cDNA for iNOS under the control of the insulin promoter	T1DM, hyperglycemia, albuminuria, and increased serum creatinine	Mesangial expansion, diffuse glomerulosclerosis
Megsin/RAGE/iNOS mice [69]	C57BL/6N × CD1	Triple transgenic mice overexpressing megsin, RAGE, and iNOS (megsin transgenic mice crossbreed with RAGE/iNOS transgenic mice)	T1DM, hyperglycemia, albuminuria, increased serum creatinine, and urea nitrogen	Glomerular hypertrophy, diffuse mesangial expansion, GBM thickening, global mesangial sclerosis, some segmental sclerotic lesions that resemble K-W nodules, inflammatory cell infiltration, interstitial fibrosis, and immune complexes depositions

eNOS: endothelial nitric oxide synthase; GBM: glomerular basement membrane; GFR: glomerular filtration rate; iNOS: inducible nitric oxide synthase; K-W nodules: Kimmelstiel-Wilson nodules; RAGE: the receptor for advanced glycation endproducts.

ZDF rat exhibits a physiological and metabolic profile similar to human T2DM and functional and morphological renal lesions that resemble human DN. Thus, ZDF rat is considered as an excellent animal model of T2DM and DN.

4. Genetically Engineered (Knockout and Transgenic) Murine Models of DN

Diabetes is the major cause of ESRD worldwide. Despite of the high incidence, only a minority of patients with diabetes develop renal lesions. Family-based studies show that a significant genetic component confers risk for DN. All the above studies indicate the importance of genetic factors in differential susceptibility to DN, whereas limited progress has been made in identifying specific genetic factors that contribute to DN due to genetic heterogeneity and multigenic pathogenesis. Recently, investigators have developed genetically engineered murine models in combination with genetic manipulations, including transgenic and knockout mice bearing defined alterations in a single gene or in a series of candidate genes. Studies *in vivo* using these models show that the genes coding TGF-β, plasma prorenin, inducible cAMP early repressor, receptor for advanced glycation endproducts (RAGE), endothelial nitric oxide synthase (eNOS), and aldose reductase involve in the origin and progression of DN, corroborating experimental findings from human association studies. Genetically engineered murine models provide valuable insight into the role of pathogenetic genes and molecular mechanisms responsible for DN, thus opening new avenues to develop novel therapeutic strategies. Table 2 lists some of the genetically engineered murine models that develop advanced DN-like human disease. Here we emphasize more on the OVE26 and the eNOS$^{-/-}$/*db/db* mice, of type 1 and type 2 diabetes, that develop kidney injury most resembling that seen in human.

4.1. OVE26 Mouse. The OVE26 mouse on the FVB inbred strain is a transgenic mouse model of severe early-onset type 1 diabetes [63]. These mice exhibit severe hyperglycemia 2-3 weeks after birth due to β-cell-specific damage in response to overexpression of calmodulin transgene regulated by the insulin promoter. Zheng et al. has reported progressively increasing albuminuria which is 305 μg/24 h by 2 months and 15,000 μg/24 h by 9 months of age [64]. They also detect hypoalbuminemia, increased GFR from 2-3 months, and the

following decreased GFR from 5–9 months, as well as hypertension which coincided with increasing albuminuria. The OVE26 mice develop morphological changes of advanced DN including enlarged glomeruli, enlarging mesangium with diffuse and nodular expansion of mesangial matrix, GBM thickening, diffuse and nodular glomerulosclerosis, nodules similar to typical K-W nodules, expansion of the tubules, atrophy of tubular cells, interstitial infiltration of mononuclear cells, and tubulointerstitial fibrosis. A low level of pancreatic beta cell survival allows OVE26 mice to survive well over a year with no insulin treatment and maintain near normal body weight. The functional and morphological changes in OVE26 mice closely resemble human DN. Therefore, OVE26 mice provide a valuable model of advanced human DN. However, severe albuminuria in OVE26 mice highly depends on FVB background. Albuminuria, mesangial matrix expansion, and fibrosis are all significantly diminished when OVE26 mice were crossbred with C57BL6 or DBA2 mice [65]. This strain dependence makes it difficult to introduce other genetic mutations from other backgrounds into this model.

4.2. eNOS$^{-/-}$/db/db Mouse. The eNOS$^{-/-}$/*db/db* mouse is a model of type 2 diabetes generated by backcrossing of eNOS knockout mouse on the C57/B6 background with *db/db* mouse on the C57BLKS/J (BKS) background [66]. The eNOS$^{-/-}$/lepr$^{db/db}$ double-knockout mice exhibit obesity, hyperglycemia, hyperinsulinemia, hypertension, dramatic albuminuria, and decreased GFR [67, 68]. These mice develop histopathological changes of DN-like human disease such as mesangial expansion, GBM thickening, mesangiolysis, focal segmental and nodular glomerulosclerosis, nodules that resemble K-W nodules, striking fibronectin accumulation in glomeruli, arteriolar hyalinosis, minimal tubulointerstitial fibrosis, and microaneurysms. These features establish this mouse model as one of the very few to develop features of advanced DN.

5. Conclusions

With increasing incidence of DN, development of an ideal animal model becomes one of the top priorities in combating this health crisis. Murine models have significant advantages over other species in pathogenesis investigation. Impact of genetic background on several murine models of DN is evident on the susceptibility to diabetes-associated renal injury, the severity and histopathology of renal lesions. STZ-treated mice and rats are widely used as animal models of early DN due to their cost effectiveness and the absence of advanced pathological lesions. Some mutations in spontaneous murine models enhance our understanding of pathophysiological mechanisms of DN. Genetic engineering enables us to insert or delete a specific gene or a series of candidate genes, providing valuable insight into the role of pathogenetic genes and molecular mechanisms responsible for DN, as well as opening new avenues to develop novel therapeutic strategies. However, it is difficult to establish an animal model that recapitulates all the features of human DN. Few models develop morphologically advanced DN; among these, OLETF rats, OVE26 mice, BTBR *ob/ob* mice, eNOS$^{-/-}$/*db/db* mice, RAGE/iNOS mice, and megsin/RAGE/iNOS mice seem to be the most robust. Perhaps the last four models suggest to us that more robust murine models of DN can be established by superimposed genetic mutations or crossbreeding with an entirely different strain. Novel animal models that reproduce human DN have yet to be established in the future.

Acknowledgments

The authors would like to express their gratitude to all the physicians participating in this work. The authors declare no conflict of interests. This study was supported by the National Natural Science Foundation of China (81170669, 81000300, and 81200525) and Natural Science Foundation of Jilin Province (201215068).

References

[1] T. Szkudelski, "The mechanism of alloxan and streptozotocin action in B cells of the rat pancreas," *Physiological Research*, vol. 50, no. 6, pp. 537–546, 2001.

[2] S. Lenzen, "The mechanisms of alloxan- and streptozotocin-induced diabetes," *Diabetologia*, vol. 51, no. 2, pp. 216–226, 2008.

[3] K. Susztak, K. Sharma, M. Schiffer, P. McCue, E. Ciccone, and E. P. Böttinger, "Genomic strategies for diabetic nephropathy," *Journal of the American Society of Nephrology*, vol. 14, no. 3, pp. S271–S278, 2003.

[4] G. H. Tesch and T. J. Allen, "Rodent models of streptozotocin-induced diabetic nephropathy (methods in renal research)," *Nephrology*, vol. 12, no. 3, pp. 261–266, 2007.

[5] S. Itagaki, E. Nishida, M.-J. Lee, and K. Doi, "Histopathology of subacute renal lesions in mice induced by streptozotocin," *Experimental and Toxicologic Pathology*, vol. 47, no. 6, pp. 485–491, 1995.

[6] A. G. Farr, J. W. Mannschreck, and S. K. Anderson, "Expression of Ia antigens by murine kidney epithelium after exposure to streptozotocin," *American Journal of Pathology*, vol. 126, no. 3, pp. 561–568, 1987.

[7] P. Schmezer, C. Eckert, and U. M. Liegibel, "Tissue-specific induction of mutations by streptozotocin *in vivo*," *Mutation Research*, vol. 307, no. 2, pp. 495–499, 1994.

[8] M. Hall-Craggs, D. E. Brenner, R. D. Vigorito, and J. C. Sutherland, "Acute renal failure and renal tubular squamous metaplasia following treatment with streptozotocin," *Human Pathology*, vol. 13, no. 6, pp. 597–601, 1982.

[9] Y. Tay, Y. Wang, L. Kairaitis, G. K. Rangan, C. Zhang, and D. C. H. Harris, "Can murine diabetic nephropathy be separated from superimposed acute renal failure?" *Kidney International*, vol. 68, no. 1, pp. 391–398, 2005.

[10] M. D. Breyer, E. Bottinger, F. C. Brosius III et al., "Mouse models of diabetic nephropathy," *Journal of the American Society of Nephrology*, vol. 16, no. 1, pp. 27–45, 2005.

[11] A. R. Kraynak, R. D. Storer, R. D. Jensen et al., "Extent and persistence of streptozotocin-induced DNA damage and cell proliferation in rat kidney as determined by *in vivo* alkaline elution and BrdUrd labeling assays," *Toxicology and Applied Pharmacology*, vol. 135, no. 2, pp. 279–286, 1995.

[12] E. H. Leiter, "Multiple low-dose streptozotocin-induced hyperglycemia and insulitis in C57BL mice: influence of inbred background, sex, and thymus," *Proceedings of the National Academy of Sciences of the United States of America*, vol. 79, no. 2, pp. 630–634, 1982.

[13] E. H. Leiter, "Differential susceptibility of BALB/c sublines to diabetes induction by multi-dose streptozotocin treatment," *Current Topics in Microbiology and Immunology*, vol. 122, pp. 78–85, 1985.

[14] S. Sun, Y. Wang, Q. Li, Y. Tian, M. Liu, and Y. Yu, "Effects of benazepril on renal function and kidney expression of matrix metalloproteinase-2 and tissue inhibitor of metalloproteinase-2 in diabetic rats," *Chinese Medical Journal*, vol. 119, no. 10, pp. 814–821, 2006.

[15] A. A. Like, M. C. Appel, R. M. Williams, and A. A. Rossini, "Streptozotocin-induced pancreatic insulitis in mice morphologic and physiologic studies," *Laboratory Investigation*, vol. 38, no. 4, pp. 470–486, 1978.

[16] A. A. Like and A. A. Rossini, "Streptozotocin induced pancreatic insulitis: new model of diabetes mellitus," *Science*, vol. 193, no. 4251, pp. 415–417, 1976.

[17] A. A. Rossini, M. C. Appel, R. M. Williams, and A. A. Like, "Genetic influence of the streptozotocin-induced insulitis and hyperglycemia," *Diabetes*, vol. 26, no. 10, pp. 916–920, 1977.

[18] S. B. Gurley, S. E. Clare, K. P. Snow, A. Hu, T. W. Meyer, and T. M. Coffman, "Impact of genetic background on nephropathy in diabetic mice," *American Journal of Physiology*, vol. 290, no. 1, pp. F214–F222, 2006.

[19] W. Huang, Y. Gallois, N. Bouby et al., "Genetically increased angiotensin I-converting enzyme level and renal complications in the diabetic mouse," *Proceedings of the National Academy of Sciences of the United States of America*, vol. 98, no. 23, pp. 13330–13334, 2001.

[20] K. Susztak, E. Böttinger, A. Novetsky et al., "Molecular profiling of diabetic mouse kidney reveals novel genes linked to glomerular disease," *Diabetes*, vol. 53, no. 3, pp. 784–794, 2004.

[21] R. S. Surwit, M. N. Feinglos, J. Rodin et al., "Differential effects of fat and sucrose on the development of obesity and diabetes in C57BL/6J and A/J mice," *Metabolism*, vol. 44, no. 5, pp. 645–651, 1995.

[22] R. S. Surwit, C. M. Kuhn, C. Cochrane, J. A. McCubbin, and M. N. Feinglos, "Diet-induced type II diabetes in C57BL/6J mice," *Diabetes*, vol. 37, no. 9, pp. 1163–1167, 1988.

[23] A. E. Petro, J. Cotter, D. A. Cooper, J. C. Peters, S. J. Surwit, and R. S. Surwit, "Fat, carbohydrate, and calories in the development of diabetes and obesity in the C57BL/6J mouse," *Metabolism*, vol. 53, no. 4, pp. 454–457, 2004.

[24] S. A. Schreyer, D. L. Wilson, and R. C. Leboeuf, "C57BL/6 mice fed high fat diets as models for diabetes-accelerated atherosclerosis," *Atherosclerosis*, vol. 136, no. 1, pp. 17–24, 1998.

[25] D. A. Towler, M. Bidder, T. Latifi, T. Coleman, and C. F. Semenkovich, "Diet-induced diabetes activates an osteogenic gene regulatory program in the aortas of low density lipoprotein receptor-deficient mice," *Journal of Biological Chemistry*, vol. 273, no. 46, pp. 30427–30434, 1998.

[26] J. Mu, J. K. Naggert, K. L. Svenson et al., "Quantitative trait loci analysis for the differences in susceptibility to atherosclerosis and diabetes between inbred mouse strains C57BL/6J and C57BLKS/J," *Journal of Lipid Research*, vol. 40, no. 7, pp. 1328–1335, 1999.

[27] M. Sugano, H. Yamato, T. Hayashi et al., "High-fat diet in low-dose-streptozotocin-treated heminephrectomized rats induces all features of human type 2 diabetic nephropathy: a new rat model of diabetic nephropathy," *Nutrition, Metabolism and Cardiovascular Diseases*, vol. 16, no. 7, pp. 477–484, 2006.

[28] S. Makino, K. Kunimoto, Y. Muraoka, Y. Mizushima, K. Katagiri, and Y. Tochino, "Breeding of a non-obese, diabetic strain of mice," *Jikken Dobutsu*, vol. 29, no. 1, pp. 1–13, 1980.

[29] C. E. Mathews, "Utility of murine models for the study of spontaneous autoimmune type 1 diabetes," *Pediatric Diabetes*, vol. 6, no. 3, pp. 165–177, 2005.

[30] L. S. Wicker, G. Chamberlain, K. Hunter et al., "Fine mapping, gene content, comparative sequencing, and expression analyses support Ctla4 and Nramp1 as candidates for Idd5.1 and Idd5.2 in the nonobese diabetic mouse," *Journal of Immunology*, vol. 173, no. 1, pp. 164–173, 2004.

[31] J. P. Driver, D. V. Serreze, and Y. Chen, "Mouse models for the study of autoimmune type 1 diabetes: a NOD to similarities and differences to human disease," *Seminars in Immunopathology*, vol. 33, no. 1, pp. 67–87, 2011.

[32] T. Doi, L. Y. C. Agodoa, T. Sato et al., "Glomerular lesions in nonobese diabetic mouse: before and after the onset of hyperglycemia," *Laboratory Investigation*, vol. 63, no. 2, pp. 204–212, 1990.

[33] C. E. Alpers and K. L. Hudkins, "Mouse models of diabetic nephropathy," *Current Opinion in Nephrology and Hypertension*, vol. 20, no. 3, pp. 278–284, 2011.

[34] M. P. Cohen, G. T. Lautenslager, and C. W. Shearman, "Increased urinary type IV collagen marks the development of glomerular pathology in diabetic d/db mice," *Metabolism*, vol. 50, no. 12, pp. 1435–1440, 2001.

[35] K. Arakawa, T. Ishihara, A. Oku et al., "Improved diabetic syndrome in C57BL/KsJ-db/db mice by oral administration of the Na^+-glucose cotransporter inhibitor T-1095," *British Journal of Pharmacology*, vol. 132, no. 2, pp. 578–586, 2001.

[36] R. Mishra, S. N. Emancipator, C. Miller, T. Kern, and M. S. Simonson, "Adipose differentiation-related protein and regulators of lipid homeostasis identified by gene expression profiling in the murine db/db diabetic kidney," *American Journal of Physiology*, vol. 286, no. 5, pp. F913–F921, 2004.

[37] D. Koya, M. Haneda, H. Nakagawa et al., "Amelioration of accelerated diabetic mesangial expansion by treatment with a PKC β inhibitor in diabetic db/db mice, a rodent model for type 2 diabetes," *FASEB Journal*, vol. 14, no. 3, pp. 439–447, 2000.

[38] D. H. Moralejo, T. Ogino, M. Zhu et al., "A major quantitative trait locus co-localizing with cholecystokinin type A receptor gene influences poor pancreatic proliferation in a spontaneously diabetogenic rat," *Mammalian Genome*, vol. 9, no. 10, pp. 794–798, 1998.

[39] R. Choi, B. H. Kim, J. Naowaboot et al., "Effects of ferulic acid on diabetic nephropathy in a rat model of type 2 diabetes," *Experimental and Molecular Medicine*, vol. 43, no. 12, pp. 676–683, 2011.

[40] P. Li, H. Zhang, F. J. Burczynski et al., "Attenuation of diabetic nephropathy in Otsuka long-evans Tokushima fatty (OLETF) rats with a combination of Chinese herbs (tangshen formula)," *Evidence-Based Complementary and Alternative Medicine*, vol. 2011, Article ID 613737, 8 pages, 2011.

[41] A. O. Phillips, K. Baboolal, S. Riley et al., "Association of prolonged hyperglycemia with glomerular hypertrophy and renal basement membrane thickening in the Goto Kakizaki model of non-insulin-dependent diabetes mellitus," *American Journal of Kidney Diseases*, vol. 37, no. 2, pp. 400–410, 2001.

[42] S. G. Riley, R. A. Evans, M. Davies, J. Floege, and A. O. Phillips, "Goto-Kakizaki rat is protected from proteinuria after induction of anti-Thy1 nephritis," *American Journal of Kidney Diseases*, vol. 39, no. 5, pp. 985–1000, 2002.

[43] S. G. Riley, R. Steadman, J. D. Williams, J. Floege, and A. O. Phillips, "Augmentation of kidney injury by basic fibroblast growth factor or platelet-derived growth factor does not induce progressive diabetic nephropathy in the Goto Kakizaki model of non-insulin-dependent diabetes," *Journal of Laboratory and Clinical Medicine*, vol. 134, no. 3, pp. 304–312, 1999.

[44] N. Sato, K. Komatsu, and H. Kurumatani, "Late onset of diabetic nephropathy in spontaneously diabetic GK rats," *American Journal of Nephrology*, vol. 23, no. 5, pp. 334–342, 2003.

[45] Y. Yamamoto, I. Kato, T. Doi et al., "Development and prevention of advanced diabetic nephropathy in RAGE-overexpressing mice," *Journal of Clinical Investigation*, vol. 108, no. 2, pp. 261–268, 2001.

[46] S. C. Chua Jr., W. K. Chung, X. S. Wu-Peng et al., "Phenotypes of mouse diabetes and rat fatty due to mutations in the OB (leptin) receptor," *Science*, vol. 271, no. 5251, pp. 994–996, 1996.

[47] S. M. Clee, S. T. Nadler, and A. D. Attie, "Genetic and genomic studies of the BTBR ob/ob mouse model of type 2 diabetes," *American Journal of Therapeutics*, vol. 12, no. 6, pp. 491–498, 2005.

[48] K. L. Hudkins, W. Pichaiwong, T. Wietecha et al., "BTBR Ob/Ob mutant mice model progressive diabetic nephropathy," *Journal of the American Society of Nephrology*, vol. 21, no. 9, pp. 1533–1542, 2010.

[49] K. A. Melez, L. C. Harrison, J. N. Gilliam, and A. D. Steinberg, "Diabetes is associated with autoimmunity in the New Zealand Obese (NZO) mouse," *Diabetes*, vol. 29, no. 10, pp. 835–840, 1980.

[50] D. Lu, D. Willard, I. R. Patel et al., "Agouti protein is an antagonist of the melanocyte-stimulating-hormone receptor," *Nature*, vol. 371, no. 6500, pp. 799–802, 1994.

[51] M. M. Ollmann, B. D. Wilson, Y. Yang et al., "Antagonism of Central Melanocortin receptors *in vitro* and *in vivo* by agouti-related protein," *Science*, vol. 278, no. 5335, pp. 135–138, 1997.

[52] M. Okazaki, Y. Saito, Y. Udaka et al., "Diabetic nephropathy in KK and KK-Ay mice," *Experimental Animals*, vol. 51, no. 2, pp. 191–196, 2002.

[53] H. Ninomiya, T. Inomata, and K. Ogihara, "Obstructive uropathy and hydronephrosis in male KK-Ay mice: a report of cases," *Journal of Veterinary Medical Science*, vol. 61, no. 1, pp. 53–57, 1999.

[54] M. S. Phillips, Q. Liu, H. A. Hammond et al., "Leptin receptor missense mutation in the fatty Zucker rat," *Nature Genetics*, vol. 13, no. 1, pp. 18–19, 1996.

[55] Y. Li, Y. Qi, M. S. Kim et al., "Increased renal collagen cross-linking and lipid accumulation in nephropathy of Zucker diabetic fatty rats," *Diabetes/Metabolism Research and Reviews*, vol. 24, no. 6, pp. 498–506, 2008.

[56] S. Hoshi, Y. Shu, F. Yoshida et al., "Podocyte injury promotes progressive nephropathy in zucker diabetic fatty rats," *Laboratory Investigation*, vol. 82, no. 1, pp. 25–35, 2002.

[57] T. M. Coimbra, U. Janssen, H. J. Gröne et al., "Early events leading to renal injury in obese Zucker (fatty) rats with type II diabetes," *Kidney International*, vol. 57, no. 1, pp. 167–182, 2000.

[58] Y. Izuhara, T. Sada, H. Yanagisawa et al., "A novel sartan derivative with very low angiotensin II type 1 receptor affinity protects the kidney in type 2 diabetic rats," *Arteriosclerosis, Thrombosis, and Vascular Biology*, vol. 28, no. 10, pp. 1767–1773, 2008.

[59] A. B. Magil and J. J. Frohlich, "Monocytes and macrophages in focal glomerulosclerosis in Zucker rats," *Nephron*, vol. 59, no. 1, pp. 131–138, 1991.

[60] A. B. Magil, "Tubulointerstitial lesions in young zucker rats," *American Journal of Kidney Diseases*, vol. 25, no. 3, pp. 478–485, 1995.

[61] D. Chen and M. Wang, "Development and application of rodent models for type 2 diabetes," *Diabetes, Obesity and Metabolism*, vol. 7, no. 4, pp. 307–317, 2005.

[62] J. L. Figarola, S. Loera, Y. Weng, N. Shanmugam, R. Natarajan, and S. Rahbar, "LR-90 prevents dyslipidaemia and diabetic nephropathy in the Zucker diabetic fatty rat," *Diabetologia*, vol. 51, no. 5, pp. 882–891, 2008.

[63] W. P. Cui, B. Li, Y. Bai et al., "Potential role for Nrf2 activation in the therapeutic effect of MG132 on diabetic nephropathy in OVE26 diabetic mice," *American Journal of Physiology*, vol. 304, no. 1, pp. E87–E99, 2013.

[64] S. Zheng, W. T. Noonan, N. S. Metreveli et al., "Development of late-stage diabetic nephropathy in OVE26 diabetic mice," *Diabetes*, vol. 53, no. 12, pp. 3248–3257, 2004.

[65] J. Xu, Y. Huang, F. Li, S. Zheng, and P. N. Epstein, "FVB mouse genotype confers susceptibility to OVE26 diabetic albuminuria," *American Journal of Physiology*, vol. 299, no. 3, pp. 487–494, 2010.

[66] H. J. Zhao, S. Wang, H. Cheng et al., "Endothelial nitric oxide synthase deficiency produces accelerated nephropathy in diabetic mice," *Journal of the American Society of Nephrology*, vol. 17, no. 10, pp. 2664–2669, 2006.

[67] S. Mohan, R. L. Reddick, N. Musi et al., "Diabetic eNOS knockout mice develop distinct macro- and microvascular complications," *Laboratory Investigation*, vol. 88, no. 5, pp. 515–528, 2008.

[68] F. C. Brosius III, C. E. Alpers, E. P. Bottinger et al., "Mouse models of diabetic nephropathy," *Journal of the American Society of Nephrology*, vol. 20, no. 12, pp. 2503–2512, 2009.

[69] R. Inagi, Y. Yamamoto, M. Nangaku et al., "A severe diabetic nephropathy model with early development of nodule-like lesions induced by megsin overexpression in RAGE/iNOS transgenic mice," *Diabetes*, vol. 55, no. 2, pp. 356–366, 2006.

[70] M. Maeda, A. Yabuki, S. Suzuki, M. Matsumoto, K. Taniguchi, and H. Nishinakagawa, "Renal lesions in spontaneous insulin-dependent diabetes mellitus in the nonobese diabetic mouse: acute phase of diabetes," *Veterinary Pathology*, vol. 40, no. 2, pp. 187–195, 2003.

[71] C.-J. He, F. Zheng, A. Stitt, L. Striker, M. Hattori, and H. Vlassara, "Differential expression of renal AGE-receptor genes in NOD mice: possible role in nonobese diabetic renal disease," *Kidney International*, vol. 58, no. 5, pp. 1931–1940, 2000.

[72] O. G. Pankewycz, J. Guan, W. K. Bolton, A. Gomez, and J. F. Benedict, "Renal TGF-β regulation in spontaneously diabetic NOD mice with correlations in mesangial cells," *Kidney International*, vol. 46, no. 3, pp. 748–758, 1994.

[73] K. Sharma and F. N. Ziyadeh, "Renal hypertrophy is associated with upregulation of TGF-β1 gene expression in diabetic BB rat and NOD mouse," *American Journal of Physiology*, vol. 267, no. 6, part 2, pp. F1094–F1101, 1994.

[74] F. Y. Chow, D. J. Nikolic-Paterson, E. Ozols, R. C. Atkins, and G. H. Tesch, "Intercellular adhesion molecule-1 deficiency is protective against nephropathy in type 2 diabetic db/db mice,"

Journal of the American Society of Nephrology, vol. 16, no. 6, pp. 1711–1722, 2005.

[75] F. R. DeRubertis, P. A. Craven, M. F. Melhem, and E. M. Salah, "Attenuation of renal injury in db/db mice overexpressing superoxide dismutase: evidence for reduced superoxide-nitric oxide interaction," *Diabetes*, vol. 53, no. 3, pp. 762–768, 2004.

[76] K. Shima, K. Shi, T. Sano, T. Iwami, A. Mizuno, and Y. Noma, "Is exercise training effective in preventing diabetes mellitus in the Otsuka-Long-Evans-Tokushima Fatty rat, a model of spontaneous non-insulin-dependent diabetes mellitus?" *Metabolism*, vol. 42, no. 8, pp. 971–977, 1993.

[77] N. Okauchi, A. Mizuno, S. Yoshimoto, M. Zhu, T. Sano, and K. Shima, "Is caloric restriction effective in preventing diabetes mellitus in the Otsuka Long Evans Tokushima Fatty Rat, a model of spontaneous non-insulin-dependent diabetes mellitus?" *Diabetes Research and Clinical Practice*, vol. 27, no. 2, pp. 97–106, 1995.

[78] U. Janssen, A. Vassiliadou, S. G. Riley, A. O. Phillips, and J. Floege, "The quest for a model of type II diabetes with nephropathy: the Goto Kakizaki rat," *Journal of Nephrology*, vol. 17, no. 6, pp. 769–773, 2004.

[79] F. Miralles and B. Portha, "Early development of beta-cells is impaired in the GK rat model of type 2 diabetes," *Diabetes*, vol. 50, pp. S84–88, 2001.

[80] M. T. Velasquez, P. L. Kimmel, and O. E. Michaelis IV, "Animal models of spontaneous diabetic kidney disease," *FASEB Journal*, vol. 4, no. 11, pp. 2850–2859, 1990.

[81] F. Bielschowsky and M. Bielschowsky, "The New Zealand strain of obese mice; their response to stilboestrol and to insulin," *Australian Journal of Experimental Biology & Medical Science*, vol. 34, no. 3, pp. 181–198, 1956.

[82] E. H. Leiter and P. C. Reifsnyder, "Differential levels of diabetogenic stress in two new mouse models of obesity and type 2 diabetes," *Diabetes*, vol. 53, no. 1, pp. S4–S11, 2004.

[83] P. C. Reifsnyder and E. H. Leiter, "Deconstructing and reconstructing obesity-induced diabetes (diabesity) in mice," *Diabetes*, vol. 51, no. 3, pp. 825–832, 2002.

[84] J. P. Corsetti, J. D. Sparks, R. G. Peterson, R. L. Smith, and C. E. Sparks, "Effect of dietary fat on the development of non-insulin dependent diabetes mellitus in obese Zucker diabetic fatty male and female rats," *Atherosclerosis*, vol. 148, no. 2, pp. 231–241, 2000.

Hindawi Publishing Corporation
Journal of Diabetes Research
Volume 2013, Article ID 761415, 7 pages
http://dx.doi.org/10.1155/2013/761415

Review Article

Porcine Models of Accelerated Coronary Atherosclerosis: Role of Diabetes Mellitus and Hypercholesterolemia

Damir Hamamdzic and Robert L. Wilensky

Cardiovascular Division, Hospital of the University of Pennsylvania and Cardiovascular Institute, University of Pennsylvania, Philadelphia, PA 19104, USA

Correspondence should be addressed to Robert L. Wilensky; robert.wilensky@uphs.upenn.edu

Received 13 January 2013; Accepted 16 May 2013

Academic Editor: Bernard Portha

Animal models of atherosclerosis have proven to be an invaluable asset in understanding the pathogenesis of the disease. However, large animal models may be needed in order to assess novel therapeutic approaches to the treatment of atherosclerosis. Porcine models of coronary and peripheral atherosclerosis offer several advantages over rodent models, including similar anatomical size to humans, as well as genetic expression and development of high-risk atherosclerotic lesions which are similar to humans. Here we review the four models of porcine atherosclerosis, including the diabetic/hypercholesterolemic model, Rapacz-familial hypercholesterolemia pig, the (PCSK9) gain-of-function mutant pig model, and the Ossabaw miniature pig model of metabolic syndrome. All four models reliably represent features of human vascular disease.

1. Introduction

Atherosclerosis is a systemic disease affecting virtually all vascular beds. Primary and secondary prevention strategies, novel pharmaceutical treatment modalities, and early intervention have reduced mortality rates of coronary artery disease. However, cardiovascular atherosclerotic diseases such as acute coronary syndromes, stroke, and aortic disease continue to be the leading cause of death in developed countries and the incidence is rapidly increasing in developing countries. Macrovascular disease is the major cause of death with patients suffering from diabetes mellitus (DM), both type I and type II, having a 2- to 6-fold greater risk of developing atherosclerosis compared to nondiabetic patients with comparable risk factors [1]. Type II diabetic patients often exhibit increased low density lipoprotein (LDL) and decreased high density lipoprotein (HDL) cholesterol levels and hypertension (i.e., the metabolic syndrome), as well as altered platelet function. Often the diagnosis of type II DM is made at the time the patient presents with coronary artery disease.

Animal models have proven invaluable in understanding the pathophysiology of atherosclerosis as well as developing and testing treatment strategies. Genetically modified murine models have led to an understanding of the mechanisms of disease and the role of signaling pathways and genetic factors which play a major role in disease initiation and development. However, mice are limited by their varying lipid profiles, lack of spontaneous coronary artery disease, and development of disease in vascular beds which are in variance with human disease [2, 3]. DM has only a small effect on development of atherosclerosis in mice [4], and their small size limits physiologic evaluation. Rabbits are limited because they do not naturally develop atherosclerosis and require a high cholesterol diet to induce atherosclerosis resulting in cholesterol levels which often exceed 1000 mg/dL, lesions which are largely foam cell rich, and, given size considerations, the need to perform vascular studies in the aortae and iliofemoral arteries rather than coronary arteries [5].

Such differences between rodents and humans have made it incumbent for additional models to be used to assess possible treatments, whether pharmacologic or device related. Porcine models of atherosclerosis have several advantages over small animal models. Pigs are closer phylogenetically to humans and present more similar anatomy, with

a comparable size of the heart and vasculature. Like humans, pigs are omnivores and the vascular response to the increase in fat content of the diet is similar. Indeed, elderly pigs can spontaneously develop atherosclerosis [6]. In this review, we will focus on four porcine models with accelerated atherosclerosis: the induced diabetic/hypercholesterolemic (DM/HC) swine model, the LDL receptor knock-out model (or Rapacz pig), the recently described PCSK9 gain-of-function mutant cloned pig, and the Ossabaw metabolic syndrome model (Table 1).

2. Diabetic/Hypercholesterolemic Pig Model

In 2001, Gerrity et al. [7] first described superimposing DM on an HC diet in male Yorkshire domestic pigs. DM was induced by the intravenous injection of the pancreatic β-cell cytotoxin streptozotocin (STZ) which reduces the number of insulin producing β-cells, on average, by 90% at 2 weeks. Given the subsequent risk of hyperglycemic coma persistently elevated glucose levels, >350 mg/dL, are treated with administration of insulin [8]. An advantage of the model is that animals with persistently increased glucose levels grow at slower rates than normoglycemic animals. However, pigs with DM only do not develop atherosclerosis [7, 9, 10] and so in order to produce lesions DM pigs require a high fat/high cholesterol diet containing 5%–10% lard and 0.5%–1.0% cholesterol. The combination of DM and HC results in more severe lesions which are complex and humanoid in morphology [7–9].

Development of atherosclerosis in DM/HC pigs is variable in presence, severity, morphology, and vascular location of the lesions. Lesions develop in all animals in the distal, infrarenal abdominal aorta while less severe lesions are observed in thoracic aortae. Coronary arteries demonstrate variable lesion development with some animals developing severe lesions, occasionally resulting in sudden cardiac death; some animals develop single severe lesion while others develop nonhemodynamically significant lesions or no lesion at all. The most advanced lesions are observed in the proximal segment of the coronary arteries. Only a minority of carotid arteries develop lesions. Early lesions in the affected vascular beds are observed 3 months after induction [7, 11] and are characterized as either intimal thickening or xanthomas consisting of lipid deposits, foam cells, and inflammation (mainly the early recruitment of macrophages). By 3 months 61% of coronary arteries, 20% of carotids, and 89% of thoracic aortae demonstrate a lesion increasing to 96%, 31%, and 100% at 6 months, respectively. By 6 months atherosclerotic lesions in coronary arteries and abdominal aorta of DM/HC pigs progress into complex human-like atherosclerotic plaques characterized by lipid pools and lipid-rich necrotic cores, thinning of the fibrous cap, increased macrophage infiltration, calcification, and destruction of the media (Figure 1). By 9 months high-grade complex lesions consisting of smooth muscle cells, extracellular matrix, increased calcifications and necrotic cores are observed. Abdominal aortic lesions demonstrate large necrotic cores and Monckeberg's sclerosis. At 9 months all coronary arteries, one-third of carotids, and all thoracic aortae have lesion development [11]. Advanced lesions such as fibroatheromas are observed in 6% of coronary arteries at 3 months, 17% at 6 months, and 39% at 9 months and fibrocalcific plaques are noted in 0%, 2%, and 22% of lesions at the 3 time points [11]. Morphologically advanced coronary artery lesions mimic human diabetic lesions [12, 13].

Akt is a central signaling node important for inflammation and involved in vascular cell growth, proliferation, differentiation, apoptosis, and angiogenesis. Reduced Akt activation results in loss of vascular protection contributing to increased vascular inflammation and disease progression. A possible mechanism by which the combination of DM and HC produces complex lesions is through aberrant, reduced p-Akt activity. Hamamdzic et al. [10] showed that compared to control, DM only, and HC only coronary arteries, DM/HC coronary arteries demonstrate greater attenuated Akt activity resulting in decreased phosphorylation of glycogen synthetase kinase-3β (GSK-3β). This in turn was associated with increased cellular proliferation and apoptosis as well as activation of nuclear factor-kappa B (NF-κB) resulting in increased complexity of the atherosclerotic lesions. Aberrant Akt signaling also correlated with increase vasa vasorum neovasculogenesis.

Evaluation of 59 genes obtained from DM/HC coronary, carotid, and thoracic aortic arteries, 1, 3, and 6 months after DM/HC induction, showed that genes involved in cholesterol metabolism and insulin pathways were most markedly upregulated in coronary arteries; more so than in thoracic aortae and carotid arteries. At 1 month increased gene expression of insulin related pathways, such as adiponectin, leptin, PPARγ, and preproadipsin, was noted in coronary arteries [11] and early increased expression of inflammatory genes was observed only in coronary arteries [11], while at 6 months increased expression of multiple genes, including those associated with monocyte chemotaxis, progression of macrophages to foam cells, cell growth, and maintenance was observed in coronary arteries. Genes implicated in plaque instability were upregulated only in the coronary arteries at the 6-month time point.

Using intravascular ultrasound (IVUS) imaging of coronary arteries in DM/HC pigs, Koskinas et al. [14] demonstrated that low endothelial sheer stress (ESS) was an independent predictor of the development and progression of atherosclerosis and importantly with the development of high-risk coronary lesions. Furthermore, plaques with excessive remodeling in the areas of very low ESS were associated with additional plaque growth resulting in development of high-risk atherosclerotic lesions with increased expression of collagenases in the fibrous cap [14, 15]. Similar results demonstrating the relationship between low shear stress and plaque progression have been obtained in patients following an acute coronary syndrome thereby indicating the relevance of the DM/HC model for investigating lesion development [16].

Using Near Infrared Spectroscopy (NIRS) and IVUS imaging, obtained at 3, 6, and 9 months after DM/HC induction, Patel et al. [17] demonstrated that the combination of NIRS and IVUS could detect the presence of a fibroatheroma and importantly predict the future development of fibroatheromas. The early and persistent accumulation

Table 1: Relative advantages and disadvantages of the 4 atherosclerotic porcine models.

Model	Advantages	Limitations
Diabetes/ hypercholesterolemic	Well characterized. Reproducible human-like atherosclerosis. Results obtained from diagnostic and pharmacologic treatment studies corroborate data obtained in humans. Complex lesions detectable as early as 6 months after induction.	Type I diabetic model. Variable development of atherosclerosis.
Rapacz familial hypercholesterolemic	Well characterized Models a known human disease state.	Long induction period for atherosclerosis. Large size of animals (although genetic modified mini-pig has been developed). Expensive.
PCSK9 gain of function	Small size. Models a known human disease state. Reproducible lesions.	Limited commercial availability. Relatively long-term induction period (12 months).
Ossabaw	Only model of metabolic syndrome induced atherosclerosis. Small size. Relatively short induction period after a high fat diet regimen.	Limited commercial availability.

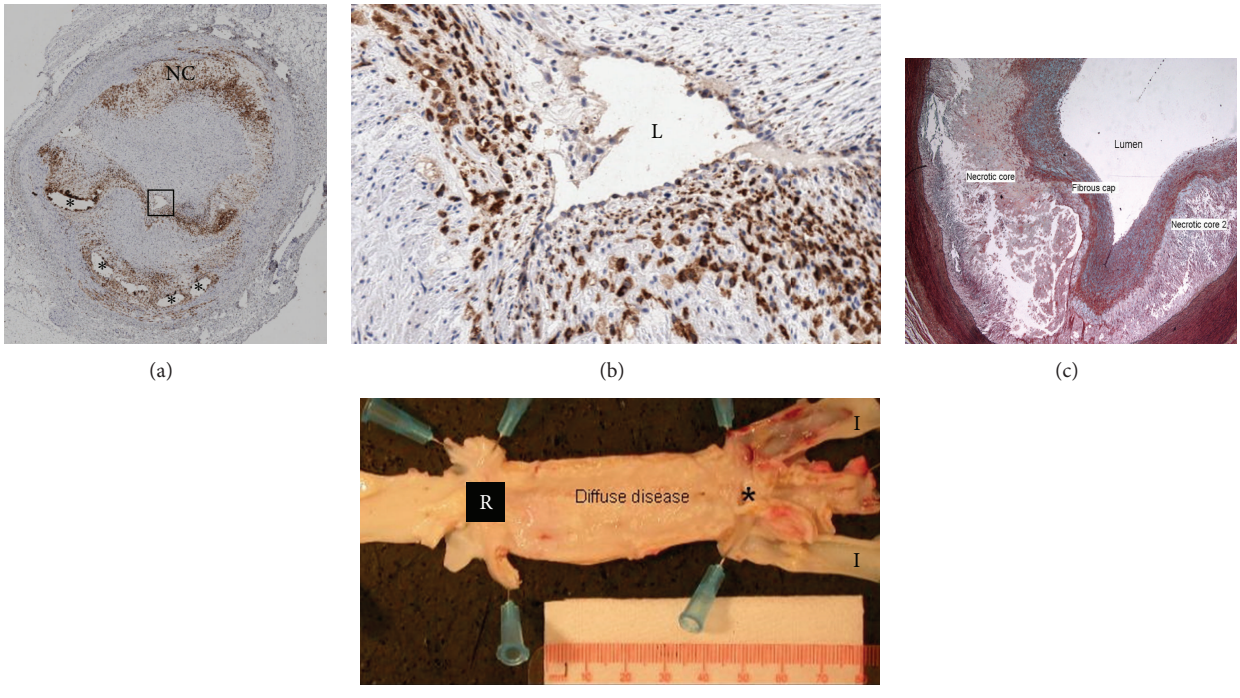

(a) (b) (c)

(d)

Figure 1: Examples of atherosclerotic lesions from DM/HC pigs. (a) Low power magnification of a coronary artery with a severe atherosclerotic lesion, obtained 6 months after DM/HC induction. Artery stained with Cathepsin S (brown cells) to denote the presence of inflammatory cells showing protease activity. Lumen is within the outlined box, *—calcification and NC-necrotic core. (b) High power view of outlined area in (a) with L denoting the arterial lumen. Cathepsin positive areas near the lumen indicate a thinned fibrous cap with increased inflammation. (c) Movat's staining of a high-risk coronary fibroatheroma showing two large necrotic cores covered by a fibrous cap. (d) Longitudinal view of the abdominal aorta demonstrating severe, diffuse atherosclerosis between the renal arteries (R) and the distal bifurcation (*) into the iliac arteries (I). The ostia of the iliac arteries are generally severely diseased in this model.

of lipid within the arterial wall of coronary arteries led to the subsequent development of fibroatheromas, often demonstrating increased inflammation in the plaque and within the fibrous cap as well as thinned fibrous caps; markers of high-risk lesions.

The vascular effects of both drug-eluting and bare-metal stenting in DM/HC porcine coronary arteries were examined and compared to implantation in nonatherosclerotic porcine arteries [18]. Increased neointimal accumulation and vascular inflammation following both bare metal and paclitaxel eluting stent implantation were observed in DM/HC swine, and use of the DM/HC model allowed for greater discrimination of the vascular effects of bare metal and drug eluting stents compared to nonatherosclerotic porcine model. DM/HC pigs also demonstrated increased platelet aggregation mimicking the findings in diabetic patients. In addition, the findings of increased vascular inflammation and delayed reendothelization in DM/HC porcine arteries as well as increased platelet reactivity lent insight into the possible mechanisms of subacute and late stent thrombosis, a potentially deadly untoward effect of drug eluting stent implantation.

Since vascular inflammation plays an important role in development of atherosclerosis and specifically high-risk lesions in human and DM/HC porcine coronary arteries, it was hypothesized that selective inhibition of lipoprotein associated phospholipase A_2 (Lp-PLA_2) could reduce lesion development in this model [8]. Darapladib, a selective inhibitor of Lp-PLA_2, inhibited plasma and vascular Lp-PLA_2 activity thereby reducing levels of lysophosphatidylcholine and oxidized nonesterified fatty acids, inflammatory mediators which are released by the action of Lp-PLA_2 on intramural oxidized fatty acids. Analysis of coronary gene expression showed that darapladib exhibited a general anti-inflammatory action by reducing the expression of the genes associated with macrophage and T lymphocyte functioning, independent of an effect on blood cholesterol levels. Morphologically, selective Lp-PLA_2 inhibition resulted in decreased plaque and necrotic core area and medial destruction. As a consequence selective Lp-PLA_2 inhibition resulted in fewer lesions with an unstable phenotype. This study corroborated the results of the IBIS 2 study [19] in which the treatment reduced necrotic core area in human coronary artery lesions, as determined by VH-intravascular ultrasound over a year in patients with coronary artery disease and led to two large multicenter, international Phase III clinical trials examining the use of darapladib to prevent primary and secondary cardiovascular events.

3. LDLR−/− Pig Model of Familial Hypercholesterolemia

An unique strain of pigs exhibiting elevated LDL levels and spontaneous atherosclerosis, due to a mutation in genes coding for apolipoproteins and LDL receptor, akin to familial hypercholesterolemia, has been described and has become known a Rapacz-FH pigs [20, 21]. When fed low fat/low cholesterol diet, total blood cholesterol values in these animals ranged from 234 to 464 mg/dL, compared to 96 to 113 mg/dL in the control pigs [22]. Blood levels of triglycerides were 48 ± 10.8 mg/dL in FH animals, compared to 29 ± 5.7 mg/dL in control group, while apoB levels in FH group were 152 ± 32.5 mg/dL, compared to 48 ± 5.7 mg/dL in control group.

Figure 2: Photomicrograph of a lesion from an eccentric 13-month-old Rapacz-FH minipig coronary artery. Arrow denotes a thin fibrous cap covering a foam cell rich area with necrotic cores (empty areas within the lesion). The pig was fed a mixed high/fat, low/fat diet. Photomicrograph kindly provided by Dr. Erling Falk.

Immature atherosclerotic lesions were identified at 12 months of age and were characterized by the presence of macrophage derived foam cells and smooth muscle cell proliferation in the coronary arteries, iliofemoral arteries, and aorta. By 18 months of age 60% of animals exhibited atheromas. Lesions were most prominent in the coronary arteries (Figure 2), but peripheral lesions were also observed in thoracic aortae and at the aortoiliac bifurcation. By 24 months, fully developed atherosclerotic lesions were seen in coronary arteries, characterized by necrotic cores with thinned fibrous caps, cholesterol deposits, calcification and neovascularization. By 39–54 months advanced lesions were present in the coronary, iliac, and femoral arteries, characterized by extensive calcification, necrotic cores, fibrous caps, and inflammatory cells. Neovascularization and intraplaque hemorrhage were also present indicating a high risk of subsequent plaque rupture [20]. The pathogenesis of atherosclerosis in this model mimics the progression of human disease and is potentially very useful for testing novel treatment and imaging modalities. However, major limitations are the slow progression of the disease (12–36 months) and the size of the animals, often exceeding 200 kg. More rapid lesion development results from administration of a high cholesterol diet and balloon induced focal coronary injury [23].

Rapacz FH pigs develop peripheral arterial atherosclerosis in femoral but rarely in brachial arteries. Bahls et al. [24] investigated gene expression profiling to investigate the differences between these two vascular beds in young, disease-free pigs to determine how the expression of pro-atherogenic genes contributes to the heterogeneous distribution of atherosclerosis development. These investigators showed that the differences in gene expression between

healthy brachial (atheroprotected) and femoral (atherosusceptible) arteries exist prior to the onset of atherosclerotic disease. The gene expression profiles between the two arteries were not similar in that only 430 of 15,552 exhibited genes significantly demonstrated different levels of expression. Ribosomal structural genes essential for the formation of the large 60S ribosomal subunit which controls protein production and the small 40S ribosomal subunit which programs protein synthesis, binds mRNA, and mediates the interactions between mRNA codons and transfer RNA anticodons were differentially expressed. Even though distinct functions during translation of these proteins have been described, the possible consequence of an overexpression of either the large or the small ribosomal subunits remains unclear.

Rapacz FH swine have been used to investigate whether angioplasty with the zotarolimus coated balloon (ZCB) would inhibit neointimal hyperplasia in balloon injured superficial femoral arteries [25]. Zotarolimus, a molecular target of rapamycin (m-TOR) inhibitor, has been shown to inhibit cell-cycle progression and is used clinically, from a stent platform, to reduce restenosis. Pharmacokinetic studies after balloon denudation in superficial femoral artery segments, followed by balloon angioplasty, revealed that zotarolimus was detected in arterial tissue up to 28 days after ZCB inflation and was associated with a reduction in neointimal formation compared with controls. There was no evidence of delayed arterial healing or vascular toxicity in ZCB animals.

Given the unwieldy size and weight of full grown Rapacz pigs, a smaller, more manageable FH pig has been developed by crossing the Rapacz farm pigs with smaller Chinese Meishan pigs and then crossing the offspring with a smaller minipig [26]. Atherosclerosis in these animals was induced by high fat/high cholesterol diet and accelerated by coronary artery balloon injury. Following cholesterol feeding (resulting in a 4-fold increase in total cholesterol levels) 22 high-risk atherosclerotic lesions containing a large necrotic core and thin fibrous cap were observed in 18 arteries which developed either spontaneously and following balloon injury. Of interest, there was a high incidence of intraplaque hemorrhage and neovascularization as well as expansive remodeling in the lesions, signs of rapidly progressing, unstable lesions. The lesions are similar morphologically to the DM/HC coronary lesions despite the absence of DM.

4. (PCSK9) Gain-of-Function Mutant Pig

Recently, a new Yucatan minipig model of familial hypercholesterolemia was created by DNA transposition of human D374Y-proprotein convertase subtilisin/kexin type 9 (PCSK9) gain-of-function mutant [27]. The D374Y-PSSK9 gain-of-function mutation in the proprotein convertase subtilisin/kexin type 9 (PCSK9) gene causes severe autosomal dominant hypercholesterolemia and early development of atherosclerosis in humans. Clinical studies have shown that the subcutaneous administration of a monoclonal antibody to PCSK9 reduced LDL levels in a dose-dependent manner in up to 61% in patients with familial or nonfamilial hypercholesterolemia [28].

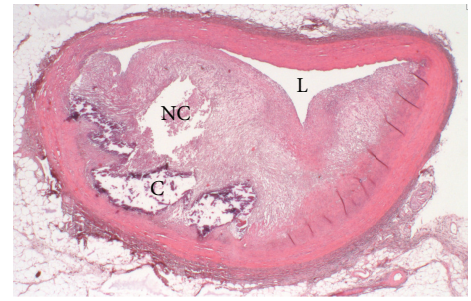

Figure 3: Photomicrograph of a high-grade coronary atherosclerotic lesion obtained from a 13-month PCSK9 gain-of-function mutant pig fed a high cholesterol diet. C: calcifications; L: lumen; NC: necrotic core; Photomicrograph kindly provided by Dr. Erling Falk.

Al-Mashhadi et al. [27] showed that Yucatan minipigs expressing human, liver specific D374Y-PCSK9 exhibited reduced LDL receptor levels, resulting in impaired LDL clearance and increased plasma LDL levels. The administration of a high fat/high cholesterol diet for 46 weeks led to greatly increased cholesterol (approximately 772 mg/dL or 20 mM) and LDL (425 mg·dL or 11 mM) levels. At approximately 1 year of age complex progressive human-like atherosclerotic lesions in the aortae and iliofemoral and left anterior descending coronary arteries were observed. Mean aortic surface area covered by atherosclerosis increased by 2.1-fold in transgenic pigs compared with wild type. In the abdominal aorta lesions characterized as intimal thickening or fibroatheromas were present in all transgenic males, while only 28% of control wild-type (w/t) animals exhibited similar type lesions. In the iliofemoral arteries there was a 7.6-median-fold increase in atherosclerosis, while the left anterior descending coronary arteries demonstrated a 1.8-fold increase compared to wild-type males. All left anterior descending coronary arteries demonstrated at least one advanced lesion compared to only 28% in the wild-type pigs. An example of the lesions is noted in Figure 3. [18^F] Fluorodeoxyglucose (FDG) Positron emission tomography (PET) detected inflammatory activity in the aorta. As such, the (PCSK9) gain-of-function mutant pig is a potentially important large-animal translational research model.

5. Metabolic Disease Pig Model (Ossabaw Pig)

The DM/HC porcine model is a type I diabetic model while the majority of DM patients with diabetes suffer from type II diabetes and metabolic syndrome (MetSyn). The lack of a viable and reproducible, human-like animal model of MetSyn with type II DM has hampered the advances in this area of research. However, the Ossabaw strain of pigs offers promise in lending itself to advancing the understanding of the pathophysiology of MetSyn as well as the testing of novel treatment strategies.

In the early 16th century Spanish explorers left a small herd of pigs on Ossabaw Island located off the coast of Georgia (USA). As a result of their geographic isolation

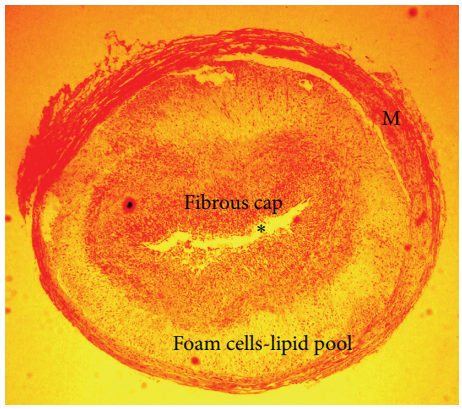

Figure 4: Photomicrograph of a coronary lesion obtained from an Ossabaw pig on a high fat diet. Lumen denoted by *, and M indicates medial layer. Kindly provided by Drs. Michael Sturek and Mouhamad Alloosh, Department of Cellular and Integrative Physiology, Indiana University School of Medicine.

the pigs adapted to conditions on the island, characterized by extreme seasonal tides, by evolving a smaller phenotype (insular dwarfism) while adapting to the food cycle which provided minimal amount of nutrition during the spring season. The development of a unique, thrifty genotype afforded these pigs the ability to store large amounts of fat which was used for survival during periods of famine but also increased the propensity for obesity. As a result this strain has developed low-grade, non-insulin-dependent diabetes when fed an atherogenic diet of cholesterol and fat derived from hydrogenated soybean oil and fructose. In addition to the increased risk of developing diabetes, Ossabaw swine fed this type of diet nearly double their percentage body fat in only 9 weeks showing signs of MetSyn including obesity, insulin resistance, hypertension, and dyslipidemia with an increase in the LDL/HDL cholesterol ratio and hypertriglyceridemia [29]. Female obese pigs compared with lean pigs demonstrated a 2-fold increase in insulin × glucose concentrations and an over 4-fold increase in total cholesterol (156.6 ± 13.4 mg/dL versus 479.0 ± 46.7 mg/dL) with the greatest increase in LDL levels (104.2 ± 13.2 mg/dL versus 430.8 ± 48.0 mg/dL). The mean blood pressure was increased from 92 ± 9 mmHg to 113 ± 8 mmHg [30].

Mild, early coronary atherosclerosis, characterized as intimal thickening, was also observed [28]. Neeb et al. compared the features of MetSyn, coronary artery disease, and stent induced restenosis in Ossabow pigs to a Yucatan miniature pigs, both fed either a control or high fat diet with calorie-matching for 40 weeks [31]. An example is shown in Figure 4. Ossabaw pigs with MetSyn had more extensive and diffuse native CAD, defined as wall coverageas well as a 2.5-fold greater accumulation of neointimal hyperplasia, 3 weeks following stent implantation. There was little difference in the severity of the in-stent restenotic lesions between those Ossabaw pigs on a control diet and those on a high fat diet. Of interest was that Ossabaw coronary arteries were less fibrous and more cellular, compared to Yucatan coronary arteries, indicating a potentially higher risk for the plaque instability and subsequent thrombosis. Increased platelet activity has been shown in the MetSyn Ossabaw pigs compared to lean non-MetSyn pigs [32], mimicking that observed in patients with diabetes.

6. Conclusion

Large animal models of human-like atherosclerosis are of increasing importance in preclinical studies evaluating novel treatments and imaging techniques and further elucidating the pathophysiology of cardiovascular diseases. We have described here the four viable pig models that hold promise in translating preclinical results to human treatment. The major limitations for the pig studies remain the size of the animal (relevant to housing requirements), length of the studies, and cost. While each of these models has specific uses as well as potential limitations, continuing elaboration and optimization of these models is ongoing.

References

[1] S. M. Haffner, S. Lehto, T. Rönnemaa, K. Pyörälä, and M. Laakso, "Mortality from coronary heart disease in subjects with type 2 diabetes and in nondiabetic subjects with and without prior myocardial infarction," *The New England Journal of Medicine*, vol. 339, no. 4, pp. 229–234, 1998.

[2] C. F. Howard Jr., "Diabetes mellitus: relationships of nonhuman primates and other animal models to human forms of diabetes," *Advances in veterinary science and comparative medicine*, vol. 28, pp. 115–149, 1984.

[3] J. L. Breslow, "Mouse models of atherosclerosis," *Science*, vol. 272, no. 5262, pp. 685–688, 1996.

[4] Y. Kako, L.-S. Huang, J. Yang, T. Katopodis, R. Ramakrishnan, and I. J. Goldberg, "Streptozotocin-induced diabetes in human apolipoprotein B transgenic mice: effects on lipoproteins and atherosclerosis," *Journal of Lipid Research*, vol. 40, no. 12, pp. 2185–2194, 1999.

[5] R. L. Wilensky, K. L. March, I. Gradus-Pizlo, G. Sandusky, N. Fineberg, and D. R. Hathaway, "Vascular injury, repair, and restenosis after percutaneous transluminal angioplasty in the atherosclerotic rabbit," *Circulation*, vol. 92, no. 10, pp. 2995–3005, 1995.

[6] B. H. Skold, R. Getty, and F. K. Ramsey, "Spontaneous atherosclerosis in the arterial system of aging swine," *The American Journal of Veterinary Research*, vol. 27, no. 116, pp. 257–273, 1966.

[7] R. G. Gerrity, R. Natarajan, J. L. Nadler, and T. Kimsey, "Diabetes-induced accelerated atherosclerosis in Swine," *Diabetes*, vol. 50, no. 7, pp. 1654–1665, 2001.

[8] R. L. Wilensky, Y. Shi, E. R. Mohler III et al., "Inhibition of lipoprotein-associated phospholipase A_2 reduces complex coronary atherosclerotic plaque development," *Nature Medicine*, vol. 14, no. 10, pp. 1059–1066, 2008.

[9] L. Zhang, A. Zalewski, Y. Liu et al., "Diabetes-induced oxidative stress and low-grade inflammation in porcine coronary arteries," *Circulation*, vol. 108, no. 4, pp. 472–478, 2003.

[10] D. Hamamdzic, R. S. Fenning, D. Patel et al., "Akt pathway is hypoactivated by synergistic actions of diabetes mellitus and hypercholesterolemia resulting in advanced coronary artery disease," *The American Journal of Physiology—Heart and Circulatory Physiology*, vol. 299, no. 3, pp. H699–H706, 2010.

[11] E. R. Mohler III, L. Sarov-Blat, Y. Shi et al., "Site-specific atherogenic gene expression correlates with subsequent variable lesion development in coronary and peripheral vasculature," *Arteriosclerosis, Thrombosis, and Vascular Biology*, vol. 28, no. 5, pp. 850–855, 2008.

[12] P. R. Moreno, A. M. Murcia, I. F. Palacios et al., "Coronary composition and macrophage infiltration in atherectomy specimens from patients with diabetes mellitus," *Circulation*, vol. 102, no. 18, pp. 2180–2184, 2000.

[13] A. P. Burke, F. D. Kolodgie, A. Zieske et al., "Morphologic findings of coronary atherosclerotic plaques in diabetics: a postmortem study," *Arteriosclerosis, Thrombosis, and Vascular Biology*, vol. 24, no. 7, pp. 1266–1271, 2004.

[14] K. C. Koskinas, C. L. Feldman, Y. S. Chatzizisis et al., "Natural history of experimental coronary atherosclerosis and vascular remodeling in relation to endothelial shear stress: a serial, in vivo intravascular ultrasound study," *Circulation*, vol. 121, no. 19, pp. 2092–2101, 2010.

[15] Y. S. Chatzizisis, A. B. Baker, G. K. Sukhova et al., "Augmented expression and activity of extracellular matrix-degrading enzymes in regions of low endothelial shear stress colocalize with coronary atheromata with thin fibrous caps in pigs," *Circulation*, vol. 123, no. 6, pp. 621–630, 2011.

[16] P. Stone, S. Saito, S. Takahashi et al., "Prediction of progression of coronary artery disease and clinical outcomes using vascular profiling of endothelial shear stress and arterial plaque characteristics. The PREDICTION study," *Circulation*, vol. 126, no. 2, pp. 172–181, 2012.

[17] D. Patel, D. Hamamdzic, R. Llano et al., "Subsequent development of fibroatheromas with inflamed fibrous caps can be predicted by intracoronary near-IR spectroscopy," *Arteriosclerosis, Thrombosis, and Vascular Biology*, vol. 33, no. 2, pp. 346–353, 2013.

[18] R. Llano, D. Winsor-Hines, D. B. Patel et al., "Vascular responses to drug-eluting and bare metal stents in diabetic/hypercholesterolemic and nonatherosclerotic porcine coronary arteries," *Circulation*, vol. 4, no. 5, pp. 438–446, 2011.

[19] P. W. Serruys, H. M. García-García, P. Buszman et al., "Effects of the direct lipoprotein-associated phospholipase A2 inhibitor darapladib on human coronary atherosclerotic plaque," *Circulation*, vol. 118, no. 11, pp. 1172–1182, 2008.

[20] M. F. Prescott, C. H. McBride, J. Hasler-Rapacz, J. von Linden, and J. Rapacz, "Development of complex atherosclerotic lesions in pigs with inherited hyper-LDL cholesterolemia bearing mutant alleles for apolipoprotein B," *The American Journal of Pathology*, vol. 139, no. 1, pp. 139–147, 1991.

[21] J. Hasler-Rapacz, H. Ellegren, A. K. Fridolfsson et al., "Identification of a mutation in the low density lipoprotein receptor gene associated with recessive familial hypercholesterolemia in swine," *American Journal of Medical Genetics*, vol. 76, no. 5, pp. 379–386, 1998.

[22] J. Hasler-Rapacz, M. F. Prescott, J. von Linden-Reed, J. M. Rapacz Jr., Z. Hu, and J. Rapacz, "Elevated concentrations of plasma lipids and apolipoproteins B, C-III, and E are associated with the progression of coronary artery disease in familial hypercholesterolemic swine," *Arteriosclerosis, Thrombosis, and Vascular Biology*, vol. 15, no. 5, pp. 583–592, 1995.

[23] A. Tellez, C. G. Krueger, P. Seifert et al., "Coronary bare metal stent implantation in homozygous LDL receptor deficient swine induces a neointimal formation pattern similar to humans," *Atherosclerosis*, vol. 213, no. 2, pp. 518–524, 2010.

[24] M. Bahls, C. A. Bidwell, J. Hu et al., "Gene expression differences in healthy brachial and femoral arteries of Rapacz familial hypercholesterolemic swine," *Physiological Genomics*, vol. 43, no. 12, pp. 781–788, 2011.

[25] J. F. Granada, K. Milewski, H. Zhao et al., "Vascular response to zotarolimus-coated balloons in injured superficial femoral arteries of the familial hypercholesterolemic swine," *Circulation*, vol. 4, no. 5, pp. 447–455, 2011.

[26] T. Thim, M. K. Hagensen, L. Drouet et al., "Familial hypercholesterolaemic downsized pig with human-like coronary atherosclerosis: a model for preclinical studies," *EuroIntervention*, vol. 6, no. 2, pp. 261–268, 2010.

[27] R. H. Al-Mashhadi, C. B. Sørensen, P. M. Kragh et al., "Familial hypercholesterolemia and atherosclerosis in cloned minipigs created by DNA transposition of a human PCSK9 gain-of-function mutant," *Science Translational Medicine*, vol. 5, no. 166, pp. 1–10, 2013.

[28] E. A. Stein, S. Mellis, G. D. Yancopoulos et al., "Effect of a monoclonal antibody to PCSK9 on LDL cholesterol," *The New England Journal of Medicine*, vol. 366, no. 12, pp. 1108–1118, 2012.

[29] M. Sturek, M. Alloosh, J. Wenzel, J. P. Byrd, J. M. Edwards, and P. G. Lloyd, "Ossabaw Island miniature swine: cardiometabolic syndrome assessment," in *Swine in the Laboratory: Surgery, Anesthesia, Imaging, and Experimental Techniques*, M. M. Swindle, Ed., CRC Press, Boca Raton, Fla, USA, 2007.

[30] M. C. Dyson, M. Alloosh, J. P. Vuchetich, E. A. Mokelke, and M. Sturek, "Components of metabolic syndrome and coronary artery disease in female Ossabaw swine fed excess atherogenic diet," *Comparative Medicine*, vol. 56, no. 1, pp. 35–45, 2006.

[31] Z. P. Neeb, J. M. Edwards, M. Alloosh, X. Long, E. A. Mokelke, and M. Sturek, "Metabolic syndrome and coronary artery disease in ossabaw compared with yucatan swine," *Comparative Medicine*, vol. 60, no. 4, pp. 300–315, 2010.

[32] R. P. Kreutz, M. Alloosh, K. Mansour et al., "Morbid obesity and metabolic syndrome in Ossabaw miniature swine are associated with increased platelet reactivity," *Diabetes, Metabolic Syndrome and Obesity*, vol. 4, pp. 99–105, 2011.

Hindawi Publishing Corporation
Journal of Diabetes Research
Volume 2013, Article ID 370212, 9 pages
http://dx.doi.org/10.1155/2013/370212

Research Article

Exacerbation of Glycoprotein VI-Dependent Platelet Responses in a Rhesus Monkey Model of Type 1 Diabetes

J. F. Arthur,[1] Y. Shen,[1] Y. Chen,[2] J. Qiao,[1] R. Ni,[2] Y. Lu,[2] R. K. Andrews,[1] E. E. Gardiner,[1] and J. Cheng[2]

[1] *Australian Centre for Blood Diseases, Alfred Medical Research & Education Precinct (AMREP), Monash University, Melbourne, VIC 3004, Australia*
[2] *Key Laboratory of Transplant Engineering and Immunology, West China Hospital, Ministry of Health, Sichuan University, Chengdu 610041, China*

Correspondence should be addressed to J. F. Arthur; jane.arthur@monash.edu and Y. Lu; luyanrong@scu.edu.cn

Received 19 December 2012; Accepted 7 May 2013

Academic Editor: Bernard Portha

Thrombosis is a life-threatening complication of diabetes. Platelet reactivity is crucial to thrombus formation, particularly in arterial vessels and in thrombotic complications causing myocardial infarction or ischaemic stroke, but diabetic patients often respond poorly to current antiplatelet medication. In this study, we used a nonhuman primate model of Type 1 diabetes to measure early downstream signalling events following engagement of the major platelet collagen receptor, glycoprotein (GP)VI. Diabetic monkeys were given enough insulin to maintain their blood glucose levels either at ~8 mM (well-controlled diabetes) or ~15 mM (poorly controlled diabetes). Flow cytometric analysis was used to measure platelet reactive oxygen species (ROS) generation, calcium mobilisation, receptor surface expression, and immature platelet fraction. We observed exacerbated intracellular ROS and calcium flux associated with engagement of GPVI in monkeys with poorly controlled diabetes. GPVI surface levels did not differ between healthy monkeys or the two diabetic groups. Treatment of platelets with the specific Syk inhibitor BAY61-3606 inhibited GPVI-dependent ROS and, importantly, reduced ROS generation in the poorly controlled diabetes group to that observed in healthy monkeys. These data indicate that glycaemic control is important in reducing GPVI-dependent platelet hyperreactivity and point to a potential antithrombotic therapeutic benefit of Syk inhibition in hyperglycaemic diabetes.

1. Introduction

Type 2 diabetes occurs when individuals with an underlying genetic disposition develop resistance to the glucose uptake/metabolism-promoting signals of insulin. Type 1 diabetes, which accounts for 5%–10% of all diabetes cases, generally results from autoimmune destruction of insulin-secreting pancreatic islet cells [1]. One of the high risk complications of diabetes is thrombosis, and platelets are pivotal to thrombus formation, particularly in arterial vessels, and hence the resultant thrombotic complications of myocardial infarction or ischaemic stroke. Platelets from individuals with diabetes, particularly Type 2 diabetes, are more sensitive to aggregation by a variety of agonists [2, 3], and 80% of diabetic patients are likely to die from thrombotic complications [4]. Considerably less is known about platelet activation in Type 1 diabetes, although the relative risk of cardiovascular disease in Type 1 diabetic patients can be as much as 10-fold greater than that in nondiabetic individuals [1]. However, the reduction of thrombotic events in diabetic patients has proven to be only marginal in several trials of antiplatelet therapy [5–7], and diabetes is consistently associated with a high rate of adverse cardiovascular events. There is therefore a pressing need for alternative/improved antiplatelet therapy for diabetic patients.

Exogenous reactive oxygen species (ROS) can influence platelet function, and platelets themselves are able to generate ROS. We have shown that the major collagen receptor on platelets, glycoprotein (GP) VI, is linked to redox signalling pathways via its association with the adaptor molecule, tumour necrosis factor receptor-associated factor 4 (TRAF4; [8]). TRAF4 interacts with an intracellular sequence of

GPVI as well as $p47^{phox}$ of the NADPH oxidase complex, the major source of ROS in platelets. Initiation of GPVI-dependent signalling involves GPVI-associated Lyn phosphorylating an immunoreceptor tyrosine-based activation motif (ITAM) in FcRγ (in a complex with GPVI), leading to recruitment and activation of spleen tyrosine kinase (Syk). A subsequent tyrosine phosphorylation signalling cascade results in intraplatelet calcium mobilisation and activation of the integrin $\alpha_{IIb}\beta_3$, leading to platelet aggregation and metalloproteinase-dependent GPVI ectodomain shedding. Intracellular ROS generation following GPVI engagement is an early signalling event and precedes GPVI-dependent signalling leading to aggregation and shedding. We have recently shown that GPVI ROS generation is comprised of two phases: an initial Syk-independent burst followed by additional Syk-dependent generation [9]. In the current study, we investigate GPVI-dependent ROS generation and calcium mobilisation in a rhesus model of Type 1 diabetes. Compared with rodent models, monkeys are metabolically closer to humans, and a longer lifespan allows long-term disease progression to be assessed in the same animal over 3–5 years. Genetic variability in monkeys also better approximates disease in humans compared with in-bred rodents. Importantly, while the GPVI primary sequence and platelet immunoreceptor signalling pathways are significantly different in rats or mice compared with human, monkey GPVI is closely related [10] making them suitable for platelet functional analysis. Additionally, we obtain data on GPVI-dependent ROS generation in monkeys in the setting of diabetes with controlled dietary intake to eliminate this unavoidable variable associated with human studies. We assess the influence of glycaemic control (well-controlled versus poorly controlled) in this model and the effect of Syk inhibition on ROS generation in the different diabetic groups.

2. Materials and Methods

2.1. Materials. The GPVI-specific agonist, collagen-related peptide (CRP) was prepared as previously described [11, 12]. Thrombin receptor-agonist peptide (TRAP) was from Auspep (Melbourne, VIC, Australia). The potent and selective Syk inhibitor, 2-[[7-(3,4-dimethoxyphenyl)imidazo[1,2-c]pyrimidin-5-yl]amino]pyridine-3-carboxamide hydrochloride (BAY61-3606) was from Enzo Life Sciences (Farmingdale, NY, USA).

2.2. Animals. Eighteen rhesus monkeys (aged 4–9) were obtained from Chengdu Ping'an Experimental Animal Reproduction Center (Sichuan, China). All the animals had free access to water supply and were fed a primate diet twice a day. The animals were cared for in accordance with the guidelines of the Experimental Animal Center, Sichuan University, which have been approved by the Association for the Assessment and Accreditation of Laboratory Animal Care International (AAALAC). Each subject had a history, recording the general condition (body weight, food intake, and behavioural activity), a physical examination, a mental health evaluation, and laboratory testing every 1-2 months.

2.3. Induction of Diabetes. Monkeys were made to fast overnight. Streptozotocin (STZ; Yuyang High-tech Development Co. Ltd., Chengdu, China) was administered by intravenous injection after dissolution with sodium citrate (pH 4.5) at a dose of 80 mg/kg over 30 seconds (see [13]). Blood glucose levels were determined twice a day commencing 72 hours after STZ induction. The model was considered to be successfully established if the fasting blood glucose (FBG) values remained >11.1 mM for two consecutive days and the C-peptide concentration was <0.17 nM. After the successful induction of diabetes, monkeys were administered porcine insulin (Wanbang Biopharma Co. Ltd., Xuzhou, China) that included a combination of protamine zinc insulin and insulin, twice a day before feeding (9:00 AM and 4:30 PM) [14]. Diabetic monkeys were separated into two groups: treated with sufficient insulin to maintain the FBG level at <10 mM (well-controlled group, $n = 6$) and reduced insulin to maintain the FBG level at 15–20 mM (poorly controlled diabetes group, $n = 6$). Six healthy monkeys were used as normal controls. Experiments were conducted between July and August 2011. Diabetes was successfully established in the poorly controlled diabetic monkeys between 2 and 3 years prior to experimentation (July 2008–July 2009). Diabetes was established in the well-controlled diabetic monkeys 1 year prior to experimentation (June 2010).

2.4. Blood Collection. Platelet-rich plasma (PRP) was obtained from blood collected into 3.2% (w/v) trisodium citrate and centrifuged at 110 g for 20 min at room temperature.

2.5. Measurement of Intracellular ROS. Platelets in PRP from healthy, low glucose diabetic, and high glucose diabetic rhesus monkeys were loaded with 2′,7′-dichlorofluorescein (H_2DCF-DA; Sigma, St. Louis, MO, USA), a cell-permeable nonfluorescent dye that is cleaved by intracellular esterases to H_2DCF rendering it membrane-impermeable and then emits fluorescent energy in the presence of ROS [15–17]. H_2DCF-DA (10 μM final concentration) was incubated with PRP for 30 min at 37°C. Samples were then treated with (final concentrations) 10 μg/mL CRP or 5 μM TRAP, then diluted tenfold in Ca^{2+}-free Tyrode's buffer (0.36 mM NaH_2PO_4, 5 mM HEPES, 137 mM NaCl, 5.6 mM glucose, and 2.7 mM KCl, pH 7.4) containing 0.1% (w/v) BSA and 10 μM H_2DCF-DA, and analysed in a Beckman Elite ESP flow cytometer (Beckman Coulter). Experiments were carried out in the presence or absence of Syk inhibitor (pretreatment with 5 μM BAY61-3606 for 15 min) to represent the initial and secondary phases of ROS, respectively [9].

2.6. Measurement of Intracellular Calcium Mobilisation. The method was modified for platelet-rich plasma (PRP) from previous studies [18, 19]. In brief, Fluo-3-AM- (fluo-3 acetoxymethyl ester) labelled PRP containing 1-2 $\times$ 10^6 platelets/mL was diluted in 290 μL HEPES-Tyrode's buffer (see measurement of intracellular ROS) containing 1 mM $CaCl_2$. The GPVI agonist CRP (10 μg/mL) was added to the platelet/buffer sample. Platelet intracellular calcium mobilisation was measured from 10 seconds (initial calcium mobilisation) to 2.5 minutes of agonist treatment (maximal calcium

Table 1: Comparison of monkey parameters.

	Healthy	Well-controlled diabetes	Poorly-controlled diabetes
n	6	6	6
Age (years)†	5.50 ± 0.96 (4–9)	4.17 ± 0.17 (4–5)	5.67 ± 0.21 (5–6)
Recent weight (kg) (July-Aug. 2011)	7.25 ± 2.06	5.70 ± 0.54*	8.47 ± 2.09
Gender	4 M, 2 F	2 M, 4 F	6 M
Monthly blood glucose level (mM)† (July-Aug. 2011)	4.7 ± 0. 15 (4.2–5.2)	7.87 ± 0.53* (2.6–18.20)	16.17 ± 1.65*** (8.0–31.2)
Platelet count in whole blood†	213.5 ± 31.5 (139–330)	192.8 ± 17.5 (137–241) $n = 5$	193.4 ± 15.3 (150–230) $n = 5$
MPV†	7.78 ± 0.86 (7.3–9.31) $n = 5$	7.98 ± 1.67 (7.07–10.7) $n = 5$	7.01 ± 0.54 (6.56–7.95) $n = 5$
Basal ROS (X-mean)	0.82 ± 0.05	0.80 ± 0.06	0.85 ± 0.05
Immature platelet fraction (TO staining; X-mean)	30.8 ± 3.6	29.8 ± 3.7	27.4 ± 3.9

†Mean ± standard error (range).
*$P < 0.05$; ***$P < 0.001$ compared with control.

mobilisation). Platelets were specifically gated on forward and side scatter characteristics and CD41a positive staining. The Fluo-3 intensity log ratio of the agonist-induced Fluo-3 positive platelets to basal (resting) level Fluo-3-labelled platelets was used for calcium mobilisation analysis.

2.7. Analysis of Receptor Surface Expression. Platelet surface levels of GPVI were assessed using anti-GPVI mAb 1G5 [20, 21] directly conjugated to phycoerythrin (PE) using the Lightning-Link R-PE antibody labelling kit (Novus Biologicals, CO, USA). GPIbα levels were measured using PE-conjugated AK2 [22]. Integrin $\alpha_{IIb}\beta_3$ and platelet tetraspanin CD9 levels were measured by PE-conjugated anti-CD41a against integrin chain α_{IIb} and anti-CD9 mAb (PE-CD9), both from BD Biosciences, San Jose, CA, USA.

2.8. Measurement of Immature Platelet Fraction. Immature platelets recently released from the bone marrow contain more RNA than platelets that have been in the circulation for longer periods of time (average platelet lifespan 7–10 days). The immature platelet fraction is determined by staining platelets with the RNA dye thiazole orange (TO) and reflects platelet production and the rate of platelet turnover [23]. Platelets in PRP were fixed with 1% (w/v) paraformaldehyde for 10 min at RT. TO (0.5 μg/mL final concentration in PBS containing 5 mM EDTA) was added to the fixed sample, incubated in the dark for 1 h at RT, and then analysed by flow cytometry on the FL-1 channel.

2.9. Statistical Analyses. For comparison of ROS generation by various treatments, data were assessed by linear mixed model using SAS System Software Version 9.2 (SAS Institute, Cary, NC, USA). For comparison of basal ROS, peak calcium mobilisation, body weight, platelet count, mean platelet volume (MPV), platelet distribution width (PDW), and receptor levels, data were assessed by one-way ANOVA with Newman-Keuls multiple comparison post hoc test using GraphPad Prism 5.

3. Results

3.1. Haematological Parameters. Monkeys receiving sufficient insulin per day to control their blood glucose level (well-controlled diabetes) still had elevated glucose compared with healthy monkeys; however the blood glucose level of monkeys receiving a reduced insulin regime (poorly controlled diabetes) was significantly greater than healthy monkeys or monkeys with well-controlled diabetes (Figure 1(a)). Platelet count (Figure 1(b)) and platelet morphology markers (including mean platelet volume, Figure 1(c) and platelet distribution width, Figure 1(d)) displayed no significant difference between all three groups. Although well-controlled diabetic animals had lower average body weights than poorly controlled diabetic animals (5.7 ± 0.5 and 8.5 ± 2.1 kg for well-controlled and poorly controlled diabetic monkeys, resp.; $P < 0.05$), there was no significant difference between the average weight of healthy monkeys (7.3 ± 2.1 kg) and either diabetes group. Similarly, there was no significant difference between the mean age within each group (Table 1).

3.2. Intracellular ROS Generation. To evaluate the effect of glucose control on early GPVI-mediated ROS generation in diabetic monkeys, we utilised a flow cytometry-based assay to rapidly assess intracellular ROS using the fluorescent dye, H_2DCF-DA. Basal ROS in platelet-rich plasma (PRP) from all three monkey groups was similar (Table 1). Treatment of platelets with 10 μg/mL of the GPVI-specific agonist collagen-related peptide (CRP) for 2 min increased intraplatelet ROS in all groups, but there was a significant exacerbation of CRP-induced ROS generation in the poorly controlled diabetic

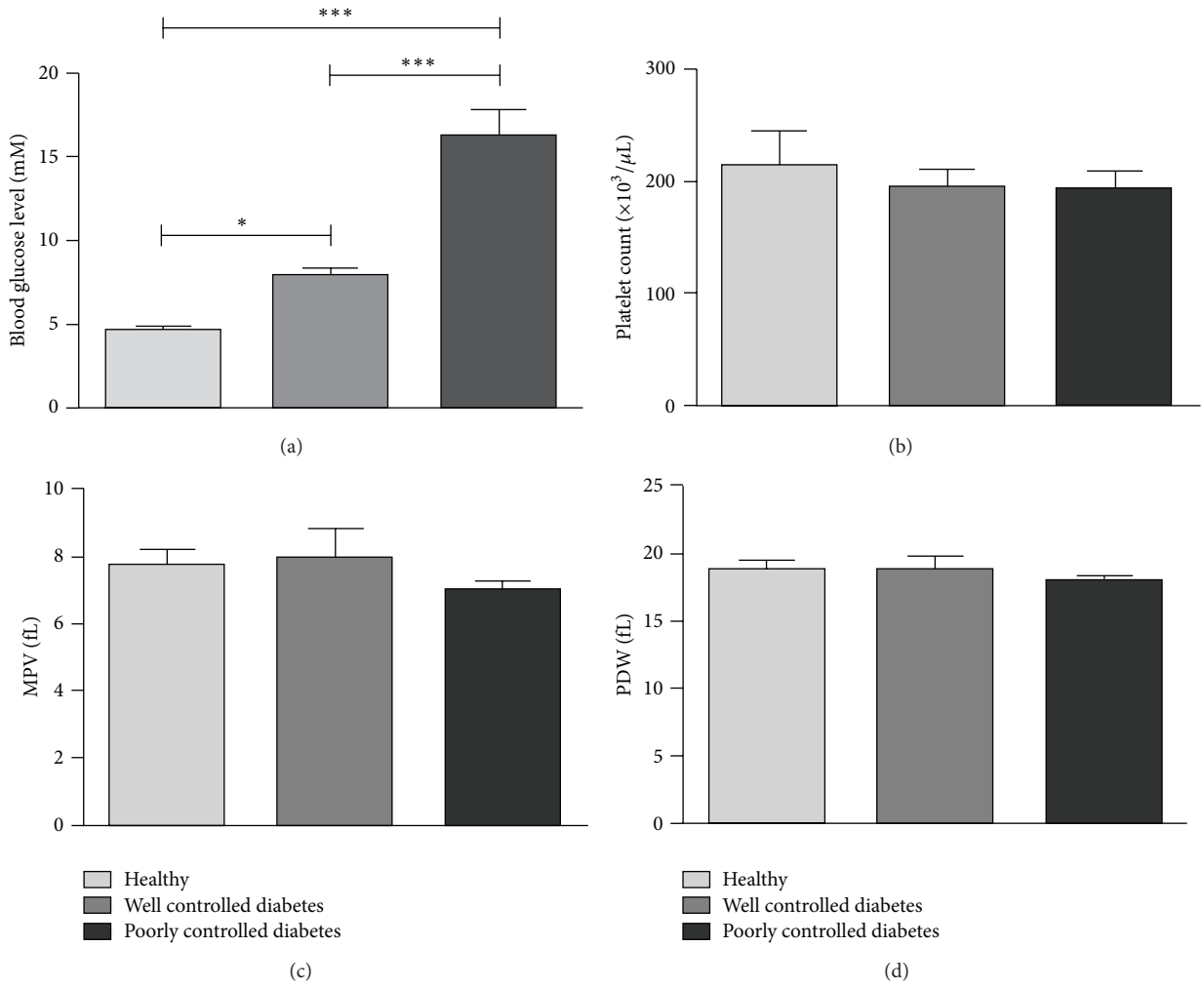

Figure 1: Haematological parameters for healthy and diabetic monkeys. (a) Blood glucose, (b) platelet count, (c) mean platelet volume, and (d) platelet distribution width. Data are from six monkeys in each group. $^{*}P < 0.05$, $^{***}P < 0.001$.

monkeys (Figure 2). There was a tendency for intracellular ROS generation in the well-controlled diabetic monkeys to be lower compared with healthy or poorly controlled diabetic monkeys, but this did not achieve statistical significance ($P = 0.094$). As seen previously in healthy human donors, there was no intracellular ROS generated by treatment of platelets with the thrombin receptor agonist, TRAP (5 μM).

To examine early GPVI signalling events, platelets were treated with GPVI agonist in the presence and absence of 5 μM BAY61-3606, a potent, specific inhibitor of Syk [24]. Increased DCF fluorescence in response to CRP occurs in two distinct phases: an initial burst of ROS occurring within 2 min followed by additional ROS generation as a consequence of downstream signalling [9]. Syk inhibition reduced CRP-induced ROS in all monkey groups and, critically, reduced the exacerbated ROS in poorly controlled diabetic monkeys to levels observed in healthy monkeys (Figure 2).

3.3. Intracellular Calcium Flux. As an additional readout of downstream signalling following agonist treatment of platelets, intracellular calcium mobilisation was measured by flow cytometry following treatment of platelets with 10 μg/mL CRP or 10 μM TRAP. Although measurements were unable to be obtained in all monkeys, calcium flux was measured in five healthy, five well-controlled diabetic and three poorly controlled diabetic animals (Figure 3). Mirroring the results obtained for intracellular ROS, peak intracellular calcium, measured 30 sec after CRP treatment, was significantly increased in poorly controlled diabetic monkeys (Figure 3(a); $P < 0.001$ compared with healthy or well-controlled diabetes). Control of blood glucose levels in diabetic monkeys reduced the peak calcium flux to below that observed in healthy monkeys ($P < 0.05$). In contrast, peak calcium flux induced by the PAR-1 agonist TRAP (measured at 10 sec after treatment) was equivalent in all monkey groups (Figure 3(b)).

3.4. Receptor Surface Expression. Functional GPVI responses are determined at least in part by surface density of GPVI [25, 26], so to assess whether variation in surface expression

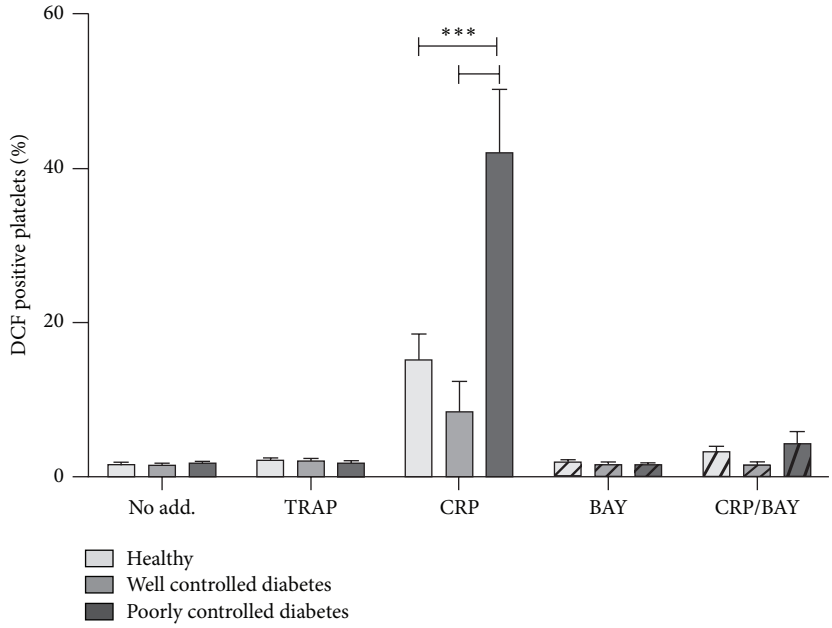

FIGURE 2: Effect of well-controlled or poor glycaemic control on intracellular ROS measurements in diabetes. Flow cytometry of H_2DCF-DA-loaded monkey platelets in PRP either untreated (no add.) or treated with 10 μg/mL CRP or 5 μM TRAP. Syk inhibition by 5 μM BAY61-3606 (BAY) reduces GPVI-induced ROS generation in all monkey groups. Data are from six monkeys in each group. $^{***}P < 0.001$.

could account for differences in intracellular ROS production or calcium flux observed between the diabetes groups, receptor surface levels of GPVI and three other platelet receptors were measured. Expression of glycoprotein receptors (GPVI, GPIbα) using in-house PE-labelled antibodies displayed lower mean fluorescence intensity than that of the corresponding measurements of CD9 (anti-tetraspanin antibody) or $\alpha_{IIb}\beta_3$ using commercial PE-labelled antibodies. GPVI surface expression was similar between all three monkey groups: healthy, well-controlled diabetes, and poorly controlled diabetes (Figure 4(a)). Although an outlier in the healthy group (confirmed by extreme studentized deviate method (ESD, Grubbs' test, GraphPad)) raised the average expression level of this group, exclusion of the outlier did not alter the overall outcome but did highlight the tendency for GPVI expression in the poorly controlled diabetic animals to be higher than in the other two groups. There was no difference in surface levels of GPIbα, CD9, or $\alpha_{IIb}\beta_3$ between groups (Figures 4(b)–4(d)). TO staining of platelets to detect the immature platelet fraction similarly revealed no differences (Table 1) suggesting that platelet hyperactivity was not likely to be due to aberrant platelet production or clearance.

4. Discussion

Type 1 diabetic patients have increased risk of cardiovascular disease compared with non-diabetic individuals [1]. Platelet hyperreactivity plays a key role in prothrombotic complications. Increased platelet responsiveness to collagen has been proposed as a contributing factor to the increased incidence of vascular disease seen in diabetes. In a non-human primate model of Type 1 diabetes, we observed exacerbated intracellular ROS and calcium flux associated with engagement of GPVI, the major platelet collagen receptor on platelets.

Basal levels of intraplatelet ROS were not different between healthy monkeys and monkeys receiving sufficient insulin to control their diabetes (well-controlled) or those receiving less insulin (poorly controlled). This was not the case in a study of non-insulin-dependent diabetic patients in whom resting platelets had a basal level of ROS that was significantly higher than in controls [27]. The patients in that study had an average age of 60 years so it is likely that their platelets had been subjected to longer periods of hyperglycaemia than our monkeys. It will be interesting to perform follow-up studies in our monkeys to determine whether the oxidative status of their platelets is altered with time.

In diabetic monkeys with higher levels of blood glucose, there was a significant increase in GPVI-dependent ROS generation compared with normoglycaemic monkeys or diabetic monkeys with lower levels of blood glucose. Hyperglycaemia is the diagnostic feature of Type 1 and Type 2 diabetes, yet the role of glycaemic control in preventing thrombotic events is not easily defined. Randomised controlled trials involving Type 1 and Type 2 diabetic patients have found that improved glycaemic control might stabilise macrovascular disease or prevent progression in those at risk [28]. In Type 1 diabetic patients with established microvascular complications of nephropathy, however, a significant improvement in glycaemic control did not improve hyperreactivity of platelets *in vitro* [29]. In a study involving Type 2 diabetic patients, Davi and colleagues [30] found that only with tight

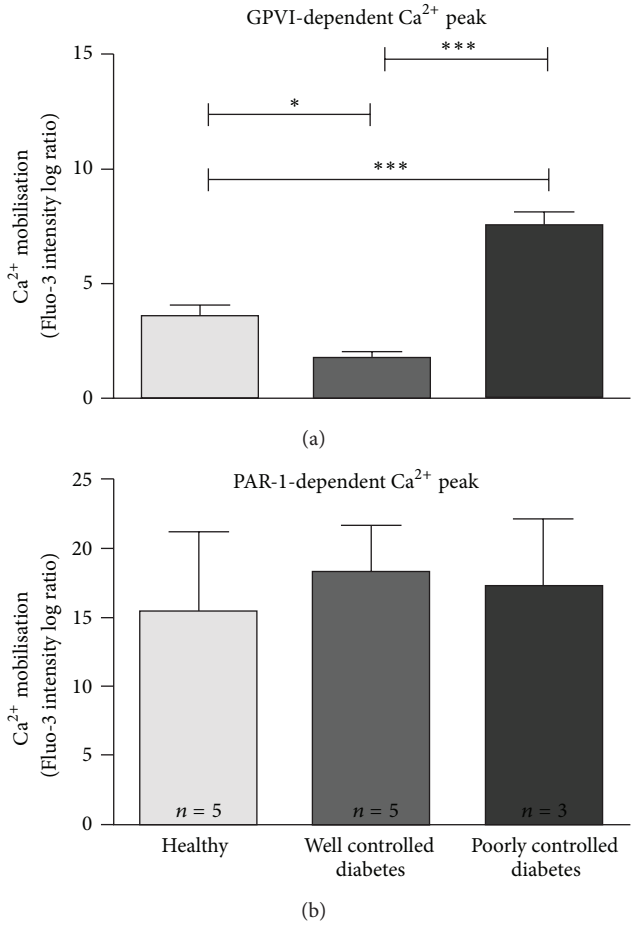

Figure 3: Influence of well- and poorly controlled diabetes on intracellular calcium mobilisation. Flow cytometry of Fluo-3-AM-loaded monkey platelets in PRP treated with 10 μg/mL CRP (a) or 10 μM TRAP (b). Data are from three to five monkeys in each group. $^{*}P < 0.05$, $^{***}P < 0.001$.

glycaemic control there was resultant improvement in platelet function. Our data indicate that specific hyperreactivity to GPVI engagement is an early event in the progression of Type 1 diabetes and is linked to high blood glucose levels. This is in agreement with a recent study in which moderately controlled diabetes (~10–13 mM blood glucose) was induced in cynomolgus monkeys fed an atherogenic diet, and an increase in ROS was detected prior to atherosclerotic changes [31], supporting ROS elevation as an initiating event in diabetic vascular disease.

Of interest, monkeys with well-controlled diabetes in our study had reduced GPVI-dependent platelet responses relative to the healthy controls, despite having elevated glucose levels. The reduction was statistically significant for calcium responses but did not achieve significance for the ROS measurements. Insulin has been reported to have antiplatelet effects, inhibiting platelet interaction with collagen-coated coverslips following *in vivo* perfusion in nonobese, non-diabetic individuals and reducing aggregation induced by several agonists [32]. Although there is still considerable debate over whether insulin has a direct effect on platelet function [33, 34], our data could point to a role for insulin administration specifically reducing GPVI-dependent signalling (ROS generation and calcium mobilisation). Although it is possible that monkey characteristics in the well-controlled diabetes group (i.e., more females, lower average weight and age) could have contributed to the observed reduced platelet responsiveness, it was not a global platelet phenomenon because signalling downstream of G protein-coupled PAR-1 receptors was not diminished under the same conditions (Figure 3).

Mean platelet volume (MPV) is probably the most extensively studied morphological marker of platelet activation. Platelet distribution width (PDW) indicates the variation in platelet size and is also used as an indication of platelet activation, with both increased MPV and higher PDW associated with increased platelet activation. In a recent study evaluating platelet indices in diabetic and non-diabetic patients, MPV and PDW were significantly higher in diabetic patients compared to the control subjects [35]. Among the diabetic patients, PDW was found to be higher in those with microvascular complications (retinopathy, nephropathy, and neuropathy) compared to those without. In our monkey model, there was no difference in either MPV or PDW between healthy animals or the two diabetic groups. In accordance with these observations, there was also no difference in TO staining (a measure of the immature platelet fraction which usually comprises larger, more haemostatically active platelets) between the different monkey cohorts indicating that there was no difference in platelet turnover. Diabetic patients have been reported to have accelerated platelet consumption/production and hence an increase in immature platelets [36]. Given that our diabetic models have been established no longer than three years (the earliest established was a poorly controlled diabetic monkey, in July 2008, 3 years prior to our laboratory tests), the increase in MPV, PDW, and immature platelets associated with diabetes with/without vascular problems could be a later development of the disease.

Surface expression of FcRγ/GPVI is reportedly enhanced on platelets of Type 2 diabetic individuals, although only FcRγ chain levels correlated significantly with diabetes [37]. No data has been obtained in Type 1 diabetic patients. In the current study, there was a tendency for monkeys with poorly controlled diabetes to have higher levels of GPVI on the platelet surface; however this did not reach statistical significance. The reason for exacerbated GPVI-dependent signalling in the hyperglycaemic monkeys was therefore unlikely to be due to a higher density of receptors. There was no difference in expression of other platelet receptors, GPIbα, CD9, or integrin $\alpha_{IIb}\beta_3$, between the groups.

Enhanced calcium mobilisation has been observed in platelets from Type 1 and Type 2 diabetic patients [17, 38]. Intracellular calcium homeostasis in platelets of patients with non-insulin-dependent diabetes is altered, leading to increased adhesiveness and spontaneous aggregation [39]. In our poorly controlled Type 1 diabetic monkeys, peak calcium mobilisation was significantly increased relative to healthy or well-controlled diabetic monkeys following treatment with the GPVI-specific ligand, CRP. No such hyperreactivity was

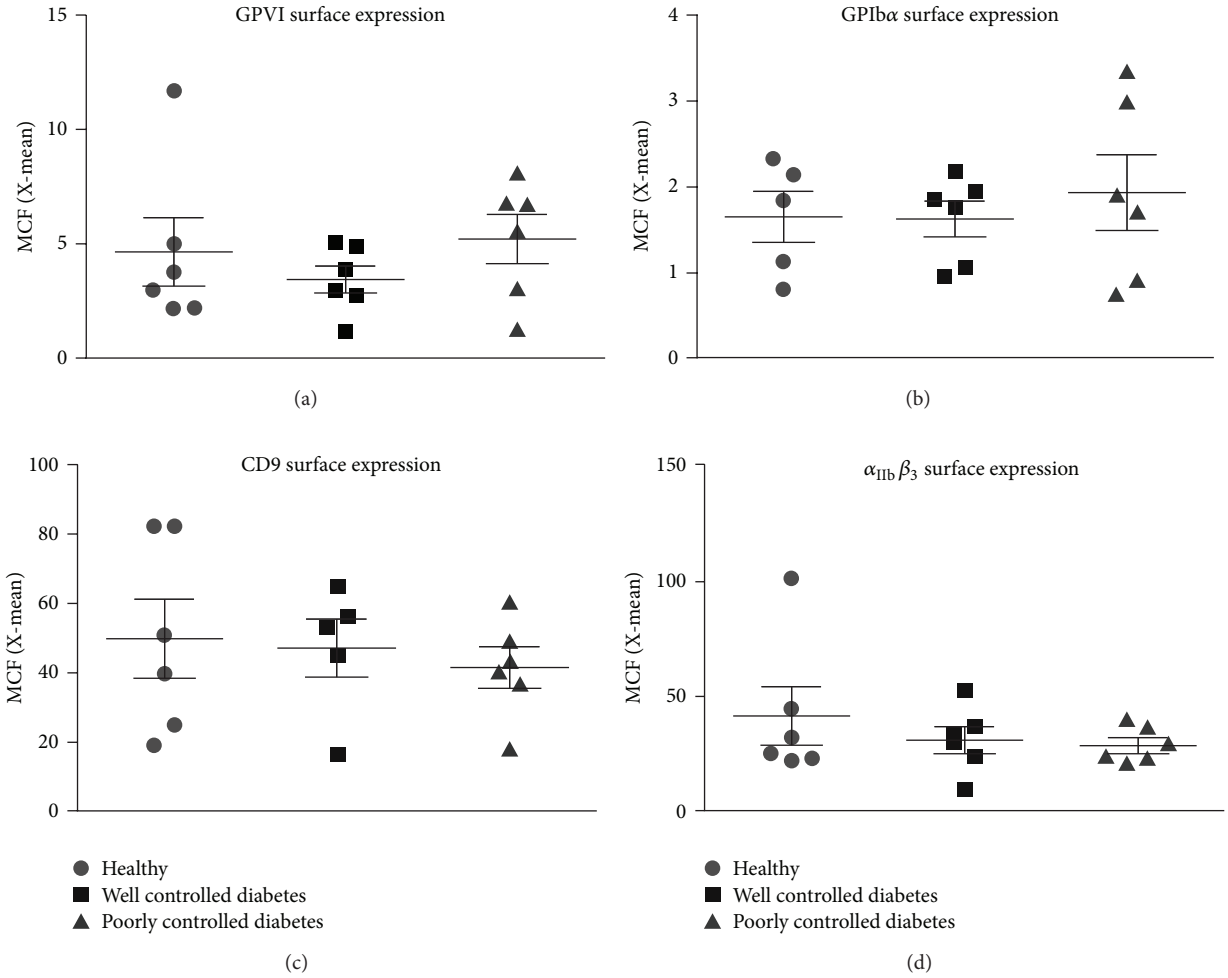

Figure 4: Effect of diabetes on platelet receptor surface levels. Platelet surface expression of (a) GPVI, (b) GPIbα, (c) CD9, and (d) $\alpha_{IIb}\beta_3$. Data are from five to six monkeys in each group.

observed when platelets were treated with the PAR-1 agonist, TRAP, indicating that the exaggerated calcium response is specific for GPVI engagement at this time (≤3 years) of disease progression.

Upon GPVI engagement, phosphorylation of the ITAM motif of the associated FcRγ chain initiates a tyrosine phosphorylation-dependent signalling cascade that involves Syk activation as an early event and leads to platelet activation. Unlike the initial burst of ROS production following GPVI engagement, the secondary phase is completely blocked by the Syk inhibitor, BAY 61-3606, which inhibits GPVI-dependent signalling leading to activation of $\alpha_{IIb}\beta_3$ [9]. Inhibition of Syk in the current study reduced CRP-induced ROS generation regardless of the level of glycaemic control. Early ROS generation in poorly controlled diabetic animals was indistinguishable from that in healthy animals. Basal ROS levels were similar in all groups so this indicates that the hyperreactivity associated with hyperglycaemia in this model of diabetes was due to increased signalling downstream of Syk rather than an upregulation of receptor proximal signalling. Syk inhibition could prove to be an effective antiplatelet strategy for diabetic patients because of its minimal impact on primary haemostasis while providing significant protection from arterial thrombosis [40]. The potential for targeting Syk in autoimmune diabetes has been evaluated in a recent mouse study. Oral administration of the Syk inhibitor R788 delayed the onset of spontaneous diabetes in nonobese diabetic (NOD) mice and the progression of early-established diabetes even when treatment was initiated after the development of glucose intolerance in those animals [41]. The mechanism in that study was reportedly blockage of B cell receptor- and FcγR-mediated antigen presentation due to Syk inhibition although R788 treatment was not associated with large reductions in autoantibody levels, suggesting that perhaps a reduction in B cell development and activation was not the main reason for the antidiabetic effect of Syk inhibition.

Mechanistically, what could be the link between GPVI and hyperglycaemia? Aldose reductase (AR) is the first enzyme of the polyol pathway, which converts excess glucose to sorbitol accompanied by an increase in the cytosolic NADH/NAD+ ratio. Under normal glycaemic conditions, AR is only a minor consumer of glucose; however during

hyperglycaemia AR activity is significantly enhanced and it is thought to contribute to the vascular complications associated with diabetes by increasing oxidative and osmotic stress on cells. Two important recent studies have linked AR and GPVI signalling [42, 43]. First, proteomic analysis of differentially altered proteins revealed that AR activity and expression were upregulated following GPVI-dependent platelet activation [42]. These changes were functionally relevant because inhibition of AR activity resulted in reduced GPVI-dependent platelet aggregation. Second, AR was shown to play a central role in GPVI-dependent signal transduction (increased PLCγ2 and PKC activation) and this signalling pathway was enhanced in hyperglycaemic conditions [43]. What is not known is how AR fits into the GPVI signalling cascade and how glucose metabolism through AR might enhance GPVI-dependent platelet responses. Further investigation is required and is the subject of an ongoing study.

In conclusion, we have demonstrated exacerbated platelet intracellular ROS and calcium flux associated with engagement of GPVI in monkeys with poorly controlled diabetes and that inhibition of a specific signalling protein (Syk) reduced GPVI-dependent ROS generation regardless of the level of glycaemic control in diabetic monkeys, indicating that Syk inhibition could prove to be an effective antiplatelet strategy for diabetic patients.

Abbreviations

CRP:	Collagen-related peptide
FBG:	Fasting blood glucose
GP:	Glycoprotein
H_2DCF-DA:	2′,7′-dichlorodihydrofluorescein diacetate
ITAM:	Immunoreceptor tyrosine-based activation motif
MPV:	Mean platelet volume
PAR-1:	Protease activated receptor-1
PDW:	Platelet distribution width
PE:	Phycoerythrin
PRP:	Platelet-rich plasma
ROS:	Reactive oxygen species
STZ:	Streptozotocin
Syk:	Spleen tyrosine kinase
TO:	Thiazole orange
TRAF4:	Tumour necrosis factor receptor-associated factor 4
TRAP:	Thrombin receptor-activating peptide.

Acknowledgments

The authors are grateful to Meimei Shi and Huan Li for technical assistance. They thank Dr. Antonia Miller for critical eva luation of the paper, and Catherine Smith for assistance with statistical analyses. This study was supported by the Key Program of National Nature Science Foundation of China (no. 30930088) and the National Program for High Technology Research and Development of China (no. 2011ZX09307-301). They acknowledge the National Health and Medical Research Council of Australia and Monash University Strategic Funding for financial support.

References

[1] D. Daneman, "Type 1 diabetes," *The Lancet*, vol. 367, no. 9513, pp. 847–858, 2006.

[2] V. Serebruany, I. Pokov, W. Kuliczkowski, J. Chesebro, and J. Badimon, "Baseline platelet activity and response after clopidogrel in 257 diabetics among 822 patients with coronary artery disease," *Thrombosis and Haemostasis*, vol. 100, no. 1, pp. 76–82, 2008.

[3] J. L. Ferreiro, J. A. Gomez-Hospital, and D. J. Angiolillo, "Platelet abnormalities in diabetes mellitus," *Diabetes and Vascular Disease Research*, vol. 7, no. 4, pp. 251–259, 2010.

[4] M. E. Carr, "Diabetes mellitus: a hypercoagulable state," *Journal of Diabetes and Its Complications*, vol. 15, no. 1, pp. 44–54, 2001.

[5] Antithrombotic Trialists' Collaboration, "Collaborative meta-analysis of randomised trials of antiplatelet therapy for prevention of death, myocardial infarction, and stroke in high risk patients," *British Medical Journal*, vol. 324, no. 7329, pp. 71–86, 2002.

[6] L. Hansson, A. Zanchetti, S. G. Carruthers et al., "Effects of intensive blood-pressure lowering and low-dose aspirin in patients with hypertension: principal results of the Hypertension Optimal Treatment (HOT) randomised trial. HOT Study Group," *The Lancet*, vol. 351, no. 9118, pp. 1755–1762, 1998.

[7] G. Tocci, A. Ferrucci, P. Guida et al., "Impact of diabetes mellitus on the clinical management of global cardiovascular risk: analysis of the results of the Evaluation of Final Feasible Effect of Control Training and Ultra Sensitization (EFFECTUS) educational program," *Clinical Cardiology*, vol. 34, no. 9, pp. 560–566, 2011.

[8] J. F. Arthur, Y. Shen, E. E. Gardiner et al., "TNF receptor-associated factor 4 (TRAF4) is a novel binding partner of glycoprotein Ib and glycoprotein VI in human platelets," *Journal of Thrombosis and Haemostasis*, vol. 9, no. 1, pp. 163–172, 2011.

[9] J. F. Arthur, J. Qiao, Y. Shen et al., "ITAM receptor-mediated generation of reactive oxygen species in human platelets occurs via Syk-dependent and Syk-independent pathways," *Journal of Thrombosis and Haemostasis*, vol. 10, no. 6, pp. 1133–1141, 2012.

[10] J. L. Qiao, Y. Shen, E. E. Gardiner, and R. K. Andrews, "Proteolysis of platelet receptors in humans and other species," *Biological Chemistry*, vol. 391, no. 8, pp. 893–900, 2010.

[11] E. E. Gardiner, D. Karunakaran, Y. Shen, J. F. Arthur, R. K. Andrews, and M. C. Berndt, "Controlled shedding of platelet glycoprotein (GP)VI and GPIb-IX-V by ADAM family metalloproteinases," *Journal of Thrombosis and Haemostasis*, vol. 5, no. 7, pp. 1530–1537, 2007.

[12] E. E. Gardiner, J. F. Arthur, M. L. Kahn, M. C. Berndt, and R. K. Andrews, "Regulation of platelet membrane levels of glycoprotein VI by a platelet-derived metalloproteinase," *Blood*, vol. 104, no. 12, pp. 3611–3617, 2004.

[13] X. Jin, L. Zeng, S. Rong et al., "Comparison of single high-dose STZ with partial pancreatectomy combined with low-dose STZ for diabetes induction in rhesus monkeys," *Experimental Biology and Medicine*, vol. 235, pp. 877–885, 2010.

[14] C. F. Qiao, B. L. Tian, G. Mai et al., "Induction of diabetes in rhesus monkeys and establishment of insulin administration strategy," *Transplantation Proceedings*, vol. 41, no. 1, pp. 413–417, 2009.

[15] N. Bakdash and M. S. Williams, "Spatially distinct production of reactive oxygen species regulates platelet activation," *Free Radical Biology and Medicine*, vol. 45, no. 2, pp. 158–166, 2008.

[16] A. J. Begonja, S. Gambaryan, J. R. Geiger et al., "Platelet NAD (P)H-oxidase-generated ROS production regulates αIIbβ3-integrin activation independent of the NO/cGMP pathway," *Blood*, vol. 106, no. 8, pp. 2757–2760, 2005.

[17] P. C. Redondo, I. Jardin, J. M. Hernández-Cruz, J. A. Pariente, G. M. Salido, and J. A. Rosado, "Hydrogen peroxide and peroxynitrite enhance Ca^{2+} mobilization and aggregation in platelets from type 2 diabetic patients," *Biochemical and Biophysical Research Communications*, vol. 333, no. 3, pp. 794–802, 2005.

[18] L. K. Jennings, M. E. Dockter, C. D. Wall, C. F. Fox, and D. M. Kennedy, "Calcium mobilization in human platelets using indo-1 and flow cytometry," *Blood*, vol. 74, no. 8, pp. 2674–2680, 1989.

[19] M. D. Monteiro, M. J. Goncalves, F. Sansonetty, and J. E. O'Connor, "Flow cytometric analysis of calcium mobilization in whole-blood platelets," *Current Protocols in Cytometry*, chapter 9:unit 9.20, 2003.

[20] M. Al-Tamimi, F. Mu, J. F. Arthur et al., "Anti-glycoprotein VI monoclonal antibodies directly aggregate platelets independently of FcγRIIa and induce GPVI ectodomain shedding," *Platelets*, vol. 20, no. 2, pp. 75–82, 2009.

[21] E. E. Gardiner, D. Karunakaran, J. F. Arthur et al., "Dual ITAM-mediated proteolytic pathways for irreversible inactivation of platelet receptors: De-ITAM-izing FcγRIIa," *Blood*, vol. 111, no. 1, pp. 165–174, 2008.

[22] Y. Shen, G. M. Romo, J. Dong et al., "Requirement of leucine-rich repeats of glycoprotein (GP) Ibα for shear- dependent and static binding of von willebrand factor to the platelet membrane GP Ib-IX-V complex," *Blood*, vol. 95, no. 3, pp. 903–910, 2000.

[23] S. J. Barsam, B. Psaila, M. Forestier et al., "Platelet production and platelet destruction: assessing mechanisms of treatment effect in immune thrombocytopenia," *Blood*, vol. 117, no. 21, pp. 5723–5732, 2011.

[24] N. Yamamoto, K. Takeshita, M. Shichijo et al., "The orally available spleen tyrosine kinase inhibitor 2-[7-(3,4-dimethoxyphenyl)-imidazo[1,2-c]pyrimidin-5-ylamino]-nicotinamide dihydrochloride (BAY 61-3606) blocks antigen-induced airway inflammation in rodents," *Journal of Pharmacology and Experimental Therapeutics*, vol. 306, no. 3, pp. 1174–1181, 2003.

[25] D. Best, Y. A. Senis, G. E. Jarvis et al., "GPVI levels in platelets: relationship to platelet function at high shear," *Blood*, vol. 102, no. 8, pp. 2811–2818, 2003.

[26] H. Chen, D. Locke, Y. Liu, C. Liu, and M. L. Kahn, "The platelet receptor GPVI mediates both adhesion and signaling responses to collagen in a receptor density-dependent fashion," *Journal of Biological Chemistry*, vol. 277, no. 4, pp. 3011–3019, 2002.

[27] G. Leoncini, M. G. Signorello, A. Piana, M. Carrubba, and U. Armani, "Hyperactivity and increased hydrogen peroxide formation in platelets of NIDDM patients," *Thrombosis Research*, vol. 86, no. 2, pp. 153–160, 1997.

[28] M. L. Lawson, H. C. Gerstein, E. Tsui, and B. Zinman, "Effect of intensive therapy on early macrovascular disease in young individuals with type 1 diabetes: a systematic review and meta-analysis," *Diabetes Care*, vol. 22, no. 2, pp. B35–B39, 1999.

[29] B. Roshan, G. H. Tofler, L. A. Weinrauch et al., "Improved glycemic control and platelet function abnormalities in diabetic patients with microvascular disease," *Metabolism*, vol. 49, no. 1, pp. 88–91, 2000.

[30] G. Davi, M. Averna, I. Catalano et al., "Platelet function in patients with type 2 diabetes mellitus: the effect of glycaemic control," *Diabetes Research*, vol. 10, no. 1, pp. 7–12, 1989.

[31] P. A. Rowe, K. Kavanagh, L. Zhang, H. J. Harwood Jr., and J. D. Wagner, "Short-term hyperglycemia increases arterial superoxide production and iron dysregulation in atherosclerotic monkeys," *Metabolism*, vol. 60, no. 8, pp. 1070–1080, 2011.

[32] J. Westerbacka, H. Yki-Järvinen, A. Turpeinen et al., "Inhibition of platelet-collagen interaction: an in vivo action of insulin abolished by insulin resistance in obesity," *Arteriosclerosis, Thrombosis, and Vascular Biology*, vol. 22, no. 1, pp. 167–172, 2002.

[33] S. Rauchfuss, J. Geiger, U. Walter, T. Renne, and S. Gambaryan, "Insulin inhibition of platelet-endothelial interaction is mediated by insulin effects on endothelial cells without direct effects on platelets," *Journal of Thrombosis and Haemostasis*, vol. 6, no. 5, pp. 856–864, 2008.

[34] J. W. Akkerman, A. J. Gerrits, I. A. Ferreira, and J. W. M. Heemskerk, "Insulin inhibition of platelet-endothelial interaction is mediated by insulin effects on endothelial cells without direct effects on platelets: a rebuttal," *Journal of Thrombosis and Haemostasis*, vol. 7, no. 2, pp. 369–371, 2009.

[35] S. Jindal, S. Gupta, R. Gupta et al., "Platelet indices in diabetes mellitus: indicators of diabetic microvascular complications," *Hematology*, vol. 16, no. 2, pp. 86–89, 2011.

[36] C. Watala, M. Boncler, T. Pietrucha, and Z. Trojanowski, "Possible mechanisms of the altered platelet volume distribution in type 2 diabetes: does increased platelet activation contribute to platelet size heterogeneity?" *Platelets*, vol. 10, no. 1, pp. 52–60, 1999.

[37] N. Cabeza, Z. Li, C. Schulz et al., "Surface expression of collagen receptor Fc receptor-γ/glycoprotein VI is enhanced on platelets in type 2 diabetes and mediates release of CD40 ligand and activation of endothelial cells," *Diabetes*, vol. 53, no. 8, pp. 2117–2121, 2004.

[38] J. Takaya, Y. Iwamoto, H. Higashino, R. Ishihara, and Y. Kobayashi, "Increased intracellular calcium and altered phorbol dibutyrate binding to intact platelets in young subjects with insulin-dependent and non-insulin- dependent diabetes mellitus," *Metabolism*, vol. 46, no. 8, pp. 949–953, 1997.

[39] I. Jardín, P. C. Redondo, G. M. Salido, J. A. Pariente, and J. A. Rosado, "Endogenously generated reactive oxygen species reduce PMCA activity in platelets from patients with non-insulin-dependent diabetes mellitus," *Platelets*, vol. 17, no. 5, pp. 283–288, 2006.

[40] P. Andre, T. Morooka, D. Sim et al., "Critical role for Syk in responses to vascular injury," *Blood*, vol. 118, no. 18, pp. 5000–5010, 2011.

[41] L. Colonna, G. Catalano, C. Chew et al., "Therapeutic targeting of Syk in autoimmune diabetes," *Journal of Immunology*, vol. 185, no. 3, pp. 1532–1543, 2010.

[42] C. Schulz, N. V. Leuschen, T. Fröhlich et al., "Identification of novel downstream targets of platelet glycoprotein VI activation by differential proteome analysis: implications for thrombus formation," *Blood*, vol. 115, no. 20, pp. 4102–4110, 2010.

[43] W. H. Tang, J. Stitham, S. Gleim et al., "Glucose and collagen regulate human platelet activity through aldose reductase induction of thromboxane," *Journal of Clinical Investigation*, vol. 121, no. 11, pp. 4462–4476, 2011.

Hindawi Publishing Corporation
Journal of Diabetes Research
Volume 2013, Article ID 986906, 8 pages
http://dx.doi.org/10.1155/2013/986906

Methodology Report

Methods and Models for Metabolic Assessment in Mice

G. Pacini,[1] B. Omar,[2] and B. Ahrén[2]

[1] *Metabolic Unit, ISIB CNR, 35127 Padova, Italy*
[2] *Department of Medicine, Lund University, 221 84 Lund, Sweden*

Correspondence should be addressed to G. Pacini; giovanni.pacini@isib.cnr.it

Received 28 December 2012; Accepted 23 April 2013

Academic Editor: Daisuke Koya

The development of new therapies for the treatment of type 2 diabetes requires robust, reproducible and well validated *in vivo* experimental systems. Mice provide the most ideal animal model for studies of potential therapies. Unlike larger animals, mice have a short gestational period, are genetically similar, often give birth to many offspring at once and can be housed as multiple groups in a single cage. The mouse model has been extensively metabolically characterized using different tests. This report summarizes how these tests can be executed and how arising data are analyzed to confidently determine changes in insulin resistance and insulin secretion with high reproducibility. The main tests for metabolic assessment in the mouse reviewed here are the glucose clamp, the intravenous and the oral glucose tolerance tests. For all these experiments, including some commonly adopted variants, we describe: (i) their performance; (ii) their advantages and limitations; (iii) the empirical formulas and mathematical models implemented for the analysis of the data arising from the experimental procedures to obtain reliable measurements of peripheral insulin sensitivity and beta cell function. Finally, a list of previous applications of these methods and analytical techniques is provided to better comprehend their use and the evidences that these studies yielded.

1. Introduction

The global incidence of type 2 diabetes is predicted to grow rapidly also in the coming decades as more countries develop economically and overweight and obesity spread to populations with a genetic predisposition to the development of the disease [1]. These factors make the need for effective diabetes therapies that much greater. The development of new therapies for the treatment of type 2 diabetes requires robust, reproducible, and well validated *in vivo* experimental systems. Of particular importance are preclinical *in vivo* models, since these may select and refine experimental models for further studies and drug development in humans. There are multiple animal models of insulin resistance and decreased beta cell function including genetically deficient mice and rats as well as mouse and rat strains fed a high energy diet. Mice may provide the most ideal animal model for studies of potential type 2 diabetes therapies. Unlike larger animals, mice have a short gestational period, often give birth to many offspring at once, and can be housed in multiple groups in a single cage. This makes "in house" breeding less expensive and makes it easier to generate larger numbers to obtain well-powered studies. Gene deletion and overexpression technology have been well established in mice for over two decades, allowing researchers to create single gene mutant mice that display phenotypes which are useful in the development of type 2 diabetes therapy [2]. There are also mouse models of type 2 diabetes that have arisen due to spontaneous mutations such as the leptin deficient ob/ob and leptin receptor deficient db/db mice [3].

The C57/BL6 mouse strain fed a high-fat diet is a commonly used animal model in the development of potential therapies for type 2 diabetes [4]. These mice fed a high-fat diet for a short period of time (3–8 weeks) become obese and severely insulin resistant and develop postglucose load hyperglycemia, fasting hyperinsulinemia, and a diminished first phase insulin response [4, 5]. These phenotypic characteristics resemble some of the phenotypic characteristics of type 2 diabetes in humans and as such make the model a useful tool for studying potential type 2 diabetes therapies.

The advantages of the C57/BL6 high-fat diet mouse model in studies of potential type 2 diabetes treatments are numerous. The strain itself has been inbred for hundreds of generations and its genome has been sequenced, resulting

in no interindividual variation in genetic background and very little phenotypic variability. With little interindividual variation, studies can be done on fewer animals without losing statistical power which makes it a very cost effective model system. Unlike single gene mutant models of type 2 diabetes, the high-fat diet models have no deficiency of a single gene meaning that all therapeutic approaches can be applied regardless of mode of action. Additional advantages include a short generation time. Upon delivery a study can be executed in as little as five weeks and the availability of precondition high-fat diet mice, which are ready for experimentation on delivery, has also become more widely available. The high-fat diet mouse model has been extensively metabolically characterized using different metabolic tests [6]. This report aims to summarize how these tests are performed and how arising data are analyzed to confidently determine changes in peripheral insulin sensitivity and beta cell function with high reproducibility.

2. Experimental Tests

In general, we refer to animals weighting 20 to 25 grams. All the following considerations apply to the mouse in general, regardless of the specific strain and whether is a wild type or transgenic. Mice should be handled under anesthesia to allow serial sampling from the preorbital plexus with a lower degree of stress. Example of anesthesia is intraperitoneal injection of midazolam (0.4 mg/mouse) and a combination of fluanison (0.9 mg/mouse) and fentanyl (0.02 mg/mouse). This kind of anesthesia persists for approximately 1 h. If the experimental procedure is longer (for instance the clamp experiments; see below), the administration of anesthetics is repeated every 60 min. During the whole procedure, animals should be kept on a heating pad.

3. Metabolic Tests for Insulin Sensitivity and Secretion

3.1. Five-Hour Fasting Measurements. Sometimes, performing a dynamic test may not be possible and the investigator must only rely on a single sample drawn in a steady-state condition for which both glucose (G_0) and insulin (I_0) are measured. In humans, in such conditions, insulin resistance is evaluated with the HOMA model and insulin sensitivity with the log-reciprocal QUICKI formula [7] by using overnight fasting measurements. In the mouse, a long fasting means starvation with profound exhaustion of glycogen reserves and also the counterregulatory implications that this condition implies. Instead, a period of 5 hours fasting is considered to be adequate for a definition of fasting in the small rodents since it avoids massive reduction in body fat content and glycogen [8, 9].

Recent studies proposed that HOMA (and thus QUICKI) measurements refer mostly to the liver (insulin mediated inhibition of hepatic glucose production) rather than describing peripheral insulin sensitivity [10]. Extending these concepts to the mice, liver insulin sensitivity [11] can be then calculated as $1/(\log G_0 + \log I_0)$. With the same approach, beta cell secretion is represented by I_0, while beta cell function can be described by I_0/G_0. Of course, these measurements refer to posthepatic hormone appearance. For a better determination of true beta cell activity, measuring C-peptide is advisable. In fact, it is equimolarly released with insulin but not degraded in the liver; thus, its peripheral concentration reflects directly the islet release of insulin.

3.2. Glucose Clamp

3.2.1. Rationale. In humans the gold standard test is the euglycemic-hyperinsulinemic glucose clamp [12]. By maintaining glucose concentration basically constant at a target level by means of glucose infusion despite exogenously produced elevated insulin levels, this test provides an absolute index of insulin sensitivity, given by the glucose infusion rate when glucose concentration is kept at a constant steady state. The more glucose is needed, the higher is the insulin action (insulin sensitivity) on glucose uptake by peripheral tissues. If insulin levels are different among the various animals, glucose infusion must be normalized to the prevailing steady-state insulin concentration.

3.2.2. Experimental Procedure. In the anesthetized mouse, the right jugular vein and the left carotid artery are catheterized. The venous catheter is used for infusion of glucose and insulin, and the arterial catheter is used for sampling. Thirty minutes after introduction of the catheters, synthetic human insulin is infused at a rate of 60 mU/kg min^{-1} for 1 min, followed by a continuous and constant infusion of 30 mU/kg min^{-1}. The volume load is 4 mL for the 1st min, followed by 2 mL/min thereafter. Blood glucose levels are determined at 5 min intervals for 120 min. A variable rate of glucose (solution of 40 g/dL) is infused to maintain blood glucose levels at 100–120 mg/dL. A blood sample is taken at 60, 90, and 120 min for determination of plasma insulin. More details can be found in previous reports [13, 14]. When the purpose of a work is examining insulin sensitivity, the glucose level during the steady state is targeting euglycemia, that is, ≈6 mmol/L. The glucose clamp technique may, however, be used also for other purposes than determining insulin sensitivity. One such possibility is to evaluate glucose counter-regulatory mechanisms during hypoglycemia. Then, levels below baseline are targeted, for example, 2.5 mmol/L, and factors involved in the counterregulation, like glucagon, may be measured. Alternatively, the clamp may be used to estimate insulin secretory responses to standardized raised glucose levels by targeting hyperglycemia values, like 8.3 or 11.1 mmol/L. Therefore, although the main purpose of the clamp technique is usually that of maintaining euglycemia in spite of hyperinsulinemia for measurements of insulin sensitivity, the glucose clamp technique may be used for a variety of other scientific purposes with only slight modifications. Examples of eu- and hypoglycemic clamps are shown in Figure 1. The technique may also be used for distinguishing between hepatic versus peripheral insulin sensitivity by administering radiolabelled glucose in the infusate. Then, a bolus injection of [3-^{3}H]glucose is given, followed by

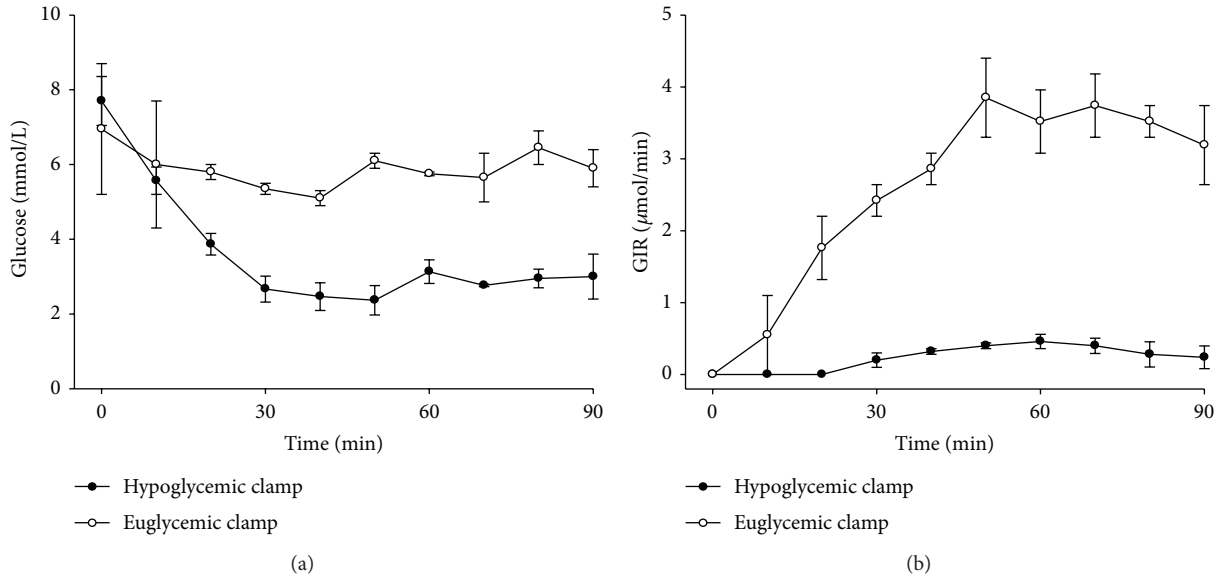

Figure 1: Example of glucose clamp experiments. Glucose levels and glucose infusion rates (mean ± SEM) during euglycemic clamp (aiming at the target level of 6 mmol/L glucose, $n = 4$) and hypoglycemic clamp (aiming at 2.5 mmol/L glucose, $n = 3$) in C58BL/6J mice. GIR is glucose infusion rate in the two cases.

a continuous infusion of [3-^{3}H]glucose throughout the study period. Blood samples are taken at steady state (60 and 90 min after the start of the infusion) for the determination of [3-^{3}H]glucose concentration [15].

3.2.3. Data Analysis. Insulin sensitivity is calculated as the glucose infusion rate during the second hour (M) divided by the mean insulin concentration at 60, 90, and 120 min (I), and the clamp glucose clearance per unit of insulin is calculated as M/I divided by the clamped glucose concentration. Since insulin is exogenously administered, this test does not provide any assessment of beta cell secretion for which a hyperglycemic clamp test needs to be performed. When using tritiated glucose, basal endogenous glucose production (EGP) is calculated by dividing the rate of infusion of [3-^{3}H]glucose by the plasma glucose specific activity; glucose appearance at 90 min is measured by dividing the infusion rate in dpm by the plasma glucose specific activity at this time point. EGP at this time is calculated by subtracting the glucose infusion rate from the glucose appearance rate. Finally, the glucose disposal rate is calculated as the glucose appearance rate divided by the glucose concentration.

3.3. Intravenous Glucose Tolerance Test (IVGTT)

3.3.1. Rationale. With this test, the steady state is perturbed by an injection of glucose; this directly stimulates insulin release which makes glucose to be taken up by peripheral tissues and hepatic glucose production to be inhibited. The rate of lowering of the glucose concentration for the prevailing insulin concentration is an index of insulin action. The insulin concentration is at the same time an index of the ability of the pancreas to release the hormone under the glucose stimulation.

3.3.2. Experimental Procedure. In the anesthetized mouse, a blood sample is taken from the retrobulbar intraorbital capillary plexus into a 100 mL pipette that had been prerinsed in heparin solution (100 U/mL in 0.9% NaCl). Thereafter, D-glucose (solution of 10 g/dL) is injected intravenously over 3 sec at a dose of 1 g/kg in a tail vein without flushing of the 27-gauge needle after injection. The volume load is 10 mL/g body wt. The dose of 1 g/kg is quite high, because of the rapid metabolism in mice; in fact, a rise in insulin is observed only at 1 min, and rarely at 5 min, when giving lower doses of glucose such as 0.3 or 0.25 g/kg. At 1, 5, 10, 20, 30, and 50 min after injection, blood samples (75 mL each) are collected. The first sample is at 1 min, because by that time, the mixing phase of the glucose bolus could be considered terminated; the last sample is at 50 min to avoid possible influence on the measurements of awakening from anesthesia. An example is depicted in the left panel of Figure 2.

3.3.3. Data Analysis. The net glucose elimination rate after the glucose injection (K_G, the glucose tolerance index) is calculated as the slope for the interval 1–20 min after glucose injection of the logarithmic transformation of the individual plasma glucose values. Insulin sensitivity is estimated with the minimal-model technique. The model assumes first-order, nonlinear, insulin-controlled kinetics and accounts for the effect of insulin and glucose alone on net glucose disappearance. This modeling analysis that uses the whole data set from 0 to the end of the experiment provides the parameter S_I (insulin sensitivity index), which is defined as the ability of insulin to enhance net glucose disappearance and inhibit glucose production, and the parameter S_G, which is the glucose effectiveness, representing net glucose disappearance per se from plasma without any change in dynamic insulin. The glucose distribution volume is calculated as the ratio of

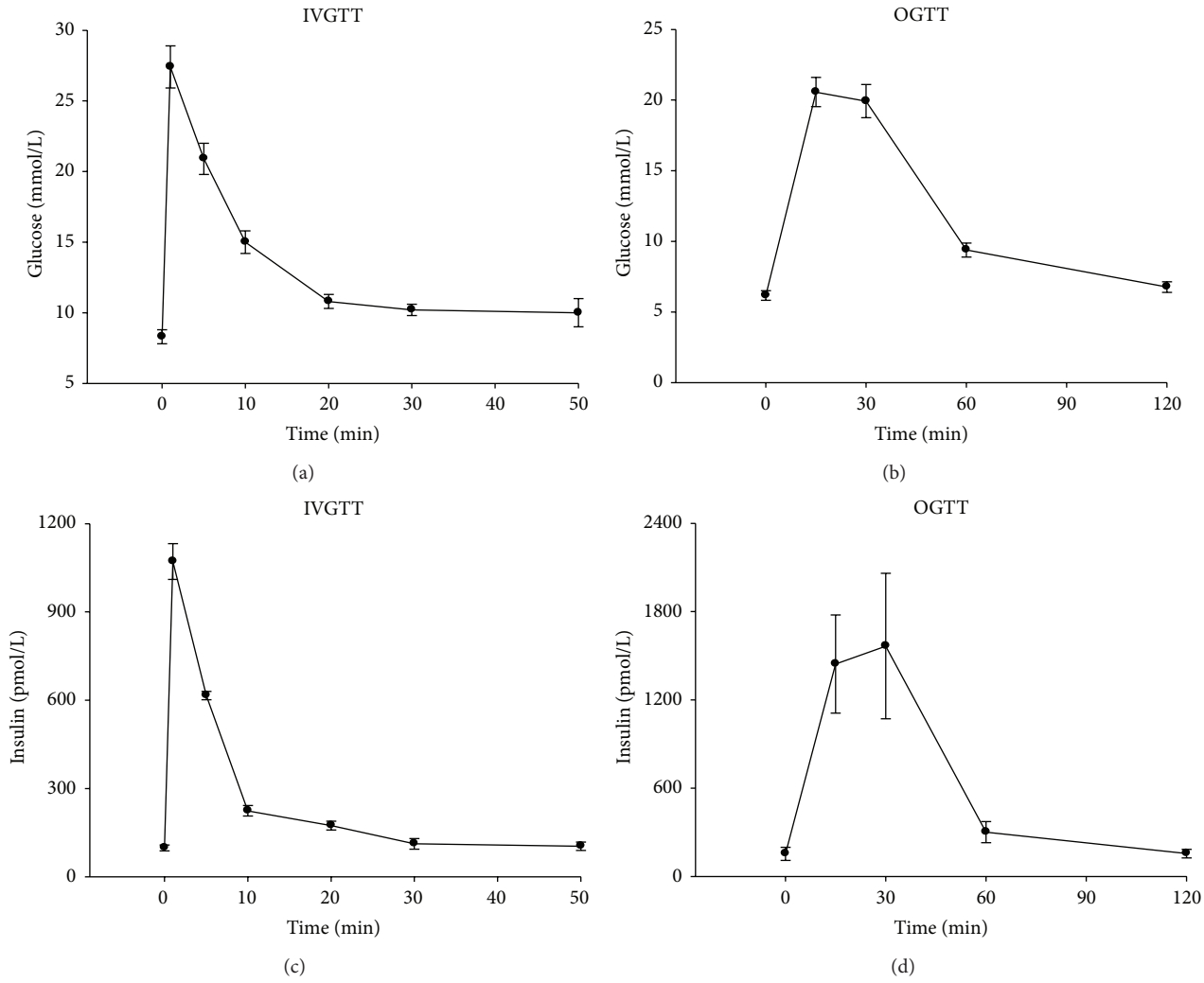

Figure 2: Example of outcomes from metabolic tests. Glucose and insulin levels (means ± sem) after intravenous (1 g/kg; $n = 18$) or oral (75 mg; $n = 27$) glucose administration in normal C57/BL6 mice.

the glucose dose to the difference between the extrapolated zero intercept (a model parameter) and glucose basal level.

In order to simplify the procedure for obtaining an insulin sensitivity index, a simple formula has been developed. In previous studies, it has been shown that the tolerance index K_G (see above) is linearly related to the disposition index, which is a function of insulin sensitivity. In addition, it has been clearly demonstrated that the insulin sensitivity index depends upon the glucose disappearance rate and the suprabasal concentration that follows the glucose stimulation. We applied a similar approach to relate K_G to the metabolic parameter under the assumption that an index of insulin sensitivity should be linearly related to the ratio of $K_G/\Delta\text{AUC}_{\text{ins}}$. $\Delta\text{AUC}_{\text{ins}}$ is defined in this case as the dynamic area under the insulin curve in the IVGTT interval 0–50 min divided by the length of the interval. This ratio, called computed insulin sensitivity (*CSI*) has been shown to be a valid surrogate of S_I from the minimal model for an easy use of IVGTT data. For further details on the exploitation of this method, we refer to the original publication [16], where also the additional calculation of S_G is clearly explained.

Acute insulin secretion (AIR), calculated as the mean of suprabasal 1 and 5 min insulin levels, represents the early phase insulin response, while the total area under the insulin curve ($\text{AUC}_{\text{insulin}}$) describes the total insulin release. When $\text{AUC}_{\text{insulin}}$ is divided by $\text{AUC}_{\text{glucose}}$, an index of glucose-mediated beta cell function can be obtained.

The IVGTT technique just described, however, requires a sufficient insulin response to the intravenous administration of glucose for a reliable estimation of the parameters. When the animals exhibit severe bluntness of glucose-stimulated insulin secretion and low serum levels of insulin in association with hyperglycemia, it is not possible to quantify S_I from a regular IVGTT. In fact, the suppression of insulin secretion may be so severe that hardly any suprabasal elevation of plasma insulin followed the glucose challenge is observed, making it impossible to use the model. In this case, insulin can be injected exogenously along with glucose (insulin-modified IVGTT) [17] or substances stimulating insulin release [18, 19]. However, the achieved peripheral concentration could be too high if some residual beta cell capacity has remained. In order to achieve the desired insulin levels, it is

recommended to use the diazoxide-supplemented glucose-insulin test (DSGIT), for the establishment of dynamic insulin sensitivity in mice. This technique was applied for exploring insulin sensitivity in the RIP-DN HNF-1α mice [20]. The DSGIT is based on the potent action of diazoxide to suppress insulin secretion [17]. The procedure is the following: 30 min after anesthesia, diazoxide (25 mg/kg) is given as a subcutaneous injection. Then, 10 min later, D-glucose (1 g/kg) is given intravenously together with human insulin (doses ranging 0.1–0.4 U/kg). The volume load is in this case 10 μL/g body wt. the performance of the IVGTT (sampling and assays) occurs as previously described.

It is known that insulin resistance such as in obesity is associated with an increased insulin secretion. Several studies in humans have demonstrated that a nonlinear inverse relationship (hyperbola-like) describes the physiological regulating system which allows insulin sensitivity and secretion to move in opposite directions, so that the ability of the normal subject to dispose of glucose remains relatively constant [21–23]. This constant with the IVGTT is called *disposition index* and is calculated with the product of the insulin sensitivity index times the acute insulin response, as the average of the insulin concentration during the first minutes after the glucose bolus. The hyperbolic relationship also means that a change in one of the variables is mirrored by a reciprocal change in the other variable and the understanding of this relationship is fundamental for an accurate comprehension of the nature of type 2 diabetes. Also in mice, a hyperbolic relationship was evident when plotting insulin sensitivity versus insulin secretion [17, 24] and therefore also in mice it was possible to calculate a disposition index. This has offered a tool for experimental analysis of the mechanisms regulating the interrelationships between insulin action and secretion and for studies of potential treatment modalities in mice [19].

The use of measurements related to circulating insulin concentration, however, does not necessarily allow information on insulin secretion, since only posthepatic insulin delivery is considered. The role of hepatic insulin extraction should in fact also be taken into account if we are interested in evaluating the beta cell function, that is, how the cell directly changes hormone release in response to changes in insulin sensitivity. To this aim, it is necessary to include in the analysis also C-peptide, which can be evaluated with either the area under the curve or concentration values at specific time points. Therefore, as a further development of the use of the hyperbolic relationship, by using S_I from the minimal model or *CSI* and beta cell parameters from C-peptide analysis, an index of how capable the beta cell is of adapting its secretion to changes in insulin resistance can be derived. This index thus assesses true insulin secretion in relation to insulin sensitivity; it has been called *adaptation index* and, together with the classic disposition index, provides a comprehensive picture of the mechanism of the beta cell functioning in relation to the prevailing insulin resistance.

3.4. Oral Glucose Tolerance Test (OGTT)

3.4.1. Rationale. This should be considered the most physiological test, since it mimics the correct route (i.e., orally) of assuming carbohydrates. The ingested glucose (usually instilled into the stomach) is absorbed in the intestinal tract and enters the splanchnic circulation and then into the systemic circulation. The increased blood glucose concentration stimulates the pancreatic beta cell to release insulin, which stimulates glucose uptake by peripheral tissues. The passage of the nutrients through the early part of the intestine stimulates the release of the gut hormones (e.g., glucose-dependent insulinotropic polypeptide, GIP, and glucagon-like peptide-1, GLP-1), which in turn augment the beta cell sensitivity to glucose, increasing the production of insulin.

3.4.2. Experimental Procedure. In the 30 min period after anesthesia, a gavage tube (outer diameter 1.2 mm) is placed in the stomach to be used to administer glucose (dose 75 mg/mouse) in few seconds (standardized volume of 0.5 mL, approximate energy content 0.171 kcal). Blood samples are collected from the retrobulbar, intraorbital, capillary plexus into heparinized tubes before and either 5, 10, and 20 min or 15, 30, 60, and 90 min after oral gavage. An example is depicted in the right panel of Figure 2.

3.4.3. Data Analysis. Several different possibilities exist to estimate insulin sensitivity by using empirical methods and mathematical modeling.

ISI Comp. This empirical method is the application in rodents of the widely used formula in humans, called also Matsuda's method [25]. It is simply calculated as $10000/(\sqrt{[G_0 \times I_0 \times G_{\text{mean}} \times I_{\text{mean}}]})$, where the suffix *mean* indicates the average value of glucose and insulin concentration measurements during the whole length of the test. This formula provides a measure of insulin sensitivity.

OGIS. Modeling glucose-insulin interrelationships are the basis of this method that provides a value of insulin-mediated glucose clearance that reflects insulin action. The final formula is quite complex [26], but its exploitation is easy, offering the possibility of downloading it from internet (http://webmet.pd.cnr.it/ogis/, last checked May 15, 2013). The formula requires the animal's body weight, the exact dose of administered glucose, and glucose and insulin concentration at specific samples.

However, there is not yet validated model-derived method to assess insulin secretion or beta cell function, except the use of the area under the concentration curves (AUC). Insulin secretion can be evaluated by AUC_{ins}, while beta cell function can be obtained by $\text{BCI}_{\text{oral}} = \text{AUC}_{\text{ins}}/\text{AUC}_{\text{gluc}}$. It is interesting to note that, if also GIP and/or GLP-1 have been measured during the test, it is possible to evaluate an index for the incretin effect as $\text{BCI}_{\text{oral}}/\text{AUC}_{\text{incr}}$ where AUC_{incr} is the AUC of the measured incretin concentration. If the main purpose of this study is the evaluation of the performance of the beta cell, it is again advisable to measure C-peptide, instead of insulin, under the premises that in these small animals blood withdrawn must be limited and only two compounds can be measured at one time. A more direct figure of the beta cell function can therefore be obtained from C-peptide as

$BCP_{oral} = AUC_{cp}/AUC_{gluc}$. Similarly, the incretin effect on the real beta cell release is obtained by BCP_{oral}/AUC_{incr}.

Even though a definition of disposition index during OGTT has never been provided, it is accepted that the product of insulin sensitivity times insulin secretion still yields a quantitative figure of the adaptive mechanism between beta cell function and insulin resistance. Albeit these indices have never been thoroughly validated during the OGTT, a possible disposition index is the product of $OGIS \times BCI_{oral}$, while the adaptation index can be derived as $OGIS \times BCP_{oral}$.

3.5. Combining Oral and Intravenous Glucose Tests. An interesting and important physiological implication of oral glucose administration is the marked increase in gut hormones elicited by the glucose. These hormones are the so-called incretin hormones which stimulate insulin secretion in a glucose-dependent manner, for example, GIP and GLP-1. In humans, the incretin concept was initially demonstrated in 1964 by two studies showing that an oral glucose administration elicited a much higher insulin response than an intravenous glucose administration, in spite of a lower glucose level [27, 28]. By combining oral and intravenous glucose administration and thereby adjust the intravenous glucose infusion rate to achieve matching glucose concentration allows for a quantification of the importance of incretin factors (mainly GIP and GLP-1) for islet function after oral glucose. Such a study in mice shows that approximately 50% of the insulin secretory response (measured by C-peptide) following oral glucose administration is due to the incretin effect and not to glucose and, interestingly, that this relative contribution of incretin hormones is higher in high-fat fed mice, suggesting that the incretin factors behave as an adaptation mechanism [6].

4. Discussion

We have presented the most common methods to carry out metabolic studies in the mouse, particularly to obtain the main parameters related to glucose tolerance, that is, insulin sensitivity and beta cell function, and the variables describing the mechanisms of the beta cell to adapt insulin secretion to the prevailing insulin resistance. The value of the use of the tests in these animals is that the mouse is a good model for specific diseases (diabetes), for basic physiology (aging and obesity), and for the development of new drugs. All the above tests in fact can be performed in any different mouse strain and in several conceivable conditions. The overarching goal of the metabolic tests is the understanding of the etiology of diabetes and of its complications, by exploring different situations and the effects of several endogenously produced or exogenously given compounds. For instance, both the IVGTT and OGTT have been used for evaluating the insulin secretory capacity of different doses of pituitary adenylate cyclase-activating polypeptide (PACAP) [18] and glucagon-like peptide-1 (GLP-1) [19]; for the assessment of GLP-1 effects on different processes involved in glucose homeostasis [29–31]; for a metabolic picture of gastrin-releasing peptide receptor gene-deficient mice [32] and of IGF-I [33] and hepatocyte nuclear factor (HNF)-1α [19] transgenic mice; for assessing the effect on insulin secretion and sensitivity of different compounds such as ghrelin [34], galanin [35], and acylation stimulating protein [36]; and for estimating the role of different nutrients on insulin resistance and beta cell function in different mouse strains [37–39]. The techniques have also been used in mice metabolically challenged with high-fat diets resulting in insulin resistance with islet adaptation [6, 24, 38].

The application of mouse models to the studying of metabolic derangements due to overfeeding and obesity recently assumed even more importance. In fact, with the economic, technological, and agricultural developments of the last century, access to adequate food supplies is the most widespread in human history. Unfortunately, this has, together with increasing sedentary life style with less physical activity, led to a global increase in the incidence of overweight and obesity. The global increase in overweight and obesity has created near epidemics in obesity related diseases such as cardiovascular disease and type 2 diabetes [40]. Overweight and obesity correlate strongly with diminished insulin sensitivity [41] and it is known since long time that most individuals are able to counteract the decreased insulin sensitivity by increasing insulin secretion and beta cell function [42]. In many individuals, the improvements in beta cell function are not maintained over a longer period, however, and a slow decline of beta cell function is the result [43]. The result of the decline in beta cell function is a progressive increase in fasting and postprandial hyperglycemia and the development of diabetes. Mice studies, given the relative easiness of inducing different adiposity conditions, may reveal paramount to understand the etiology, progress, and possible remedies against the obesity pandemic.

It is worth noting that no specific test has been created for the mouse, but all of them are just tests developed in humans and then adapted to animals. In some cases, like in the OGTT, the data analysis is totally similar to that for human data, while the this simplified IVGTT and the minimal model have been tailored to the size of the animal which allows only the collection of a limited number of samples. In this case, being the IVGTT in mice a sort of unexplored test, it has been necessary validating it against the gold standard (even in the animals) glucose clamp [17]. However, the IVGTT with minimal modeling assessment of insulin sensitivity and glucose effectiveness still remains a quite complex method that requires a certain skill of the operator and a wise interpretation of the modeling outputs. For this reason, a simplified, but still validated, method has been devised [16] for a reliable assessment of those fundamental parameters. It is interesting to note that, at variance with the common procedure, this simplified method developed in the mouse has been then successfully extended to humans [44].

In summary, we reviewed the main tests for metabolic assessment in the mouse and analyzed the corresponding techniques for obtaining the needed information from the data arising from the experimental procedures. We provided a list of previous applications of these methods to better comprehend their use and the evidences that these studies yielded.

References

[1] H. King, R. E. Aubert, and W. H. Herman, "Global burden of diabetes, 1995–2025: prevalence, numerical estimates, and projections," *Diabetes Care*, vol. 21, no. 9, pp. 1414–1431, 1998.

[2] T. Kadowaki, "Insights into insulin resistance and type 2 diabetes from knockout mouse models," *Journal of Clinical Investigation*, vol. 106, no. 4, pp. 459–465, 2000.

[3] R. C. Davis, L. W. Castellani, M. Hosseini et al., "Early hepatic insulin resistance precedes the onset of diabetes in obese C57BLKS-db/db mice," *Diabetes*, vol. 59, pp. 1616–1625, 2010.

[4] M. S. Winzell, G. Pacini, C. B. Wollheim, and B. Ahrén, "β-cell-targeted expression of a dominant-negative mutant of hepatocyte nuclear factor-1α in mice: diabetes model with β-cell dysfunction partially rescued by nonglucose secretagogues," *Diabetes*, vol. 53, no. 3, pp. S92–S96, 2004.

[5] M. S. Winzell, C. Magnusson, and B. Ahrén, "Temporal and dietary fat content-dependent islet adaptation to high-fat feeding-induced glucose intolerance in mice," *Metabolism*, vol. 56, no. 1, pp. 122–128, 2007.

[6] B. Ahrén, M. S. Winzell, and G. Pacini, "The augmenting effect on insulin secretion by oral versus intravenous glucose is exaggerated by high-fat diet in mice," *Journal of Endocrinology*, vol. 197, no. 1, pp. 181–187, 2008.

[7] G. Pacini and A. Mari, "Methods for clinical assessment of insulin sensitivity and β-cell function," *Best Practice and Research: Clinical Endocrinology and Metabolism*, vol. 17, no. 3, pp. 305–322, 2003.

[8] A. Agouni, C. Owen, A. Czopek, N. Mody, and M. Delibegovic Mirela, "*In vivo* differential effects of fasting, re-feeding, insulin and insulin stimulation time course on insulin signaling pathway components in peripheral tissues," *Biochemical and Biophysical Research Communications*, vol. 401, no. 1, pp. 104–111, 2010.

[9] E. Mutel, A. Gautier-Stein, A. Abdul-Wahed et al., "Control of blood glucose in the absence of hepatic production during prolonged fasting in mice," *Diabetes*, vol. 60, pp. 3121–3131, 2011.

[10] M. A. Abdul-Ghani, C. P. Jenkinson, D. K. Richardson, D. Tripathy, and R. A. DeFronzo, "Insulin secretion and action in subjects with impaired fasting glucose and impaired glucose tolerance: results from the veterans administration genetic epidemiology study," *Diabetes*, vol. 55, no. 5, pp. 1430–1435, 2006.

[11] P. D. Home and G. Pacini, "Hepatic dysfunction and insulin insensitivity in type 2 diabetes mellitus: a critical target for insulin-sensitizing agents," *Diabetes, Obesity and Metabolism*, vol. 10, no. 9, pp. 699–718, 2008.

[12] R. A. DeFronzo, J. D. Tobin, and R. Andres, "Glucose clamp technique: a method for quantifying insulin secretion and resistance," *The American Journal of Physiology*, vol. 237, no. 3, pp. E214–E223, 1979.

[13] R. O. Deems, J. L. Evans, R. W. Deacon et al., "Expression of human GLUT4 in mice results in increased insulin action," *Diabetologia*, vol. 37, no. 11, pp. 1097–1104, 1994.

[14] K. D. Niswender, M. Shiota, C. Postic, A. D. Cherrington, and M. A. Magnuson, "Effects of increased glucokinase gene copy number on glucose homeostasis and hepatic glucose metabolism," *Journal of Biological Chemistry*, vol. 272, no. 36, pp. 22570–22575, 1997.

[15] G. Bryzgalova, H. Gao, B. Ahrén et al., "Evidence that oestrogen receptor-α plays an important role in the regulation of glucose homeostasis in mice: insulin sensitivity in the liver," *Diabetologia*, vol. 49, no. 3, pp. 588–597, 2006.

[16] G. Pacini, M. Ahrén, and B. Ahrén, "Reappraisal of the intravenous glucose tolerance index for a simple assessment of insulin sensitivity in mice," *American Journal of Physiology—Regulatory Integrative and Comparative Physiology*, vol. 296, no. 5, pp. R1316–R1324, 2009.

[17] G. Pacini, K. Thomaseth, and B. Ahrén, "Contribution to glucose tolerance of insulin-independent vs. insulin-dependent mechanisms in mice," *American Journal of Physiology—Endocrinology and Metabolism*, vol. 281, no. 4, pp. E693–E703, 2001.

[18] K. Filipsson, G. Pacini, A. J. W. Scheurink, and B. Ahrén, "PACAP stimulates insulin secretion but inhibits insulin sensitivity in mice," *American Journal of Physiology—Endocrinology and Metabolism*, vol. 274, no. 5, pp. E834–E842, 1998.

[19] B. Ahrén and G. Pacini, "Dose-related effects of GLP-1 on insulin secretion, insulin sensitivity, and glucose effectiveness in mice," *American Journal of Physiology—Endocrinology and Metabolism*, vol. 277, no. 6, pp. E996–E1004, 1999.

[20] B. Ahrén and G. Pacini, "A novel approach to assess insulin sensitivity reveals no increased insulin sensitivity in mice with a dominant-negative mutant hepatocyte nuclear factor-1α," *American Journal of Physiology—Regulatory Integrative and Comparative Physiology*, vol. 291, no. 1, pp. R131–R137, 2006.

[21] S. E. Kahn, R. L. Prigeon, D. K. McCulloch et al., "Quantification of the relationship between insulin sensitivity and β-cell function in human subjects: evidence for a hyperbolic function," *Diabetes*, vol. 42, no. 11, pp. 1663–1672, 1993.

[22] B. Ahrén and G. Pacini, "Importance of quantifying insulin secretion in relation to insulin sensitivity to accurately assess beta cell function in clinical studies," *European Journal of Endocrinology*, vol. 150, no. 2, pp. 97–104, 2004.

[23] B. Ahrén and G. Pacini, "Islet adaptation to insulin resistance: mechanisms and implications for intervention," *Diabetes, Obesity and Metabolism*, vol. 7, no. 1, pp. 2–8, 2005.

[24] B. Ahrén and G. Pacini, "Insufficient islet compensation to insulin resistance vs. reduced glucose effectiveness in glucose-intolerant mice," *American Journal of Physiology—Endocrinology and Metabolism*, vol. 283, no. 4, pp. E738–E744, 2002.

[25] M. Matsuda and R. A. DeFronzo, "Insulin sensitivity indices obtained from oral glucose tolerance testing: comparison with the euglycemic insulin clamp," *Diabetes Care*, vol. 22, no. 9, pp. 1462–1470, 1999.

[26] A. Mari, G. Pacini, E. Murphy, B. Ludvik, and J. J. Nolan, "A model-based method for assessing insulin sensitivity from the oral glucose tolerance test," *Diabetes Care*, vol. 24, no. 3, pp. 539–548, 2001.

[27] H. Elrick, L. Stimmler, C. J. Hlad, and Y. Arai, "Plasma insulin responses to oral and intravenous glucose administration," *The Journal of Clinical Endocrinology and Metabolism*, vol. 24, pp. 1076–1082, 1964.

[28] N. Mcintyre, C. D. Holdsworth, and D. S. Turner, "New interpretation of oral glucose tolerance," *The Lancet*, vol. 284, no. 7349, pp. 20–21, 1964.

[29] B. Ahrén, K. Thomaseth, and G. Pacini, "Reduced insulin clearance contributes to the increased insulin levels after administration of glucagon-like peptide 1 in mice," *Diabetologia*, vol. 48, no. 10, pp. 2140–2146, 2005.

[30] K. Thomaseth, A. Pavan, G. Pacini, and B. Ahrén, "Glucagon-like peptide-1 accelerates the onset of insulin action on glucose disappearance in mice," *American Journal of Physiology—Endocrinology and Metabolism*, vol. 292, no. 6, pp. E1808–E1814, 2007.

[31] G. Pacini, K. Thomaseth, and B. Ahrén, "Dissociated effects of glucose-dependent insulinotropic polypeptide vs glucagon-like peptide-1 on β-cell secretion and insulin clearance in mice," *Metabolism*, vol. 59, no. 7, pp. 988–992, 2010.

[32] K. Persson, G. Pacini, F. Sundler, and B. Ahrén, "Islet function phenotype in gastrin-releasing peptide receptor gene-deficient mice," *Endocrinology*, vol. 143, no. 10, pp. 3717–3726, 2002.

[33] K. Sjögren, K. Wallenius, J. L. Liu et al., "Liver-derived IGF-I is of importance for normal carbohydrate and lipid metabolism," *Diabetes*, vol. 50, no. 7, pp. 1539–1545, 2001.

[34] M. K. Reimer, G. Pacini, and B. Ahrén, "Dose-dependent inhibition by ghrelin of insulin secretion in the mouse," *Endocrinology*, vol. 144, no. 3, pp. 916–921, 2003.

[35] B. Ahrén, G. Pacini, D. Wynick, N. Wierup, and F. Sundler, "Loss-of-function mutation of the galanin gene is associated with perturbed islet function in mice," *Endocrinology*, vol. 145, no. 7, pp. 3190–3196, 2004.

[36] B. Ahrén, P. J. Havel, G. Pacini, and K. Cianflone, "Acylation stimulating protein stimulates insulin secretion," *International Journal of Obesity*, vol. 27, no. 9, pp. 1037–1043, 2003.

[37] M. S. Winzell, G. Pacini, and B. Ahrén, "Insulin secretion after dietary supplementation with conjugated linoleic acids and n-3 polyunsaturated fatty acids in normal and insulin-resistant mice," *American Journal of Physiology—Endocrinology and Metabolism*, vol. 290, no. 2, pp. E347–E354, 2006.

[38] B. Omar, G. Pacini, and B. Ahrén, "Differential development of glucose intolerance and pancreatic islet adaptation in multiple diet induced obesity models," *Nutrients*, vol. 4, pp. 1367–1381, 2012.

[39] L. Ahlkvist, J. Vikman, G. Pacini, and B. Ahrén, "Synergism by individual macronutrients explains the marked early GLP-1 and islet hormone responses to mixed meal challenge in mice," *Regulatory Peptides*, vol. 178, no. 1–3, pp. 29–35, 2012.

[40] D. W. Lam and D. LeRoith, "The worldwide diabetes epidemic," *Current Opinion in Endocrinology, Diabetes and Obesity*, vol. 19, pp. 93–96, 2012.

[41] B. B. Kahn and J. S. Flier, "Obesity and insulin resistance," *The Journal of Clinical Investigation*, vol. 106, pp. 473–481, 2000.

[42] S. E. Kahn, J. C. Beard, M. W. Schwartz et al., "Increased β-cell secretory capacity as mechanism for islet adaptation to nicotinic acid-induced insulin resistance," *Diabetes*, vol. 38, no. 5, pp. 562–568, 1989.

[43] R. J. Heine, M. Diamant, J. C. Mbanya, and D. M. Nathan, "Management of hyperglycaemia in type 2 diabetes," *British Medical Journal*, vol. 333, no. 7580, pp. 1200–1204, 2006.

[44] A. Tura, S. Sbrignadello, E. Succurro, L. Groop, G. Sesti, and G. Pacini, "An empirical index of insulin sensitivity from short IVGTT: validation against the minimal model and glucose clamp indices in patients with different clinical characteristics," *Diabetologia*, vol. 53, no. 1, pp. 144–152, 2010, Erratum in *Diabetologia* vol. 53, p. 1245, 2010.

Hindawi Publishing Corporation
Journal of Diabetes Research
Volume 2013, Article ID 498925, 13 pages
http://dx.doi.org/10.1155/2013/498925

Research Article

Glomerulopathy in the KK.Cg-A^y/J Mouse Reflects the Pathology of Diabetic Nephropathy

Stephen P. O'Brien, Mandy Smith, Hong Ling, Lucy Phillips, William Weber, John Lydon, Colleen Maloney, Steven Ledbetter, Cynthia Arbeeny, and Stefan Wawersik

Tissue Protection and Repair, Genzyme, A Sanofi Company, 49 New York Ave., Framingham, MA 01701, USA

Correspondence should be addressed to Stephen P. O'Brien; stephen.obrien@genzyme.com

Received 23 January 2013; Accepted 15 March 2013

Academic Editor: Daisuke Koya

The KK.Cg-A^y/J (KK-A^y) mouse strain is a previously described model of type 2 diabetes with renal impairment. In the present study, female KK-A^y mice received an elevated fat content diet (24% of calories), and a cohort was uninephrectomized (Unx) to drive renal disease severity. Compared to KK-a/a controls, 26-week-old KK-A^y mice had elevated HbA1c, insulin, leptin, triglycerides, and cholesterol, and Unx further elevated these markers of metabolic dysregulation. Unx KK-A^y mice also exhibited elevated serum BUN and reduced glomerular filtration, indicating that reduction in renal mass leads to more severe impairment in renal function. Glomerular hypertrophy and hypercellularity, mesangial matrix expansion, podocyte effacement, and basement membrane thickening were present in both binephric and uninephrectomized cohorts. Glomerular size was increased in both groups, but podocyte density was reduced only in the Unx animals. Consistent with functional and histological evidence of increased injury, fibrotic (fibronectin 1, MMP9, and TGFβ1) and inflammatory (IL-6, CD68) genes were markedly upregulated in Unx KK-A^y mice, while podocyte markers (nephrin and podocin) were significantly decreased. These data suggest podocyte injury developing into glomerulopathy in KK-A^y mice. The addition of uninephrectomy enhances renal injury in this model, resulting in a disease which more closely resembles human diabetic nephropathy.

1. Introduction

Diabetic nephropathy (DN) is the leading cause of end-stage renal disease (ESRD) and is associated with high cardiovascular risk and significant morbidity and mortality [1, 2]. Disease progression is difficult to predict, as rates of decline in glomerular filtration rate (GFR) are variable in this patient population and only one-third of diabetic patients, the majority of whom have type 2 diabetes (T2D), develop progressive renal failure. The pathogenesis of DN is mediated by a complex interplay of genetic and environmental modifiers resulting in hemodynamic and structural changes in the kidney that contribute to progressive functional loss in both the glomerulus and tubular-interstitial epithelium [3, 4]. Central to disease progression is glomerular injury, with pathological changes including glomerular hypertrophy, glomerular basement membrane (GBM) thickening, mesangial matrix expansion, and subsequent glomerulosclerosis [3]. Podocytes are critical to the functional glomerular filtration barrier and are particularly sensitive to damage by the "diabetic milieu" of dysglycemia, dyslipidemia, hemodynamic changes, and inflammation [5, 6]. In both T1 and T2D patients, podocyte detachment and loss are associated with decline in glomerular function [7–9].

While rodent DN models have provided significant insight into renal disease pathophysiology, no model captures all the features of human DN [10–13], creating an obstacle to understanding disease etiology and to developing effective treatments [14]. To address this, the NIH-sponsored Animal Models of Diabetic Complications Consortium (AMDCC) committee was formed to establish phenotyping standards and validation criteria for available murine models of DN (http://www.diacomp.org/). The committee defined criteria for mouse models of DN that reflect human disease, including greater than 50% decline in GFR over the lifetime of the animal model, 10-fold increase in albuminuria relative to age-

and gender- matched controls, and renal pathology characterized by advanced mesangial matrix expansion, arteriolar hyalinosis, and glomerular basement membrane thickening [10, 11]. While numerous diabetic murine models were phenotyped and met some of the criteria, no one model fulfilled all of the AMDCC criteria. The committee consequently recommended the use of a "suite" of mouse models, each recapitulating individual features of renal disease in diabetic patients [11, 15].

One of the mouse models not extensively examined by the AMDCC is the KK-A^y strain. This model exhibits marked obesity, glucose intolerance, severe insulin resistance, dyslipidemia, and hypertension [16–18]. KK-A^y mice also develop renal disease characterized by moderate albuminuria with mild glomerular pathology and podocyte loss [19–21]. Several therapeutic interventions have been reported to reduce albuminuria and improve renal pathology in this model, including renin-angiotensin blockage [18, 22, 23], statin therapy [24], and vitamin D [25]. However, direct measurement of GFR in this model has not been reported and is an important component, as decline in GFR is the benchmark of disease progression, and prevention of decline in GFR is a key efficacy endpoint in therapeutic clinical trials [26, 27].

The goal of this study was to increase renal disease severity in the KK-A^y model by multiple "hits," each reflecting a known factor contributing to diabetes and its complications in humans. We combined dietary manipulation and reduction in renal mass to increase renal injury in this model. Together, these environmental modifiers exacerbate glomerular and tubulointerstitial pathology, increase podocyte loss, and reduce GFR in KK-A^y mice, and our findings support the use of this multifactorial approach in developing appropriate models for human diabetic nephropathy.

2. Materials and Methods

2.1. Experimental Animals. All animal studies followed the principles of laboratory animal care established by the National Institutes of Health and the Institutional Animal Care and Use Committee (IACUC). Female KK.Cg-A^y/J (further referred as KK-A^y) and littermate control KK-*a/a* mice were purchased from Jackson Laboratories (Bar Harbor, ME, USA) and acclimated for 3 weeks before the beginning of the study. Cohorts of mice were uninephrectomized at 8 weeks of age. At 9 weeks, animals were placed on semipurified control diet (D08112307) containing 12% k/cal fat or a moderately high-fat diet containing 24% k/cal fat and 0.2% cholesterol (D10011701) (Research Diets Inc., St. Louis, MO, USA). Mice were randomized according to albumin/creatinine at 12 weeks of age and were sacrificed at 26 weeks of age.

2.2. Physiological and Biochemical Characterization. Blood pressure was measured at 11 and 22 weeks of age by a noninvasive tail cuff CODA system (Kent Scientific, Torrington, CT, USA) after the mice were externally prewarmed for 10 min at 37°C. Animals were trained once daily, 4 days prior to recorded measurements. Eight to twenty recordings were taken for each measurement.

Fasting blood samples were collected by retroorbital sinus bleeds. Collected samples were separated to serum or EDTA plasma or kept as whole blood. Glycated hemoglobin (HbA1c), serum and urine creatinine, blood urea nitrogen (BUN), serum cholesterol, and triglycerides were measured using a Cobas 400 plus bioanalyzer (Roche Diagnostics, IN, USA). Blood was also collected from the tail vein from unanesthetized, nonfasted animals for the measurement of blood glucose using a glucometer. Body weight (BW) was measured weekly. Urine samples were collected for 24 h using metabolic cages. Urine albumin was measured by immunoassay Albuwell M (Exocell Inc., Philadelphia, PA, USA). Immuno-ELISA according to manufacturer's instructions was used to measure serum adiponectin and insulin (ALPCO Diagnostics, Salem, NH, USA), PAI-1 (Molecular Innovations, Novi, MI, USA), urine nephrin (Exocell Inc., Philadelphia, PA, USA), and KIM-1 (Immunology Consultants Laboratory, Inc. Portland, OR, USA).

2.3. Glomerular Filtration Rate. Glomerular filtration rate (GFR) was performed at 23 weeks of age using a FITC-GFR Test Kit for Inulin according to the manufacturer's instructions (BioPal, Worcester, MA, USA). A 5 mg/kg bolus intraperitoneal injection of inulin was given, followed by serial saphenous bleeds at 30, 60, and 90 minutes. Serum was isolated and quantified on inulin ELISA. Inulin serum clearance was determined by nonlinear regression using a one-phase exponential decay formula ($y = Be^{-bx}$), and GFR was calculated (GFR = $((I)/(B/b))$/KW, where I is the amount of inulin delivered by the bolus injection, B is y-intercept, b is the decay constant, x is time, and KW is kilo weight of the animal).

2.4. Histological Assessment. Formalin-fixed, paraffin-embedded kidneys were sectioned at 3 microns and stained with hematoxylin and eosin (H&E), periodic acid-Schiff (PAS), and Masson's Trichrome for histological analysis. Slides were evaluated by a veterinary pathologist. Glomerular and tubular pathology, interstitial inflammation including presence of CD68 immunolabeled macrophages, and interstitial fibrosis were semiquantitatively scored on a scale of 0–4 as follows: 0 = normal; 1 = mild; 2 = moderate; 3 = marked; 4 = severe. Statistical analysis was performed using the nonparametric Kruskal-Wallis test followed by Dunn's multiple comparison test.

2.5. Immunohistochemistry. Immunohistochemistry was performed on paraffin-embedded kidney sections. Anti-CD68 immunohistochemistry staining was performed on a Leica Bond MAX automated immunostainer (Leica Microsystems Inc. Buffalo Grove, IL, USA). Tissue sections were dewaxed, treated with Proteinase K enzyme, and followed by blocking with peroxidase and then serum. Slides were incubated in CD68 Clone Fa-11 (Abcam, Cambridge, MA, USA) antibody for 30 minutes, followed by rabbit anti-rat antibody, then a goat anti-rabbit HRP polymer for 15

minutes. Chromogen visualization was performed using 3,3′-diaminobenzidine tetrahydrochloride (DAB) for 3–5 minutes, followed by hematoxylin counterstain (all components were from Leica, unless otherwise noted). 0.05% Tween 20/Tris-buffered saline (DAKO, Carpinteria, CA, USA) washes were performed between all steps. Podocyte counting was assessed using anti-WT1 (Wilms Tumor 1) clone 6F-H2 at 1 : 100 dilution (Dako). Immunohistochemistry was performed on a Leica Bond MAX automated immunostainer (Leica Microsystems Inc. Bannockburn, IL, USA). 0.05% Tween 20/Tris-buffered saline (DAKO) washes were performed between all steps. Tissue sections were dewaxed and treated with Proteinase K enzyme then peroxidase. Tissues were then treated with rodent block (BioGenex, Fremont, CA, USA), anti-WT-1 primary antibody was detected using mouse on mouse HRP polymer. Chromogen visualization was performed using 3,3′-diaminobenzidine tetrahydrochloride (DAB) for 5 minutes, followed by hematoxylin counterstain and dehydration through increasing ethanol-water gradient to xylene and mounted in Permount (Fisher Scientific, Pittsburg, PA, USA). Whole kidney sections were imaged using Aperio ScanScope (Aperio Technologies, Vista, CA, USA). Greater than 50 glomeruli per kidney section were quantitated for the number of WT-1-positive (brown) and WT-1-negative cells (blue). Software analysis was done using custom algorithm on Spectrum Version 11.0.0.725 (Aperio Technologies).

2.6. Transmission Electron Microscopy. For ultrastructural analysis, 1 mm^3 samples of kidney cortex were fixed in 3% glutaraldehyde in 0.2 M cacodylate buffer (Electron Microscopy Sciences, Hatfield, PA, USA) and embedded in epon. Semithin 1 micron sections were stained with Richardson's stain (made up of methylene blue CI-52015, azure II, and borax, (Sigma, St. Louis, MO, USA)) and evaluated via high resolution light microscopy. Ultrathin sections were cut at 70 nm and mounted on 200 mesh copper grids. The grids were stained on a Leica EM AC20 Stainer (Leica Microsystems) with 0.5% aqueous uranyl acetate and 3% lead citrate solution (Leica). Images were acquired on a JEOL JEM-1400 transmission electron microscope (JEOL; Peabody, MA, USA) using a Gatan 785 Erlangshan ESW1000 digital camera (Gatan, Inc.; Pleasanton, CA, USA).

2.7. Transcriptional Analysis. Quantitative transcriptional analysis of kidney tissue from animals at 26 weeks of age was performed on TaqMan Custom Array microarrays using 7900HT Fast real-time PCR system. Kidney mRNA purification was performed by homogenizing 50–100 mg of tissue in 1 mL of TRIzol reagent. Samples were left for 5 minutes at 15 to 30°C followed by the addition of 0.2 mL chloroform (Sigma). Samples were mixed vigorously, left at room temperature for 3 minutes followed by centrifugation at 12,000 ×g for 15 minutes at 4°C. The aqueous phase was taken, and RNA was precipitated with 0.5 mL of isopropyl alcohol (Sigma). The pellet was washed once with 1 mL 75% ethanol, air-dried, and redissolved in RNase-free water. Samples were DNAse treated using TurboDNase according to manufacturer's instructions. RNA was qualified on an Agilent 2100 Bioanalyzer (Agilent Technologies, Santa Clara, CA, USA). All items were obtained from Life Technologies, Grand Island, NY, USA unless otherwise noted.

3. Results

3.1. Uninephrectomized KK-A^y Mice Are Obese and Exhibit Evidence of Metabolic Abnormalities. Diabetes and renal injury are more severe in male versus female KK-A^y mice [28] and, as a consequence, preclinical studies typically focus on males. However, male KK-A^y develop obstructive uropathy and hydronephrosis [29] and exhibit impaired glucose tolerance [28]. To avoid these urological issues, all studies described here use female mice. This also allowed us to use KK-*a/a* females as nondiabetic, strain-matched controls, as female KK-*a/a* mice maintain normal glycemic control, while male KK-*a/a* are insulin resistant [30].

While on standard chow, KK-A^y mice were significantly heavier than control or uninephrectomized (Unx) KK-*a/a* animals (Figure 1(a)). After switching to the elevated fat diet, KK-*a/a* + Unx mice gained weight relative to KK-*a/a* controls, but were less obese than both KK-A^y groups. Blood pressure, measured in 11-and 22-week-old mice, was unchanged in both the KK-*a/a* and KK-A^y + Unx groups, and no difference was observed between the two cohorts. At 11 weeks, KK-*a/a* mean arterial pressure (MAP) was 85.6±3.7 mmHg, while KK-A^y + Unx MAP was 83.5 ± 2.2 mmHg. At 22 weeks, MAP in KK-*a/a* mice was 84.0 ± 3.3 mmHg and KK-A^y + Unx MAP was 86.5 ± 3.5 mmHg.

In KK-*a/a* controls, glycated hemoglobin (HbA1c) was unaffected by the switch to an elevated fat diet (Figure 1(b)). Serum HbA1c levels were elevated in all KK-A^y mice on standard chow, and serum HbA1c further increased after the switch to the elevated fat diet, with peak levels occurring between 5 and 10 weeks after diet change. While serum HbA1c levels were higher in uninephrectomized KK-A^y (KK-A^y + Unx) mice than in KK-*a/a*, these levels were consistently lower compared to birenal KK-A^y, a likely consequence of elevated insulin levels in the KK-A^y + Unx animals (Figure 1(c)). Consistent with the HbA1c levels, blood glucose in nonfasted, unanesthetized animals was also significantly elevated in the KK-A^y + Unx group relative to KK-*a/a* mice (318.8+/26.3 versus 222.3+/−20.3, $P < 0.01$). However, to avoid undue stress caused by unanesthetized blood collection, and because we note short-term variability in glucose values as mice are moved into the metabolic cages for urine collection, glycemia was followed in this study using HbA1c. Serum adiponectin levels were reduced at 16 weeks of age in both KK-A^y groups, which were further decreased at 26 weeks (Figure 1(d)). Interestingly, uninephrectomy in the KK-*a/a* mice was also associated with a sharp decline in adiponectin levels between 20 and 26 weeks of age.

Consistent with increased body weight, serum lipids and adiposity-associated cytokines were elevated in KK-A^y mice. Serum leptin was elevated 2-fold relative to KK-*a/a* controls in binephric KK-A^y mice and approximately 5-fold in KK-A^y + Unx animals (Figure 2(a)). Serum leptin was

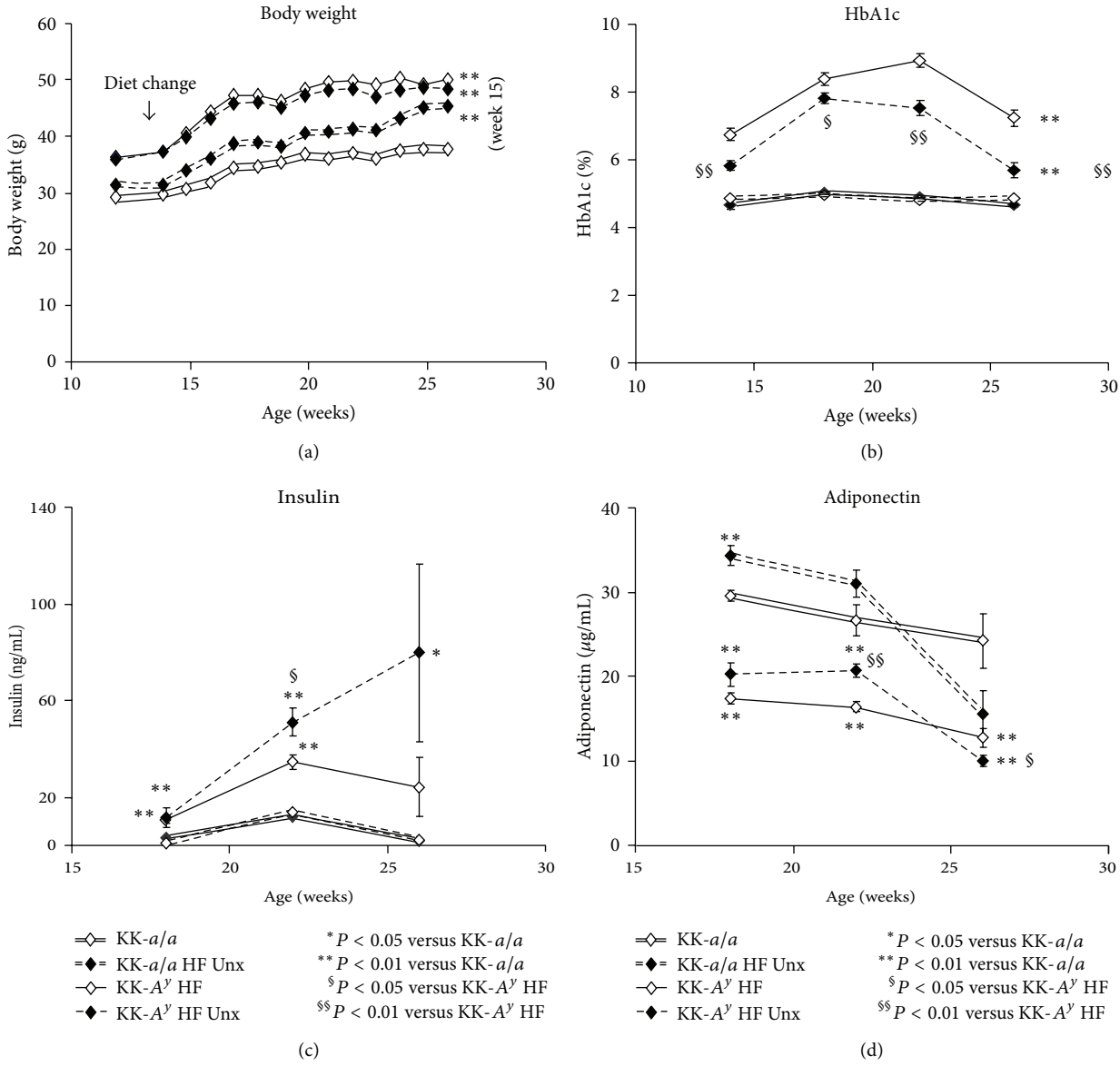

Figure 1: Obesity, glucose intolerance, insulin resistance, and hypoadiponectinemia in KK-A^y mice. (a) Prior to diet change of a moderately high-fat diet at 12 weeks, KK-A^y were significantly heavier than KK-*a/a* control animals. After 3 weeks on modified diet, KK-*a/a* control animals became obese, but never reached the same level as KK-A^y ($P < 0.01$). (b) Throughout the study, glycated hemoglobin was elevated in KK-A^y mice (compared to KK-*a/a* controls, $P < 0.01$). KK-*a/a* mice maintain normal long-term glucose homeostasis. Hyperglycemic uninephrectomized KK-A^y (KK-A^y + Unx) animals had lower HbA1c than birenal KK-A^y ($P < 0.05$). (c) All KK-A^y had elevated insulin, but greater hyperinsulinemia was evident in the KK-A^y + Unx group, where insulin increased progressively throughout the study. (d) Consistent with obesity, all KK-A^y mice had lower adiponectin levels at 16 weeks of age, which were further decreased by 26 weeks. The observed decline in adiponectin levels in KK-*a/a* Unx and high-fat diet between 22–26 weeks was not statistically different from the KK-*a/a* control. The KK-A^y + Unx adiponectin levels were significantly lower than KK-A^y binephric mice.

also elevated by Unx in both KK-*a/a* and KK-A^y. Serum triglyceride levels show a similar profile: both KK-*a/a* and KK-A^y uninephrectomized mice were hypertriglyceridemic compared to binephric animals, and triglycerides were higher in KK-A^y mice than in comparable KK-*a/a*. KK-A^y + Unx triglycerides were elevated 4.5-fold versus binephric KK-*a/a* controls (Figure 2(b)). Serum cholesterol levels were also markedly elevated in KK-A^y + Unx mice (Figure 2(c)) and further increased by uninephrectomy, an effect consistent with that observed for serum leptin and triglycerides. In contrast, serum PAI-1 levels were not affected by uninephrectomy (Figure 2(d)), but were significantly elevated in KK-A^y mice relative to KK-*a/a*. Taken together, these data are consistent with the metabolic profile of human T2DN [2, 31, 32].

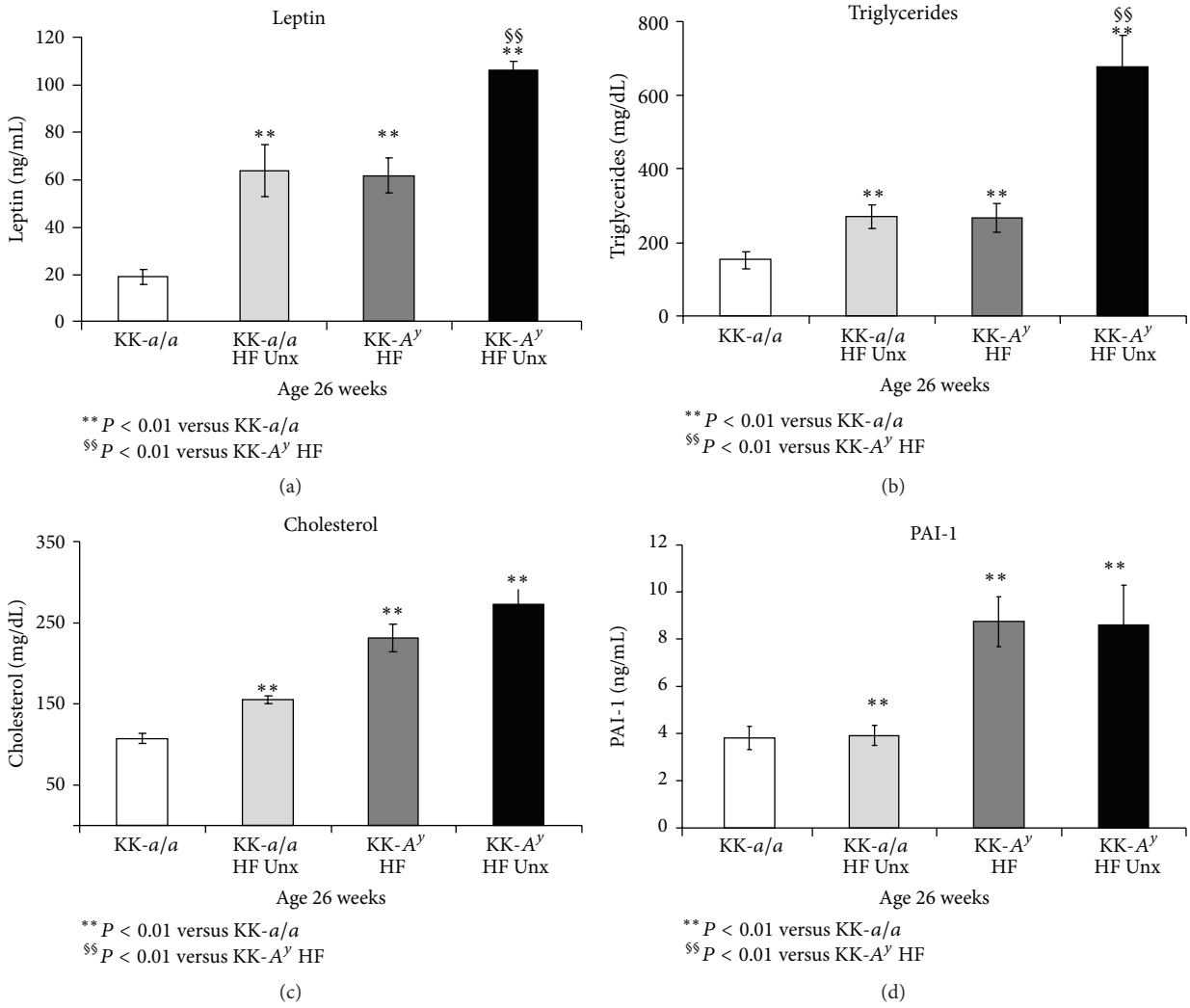

Figure 2: Altered serum cytokines and serum lipids in KK-A^y mice. (a) Leptin levels were elevated in KK-A^y (versus KK-*a/a* control). Addition of uninephrectomy (Unx) elevated serum leptin, both in KK-*a/a* and in KK-A^y mice ($P < 0.01$). (b) A similar profile was observed for serum triglycerides, which were elevated in KK-A^y (versus KK-*a/a* control). As with leptin, Unx further elevated triglycerides both in KK-*a/a* and in KK-A^y mice ($P < 0.01$). (c) Relative to KK-*a/a* controls, KK-*a/a* + Unx, KK-A^y, and KK-A^y + Unx mice all showed markedly elevated serum cholesterol ($P < 0.001$). (d) Serum PAI-1 levels were elevated in KK-A^y mice compared to age-matched KK-*a/a* animals ($P < 0.01$). However, PAI-1 levels in KK-A^y were unaffected by Unx.

3.2. Urine and Serum Biomarkers Indicate Renal Injury in KK-A^y and KK-A^y + Unx Mice. KK-A^y mice exhibit consistent and progressive albuminuria, measured as albumin/creatinine ratio (ACR) (Figure 3(a)). ACRs were comparable in both KK-A^y and KK-A^y + Unx, suggesting that uninephrectomy does not affect albuminuria in KK-A^y animals. Urinary excretion of the podocyte protein nephrin, recently identified as a biomarker of glomerular injury in both humans and mice [33, 34], was elevated in both KK-A^y and KK-A^y + Unx mice at 26 weeks (14 weeks after the switch to elevated fat diet), with a trend towards nephrinuria first detected at 22 weeks (Figure 3(b)). As with ACR, we observed no difference in urinary nephrin/creatinine ratio in intact and uninephrectomized mice, suggesting glomerular injury in both KK-A^y groups.

We also examined the concentration of KIM-1, a marker of ongoing renal tubular injury [35, 36], in urine collected from 26-week-old mice (Figure 3(c)). Relative to KK-*a/a* animals, KIM-1 was elevated in both KK-A^y and KK-A^y + Unx mice. Interestingly, KIM-1 levels in KK-A^y + Unx animals were lower than in their binephric counterparts, possibly as a consequence of the reduced renal mass in uninephrectomized mice.

Elevated ACR and urine nephrin and KIM-1 concentrations suggest renal glomerular and tubular injury in KK-A^y mice. To determine whether renal function was affected, we examined serum blood urea nitrogen (BUN) levels in these animals (Figure 4(a)). BUN was of normal range in KK-*a/a* mice, but was slightly elevated in KK-*a/a* + Unx and KK-A^y animals. Mice in the KK-A^y + Unx group, however, showed substantially greater increases in BUN, reaching an average of 45.3 mg/dL at 26 weeks ($P < 0.0001$ versus both KK-A^y and KK-*a/a*). These BUN values suggest impaired renal function in KK-A^y + Unx mice, and we therefore directly measured

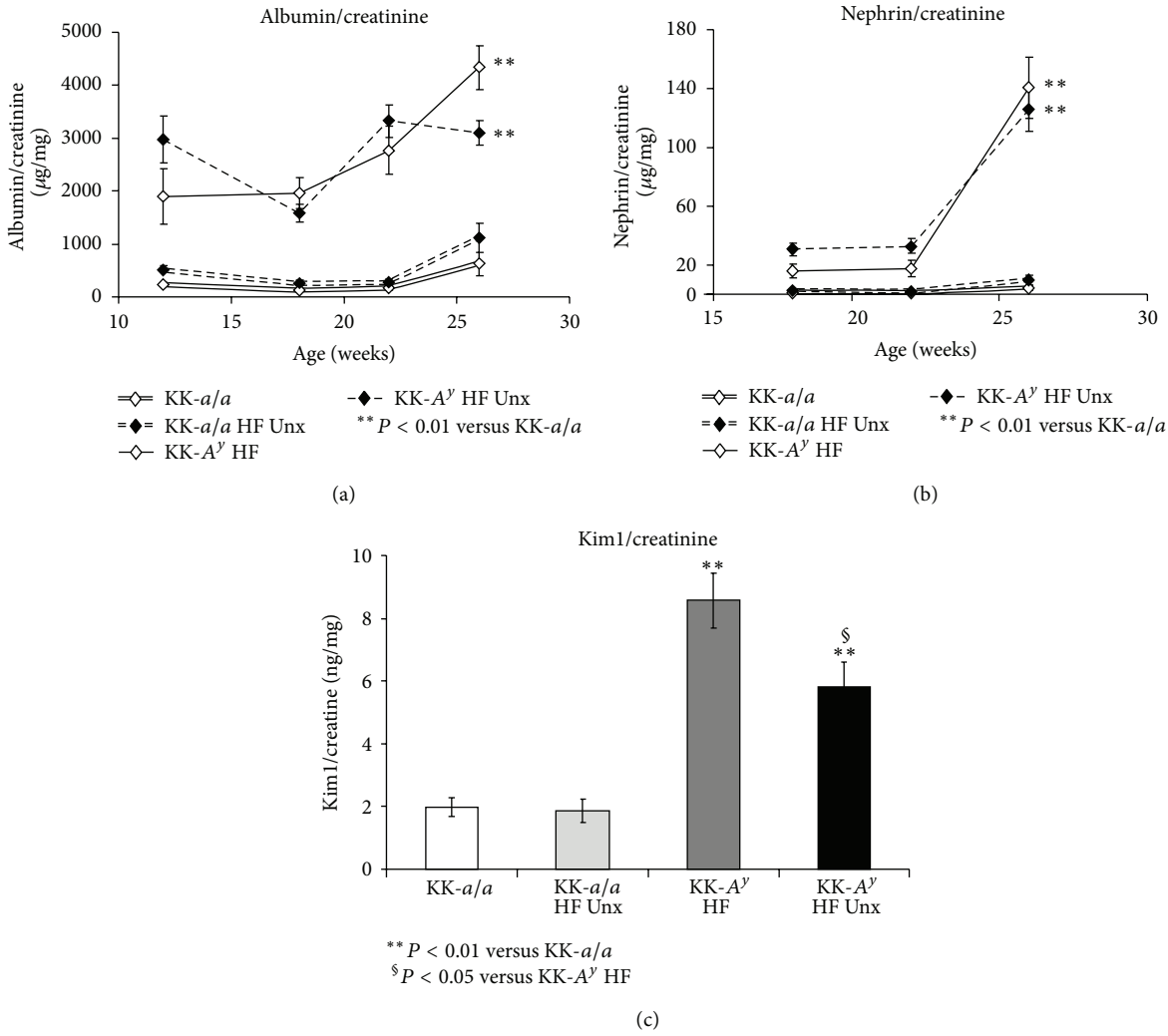

Figure 3: Urine markers indicate glomerular injury in KK-A^y. (a) KK-A^y mice exhibited consistent and progressive albuminuria, measured as albumin/creatinine ratio (ACR) ($P < 0.01$ at all timepoints versus KK-*a/a*). No difference was observed in ACR between KK-A^y and KK-A^y + Unx. (b) Glomerular injury in KK-A^y mice was suggested by progressive elevation of the podocyte-specific protein nephrin in the urine. Again, urine nephrin levels were comparable in KK-A^y and KK-A^y + Unx mice ($P < 0.01$ versus KK-*a/a*). (c) When compared to KK-*a/a*, the renal tubular marker Kim1 was also elevated in KK-A^y mice. Interestingly, Kim1 levels in KK-A^y + Unx animals were lower than in KK-A^y mice.

glomerular filtration rate (GFR) in this group. We found a 32% reduction in GFR in KK-A^y + Unx mice compared to KK-*a/a* littermate controls, a reduction roughly equivalent to late stage 2 CKD in human patients. Thus, despite the finding that urine biomarkers revealed little difference in the extent of renal damage between KK-A^y and KK-A^y + Unx mice, changes in BUN and GFR, both direct indicators of renal function, indicated substantial renal impairment only in KK-A^y + Unx mice.

3.3. Uninephrectomy Exacerbates Glomerulopathy and Renal Fibrosis Markers in KK-A^y Mice. On histologic assessment, nondiabetic KK-*a/a* control mice exhibited minimal to mild glomerulopathy that was unchanged by elevated fat diet and Unx (Figures 5(a) and 5(b)). In contrast, diabetic KK-A^y mice fed elevated fat diet exhibited a moderate to marked glomerulopathy (Figure 5(c)), characterized predominantly by segmental to global expansion of the mesangial matrix by PAS positive material and hypercellularity of the glomerular tuft. Semiquantitative scoring (Figure 5(i)) demonstrated a significant increase in the glomerulopathy in binephric diabetic KK-A^y mice versus KK-*a/a* controls ($P < 0.01$), and this was further exacerbated by uninephrectomy in the KK-A^y + Unx group ($P < 0.001$ vs. KK-*a/a* controls). Tubular lesions were rare to nonexistent in nondiabetic KK-*a/a* groups (Figures 5(e) and 5(f)). However, uninephric and binephric KK-A^y groups exhibited multifocal tubular atrophy with thickened tubular basement membranes (Figures 5(g) and 5(h)), tubular dilation with or without luminal protein casts, and tubular mineralization at the corticomedullary junction. Overall, the tubular pathology was significantly

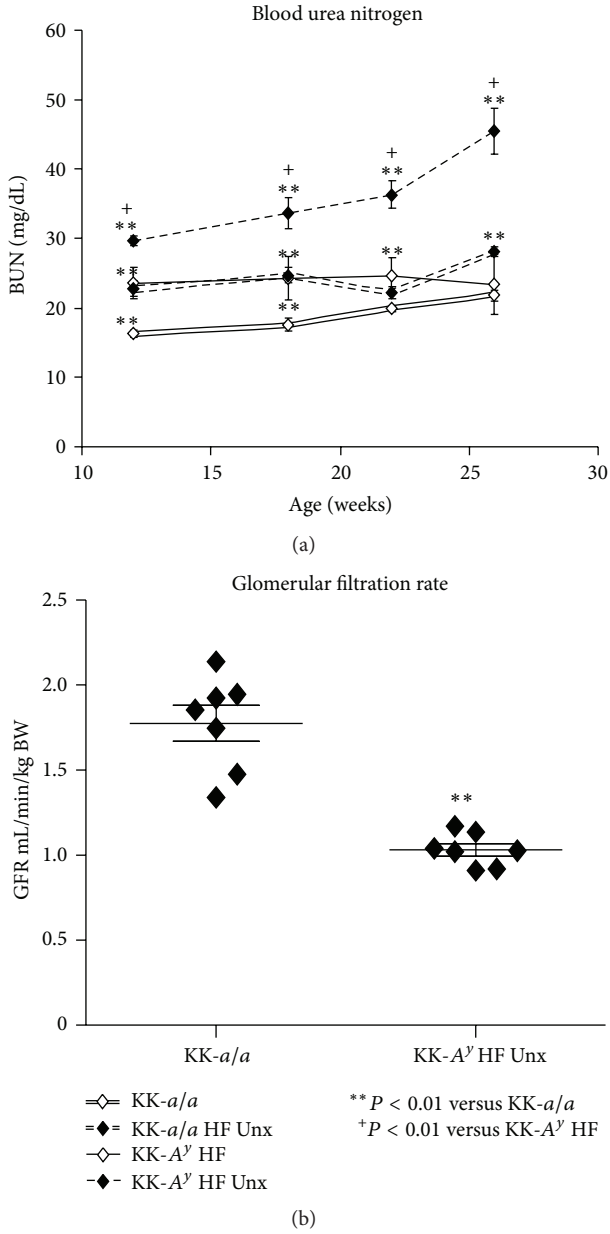

Figure 4: Decreased renal function in KK-A^y is exacerbated by uninephrectomy. (a) Compared to KK-*a/a* mice, blood urea nitrogen (BUN) is slightly elevated in KK-A^y and KK-*a/a* + Unx, though this difference is not statistically significant at later time points in the KK-*a/a* + Unx group. Uninephrectomy further elevates BUN in KK-A^y, with BUN increased by twofold, indicating mild uremia in KK-A^y + Unx animals. (b) Renal function, as measured by glomerular filtration rate (GFR), is reduced by 32% in KK-A^y + Unx mice compared to KK-*a/a* littermate controls ($P < 0.001$).

greater in binephric KK-A^y ($P < 0.01$) and uninephric KK-A^y mice ($P < 0.001$, Figure 5(j)) relative to the KK-*a/a* controls. In the interstitium, KK-A^y diabetic mice in both groups had multifocal infiltration of mixed inflammatory cells and mild fibrosis which typically surrounded severely affected glomeruli and/or tubules (Figures 5(g) and 5(h)). Inflammatory infiltrates were composed of macrophages, lymphocytes, and plasma cells admixed with occasional neutrophils. Although group median scores for interstitial fibrosis were similar in binephric and uninephric KK-A^y groups, only the uninephric group showed a statistically significant increase relative to the KK-*a/a* controls ($P < 0.001$, not shown).

To further examine whether uninephrectomy affects fibrosis in KK-A^y mice, we measured transcription of fibrosis-related genes in total kidney mRNA (Figure 5(k)). In KK-A^y animals, we observed the upregulation of RNA encoding *Col3a1, Fn1, PAI-1, Mmp9,* and RNA encoding the TGFβ1-3 ligands relative to KK-*a/a* controls. In KK-A^y + Unx mice, we saw an additional statistically significant increase in *Col3a1* and *Mmp9* expression relative to binephric KK-A^y animals, as well as a trend towards increased expression of the remaining fibrotic genes assessed. Taken together, these data indicate renal fibrosis in KK-A^y mice and that uninephrectomy further exacerbates renal damage in this model.

3.4. Podocyte Injury in KK-A^y + Unx Mice. At the ultrastructural level, KK-*a/a* mice showed normal podocyte foot processes (Figure 6(a)) and a smooth, trilaminar glomerular basement membrane (GBM). Both KK-A^y and KK-A^y + Unx animals exhibited multifocal podocyte foot process effacement and areas of irregular thickening in the lamina densa of the GBM (Figures 6(b) and 6(c)). Because podocyte foot process effacement is reversible [37, 38], we used morphometric analysis of sections immunostained for the podocyte marker WT-1 to assess podocyte loss in KK-A^y mice. No change was observed in average cell density per glomerulus in any of the groups examined (Figure 6(d)). However, we noted increased glomerular area in KK-A^y and KK-A^y + Unx mice. Furthermore, we observed a 28% decrease in the density of WT-1 positive cells per mm^2 glomerular area in uninephrectomized KK-A^y animals compared to KK-*a/a* mice (Figure 6(f)). This decrease in podocyte density was not observed in binephric KK-A^y animals, a distinction consistent with the higher glomerular pathology scores in KK-A^y + Unx mice (Figure 5(i)) and suggesting that addition of uninephrectomy exacerbates glomerular injury in the KK-A^y model of diabetic nephropathy.

Examination of podocyte-specific transcripts further supports the conclusion that podocyte loss is observed only in KK-A^y + Unx mice. Using quantitative RT-PCR, we measured expression of the podocyte-specific genes nephrin (*Nphs1),* podocin *(Nphs2)*, and WT-1 in total kidney mRNA (Figure 6(g)). We observed no difference in the expression of any of these genes between KK-*a/a* and binephric KK-A^y mice, but note a statistically significant decrease in all three podocyte markers in KK-A^y + Unx animals. These data are consistent with the decrease in podocyte density in KK-A^y + Unx mice and suggest that uninephrectomy is necessary to induce podocyte loss in this model.

3.5. Increased Macrophage Infiltration and Inflammation in Uninephrectomized KK-A^y Mice. Macrophage infiltration and inflammation are increasingly recognized as important elements in diabetic glomerular disease [39]. To examine

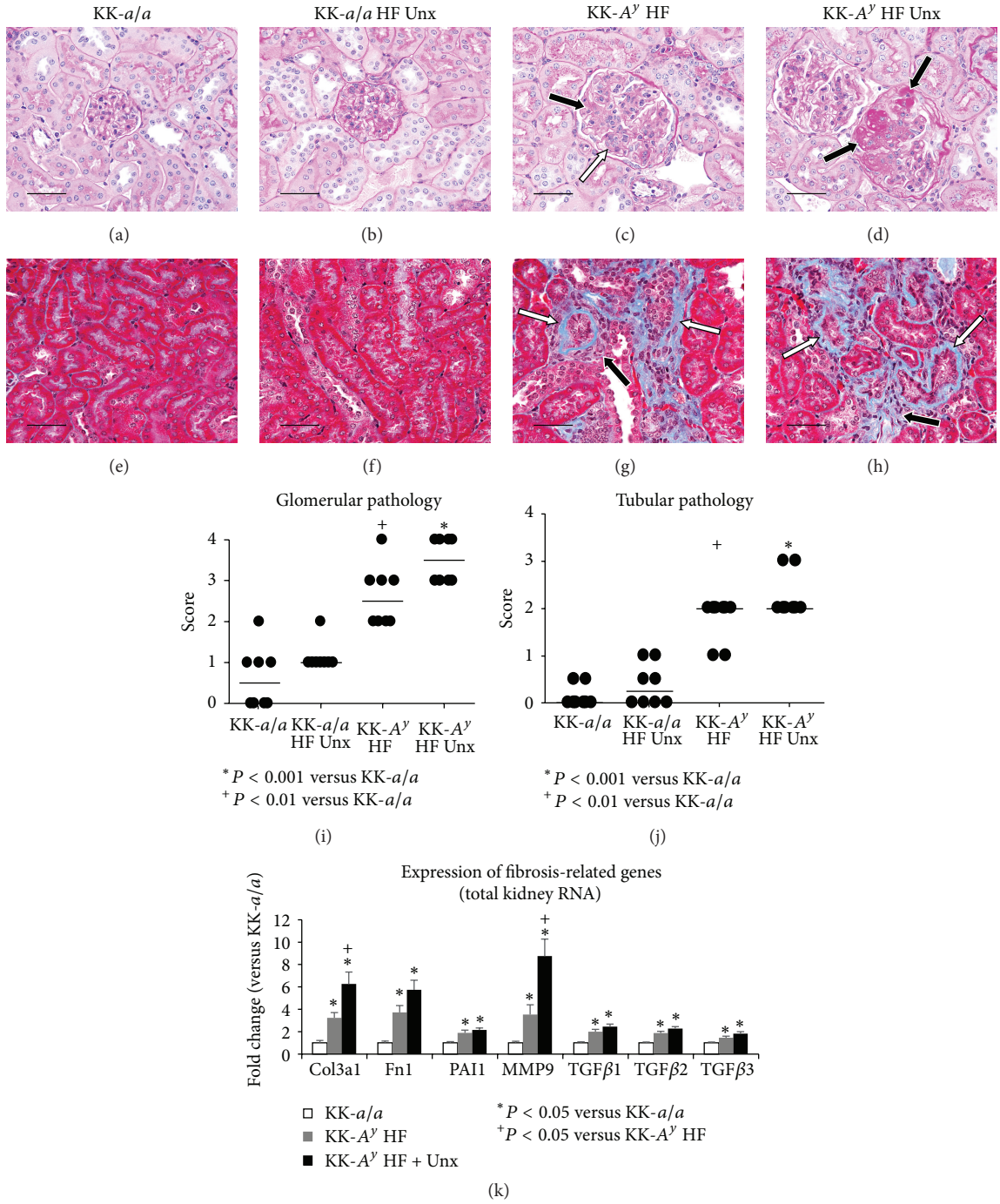

Figure 5: Glomerular injury in KK-A^y diabetic mice. PAS staining in KK-*a/a* (a) and KK-*a/a* + Unx (b) mice revealed normal glomeruli. KK-A^y mice (c) exhibited glomerular hypercellularity (white arrow) and mesangial matrix expansion (black arrow). KK-A^y + Unx (d) had more severe glomerular mesangial matrix expansion (black arrow). Trichrome staining revealed normal tubules and interstitium in KK-*a/a* (e) and KK-*a/a* + Unx (f), whereas KK-A^y (g) and KK-A^y + Unx (h) had multifocal tubular atrophy with thickened basement membranes (white arrows) and mild interstitial fibrosis (black arrows). Scale bars represent 50 μm. (i) In the semiquantitative pathological scoring, horizontal bars indicate group median score. The binephric KK-A^y diabetic mice had a significantly greater group median score for glomerular pathology ($P < 0.01$ versus KK-*a/a* controls), with a trend toward exacerbation of pathology by uninephrectomy in the KK-A^y + Unx group ($P < 0.001$ versus KK-*a/a* controls). (j) Both KK-A^y groups had a significant increase in tubular pathology relative to KK-*a/a* controls ($P < 0.01$ KK-A^y; $P < 0.001$ KK-A^y + Unx). (k) Whole kidney qRT-PCR indicated increased expression of fibrosis related genes by uninephrectomy in KK-A^y versus KK-*a/a*. Expression of mRNA encoding Collagen 3a1 (Col3a1), fibronectin (FN1), serpine-1 (PAI-1), *matrix* metallopeptidase *9 (MMP9)*, and the transforming growth factor beta-proteins (TGFβ) 1–3 was significantly elevated in KK-A^y versus KK-a/a. Addition of Unx to KK-A^y significantly elevated expression of Col3a and MMP9 versus KK-A^y ($P < 0.01$).

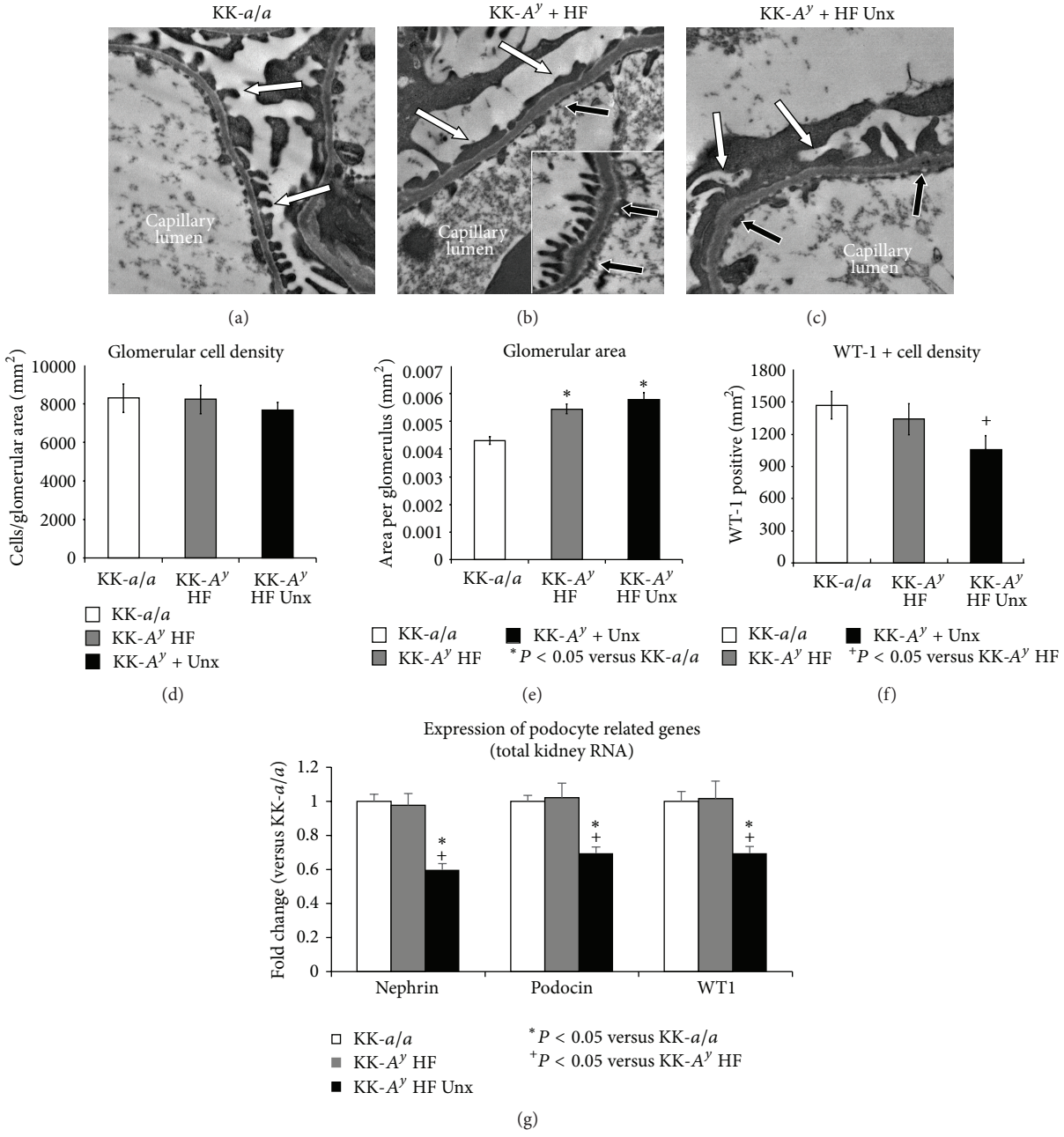

FIGURE 6: Podocyte injury in KK-A^y + Unx mice. (a) At the ultrastructural level, KK-*a/a* controls had normal podocyte foot processes (white arrows) and a smooth, trilaminar glomerular basement membrane. In KK-A^y (b) and KK-A^y + Unx (c) mice, there was podocyte foot process effacement (white arrows) and areas of mild irregular GBM thickening (black arrows). Regions of uneffaced foot processes ((b), inset) were present in both KK-A^y cohorts, and uninephrectomy did not induce discernable differences in the severity of glomerular basement membrane thickening. Podocyte counting was carried out using WT-1 as a specific podocyte marker. The total number of cells per glomerular area (d) was unchanged between any of the groups, but glomerular area was significantly increased in all KK-A^y animals (e). In uninephrectomized KK-A^y mice, the number of WT-1-positive cells per glomerular area was reduced by 28% ($P < 0.05$). The number of podocytes per glomerulus (independent of area) was also decreased in KK-A^y (18% of total cells in KK-*a/a*, 16% in KK-A^y HF, and 13% in KK-A^y HF Unx (data not shown)) suggesting that loss of podocytes is not simply due to increased glomerular area. (g) qRT-PCR analysis of podocyte-specific genes further supports podocyte loss, revealing statistically significant decreases in nephrin, podocin, and WT-1 RNA expression in KK-A^y HF Unx kidneys.

whether renal macrophage infiltration is present in the KK-A^y model, immunohistochemistry for the macrophage marker CD68 was performed on kidney sections (Figure 7). In KK-*a/a* or KK-*a/a* + Unx mice, there were scattered $CD68^+$ macrophages in the interstitium (Figures 7(a) and 7(b)) and rare CD68 positive cells in glomeruli. In contrast, binephric KK-A^y mice (Figure 7(c)) exhibited a significant increase in interstitial $CD68^+$ macrophages ($P < 0.05$ versus KK-*a/a* controls) and this was enhanced in the KK-A^y + Unx group ($P < 0001$ versus KK-*a/a* controls, Figure 7(f)). Both KK-A^y diabetic groups had low numbers of $CD68^+$ cells within glomeruli (Figure 7(e)). These may represent infiltrating macrophages or, alternatively, mesangial cells transforming to a macrophage phenotype.

Immunohistochemical findings were corroborated by quantitative RT-PCR from total kidney mRNA which indicated a significant increase in the expression of CD68 and inflammation-associated markers IL-6, MCP-1, and CD44 in both KK-A^y and KK-A^y + Unx animals (Figure 7(g)). Expression of each of these markers was further increased in KK-A^y + Unx mice, pointing to increased renal inflammation in this group.

4. Discussion

The KK-A^y mouse strain is glucose intolerant, severely insulin resistant, dyslipidemic, and hypertensive; all are characteristics of the "metabolic syndrome" phenotype of T2D patients [24–26]. Evidence of kidney injury is also present, including albuminuria, mesangial matrix accumulation, and GBM thickening [20]. However, as with many mouse models of diabetic nephropathy [10, 11], renal damage in KK-A^y mice is mild and does not adequately capture key aspects of the human disease. To drive disease severity in KK-A^y, we provided a diet containing 24% of calories from fat and examined the effects of uninephrectomy (Unx) on metabolic and renal endpoints in this model. We found that while urinary markers of renal injury (albuminuria, nephrinuria, and urine Kim-1) were similar in KK-A^y and KK-A^y + Unx mice, uninephrectomized animals exhibited increased glomerular pathology, podocyte damage and loss, and renal inflammation. Furthermore, KK-A^y + Unx mice had elevated serum BUN and reduced GFR, indicating the impairment of renal function. Our findings indicate that KK-A^y + Unx mice have a more severe phenotype than previously reported in other DN models and, therefore, is a representative model of progressive glomerular injury and podocyte loss.

Our strategy was to use reduction in renal mass and dietary manipulation in a strain which is genetically susceptible to renal disease to further exacerbate renal injury. First, KK-A^y mice were uninephrectomized to induce glomerular hypertrophy, distortion of capillary architecture, and increased mechanical stress on the podocyte, factors which have been shown to exacerbate glomerulosclerosis [40, 41]. KK-A^y mice were then fed a semipurified diet that is more representative of a normal human diet, with 24% of calories derived from fat. Excess dietary fat promotes tissue injury [42], and the very low fat content in normal rodent chow may consequently be protective. This elevated fat diet is also low in phytoestrogens, which are present in high levels in normal rodent chow [43] and can induce hormonal and antioxidant effects [44] that may blunt progressive injury.

A significant advantage to using the KK-A^y strain is that diabetes is polygenic and not due to a defect in leptin receptor signaling. This is analogous to human disease and in contrast to other obese diabetic models such as *db/db* and *ob/ob* mice [10, 17]. We found that both binephric and uninephrectomized KK-A^y animals have elevated HbA1c, insulin, and leptin levels, suggesting both insulin and leptin resistance. We also observed a reduction in serum levels of the anti-inflammatory cytokine adiponectin [31, 45] and elevation of the proinflammatory cytokine PAI-1 [32, 46] in both cohorts of KK-A^y mice, suggesting the presence of a proinflammatory state similar to human diabetic patients [47]. Inflammation may be exacerbated in KK-A^y + Unx mice, as serum insulin and leptin levels (and, consequently, triglycerides) were further elevated in these animals. Taken together, these data indicate metabolic dysfunction and inflammation in both KK-A^y and KK-A^y + Unx cohorts, and suggest that uninephrectomy heightens inflammation in this model.

Urinalysis of KK-A^y and KK-A^y + Unx mice indicated renal injury in both groups. Albumin/creatinine ratios (ACRs) were elevated relative to KK-*a/a* controls, and increased levels of urine nephrin, a marker of podocyte injury in preclinical models and in human patients [48, 49], were also detected. Together, these findings suggest the impairment of the glomerular filtration barrier in KK-A^y mice. Kim-1, a marker of proximal tubule injury [36], was also elevated in KK-A^y and KK-A^y + Unx. We note, however, that Kim-1 in urine from KK-A^y + Unx mice was slightly, but statistically significantly, decreased relative to KK-A^y, possibly reflecting the reduced renal mass in the uninephrectomized mice.

While urine markers of renal injury were similar in both KK-A^y cohorts, renal function appeared to be more significantly impaired in the Unx group. Serum BUN is a routine laboratory test for diagnosis and routine followup of patients with CKD [50] and was elevated in KK-A^y + Unx mice. Furthermore, glomerular filtration rate (GFR) was decreased by 33% versus nondiabetic KK-*a/a*. Such loss of renal function, roughly comparable to late stage CKD stage 2 [51], suggests that KK-A^y + Unx mice exhibit the progressive renal injury characteristic of human diabetic nephropathy.

Consistent with previous reports [20, 21], nonnephrectomized KK-A^y mice displayed significant glomerulopathy and mild to moderate tubulointerstitial pathology. KK-A^y + Unx animals had higher median glomerular pathology scores, indicating that addition of Unx exacerbates the severity of glomerulopathy in this model. While tubulointerstitial pathology is not quantifiably different in the two KK-A^y groups, expression of the fibrotic markers *Col3a1* and *Mmp9* is statistically significantly elevated, and we note a trend towards increased expression of a number of additional fibrotic genes.

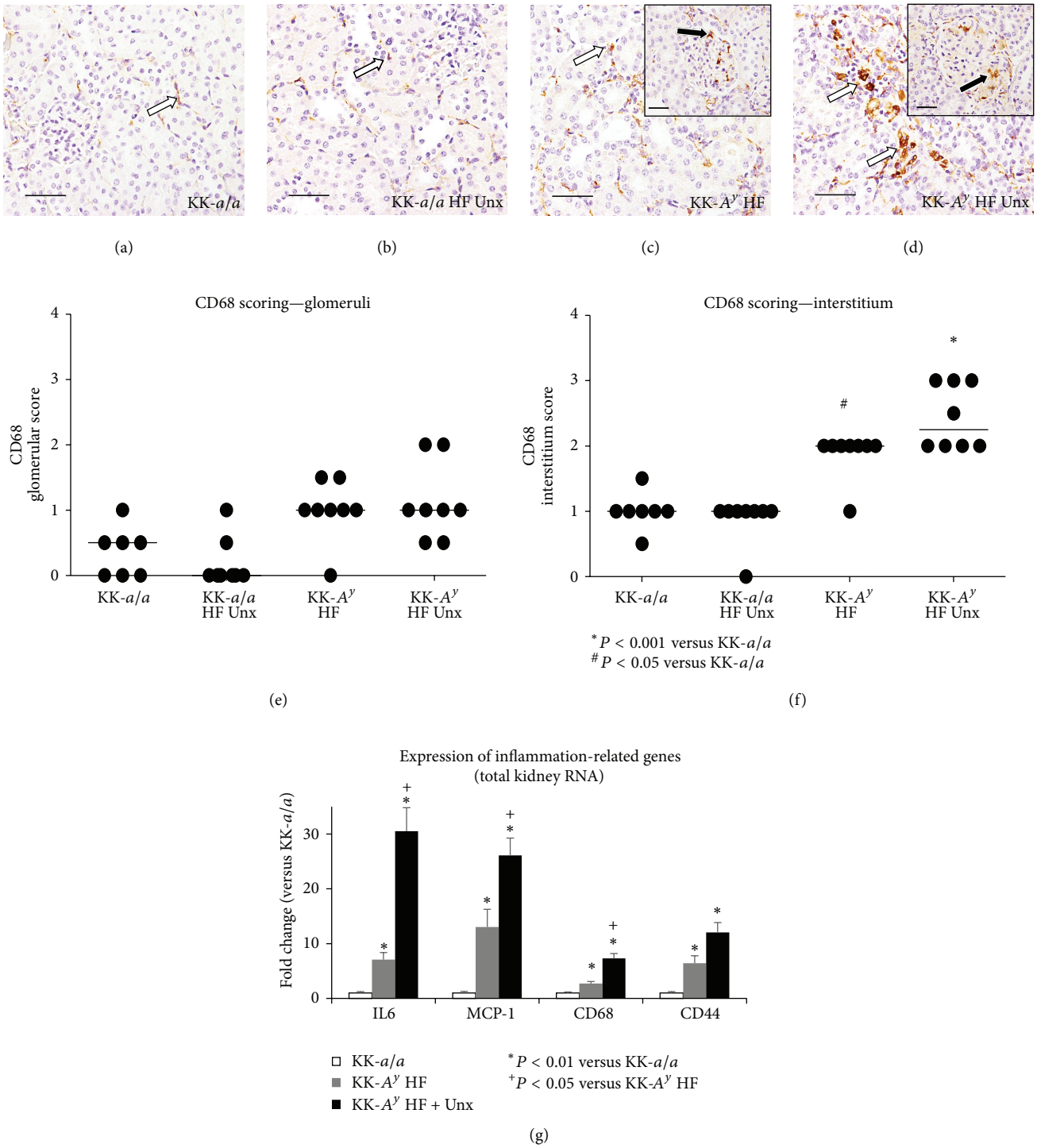

FIGURE 7: Increased inflammation in KK-A^y mice.Macrophage infiltration was evaluated by CD68 immunohistochemistry. KK-*a/a* (a) and KK-*a/a* + Unx (b) mice had scattered $CD68^+$ macrophages in the interstitium (white arrows) and rare $CD68^+$ cells in the glomeruli. KK-A^y (c) and KK-A^y + Unx (d) mice showed increased $CD68^+$ macrophage infiltration in the interstitium (white arrows) and occasional $CD68^+$ cells in glomeruli (inset, black arrows). Scale bars represent 50 μm. Semiquantitative scoring of $CD68^+$ cells revealed a modest increase in positively stained cells within glomeruli of KK-A^y relative to the KK-*a/a* controls (e), additionally a statistically significant increase in interstitial $CD68^+$ macrophages in both groups, with a slight enhancement in the KK-A^y + Unx group (f). Horizontal bars indicate group median score and asterisk represents P value <0.001. (g) Gene expression was assayed by qRT-PCR using total kidney RNA from 26 week old mice KK-A^y, uninephrectomized KK-A^y, and control KK-*a/a* animals. qRT-PCR revealed increased expression of IL-6, MCP-1, CD68, and CD44 were significantly upregulated in KK-A^y versus KK-*a/a* ($P < 0.01$). Uninephrectomy further exacerbated IL-6, MCP-1, and CD68 mRNA upregulation versus KK-A^y ($P < 0.05$).

Both KK-A^y and KK-A^y + Unx animals exhibited multifocal podocyte foot process effacement and areas of irregular GBM thickening, but we observed a 28% decrease in the density of WT-1^+ cells only in the KK-A^y + Unx group, indicating podocyte loss in these mice. Reduced RNA expression of WT-1 and of the podocyte-specific markers nephrin (nphs1) and podocin (nphs2) in KK-A^y + Unx further support this conclusion. We note, however, that despite the evidence of podocyte loss in KK-A^y + Unx mice, the concentration of urine nephrin was similar in both KK-A^y cohorts, suggesting that, while elevated urine nephrin indicated ongoing glomerular injury, the absolute level of nephrinuria may not distinguish relative degrees of podocyte injury. Alternatively, because reduction of renal mass in KK-A^y + Unx animals halves the total number of podocytes, potentially contributing to urinary nephrin, equivalent levels of nephrinuria may actually reflect a much higher rate of podocyte loss in KK-A^y + Unx mice. Nevertheless, taken together, these data attest measurable podocyte loss only in the KK-A^y + Unx group, suggesting that uninephrectomy is necessary to induce podocyte loss in the KK-A^y model.

Our data also indicate that uninephrectomy heightened renal inflammation in this model. Immunostaining for the macrophage marker CD68 revealed a statistically significant increase in $CD68^+$macrophages in the interstitium of diabetic mice, with a trend for greater infiltration in the uninephric versus the binephric KK-A^y group. Furthermore, RNA expression of CD68, as well as of the inflammation-associated markers IL-6 and MCP-1, was significantly greater in the KK-A^y + Unx group. These data all point to increased renal inflammation in Unx-KK-A^y mice as a contributory factor in the enhanced renal phenotype in this model.

The results of this study support a strategy for DN model development, complementary to the AMDCC's recommendation, in which multiple "hits" were layered together to exacerbate renal pathology in mouse models genetically predisposed to diabetes. Such an approach may more realistically capture the interaction between genetics and environment contributing to the complex pathogenesis of diabetic nephropathy.

Conflict of Interests

All authors are employed by Genzyme, a Sanofi company. There are no other competing interests to disclose.

References

[1] A. J. Collins, R. N. Foley, B. Chavers et al., "US renal data system 2011 Annual data report," *American Journal of Kidney Diseases*, vol. 59, no. 1, pp. e1–e26, 2012.

[2] A. Whaley-Connell, J. R. Sowers, P. A. McCullough et al., "Diabetes mellitus and CKD awareness: the kidney early evaluation program (KEEP) and national health and nutrition examination survey (NHANES)," *American Journal of Kidney Diseases*, vol. 53, no. 4, pp. S11–S21, 2009.

[3] P. Fioretto and M. Mauer, "Histopathology of diabetic nephropathy," *Seminars in Nephrology*, vol. 27, no. 2, pp. 195–207, 2007.

[4] T. W. C. Tervaert, A. L. Mooyaart, K. Amann et al., "Pathologic classification of diabetic nephropathy," *Journal of the American Society of Nephrology*, vol. 21, no. 4, pp. 556–563, 2010.

[5] G. R. Reddy, K. Kotlyarevska, R. F. Ransom, and R. K. Menon, "The podocyte and diabetes mellitus: is the podocyte the key to the origins of diabetic nephropathy?" *Current Opinion in Nephrology and Hypertension*, vol. 17, no. 1, pp. 32–36, 2008.

[6] H. Makino, Y. Miyamoto, K. Sawai et al., "Altered gene expression related to glomerulogenesis and podocyte structure in early diabetic nephropathy of db/db mice and its restoration by pioglitazone," *Diabetes*, vol. 55, no. 10, pp. 2747–2756, 2006.

[7] M. Toyoda, B. Najafian, Y. Kim, M. L. Caramori, and M. Mauer, "Podocyte detachment and reduced glomerular capillary endothelial fenestration in human type 1 diabetic nephropathy," *Diabetes*, vol. 56, no. 8, pp. 2155–2160, 2007.

[8] M. E. Pagtalunan, P. L. Miller, S. Jumping-Eagle et al., "Podocyte loss and progressive glomerular injury in type II diabetes," *Journal of Clinical Investigation*, vol. 99, no. 2, pp. 342–348, 1997.

[9] K. E. White, R. W. Bilous, and On Behalf of the Diabiopsies Study Group, "Structural alterations to the podocyte are related to proteinuria in type 2 diabetic patients," *Nephrology Dialysis Transplantation*, vol. 19, no. 6, pp. 1437–1440, 2004.

[10] M. D. Breyer, E. Böttinger, F. C. Brosius et al., "Mouse models of diabetic nephropathy," *Journal of the American Society of Nephrology*, vol. 16, no. 1, pp. 27–45, 2005.

[11] F. C. Brosius, C. E. Alpers, E. P. Bottinger et al., "Mouse models of diabetic nephropathy," *Journal of the American Society of Nephrology*, vol. 20, no. 12, pp. 2503–2512, 2009.

[12] C. Rüster and G. Wolf, "Models of diabetic nephropathy," *Drug Discovery Today*, vol. 7, no. 1-2, pp. 35–41, 2010.

[13] M. J. Soler, M. Riera, and D. Batlle, "New experimental models of diabetic nephropathy in mice models of type 2 diabetes: efforts to replicate human nephropathy," *Experimental Diabetes Research*, vol. 2012, Article ID 218917, 9 pages, 2012.

[14] M. D. Breyer, "Progress in progression?" *Journal of the American Society of Nephrology*, vol. 21, no. 9, pp. 1414–1416, 2010.

[15] D. Schlöndorff, "Choosing the right mouse model for diabetic nephropathy," *Kidney International*, vol. 77, no. 9, pp. 749–750, 2010.

[16] A. R. Diani, G. A. Sawada, B. A. Hannah et al., "Analysis of pancreatic islet cells and hormone content in the spontaneously diabetic KK A^y mouse by morphometry, immunocytochemistry and radioimmunoassay," *Virchows Archiv*, vol. 412, no. 1, pp. 53–61, 1987.

[17] G. Chakraborty, S. Thumpayil, D. E. Lafontant, W. Woubneh, and J. H. Toney, "Age dependence of glucose tolerance in adult KK-A y mice, a model of non-insulin dependent diabetes mellitus," *Lab Animal*, vol. 38, no. 11, pp. 364–368, 2009.

[18] T. Yamazaki, M. Tanimoto, T. Gohda et al., "Combination effects of enalapril and losartan on lipid peroxidation in the kidneys of KK-A^y/Ta mice," *Nephron*, vol. 113, no. 2, pp. e66–e76, 2009.

[19] A. R. Diani, G. A. Sawada, N. Y. Zhang et al., "The KKA(y) mouse: a model for the rapid development of glomerular capillary basement membrane thickening," *Blood Vessels*, vol. 24, no. 6, pp. 297–303, 1987.

[20] M. Okazaki, Y. Saito, Y. Udaka et al., "Diabetic nephropathy in KK and KK-A^y mice," *Experimental Animals*, vol. 51, no. 2, pp. 191–196, 2002.

[21] T. Ito, M. Tanimoto, K. Yamada et al., "Glomerular changes in the KK-A^y/Ta mouse: a possible model for human type 2 diabetic nephropathy," *Nephrology*, vol. 11, no. 1, pp. 29–35, 2006.

[22] T. Shiuchi, T. X. Cui, L. Wu et al., "ACE inhibitor improves insulin resistance in diabetic mouse via bradykinin and NO," *Hypertension*, vol. 40, no. 3, pp. 329–334, 2002.

[23] M. Sasaki, S. Uehara, H. Ohta et al., "Losartan ameliorates progression of glomerular structural changes in diabetic KK A^y mice," *Life Sciences*, vol. 75, no. 7, pp. 869–880, 2004.

[24] M. Matsumoto, M. Tanimoto, T. Gohda et al., "Effect of pitavastatin on type 2 diabetes mellitus nephropathy in KK-A^y/Ta mice," *Metabolism*, vol. 57, no. 5, pp. 691–697, 2008.

[25] I. Ohara, M. Tanimoto, T. Gohda et al., "Effect of combination therapy with angiotensin receptor blocker and 1,25-dihydroxyvitamin D3 in type 2 diabetic nephropathy in KK-A y/Ta mice," *Nephron*, vol. 117, no. 4, pp. e124–e132, 2011.

[26] L. F. Fried, W. Duckworth, J. H. Zhang et al., "Design of combination angiotensin receptor blocker and angiotensin- converting enzyme inhibitor for treatment of diabetic nephropathy (VA NEPHRON-D)," *Clinical Journal of the American Society of Nephrology*, vol. 4, no. 2, pp. 361–368, 2009.

[27] H.-H. Parving, B. M. Brenner, J. J. V. McMurray et al., "Aliskiren trial in type 2 diabetes using cardio-renal endpoints (ALTITUDE): rationale and study design," *Nephrology Dialysis Transplantation*, vol. 24, no. 5, pp. 1663–1671, 2009.

[28] J. I. Suto, S. Matsuura, K. Imamura, H. Yamanaka, and K. Sekikawa, "Genetic analysis of non-insulin-dependent diabetes mellitus in KK and KK-A(y) mice," *European Journal of Endocrinology*, vol. 139, no. 6, pp. 654–661, 1998.

[29] H. Ninomiya, T. Inomata, and K. Ogihara, "Obstructive uropathy and hydronephrosis in male KK-A^y mice: a report of cases," *Journal of Veterinary Medical Science*, vol. 61, no. 1, pp. 53–57, 1999.

[30] M. Nakamura and K. Yamada, "Studies on a diabetic (KK) strain of the mouse," *Diabetologia*, vol. 3, no. 2, pp. 212–221, 1967.

[31] B. Becker, F. Kronenberg, J. T. Kielstein et al., "Renal insulin resistance syndrome, adiponectin and cardiovascular events in patients with kidney disease: the mild and moderate kidney disease study," *Journal of the American Society of Nephrology*, vol. 16, no. 4, pp. 1091–1098, 2005.

[32] H. Ha, E. Y. Oh, and H. B. Lee, "The role of plasminogen activator inhibitor 1 in renal and cardiovascular diseases," *Nature Reviews Nephrology*, vol. 5, no. 4, pp. 203–211, 2009.

[33] J. H. Chang, S. Y. Paik, L. Mao et al., "Diabetic kidney disease in FVB/NJ Akita mice: temporal pattern of kidney injury and urinary nephrin excretion," *PLoS ONE*, vol. 7, no. 4, Article ID e33942.

[34] Y. Wang, S. Zhao, S. Loyd, and L. J. Groome, "Increased urinary excretion of nephrin, podocalyxin, and betaig-h3 in women with preeclampsia," *American Journal of Physiology*, vol. 302, no. 9, pp. F1084–F1089, 2012.

[35] V. S. Vaidya, V. Ramirez, T. Ichimura, N. A. Bobadilla, and J. V. Bonventre, "Urinary kidney injury molecule-1: a sensitive quantitative biomarker for early detection of kidney tubular injury," *American Journal of Physiology*, vol. 290, no. 2, pp. F517–F529, 2006.

[36] V. S. Sabbisetti, K. Ito, C. Wang et al., "Novel assays for detection of urinary Kim-1 in mouse models of kidney injury," *Toxicological Sciences*, vol. 131, no. 1, pp. 13–25, 2013.

[37] P. Ronco, "Proteinuria: is it all in the foot?" *Journal of Clinical Investigation*, vol. 117, no. 8, pp. 2079–2082, 2007.

[38] V. D. D'Agati, "Podocyte injury in focal segmental glomerulosclerosis: lessons from animal models (a play in five acts)," *Kidney International*, vol. 73, no. 4, pp. 399–406, 2008.

[39] F. T. H. Lee, Z. Cao, D. M. Long et al., "Interactions between angiotensin II and NF-κB-dependent pathways in modulating macrophage infiltration in experimental diabetic nephropathy," *Journal of the American Society of Nephrology*, vol. 15, no. 8, pp. 2139–2151, 2004.

[40] M. Nagata, K. Scharer, and W. Kriz, "Glomerular damage after uninephrectomy in young rats. I. Hypertrophy and distortion of capillary architecture," *Kidney International*, vol. 42, no. 1, pp. 136–147, 1992.

[41] J. M. Turner, C. Bauer, M. K. Abramowitz, M. L. Melamed, and T. H. Hostetter, "Treatment of chronic kidney disease," *Kidney International*, vol. 81, pp. 351–362, 2012.

[42] J. A. Chavez and S. A. Summers, "Lipid oversupply, selective insulin resistance, and lipotoxicity: molecular mechanisms," *Biochimica et Biophysica Acta*, vol. 1801, no. 3, pp. 252–265, 2010.

[43] M. N. Jensen and M. Ritskes-Hoitinga, "How isoflavone levels in common rodent diets can interfere with the value of animal models and with experimental results," *Laboratory Animals*, vol. 41, no. 1, pp. 1–18, 2007.

[44] K. D. R. Setchell, "Phytoestrogens: the biochemistry, physiology, and implications for human health of soy isoflavones," *American Journal of Clinical Nutrition*, vol. 68, supplement 6, pp. 1333S–1346S, 1998.

[45] K. Sharma, S. RamachandraRao, G. Qiu et al., "Adiponectin regulates albuminuria and podocyte function in mice," *Journal of Clinical Investigation*, vol. 118, no. 5, pp. 1645–1656, 2008.

[46] A. A. Eddy and A. B. Fogo, "Plasminogen activator inhibitor-1 in chronic kidney disease: evidence and mechanisms of action," *Journal of the American Society of Nephrology*, vol. 17, no. 11, pp. 2999–3012, 2006.

[47] R. B. Goldberg, "Cytokine and cytokine-like inflammation markers, endothelial dysfunction, and imbalanced coagulation in development of diabetes and its complications," *Journal of Clinical Endocrinology and Metabolism*, vol. 94, no. 9, pp. 3171–3182, 2009.

[48] D. P. K. Ng, B. C. Tai, E. Tan et al., "Nephrinuria associates with multiple renal traits in type 2 diabetes," *Nephrology Dialysis Transplantation*, vol. 26, no. 8, pp. 2508–2514, 2011.

[49] M. A. Saleh, E. I. Boesen, J. S. Pollock, V. J. Savin, and D. M. Pollock, "Endothelin receptor A-specific stimulation of glomerular inflammation and injury in a streptozotocin-induced rat model of diabetes," *Diabetologia*, vol. 54, no. 4, pp. 979–988, 2011.

[50] Group CKDW, "VA/DoD clinical practice guideline for the management of chronic kidney disease in primary care. Version 2.0," in *Veterans Health Administration (VHA) DoVAV*, Department of Defense (DoD), Ed., Veterans Health Administration and Department of Defense, Washingon DC, USA, 2008.

[51] National Kidney Foundation, "K/DOQI clinical practice guidelines for chronic kidney disease: evaluation, classification, and stratification," *American Journal of Kidney Diseases*, vol. 39, no. 2, supplement 1, pp. S1–S266, 2002.

Hindawi Publishing Corporation
Journal of Diabetes Research
Volume 2013, Article ID 620313, 7 pages
http://dx.doi.org/10.1155/2013/620313

Research Article

Nearby Construction Impedes the Progression to Overt Autoimmune Diabetes in NOD Mice

Erin E. Hillhouse,[1,2] Roxanne Collin,[1,2] Geneviève Chabot-Roy,[1] Marie-Josée Guyon,[1] Nathalie Tessier,[1] Maryse Boulay,[1,3] Patricia Liscourt,[1] and Sylvie Lesage[1,2]

[1] *Maisonneuve-Rosemont Hospital Research Center, Montréal, QC, Canada H1T 2M4*
[2] *Department of Microbiology and Immunology, University of Montreal, Montréal, QC, Canada H3C 3J7*
[3] *Centre de Recherche du Centre Hospitalier de l'Université de Montréal, Montréal, QC, Canada H2L 2W5*

Correspondence should be addressed to Sylvie Lesage; sylvie.lesage@gmail.com

Received 19 December 2012; Revised 19 March 2013; Accepted 29 March 2013

Academic Editor: Shahidul Islam

Construction nearby animal houses has sporadically been reported to affect various aspects of animal health. Most of the reports have focussed on the impact on stress hormone levels and the hypersensitivity of animals relative to humans. There has also been an anecdotal report on the impact of construction on autoimmune diabetes in NOD mice. Here, we describe that nearby construction significantly impedes the progression to overt diabetes in female NOD mice offspring. We demonstrate that this was not due to a genetic drift or to particularities associated with our specific mouse colony. Interestingly, although the glycemia levels remained low in mice born from mothers subject to construction stress during gestation, we detected an active autoimmune reaction towards pancreatic islet cells, as measured by both the degree of insulitis and the presence of insulin autoantibody levels in the serum. These results suggest that the external stress imposed during embryonic development does not prevent but significantly delays the autoimmune process. Together, our findings emphasize the impact of surrounding factors during *in vivo* studies and are in agreement with the hypothesis that both environmental and genetic cues contribute to autoimmune diabetes development.

1. Introduction

The NOD mouse was developed in the 1970s in Japan and has since become the animal model of choice to investigate the genetic, cellular, and molecular mechanisms involved in the development of autoimmune diabetes [1]. This inbred strain spontaneously develops an autoimmune reaction towards pancreatic islet antigens, destroying the insulin-producing pancreatic beta cells. The spontaneous disease process in the NOD mouse parallels that observed in humans and, consequently, the NOD mouse model provides an important tool to dissect and better understand the complex pathophysiological process leading to disease onset [2, 3].

Two main factors are known to contribute to disease susceptibility of this complex trait, namely, genetic and environmental factors. First, autoimmune diabetes is a complex genetic trait, with over 50 genetic loci contributing to disease susceptibility [4, 5]. Interestingly, a direct parallel can be made between most of the diabetes susceptibility genetic risk factors currently identified in humans and mice [6]. However, a notable difference is that although the prevalence of autoimmune diabetes in humans is not influenced by gender, the incidence in female NOD mice is consistently higher than that of male mice [1]. Nevertheless, the NOD strain constitutes a valid model to investigate the pathophysiology and the genetic susceptibility towards the spontaneous occurrence of autoimmune diabetes. Second, the contribution of environmental factors to diabetes susceptibility in humans is less well understood and include, but are not limited to, viral infections, diet and epigenetic modifications [7, 8].

Interestingly, environmental factors are not only at play in defining susceptibility to autoimmune diabetes in humans but also exhibit a major impact on susceptibility to disease in the inbred NOD strain. Indeed, the incidence of diabetes is known to vary depending on the barrier status of the animal house, where the incidence of disease

Table 1: Description of the mothers and litters from the NOD/LtJ-HMR mouse colony used in this study.

Breeding pair (#)	Date of birth of the mother	Became diabetic	Number of litters produced	In gestation during construction	Age of mothers at postpartum, first litter	Litters included in the study
142	June 16, 2010	Unknown	2 litters	Yes	15 weeks	1st litter born October 1, 2010
143	June 16, 2010	Yes	6 litters	No	8 weeks	N/A, not included
144	July 25, 2010	Yes	5 litters	Yes	10 weeks	1st litter born October 5, 2010 After construction born Dec 9 2010

is the highest in specific pathogen-free facilities relative to conventional facilities [9–11]. The type of diet provided to NOD mice or the ambient temperature in which the mouse colonies are kept can both impact the incidence of disease [12–15]. Finally, the Jackson Laboratory has reported modest changes in the incidence of disease in their large NOD mouse cohorts due to alterations in light cycles or to nearby construction and earthquake tremors (http://type1diabetes.jax.org/images/fine-mapping/1976%20cumulative%20inc.jpg).

We currently hold a NOD mouse colony in our specific pathogen-free facility, for which we routinely monitor the incidence of diabetes in female mice. These data serve as a control for ongoing experiments, wherein we administer different products to female NOD mice to determine the impact of these products on the pathophysiology of the disease as well as the incidence of diabetes [16]. In our small animal cohort, we show that nearby construction significantly delayed diabetes onset in NOD mice and almost completely impeded the progression to overt diabetes. We also demonstrate that this is not a consequence of a genetic drift in our NOD mouse colony. The results emphasize the importance of considering the surrounding environment when performing experiments in animal models.

2. Methods

2.1. Ethics Statement. All experiments were performed in line with the rules and regulations of the Canadian Council for Animal Protection, and the experimental procedure was approved by the Maisonneuve-Rosemont Hospital Animal Care Committee.

2.2. Mice. NOD mice from the NOD/LtJ colony were purchased from Jackson Labs in 2006 and were maintained by intercrossing nondiabetic 6-week-old male and female mice at the Hôpital Maisonneuve-Rosemont (HMR) specific pathogen-free facility. Routine microbiological monitoring of dirty bedding exposed sentinel animals was performed for the following murine pathogens: mouse hepatitis virus, Sendai virus, pneumonia virus of mice, reovirus-3, Theiler's murine encephalomyelitis virus, *Mycoplasma pulmonis*, mouse parvovirus, mice minute virus, mouse rotavirus, murine norovirus, *Helicobacter genus, Helicobacter bilis, Helicobacter hepaticus*, *Bordetella bronchiseptica, Corynebacterium kutscheri, Klebsiella oxytoca, Klebsiella pneumoniae, Pasteurella multocida, Pasteurella pneumotropica (Heyl and Jawetz), Pseudomonas aeruginosa, Staphylococcus aureus, Streptococcus pneumonia, Beta Strep* spp., *Beta Strep.* sp.-*Group B, Beta Strep.* sp.-*Group G, Salmonella, Citrobacter rodentium, Clostridium piliforme*. The colony was also free of the following endo- and ectoparasites: lice, mites, *Aspicularis tetraptera*, *Syphacia murisSyphacia obvelata*, *Chilomastix* sp. *Entamoeba* sp., *Giardia, Hexamastix* sp., *Monocercomonoides* sp., *Retortamonas* sp., *Spironucleus* sp., and *Trichomonads*. The colony remained free of these specific pathogens for the period of interest, aside from one report of *Entamoeba* sp. in July 2011. Animals were kept under a photoperiod of 14 hours of light/10 hours of darkness and ambient temperatures set at a range of 21°C to 24°C. Animals had unlimited access to distilled and acidified water and standard rodent diet (2018 Teklad Global 18% Protein Rodent Diet, or 2019 Teklad Global 19% Protein Extruded Rodent Diet, Harlan Laboratories Inc., Indianapolis, IN, USA). Mice were maintained in polycarbonate individually ventilated cages with hardwood bedding (7090A Teklad Aspen SaniChips, Harlan Laboratories Indianapolis Inc., IN, USA).

The breeding couples have been renewed, on average, every 14 weeks in an attempt to minimize potential genetic drifts [17]. The incidence of diabetes was monitored when the colony was at the HMR F11 to F13 generations. This mouse colony is hereafter referred to as NOD/LtJ-HMR. NOD mice were also purchased from the NOD/ShiLtJ colony at Jackson Labs in January 2011 and were maintained at the HMR under the same conditions as the NOD/LtJ-HMR colony. All our NOD mouse colonies were maintained by on-site breeding, in the same barrier status from 2006 to 2012, with no change in the housing conditions, husbandry practices, feed, or water. No embryo transfer or cross-fostering was undertaken in these colonies.

2.3. Construction. Asphalt and part of the sidewalk were repaired from September 15 to 18, 2010. The animal house where all the NOD mice are kept is located in the basement immediately adjacent to this construction site. At that time, we held three breeder pairs, for which the details are provided in Table 1.

2.4. Monitoring Diabetes Incidence. Diabetes incidence was monitored daily for overt signs of diabetes (wet cage, hunched posture) and every two weeks for urine glucose levels using Diastix (Bayer) starting at between 8 to 10 weeks of age. Mice

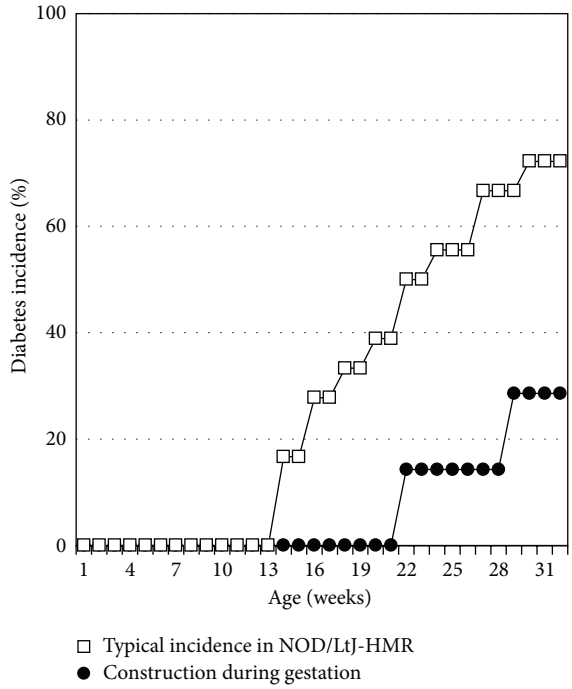

Figure 1: Nearby construction during the gestation period impacts diabetes onset and cumulative incidence in offspring. Depicted is a typical cumulative incidence of diabetes for eighteen female NOD/LtJ-HMR mice (open squares). Two NOD/LtJ-HMR female mice were in gestation while asphalt and sidewalk repairs were being carried out immediately outside the facility. The incidence of diabetes was closely monitored in the seven female offspring from these mothers (closed circles), where the onset is observed at 22 weeks of age and the cumulative incidence reaches approximately 30% at 32 weeks of age. Log-rank test, P value < 0.05.

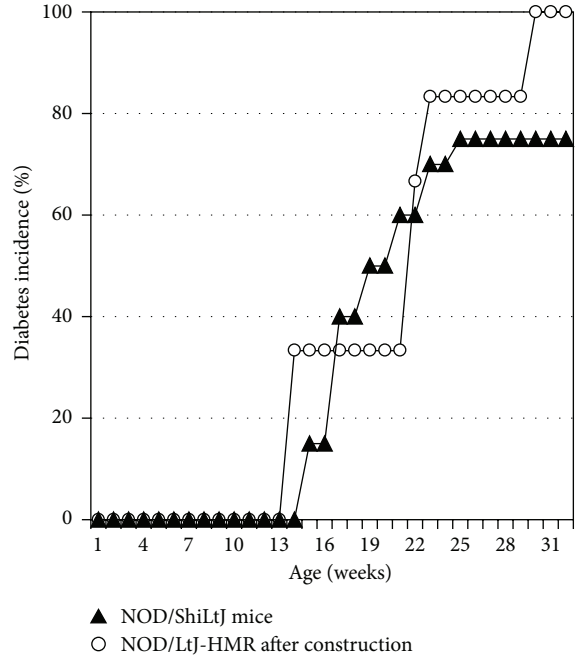

Figure 2: The lower incidence of diabetes is not due to a genetic drift in our colony. The onset of diabetes was monitored in six female NOD mice from the NOD/LtJ-HMR mouse colony born more than two months after the construction had been completed (open circles) as well as from twenty female NOD/ShiLtJ mice bought from Jackson Labs and maintained at the HMR facility (closed triangles). The cumulative diabetes incidence shows no difference between these two colonies. Log-rank test, P value = 0.4142.

were called diabetic upon two consecutive positive urine glucose readings. Blood glucose measurements >12 mM were used to confirm diabetes. Mice presenting with >12 mM of blood glucose were sacrificed within one week. All other mice were sacrificed at 32 weeks of age. At sacrifice, the pancreas was collected and frozen in Optimal Cutting Temperature Compound (OCT, Fisher) and the serum was collected and stored at −80°C.

2.5. Insulitis. Frozen pancreases were cut to 7 μm sections, pressed against slides, fixed in acetone, and stored overnight at 4°C prior to hematoxylin and eosin staining. Three to six nonconsecutive sections of pancreas were analysed per mouse. The number of islets as well as the degree of insulitis was quantified according to the following scale (see Figure 4): 0, no infiltration; 1, lymphocytes surrounding the islets; 2, lymphocytes surrounding the islets and break of barrier (less than 50% infiltration); 3, lymphocytes within the islets (over 50% infiltration); 4 extensive lymphocytic infiltrate with few or no detectable pancreatic islet cells.

2.6. Insulin Autoantibodies (IAA). The serum levels of IAA were measured by ELISA in a protocol adapted from previous work [18–20]. Insulin (Insulin B (9–23), Anaspec) was immobilized onto microwells in 96 well plates. As a negative control, half of each serum sample was previously incubated with insulin for 7 days. All serum samples (preincubated with insulin or not) were diluted 1/10 and were added to the insulin-coated microwells. Horseradish peroxidase-labeled polyclonal goat anti-mouse IgG (Biolegend) followed by TMB substrate solution (Biolegend) was used to quantify insulin-specific IgG antibodies. The optical density (OD) is directly proportional to the concentration of IAA in the sample. All samples were run in duplicate. The level of IAA in the sample = (average of sample OD) − (average of background control OD).

2.7. Statistics. Log rank Mantel-Cox tests were performed using GraphPad Prism 5 to determine the statistical significance of the difference in the incidence of diabetes.

3. Results and Discussion

Jackson Labs had previously reported that nearby construction partially affected the diabetes incidence in their NOD/LtJ colony in 2006 (http://type1diabetes.jax.org/images/fine-mapping/1976%20cumulative%20inc.jpg). Therefore, as we were aware of nearby construction upon undertaking a new diabetes incidence study in September 2010, we closely monitored the diabetes onset and incidence in the female

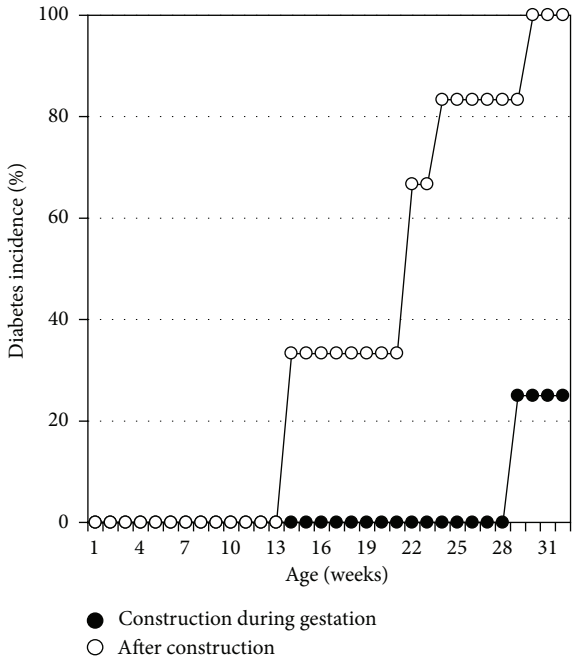

Figure 3: Nearby construction affects diabetes onset and cumulative incidence in NOD mice born from the same breeder pair. The cumulative incidence of diabetes is compared for female NOD mice born from the same breeder pair at different times, namely, those who nearby construction occurred during their embryonic development (closed circles, $n = 4$) and those born over two months after the construction event (open circles, $n = 6$). Log-rank test, P value < 0.05.

NOD mouse experimental control group. Notably, at the HMR-specific pathogen-free animal house facility, diabetes onset in female NOD mice from the NOD/LtJ-HMR colony is typically between 12 to 14 weeks of age, and the incidence of diabetes reaches approximately 70%–80% at 32 weeks of age (Figure 1).

Two of the three female NOD mice, that had been placed in breeding pairs, were in gestation during the construction period—September 15 to 18, 2010 (Table 1). We monitored the incidence of diabetes in the seven female offspring born in October 2010 from these mothers. We observed a delay in diabetes onset, which now initiated at 22 weeks of age for female NOD mice born from mothers subject to construction stress during gestation (Figure 1). Moreover, we found a significantly reduced cumulative incidence of diabetes, where only two of the seven female NOD mice developed diabetes within 32 weeks in the NOD/LtJ-HMR mouse colony (Figure 1).

Notably, the incidence of diabetes in Figure 1 was monitored in female NOD mice inbred for 11 to 13 generations in a relatively small animal house cohort, generally comprised of 3 to 5 breeder pairs. Although breeder replacement is performed on average every 14 weeks to prevent potential genetic selection for diabetes resistance, we could not entirely exclude the possibility of a genetic drift in the NOD/LtJ-HMR mouse colony [17, 21–23]. Indeed, as diabetes onset normally occurs between 12 to 14 weeks of age in female NOD mice of the NOD/LtJ-HMR mouse colony, and since we maintained a few breeder pairs beyond that time point, there is a risk that we selected mice carrying a genetic polymorphism conferring resistance to diabetes.

We thus went on to test the hypothesis that the diabetes onset was delayed and that the incidence was reduced in the NOD/LtJ-HMR mouse colony as a consequence of a genetic drift. We undertook a second diabetes incidence study with six female NOD mice of the NOD/LtJ-HMR colony born in December 2010, more than two months after the construction had been completed. In addition, we purchased twenty 7-week-old female NOD mice from the Jackson Labs NOD/ShiLtJ mouse colony and maintained them in the same conditions as the mice from the NOD/LtJ-HMR colony. The onset of diabetes for female NOD mice from both the NOD/LtJ-HMR and NOD/ShiLtJ mouse colonies was between 12–15 weeks of age and the cumulative incidence of diabetes also reached 70–100% in both mouse colonies by 32 weeks of age (Figure 2). Together, our data demonstrate that the decrease in disease onset and cumulative incidence observed in the female NOD mice born in October 2010 was not due to a genetic drift in our mouse colony and is likely attributable to the effect of nearby construction.

Of interest, all of the six female NOD mice of the NOD/LtJ-HMR colony from Figure 2 were born from one of the two original breeders, wherein the mothers had been subject to construction stress during the gestation two months before. We thus opted to directly compare the diabetes incidence from the four female NOD mice born in early October 2010 (i.e., subject to construction stress during their embryonic development) to the six female NOD mice born in December 2010, where all 10 offspring are of the same breeder pair. We again find a statistical difference in the incidence of diabetes as well as a delay in disease onset (Figure 3). These results demonstrate that the biological effects causing alterations in diabetes susceptibility due to construction stress are rapidly dissipated overtime and are unlikely to cause permanent modifications to the phenotype.

As mentioned previously, of the seven NOD female offspring born from mothers subject to construction stress during gestation, only two mice progressed to overt diabetes. Therefore, the environmental stress imposed by the construction during embryonic development appears to delay, but not necessarily impede, the autoimmune reaction towards pancreatic islet antigens. As such, we evaluated the subclinical progression of autoimmunity by quantifying the degree of insulitis and islet cell destruction. As expected, all diabetic NOD mice presented with few pancreatic islets and heavy lymphocyte infiltrates, suggesting an active autoimmune process (Figure 4). In contrast, the 32-week-old nondiabetic NOD/ShiLtJ mice presented with a greater number of pancreatic islets and with fewer lymphocytic infiltrates than the diabetic NOD mice (Figure 4). Surprisingly, few pancreatic islets were found in the nondiabetic NOD/LtJ-HMR mice which were subject to construction stress during embryonic development (Figure 4). Moreover, the few remaining pancreatic islets were heavily infiltrated with

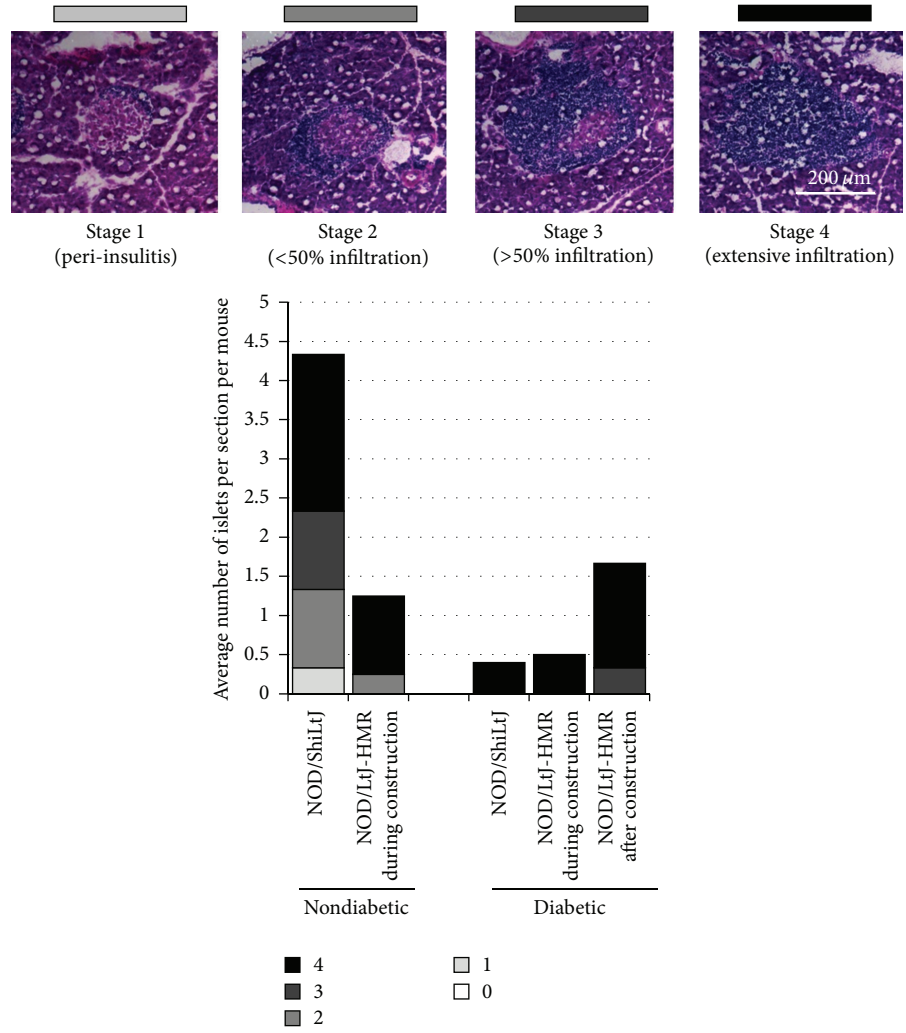

Figure 4: Islet destruction and lymphocytic infiltration in nondiabetic NOD mice subject to construction stress. The number of islets per pancreatic section was scored as exemplified by the histology sections presented (scale 200 μm). At least three mice per group were included except for the diabetic NOD/LtJ-HMR mice during construction, which included only two mice. Note that there are no nondiabetic mice from the NOD/LtJ-HMR mice born after construction.

lymphocytes (Figure 4). These results suggest that the stress imposed by the construction did not prevent the onset of the autoimmune response and that the mice were slowly progressing towards overt diabetes.

To further define whether an active autoimmune response was ongoing in the five nondiabetic NOD/LtJ-HMR mice which were subject to construction stress during embryonic development, we determined the serum insulin autoantibody (IAA) levels. Serum IAA levels correlate with autoimmune diabetes onset in both humans and NOD mice and the serum IAA levels eventually decline with disease progression [18, 24, 25]. Expectedly, the 32-week-old nondiabetic NOD/ShiLtJ mice did not show detectable levels of serum IAA levels, while the diabetic NOD mice exhibited a variable range of serum IAA (Figure 5). In agreement with the histological observations suggestive of an active autoimmune response in the nondiabetic NOD/LtJ-HMR mice, IAA were present in the serum of these mice (Figure 5). Taken together, these results suggest that the nondiabetic NOD/LtJ-HMR mice were likely progressing towards overt diabetes. The stress imposed by the nearby construction during the embryonic development, therefore, does not preclude the onset of an autoimmune response towards pancreatic islets, although it significantly delays the progression to overt diabetes.

Limits of this current study include the low number of mice analyzed in our cohorts and the difficulty in reproducing similar events. However, similar variations in diabetes incidence have previously been documented by the Jackson Laboratory in much larger NOD animal cohorts. Indeed, the Jackson Laboratory has previously reported a modest effect of nearby construction on the incidence of diabetes in their NOD/ShiLtJ mouse colony (http://type1diabetes.jax.org/images/fine-mapping/1976%20cumulative%20inc.jpg). In contrast, we report a striking and significant delay in disease onset as well as in the cumulative incidence of

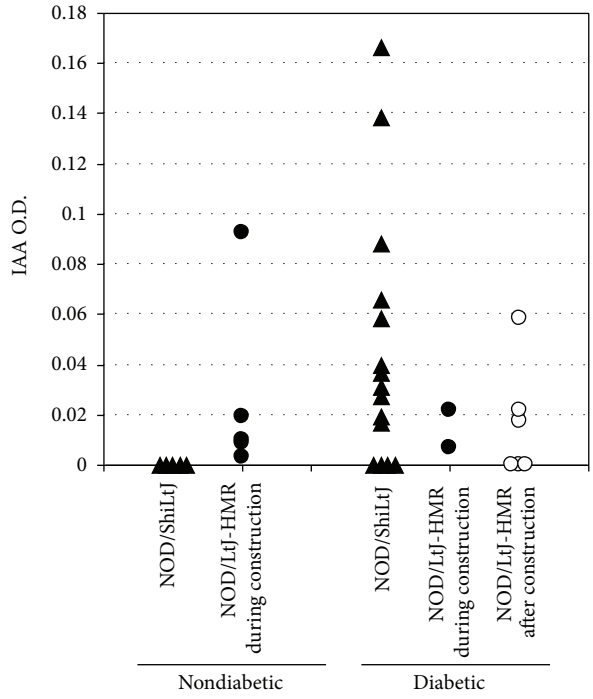

Figure 5: Serum IAA levels as an indication of an ongoing autoimmune response towards pancreatic islets. The serum IAA levels are shown for every mouse group and segregated according to the health status (i.e., diabetic versus nondiabetic). Note that there are no nondiabetic mice from the NOD/LtJ-HMR mice born after construction. Each dot represents one mouse.

disease. The main difference between these two studies lies in the stratification of data. Whereas we stratified the mice according to whether the mothers were subject to construction stress during gestation or not, the data reported by the Jackson Laboratory presents a cumulative incidence study of a larger cohort over an entire year and they did not stratify their data relative to construction events. It is thus likely that the reason we observe a more striking effect of nearby construction on both the onset and incidence of diabetes is due to a stricter stratification of affected mice. To that effect, in our hands, the nearby construction only affected mice that were born from mothers subject to construction stress during gestation and not from mice born from the same parents at a later date. The effect is thus not permanent and unlikely to cause permanent changes in a mouse colony. Together with the results of the larger NOD mouse cohort study from the Jackson Laboratory, the current study performed on a limited number of NOD mice supports the view that nearby construction can significantly affect the incidence of diabetes.

Another factor which could have influenced the incidence of diabetes in our study includes variations in the microbiome of the mouse colony over time. The animal house barrier status is known to influence the incidence of diabetes in NOD mice [1]. More recently, the microbiome was shown to influence diabetes incidence by causing variations in testosterone hormone levels and other metabolomic changes [11]. We have not directly characterized the microbiome or the hormone levels of our NOD mouse colony before and after construction. However, the routine sentinel health report status did not vary overtime, nor did the feeding, water, bedding, or procedures for the animal handling (as described in the Methods section). In addition, the fertility of NOD mice was not apparently affected by the construction stress (Table 1), suggesting that the potential changes in hormone levels were insufficient to affect the fertility. Admittedly, these represent very crude and indirect measures of the microbiome and hormone levels, and thus we cannot fully exclude the possibility that the variations in diabetes incidence in our study were due to modifications in these parameters. Of interest, changes in the microbiome have been reported to significantly alter testosterone levels without affecting NOD mouse fertility [11].

In addition to the microbiome and hormone levels, elevated serum IAA levels from the mothers have also been shown to significantly impact diabetes incidence [26, 27]. At postpartum, the NOD mothers were 10 and 15 weeks of age for the first litters subject to construction stress (Table 1). The serum IAA levels typically peak at 8 weeks of age and slowly wane off overtime [18], suggesting that the mothers were likely to present detectable serum IAA levels. Notably, first litters of NOD mothers in our animal house facility typically present with a normal incidence of diabetes (not shown). Still, the fact that we did not monitor the serum IAA levels from the mothers presents a limitation of our study.

In summary, many parameters can influence diabetes incidence in NOD mice and there are possible alternative explanations as to why the mouse cohorts subject to construction stress during gestation showed a reduced incidence of diabetes. Nevertheless, the fact that litters born from the same mother, where one litter was subject to construction stress and the other was not, exhibited a significant difference in diabetes incidence suggests that construction stress during gestation modulates biological responses. Our results thus add to the observations from the Jackson Laboratory documenting a potential influence of nearby construction on the incidence of diabetes in NOD mice.

4. Conclusions

Altogether, these results emphasize the importance of surrounding factors which should be taken into consideration when performing long-term *in vivo* studies and are in agreement with the hypothesis that both environmental and genetic cues contribute to autoimmune diabetes development. Our data lend further support to the view that environmental stress caused by nearby construction severely impacts biological processes. Of interest, NOD mice suffer from significant hearing loss [28, 29] suggesting that vibrations, rather than noise, emitted as a consequence of the nearby construction provoke physiological changes in rodents. We would thus caution investigators that, prior to undertaking long-term *in vivo* studies, alterations in the surrounding environment must be carefully considered and appropriately controlled.

Acknowledgments

The authors wish to thank Adam-Nicolas Pelletier for expert help with statistical analyses. E. E. Hillhouse and R. Collin currently hold a Diabète Québec scholarship. E. E. Hillhouse was also a recipient of a CIHR Ph.D. scholarship. S. Lesage holds a CIHR New Investigator Award and is currently funded by the Canadian Foundation for Innovation and the Natural Sciences and Engineering Research Council of Canada. The weblink in the manuscript presents data obtained by The Jackson Laboratory, which was funded by The National Center for Research Resources (NCRR) at NIH.

References

[1] M. S. Anderson and J. A. Bluestone, "The NOD mouse: a model of immune dysregulation," *Annual Review of Immunology*, vol. 23, pp. 447–485, 2005.

[2] A. Lehuen, J. Diana, P. Zaccone, and A. Cooke, "Immune cell crosstalk in type 1 diabetes," *Nature Reviews Immunology*, vol. 10, no. 7, pp. 501–513, 2010.

[3] M. Kornete and C. A. Piccirillo, "Critical co-stimulatory pathways in the stability of Foxp3$^+$ Treg cell homeostasis in Type I diabetes," *Autoimmunity Reviews*, vol. 11, pp. 104–111, 2011.

[4] J. C. Barrett, D. G. Clayton, P. Concannon et al., "Genome-wide association study and meta-analysis find that over 40 loci affect risk of type 1 diabetes," *Nature Genetics*, vol. 41, no. 6, pp. 703–707, 2009.

[5] L. S. Wicker, J. A. Todd, and L. B. Peterson, "Genetic control of autoimmune diabetes in the NOD mouse," *Annual Review of Immunology*, vol. 13, pp. 179–200, 1995.

[6] L. S. Wicker, J. Clark, H. I. Fraser et al., "Type 1 diabetes genes and pathways shared by humans and NOD mice," *Journal of Autoimmunity*, vol. 25, supplement, pp. 29–33, 2005.

[7] M. Knip, R. Veijola, S. M. Virtanen, H. Hyöty, O. Vaarala, and H. K. Åkerblom, "Environmental triggers and determinants of type 1 diabetes," *Diabetes*, vol. 54, supplement 2, pp. S125–S136, 2005.

[8] A. El-Osta, D. Brasacchio, D. Yao et al., "Transient high glucose causes persistent epigenetic changes and altered gene expression during subsequent normoglycemia," *The Journal of Experimental Medicine*, vol. 205, pp. 2409–2417, 2008.

[9] B. Singh and A. Rabinovitch, "Influence of microbial agents on the development and prevention of autoimmune diabetes," *Autoimmunity*, vol. 15, no. 3, pp. 209–213, 1993.

[10] L. Wen, R. E. Ley, P. Y. Volchkov et al., "Innate immunity and intestinal microbiota in the development of Type 1 diabetes," *Nature*, vol. 455, no. 7216, pp. 1109–1113, 2008.

[11] J. G. Markle, D. N. Frank, S. Mortin-Toth et al., "Sex differences in the gut microbiome drive hormone-dependent regulation of autoimmunity," *Science*, vol. 339, pp. 1084–1088, 2013.

[12] A. J. K. Williams, J. Krug, E. F. Lampeter et al., "Raised temperature reduces the incidence of diabetes in the NOD mouse," *Diabetologia*, vol. 33, no. 10, pp. 635–637, 1990.

[13] D. P. Funda, A. Kaas, T. Bock, H. Tlaskalova-Hogenova, and K. Buschard, "Gluten-free diet prevents diabetes in NOD mice," *Diabetes/Metabolism Research and Reviews*, vol. 15, no. 5, pp. 323–327, 1999.

[14] J. Hoorfar, K. Buschard, and F. Dagnaes-Hansen, "Prophylactic nutritional modification of the incidence of diabetes in autoimmune non-obese diabetic (NOD) mice," *British Journal of Nutrition*, vol. 69, no. 2, pp. 597–607, 1993.

[15] M. Furuse, C. Kimura, H. Takahashi, and J. I. Okumura, "Prevention of the incidence of diabetes by dietary sorbose in nonobese diabetic mice," *Journal of Nutrition*, vol. 121, no. 7, pp. 1135–1138, 1991.

[16] V. Dugas, C. Beauchamp, G. Chabot-Roy, E. E. Hillhouse, and S. Lesage, "Implication of the CD47 pathway in autoimmune diabetes," *Journal of Autoimmunity*, vol. 35, no. 1, pp. 23–32, 2010.

[17] P. Pozzilli, A. Signore, A. J. K. Williams, and P. E. Beales, "NOD mouse colonies around the world—recent facts and figures," *Immunology Today*, vol. 14, no. 5, pp. 193–196, 1993.

[18] L. Yu, D. T. Robles, N. Abiru et al., "Early expression of antiinsulin autoantibodies of humans and the NOD mouse: evidence for early determination of subsequent diabetes," *Proceedings of the National Academy of Sciences of the United States of America*, vol. 97, no. 4, pp. 1701–1706, 2000.

[19] E. Bonifacio, M. Atkinson, G. Eisenbarth et al., "International Workshop on Lessons From Animal Models for Human Type 1 Diabetes: identification of insulin but not glutamic acid decarboxylase or IA-2 as specific autoantigens of humoral autoimmunity in nonobese diabetic mice," *Diabetes*, vol. 50, no. 7–12, pp. 2451–2458, 2001.

[20] N. Babaya, Y. Liping, M. Dongmei et al., "Comparison of insulin autoantibody: polyethylene glycol and micro-IAA 1-day and 7-day assays," *Diabetes/Metabolism Research and Reviews*, vol. 25, no. 7, pp. 665–670, 2009.

[21] A. G. Baxter, F. Hamilton, T. E. Mandel, C. Augustine, A. Cooke, and G. Morahan, "Genetic basis for diabetes resistance in NOD/Wehi mice," *European Journal of Immunogenetics*, vol. 20, no. 5, pp. 409–417, 1993.

[22] A. G. Baxter, M. Koulmanda, and T. E. Mandel, "High and low diabetes incidence Nonobese Diabetic (NOD) mice: origins and characterisation," *Autoimmunity*, vol. 9, no. 1, pp. 61–67, 1991.

[23] A. G. Baxter, M. A. Adams, and T. E. Mandel, "Comparison of high- and low-diabetes-incidence NOD mouse strains," *Diabetes*, vol. 38, no. 10, pp. 1296–1300, 1989.

[24] A. K. Steck, K. Johnson, K. J. Barriga et al., "Age of islet autoantibody appearance and mean levels of insulin, but not GAD or IA-2 autoantibodies, predict age of diagnosis of type 1 diabetes: diabetes autoimmunity study in the young," *Diabetes Care*, vol. 34, pp. 1397–1399, 2011.

[25] E. Bonifacio and A. G. Ziegler, "Advances in the prediction and natural history of type 1 diabetes," *Endocrinology and Metabolism Clinics of North America*, vol. 39, no. 3, pp. 513–525, 2010.

[26] S. A. W. Greeley, M. Katsumata, L. Yu et al., "Elimination of maternally transmitted autoantibodies prevents diabetes in nonobese diabetic mice," *Nature Medicine*, vol. 8, no. 4, pp. 399–402, 2002.

[27] E. Melanitou, D. Devendra, E. Liu, D. Miao, and G. S. Eisenbarth, "Early and quantal (by litter) expression of insulin autoantibodies in the nonobese diabetic mice predict early diabetes onset," *Journal of Immunology*, vol. 173, no. 11, pp. 6603–6610, 2004.

[28] M. Atkinson, P. Gendreau, T. Ellis, and J. Petitto, "NOD mice as a model for inherited deafness," *Diabetologia*, vol. 40, no. 7, article 868, 1997.

[29] A. Lonyai, S. Kodama, D. Burger, and D. L. Faustman, "Fetal Hox11 expression patterns predict defective target organs: a novel link between developmental biology and autoimmunity," *Immunology and Cell Biology*, vol. 86, no. 4, pp. 301–309, 2008.

Hindawi Publishing Corporation
Journal of Diabetes Research
Volume 2013, Article ID 906590, 12 pages
http://dx.doi.org/10.1155/2013/906590

Review Article

Animal Models of GWAS-Identified Type 2 Diabetes Genes

Gabriela da Silva Xavier,[1] Elisa A. Bellomo,[1] James A. McGinty,[2] Paul M. French,[2] and Guy A. Rutter[1]

[1] *Section of Cell Biology, Division of Diabetes, Endocrinology and Metabolism, Department of Medicine, Imperial College London, London SW7 2AZ, UK*
[2] *Biophotonics Section, Department of Physics, Imperial College London, London SW7 2AZ, UK*

Correspondence should be addressed to Guy A. Rutter; g.rutter@imperial.ac.uk

Received 4 February 2013; Accepted 18 March 2013

Academic Editor: Daisuke Koya

More than 65 *loci*, encoding up to 500 different genes, have been implicated by genome-wide association studies (GWAS) as conferring an increased risk of developing type 2 diabetes (T2D). Whilst mouse models have in the past been central to understanding the mechanisms through which more penetrant risk genes for T2D, for example, those responsible for neonatal or maturity-onset diabetes of the young, only a few of those identified by GWAS, notably *TCF7L2* and *ZnT8/SLC30A8*, have to date been examined in mouse models. We discuss here the animal models available for the latter genes and provide perspectives for future, higher throughput approaches towards efficiently mining the information provided by human genetics.

1. Introduction

The estimated global prevalence for diabetes in 2011 was 366 million, and the disease is expected to affect 552 million people by 2030 (Diabetes U.K. figures; [1] accessed 09/01/13). Type 2 diabetes (T2D) is a complex and multifactorial disease characterised by impaired insulin secretion and insulin resistance. Disease risk/progression is determined by a combination of genetic and environmental factors. It has been consistently demonstrated that lifestyle factors are associated with risk of T2D across populations [2–8], with increased adiposity being the greatest modifiable risk factor for the disease [9, 10]. Inactivity [3, 11], "bad" diet [2, 6, 8, 12–14], smoking, and other vices [8, 15, 16] and the nutritional environment during pre- and postnatal life [17] also contribute to the risk for developing diabetes.

It has been estimated that 30–70% of T2D risk may be due to genetics [18]. Whilst pedigree-based linkage analysis and the candidate gene approach led to the discovery of highly penetrant genetic defects which account for the development of diabetes [19–24], it is the advent of large scale genome-wide association studies (GWAS) which have led to the accelerated discovery of risk-variants associated with T2D [25–34]. Currently, over 60 common risk variants have been identified [30–34], with a combined disease risk of 5–10% [34, 35], suggesting the existence of many more as yet undiscovered loci [34, 36, 37]. Most of the GWAS-identified associations for T2D have high linkage disequilibrium with a causal variant with a small effect size; the largest common variant-signal identified to date is that for *TCF7L2,* which has a per allelle odds ratio of 1.35 [27–29].

Most of the common variant signals identified by GWAS are associated with defective pancreatic islet function, indicating that this is the primary driver for the development of T2D [34, 38]. However, most of the GWAS signals map to noncoding regions of the genome, making it difficult to establish functional links to specific transcripts. As a result, determination both of (a) the identity of the likely transcript(s) involved and (b) the mechanisms of actions on disease risk, require the use of genetically tractable organisms where the expression of candidate genes can be manipulated at will in a cell type-specific manner. Of the available models (which include lower organisms such as *C. elegans*, *D. melanogaster,* etc.), mice arguably represent the best compromise between ease of genetic manipulation and similarity to man, in terms of both genome structure and physiology. In this review, we discuss the use of mouse models to study the contribution of genetic variations, identified by GWAS, in the *TCF7L2* and

SLC30A8 genes to the development of T2D via their effects on pancreatic islet function.

2. *TCF7L2*

2.1. Background. The gene-encoding Transcription 7 Like-2 (*TCF7L2*, previously called TCF4) is the most important T2D susceptibility gene identified to date, with genetic variants strongly associated with diabetes in all major racial groups [27–29, 39–59]. Signals in this locus are the most consistently identified across various GWAS and are associated with the highest elevation of risk of developing adult-onset T2D. Each copy of the risk *T*-allele at rs7903146 has an increased odds ratio for T2D of 1.4-1.5 [60]. Inheritance of the risk allele is also a useful predictor for the likelihood of conversion from a state of prediabetes to T2D [61, 62]. Additionally, results from a small number of studies also indicate that *TCF7L2* variation may play an important role in cases of early onset T2D [63, 64].

TCF7L2 is a member of the TCF family of transcription factors involved in the control of cell growth and signalling downstream of wingless-type MMTV integration site family (Wnt) receptors [65]. Activation of the Wnt pathway leads to release of β-catenin from an inhibitory complex and its translocation to the nucleus, where it binds *TCF7L2* and other related TCF factors [66]. The function of this transcriptional complex is context dependent; that is it may act as either a transcriptional activator or repressor [66].

In recent years, the product of the *TCF7L2* gene has been associated with dysregulated pancreatic β cell function and T2D [25, 27, 28]. Enhanced Wnt signalling has been shown to lead to proliferation of islets [67] and the pancreatic epithelium [68]. Whilst loss of β-catenin signalling has been shown to lead to pancreatic hypoplasia [69], stabilisation of β-catenin has been shown to result in the formation of large pancreatic tumours [70].

Individuals carrying the risk alleles of rs7903146 in the *TCF7L2* gene display lowered insulin secretion [61, 71, 72], impaired insulin processing [71], and decreased sensitivity to the incretin glucagon-like peptide 1 (GLP-1) [72, 73] compared to controls. *TCF7L2* message levels were elevated in T2D patients [72, 74], whilst *TCF7L2* protein content was depressed [75]. The decrease in protein content was associated with downregulation of GLP-1 and gastric inhibitory peptide (GIP) receptor expression and impaired pancreatic β cell function [74, 76, 77]. Studies have shown that silencing of *Tcf7l2* gene expression in clonal mouse β cell lines [76] and primary islets [75] leads to increased apoptosis [75] and impaired β cell function [19, 20]. Gene expression analysis following *Tcf7l2* silencing revealed changes in the expression of a number of genes in mouse pancreatic islets [76], one of which was *Glp1r* [73, 78]. *TCF7L2* may mediate GLP-1-induced β cell proliferation through activation of the Wnt signalling pathway [79]. Since GLP-1 is implicated in β cell survival, the increased incidence of apoptosis in *TCF7L2*-silenced islets [74, 75] and in individuals carrying the variants of *TCF7L2* [73] is consistent with lowered GLP-1 signalling [73, 78]. Correspondingly, the diminished insulinotropic effect of GLP-1 in *Tcf7l2*-silenced islets may be due, at least in part, to the lack of cognate receptors on the cell surface [74].

2.2. Mouse Models for TCF7L2

2.2.1. Whole Body Knockout Model. Prior to its association with T2D, *TCF7L2* was previously best known for its association with cancer development [80–82]. Homozygous *Tcf7l2* knockout (*Tcf7l2* $^{-/-}$) mice die shortly after birth, with a lack of stem cells in their intestinal crypts [83]. Newborn *Tcf7l2* $^{-/-}$ mice have reduced body weight with significantly lower blood glucose 3 h postpartum than control littermates, which is not caused by excessive insulin release but by impaired carbohydrate and lipid metabolism in the newborn liver [84].

Heterozygote *Tcf7l2* $^{+/-}$ mice display >20% decrease in body weight compared to wild-type littermates, with decreased glucose, insulin, fatty acid, triglyceride, and cholesterol in adult mice [84]. *Tcf7l2* $^{+/-}$ mice displayed increased insulin sensitivity, improved glucose tolerance, and reduced hepatic glucose output [84, 85]. Improved glucose tolerance was also observed in heterozygote null mice generated using zinc finger nucleases [85] and insertion of a loxP site and FRT-flanked neomycin selection cassette within intron 4 and a loxP site within intron 5 [86], with data from the latter study also pointing to reduced lipogenesis and hepatic triglyceride levels and decreased peripheral fat deposition following exposure to a high fat diet in heterozygote mice compared to control littermates.

Pancreatic development is grossly normal in *Tcf7l2* $^{-/-}$ mice [83, 84]. This observation and a report suggesting that *TCF7L2* was not expressed in the pancreas [87] led to the proposal that the principle defect underlying decreased insulin production in TC- or TT-bearing individuals may be inadequate production of GLP-1, from gut L-cells [88]. However, evidence for differences in GLP-1 level in individuals with the common *versus* the at-risk *TCF7L2* allele is currently absent [89], and patient studies have indicated that the primary defect lies in pancreatic β cells [71, 72, 75]. For this reason, mouse models which allow *Tcf7l2* gene expression to be selectively ablated in the islet were required.

2.2.2. Pancreas Knockout Model. We used the *Pdx1* promoter-driven Cre recombinase (PDX1.*Cre)* deleter strain [90] to effect deletion in all cells of pancreatic lineage in transgenic mice with a floxed *Tcf7l2* exon 1 to address the question whether selective deletion of *Tcf7l2* in pancreas impairs or improves glucose homeostasis and insulin secretion [77]. This approach allowed us to detect the potential effects of *Tcf7l2* deletion early in pancreatic development, as *TCF7L2* has previously been shown to regulate cell proliferation during development: the *Tcf7l2* $^{-/-}$ mouse exhibited defects in the accumulation of stem cells in the intestinal crypt [83]. This approach also offered an advantage over the use of the commonly deployed rat insulin 2-promoter-driven Cre recombinase (RIP2.*Cre*) deleter strain since the latter also leads to deletion in the central nervous system [91–93]. Pancreas-specific *Tcf7l2* $^{-/-}$ (pTcf7l2) mice showed age-dependent glucose intolerance by 20 weeks of age when

challenged with an intraperitoneal glucose bolus [77]. Glucose intolerance was detected from 12 weeks of age when glucose was administered by the oral route, indicating that the incretin response was impaired [77]. Tolerance to glucose introduced by both the oral and intraperitoneal route was exacerbated in pTcf7l2 mice that were exposed to a high fat diet, with a concomitant decrease in β cell mass [77]. The latter observation is consistent with observations by Shu and colleagues in high-fat-fed rats [94], where the authors found a correlation of *Tcf7l2* expression and β cell regeneration from pancreatic ductal cells and may reflect the inability of β cells to proliferate or regenerate from progenitor cells in the absence of functional *Tcf7l2*. The decreased expression of the *cyclin D1* gene [77] from islets of Langerhans extracted from 20-week-old pTcf7l2 mice may contribute towards the lack of cell proliferation.

pTcf7l2 $^{-/-}$ islets displayed impaired glucose and GLP-1-stimulated insulin secretion and decreased expression of the gene encoding for the GLP-1 receptor [77], consistent with *in vitro* human and mouse islet and cell line siRNA-mediated-silencing experiments [74–76]. Whilst the PDX1.*Cre* strain is likely to result in deletion in other (non-β) cell types [95], we observed no difference in plasma glucagon and GLP-1 levels and in insulin sensitivity in pTcf7l2 mice [77]. Our preliminary data obtained using a more β cell selective deleter strain (Ins1.*Cre*; J. Ferrer, B. Thorens, unpublished) also indicate deficiencies in insulin secretion and glucose tolerance, suggesting that *TCF7L2* plays a critical and cell autonomous role in the β cell compartment.

2.2.3. β Cell Knockout Model. Recently, Boj and colleagues generated a β cell *Tcf7l2* knockout (βTCF4KO) mouse using the tamoxifen inducible RIP2.*Cre*-ER^{T2} deleter strain [96] bred against a conditional mouse-bearing *Tcf7l2* alleles with a *flox*ed exon 10 [84]. Although the use of the RIP2.Cre-ER^{T2} may affect metabolic phenotype through the expression of *Cre* recombinase in islet cells as well as in hypothalamic neurons [95], it is unclear whether *Tcf7l2* expression was affected in the hypothalamus of βTCF4KO mice.

βTCF4KO mice on normal or high fat diet displayed normal glucose tolerance when glucose was introduced by the intraperitoneal route [84]. There was no difference in plasma insulin and insulin release from isolated islets of βTCF4KO mice, *versus* control littermates, in response to glucose challenge [84]. Importantly, however, mice were not examined beyond 12 weeks of age, and oral glucose tolerances were not reported in this later study.

2.2.4. Transgenic Models. In the three previous mouse models described in this section, *Tcf7l2* gene expression was ablated either constitutively [83] or specifically in islet cells [77, 84]. Savic and colleagues took a different approach whereby they engineered mice that expressed LacZ under the control of human bacterial artificial chromosomes (BACs) containing the genomic interval encompassing the diabetes associated SNPs (which are intronic) for *TCF7L2* [85]. Using this technique, they demonstrated the presence of enhancer function in the SNPs-containing region which drives expression in, for example, intestine and pancreas, but not in adult islets [85]. Transgenic mice with *Tcf7l2* overexpression driven by the human BAC sequence exhibited glucose intolerance when placed on a high fat diet [85]. These data are consistent with that presented by Gaulton and colleagues [103] indicating that the chromatin of the *TCF7L2* intronic variant is in an islet-specific "open" conformation, and reporter assays demonstrated increased enhancer activity of the at-risk *T*-allelle compared with the *C*-allelle in β cell lines.

The discrepancy in data between the various mouse models could be partly due to the involvement of *TCF7L2* in glucose homeostasis in more than one tissue, and at different times during development. The *Tcf7l2* gene was manipulated in different ways in the various experimental models and this may alter the tissue-specific splicing of the gene [104–107]. The expression of different variants may lead to different outcomes in different tissue types [104–107]. Analysis of glucose homeostasis at different time points during the life time of the animals and exposure to differing amounts of time to diets with different fat composition could all contribute to the differences in observations.

3. ZnT8 (SLC30A8)

3.1. Background. ZnT8 (encoding by the *SLC30A8* gene) is a member of the zinc transporter family (ZnTs) important for extruding zinc from the cytosol into either the extracellular space or intracellular organelles [108]. In particular, the expression of ZnT8 is largely (but not exclusively) restricted to α and β cells of the islets of Langerhans, where the mature protein resides chiefly on the limiting membrane of dense core secretory granule [97, 109, 110]. Its function thus, appears to be chiefly to transport Zn^{2+} from the cytosol into the granules where, in beta cells, this is required for insulin crystallisation [111]. By contrast, the role of Zn^{2+} in glucagon storage in the pancreatic alpha cell granule is not fully understood.

From the discovery that a single nucleotide polymorphism in the *SLC30A8* gene leads to an increased risk of developing T2D [27, 29], much work has been done to elucidate the function of the encoded protein and the role that ZnT8 plays in the pathogenesis of the disease. In contrast with the majority of GWAS-identified polymorphisms, rs13266634 in the *SLC30A8* gene encodes the replacement of Trp for Arg at position 325 (R325W) at the C-terminus of the protein and is associated with a ~20% increased risk of developing T2D per allele [28]. Given the highly restricted expression pattern of the transporter, hopes have been raised that ZnT8 may provide an exciting new drug target to enhance insulin release in diabetic patients.

3.2. Mouse Models Exploring ZnT8/SLC30A8 Function. A number of mouse models have been generated in order to elucidate the function of this molecule and its role in the pathogenesis of diabetes. These include whole body [97, 99–101] and cell type-specific (α or β cell) [102] ZnT8 knockout animals. Systemic ZnT8 knockout models have up to now been investigated by three different groups [97, 99–101]. These studies have revealed gross abnormalities (albeit age

Table 1: Summary of the major phenotype of the different colonies of ZnT8 KO mice. ZnT8-αKO and ZnT8-βKO for α and β-cell-specific knockout mice, respectively; GSIS for glucose-stimulated insulin secretion.

Phenotype/model	ZnT8KO-London [97]	ZnT8KO-Toronto [98]	ZnT8KO-Leuven [99]	ZnT8KO-Vanderbilt [100] (129SvEv^{Brd} × C57BL/6J)	ZnT8KO-Vanderbilt [101] (C57BL/6J)	ZnT8-αKO	ZnT8-βKO [102]
Glucose tolerance							
≤6 weeks	♂ intolerant	♂ intolerant ♀ intolerant	Normal		♂ intolerant	Normal	Intolerant
12 weeks	♂ intolerant ♀ normal	♂ normal ♀ intolerant	Normal				
≥18 weeks			Normal	Normal	Normal		
Insulin sensitivity	Normal	Normal	Normal	Normal	Normal		
Plasma glucose		♂: Elevated (fasting) at 6 wks, normal afterwards. ♀: Normal	Normal	Normal	Normal (fasting)		
Plasma insulin		Decreased	Normal	Decreased	Normal (fasting)	Normal. (Plasma glucagon normal.)	Normal
Islet insulin content			Normal (glucagon content was normal.)	Normal	Normal		
Insulin secretion							
In vivo		Reduced					
In vitro	Basal secretion enhanced GSIS normal	GSIS enhanced	GSIS normal	GSIS reduced	GSIS normal		Reduced first phase
Glucagon secretion		Unaffected					
Insulin processing	Normal		Normal				
Granule morphology	Abnormal	Abnormal	Abnormal		Normal	Normal	Abnormal

and gender dependent) in insulin crystallisation and storage [97, 99] (Figure 1(a)), confirming the importance of ZnT8 in granular zinc accumulation. Nonetheless, significant differences were apparent both in terms of the regulation of insulin secretion and whole body glucose homeostasis. These differences are likely the result of subtle differences in genetic background, gender, and the age of the animals. Local environmental factors including diet and gut microbiome may also play a role [112]. Thus, glucose tolerance was found to be impaired at an early age (4–6 weeks of age) in three of these studies but not at an older age (>18 weeks) [97, 99, 100], suggesting that the penetrance of the phenotype decreases with age. While insulin sensitivity was unaltered in all of the studies, defects in insulin secretion were reported in two of the studies [97, 100]. None of these changes was associated with altered beta cell mass (Figures 1(b) and 1(c)) These data support the view that decreased ZnT8 activity is likely to influence glucose homeostasis in man and may underlie the defects which increase the risk of developing T2D. Differences in the phenotype are summarised in Table 1.

Of note, the two recent studies of Pound et al. stress the importance of the genetic background. In the first [100], the genetically modified animals were maintained on a mixed background, while in the second [101], the mice were backcrossed onto a pure C57BL/6 background. Strikingly, whereas glucose-stimulated insulin secretion was unaltered in islets from ZnT8 knockout mice on a pure C57BL/6 background, islets from mice on the mixed background showed clear abnormalities in this parameter. Again, plasma insulin was decreased in the mixed background animals, while it was found normal in mice on a pure background. Since these mice were generated and kept in the same animal facility, it seems reasonable to exclude environmental differences as playing a role. Instead, these data support the view that background is a critical determinant of the penetrance of null ZnT8 alleles. Whether this impacts the preservation of functional β cell

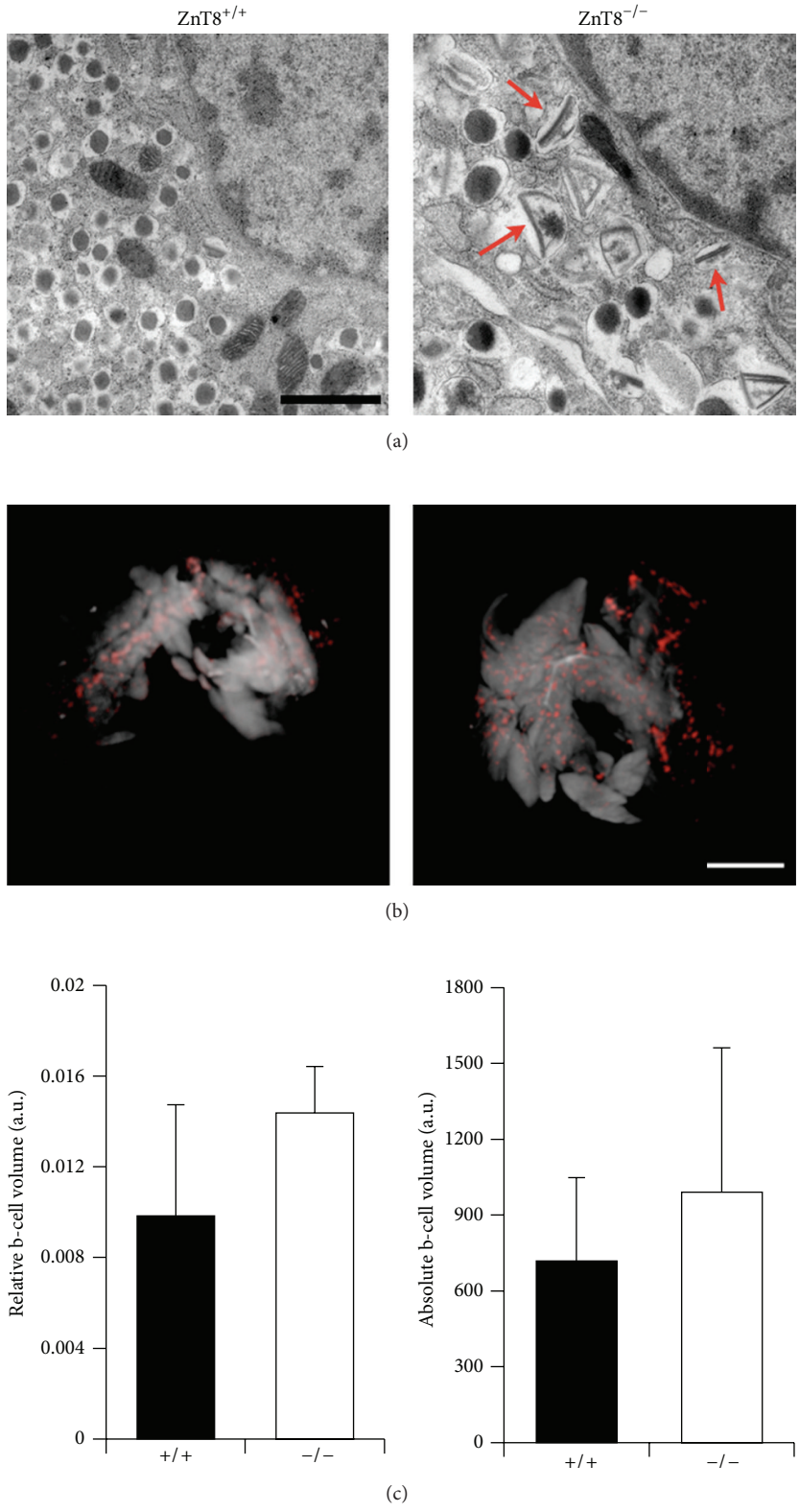

Figure 1: Electron Micrographs and Optical Projection Tomography (OPT) in $ZnT8^{+/+}$ and $ZnT8^{-/-}$ mice. (a) Transmission electron microscopy images of isolated islets from $ZnT8^{+/+}$ and $ZnT8^{-/-}$ male mice at high magnification (scale bar 1 mm) reveals the appearance of rod-shaped core granules in $ZnT8^{-/-}$ cells, indicated by red arrows ($n = 3$ mice). Sections were cut and images were acquired by Dr. Raffaella Carzaniga and Ms. Katrin Kronenberger. (b) Representative three-dimensional OPT projections of whole fixed and permeabilised pancreas from $ZnT8^{-/-}$ and $ZnT8^{+/+}$ mice. In red are the insulin positive structures (β cells). The overall shape of the whole pancreas was visualized as autofluorescence and is apparent as white/grey shading. Scale bar = 1 cm. (c) Relative (right panel) and absolute (left panel) β-cell volume ($n = 2$ pancreata per genotype).

mass in the face of differing insulin sensitivities between the strains, altered intracellular Zn^{2+} handling, or defective auto/paracrine Zn^{2+} signalling between islets cells remains to be elucidated.

As mentioned above, ZnT8 is present in both α and β cells such that the systemic knockout model reflects the impact of deletion from both cell types (and perhaps others where ZnT8 is expressed at low but detectable levels). The generation of cell-specific knockout models has therefore helped in understanding the contribution of each cell type to the overall phenotype observed. Wijesekara et al. described both the animal models in a recent paper [102]. Deletion of ZnT8 selectively from β cells (βZnT8 null mice; using the RIP2 promoter) led to similar effects on glucose homeostasis as those observed in the systemic knockout developed by the same group and by ourselves [97], confirming that the transporter is required for proper insulin processing, crystallization, and packaging. However, βZnT8 null mice displayed additional abnormalities in the expression of key genes required for normal glucose sensing in β cells. Whilst the underlying reasons for this greater penetrance are unclear, it is possible that changes in intracellular free Zn^{2+} levels are more marked in the β cell selective model since the α cell complement remains as an efficient sink for Zn^{2+} release, thus, more efficiently depleting β cell Zn^{2+}. Nonetheless, the broad similarities between ZnT8 whole body knockout and the β-cell-specific mouse model suggest that the phenotype of the former is primarily a consequence of ZnT8 deletion in β and not α cells; α cell-selective ZnT8 null mouse displayed unaltered glucose tolerance. However, glucagon secretion was not measured in these animals under conditions where the latter is likely to be physiologically important that is hypoglycaemia. It therefore remains possible that ZnT8 plays a significant role in the α cell, a possibility which awaits more detailed examination of α cell-selective null mice in the future.

Because T2D is a polygenic disease that is also influenced by environmental factors, it is important to mention new studies where ZnT8 knockout animals were maintained on a high fat content diet (HFD) [98, 99]. In both of these studies, ZnT8 null mice displayed an increase in body weight as well as fasting blood glucose and insulin levels compared to wild type controls. In particular, in one of these studies, 50% of the ZnT8 knockout animals became hyperglycemic after exposure to HFD, while none of the controls did so [99]. Each of these studies was performed using animals on a mixed (sv129/C57BL6) background. On the other hand, a further recent study using animals backcrossed onto a C57BL6 background [101] revealed that ZnT8 null animals were protected against the effects of high fat, again stressing the likely importance of modifier genes in determining the final penetrance of the effect. Although it is difficult to provide a straightforward rationalisation for these differences, it is noteworthy that sv129 mice are more insulin sensitive than C57BL6 animals [113], with the latter producing more insulin in hyperglycemic clamps. It is possible, therefore, that C57BL6 mice are better equipped to tolerate perturbations in insulin storage and secretion following *ZnT8* deletion.

These data reinforce the idea that mice, at least, are able to adapt metabolically to the loss of ZnT8 alleles under many circumstances. However, under metabolic stress, such as in the case of a diet rich in fat, the impact of defective insulin storage and or secretion are more apparent at least for mice on a mixed genetic background.

Whilst complete inactivation of ZnT8 in the mouse has been useful as a means of understanding the function of this protein, it is clear that more work needs to be done in order to elucidate the significance of the diabetes-associated polymorphism *in vivo*. At present, knock-in models for either the protective (W325) or risk (R325) forms of ZnT8 are missing and may be revealing, provided that the impact on transporter activity is sufficiently large [97]. Of note, such models would more closely mimic the situation in humans and help us to better understand the metabolic, signaling, and other pathways that are altered in tissues which express the transporter.

4. Perspectives

4.1. Better Mouse Models. A key point to bear in mind in assessing the usefulness of mouse models is the relative plasticity displayed by rodents faced with gene deletions. Thus, differences between the penetrance of mutations in human genes linked to monogenic forms of diabetes, including maturity onset diabetes of the young (MODY), between humans and mice, are usually observed [114] with the mouse equivalents showing far less marked disturbances in glycemia or changes which are seen only after deletion of both alleles. This clearly reflects the limitations of the use of mice (weight ~25 g, life expectancy ~3 years) for comparisons with human subjects. Nonetheless, and although the phenotypes of the above murine models are thus often more subtle than the human counterparts, they remain useful models for the study of diabetes, allowing single-targeted gene deletions which are impossible in man. For example, human populations with different genetic backgrounds have different susceptibility to the R235W ZnT8 polymorphism. We should not, therefore, find surprising the results that different genetic backgrounds and different diet reveal different phenotypes in ZnT8 knockout models.

The study of knockout mouse models is most useful if the likely target gene is clearly defined, as is the case when a SNP lies in an exon and encodes a nonsense or missense mutation (as for *SLC30A8*). One of the difficulties in studying the contribution of the SNPs identified for increased risk of T2D is that many of the SNPs identified to date mainly reside in intronic regions. This may be due to the technical limitations of identifying the disease-causing gene using current methods for GWAS, or that the disease-inducing variation may indeed reside in the intronic region of the gene, which may have regulatory function, as may be the case for *TCF7L2* [85]. Frequently, the sequences within the SNP regions are poorly conserved between mouse and man, for example, the sequences spanning SNP rs7903146 for *TCF7L2* lies within a repetitive element that is absent in mice. One possibility is to conduct physiological studies in "humanized" mice [85], but it is difficult to fully replicate the human

genetic environment in mouse models. Additionally, it is technically difficult to introduce targeted changes at high efficiency at precise locations. The emergence of genome modification technologies such as transcription activator-like effector nucleases (TALENs) [115–117] can substantially speed up the making of a tailored mutant animal model for whole system approaches to study the contribution of risk variants identified by GWAS to disease progression and may be useful in those instances where the region containing the variation is sufficiently similar to that found in humans. Importantly, such gene-editing approaches may also facilitate the use of alternative species (such as the rat or even the pig) whose physiology more closely resembles that of man.

An additional complication is that disease-causing SNPs do not exist in isolation. The genetic landscape of each individual may play a part in an individual's risk of developing a certain disease. For example, the risk of T2D is additive: the larger the number of risk SNPs present in an individual's genome, the higher the risk for the development of T2D [37, 118–121]. Thus, future animal models may require careful mapping of the genetic variations present in the model animal and the introduction of more than one genetic variation to model the diabetic phenotype conferred by these combined genetic variations.

4.2. Gene-Environment Interactions. An individual's risk of developing T2D is the product of interaction between the individual's genetic constitution and the environment inhabited by the individual. Whilst the contribution of genetic factors to disease risk is relatively easy to quantify, the impact of environmental exposure is less easily measured in a clinical setting. Nevertheless, efforts have been made to study the interactions between some of the known susceptibility *loci* for T2D and the environment, and these findings may be useful for the development of prediction models and tailoring clinical treatment for T2D [122, 123]. For example, for carriers of the risk allele for *TCF7L2*, diets of low glycaemic load [124, 125] and a more intensive lifestyle modification regime (*versus* that recommended for nonrisk carriers) [61, 62, 126, 127] have been shown to reduce the risk of T2D. Meaningful studies for gene-environment interactions will require samples of sufficient size to increase statistical power [128] and accurate methods for measuring environmental exposure, for example, the use of metabolomics to identify and assess metabolic characteristics, changes, and phenotypes in response to the environment, diet, lifestyle, and pathophysiological states. This information will allow the generation of better risk prediction models and personalisation/stratification of treatment, the holy grail of GWAS.

4.3. Cancer versus Diabetes (Opposing Mechanisms Hypothesis). One other observation from GWAS that should be mentioned, as it may have implications on treatment, is the link between cancer and T2D. There is epidemiological evidence that links T2D and cancer [129]. A large number of T2D genes found via GWAS are involved in cell cycle regulation [34], for example, the T2D association SNP mapping to chromosome 9p21 in the vicinity of the tumour suppressor genes CDKN2A and CDKN2B [130–132] and the CDKN2B regulator ANRIL [133–135]. Recent genetic data suggest that common genetic variants influence cancer and diabetes in opposite directions [136, 137].

4.4. Which Genes Do We Study? A fundamental challenge facing those wishing to determine which of the genes in a particular locus is responsible for affecting disease risk, and dissect how this/these act, is the very scale of the problem (currently more than 500 genes in total to interrogate, with others emerging) [35] (and McCarthy M, personal communication). Clearly, new strategies will be required both to prioritise genes and thus develop models for those most likely to be involved: assessment of the impact of a particular variant (odds ratio) as well as expression profile (notably expression in β cells for those genes affecting insulin secretion), and finally, the likely biological impact of variations in a particular gene based on published knowledge are all essential to this process. Further, "experimental filtration" through higher throughput approaches (e.g., siRNA in β cell lines, including novel human lines [138]) are likely to be needed. Finally, more high throughput means to inactivate or overexpress genes in specific tissues in living mice without the need to engineer the latter via conventional recombination-based engineering of embryonic stem cells (e.g., through virus-mediated delivery) [139] and are likely to be increasingly important. A further challenge is that of understanding how the identified genes affect disease risk work via different tissues; systems and computational biology are likely to be highly important here.

Acknowledgments

This work is supported by Wellcome Trust Senior Investigator (WT098424AIA), Royal Society Wolfson Research Merit, MRC Programme (MR/J0003042/1), and Diabetes UK Studentship grants to Guy A. Rutter. Gabriela da Silva Xavier and Guy A. Rutter thank the European Foundation for the Study of Diabetes (EFSD) for Project grants. The work leading to this publication has also received support from the Innovative Medicines Initiative Joint Undertaking under Grant Agreement no. 155005 (IMIDIA), resources of which are composed of financial contribution from the European Union's Seventh Framework Programme (FP7/2007–2013) and EFPIA companies' in kind contribution.

References

[1] Diabetes UK, "Diabetes in the UK 2012: key statistics on diabetes," 2013.

[2] F. B. Hu, "Globalization of diabetes: the role of diet, lifestyle, and genes," *Diabetes Care*, vol. 34, pp. 1249–1257, 2011.

[3] F. B. Hu, T. Y. Li, G. A. Colditz, W. C. Willett, and J. E. Manson, "Television watching and other sedentary behaviors in relation to risk of obesity and type 2 diabetes mellitus in women," *Journal of the American Medical Association*, vol. 289, no. 14, pp. 1785–1791, 2003.

[4] W. C. Knowler, E. Barrett-Connor, S. E. Fowler et al., "Reduction in the incidence of type 2 diabetes with lifestyle intervention or metformin," *New England Journal of Medicine*, vol. 346, no. 6, pp. 393–403, 2002.

[5] A. Ramachandran, C. Snehalatha, S. Mary, B. Mukesh, A. D. Bhaskar, and V. Vijay, "The Indian Diabetes Prevention Programme shows that lifestyle modification and metformin prevent type 2 diabetes in Asian Indian subjects with impaired glucose tolerance (IDPP-1)," *Diabetologia*, vol. 49, no. 2, pp. 289–297, 2006.

[6] J. Salas-Salvadó, M. Bulló, N. Babio et al., "Reduction in the incidence of type 2 diabetes with the mediterranean diet: results of the PREDIMED-Reus nutrition intervention randomized trial," *Diabetes Care*, vol. 34, no. 1, pp. 14–19, 2011.

[7] J. Tuomilehto, J. Lindström, J. G. Eriksson et al., "Prevention of type 2 diabetes mellitus by changes in lifestyle among subjects with impaired glucose tolerance," *New England Journal of Medicine*, vol. 344, no. 18, pp. 1343–1350, 2001.

[8] R. M. Van Dam, "The epidemiology of lifestyle and risk for type 2 diabetes," *European Journal of Epidemiology*, vol. 18, no. 12, pp. 1115–1125, 2003.

[9] D. Yach, D. Stuckler, and K. D. Brownell, "Epidemiologic and economic consequences of the global epidemics of obesity and diabetes," *Nature Medicine*, vol. 12, pp. 62–66, 2006.

[10] P. W. F. Wilson, J. B. Meigs, L. Sullivan, C. S. Fox, D. M. Nathan, and R. B. D'Agostino Sr., "Prediction of incident diabetes mellitus in middle-aged adults: the framingham offspring study," *Archives of Internal Medicine*, vol. 167, no. 10, pp. 1068–1074, 2007.

[11] J. S. Rana, T. Y. Li, J. E. Manson, and F. B. Hu, "Adiposity compared with physical inactivity and risk of type 2 diabetes in women," *Diabetes Care*, vol. 30, no. 1, pp. 53–58, 2007.

[12] V. S. Malik, B. M. Popkin, G. A. Bray, J. P. Després, W. C. Willett, and F. B. Hu, "Sugar-sweetened beverages and risk of metabolic syndrome and type 2 diabetes: a meta-analysis," *Diabetes Care*, vol. 33, no. 11, pp. 2477–2483, 2010.

[13] U. Risérus, W. C. Willett, and F. B. Hu, "Dietary fats and prevention of type 2 diabetes," *Progress in Lipid Research*, vol. 48, no. 1, pp. 44–51, 2009.

[14] A. W. Barclay, P. Petocz, J. McMillan-Price et al., "Glycemic index, glycemic load, and chronic disease risk—a metaanalysis of observational studies," *American Journal of Clinical Nutrition*, vol. 87, no. 3, pp. 627–637, 2008.

[15] N. A. Christakis and J. H. Fowler, "The spread of obesity in a large social network over 32 years," *New England Journal of Medicine*, vol. 357, no. 4, pp. 370–379, 2007.

[16] C. Willi, P. Bodenmann, W. A. Ghali, P. D. Faris, and J. Cornuz, "Active smoking and the risk of type 2 diabetes: a systematic review and meta-analysis," *Journal of the American Medical Association*, vol. 298, no. 22, pp. 2654–2664, 2007.

[17] G. C. Burdge and K. A. Lillycrop, "Nutrition, epigenetics, and developmental plasticity: implications for understanding human disease," *Annual Review of Nutrition*, vol. 30, pp. 315–339, 2010.

[18] P. Poulsen, K. Ohm Kyvik, A. Vaag, and H. Beck-Nielsen, "Heritability of type II (non-insulin-dependent) diabetes mellitus and abnormal glucose tolerance—a population-based twin study," *Diabetologia*, vol. 42, no. 2, pp. 139–145, 1999.

[19] K. Owen and A. T. Hattersley, "Maturity-onset diabetes of the young: from clinical description to molecular genetic characterization," *Best Practice and Research*, vol. 15, no. 3, pp. 309–323, 2001.

[20] I. S. Farooqi and S. O'Rahilly, "Genetics of obesity in humans," *Endocrine Reviews*, vol. 27, no. 7, pp. 710–718, 2006.

[21] N. Risch and K. Merikangas, "The future of genetic studies of complex human diseases," *Science*, vol. 273, no. 5281, pp. 1516–1517, 1996.

[22] D. Altshuler, J. N. Hirschhorn, M. Klannemark et al., "The common PPARγ Pro12Ala polymorphism is associated with decreased risk of type 2 diabetes," *Nature Genetics*, vol. 26, no. 1, pp. 76–80, 2000.

[23] J. M. Lehmann, L. B. Moore, T. A. Smith-Oliver, W. O. Wilkison, T. M. Willson, and S. A. Kliewer, "An antidiabetic thiazolidinedione is a high affinity ligand for peroxisome proliferator-activated receptor γ (PPARγ)," *Journal of Biological Chemistry*, vol. 270, no. 22, pp. 12953–12956, 1995.

[24] A. L. Gloyn, M. N. Weedon, K. R. Owen et al., "Large-scale association studies of variants in genes encoding the pancreatic β-cell KATP channel subunits Kir6.2 (KCNJ11) and SUR1 (ABCC8) confirm that the KCNJ11 E23K variant is associated with type 2 diabetes," *Diabetes*, vol. 52, no. 2, pp. 568–572, 2003.

[25] S. F. A. Grant, G. Thorleifsson, I. Reynisdottir et al., "Variant of transcription factor 7-like 2 (TCF7L2) gene confers risk of type 2 diabetes," *Nature Genetics*, vol. 38, no. 3, pp. 320–323, 2006.

[26] R. Saxena, B. F. Voight, V. Lyssenko et al., "Genome-wide association analysis identifies loci for type 2 diabetes and triglyceride levels," *Science*, vol. 316, no. 5829, pp. 1331–1336, 2007.

[27] L. J. Scott, K. L. Mohlke, L. L. Bonnycastle et al., "A genome-wide association study of type 2 diabetes in finns detects multiple susceptibility variants," *Science*, vol. 316, no. 5829, pp. 1341–1345, 2007.

[28] R. Sladek, G. Rocheleau, J. Rung et al., "A genome-wide association study identifies novel risk loci for type 2 diabetes," *Nature*, vol. 445, no. 7130, pp. 881–885, 2007.

[29] E. Zeggini, M. N. Weedon, C. M. Lindgren et al., "Replication of genome-wide association signals in UK samples reveals risk loci for type 2 diabetes," *Science*, vol. 316, pp. 1336–1341, 2007.

[30] Y. S. Cho, C. H. Chen, C. Hu et al., "Meta-analysis of genome-wide association studies identifies eight new loci for type 2 diabetes in east Asians," *Nature Genetics*, vol. 44, pp. 67–72, 2012.

[31] J. Dupuis, C. Langenberg, I. Prokopenko et al., "New genetic loci implicated in fasting glucose homeostasis and their impact on type 2 diabetes risk," *Nature Genetics*, vol. 42, pp. 105–116, 2010.

[32] J. S. Kooner, D. Saleheen, X. Sim et al., "Genome-wide association study in individuals of South Asian ancestry identifies six new type 2 diabetes susceptibility loci," *Nature Genetics*, vol. 43, pp. 984–989, 2011.

[33] N. D. Palmer, C. W. McDonough, P. J. Hicks et al., "A genome-wide association search for type 2 diabetes genes in African Americans," *PLoS ONE*, vol. 7, Article ID e29202, 2012.

[34] B. F. Voight, L. J. Scott, V. Steinthorsdottir et al., "Twelve type 2 diabetes susceptibility loci identified through large-scale association analysis," *Nature Genetics*, vol. 42, pp. 579–589, 2010.

[35] A. P. Morris, B. F. Voight, T. M. Teslovich et al., "Large-scale association analysis provides insights into the genetic architecture and pathophysiology of type 2 diabetes," *Nature Genetics*, vol. 44, pp. 981–990, 2012.

[36] M. C. Cornelis, L. Qi, C. Zhang et al., "Joint effects of common genetic variants on the risk for type 2 diabetes in U.S. men and women of European ancestry," *Annals of Internal Medicine*, vol. 150, no. 8, pp. 541–550, 2009.

[37] J. M. De Miguel-Yanes, P. Shrader, M. J. Pencina et al., "Genetic risk reclassification for type 2 diabetes by age below or above 50 years using 40 type 2 diabetes risk single nucleotide polymorphisms," *Diabetes Care*, vol. 34, no. 1, pp. 121–125, 2011.

[38] J. C. Florez, "Newly identified loci highlight beta cell dysfunction as a key cause of type 2 diabetes: where are the insulin resistance genes?" *Diabetologia*, vol. 51, no. 7, pp. 1100–1110, 2008.

[39] S. Cauchi, D. Meyre, C. Dina et al., "Transcription factor TCF7L2 genetic study in the French population: expression in human β-cells and adipose tissue and strong association with type 2 diabetes," *Diabetes*, vol. 55, no. 10, pp. 2903–2908, 2006.

[40] S. Maeda, N. Osawa, T. Hayashi, S. Tsukada, M. Kobayashi, and R. Kikkawa, "Genetic variations associated with diabetic nephropathy and type II diabetes in a Japanese population," *Kidney International*, vol. 72, no. 106, supplement, pp. S43–S48, 2007.

[41] J. B. Meigs, M. K. Rutter, L. M. Sullivan, C. S. Fox, R. B. D'Agostino, and P. W. F. Wilson, "Impact of insulin resistance on risk of type 2 diabetes and cardiovascular disease in people with metabolic syndrome," *Diabetes Care*, vol. 30, no. 5, pp. 1219–1225, 2007.

[42] C. Herder, W. Rathmann, K. Strassburger et al., "Variants of the PPARG, IGF2BP2, CDKAL1, HHEX, and TCF7L2 genes confer risk of type 2 diabetes independently of BMI in the German KORA studies," *Hormone and Metabolic Research*, vol. 40, no. 10, pp. 722–726, 2008.

[43] D. K. Sanghera, L. Ortega, S. Han et al., "Impact of nine common type 2 diabetes risk polymorphisms in Asian Indian Sikhs: PPARG2 (Pro12Ala), IGF2BP2, TCF7L2 and FTO variants confer a significant risk," *BMC Medical Genetics*, vol. 9, article 59, 2008.

[44] Y. M. Cho, T. H. Kim, S. Lim et al., "Type 2 diabetes-associated genetic variants discovered in the recent genome-wide association studies are related to gestational diabetes mellitus in the Korean population," *Diabetologia*, vol. 52, no. 2, pp. 253–261, 2009.

[45] Y. Tabara, H. Osawa, R. Kawamoto et al., "Replication study of candidate genes associated with type 2 diabetes based on genome-wide screening," *Diabetes*, vol. 58, no. 2, pp. 493–498, 2009.

[46] G. F. Marquezine, A. C. Pereira, A. G. P. Sousa, J. G. Mill, W. A. Hueb, and J. E. Krieger, "TCF7L2 variant genotypes and type 2 diabetes risk in Brazil: significant association, but not a significant tool for risk stratification in the general population," *BMC Medical Genetics*, vol. 9, article 106, 2008.

[47] I. Ezzidi, N. Mtiraoui, S. Cauchi et al., "Contribution of type 2 diabetes associated loci in the Arabic population from Tunisia: a case-control study," *BMC Medical Genetics*, vol. 10, article 33, 2009.

[48] F. Takeuchi, M. Serizawa, K. Yamamoto et al., "Confirmation of multiple risk loci and genetic impacts by a genome-wide association study of type 2 diabetes in the Japanese population," *Diabetes*, vol. 58, no. 7, pp. 1690–1699, 2009.

[49] S. Ereqat, A. Nasereddin, S. Cauchi, K. Azmi, Z. Abdeen, and R. Amin, "Association of a common variant in TCF7L2 gene with type 2 diabetes mellitus in the Palestinian population," *Acta Diabetologica*, vol. 47, no. 1, supplement, pp. S195–S198, 2010.

[50] J. Wen, T. Rönn, A. Olsson et al., "Investigation of type 2 diabetes risk alleles support CDKN2A/B, CDKAL1, and TCF7L2 as susceptibility genes in a Han Chinese cohort," *PLoS ONE*, vol. 5, no. 2, Article ID e9153, 2010.

[51] G. Chauhan, C. J. Spurgeon, R. Tabassum et al., "Impact of common variants of PPARG, KCNJ11, TCF7L2, SLC30A8, HHEX, CDKN2A, IGF2BP2, and CDKAL1 on the risk of type 2 diabetes in 5,164 Indians," *Diabetes*, vol. 59, no. 8, pp. 2068–2074, 2010.

[52] R. Karns, G. Zhang, N. Jeran et al., "Replication of genetic variants from genome-wide association studies with metabolic traits in an island population of the Adriatic coast of Croatia," *European Journal of Human Genetics*, vol. 19, no. 3, pp. 341–346, 2011.

[53] E. Ramos, G. Chen, D. Shriner et al., "Replication of genome-wide association studies (GWAS) loci for fasting plasma glucose in African-Americans," *Diabetologia*, vol. 54, no. 4, pp. 783–788, 2011.

[54] S. D. Rees, M. Z. Hydrie, A. S. Shera et al., "Replication of 13 genome-wide association (GWA)-validated risk variants for type 2 diabetes in Pakistani populations," *Diabetologia*, vol. 54, pp. 1368–1374, 2011.

[55] R. Saxena, C. C. Elbers, Y. Guo et al., "Large-scale gene-centric meta-analysis across 39 studies identifies type 2 diabetes loci," *American Journal of Human Genetics*, vol. 90, pp. 410–425, 2012.

[56] S. Cauchi, I. Ezzidi, A. Y. El et al., "European genetic variants associated with type 2 diabetes in North African Arabs," *Diabetes & Metabolism*, vol. 38, pp. 316–323, 2012.

[57] N. Mtiraoui, A. Turki, R. Nemr et al., "Contribution of common variants of ENPP1, IGF2BP2, KCNJ11, MLXIPL, PPARgamma, SLC30A8 and TCF7L2 to the risk of type 2 diabetes in Lebanese and Tunisian Arabs," *Diabetes & Metabolism*, vol. 38, pp. 444–449, 2012.

[58] A. Turki, G. S. Al-Zaben, N. Mtiraoui, H. Marmmuoch, T. Mahjoub, and W. Y. Almawi, "Transcription factor-7-like 2 gene variants are strongly associated with type 2 diabetes in Tunisian Arab subjects," *Gene*, vol. 513, pp. 244–248, 2013.

[59] J. Long, T. Edwards, L. B. Signorello et al., "Evaluation of genome-wide association study-identified type 2 diabetes loci in African Americans," *American Journal of Epidemiology*, vol. 176, pp. 995–1001, 2012.

[60] A. Helgason, S. Pálsson, G. Thorleifsson et al., "Refining the impact of TCF7L2 gene variants on type 2 diabetes and adaptive evolution," *Nature Genetics*, vol. 39, no. 2, pp. 218–225, 2007.

[61] J. C. Florez, K. A. Jablonski, N. Bayley et al., "TCF7L2 polymorphisms and progression to diabetes in the Diabetes Prevention Program," *New England Journal of Medicine*, vol. 355, no. 3, pp. 241–250, 2006.

[62] J. Wang, J. Kuusisto, M. Vänttinen et al., "Variants of transcription factor 7-like 2 (TCF7L2) gene predict conversion to type 2 diabetes in the Finnish Diabetes Prevention Study and are associated with impaired glucose regulation and impaired insulin secretion," *Diabetologia*, vol. 50, no. 6, pp. 1192–1200, 2007.

[63] D. Dabelea, L. M. Dolan, R. D'Agostino et al., "Association testing of TCF7L2 polymorphisms with type 2 diabetes in multi-ethnic youth," *Diabetologia*, vol. 54, no. 3, pp. 535–539, 2011.

[64] O. T. Raitakari, T. Rönnemaa, R. Huupponen et al., "Variation of the transcription factor 7-like 2 (TCF7L2) gene predicts impaired fasting glucose in healthy young adults. The Cardiovascular Risk in Young Finns Study," *Diabetes Care*, vol. 30, pp. 2299–2301, 2007.

[65] T. Jin and L. Liu, "The Wnt signaling pathway effector TCF7L2 and type 2 diabetes mellitus," *Molecular Endocrinology*, vol. 22, no. 11, pp. 2383–2392, 2008.

[66] T. Reya and H. Clevers, "Wnt signalling in stem cells and cancer," *Nature*, vol. 434, no. 7035, pp. 843–850, 2005.

[67] I. C. Rulifson, S. K. Karnik, P. W. Heiser et al., "Wnt signaling regulates pancreatic β cell proliferation," *Proceedings of the National Academy of Sciences of the United States of America*, vol. 104, no. 15, pp. 6247–6252, 2007.

[68] S. Papadopoulou and H. Edlund, "Attenuated Wnt signaling perturbs pancreatic growth but not pancreatic function," *Diabetes*, vol. 54, no. 10, pp. 2844–2851, 2005.

[69] J. M. Wells, F. Esni, G. P. Boivin et al., "Wnt/β-catenin signaling is required for development of the exocrine pancreas," *BMC Developmental Biology*, vol. 7, article 4, 2007.

[70] P. W. Heiser, J. Lau, M. M. Taketo, P. L. Herrera, and M. Hebrok, "Stabilization of β-catenin impacts pancreas growth," *Development*, vol. 133, no. 10, pp. 2023–2032, 2006.

[71] R. J. F. Loos, P. W. Franks, R. W. Francis et al., "TCF7L2 polymorphisms modulate proinsulin levels and β-cell function in a British europid population," *Diabetes*, vol. 56, no. 7, pp. 1943–1947, 2007.

[72] V. Lyssenko, R. Lupi, P. Marchetti et al., "Mechanisms by which common variants in the TCF7L2 gene increase risk of type 2 diabetes," *Journal of Clinical Investigation*, vol. 117, no. 8, pp. 2155–2163, 2007.

[73] D. T. Villareal, H. Robertson, G. I. Bell et al., "TCF7L2 variant rs7903146 affects the risk of type 2 diabetes by modulating incretin action," *Diabetes*, vol. 59, no. 2, pp. 479–485, 2010.

[74] L. Shu, A. V. Matveyenko, J. Kerr-Conte, J. H. Cho, C. H. S. McIntosh, and K. Maedler, "Decreased TCF7L2 protein levels in type 2 diabetes mellitus correlate with downregulation of GIP- and GLP-1 receptors and impaired beta-cell function," *Human Molecular Genetics*, vol. 18, no. 13, pp. 2388–2399, 2009.

[75] L. Shu, N. S. Sauter, F. T. Schulthess, A. V. Matveyenko, J. Oberholzer, and K. Maedler, "Transcription factor 7-like 2 regulates β-cell survival and function in human pancreatic islets," *Diabetes*, vol. 57, no. 3, pp. 645–653, 2008.

[76] G. Da Silva Xavier, M. K. Loder, A. McDonald et al., "TCF7L2 regulates late events in insulin secretion from pancreatic islet β-cells," *Diabetes*, vol. 58, no. 4, pp. 894–905, 2009.

[77] G. da Silva Xavier, A. Mondragon, G. Sun et al., "Abnormal glucose tolerance and insulin secretion in pancreas-specific Tcf7l2-null mice," *Diabetologia*, vol. 55, pp. 2667–2676, 2012.

[78] L. Prokunina-Olsson, C. Welch, O. Hansson et al., "Tissue-specific alternative splicing of TCF7L2," *Human Molecular Genetics*, vol. 18, no. 20, pp. 3795–3804, 2009.

[79] Z. Liu and J. F. Habener, "Glucagon-like peptide-1 activation of TCF7L2-dependent Wnt signaling enhances pancreatic beta cell proliferation," *Journal of Biological Chemistry*, vol. 283, no. 13, pp. 8723–8735, 2008.

[80] M. L. Slattery, A. R. Folsom, R. Wolff, J. Herrick, B. J. Caan, and J. D. Potter, "Transcription factor 7-like 2 polymorphism and colon cancer," *Cancer Epidemiology Biomarkers and Prevention*, vol. 17, no. 4, pp. 978–982, 2008.

[81] A. Saadeddin, R. Babaei-Jadidi, B. Spencer-Dene, and A. S. Nateri, "The links between transcription, β-catenin/JNK signaling, and carcinogenesis," *Molecular Cancer Research*, vol. 7, no. 8, pp. 1189–1196, 2009.

[82] J. Roose and H. Clevers, "TCF transcription factors: molecular switches in carcinogenesis," *Biochimica et Biophysica Acta*, vol. 1424, no. 2-3, pp. M23–M37, 1999.

[83] V. Korinek, N. Barker, P. Moerer et al., "Depletion of epithelial stem-cell compartments in the small intestine of mice lacking Tcf-4," *Nature Genetics*, vol. 19, no. 4, pp. 379–383, 1998.

[84] S. F. Boj, J. H. van Es, M. Huch et al., "Diabetes risk gene and Wnt effector Tcf7l2/TCF4 controls hepatic response to perinatal and adult metabolic demand," *Cell*, vol. 151, no. 7, pp. 1595–1607, 2012.

[85] D. Savic, H. Ye, I. Aneas, S. Y. Park, G. I. Bell, and M. A. Nobrega, "Alterations in TCF7L2 expression define its role as a key regulator of glucose metabolism," *Genome Research*, vol. 21, pp. 1417–1425, 2011.

[86] H. Yang, Q. Li, J. H. Lee, and Y. Shu, "Reduction in Tcf7l2 expression decreases diabetic susceptibility in mice," *International Journal of Biological Sciences*, vol. 8, pp. 791–801, 2012.

[87] N. Barker, G. Huls, V. Korinek, and H. Clevers, "Restricted high level expression of Tcf-4 protein in intestinal and mammary gland epithelium," *American Journal of Pathology*, vol. 154, no. 1, pp. 29–35, 1999.

[88] M. Horikoshi, K. Hara, C. Ito, R. Nagai, P. Froguel, and T. Kadowaki, "A genetic variation of the transcription factor 7-like 2 gene is associated with risk of type 2 diabetes in the Japanese population," *Diabetologia*, vol. 50, no. 4, pp. 747–751, 2007.

[89] S. A. Schäfer, O. Tschritter, F. Machicao et al., "Impaired glucagon-like peptide-1-induced insulin secretion in carriers of transcription factor 7-like 2 (TCF7L2) gene polymorphisms," *Diabetologia*, vol. 50, no. 12, pp. 2443–2450, 2007.

[90] G. Gu, J. Dubauskaite, and D. A. Melton, "Direct evidence for the pancreatic lineage: NGN3+ cells are islet progenitors and are distinct from duct progenitors," *Development*, vol. 129, no. 10, pp. 2447–2457, 2002.

[91] K. Hisadome, M. A. Smith, A. I. Choudhury, M. Claret, D. J. Withers, and M. L. J. Ashford, "5-HT inhibition of rat insulin 2 promoter Cre recombinase transgene and proopiomelanocortin neuron excitability in the mouse arcuate nucleus," *Neuroscience*, vol. 159, no. 1, pp. 83–93, 2009.

[92] G. Sun, A. I. Tarasov, J. A. McGinty et al., "LKB1 deletion with the RIP2.Cre transgene modifies pancreatic β-cell morphology and enhances insulin secretion in vivo," *American Journal of Physiology: Endocrinology and Metabolism*, vol. 298, no. 6, pp. E1261–E1273, 2010.

[93] G. Sun, R. Reynolds, I. Leclerc, and G. A. Rutter, "RIP2-mediated LKB1 deletion causes axon degeneration in the spinal cord and hind-limb paralysis," *DMM Disease Models and Mechanisms*, vol. 4, no. 2, pp. 193–202, 2011.

[94] L. Shu, K. Zien, G. Gutjahr et al., "TCF7L2 promotes beta cell regeneration in human and mouse pancreas," *Diabetologia*, vol. 55, pp. 3296–3307, 2012.

[95] B. Wicksteed, M. Brissova, W. Yan et al., "Conditional gene targeting in mouse pancreatic β-cells: analysis of ectopic cre transgene expression in the brain," *Diabetes*, vol. 59, no. 12, pp. 3090–3098, 2010.

[96] Y. Dor, J. Brown, O. I. Martinez, and D. A. Melton, "Adult pancreatic β-cells are formed by self-duplication rather than stem-cell differentiation," *Nature*, vol. 429, no. 6987, pp. 41–46, 2004.

[97] T. J. Nicolson, E. A. Bellomo, N. Wijesekara et al., "Insulin storage and glucose homeostasis in mice null for the granule zinc transporter ZnT8 and studies of the type 2 diabetes-associated variants," *Diabetes*, vol. 58, no. 9, pp. 2070–2083, 2009.

[98] A. B. Hardy, N. Wijesekara, I. Genkin et al., "Effects of high-fat diet feeding on Znt8-null mice: differences between beta-cell and global knockout of Znt8," *American Journal of Physiology: Endocrinology and Metabolism*, vol. 302, pp. E1084–E1096, 2012.

[99] K. Lemaire, M. A. Ravier, A. Schraenen et al., "Insulin crystallization depends on zinc transporter ZnT8 expression, but is not required for normal glucose homeostasis in mice," *Proceedings of the National Academy of Sciences of the United States of America*, vol. 106, no. 35, pp. 14872–14877, 2009.

[100] L. D. Pound, S. A. Sarkar, R. K. P. Benninger et al., "Deletion of the mouse Slc30a8 gene encoding zinc transporter-8 results in impaired insulin secretion," *Biochemical Journal*, vol. 421, no. 3, pp. 371–376, 2009.

[101] L. D. Pound, S. A. Sarkar, A. Ustione et al., "The physiological effects of deleting the mouse SLC30A8 gene encoding zinc transporter-8 are influenced by gender and genetic background," *PLoS ONE*, vol. 7, Article ID e40972, 2012.

[102] N. Wijesekara, F. F. Dai, A. B. Hardy et al., "Beta cell-specific Znt8 deletion in mice causes marked defects in insulin processing, crystallisation and secretion," *Diabetologia*, vol. 53, no. 8, pp. 1656–1668, 2010.

[103] K. J. Gaulton, T. Nammo, L. Pasquali et al., "A map of open chromatin in human pancreatic islets," *Nature Genetics*, vol. 42, no. 3, pp. 255–259, 2010.

[104] A. Duval, S. Rolland, E. Tubacher, H. Bui, G. Thomas, and R. Hamelin, "The human T-cell transcription factor-4 gene: structure, extensive characterization of alternative splicings, and mutational analysis in colorectal cancer cell lines," *Cancer Research*, vol. 60, no. 14, pp. 3872–3879, 2000.

[105] O. Le Bacquer, L. Shu, M. Marchand et al., "TCF7L2 splice variants have distinct effects on β-cell turnover and function," *Human Molecular Genetics*, vol. 20, no. 10, pp. 1906–1915, 2011.

[106] A. K. Mondal, S. K. Das, G. Baldini et al., "Genotype and tissue-specific effects on alternative splicing of the transcription factor 7-like 2 gene in humans," *Journal of Clinical Endocrinology and Metabolism*, vol. 95, no. 3, pp. 1450–1457, 2010.

[107] A. Weise, K. Bruser, S. Elfert et al., "Alternative splicing of Tcf7l2 transcripts generates protein variants with differential promoter-binding and transcriptional activation properties at Wnt/β-catenin targets," *Nucleic Acids Research*, vol. 38, no. 6, pp. 1964–1981, 2009.

[108] L. A. Lichten and R. J. Cousins, "Mammalian zinc transporters: nutritional and physiologic regulation," *Annual Review of Nutrition*, vol. 29, pp. 153–176, 2009.

[109] F. Chimienti, S. Devergnas, A. Favier, and M. Seve, "Identification and cloning of a β-cell-specific zinc transporter, ZnT-8, localized into insulin secretory granules," *Diabetes*, vol. 53, no. 9, pp. 2330–2337, 2004.

[110] F. Chimienti, A. Favier, and M. Seve, "ZnT-8, a pancreatic beta-cell-specific zinc transporter," *BioMetals*, vol. 18, no. 4, pp. 313–317, 2005.

[111] S. O. Emdin, G. G. Dodson, J. M. Cutfield, and S. M. Cutfield, "Role of zinc in insulin biosynthesis. Some possible zinc-insulin interactions in the pancreatic B-cell," *Diabetologia*, vol. 19, no. 3, pp. 174–182, 1980.

[112] G. A. Rutter, "Think zinc: new roles for zinc in the control of insulin secretion," *Islets*, vol. 2, no. 1, pp. 49–50, 2010.

[113] E. D. Berglund, C. Y. Li, G. Poffenberger et al., "Glucose metabolism in vivo in four commonly used inbred mouse strains," *Diabetes*, vol. 57, no. 7, pp. 1790–1799, 2008.

[114] A. T. Hattersley, "Unlocking the secrets of the pancreatic β cell: man and mouse provide the key," *Journal of Clinical Investigation*, vol. 114, no. 3, pp. 314–316, 2004.

[115] D. Reyon, S. Q. Tsai, C. Khayter, J. A. Foden, J. D. Sander, and J. K. Joung, "FLASH assembly of TALENs for high-throughput genome editing," *Nature Biotechnology*, vol. 30, pp. 460–465, 2012.

[116] C. Mussolino and T. Cathomen, "TALE nucleases: tailored genome engineering made easy," *Current Opinion in Biotechnology*, vol. 23, pp. 644–650, 2012.

[117] D. Hockemeyer, H. Wang, S. Kiani et al., "Genetic engineering of human pluripotent cells using TALE nucleases," *Nature Biotechnology*, vol. 29, no. 8, pp. 731–734, 2011.

[118] J. B. Meigs, P. Shrader, L. M. Sullivan et al., "Genotype score in addition to common risk factors for prediction of type 2 diabetes," *New England Journal of Medicine*, vol. 359, no. 21, pp. 2208–2219, 2008.

[119] V. Lyssenko, A. Jonsson, P. Almgren et al., "Clinical risk factors, DNA variants, and the development of type 2 diabetes," *New England Journal of Medicine*, vol. 359, no. 21, pp. 2220–2232, 2008.

[120] P. J. Talmud, A. D. Hingorani, J. A. Cooper et al., "Utility of genetic and non-genetic risk factors in prediction of type 2 diabetes: whitehall II prospective cohort study," *British Medical Journal*, vol. 340, article b4838, 2010.

[121] H. Langothe, C. N. A. Palmer, A. D. Morris et al., "Assessing the combined impact of 18 common genetic variants of modest effect sizes on type 2 diabetes risk," *Diabetes*, vol. 57, no. 11, pp. 3129–3135, 2008.

[122] R. K. Simmons, A. H. Harding, N. J. Wareham, and S. J. Griffin, "Do simple questions about diet and physical activity help to identify those at risk of Type 2 diabetes?" *Diabetic Medicine*, vol. 24, no. 8, pp. 830–835, 2007.

[123] J. Lindström and J. Tuomilehto, "The diabetes risk score: a practical tool to predict type 2 diabetes risk," *Diabetes Care*, vol. 26, no. 3, pp. 725–731, 2003.

[124] M. C. Cornelis, L. Qi, P. Kraft, and F. B. Hu, "TCF7L2, dietary carbohydrate, and risk of type 2 diabetes in US women," *American Journal of Clinical Nutrition*, vol. 89, no. 4, pp. 1256–1262, 2009.

[125] E. Fisher, H. Boeing, A. Fritsche, F. Doering, H. G. Joost, and M. B. Schulze, "Whole-grain consumption and transcription factor-7-like 2 (TCF7L2) rs7903146: gene-diet interaction in modulating type 2 diabetes risk," *British Journal of Nutrition*, vol. 101, no. 4, pp. 478–481, 2009.

[126] A. Haupt, C. Thamer, M. Heni et al., "Gene variants of TCF7L2 influence weight loss and body composition during lifestyle intervention in a population at risk for type 2 diabetes," *Diabetes*, vol. 59, no. 3, pp. 747–750, 2010.

[127] T. Reinehr, S. Friedel, T. D. Mueller, A. M. Toschke, J. Hebebrand, and A. Hinney, "Evidence for an influence of TCF7L2 polymorphism rs7903146 on insulin resistance and sensitivity indices in overweight children and adolescents during a lifestyle intervention," *International Journal of Obesity*, vol. 32, no. 10, pp. 1521–1524, 2008.

[128] D. Thomas, "Gene—environment-wide association studies: emerging approaches," *Nature Reviews Genetics*, vol. 11, no. 4, pp. 259–272, 2010.

[129] U. Smith and E. A. M. Gale, "Cancer and diabetes: are we ready for prime time?" *Diabetologia*, vol. 53, no. 8, pp. 1541–1544, 2010.

[130] W. Y. Kim and N. E. Sharpless, "The Regulation of INK4/ARF in Cancer and Aging," *Cell*, vol. 127, no. 2, pp. 265–275, 2006.

[131] J. Krishnamurthy, M. R. Ramsey, K. L. Ligon et al., "p16INK4a induces an age-dependent decline in islet regenerative potential," *Nature*, vol. 443, no. 7110, pp. 453–457, 2006.

[132] S. G. Rane, P. Dubus, R. V. Mettus et al., "Loss of Cdk4 expression causes insulin-deficient diabetes and Cdk4 activation results in β-islet cell hyperplasia," *Nature Genetics*, vol. 22, no. 1, pp. 44–54, 1999.

[133] L. M. Holdt and D. Teupser, "Recent studies of the human chromosome 9p21 locus, which is associated with atherosclerosis in

human populations," *Arteriosclerosis, Thrombosis, and Vascular Biology*, vol. 32, pp. 196–206, 2012.

[134] E. Pasmant, I. Laurendeau, D. Héron, M. Vidaud, D. Vidaud, and I. Bièche, "Characterization of a germ-line deletion, including the entire INK4/ARF locus, in a melanoma-neural system tumor family: identification of ANRIL, an antisense noncoding RNA whose expression coclusters with ARF," *Cancer Research*, vol. 67, no. 8, pp. 3963–3969, 2007.

[135] A. Visel, Y. Zhu, D. May et al., "Targeted deletion of the 9p21 non-coding coronary artery disease risk interval in mice," *Nature*, vol. 464, no. 7287, pp. 409–412, 2010.

[136] J. Gudmundsson, P. Sulem, V. Steinthorsdottir et al., "Two variants on chromosome 17 confer prostate cancer risk, and the one in TCF2 protects against type 2 diabetes," *Nature Genetics*, vol. 39, no. 8, pp. 977–983, 2007.

[137] G. Thomas, K. B. Jacobs, M. Yeager et al., "Multiple loci identified in a genome-wide association study of prostate cancer," *Nature Genetics*, vol. 40, pp. 310–315, 2008.

[138] P. Ravassard, Y. Hazhouz, S. Pechberty et al., "A genetically engineered human pancreatic beta cell line exhibiting glucose-inducible insulin secretion," *Journal of Clinical Investigation*, vol. 121, pp. 3589–3597, 2011.

[139] B. Seidler, A. Schmidt, U. Mayr et al., "A Cre-loxP-based mouse model for conditional somatic gene expression and knockdown in vivo by using avian retroviral vectors," *Proceedings of the National Academy of Sciences of the United States of America*, vol. 105, no. 29, pp. 10137–10142, 2008.

Hindawi Publishing Corporation
Journal of Diabetes Research
Volume 2013, Article ID 165327, 7 pages
http://dx.doi.org/10.1155/2013/165327

Review Article

Comparison of Two New Mouse Models of Polygenic Type 2 Diabetes at the Jackson Laboratory, NONcNZO10Lt/J and TALLYHO/JngJ

Edward H. Leiter, Marjorie Strobel, Adam O'Neill, David Schultz, Andrew Schile, and Peter C. Reifsnyder

The Jackson Laboratory, 600 Main Street, Bar Harbor, ME 04609, USA

Correspondence should be addressed to Edward H. Leiter; ehl@jax.org

Received 4 February 2013; Accepted 14 March 2013

Academic Editor: Daisuke Koya

This review compares two novel polygenic mouse models of type 2 diabetes (T2D), TALLYHO/JngJ and NONcNZO10/LtJ, and contrasts both with the well-known C57BLKS/J-*Lepr*^{db} (*db*/*db*) monogenic diabesity model. We posit that the new polygenic models are more representative of the "garden variety" obesity underlying human T2D in terms of their polygenetic rather than monogenic etiology. Moreover, the clinical phenotypes in these new models are less extreme, for example, more moderated development of obesity coupled with less extreme endocrine disturbances. The more progressive development of obesity produces a maturity-onset development of hyperglycemia in contrast to the juvenile-onset diabetes observed in the morbidly obese *db*/*db* model. Unlike the leptin receptor-deficient *db*/*db* models with central leptin resistance, the new models develop a progressive peripheral leptin resistance and are able to maintain reproductive function. Although the T2D pathophysiology in both TALLYHO/JngJ and NONcNZO10/LtJ is remarkably similar, their genetic etiologies are clearly different, underscoring the genetic heterogeneity underlying T2D in humans.

1. Introduction

The purpose of this review is to introduce two new polygenic mouse models of type 2 diabetes (T2D) and to contrast them with the most commonly studied monogenic model, the leptin receptor-deficient C57BLKS/J-*Lepr*^{db}/*Lepr*^{db} (hereafter abbreviated as *db*/*db*) mouse. On the basis of their polygenic etiologies, the absence of juvenile-onset morbid obesity, their more protracted maturity-onset development of hyperglycemia, and the absence of severe endocrine/neuroendocrine disturbances, the two polygenic models more closely reflect the phenotypes associated with the "garden variety" obesity and obesity-induced diabetes (diabesity) in humans. The genetic origins of each model will be described separately, and then their diabesity phenotypes will be compared.

2. The C57BLKS/J-*db*/*db* Mouse (JAX Stock 642)

Great interest accompanied the publication of the "diabetes" mouse in 1966 [1]. A recessive mutation occurring spontaneously in the C57BLKS/J (BKS) strain produces early onset diabesity with initial moderate hyperinsulinemia followed by insulinopenia as the pancreatic islets undergo atropy due to beta-cell degeneration [1]. The mutation was identified in 1996 [2, 3] as the receptor for leptin, the adipokine hormone missing in the *ob*/*ob* (now designated *Lep*^{ob}) mouse [4]. Leptin sensing in hypothalamic nuclei is essential for normal regulation of satiety as well as multiple metabolic and neuroendocrine/reproduction pathways. Hence, the extreme leptin resistance produced by the absence of an intracellular signaling domain in leptin receptor of the *db*/*db* mouse produces hyperphagia and morbid obesity, reproductive

failure, and severe insulin resistance. The juvenile-onset of hyperglycemia (within a week of weaning onto carbohydrate-containing chow), coupled with the massive beta-cell loss and early mortality as hyperglycemia progressed, suggested an amalgam between type 2 and type 1 diabetes. Although the origin of the diabesity is clearly monogenic, the development of severe diabetes is dependent upon multiple other background genes. The same mutation transferred onto the related C57BL/6J (B6) background produces an even more severe insulin resistance obesity syndrome, but not chronic, severe diabetes. The BKS strain is a black-pigmented strain representing an admixture of B6 and, apparently, DBA/2 genomes [5]. In the latter strain, *db* mutation homozygosity produces severe diabetes with high mortality, like BKS [6]. The identification of these genetic background modifiers has yet to be established. The *db*/*db* model has been widely used in the evaluation of antiobesity and antidiabetic compounds and therapies because the penetrance of the mutation is almost 100% (e.g., all mutants become reproducibly obese and diabetic at an early age). Further, mutants of both sexes develop diabesity and either the lean littermates from heterozygous matings (designated +/+ or +/*db*) or standard BKS mice can be used as controls. The mutant mice are not particularly stress sensitive such that pharmaceuticals can be administered by gavage when necessary. Hence, this mouse model has remained a mainstay for pharmaceutical efficacy testing. An extensive bibliographic listing of phenotypic and husbandry information, as well as a photograph of the obese mutant mouse and a lean control, may be found at http://jaxmice.jax.org/strain/000642.html.

3. The NONcNZO10/LtJ Male Mouse (JAX Stock 4456)

The nomenclature descriptor denotes a recombinant congenic strain comprising approximately 88% genome contribution from the NON/LtJ strain (JAX Stock 2423) and 12% from the New Zealand obese (NZO/HlJ, JAX Stock 2105) strain. NZO/HlJ mice of both sexes develop polygenic, morbid obesity with marked insulin resistance. However, the leptin-leptin receptor axis appears intact, such that leptin resistance is peripheral, not central [7]. As in BKS-*db*/*db* mice, NZO/HlJ males show postpubertal development of hyperleptinemia, hyperinsulinemia, thermoregulatory defects, hypertension, and impaired glucose tolerance [8, 9]. Unlike the monogenic obesity of BKS-*db*/*db* mice, NZO obesity is under complex polygenic control. Moreover, diabesity development is male sex limited, maturity onset, and represents a threshold phenomenon predicated on early rate of weight gain [9]. Although NZO/HlJ mice outbreed well, breeding within strain is poor.

The polygenic NONcNZO10/LtJ model (hereafter abbreviated as NcZ10) was specifically developed at The Jackson Laboratory over the past decade to circumvent the extreme NZO phenotypes shared with BKS-*db*/*db* mice and that distinguished both from human "garden variety" obesity while at the same time increasing the frequency of male hyperglycemia development and improving within-strain reproduction. The NON/LtJ strain was used as a "genetic scaffold" on which to build the new model. This strain was selected in Japan for high nonfasting blood glucose [10] and unpublished studies at The Jackson Laboratory showed that NON/LtJ males were markedly more sensitive to high fat diet induced obesity than B6 males. The strategy used was to outcross agouti NZO and albino NON mice and identify by genetic segregation analysis in the F2 and first backcross generations the quantitative trait loci (QTL) contributing both to obesity and diabesity. At least 10 codominant or additive polygenes capable of complex epistatic interactions and derived from both parental genomes were identified [11]. This genetic information was used to transfer as many diabesity QTL as possible onto the NON genetic background at a second backcross, followed by inbreeding to fix these QTL to homozygosity [11]. The result, as will be seen below, was creation of an albino strain that reproduced well, exhibited a more moderate obesity than NZO, and exhibited a male diabesity frequency of 90–100%. A genetic control strain, NONcNZO5/LtJ (JAX Stock 4455), was developed to contain the reciprocal (diabesity resistance) QTL of those in NcZ10 [12]; unfortunately, this obese but diabetes-free strain exhibits the poor reproduction characteristic of NZO/HlJ. Thus, the NON/LtJ or other related Swiss-derived albino inbred strains (SWR/J, SJL/J, FVB/NJ, and ICR/HaJ) are suggested as nonobese controls for physiologic comparisons. When NON/LtJ is used, it must be kept on a low fat diet to avoid diet induced obesity. As will be demonstrated below, NcZ10/LtJ males must be placed on an elevated fat diet for diabesity to develop.

Hyperinsulinemic-euglycemic clamping demonstrated insulin resistance in liver and skeletal muscle in prediabetic 8-week-old males prior to later increases in hepatic lipid content. The muscle resistance was associated with reduced GLUT4 protein, but not IRS-1 [13]. Livers of chronically hyperglycemic males show moderate to severe hepatosteatosis on a chow diet containing 6% fat [12]. Islet histopathology in NcZ10 males shows an early islet hypertrophy followed by beta-cell degranulation and beta-cell atrophy as hyperglycemia becomes chronic [11, 12]. After transfer of the colony from a research colony at The Jackson Laboratory to a high barrier production facility on campus, a 6% fat containing chow diet was found to no longer support attainment of the early body weight gain thresholds required for diabesity development. Raising the fat content of the chow to 10-11% restored diabesity development to expected frequencies. The reason for the higher dietary fat requirement for diabesity is assumed to be a more refined enteric flora in the high barrier colony. Additional phenotypic information, husbandry details, bibliographic information, and a photograph of the mouse may be found on the web at http://jaxmice.jax.org/strain/004456.html.

4. TALLYHO/JngJ Male Mice (JAX Stock 5314)

TALLYHO/Jng (hereafter abbreviated TH) males represent another recently developed polygenic T2D model at The Jackson Laboratory that also expresses less extreme diabesity

phenotypes more consistent with the common forms of human T2D. This albino strain derives from the progeny of two diabetic males discovered in an outbred colony of Theiler's original mice in the United Kingdom and imported to The Jackson Laboratory in 1992 [14]. Inbreeding with selection of progeny of diabetic males has produced a polygenic diabesity model that is very similar to NcZ10 in many respects. However, the combination of polygenes interacting to produce diabesity in TH, for the most part, appears distinct from in NcZ10, attesting to the genetic heterogeneity that clearly must also underlie a very common disease in a very genetically heterogeneous human T2D population. Outcross of TH to B6 identified multiple obesity and diabesity QTL, with a major hyperglycemia QTL on chromosome 19 and a hyperlipemia QTL on chromosome 1 (reviewed in [14]). Pancreatic islet histopathology of diabetic TH males also shows early islet hypertrophy/hyperplasia followed by beta-cell degranulation and some beta-cell loss [15]. Hyperinsulinemic-euglycemic clamping indicated peripheral insulin resistance at 10 weeks of age in prehyperglycemic males, with hepatic insulin resistance developing with hyperglycemia at 16 weeks of age [16]. Insulin resistance in white adipose tissue was associated with reduced GLUT-4 cycling and increased IRS-1 degradation [17]. Significant heart diastolic dysfunction (Sartoretto et al., 2010) [18] and cerebral vascular anomalies [19] were documented in diabetic TH males. This strain is characterized by age-associated bilateral hydronephrosis in both sexes (Dr. J. K. Naggert and Y. Wang, personal communication). Additional phenotypic information, husbandry details, bibliographic information, and a photograph of the mouse may be found on the web at http://jaxmice.jax.org/strain/005314.html.

5. Comparison of New Polygenic Models to the Monogenic BKS-*db/db* Model

Body weight gain data in Figure 1 contrasts the rapid juvenile-onset weight gain and eventual morbid obesity in BKS-*db/db* males versus the more moderate and maturity-onset weight gains in TH and NcZ10 males. Data in Figures 1 and 2 also demonstrate the unusual sensitivity of the NcZ10 strain to the diabetogenic action of dietary fat. As seen in Figure 2, the significantly slower and lower weight gains experienced by NcZ10 males fed the 4% fat-containing chow diet failed to allow them to achieve the degree of obesity necessary to trigger development of hyperglycemia (defined here as a nonfasting blood glucose of >250 mg/dL). Although the TH males fed a 6% fat-containing chow diet showed an initial high weight gain within a week of weaning, this rate moderated after puberty and was comparable to NcZ10 males, but much lower than BKS-*db/db* males. The cohort of TH males aged at The Jackson Laboratory on a 6% fat-containing chow diet showed an earlier onset of hyperglycemia than reported in the literature (10–12 weeks), with glucose values over time similar to the progressive rise seen in BKS-*db/db* males. In the NcZ10 male cohort fed the 11% fat-containing chow, chronic hyperglycemia was only established at 12 weeks. Notably, hyperglycemia did not develop in the

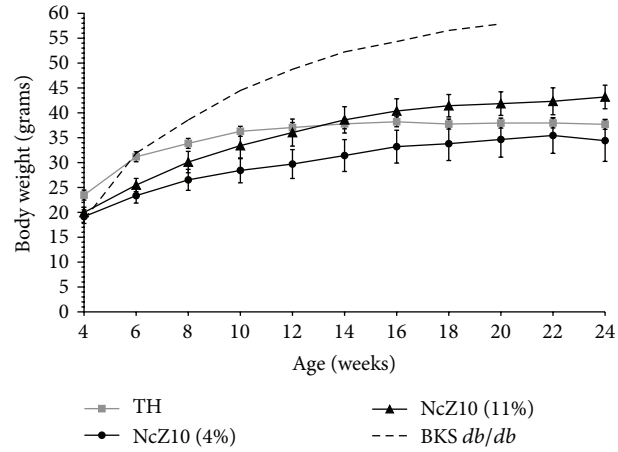

Figure 1: Comparative weight gains of groups of 20 BKS-*db/db* and TH males fed standard 6% fat-containing chow, and the same number of NcZ10 males fed either 4% or 11% fat-containing chow. Data are means ± SD.

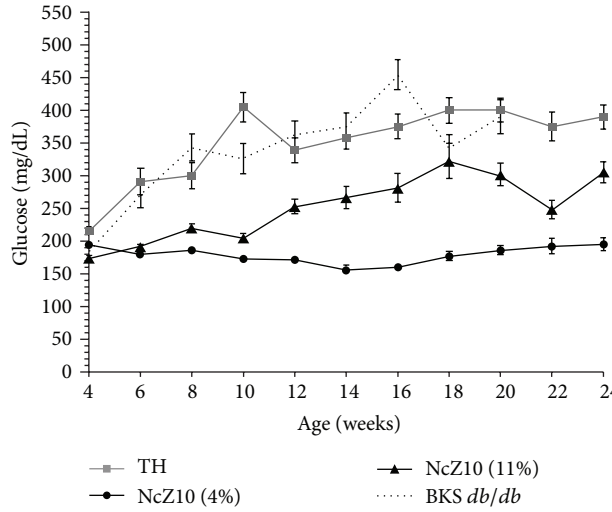

Figure 2: Development of hyperglycemia (defined as nonfasting serum glucose ≥250 mg/dL) in the same cohorts shown in Figure 1. Data are means ± SEM.

4% fat-containing chow-fed males (Figure 2) that failed to attain the requisite body weight thresholds for diabesity development. Oral glucose tolerance data in Figure 3 show that TH and NcZ10 males develop glucose intolerance at different rates. TH males already exhibited impaired glucose tolerance at 8 weeks compared to age-matched NcZ10 males fed either 4% or 11% fat-containing chow (Figure 3(a)). At 24 weeks of age, chronically diabetic TH and NcZ10 males fed the 11% fat chow exhibited comparable, severe impairment in oral glucose tolerance (Figure 3(b)). In nondiabetic 24-week-old NcZ10 males maintained on the 4% fat-containing chow (Figure 3(b)), glucose tolerance had deteriorated, but impairment was still significantly less severe than for either group of diabetic males.

Comparative clinical chemistries of the two polygenic models also distinguish them from the BKS-*db/db* model

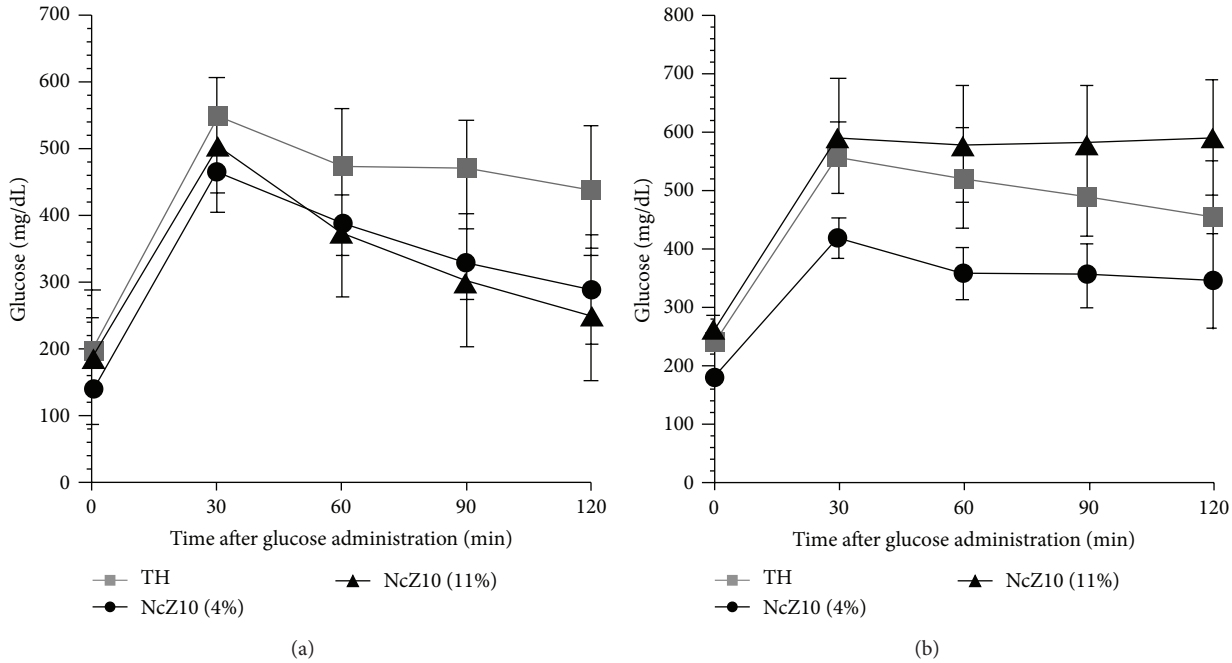

Figure 3: Oral glucose tolerance tests (2 g glucose/kg) of TH and NcZ10 males (a) at 8 weeks of age and (b) at 24 weeks of age (n = 10/group).

Table 1: Comparison of selected serum analytes in the male cohorts shown in the figures. Data show mean ± SEM for 8–10 males at 20 weeks of age. Lean age-matched BKS males are shown for comparison. Groups were maintained on 6% fat chow except for NcZ10 males that were fed 11% fat chow. Hemoglobin A1c (HbA1c) values are shown to document chronic hyperglycemia in the 3 diabetic stocks.

Strain	Glucose mg/dL	HbA1c % NGSP units	Triglyceride mg/dL	Total cholesterol mg/dL	HDL cholesterol mg/dL	Nonesterified fatty acids mEq/L	ALT[f] (IU/L)
NcZ10	475 ± 30	10.4 ± 0.2	255 ± 12[e]	128 ± 4[e]	97 ± 3	1.90 ± 0.08[e]	44.2 ± 1.1
TH	520 ± 36	9.0 ± 0.5	491 ± 57	151 ± 3	106 ± 3	2.47 ± 0.09	44.6 ± 4.1
BKS-*db/db*	444 ± 48	12.8 ± 0.8[d]	141 ± 12[b]	163 ± 6	127 ± 5[d]	2.82 ± 0.17	125.1 ± 9.8[f]
BKS-*m*+/*m*+[a]	167 ± 14[c]	5.7 ± 0.2[c]	131 ± 7[b]	98 ± 6[c]	71 ± 2[c]	1.92 ± 0.08	39.2 ± 5.3

[a] *m*+/*m*+ from the cross with the *db* gene in repulsion with the misty (*m*) gene.
[b] *db/db* and lean control significantly lower ($P \leq 0.05$) than TH and NcZ10.
[c] Lean control significantly lower ($P \leq 0.05$) than all 3 diabetic stocks.
[d] *db/db* significantly higher ($P \leq 0.05$) than TH and NcZ10.
[e] NcZ10 significantly lower ($P \leq 0.05$) than TH and *db/db*.
[f] Alanine aminotransferase; *db/db* significantly higher ($P \leq 0.05$) than control, TH, and NcZ10.

(Table 1). Circulating concentrations of insulin and leptin for all three models are available from the literature. Plasma insulin content in the BKS-*db/db* model shows temporal changes. Marked hyperinsulinemia (mean ~ 55 ng/mL at 6 weeks) develops in the early phase of the syndrome as the islet mass undergoes initial hyperplasia and beta cells hypersecrete insulin [20]. However, after 8 weeks of age, plasma insulin drops sharply to normal or subnormal concentrations (≤1 ng/mL) as beta-cell loss and islet atrophy occur [20]. In contrast, the combination of permanent adiposity coupled with deficient leptin receptor signaling in BKS-*db/db* produces a permanent, severe hyperleptinemia, with concentrations reaching >200 ng/mL [21]. Published plasma insulin and leptin concentrations for both NcZ10 and TH contrast sharply with BKS-*db/db* while being very comparable to each other. Published plasma insulin for hyperglycemic 24-week-old NcZ10 males was 6 ng/mL, only slightly higher than the 4 ng/mL in normoglycemic NON/Lt control males. Similarly, leptin concentration (17.5 ng/mL) was only 2-fold higher than the NON/Lt parental control and at least 3-fold lower than the 60 ng/mL reported in morbidly obese NZO parental males at the same age [12]. Published values for plasma insulin in diabetic 16-week-old TH males closely reflect those reported for NcZ10 males, with insulin reaching peak values of 12 ng/mL at 12 weeks and remaining elevated at 16 weeks [15]. Plasma leptin values in TH males are reported to be variable, but modestly elevated compared to normal B6 males [14]. Thus, both polygenic models differ from both the monogenic obesity in BKS-*db/db* males and the polygenic obesity in NZO males with only moderate elevations in these two endocrines.

Dyslipidemia characterized by marked hypertriglyceridemia on a standard chow diet has been reported in diabetic males in all three models. However, despite the

finding of significantly elevated total cholesterol and non-esterified free fatty acids (NEFA) in the 20-week-old BKS-*db*/*db* male cohort from The Jackson Laboratory's production colony, we were unable to replicate a significant elevation in serum triglycerides compared to lean BKS-*m*+/*m*+ male controls (Table 1). Given a previous study reporting a plasma triglyceride value of 400 ± 19 mg/dL for diabetic BKS-*db*/*db* males at this age [22], we cannot explain the difference. In contrast, data in Table 1 do confirm the literature reporting marked hypertriglyceridemia in both polygenic models, with TH mean concentration significantly higher than in NcZ10 males. High hemoglobin A1c concentrations are present at 20 weeks of age in blood of BKS-*db*/*db*, TH, and NcZ10 males (the latter fed the 11% fat chow). NcZ10 males fed the 4% fat-containing diet, although not overtly hyperglycemic at 24 weeks, exhibited plasma triglycerides as high as hyperglycemic males fed the 11% fat chow (data not shown). Thus, in the NcZ10 model, the dyslipidemia develops independently of chronic hyperglycemia. Hepatic steatosis has been described in both diabetic BKS-*db*/*db* [21] and NcZ10 males [12] and is also present in diabetic TH males (Dr. J. K. Naggert, personal communication). The significantly higher alanine aminotransferase concentrations in serum of BKS-*db*/*db* males may reflect not only increased liver pathology, but also ongoing endocrine pancreatic tissue destruction.

6. Discussion

The phenotypes of the diabesity syndromes developing in the two new polygenic models, NcZ10 and TH, are very similar to each other despite the distinct polygenetic etiologies. Although the dyslipidemias in each are very comparable to those of the BKS-*db*/*db* mouse, the new polygenic models are clearly differentiated from the latter by the absence of uncontrolled hyperphagia. Further, less severe disturbances in the hypothalamic-pituitary-adrenal axis in the polygenic models are evidenced by their retention of normal reproductive function. Finally, the maturity-onset nature of hyperglycemia coupled with the less extreme plasma concentrations of insulin and leptin makes the polygenic models much more reflective of the most common forms of human T2D.

An obvious advantage of a monogenic diabesity model is the availability of a wild-type genetic control not available in a polygenic model. In both TH and NcZ10 strains, females do not develop hyperglycemia and thus can be used for comparison to the effects of hyperglycemia in males. As shown in this review for the NcZ10 model, manipulation of either the total amount of dietary fat or its composition [23] can be used to provide normoglycemic controls. Likewise, normoglycemic NONcNZO5LtJ males are matched with NcZ10 for obesity, but have a less diabetogenic adiposity [24]. Initially, these two stocks were phenotyped on a 6% fat-containing chow diet that was sufficient for diabesity development in NcZ10 in a low barrier research colony at The Jackson Laboratory. However, this diet failed to support requisite weight gains for diabesity development after rederivation of NcZ10 into a high barrier production colony. The need to increase total dietary fat to reconstitute diabesity is assumed to reflect a more refined enteric flora of mice in the production colony phenotyped for this review. The use of dietary manipulation to generate normoglycemic controls for TH males has not yet been reported; possibly high fat and carbohydrate-free diet demonstrated to block diabesity in the NZO diabesity model [25] may generate such controls.

Given the phenotypic similarities of the diabesity syndromes in TH and NcZ10 males, it is perhaps not surprising that both more closely replicate the defects in wound healing that characterizes diabetic human patients than does the BKS-*db*/*db* model [26, 27]. Differences do distinguish the two polygenic models in their responses to antidiabetic drugs administered by gavage. The Jackson Laboratory tested the responses of diabetic males from all 3 models to the gavage-administered thiazolidinedione, rosiglitazone. This compound fed in the chow diet had previously been shown to exert potent antihyperglycemic action in diabetic NcZ10 males [28]. However, when treatment entailed multiple gavages, NcZ10 males unlike both the BKS-*db*/*db* and TH diabetic models in which antihyperglycemic responses were limited to drug-treated recipients showed a strong placebo response to the vehicle. Shipment-associated weight loss and consequent failure to achieve requisite thresholds for diabesity development [11] have characterized some shipments of prediabetic NcZ10 males, but not TH males from the production facility of The Jackson Laboratory. The basis for this enhanced stress sensitivity affecting penetrance of the diabesity phenotype of the NcZ10 compared to the TH model remains to be elucidated.

7. Summary and Conclusions

The newer TH and NcZ10 models are important additions to mouse models of T2D. The major features distinguishing these two polygenic obesity/diabesity models from the better-known BKS-*db*/*db* model are summarized in Table 2.

TH and NcZ10 males more accurately model the human condition in terms of the polygenic basis for their obesity syndromes, coupled with their maturity onset development of hyperglycemia without the extreme disruptions in neuroendocrine pathways associated with mutations in either the leptin or leptin receptor genes. Because they have become available only quite recently, the TH and NcZ10 polygenic diabesity models are not that well known to the diabetes research community. Clearly, much more research on both models is warranted. Although the T2D pathophysiology in both TH and NcZ10 is remarkably similar, their genetic etiologies are clearly different [12, 29]. This certainly models the situation in human T2D, wherein genetic analysis of patients with common disease pathophysiology reveals complex interactions between a large and variable number of genes and the environment. The newer models should certainly not be considered as replacements of the monogenic models such as BKS-*db*/*db* which has become a reference strain for drug testing. Given the genetic heterogeneity underlying T2D in humans [30, 31], the newer models discussed in this review should not supplant the "tried and true" older models, but rather extend them. A new drug that

Table 2: Summary comparison of the 3 models.

	BKS-*db*/*db*	NONcNZO10/LtJ	TALLYHO/JngJ
Obesity	Monogenic, morbid	Polygenic, moderate	Polygenic, moderate
Diabetes	Juvenile onset	Maturity onset	Maturity onset
Leptin resistance	Central, total	Peripheral, moderate	Peripheral, moderate
Insulin resistance	Severe	Moderate	Moderate
Sex bias	None	Males	Males
Littermate controls	Yes	No	No
Fertile	No	Yes	Yes

shows efficacy without toxicity in one model may or may not prove widely therapeutic in a genetically heterogeneous human T2D patient population. However, if the same drug shows equal efficacy in multiple available models, each with a distinct genetic underpinning, confidence that the drug would safely and effectively treat a broader spectrum of human patients surely is increased.

Acknowledgment

This review was supported by intramural funds of The Jackson Laboratory. All procedures involving the use of mice were approved by the Animal Care and Use Committee of The Jackson Laboratory.

References

[1] K. P. Hummel, M. M. Dickie, and D. L. Coleman, "Diabetes, a new mutation in the mouse," *Science*, vol. 153, no. 3740, pp. 1127–1128, 1966.

[2] H. Chen, O. Charlat, L. A. Tartaglia et al., "Evidence that the diabetes gene encodes the leptin receptor: identification of a mutation in the leptin receptor gene in *db*/*db* mice," *Cell*, vol. 84, no. 3, pp. 491–495, 1996.

[3] G. H. Lee, R. Proenca, J. M. Montez et al., "Abnormal splicing of the leptin receptor in diabetic mice," *Nature*, vol. 379, no. 6566, pp. 632–635, 1996.

[4] Y. Zhang, R. Proenca, M. Maffei, M. Barone, L. Leopold, and J. M. Friedman, "Positional cloning of the mouse obese gene and its human homologue," *Nature*, vol. 372, no. 6505, pp. 425–432, 1994.

[5] J. K. Naggert, J. L. Mu, W. Frankel, D. W. Bailey, and B. Paigen, "Genomic analysis of the C57BL/Ks mouse strain," *Mammalian Genome*, vol. 6, no. 2, pp. 131–133, 1995.

[6] E. H. Leiter, D. L. Coleman, and K. P. Hummel, "The influence of genetic background on the expression of mutations at the diabetes locus in the mouse. III. Effect of H-2 haplotype and sex," *Diabetes*, vol. 30, no. 12, pp. 1029–1034, 1981.

[7] J. L. Halaas, C. Boozer, J. Blair-West, N. Fidahusein, D. A. Denton, and J. M. Friedman, "Physiological response to long-term peripheral and central leptin infusion in lean and obese mice," *Proceedings of the National Academy of Sciences of the United States of America*, vol. 94, no. 16, pp. 8878–8883, 1997.

[8] R. A. Koza, K. Flurkey, D. M. Graunke et al., "Contributions of dysregulated energy metabolism to type 2 diabetes development in NZO/H1lt mice with polygenic obesity," *Metabolism*, vol. 53, no. 6, pp. 799–808, 2004.

[9] P. C. Reifsnyder, G. Churchill, and E. H. Leiter, "Maternal environment and genotype interact to establish diabesity in mice," *Genome Research*, vol. 10, no. 10, pp. 1568–1578, 2000.

[10] S. Makino, H. Yamashita, K. Kunimoto, K. Tsukahara, and K. Uchida, "Breeding of the NON mouse and its genetic characteristics," in *Current Concepts of a New Animal Model: The NON Mouse*, N. Sakamoto, N. Hotta, and K. Uchida, Eds., pp. 4–10, Elsevier Science Publishers B. V., Tokyo, Japan, 1992.

[11] P. C. Reifsnyder and E. H. Leiter, "Deconstructing and reconstructing obesity-induced diabetes (diabesity) in mice," *Diabetes*, vol. 51, no. 3, pp. 825–832, 2002.

[12] E. H. Leiter and P. C. Reifsnyder, "Differential levels of diabetogenic stress in two new mouse models of obesity and type 2 diabetes," *Diabetes*, vol. 53, no. 1, pp. S4–S11, 2004.

[13] Y. R. Cho, H. J. Kim, S. Y. Park et al., "Hyperglycemia, maturity-onset obesity, and insulin resistance in NONcNZO10/LtJ males, a new mouse model of type 2 diabetes," *American Journal of Physiology*, vol. 293, no. 1, pp. E327–E336, 2007.

[14] J. H. Kim and A. M. Saxton, "The Tallyho mouse as a model of human type 2 diabetes," *Methods in Molecular Biology*, vol. 933, pp. 75–87, 2012.

[15] J. H. Kim, T. P. Stewart, M. Soltani-Bejnood et al., "Phenotypic characterization of polygenic type 2 diabetes in TALLYHO/JngJ mice," *Journal of Endocrinology*, vol. 191, no. 2, pp. 437–446, 2006.

[16] D. Y. Jung, H. Ong, Y. J. Lee, K. Ju, X. Hu, and J. K. Kim, "TALLYHO/JngJ mice develop maturity-onset obesity, insulin resistance, and hyperglycemia: a polygenic mouse model of Type 2 diabetes," *Diabetes*, vol. 59, supplement 1, Article ID A231, 2010.

[17] Y. Wang, P. M. Nishina, and J. K. Naggert, "Degradation of IRS1 leads to impaired glucose uptake in adipose tissue of the type 2 diabetes mouse model TALLYHO/Jng," *Journal of Endocrinology*, vol. 203, no. 1, pp. 65–74, 2009.

[18] J. L. Sartoretto, T. P. Fitzgibbons, J. Hill, G. P. Aurigemma, M. P. Cooper, and J. K. Kim, "Heart dysfunction in obese and diabetic TALLYHO/JngJ mice: a new model of diabetic heart disease," *Diabetes*, vol. 59, supplement 1, p. A472, 2010.

[19] S. P. Didion, C. M. Lynch, and F. M. Faraci, "Cerebral vascular dysfunction in TallyHo mice: a new model of Type II diabetes," *American Journal of Physiology*, vol. 292, no. 3, pp. H1579–H1583, 2007.

[20] A. A. Like and W. L. Chick, "Studies in the diabetic mutant mouse: I. Light microscopy and radioautography of pancreatic islets," *Diabetologia*, vol. 6, no. 3, pp. 207–215, 1970.

[21] V. Trak-Smayra, V. Paradis, J. Massart, S. Nasser, V. Jebara, and B. Fromenty, "Pathology of the liver in obese and diabetic ob/ob and *db*/*db* mice fed a standard or high-calorie diet,"

International Journal of Experimental Pathology, vol. 92, no. 6, pp. 413–421, 2011.

[22] R. W. Tuman and R. J. Doisy, "The influence of age on the development of hypertriglyceridaemia and hypercholesterolaemia in genetically diabetic mice," *Diabetologia*, vol. 13, no. 1, pp. 7–11, 1977.

[23] N. C. Adi, J. N. Adi, L. Cesar, A. S. Agatston, P. Kurlansky, and K. A. Webster, "Influence of diet on visceral Adipose remodeling in NONcNZO10 mice with polygenic susceptibility for type 2 diabetes," *Obesity*, vol. 20, no. 10, pp. 2142–2146, 2012.

[24] E. H. Leiter, P. C. Reifsnyder, Q. Xiao, and J. Mistry, "Adipokine and insulin profiles distinguish diabetogenic and non-diabetogenic obesities in mice," *Obesity*, vol. 15, no. 8, pp. 1961–1968, 2007.

[25] O. Kluth, F. Mirhashemi, S. Scherneck et al., "Dissociation of lipotoxicity and glucotoxicity in a mouse model of obesity associated diabetes: role of forkhead box O1 (FOXO1) in glucose-induced beta cell failure," *Diabetologia*, vol. 54, no. 3, pp. 605–616, 2011.

[26] D. W. Buck II, P. Jin da, M. Geringer, S. J. Hong, R. D. Galiano, and T. A. Mustoe, "The TallyHo polygenic mouse model of diabetes: implications in wound healing," *Plastic and Reconstructive Surgery*, vol. 128, no. 5, pp. 427e–437e, 2011.

[27] R. C. Fang, Z. B. Kryger, D. W. Buck II, M. De La Garza, R. D. Galiano, and T. A. Mustoe, "Limitations of the *db/db* mouse in translational wound healing research: is the NONcNZO10 polygenic mouse model superior?" *Wound Repair and Regeneration*, vol. 18, no. 6, pp. 605–613, 2010.

[28] H. J. Pan, P. Reifsnyder, D. E. Vance, Q. Xiao, and E. H. Leiter, "Pharmacogenetic analysis of rosiglitazone-induced hepatosteatosis in new mouse models of type 2 diabetes," *Diabetes*, vol. 54, no. 6, pp. 1854–1862, 2005.

[29] J. H. Kim, A. Sen, C. S. Avery et al., "Genetic analysis of a new mouse model for non-insulin-dependent diabetes," *Genomics*, vol. 74, no. 3, pp. 273–286, 2001.

[30] N. D. Palmer, C. W. McDonough, P. J. Hicks, B. H. Roh, M. R. Wing, S. S. An et al., "A genome-wide association search for type 2 diabetes genes in African Americans," *PLoS ONE*, vol. 7, no. 1, Article ID e29202, 2012.

[31] K. Suhre, S. Y. Shin, A. K. Petersen, R. P. Mohney, D. Meredith, B. Wagele et al., "Human metabolic individuality in biomedical and pharmaceutical research," *Nature*, vol. 477, no. 7362, pp. 54–60, 2011.

Hindawi Publishing Corporation
Journal of Diabetes Research
Volume 2013, Article ID 598603, 8 pages
http://dx.doi.org/10.1155/2013/598603

Research Article

Deoxycholic Acid as a Modifier of the Permeation of Gliclazide through the Blood Brain Barrier of a Rat

Mladena Lalić-Popović,[1] Velibor Vasović,[2] Boris Milijašević,[2] Svetlana Goločorbin-Kon,[1,3] Hani Al-Salami,[4] and Momir Mikov[2,3]

[1] *Department of Pharmacy, Medical Faculty, University of Novi Sad, 2100 Novi Sad, Serbia*
[2] *Department of Pharmacology, Toxicology and Clinical Pharmacology, Medical Faculty, University of Novi Sad, 2100 Novi Sad, Serbia*
[3] *Faculty of Pharmacy, University of Montenegro Podgorica, 8100 Podgorica, Montenegro*
[4] *School of Pharmacy, Curtin University, Perth, WA 6845, Australia*

Correspondence should be addressed to Mladena Lalić-Popović; mladena.l@hotmail.com

Received 30 October 2012; Revised 13 February 2013; Accepted 15 February 2013

Academic Editor: Shahidul Islam

Major problem for diabetic patients represents damage of blood vessels and the oxidative stress of the brain cells due to increased concentration of free radicals and poor nutrition of brain cells. Gliclazide has antioxidative properties and poor blood brain barrier (BBB) penetration. Bile acids are known for their hypoglycemic effect and as promoters of drug penetration across biological membranes. Accordingly, the aim of this study is to investigate whether the bile acid (deoxycholic acid) can change the permeation of gliclazide, through the blood brain barrier of a rat model type-1 diabetes. Twenty-four male Wistar rats were randomly allocated to four groups, of which, two were given alloxan intraperitoneally (100 mg/kg) to induce diabetes. One diabetic group and one healthy group were given a bolus gliclazide intra-arterially (20 mg/kg), while the other two groups apart from gliclazide got deoxycholic acid (4 mg/kg) subcutaneously. Blood samples were collected 30, 60, 150, and 240 seconds after dose, brain tissues were immediately excised and blood glucose and gliclazide concentrations were measured. Penetration of gliclazide in groups without deoxycholic acid pretreatment was increased in diabetic animals compared to healthy animals. Also in both, the healthy and diabetic animals, deoxycholic acid increased the permeation of gliclazide through that in BBB.

1. Introduction

Blood brain barrier (BBB) is selective barrier that eclipsed the brain and isolates it from the circulating blood. It is composed of the capillary basement membrane (BM), astrocyte end feet ensheathing the vessels, and pericytes embedded within the BM [1]. It represents a major barrier for drug permeation especially those which are highly hydrophilic and have molecular mass bigger than 400 Da. In addition, efflux protein transporters at the luminal membrane of the endothelial cells limit the penetration of hydrophobic molecules. Diabetes mellitus (DM) can lead to disruption in BBB. A small opening in BBB can have significant impact on BBB function and structure [2]. Some changes in BBB occur very fast after animal being in hyperglycemic state. Previous investigations have shown 30% decrease in brain glucose uptake in only two days after induction of DM [3]. Thus it is viable that changes occur also on some other transport systems but those connected with glucose transport. Damages of central nervous system (CNS) in DM occur due to increased concentration of the free radicals and poor nutrition of the brain cells. Thus, in recent years CNS becomes a target in the treatment of DM [4, 5].

Gliclazide is a second-generation sulfonylurea, and it is used in type 2 DM to stimulate insulin production [6]. Sulphonylurea compounds bind to sulphonylurea subunit (SUR) of ATP sensitive K^+ channel (K_{ATP}) in pancreas, which leads to their closure and release of insulin. Gliclazide has selective affinity for binding to SUR1 receptors located mostly in pancreas. Gliclazide is antidiabetic drug

with antioxidative properties that are independent of any effect on glucose level [7–9]. Also gliclazide has favorable hemobiological properties and other extrapancreatic effects which make gliclazide potentially useful in type 1 DM as well [10–12]. Because of its scavenging effect and low affinity for binding to SUR receptors in brain gliclazide is a good candidate for the investigation as a protector of brain cells in diabetes. Gliclazide is hydrophobic weak acid that shows low transfer into the brain tissue [13, 14].

Bile acids are amphiphilic steroids which have been extensively studied as permeability enhancers of various biological membranes. Bile salts induce reversible BBB opening [15]. Part of the effect is hypothesized to be mediated by tight junction (TJ) modulation [16], cell lysis [17, 18] or incorporation of bile salts into the lipid bilayer [17]. Detergent activity and hydrophobicity are properties of bile salts relevant to the ability to enhance permeability. Deoxycholic acid is natural bile acid that has good permeator capabilities, and it is widely investigated in the field of nanotechnology.

The aim of this study was to investigate the efficacy of sodium salt of deoxycholic acid (DA) as a BBB permeator of lipophilic molecule gliclazide in healthy and diabetic rats by *in vivo* study of gliclazide uptake into the brain tissue after intra-arterial application of gliclazide by retrograde bolus injection into the right *a. axillaris*.

2. Material and Methods

2.1. Animal Treatment

2.1.1. Animals. Male *Wistar* rats (aged 2-3 months, weight 200–300 g) were housed under 12 h : 12 h light-dark conditions in an experimental animal facility and have food and water *ad libitum*. All experiments conducted on animals were approved by the Animal Ethic Committee of the University of Novi Sad.

2.1.2. Induction of Diabetes. Diabetes was induced in rats by the intraperitoneal injection of alloxane (100 mg/kg body weight once a day), for two days, as previously described [19, 20]. If hyperglycemia in animals persisted for four days after the second dose of alloxan, animals were included in the experiment. Blood glucose levels were determined from the tail vein blood using a glucometer-strip system (Accucheck Active, Roche). Rats were considered diabetic if blood glucose concentrations were >20 mmol/L [21].

2.1.3. Experimental Protocol. All groups received microsuspension (particle size < 0.5 μm) of gliclazide (20 mg/kg) to the right *a. axillaris*. DA solution (4 mg/kg) was given subcutaneously 30 minutes before gliclazide dose. Before preparing blood vessels, the animals were anesthetized with urethane (1 g/kg) intraperitoneally. Animals were divided into 4 groups: (1) healthy animals given gliclazide (control), (2) healthy animals given gliclazide and DA, (3) diabetic animals given gliclazide, and (4) diabetic animals given gliclazide and DA (6 rats in each group).

2.2. Sample Preparation and Analyses

2.2.1. Serum Samples Preparation. Blood samples were taken from the left *v. jugularis* 30, 60, 150, and 240 seconds after intra-arterial injection of gliclazide and they were centrifuged for 5 minutes (10000 rpm/min). Serums were stored at −20°C until analysed. Acetonitrile was added to serum (in a 2 : 1 ratio) vortexed (30 seconds), and centrifuged for 5 minutes (10000 rpm/min), and then the supernatant (10 μL) was injected into the HPLC system.

2.2.2. Brain Samples Preparation. The animals were decapitated 240 seconds after gliclazide injection. The cranial bones were resected and the brain tissue was divided into: the left and the right cerebral hemisphere (LCH and RCH), brain stem (BS), and cerebellum (C). After being weighed brain parts were stored at −20°C until analysed. Brain parts were homogenized in a 4-fold volume of distilled water. Chloroform was added to brain samples in a 4 : 1 ratio and after vortexing for 30 seconds and centrifuging for 10 minutes on 3500 rpm/min, 1.4 mL of the lower layer was transferred into tubes, evaporated at 70°C, and before injection on HPLC system reconstituted with 100 μL of methanol.

2.2.3. HPLC Determination of Gliclazide. Gliclazide concentrations in serum and brain samples were measured by HPLC system using the modified method of Mikov et al. [21]. HPLC system (*Dionex*) consisted of Agilent column (5 μm, 100 mm × 2.1 mm, 120 A°) with guard column (Agilent; 5 μm, 20 mm × 2.1 mm). The mobile phase consisted of acetonitrile 49% and water 51%, pH 2.7 at flow rate 0.4 mL/min. The retention time for gliclazide was 2.8 minutes. UV detection was set at 229 nm. Analyses were done at room temperature (25°C). The limit of detection (LOD) for brain samples was 0.02 μg/mL and limit of quantification (LOQ) was 0.22 μg/mL with recovery of 87.64 ± 3.63 and for serum samples LOD was 0.2 μg/mL and LOQ was 0.5 μg/mL with recovery of 86.13 ± 3.16%.

2.2.4. Statistical Analysis. All data were reported as mean ± standard deviation (SD). Date were analysed by General Linear Model (Multivariate ANOVA) via SPSS 17.0 (Systat Software Inc., San Jose, CA, USA). Differences were considered significant if $P \leq 0.05$. Pharmacokinetic analyses were done using WinNonLin (version 4.1; SCI software, Pharsight Corp., Gary NC, USA).

3. Results

Gliclazide concentrations (μg/g) in the brain tissue are shown in Table 1.

Table 1 shows that gliclazide concentrations vary in different parts of the brain and between healthy and diabetic animals suggesting different extent of penetration. There is statistically significant difference of gliclazide concentrations in BS between healthy and diabetic animals without pretreatment with DA. Mean gliclazide concentrations are 7-fold higher in diabetic than those in healthy animals. Also in this

Table 1: Gliclazide concentrations (μg/g) 240 seconds after gliclazide injection (20 mg/kg) in the brain parts and total brain.

Groups		Group 1: healthy Gliclazide $n = 6$	Group 2: healthy Gliclazide + DA $n = 6$	Group 3: diabetic Gliclazide $n = 6$	Group 4: diabetic Gliclazide + DA $n = 6$
Gliclazide concentration (μg/g)—mean ± SD	BS	1.57 ± 0.77	15.49 ± 9.53*	11.51 ± 5.48$^{\#}$	33.72 ± 19.58$^{\times\times,\times}$
	C	2.22 ± 1.13	23.69 ± 11.45*	19.17 ± 8.18$^{\#}$	76.92 ± 34.82$^{\times\times,\#\#}$
	LCH	1.41 ± 0.75	1.87 ± 0.94	0.70 ± 0.38	6.93 ± 4.09$^{\times\times,\times}$
	RCH	2.46 ± 1.56	6.33 ± 4.03*	2.88 ± 1.30	10.02 ± 6.43$^{\times\times,\times}$
	B	1.71 ± 1.03	9.15 ± 5.53*	7.27 ± 3.41$^{\#}$	22.00 ± 14.15$^{\times\times,\times}$

LCH: left cerebral hemisphere; RCH: right cerebral hemisphere; BS: brain stem; C: cerebellum, B: total brain.
*Group 2 versus Group 1, $P \leq 0.05$; $^{\#}$Group 3 versus Group 1, $P \leq 0.05$; $^{\times}$Group 4 versus Group 3, $P \leq 0.05$; $^{\#\#}$Group 4 versus Group 2, $P \leq 0.05$; $^{\times\times}$Group 4 versus Group 1, $P \leq 0.05$.

Table 2: Penetration coefficient of gliclazide in the brain tissue after intra-arterial application of gliclazide ($K_{b/p}$).

Groups		Group 1: healthy Gliclazide $n = 6$	Group 2: healthy Gliclazide + DA $n = 6$	Group 3: diabetic Gliclazide $n = 6$	Group 4: diabetic Gliclazide + DA $n = 6$
$K_{b/p}$—mean ± SD	BS	0.09 ± 0.06	1.35 ± 0.92*	2.13 ± 1.41$^{\#}$	6.15 ± 4.74$^{\times\times,\times}$
	C	0.13 ± 0.06	6.23 ± 3.95*	4.40 ± 2.93$^{\#}$	14.05 ± 8.53$^{\times\times}$
	LCH	0.09 ± 0.04	0.11 ± 0.07	0.09 ± 0.04	1.10 ± 0.8$^{\times\times,\times}$
	RCH	0.15 ± 0.06	0.46 ± 0.38*	0.32 ± 0.23	1.23 ± 0.98$^{\times\times,\times}$
	B	0.12 ± 0.06	1.33 ± 1.01*	1.66 ± 0.93$^{\#}$	4.09 ± 2.87$^{\times\times,\times}$

LCH: left cerebral hemisphere; RCH: right cerebral hemisphere; BS: brain stem; C: cerebellum, B: total brain.
*Group 2 versus Group 1, $P \leq 0.05$; $^{\#}$Group 3 versus Group 1, $P \leq 0.05$; $^{\times}$Group 4 versus Group 3, $P \leq 0.05$; $^{\#\#}$Group 4 versus Group 2, $P \leq 0.05$; $^{\times\times}$Group 4 versus Group 1, $P \leq 0.05$.

part of brain pretreatment with DA leads to the elevation of concentrations of gliclazide in healthy (10-fold) and diabetic rats (3-fold) (differences are statistically significant).

Gliclazide concentrations in C are 9-fold higher in diabetic than those in healthy animals without DA pretreatment and are statistically different. Pretreatment with DA resulted in higher gliclazide concentration in healthy (10-fold) and diabetic (4-fold) rats, but this differences are not statistically significant.

In the groups treated with gliclazide only, the concentrations of gliclazide in LCH and RCH are lower than those in BS and C. It is noticeable that gliclazide concentrations in RCH are, overall, slightly higher among all treatment group, than its concentrations in the LCH part of the brain. When DA was coadministered with gliclazide, the concentrations of gliclazide in RCH were 3-fold higher in healthy and 4-fold higher in diabetic animals; differences are statistically significant. Gliclazide concentrations in LCH were 4-fold higher in diabetic animals pretreated with DA, while in healthy animals coadministration of DA had no effect on gliclazide concentrations comparing to group that received only gliclazide.

In total brain mass gliclazide concentrations are elevated in diabetic animals (4-fold, statistically significant) (Table 1). In groups pretreated with DA gliclazide concentrations are 5-fold higher in healthy and 3-fold higher in diabetic animals (differences are statistically significant).

Pretreatment with DA leads to increased variation of concentrations in all groups and brain parts.

Penetration into the CNS was calculated trough formula (1):

$$K_{b/p} = \frac{C_b}{C_p}, \quad (1)$$

where $K_{b/p}$ is coefficient of the penetration of gliclazide, C_b concentration of gliclazide in brain tissue (μg/g), and C_p total gliclazide concentration in serum 240 seconds (μg/mL).

Total drug penetration is 24-fold higher in BS in diabetic animals than that in healthy animals given gliclazide alone (Table 2). DA increased penetration of gliclazide in BS 15-fold in healthy and 3-fold in diabetic animals; both differences are statistically significant. Effect of diabetes on penetration in C is more pronounced since drug penetration is 34-fold higher in diabetic than that in healthy animals. In C DA facilitates penetration 48-fold in healthy and 3-fold in diabetic animals (differences are statistically significant). The effect of illness and bile salt on gliclazide penetration through BBB is lower in cerebral hemispheres.

Relative brain mass in group of healthy animals pretreated with DA is 1.2-fold lower than that in group of healthy animals treated only with gliclazide and is statistically different (relative brain mass: 0.69±0.05% Group 1 and 0.56±0.03 Group 2). In diabetic animals pretreated with DA relative brain mass is unchanged in comparison to that of diabetic animals treated only with gliclazide (relative brain mass: 0.60±0.09% Group 3 and 0.62±0.11% Group 4). There are no significant differences in relative brain masses between other groups.

Table 3: Gliclazide serum concentrations (μg/mL) 30, 60, 150, and 240 seconds after intra-arterial injection.

Groups	Time (s)	Group 1: healthy Gliclazide $n = 6$	Group 2: healthy Gliclazide + DA $n = 6$	Group 3: diabetic Gliclazide $n = 6$	Group 4: diabetic Gliclazide + DA $n = 6$
Gliclazide serum concentrations (μg/mL): mean ± SD	30	15.13 ± 4.79	22.77 ± 7.50	12.85 ± 5	9.44 ± 5.72
	60	23.28 ± 4.75	15.37 ± 5.20	10.65 ± 3.61	8.29 ± 4.92
	150	13.94 ± 3.44	10.98 ± 3.75	9.16 ± 4.77	7.22 ± 2.94
	240	15.99 ± 4.26	9.79 ± 3.14*	11.12 ± 4.56$^{\#}$	7.43 ± 3.92$^{\times\times}$

*Group 2 versus Group 1, $P \leq 0.05$; $^{\times\times}$Group 4 versus Group 1, $P \leq 0.05$; $^{\#}$Group 3 versus Group 1, $P \leq 0.05$.

Table 4: Areas under the curve of gliclazide serum concentrations (AUC), apparent volume of distribution (Vd), and blood glucose level (mmol/L) 240 seconds after and before intra-arterial gliclazide injection.

Groups	Mean ± SD			
	AUC ($\mu g * s * mL^{-1}$)	Vd (mL)	Glucose level (mmol/L)	
			Before gliclazide	After gliclazide (240 s)
Group 1 healthy animals: gliclazide $n = 6$	4020.43 ± 456.42	219.73 ± 13.47	7.01 ± 0.3	9.55 ± 0.34**
Group 2 healthy animals: gliclazide + DA $n = 6$	3931.02 ± 1790.13	1077.19 ± 83.43*	8.11 ± 0.60	9.53 ± 0.46**
Group 3 diabetic animals: gliclazide $n = 6$	2150.16 ± 1472.50	970.15 ± 79.97$^{\#}$	29.04 ± 4.20	30.95 ± 3.86
Group 4 diabetic animals: gliclazide + DA $n = 6$	1678.7 ± 415.21$^{\times\times}$	648.42 ± 203.65$^{\times\times}$	32.50 ± 5.75	34.3 ± 7.44
Healthy animals	/	/	7.7 ± 0.3	8.7 ± 0.35
Diabetic animals	/	/	28.83 ± 2.23	29.33 ± 2.19
Healthy animals with DA pretreatment	/	/	6.93 ± 0.6	7.45 ± 1.02
Diabetic animals with DA pretreatment	/	/	33.58 ± 4.02	29.7 ± 4.30

*Group 2 versus Group 1, $P \leq 0.05$; $^{\times\times}$Group 4 versus Group 1, $P \leq 0.05$; $^{\#}$Group 3 versus Group 1, $P \leq 0.05$; **glucose level before versus after gliclazide, $P \leq 0.05$.

Gliclazide serum concentrations are shown in Table 3. There are different changes in gliclazide serum concentrations during observed period in examined groups. Gliclazide serum concentrations 240 seconds are higher in healthy than those in diabetic animals (statistically significant difference). Also, DA pretreated groups have lower gliclazide serum concentration 240 seconds than groups without DA pretreatment.

Blood glucose levels (mmol/L) and areas under the curve of gliclazide serum concentrations (AUC) as well as apparent volume of distribution (Vd) are shown in Table 4. Correlation between differences of blood glucose levels 240 seconds after and before application of gliclazide and AUC values is shown on Figure 1.

Correlation between differences of blood glucose levels and AUCs is shown in Figure 1 and it is second-order polynomial in all groups. When AUC values of gliclazide are higher the differences of blood glucose levels 240 seconds after and before application are smaller. However, after reaching maximum AUC values the differences of blood glucose levels are getting higher again.

From Table 4 it can seen that DA alone did not change the level of glucose neither in healthy nor in diabetic animals. Treatment with gliclazide in groups of healthy and diabetic animals with and without pretreatment with DA led to an increase of blood glucose levels. Such glucose level changes were not detected in groups of healthy and diabetic animals treated with only saline solution.

Apparent volumes of distribution in the group of healthy animals treated with gliclazide alone are lower than those calculated in other three groups. Healthy animals pretreated with DA had 4.8 fold higher Vd than those in group of healthy animals treated only with gliclazide. Diabetic animals had 1.5 fold lower Vd in group pretreated with bile salt.

4. Discussion

This study showed differences in gliclazide penetration in various parts of the brain under influence of diabetes mellitus

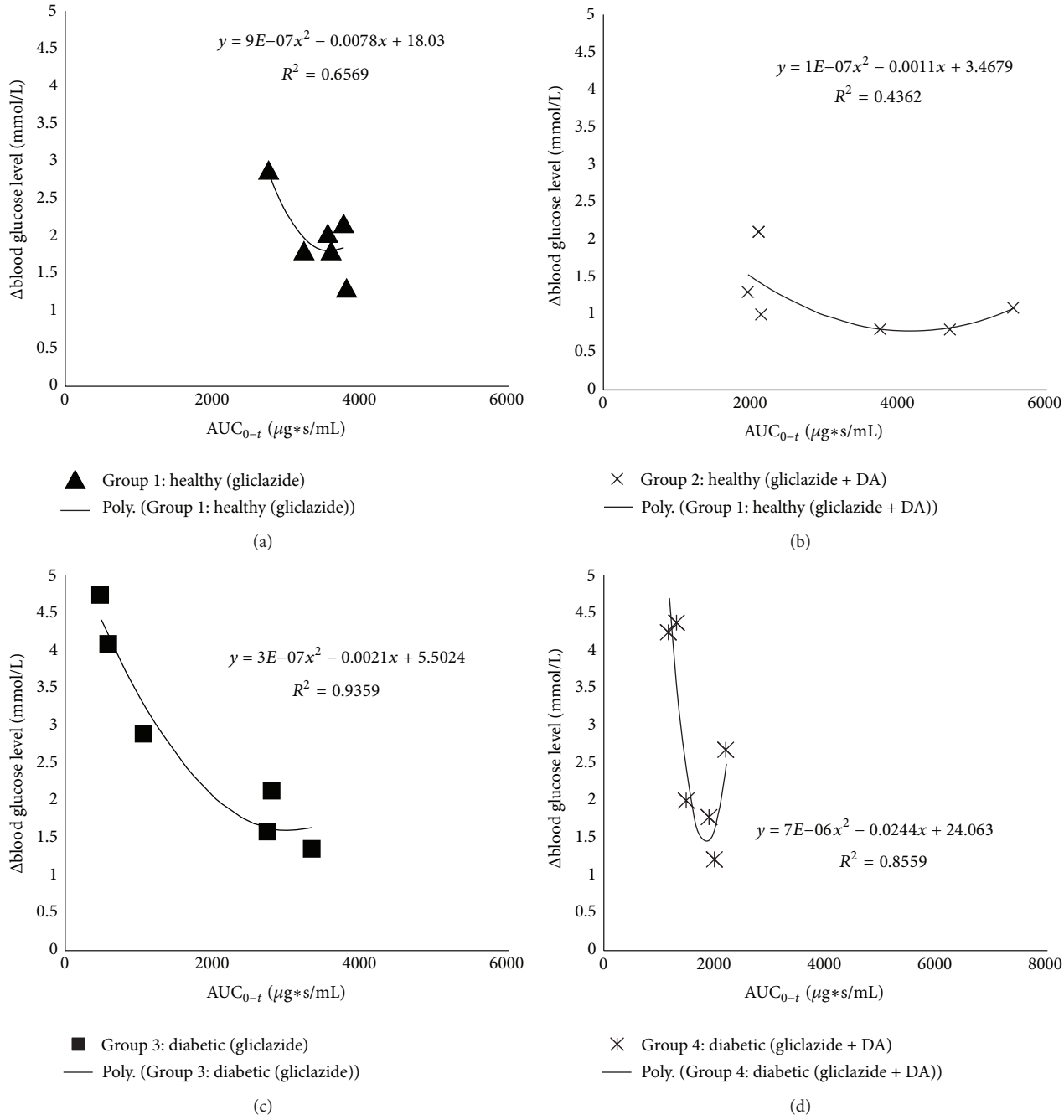

Figure 1: Scatter plots of Δ blood glucose level (mmol/L) 240 seconds after and before intra-arterial injection of gliclazide versus calculated AUC values of gliclazide.

and pretreatment with DA. There were higher concentrations of gliclazide in diabetic animals in comparison to healthy animals and they are the result of BBB disruption [22]. Also, DA had a direct permeation-enhancing effect on the antidiabetic drug gliclazide as other bile acids had in previous studies [23–31]. In group of healthy animals pretreated with DA distribution of gliclazide in all brain parts was similar to the one in group of diabetic animals treated only with gliclazide, which indicates that DA as well as diabetes mellitus had direct effect on gliclazide permeability across BBB.

In healthy animals without DA pretreatment concentrations of gliclazide were similar in all brain parts, which implies a one-compartment model of distribution. In other groups of animals data indicates existence of two compartments where one compartment is cerebellum and brain stem and the other is hemispheres of the brain. However differences in gliclazide brain concentrations could be explained in terms of the distribution of blood vessels and used method of drug application [32]. Higher concentrations of gliclazide in brain stem and cerebellum than those in hemispheres could

be due to the fact that gliclazide was given in right *a. axillaris* which directly through *a. vertebralis* takes larger amount of drug to cerebellum and brain stem because they are closer to the place of application, so these regions get the most of the given dose [33, 34]. Also, through the right *a. carotis* drug is taken to the brain hemispheres where it comes first to right cerebral hemisphere. Thus concentrations of gliclazide are higher in right cerebral hemisphere than left cerebral hemisphere. In group of diabetic animals these differences in gliclazide concentrations could be additionally explained with different susceptibility of BBB. It is known that BBB in brain regions with higher blood vessel density and flow, like it is in hemispheres, stays longer intact in hyperglycemic state.

Apparent volume of distribution of gliclazide is higher in diabetic animals than in healthy animals treated only with gliclazide. Also, apparent volume of distribution of gliclazide is higher in those animals pretreated with DA than that in healthy animals treated only with gliclazide. Apparent volume of distribution is in correlation with observed concentrations of gliclazide in brain tissue where volume of distribution was higher in groups of diabetic animals and those pretreated with DA than that in group of healthy animals treated only with gliclazide. Increased distribution in these groups could be explained in various ways. It is known that gliclazide is highly lipophilic small molecule ($\log P_{\text{octanol/water}} = 2.6$) and weak acid with protein binding of 94% [35]. In diabetes mellitus there is more acidic environment, and thus free fraction of gliclazide is expected to be more in its neutral form which can more easily penetrate BBB [36]. This partly could explain better penetration of gliclazide in group of diabetic animals than in healthy animals. However, the problem of this theory is low solubility of gliclazide which makes it difficult for gliclazide to diffuse through blood to BBB. It is more likely that rapid protein to membrane transfer occurred which was examined earlier for some hydrophobic drugs [37]. If rat brain blood flow is 1.25 mL/min/g and brain blood volume is 3% of brain weight [38] then transit time of blood through brain is approximately 1.5 s. In period of 240 seconds 160 transit times occur thus gliclazide could penetrate through BBB by rapid protein to membrane transfer.

Diabetic animals have better penetration of gliclazide through BBB than healthy animals. Groups of healthy and diabetic animals pretreated with DA have lower AUCs and higher CNS concentrations.

There is second-order polynomial correlation of AUCs with differences of blood glucose levels in all groups, where when AUCs are higher the differences of blood glucose levels are smaller till a breaking point when continued increase of AUCs leads to higher blood glucose level differences. This data suggests that too high gliclazide serum levels (AUCs) lead to inefficient blood glucose level control. Also DA changed pattern of the blood glucose level increase and changed polynomial function.

It is shown that DA enhances permeability through BBB in diabetic and healthy animals. Cell lysis is one of the possible mechanism of the BBB opening, which is unlikely to be the case in this investigation since concentration of bile salt at the site was lower than 1.5 mM [17, 36]. Probable mechanism of BBB opening is modification of tight junction or incorporation of bile salt in membrane bilayer. Also, previously it was found that the infusion of bile salts led to opening of the BBB and edemas of the rat brain [39]. In this study brain edemas were not observed since relative brain mass was not higher in groups of animals pretreated with DA.

5. Conclusions

Deoxycholic acid promotes gliclazide penetration across BBB in diabetic and in healthy animals. In addition, deoxycholic acid alters some pharmacokinetic properties of gliclazide in both healthy and diabetic rats. Deoxycholic acid pretreatment also changed the pattern of blood glucose level increase after gliclazide application in diabetic as well as in healthy animals. Thus deoxycholic acid should be more investigated in the treatment of diabetes mellitus and as permeation promoter of lipophilic molecules through BBB as well as other biological membranes.

Abbreviations

AUC: Areas under the curve of gliclazide serum concentrations ($\mu g * s * mL^{-1}$)
BBB: Blood brain barrier
B: Total brain
BS: Brain stem
DM: Diabetes mellitus
C_b: Concentration of gliclazide in brain tissue ($\mu g/g$)
C: Cerebellum
CNS: Central nervous system
C_p: Total gliclazide concentration in serum in 240th second ($\mu g/mL$)
DA: Sodium salt of deoxycholic acid
DCH: Right cerebral hemisphere
LCH: Left cerebral hemisphere
TJ: Tight junction
Vd: Apparent volume of distribution (mL).

References

[1] P. Ballabh, A. Braun, and M. Nedergaard, "The blood-brain barrier: an overview: structure, regulation, and clinical implications," *Neurobiology of Disease*, vol. 16, no. 1, pp. 1–13, 2004.

[2] J. D. Huber, R. L. VanGilder, and K. A. Houser, "Streptozotocin-induced diabetes progressively increases blood-brain barrier permeability in specific brain regions in rats," *American Journal of Physiology*, vol. 291, no. 6, pp. H2660–H2668, 2006.

[3] A. L. McCall, W. R. Millington, and R. J. Wurtman, "Metabolic fuel and amino acid transport into the brain in experimental diabetes mellitus," *Proceedings of the National Academy of Sciences of the United States of America*, vol. 79, no. 17 I, pp. 5406–5410, 1982.

[4] A. Pocai, T. K. T. Lam, S. Obici et al., "Restoration of hypothalamic lipid sensing normalizes energy and glucose homeostasis in overfed rats," *Journal of Clinical Investigation*, vol. 116, no. 4, pp. 1081–1091, 2006.

[5] D. A. Sandoval, S. Obici, and R. J. Seeley, "Targeting the CNS to treat type 2 diabetes," *Nature Reviews Drug Discovery*, vol. 8, no. 5, pp. 386–398, 2009.

[6] M. Rendell, "The role of sulphonylureas in the management of type 2 diabetes mellitus," *Drugs*, vol. 64, no. 12, pp. 1339–1358, 2004.

[7] R. C. O'Brien, M. Luo, N. Balazs, and J. Mercuri, "*In vitro* and *in vivo* antioxidant properties of gliclazide," *Journal of Diabetes and Its Complications*, vol. 14, no. 4, pp. 201–206, 2000.

[8] P. E. Jennings and J. J. F. Belch, "Free radical scavenging activity of sulfonylureas: a clinical assessment of the effect of gliclazide," *Metabolism*, vol. 49, no. 2, pp. 23–26, 2000.

[9] D. Fava, M. Cassone-Faldetta, O. Laurenti, O. De Luca, A. Ghiselli, and G. De Mattia, "Gliclazide improves anti-oxidant status and nitric oxide-mediated vasodilation in type 2 diabetes," *Diabetic Medicine*, vol. 19, no. 9, pp. 752–757, 2002.

[10] P. Drouin, E. Standl, T. Sechser et al., "Gliclazide modified release: results of a 2-year study in patients with type 2 diabetes," *Diabetes, Obesity & Metabolism*, vol. 6, no. 6, pp. 414–421, 2004.

[11] K. J. Palmer and R. N. Brogden, "Gliclazide: an update of its pharmacological properties and therapeutic efficacy in non-insulin-dependent diabetes mellitus," *Drugs*, vol. 46, no. 1, pp. 92–125, 1993.

[12] O. Ziegler and P. Drouin, "Hemobiological properties of gliclazide," *Journal of Diabetes and Its Complications*, vol. 8, no. 4, pp. 235–239, 1994.

[13] A. Benakis and B. Glasson, "Metabolic study of 14 C-labelled gliclazide in normal rats and in rats with streptozotocin-induced diabetes," in *Gliclazide and Treatment of Diabetes*, H. Keen, Ed., pp. 57–69, Academic Press and the Royal Society of Medicine, London, UK, 1980.

[14] H. Miyazaki, T. Fujii, and K. Yoshida, "Disposition and metabolism of [^{3}H]gliclazide in rats," *European Journal of Drug Metabolism and Pharmacokinetics*, vol. 8, no. 2, pp. 117–131, 1983.

[15] M. Mikov, S. Kevrešan, K. Kuhajda, V. Jakovljević, and V. Vasović, "3α,7α-dihydroxy-12-oxo-5β-cholanate as blood-brain barrier permeator," *Polish Journal of Pharmacology*, vol. 56, no. 3, pp. 367–371, 2004.

[16] M. A. Deli, "Potential use of tight junction modulators to reversibly open membranous barriers and improve drug delivery," *Biochimica et Biophysica Acta*, vol. 1788, no. 4, pp. 892–910, 2009.

[17] J. Greenwood, J. Adu, A. J. Davey, N. J. Abbott, and M. W. B. Bradbury, "The effect of bile salts on the permeability and ultrastructure of the perfused, energy-depleted, rat blood-brain barrier," *Journal of Cerebral Blood Flow and Metabolism*, vol. 11, no. 4, pp. 644–654, 1991.

[18] L. Yang, H. Zhang, J. P. Fawcett, M. Mikov, and I. G. Tucker, "Effect of bile salts on the transport of morphine-6-glucuronide in rat brain endothelial cells," *Journal of Pharmaceutical Sciences*, vol. 100, no. 4, pp. 1516–1524, 2011.

[19] R. E. Heikkila, "The prevention of alloxan induced diabetes in mice by dimethyl sulfoxide," *European Journal of Pharmacology*, vol. 44, no. 2, pp. 191–193, 1977.

[20] T. Szkudelski, "The mechanism of alloxan and streptozotocin action in B cells of the rat pancreas," *Physiological Research*, vol. 50, no. 6, pp. 537–546, 2001.

[21] M. Mikov, H. Al-Salami, S. Golocorbin-Kon, R. Skrbic, A. Raskovic, and J. P. Fawcett, "The influence of 3α,7α-dihydroxy-12-keto-5β-cholanate on gliclazide pharmacokinetics and glucose levels in a rat model of diabetes," *European Journal of Drug Metabolism and Pharmacokinetics*, vol. 33, no. 3, pp. 137–142, 2008.

[22] E. Tolia, I. P. Fouyas, P. A. T. Kelly, and I. R. Whittle, "The blood-brain barrier in diabetes mellitus: a critical review of clinical and experimental findings," *International Congress Series*, vol. 1277, pp. 244–256, 2005.

[23] H. Al-Salami, H. Kansara, J. King, B. Morar, B. Jayathilaka, and P. J. Fawcett, "Bile acids: a bitter sweet remedy for diabetes," *The New Zealand Pharmacy*, vol. 27, no. 10, pp. 17–20, 2007.

[24] H. Al-Salami, G. Butt, I. Tucker, R. Skrbic, S. Golocorbin-Kon, and M. Mikov, "Probiotic pre-treatment reduces gliclazide permeation (ex vivo) in healthy rats but increases it in diabetic rats to the level seen in untreated healthy rats," *Archives of Drug Information*, vol. 1, no. 1, pp. 35–41, 2008.

[25] H. Al-Salami, G. Butt, I. Tucker, and M. Mikov, "Influence of the semisynthetic bile acid (MKC) on the ileal permeation of gliclazide in healthy and diabetic rats," *Pharmacological Reports*, vol. 60, no. 4, pp. 532–541, 2008.

[26] H. Al-Salami, G. Butt, J. P. Fawcett, I. G. Tucker, S. Golocorbin-Kon, and M. Mikov, "Probiotic treatment reduces blood glucose levels and increases systemic absorption of gliclazide in diabetic rats," *European Journal of Drug Metabolism and Pharmacokinetics*, vol. 33, no. 2, pp. 101–106, 2008.

[27] H. Al-Salami, G. Butt, I. Tucker, and M. Mikov, "Probiotic treatment proceeded by a single dose of bile acid and gliclazide exert the most hypoglycemic effect in type 1 diabetic rats," *Medical Hypotheses and Research*, vol. 4, no. 2, pp. 93–101, 2008.

[28] H. Al-Salami, G. Butt, I. Tucker, and M. Mikov, "Influence of the semisynthetic bile acid MKC on the ileal permeation of gliclazide *in vitro* in healthy and diabetic rats treated with probiotics," *Methods and Findings in Experimental and Clinical Pharmacology*, vol. 30, no. 2, pp. 107–113, 2008.

[29] M. Mikov, N. S. Boni, H. Al-Salami et al., "Bioavailability and hypoglycemic activity of the semisynthetic bile acid salt, sodium 3alpha,7alpha-dihydroxy-12-oxo-5beta-cholanate, in healthy and diabetic rats," *European Journal of Drug Metabolism and Pharmacokinetics*, vol. 32, no. 1, pp. 7–12, 2007.

[30] H. Al-Salami, G. Butt, I. Tucker, J. P. Fawcett, and M. Mikov, "Probiotics decreased the bioavailability of the bile acid analog, monoketocholic acid, when coadministered with gliclazide, in healthy but not diabetic rats," *The European Journal of Drug Metabolism and Pharmacokinetics*, vol. 37, no. 2, pp. 99–108, 2009.

[31] H. Al-Salami, G. Butt, I. Tucker et al., "Gliclazide reduces MKC intestinal transport in healthy but not diabetic rats," *European Journal of Drug Metabolism and Pharmacokinetics*, vol. 34, no. 1, pp. 43–50, 2009.

[32] V. Vasović, *The influence of bile acids derivatives on drug transfer into central nervous system [Ph.D. thesis]*, Novi Sad, 1998.

[33] R. B. Chaisson, *Anatomy to the White Rat*, William C. Brown, Dubuque, Iowa, Canada, 5th edition, 1973.

[34] R. Hebei and M. W. Stamberg, *Anatomy of the Laboratory Rat*, Williams & Wilkins Company, Baltimore, Md, USA, 1976.

[35] M. Remko, "Theoretical study of molecular structure, pKa, lipophilicity, solubility, absorption, and polar surface area of some hypoglycemic agents," *Journal of Molecular Structure*, vol. 897, no. 1-3, pp. 73–82, 2009.

[36] L. Yang, H. Zhang, M. Mikov, and I. G. Tucker, "Physicochemical and biological characterization of monoketocholic acid, a novel permeability enhancer," *Molecular Pharmaceutics*, vol. 6, no. 2, pp. 448–456, 2009.

[37] R. L. Juliano, S. Daoud, H. J. Krause, and C. W. M. Grant, "Membrane-to-membrane transfer of lipophilic drugs used

against cancer or infectious disease," *Annals of the New York Academy of Sciences*, vol. 507, pp. 89–103, 1987.

[38] W. F. Ebling, D. R. Wada, and D. R. Stanski, "From piecewise to full physiologic pharmacokinetic modeling: applied to thiopental disposition in the rat," *Journal of Pharmacokinetics and Biopharmaceutics*, vol. 22, no. 4, pp. 259–292, 1994.

[39] A. Watanabe, M. Fujiwara, S. Tominaga, and H. Nagashima, "Bile acid and ammonia-induced brain edema in rats," *Hiroshima Journal of Medical Sciences*, vol. 36, no. 2, pp. 257–259, 1987.